

# Graduate Schools Yearbook 2015



Editors:

Kim Dam-Johansen

Peter Szabo

Aliff H. A. Razak



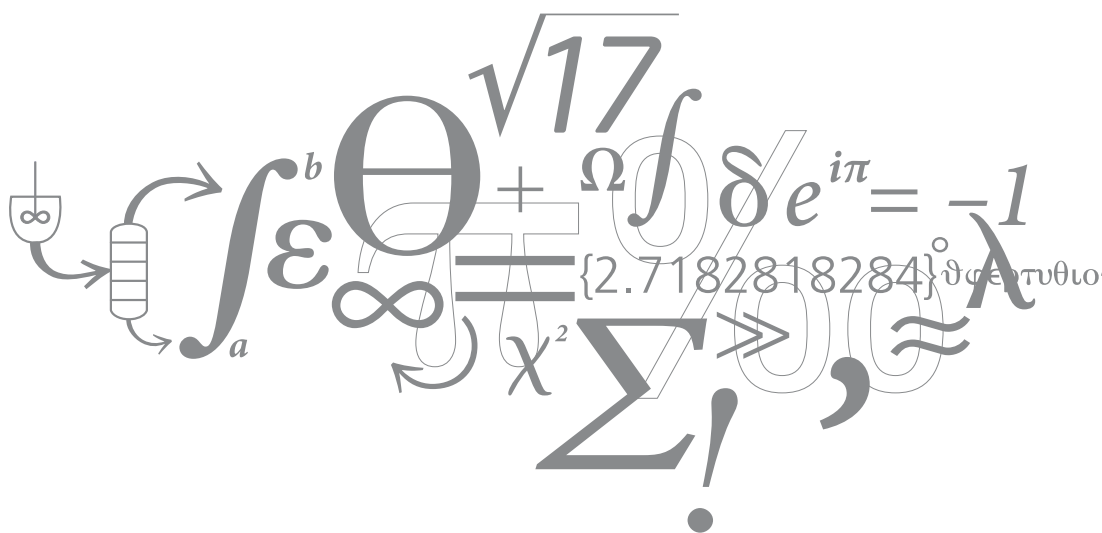
# Graduate Schools Yearbook **2015**

**Editors:**

Kim Dam-Johansen

Peter Szabo

Aliff H. A Razak



## **PREFACE**

Welcome to the Graduate Schools Yearbook of 2015. In this book, most of the PhD students of DTU Chemical Engineering present their projects. Some of the students have just initiated their work whereas others are close to writing their thesis. The work of our PhD students is of utmost importance to fulfil the mission and vision of our department.

### **Mission**

Being responsible for research, education and innovation, DTU Chemical Engineering will develop and utilize knowledge, methods, technologies and sustainable solutions within:

- Chemical and biochemical process engineering and production.
- Design of chemical and biochemical products and processes.
- Energy and environment.

### **Vision**

DTU Chemical Engineering:

- Is acknowledged as a world leading chemical engineering department.
- Is an attractive partner for university departments and research-based industry.
- Helps to retain, develop and attract knowledge-based national working places.
- Supports development of sustainable solutions in the fields of chemistry, biotechnology, food, pharma and energy through research and research based consultancy.
- Is attractive as a place to work for ambitious and technology-passionate staff members.

We hope you will find the Yearbook interesting and we invite all readers to contact us for further details.

Yours sincerely

Kim Dam-Johansen  
Professor, Head of Department

Peter Szabo & Aliff H. A Razak  
Editors

## Contents

### A

A soft and conductive PDMS-PEG block copolymer as a compliant electrode for dielectric elastomers <i>A Razak, Aliff H.</i>	1
Design and evaluation of multi-enzyme processes <i>Abu, Rohana</i>	3
CFD modeling of SNCR in cyclone reactor <i>Ahli-Gharamaleki, Mohammad</i>	5
Predictive modeling of gas diffusion and solubility in polymers for offshore pipelines <i>Almeida, Susana</i>	7
Generic model-based tailor-made design and analysis of biphasic reaction systems <i>Anantpinijwatna, Amata</i>	11
Combustion of biomass in fluidized bed reactors <i>Aničić, Božidar</i>	13
Catalytic hydrodeoxygenation of biomass pyrolysis oil for green fuels <i>Arndal, Trine Marie Hartmann</i>	15
Modeling of asphaltene system with association model <i>Arya, Alay</i>	17
<b>B</b>	
Modeling of gradients in large scale bioreactors <i>Bach, Christian</i>	19
Local enzyme production in Ghana: biodiversity of multifunctional cellulases for lignocellulose deconstruction <i>Bentil, Joseph Asankomah</i>	21
Modelling, synthesis and analysis of biorefinery networks <i>Bertran, Maria-Ona</i>	23
Operation and design of diabatic processes <i>Bisgaard, Thomas</i>	25
CO <sub>2</sub> -Hydrates - Challenges and Possibilities <i>Bjørner, Martin Gamel</i>	27
<b>C</b>	
Continuous crystallization and filtration of active pharmaceutical ingredients and intermediates for pharmaceutical production <i>Capellades Méndez, Gerard</i>	31
Model-based monitoring of bioprocessing plants <i>Caroço, Ricardo Fernandes</i>	33
Optimal model-based monitoring of tubular reactors <i>Castelán, Carlos Eduardo Ramírez</i>	35
Selective catalytic reduction of NO <sub>x</sub> on ships <i>Christensen, Steen Müller</i>	37

Computer-aided molecular, mixture and blend design <i>Cignitti, Stefano</i>	39
<b>D</b>	
Oxygen Supply Methods for Processes using Oxidases <i>Dias, Mafalda</i>	41
Fractionation and enzymatic processing of biomass for biorefinery application <i>Djajadi, Demi Tristan</i>	43
Development of highly efficient solid oxide electrolyzer cell systems <i>Duhn, Jakob Dragsbæk</i>	45
<b>F</b>	
Characterization of microbial consortia for keratin degradation processes <i>Falco, Francesco Cristino</i>	47
Model-based optimization of an industrial wastewater treatment plant combining a full scale granular sludge reactor and autotrophic nitrogen removal <i>Feldman, Hannah</i>	49
Micro scale reactor system development with integrated advanced sensor technology <i>Fernandes, Ana Carolina Oliveira</i>	51
Experimental determination of the solubility of exotic scales at high temperatures – zinc sulfide <i>Figueroa Murcia, Diana Carolina</i>	53
Sustainable process design with process intensification <i>Frauzem, Rebecca</i>	55
Computer-aided molecular design and property prediction models for working fluids of thermodynamic cycles <i>Frutiger, Jérôme</i>	57
<b>G</b>	
Investigation of oxygen-blown biomass gasification <i>Gadsbøll, Rasmus Østergaard</i>	59
Dynamic simulation and analysis of CO <sub>2</sub> post-combustion capture using piperazine and MEA <i>Gaspar, Jozsef</i>	61
Catalytic hydro-liquefaction of lignin to value-added chemicals <i>Ghafarnejad Parto, Soheila</i>	63
<b>H</b>	
Durable zeolite based catalyst systems for diesel emission control <i>Hammershøi, Peter Sams</i>	65
Simultaneous synthesis of process and water networks with superstructure-based optimization technique <i>Handani, Zainatul Bahiyah</i>	67
Development of new automotive diesel oxidation and NH <sub>3</sub> slip catalysts <i>Hansen, Thomas Klint</i>	69
Relaxation mechanism and molecular structure study of polymer blends by rheological experiments <i>Hengeller, Ludovica</i>	71
Heterogeneous surface functionalization of polysulfone membranes as a method for tailoring surface properties <i>Hoffmann, Christian</i>	75

<b>J</b>	
NO <sub>x</sub> reduction in grate-firing solid waste power plants <i>Jepsen, Morten S�e</i>	77
<b>K</b>	
Improving fermentation processes for production of bio-based chemicals and fuels <i>Kalafatakis, Stavros</i>	79
Property modeling and tailor-made mixture design involving complex chemical systems <i>Kalakul, Sawitree</i>	81
A biophysical perspective on integrated food & bioenergy systems in Ghana <i>Kamp, Andreas</i>	83
Magnetically activated microcapsules – preparation and characterization <i>Kostrzewska, Malgorzata</i>	85
<b>L</b>	
Sustainable design of biorefinery systems for biorenewables <i>L. Gargalo, Carina</i>	87
Diabatic separation of fermentation liquids <i>Larsen, Morten Jesper Greisen</i>	89
Modeling of oxygen transfer in a 1 ml microbioreactor and a 8 ml magnetically stirred reactor <i>Larsson, Hilde</i>	91
Adhesion Strength of Biomass Ash Deposits <i>Laxminarayan, Yashasvi</i>	93
Mathematical modelling of sulfuric acid accumulation in lube oil in diesel engines <i>Lejre, Kasper Hartvig</i>	95
New catalytic materials for combined particulate and NO <sub>x</sub> removal from diesel vehicles <i>Linde, Kasper</i>	97
Characterization and biological depectinization of hemp fibers originating from different stem sections <i>Liu, Ming</i>	101
Improving the manure-based anaerobic digestion by means of ammonia <i>Lymperatou, Anna</i>	103
<b>M</b>	
Integrated design, control and analysis of intensified processes <i>Mansouri, Seyed Soheil</i>	105
Biocatalytic alginate membrane by enhanced concentration polarization <i>Marpani, Fauziah</i>	107
Novel strategies for control of fermentation processes <i>Mears, Lisa</i>	109
Biocatalytic Baeyer-Villiger oxidations <i>Meissner, Murray P.</i>	111
Detoxification of a liquid stream from biomass pretreatment by nanofiltration: key role of the interaction membrane material-inhibitors on flux and retention <i>Mohd Sueb, Mohd Shafiq</i>	113

High performance separation of xylose and glucose using an integrated membrane system <i>Morthensen, Sofie Thage</i>	115
Acid and abrasive resistant coatings for the heavy duty industry <i>Møller, Victor Buhl</i>	117
Tribological studies of anti-stick coatings for adhesive raw material build-ups in the cement industry <i>Mørk, Kasper Skov</i>	119
<b>N</b>	
Multiphase flow and fuel conversion in cement calciner <i>Nakhaei, Mohammadhadi</i>	121
Measuring and modelling of chemical sulfur corrosion mechanisms in marine diesel engines <i>Nielsen, Henrik Lund</i>	123
Lignin ethanolysis: a non-catalytic route to a green diesel <i>Nielsen, Joachim Bachmann</i>	125
Release behaviour of alkali species in different atmospheres <i>Nordby, Mads Willemoes</i>	129
Mixing and oxygen transfer processes in bioreactors <i>Nørregaard, Anders</i>	131
<b>P</b>	
Hydrogen chloride (HCl) emission from cement plants <i>Pachitsas, Stylianos</i>	133
Modeling and synthesis of pharmaceutical processes: moving from batch to continuous manufacturing <i>Papadakis, Emmanouil</i>	135
Burners for cement kilns <i>Pedersen, Morten Nedergaard</i>	137
Systematic computer aided methods and tools for lipids process technology <i>Perederic, Olivia Ana</i>	139
Antifreeze proteins and a hydrophobic surface on oil and gas pipelines can better handle flow assurance issues <i>Perfeldt, Christine Malmos</i>	141
<b>Q</b>	
Morphology, rheology and mass transfer in fermentation processes <i>Quintanilla, Daniela</i>	143
<b>R</b>	
Degradation products from pretreated biomass <i>Rasmussen, Helena</i>	145
Next generation methanol to formaldehyde selective oxidation catalyst <i>Raun, Kristian Viegaard</i>	147
Seaweed polysaccharides production using enzymes technology <i>Rhein-Knudsen, Nanna</i>	149
<b>S</b>	
Development of the electrolyte cubic-plus-association equation of state <i>Schlaikjer, Anders</i>	151

Modelling of gasification of biomass in dual fluidized beds <i>Seerup, Rasmus</i>	155
Bioprocess evaluation tools <i>Seita, Catarina</i>	157
Development of advanced mathematical data interpretation methods for the description of bioprocesses in microbioreactors <i>Semenova, Daria</i>	159
The influence of hydrogen bonding on linear and nonlinear rheology of polymer melts <i>Shabbir, Aamir</i>	161
Bioprocess risk assessment using a mechanistic modelling framework <i>Spann, Robert</i>	163
Hydrogen assisted catalytic biomass pyrolysis for green fuels <i>Stummann, Magnus Zingler</i>	165
<b>T</b>	
Automating experimentation in miniaturized reactors <i>Tajsoleiman, Tannaz</i>	167
Low Temperature Thermal Gasification of marginal biomass and waste resources – coproduction of energy and fertilizer <i>Thomsen, Tobias</i>	169
Biooxidation – reactor and process design <i>Toftgaard Pedersen, Asbjørn</i>	171
Process synthesis and design using process group contribution methodology <i>Tula, Anjan Kumar</i>	173
An experimental and theoretical study of CO <sub>2</sub> hydrate formation systems <i>Tzirakis, Fragkiskos</i>	177
<b>V</b>	
Application of an association equation of state in compositional reservoir simulation <i>Vinhal, Andre</i>	181
<b>W</b>	
Experimental study of KCl capture by kaolin in an entrained flow reactor <i>Wang, Guoliang</i>	183
Low friction non-fouling coatings for high fuel efficiency at low speed <i>Wang, Xueting</i>	185
On the correlation between Young’s modulus and melt flow in fiber spinning operations <i>Wingstrand, Sara Lindeblad</i>	187
Development of optimal operating conditions for producing single cell protein <i>Wu, Mengzhe</i>	189
<b>Z</b>	
The influence of static pre-stretching on the mechanical ageing of filled silicone rubbers for dielectric elastomer applications <i>Zakaria, Shamsul</i>	191

Atmospheric hydrodeoxygenation of lignin fast pyrolysis vapor by MoO <sub>3</sub> catalyst <i>Zhou, Guofeng</i>	195
Å Modeling the automotive SCR system <i>Åberg, Andreas</i>	197



**Aliff Hisyam A Razak**

Phone: +45 4525 6819

E-mail: ahis@kt.dtu.dk

Supervisors: Anne Ladegaard Skov

Peter Szabo

PhD Study

Started: December 2013

To be completed: November 2016

## **A soft and conductive PDMS-PEG block copolymer as a compliant electrode for dielectric elastomers**

### **Abstract**

Conductive PDMS-PEG block copolymers ( $M_n = 3 - 5$  kg/mol) were chain-extended with PDMS to give extended copolymers ( $M_n = 30 - 45$  kg/mol). Subsequently, the extended copolymers were mixed with a conductive nano-filler (multi-walled carbon nanotubes – MWCNTs) in order to enhance conductivity. The combination of soft chain-extended PDMS-PEG block copolymers and conductive MWCNTs results in a soft and conductive block copolymer composite which potentially can be used as a compliant and highly stretchable electrode for dielectric elastomers. The addition of MWCNTs into the PDMS-PEG matrix not only increases the conductivity, but also increases mechanical strength by reinforcing the network. However, incorporating MWCNTs into the PDMS-PEG matrix is challenging due to strong van der Waals forces between the MWCNTs. In the present study, MWCNTs were dispersed in organic solvent (N-methyl pyrrolidinone) with 1 wt% of surfactant (Triton X-100). The conductivity of 4 phr MWCNTs is  $10^{-3}$  S/cm compared to  $10^{-1}$  S/cm of a reference conducting silicone elastomer (LR3162 from Wacker), which loses conductivity upon stretching. Furthermore, PDMS-PEG block copolymer with 4 phr MWCNTs (Young's modulus,  $Y = 0.26$  MPa) is softer and more stretchable than LR3162 ( $Y = 1.17$  MPa).

### **Introduction**

Dielectric elastomers (DEs) require inherently soft and highly conductive compliant electrodes for optimum performance. The conventional compliant electrodes, loose carbon black or carbon grease, are easy to apply on both top and bottom surfaces, but they lack adhesion to the elastomer<sup>1</sup>. Alternative compliant electrodes have been extensively explored such as silver nanowires<sup>2</sup>, ionic hydrogels<sup>3</sup>, single-walled carbon nanotubes (SWCNTs)<sup>4</sup> and polymer-carbon conductive composites<sup>5</sup>. These alternative electrodes have good adhesion to the DEs and long lifetime as well as mechanically softness corresponding to the elastomer.

Polydimethylsiloxane-polyethyleneglycol (PDMS-PEG) is a promising conductive polymer. The combination of soft and stretchable PDMS and conductive PEG in the block copolymer results in conductive properties, nearly  $10^{-8}$  S/cm, as reported by A Razak et al.<sup>6</sup> However, this conductivity is relatively low compared to other conductive polymers used for DE electrodes. Due to their conducting nature, the soft PDMS-PEG block copolymer can be further loaded with conductive nano-fillers such as multi-walled carbon nanotubes (MWCNTs) and silver (Ag) particles, incorporated in the PDMS-PEG matrix above the percolation threshold.

MWCNTs possess good mechanical properties, excellent electrical and thermal conductivities, which are suitable for many electronic applications<sup>7</sup>. However, strong van der Waals forces between the tubes cause MWCNTs to be greatly entangled and bundled. Such high interaction energies and entanglements of MWCNTs result in poor dispersibility and weak interfacial interactions with polymer matrices. Therefore, MWCNTs need to be treated either mechanically or chemically so that they are well-dispersed in the polymer network to achieve high conductivity. Treatment of MWCNT's surfaces using non-ionic surfactant does not change the structures or intrinsic properties of MWCNTs compared to other mechanical and chemical methods.

Here, conductive elastomers were prepared by extending short chain vinyl-terminated PDMS-PEG copolymers with telechelic hydride functionalized PDMS<sub>n=232</sub> (n = numbers of repeating dimethylsiloxane units) to obtain long chain copolymers (Si3PEG\_H25) with telechelic hydride-terminated. Subsequently, conductive PDMS-PEG copolymers were cross-linked with vinyl crosslinker via hydrosilylation with an addition of surface-treated MWCNTs at different concentrations.

## Results and Discussion

Due to low molecular weight of the block copolymers, they were chain-extended with PDMS232 ( $M_n = 17200$  g/mol) as a chain-extender, in the presence of 30 ppm Pt catalyst and speedmixed at 3000 rpm for 4 min at 23 °C. In order to obtain good dispersion of MWCNTs, MWCNTs were dispersed in N-methylpyrrolidone (NMP) with 1 wt% of Triton X-100 using a mechanical shaker at 180 rotations/min for 30 min and later was ultrasonicated in water bath for 6 hours.

The conductivity increased of the order of  $10^4$  from 1 phr to 2 phr of MWCNTs in chain-extended PDMS-PEG matrices as presented in figure 1. The reference sample of chain-extended PDMS-PEG without MWCNTs shows conductivity of  $10^{-10}$  S/cm coherently with a previous study<sup>6</sup>. The highest conductivity achieved by 4 phr of MWCNTs in PDMS-PEG matrix is  $10^{-3}$  S/cm, which is lower the order of  $10^2$  compared to the reference conducting silicone elastomer (LR3162).

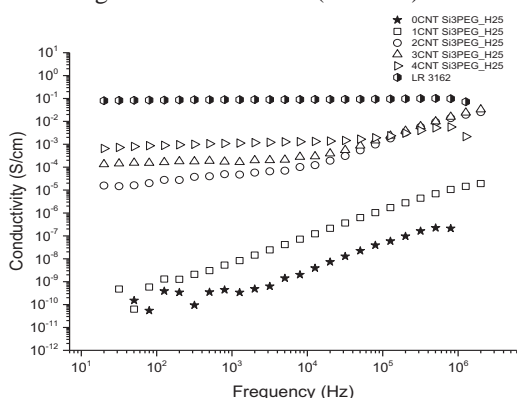


**Figure 1:** Conductivity for chain-extended PDMS-PEG copolymer with different concentration of MWCNTs at 23 °C.

Dielectric losses for chain-extended PDMS-PEG copolymers with 2 to 4 phr of MWCNTs are of the order of  $10^1$  to  $10^3$ , which are lower than the dielectric loss of LR3162 (figure 2). On the other hand, relative permittivity for chain-extended PDMS-PEG with 2 to 4 phr of MWCNTs is nearly identical to that of LR3162. Meanwhile, both chain-extended PDMS-PEG with 1 phr MWCNTs and the reference elastomer with no MWCNTs have almost identical relative permittivity ( $\sim 10$ ). They also possess low dielectric loss ( $10^{-2}$  and below).

The increased storage modulus ( $G'$ ) by adding 1 phr of MWCNTs in PDMS-PEG copolymer indicates that MWCNTs give filler-effect by reinforcing the polymer network. The elastomer shows a softening effect with the addition of 2 phr MWCNTs as the elastomers is destroyed. However, the elastomer shows brittle behaviour due to a weak network when adding above 4 phr of MWCNTs. The reference chain-extended PDMS-PEG without MWCNTs ( $G' = 10^7$  MPa) is stiffer than LR3162 conducting elastomer ( $10^5$  MPa) as shown in figure 3. The modulus loss for all samples remains low ( $\tan(\delta) < 0.3$ ).

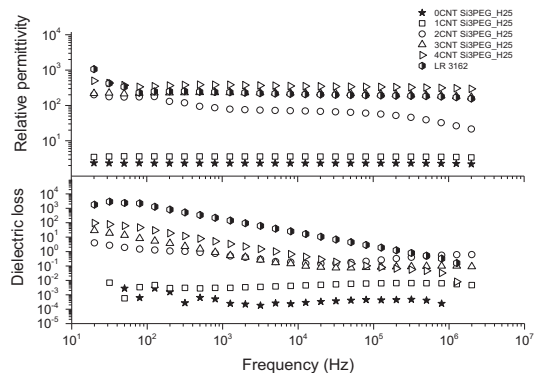


**Figure 2:** Relative permittivity and dielectric loss for chain-extended PDMS-PEG copolymer with different concentration of MWCNTs at 23 °C.

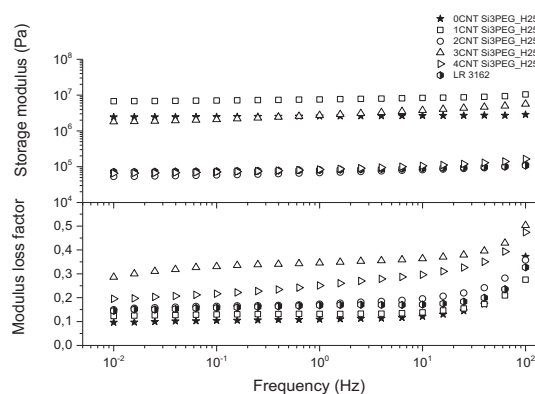


**Figure 3:** Storage modulus and modulus loss for chain-extended PDMS-PEG copolymer with different concentration of MWCNTs at 23 °C.

## Conclusion

The cross-linked conductive PDMS-PEG copolymers were successfully prepared with addition of different MWCNT concentrations. The conductivity of the chain-extended elastomers increases nearly to  $10^{-3}$  S/cm, which is lower than the conductivity of commercial conducting polymer (LR3162) –  $10^{-1}$  S/cm. The mechanical properties of chain-extended PDMS-PEG copolymers with MWCNTs ( $< 3$  phr) indicate soft networks with low modulus losses. The conductivity of soft chain-extended PDMS-PEG copolymers with MWCNTs can be improved by adding silver nanoparticles in the system if properly designed.

## References

- 1 S. Rosset and H. R. Shea, *Appl. Phys. A Mater. Sci. Process.*, 2013, **110**, 281–307.
- 2 J. Li, J. Liang, L. Li, F. Ren, W. Hu, J. Li, S. Qi and Q. Pei, *ACS Nano*, 2014, **8**, 12874–12882.
- 3 C. Keplinger, J. Sun, C. C. Foo, P. Rothmund, G. M. Whitesides and Z. Suo, *Science (80-. )*, 2013, **341**, 984–987.
- 4 S. Shian, R. M. Diebold, A. McNamara and D. R. Clarke, *Appl. Phys. Lett.*, 2012, **101**, 061101.
- 5 J. C. Huang, *Adv. Polym. Technol.*, 2002, **21**, 299–313.
- 6 A. H. A Razak, P. Szabo and A. L. Skov, *RSC Adv.*, 2015, **5**, 53054–53062.
- 7 P. C. Ma, J.-K. Kim and B. Z. Tang, *Compos. Sci. Technol.*, 2007, **67**, 2965–2972.



**Rohana Abu**

Phone: +45 4525 2926  
E-mail: roha@kt.dtu.dk

Supervisors: John M. Woodley  
Krist V. Gernaey

PhD Study  
Started: October 2013  
To be completed: September 2016

## Design and evaluation of multi-enzyme processes

### Abstract

In recent years, much interest has been shown in the application of enzymatic cascades as a useful tool in organic synthesis. Such enzymatic cascades can provide added value to a synthetic scheme by starting from cheaper raw materials or making more valuable products. Despite this interest, the feasibility study of many enzymatic cascades has not been reported and therefore difficult for process design and improvement of multi-enzyme processes.

### Introduction

To date, numerous multi-enzyme processes have been developed as a tool for the synthesis of many interesting chemical compounds. Several of the schemes have been proposed to produce a valuable chemical such as, a chiral amine from a cheap starting material, an alcohol. This is particularly interesting as in general, there is no enzyme that able to directly convert an alcohol into an amine, as the approach taken in nature in metabolic pathways.

Artificial multi-enzyme networks for the asymmetric amination of alcohols have been first developed by Wolfgang's group<sup>1</sup>. The artificial systems consist of three to five redox enzymes that provide a way to convert the alcohols to their corresponding amines. One of the schemes is shown in Fig.1a. Interestingly, the introduction of alanine dehydrogenase (AlaDH) in the cascade serves as dual purposes. Besides recycling the co-factor and co-substrate *in situ*, AlaDH reaction is energetically favourable that is also used to shift both unfavourable reactions (oxidation of alcohols as well as the amination of ketone) achieving a high conversion. However, the major challenge in this cascade is to run the oxidation and amination steps simultaneously, as it is known that amine transaminase reaction is often hindered by an adverse equilibrium position, particularly using alanine as the amino donor<sup>2-4</sup>, giving a low conversion.

Alternatively, a redox-neutral two-enzyme cascade process for the preparation of chiral amines from alcohols has been recently constructed (Fig. 1b)<sup>5,6</sup>. Here, the alcohols are oxidized by an alcohol dehydrogenase to ketones and subsequently aminated by an amine

dehydrogenase (AmDH) to produce the corresponding chiral amines. Interestingly, this approach only requires ammonia as the amino donor and water as the by-product without the addition of alanine and an external reducing agent as in Fig 1a.

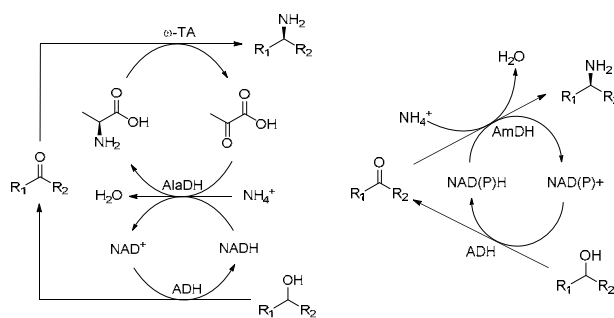


**Fig. 1:** Enzymatic toolbox of self-sufficient redox cascades. (a) ADH/ $\omega$ -TA/AlaDH and (b) ADH/AmDH coupled system. ADH: alcohol dehydrogenase,  $\omega$ -TA:  $\omega$ -transaminase, AlaDH: alanine dehydrogenase, AmDH: Amine dehydrogenase.

Besides numerous enzymatic cascades available in scientific literature, a feasibility study to develop such cascades has not been reported. The guideline to assist the combination of enzymes into a synthetic scheme as shown in Fig. 1 as well as the effective approach in reaction engineering however is not known. Therefore, in this study, the feasibility of multi-enzyme cascades is investigated in order to search for process improvement and implementation. In order to achieve this objective, case studies as mentioned above are used in order to highlight the applicability of the multi-enzyme

processes. Here, we have determined how the oxidation of alcohol and amination of ketone could be made thermodynamically feasible by the use of enzyme coupling and also how the kinetics helps to achieve a favourable conversion at a sufficient rate.

### Process evaluation

In order to improve the conversion of an otherwise thermodynamically limited reactions, the unfavourable reactions are coupled with an energetically favourable one (e.g. AlaDH in Fig. 1a). Such conversion can be determined by the Gibbs free energy and equilibrium constant  $K'$  of the overall reaction. Thus, we have determined and compared the properties of the standard Gibbs free energy of reaction  $\Delta G_r^{\circ}$  given by the group contribution method (a predictive tool) with the experimental data (Table 1). The  $\Delta G_r^{\circ}$  value was calculated based on the experimentally-determined concentration-based equilibrium constant  $K'$  as in Eq. 1.

$$\Delta G_r^{\circ} = -RT \ln K' \quad (\text{Eq. 1})$$

The equilibrium concentrations were determined by allowing the reactants to reach equilibrium from both directions. Here, the synthesis of (*S*)-phenylethylamine (PEA) from (*S*)-phenylethanol (PhEtOH) as the scheme in Fig. 1a was used. All reactions were carried out in at a 3 mL scale incubated in a thermoshaker (HCL, Bovenden, Germany) at 30°C, pH 7 with constant agitation (400 rpm). The analysis was carried out as described previously<sup>7</sup>.

**Table 1:** The  $\Delta G_r^{\circ}$  for the synthesis of PEA using L-ala as the amino donor as the scheme in Fig. 1a.

Enzyme reaction	Group contribution <sup>8</sup> (kJ/mol)	Experimental data (kJ/mol)
ADH	+9.25	+46.78±0.32
$\omega$ -TA	+16.78	+13.50±0.15
AlaDH	-36.36	-76.27±0.11
Net reaction	-10.33±5.66	-12.43±0.37

It should be noticed that AlaDH reaction has a large and negative  $\Delta G_r^{\circ}$  that can successfully shift the thermodynamics of the unfavourable reactions, ( $\omega$ -TA and ADH). The overall reaction was feasible where AlaDH reaction has been identified as a driving force that control the feasibility of the ADH/ $\omega$ -TA/AlaDH coupled system. Further analysis, we explored the feasibility of such cascade in the dependency of the  $K'$  and the overall conversion, by simplifying the individual reactions in the scheme into a net reaction (Eq. 2).

$$\Delta G_r^{\circ} = -RT \ln \frac{[PEA]}{[PhEtOH][NH_4^+]} \quad (\text{Eq. 2})$$

Equation 2 shows that the ammonium concentration is the key compound that controls the favourability of

the cascade and has the effect on the overall equilibrium. For instance, without an excess of ammonium concentration, less than 10% conversion could be expected. However, using a 50-fold excess of ammonium concentration could shift the overall equilibrium position to achieve approximately 70% conversion, assuming that the system is operated in an efficient *in-situ* re-generation system (Fig. 2).

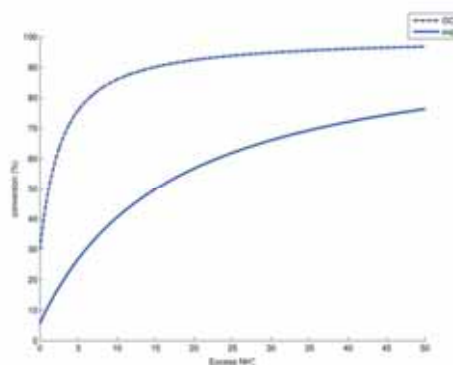


**Fig. 2:** Estimation of equilibrium conversion of ADH/ $\omega$ -TA/AlaDH coupled system in the production of PEA. GC is the group contribution method and exp is the experimental data.

Despite the value of such estimation, it remains unclear the precise effect of biocatalysts as low conversion can also be the result of biocatalyst related issues, such as low activity and stability of biocatalysts, substrate/product inhibition, and/or inefficient co-factor/co-substrate regeneration system. Therefore, kinetics study is also important for enabling high efficiency when running a multi-enzyme cascade, particularly in one-pot system. An approach to measure kinetics, by coupling with the unfavourable to favourable reaction, is currently being done.

### References

1. Tauber, K.; Fuchs, M.; Sattler, J. H.; Pitzer, J.; Pressnitz, D.; Koszelewski, D.; Faber, K.; Pfeffer, J.; Haas, T.; Kroutil, W. *Chemistry* 2013, 19, 4030–4035.
2. Shin, J. S.; Kim, B. G. *Biotechnol. Bioeng.* 1998, 60, 534–540.
3. Tufvesson, P.; Lima-ramos, J.; Jensen, J. S.; Al-Haque, N.; Neto, W.; Woodley, J. M. *Biotechnol. Bioeng.* 2011, 108, 1479–1493.
4. Abu, R.; Woodley, J. M. *ChemCatChem* 2015, 7, 3094–3105.
5. Mutti, F. G.; Knaus, T.; Scrutton, N. S.; Breuer, M.; Turner, N. J. *Science* (80). 2015, 349, 1525–1529.
6. Chen, F.F.; Liu, Y.Y.; Zheng, G.W.; Xu, J.H. *ChemCatChem* 2015, n/a – n/a.
7. Gundersen, M. T.; Abu, R.; Schürmann, M.; Woodley, J. M. *Tetrahedron: Asymmetry* 2015, 26, 567–570.
8. Jankowski, M. D.; Henry, C. S.; Broadbelt, L. J.; Hatzimanikatis, V. *Biophys. J.* 2008, 95, 1487–1499.

**Mohammad Ahli-Gharamaleki**

Phone: +45 4525 2648  
E-mail: moag@kt.dtu.dk  
Discipline: CHEC research Center

Supervisors: Kim Dam-Johansen  
Weigang Lin

PhD Study  
Started: December 2013  
To be completed: December 2016

## CFD modeling of SNCR in cyclone reactor

### Abstract

This project focuses on modelling of Selective Non-Catalytic Reduction (SNCR) of  $\text{NO}_x$  inside cyclone reactors by Computational Fluid Dynamics (CFD) by coupling fluid dynamics and chemical reactions. Cyclones have the potentiality being applied as a reactor for enhancing (because of good mixing) the conversion of reactants in short reaction time. This potential could be targeted for different applications in the chemical industry such as cement preheating stages and power plants based on CFB (Circulating Fluidized Bed) boilers. The developed model will be validated by pilot scale experiments. A pilot has been designed and manufactured for this purpose.

### Introduction

In recent years,  $\text{NO}_x$  emission control has become stricter worldwide. Selective Non-Catalytic Reduction (SNCR) with reduction capabilities from 25% to 75% over a range of industrial applications is an effective and economic method of reducing  $\text{NO}_x$  based on injecting nitrogen agents such as  $\text{NH}_3$  into flue gas containing  $\text{NO}_x$  at high temperatures [1]. In practice,  $\text{NO}_x$  reduction efficiencies are primarily dependent on three factors: mixing, temperature, and residence time. Most of the studies have been conducted on SNCR in furnaces/kilns/boilers, and there is a massive literature on different operating parameters and chemical reaction/reduced kinetics to provide better reaction conditions.

In this study the focus is put on cyclones instead of the furnaces/kilns/boilers as a preferred reactor for SNCR. Two studies have been carried out using cyclone reactor for SNCR [2], [3]. However there is still need to provide more knowledge in different aspect e.g. mixing, residence time, particle effect and etc. to achieve better understanding of the reaction inside the cyclone.

The lack of knowledge of the fluid dynamics and  $\text{NO}_x$  reduction inside cyclone is due to the fact that the fluid dynamics within a cyclone is complex. Moreover, inclusion of parameters, such as residence time, reactant concentrations distribution, as well as other relevant physical properties (e.g. viscosity, density, temperature effects, rotational effects), add further complexities. CFD simulations of the fluid and particle flows in cyclones provide an effective tool for understanding the details of the flow and reaction within the cyclones.

However, the system to be used for the simulations with detail reaction scheme is very complicated and the computation is time consuming even with powerful computers. To reach a reasonable computational time, the system needs to be simplified.

The main aim of this project is to map the relative importance of fluid dynamics and SNCR with involvement of flow pattern, transport phenomena with reduced chemical kinetics and to propose a methodology for process simplification for modelling. The results could be applied for optimisation and scale up, e.g. in cement industry and power plants.

### Methodology

The modeling is divided into three steps: 1) Develop a reliable fluid dynamic model, which will be validated by experiments. 2) Implement SNCR reactions with mass and heat transfer taken into consideration without particle injection (to start with a basic model) inside the cyclone reactor. Based on the obtained validated model and the flow patterns, the SNCR of  $\text{NO}_x$  will be implemented for a high temperature system in the second step. The model will be validated by experimental results in a pilot plan. Experiments will be performed in a pilot setup which is designed and manufactured for the project. The schematic view of the setup is shown in Figure 1.

3) Study of the effect of particles in SNCR of  $\text{NO}_x$  inside the cyclone.

The developed model would then be used to predict the performance parameters of the cyclone reactors, such as pressure drop, efficiency, temperature profile,

$\text{NO}_x$  efficiency and ammonia slip, with respect to variations in system properties (such as solid loading, gas inlet velocity, gas inlet temperature,  $\text{NH}_3/\text{NO}$  ratio and particle size).

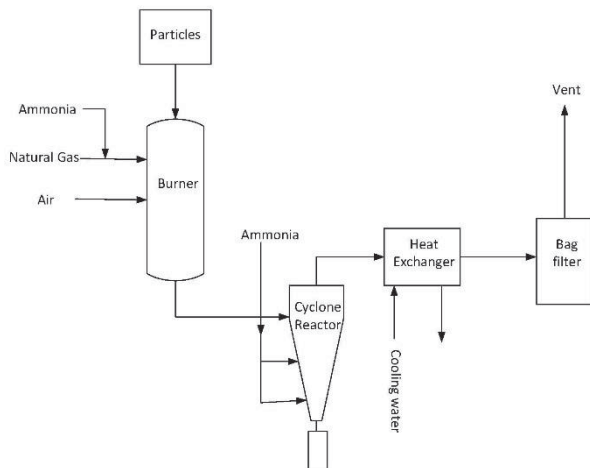


**Figure 1:** Schematic of designed pilot-plant

### Progress so far

Evaluation of CFD-Cold mode is done by Hoekstra's experimental results [4]. **Figure 2** shows the evaluation of CFD modeling of axial velocity of cyclone at an axial location ( $y=3.25D$ ) which is solved by RSM (Reynolds Stress Method).

The CFD model very well predicts the experimental results for velocity profile and pressure drop. Structure of this CFD-model such as turbulent model, boundary conditions, grid generation will be used for the next step of the project for the simulation of reaction in cyclone.

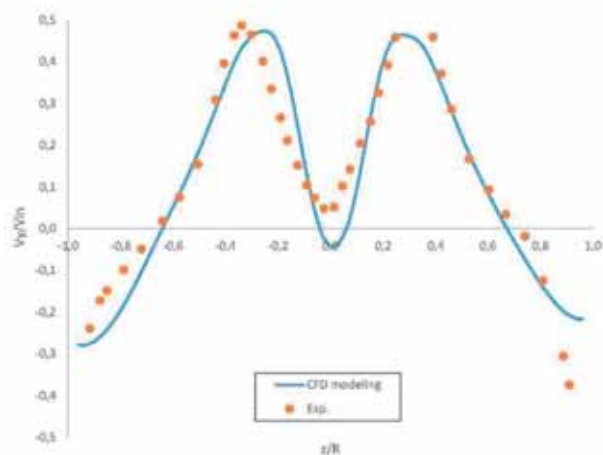


**Figure 2:** Axial velocity profile along the  $z$ -axis at  $y=3.25D$

### Future work

The future work will be model simulation to predict reduction efficiency in different conditions with change in temperature, inlet velocity, initial  $\text{NO}_x$  value, and  $\text{NH}_3/\text{NO}$  ratio. Optimum position for introducing  $\text{NH}_3$  will also be investigated. The position of injection of

$\text{NH}_3$  may affect the initial degree of mixing of  $\text{NH}_3$  stream with the main flue gas stream, and the residence time. If the  $\text{NO}_x$  reduction is the result of the competition of these two parameters, an optimum position exists. In addition, the optimum position may vary with inlet gas velocity and temperature. Mapping the optimum positions may provide valuable information for design and operation.

The optimum  $\text{NH}_3/\text{NO}$  ratio will be assessed from the result. In general, increasing  $\text{NH}_3/\text{NO}$  ratio will lead to an increase in  $\text{NO}$  reduction. However, when this ratio is higher than certain value, the  $\text{NH}_3$  slip will increase. This trade off on the  $\text{NH}_3/\text{NO}$  ratio will result in an existence of the optimum value of  $\text{NH}_3/\text{NO}$  ratio. Furthermore, it is planned to develop simulations to investigate the effect of particles on reduction. The chemistry of SNCR may change due to possible catalytic effect of the particles, especially when e.g. limestone particles are present. In this project it is planned to investigate the influence of sand (no catalytic effect) and limestone. The validation step will be expected to follow simulations with a set of experiments with changing parameters. For investigating the effect of particles, a set of experiments will be performed with and without particles to compare the particle effect in practice with the simulation results.

All the results and the validated model itself will provide general knowledge about cyclone reactor and input to scale up projects or real scale studies e.g. providing information to an existing plant. In such conditions many of the operating parameters are fixed. The model would be applied to optimize the system considering fixed parameters. In general the model could be applied to decide on how to obtain the highest degree of  $\text{NO}_x$  reduction with lowest degree of  $\text{NH}_3$  slip when implementing SNCR in different operating conditions.

### Acknowledgements

The author acknowledges the financial support from Department of Chemical and Biochemical Engineering, Technical University of Denmark.

### References

1. K. L. Richard, "Method for the reduction of the concentration of  $\text{NO}$  in combustion effluence using ammonia," U.S patent 39005541975.
2. B. Ljungdahl and J. Larfeldt, "Optimised  $\text{NH}_3$  injection in CFB boilers," *Powder Technol.*, vol. 120, no. 1–2, pp. 55–62, Oct. 2001.
3. W. G. Huang, J. J. Li, and H. R. Yang, "De $\text{NO}_x$  Technology Selection and Optimal Design of SNCR System for a 300MWe CFB Boiler," *Appl. Mech. Mater.*, vol. 492, pp. 7–12, 2014.
4. A. J. Hoekstra, "Gas flow field and collection efficiency of cyclone separators," PhD thesis, Delft University of Technology, 2000.

**Susana Almeida**

Phone: +45 4525 2891  
E-mail: susal@kt.dtu.dk

Supervisors: Nicolas von Solms  
Georgios Kontogeorgis  
Adam Rubin, NOV Flexibles  
Christian Wang, NOV Flexibles  
Jacob Sonne, NOV Flexibles

PhD Study  
Started: December 2013  
To be completed: November 2016

## Predictive modeling of gas diffusion and solubility in polymers for offshore pipelines

### Abstract

Carbon dioxide (CO<sub>2</sub>) has a crucial role in the oil and gas industry, but one of the main problematics, that is frequently forgotten in comparison with its capture and storage, is the transportation [1]. National Oilwell Varco (NOV) is a specialist in the manufacture of flexible pipes to transport gases at extreme conditions (e.g. supercritical stage) from offshore locations. The design of flexible pipes encloses several layers, being the so-called inner polymer liner the barrier to the egress of the gas being transported [2]. In order to, safely, transport supercritical gases in these pipelines, it is necessary to measure and understand several thermodynamic and transport properties of the polymer/gas system at different pressures and temperatures. The purpose of this work is to determine these key properties (solubility, permeability and swelling), for the development of flexible pipeline systems, under the direct collaboration with an industrial partner: NOV.

### Introduction

Flexible pipes are used as a key component in the oil and gas industry, especially for offshore applications. The design of a flexible pipeline consists of different layers of material, most of them metallic. But there are two types of polymeric materials of crucial importance, the first located at the outer-shell of the pipe which has the main function of protecting from sea water corrosion the inner metallic surfaces; the second polymeric layer is in permanent contact with the transported fluid and therefore reinforces from the inner side the isolation of the metal layers. Moreover, this polymeric inner layer needs to have special mechanical and chemical properties compatible with the transported fluid to avoid leakages and guarantee high safety levels. Due to its critical importance to effective transport, the inner polymer is the main object of this study. Inside the pipeline the gases are transported at high temperature and pressure, well above supercritical [2]. The critical properties of CO<sub>2</sub> are:  $T_c = 30.98\text{ }^\circ\text{C}$  and  $P_c = 73.77\text{ bar}$  [3]. There are two main issues regarding the contact of supercritical fluids with polymers: a swelling phenomenon of the polymer of variable extension depending of the type of polymer used, which could lead to rupture of the pipeline; and the gradual degradation of the polymer that can lead to a loss of some key barrier properties of the polymer.

The study and optimization of the transport properties of supercritical fluids in these pipeline systems is an experimental challenge that requires the acquisition of some thermodynamics and transport properties, such as solubility and permeability. This can be achieved using equipment, such as a Magnetic Suspension Balance (MSB) and a 2-D permeation cell for measuring the solubility and the permeability, respectively. These properties are dependent on pressure, temperature, and composition of the gas, but also on the interactions with the chain group in the polymer. Also, a particular matter to take into account is the change of the polymers physical properties during the transport at extreme conditions, such as the density, diffusivity, swollen volume and even the free volume of the polymers [2].

### Transport Phenomena

The phenomena of gas transport through a polymer can be decomposed into 5 steps, which can be summarized as follows:

- Diffusion through the limit layer on the side corresponding to the higher partial pressure (upstream side);
- Absorption of the gas (mainly due to chemical affinity or solubility) in the polymer;
- Diffusion of the gas inside the membrane polymer;

- Desorption of the gas at the side of lower partial pressure;
- Diffusion through the limit layer of the downstream side [4].

The transport phenomena can be grouped into three transport coefficients: diffusion, solubility, and permeability, where the permeability coefficient is obtained by multiplying the other two coefficients. Another important factor for gas transport in polymers to be taken into account is the crystallinity. The crystallinity fraction of polymer is attributed to the region where the molecules are well arranged, in a regular order. If in one hand the sorption and diffusion phenomena take place in the amorphous regions, on the other hand the crystalline regions act as barriers for diffusion and are not included in the sorption process. However, the existence of crystalline regions seems to not influence the sorption mode in the amorphous regions [2].

### Temperature dependence

A common approach in the literature is to use an Arrhenius equation as a descriptor of the temperature influence in the different coefficients. For example, for permeability the equation should be:

$$P_e = P_{e_0} \exp\left(\frac{-E_p}{RT}\right) \quad (1)$$

Where  $P_{e_0}$  represents the limit value of permeability for the infinite molecular agitation ( $T \rightarrow \infty$ ),  $E_p$  is the apparent activation energy of permeation,  $T$  is the absolute temperature and  $R$  is the universal gas constant. Through a linearization of Eq. 1 is possible to obtain the unknown variables using the slope and the ordinate from the trendline of the experimental data [4]-[7]

### Specific Objectives

The purpose of this study is:

1. Experimental measurements of solubility and permeability of pure CO<sub>2</sub> and its mixture with methane (90/10) in different types of polymers – PVDF, XLPE and PA11 - up to 110 °C and pressures up to 650 bar;
2. Modelling the above properties based on the equation of state sPC-SAFT. It is an objective the inclusion of the volumetric properties of the polymer (such as polymer swelling) in the model.

### Measurements and Modeling of Solubility

The MSB can be simply described as a balance that enables the weighing of the samples in almost all environments at controlled temperature and pressure conditions. The operational conditions can go up to 350 bar and 200 °C. The sample is placed in a sample container which is connected to a permanent magnet. Under the balance there is an electromagnet that attracts the magnet whenever there is an electric current passing through it. Thus, is possible to find the mass of the

polymer with the absorbed gas. The density of the gas at the current pressure and temperature conditions is acquired by MSB and after a buoyancy correction the solubility coefficient is obtained. A scheme of the set-up is represented in Figure 1.

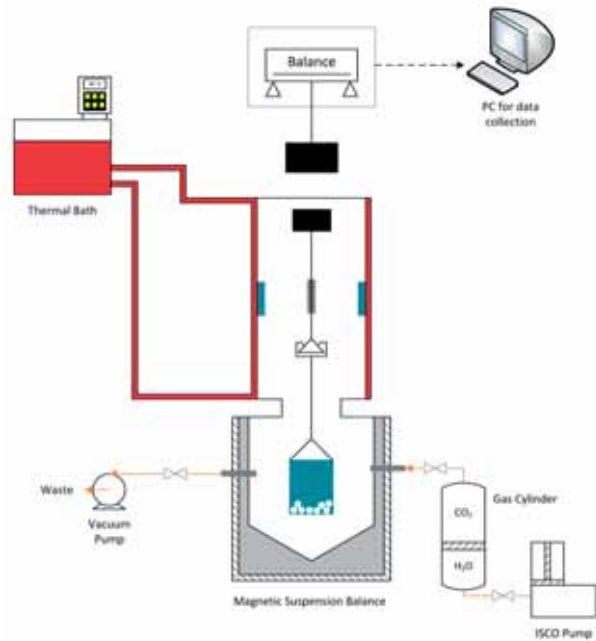


**Figure 1:** Schematic diagram of the MSB set-up.

The most versatile and successful models for predicting and correlating the thermodynamic properties (solubility and swelling) of gas/polymer mixtures, especially at elevated pressures, are equations of state [8]. In particular, the equation of state sPC-SAFT, suitable for polymers and developed at DTU [9] has been successfully applied to these and other similar systems– see Figures 2 and 3.

As a main conclusion, it was observed that the solubility is higher while increasing pressure and temperature parameters, for both polymers.

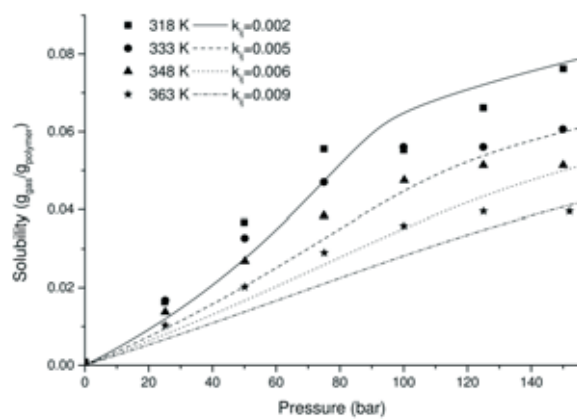


**Figure 2:** sPC-SAFT correlations for CO<sub>2</sub> solubility in PVDF at 45, 60, 75 and 90 °C. The crystallinity of the polymer used in the model prediction was estimated to be 45%. The binary interaction parameter needs to be

temperature dependent in order to capture the experimental data.

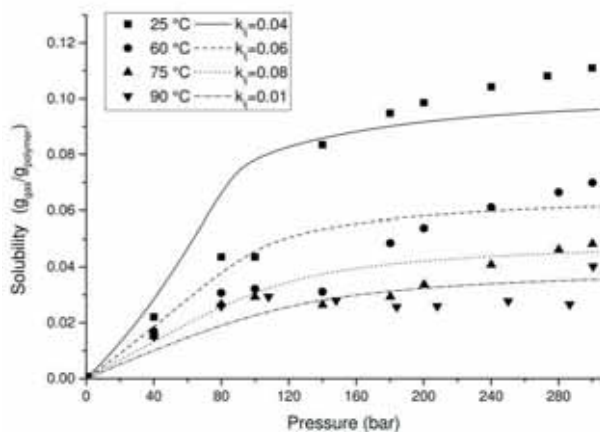


**Figure 3:** sPC-SAFT correlations for CO<sub>2</sub> solubility in XLPE at 45, 60, 75 and 90 °C. The crystallinity of the polymer used in the model prediction was estimated to be 50%. The binary interaction parameter reveals to be temperature dependent.

Around 80 bar a significant increase of the solubility is observed; one possible explanation for this phenomena is that the swelling of the polymer (caused by the passage of CO<sub>2</sub> from gas to supercritical stage) is more affected – the volume of the sample contributes for the buoyancy correction to the solubility calculation – than the change in weight caused by the gas solubility itself.

### Measurements and Modelling of Permeability

As already mentioned, the permeability is obtained from a 2-D permeation cell. The high pressure 2-D permeation cell was designed and manufactured by the Department of Chemical and Biochemical Engineering at Technical University of Denmark. The operating conditions of the cell are up to 150 °C and 700 bar. The set-up of the equipment is shown in Figure 4. The cell consists of two stainless steel chambers: a high-pressure chamber – or primary chamber – and a low pressure chamber – or secondary chamber.

Predictive theories for diffusion in polymers are rare, although Vrentas and Duda [5] have proposed a model based on the concept of free volume in a polymer, where the free volume is divided into interstitial free volume and “hole” free volume, where only the hole free volume is available for solvent diffusion. This is usually taken from a model such as Flory-Huggins, although an equation of state such as sPC-SAFT can also be used [6].

The effect of the temperature was studied in the permeability coefficient between 45 and 90 °C and a significant variation of the permeability is observed with the increasing of temperature. These results are expected because the increase of temperature causes mobility of the polymer chain, resulting in an enhancement of the gas molecules diffusion [6].

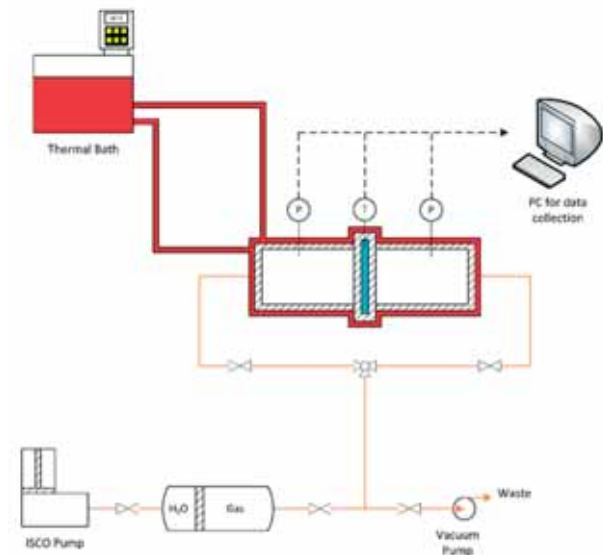


**Figure 4 -** Schematic diagram of the 2-D permeation cell set-up

Figures 5, 6 and 7 present the permeability of CO<sub>2</sub> in the three studied polymers as function of temperature and pressure, which allows to apply the Arrhenius equation linearization.

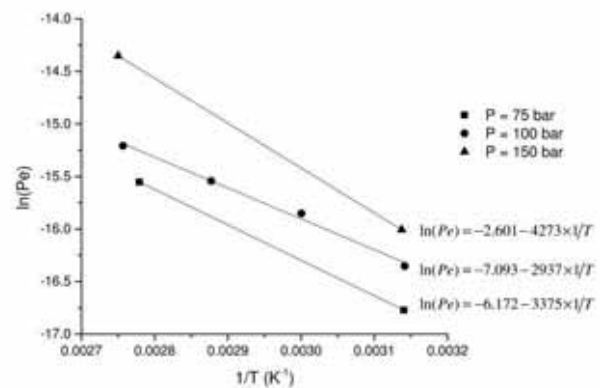


**Figure 5 –** Logarithm of the permeability coefficient as function of the inverse of the temperature for CO<sub>2</sub> in PVDF and respective Arrhenius equation for the different studied pressures.

The variation of permeability with pressure was observed to be dependent of the type of polymer – . For instance PVDF has higher permeability while increasing the pressure (Figure 5). Contrarily to this, XLPE shows a lower permeability with the pressure increase (figure 6), this former behavior can be explained by a compression of the polymer chains at higher pressures, decreasing the free space and thus limiting gas passage. PA11 shows a peculiar behavior (see Figure 7), attributed to the loss of mass that polymer experienced along the measurement due to the release of the plasticizer. The loss of mass was even more significant for higher pressures and temperatures were it reached a decrease of 3.5%.

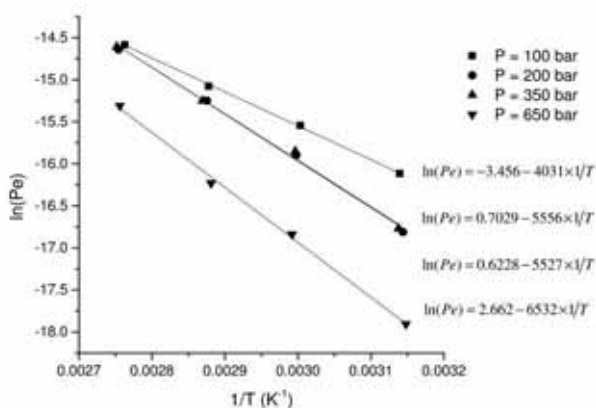


**Figure 6** - Logarithm of the permeability coefficient as function of the inverse of the temperature for CO<sub>2</sub> in XLPE and respective Arrhenius equation for the different studied pressures.

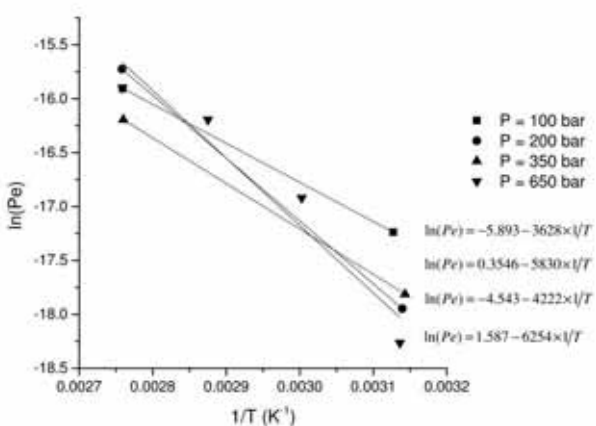


**Figure 7** - Logarithm of the permeability coefficient as function of the inverse of the temperature for CO<sub>2</sub> in PA11 and respective Arrhenius equation for the different studied pressures.

### Future Work

- Further experiments with MSB and 2-D permeation cell to measure the solubility and permeability, respectively, at different temperatures, pressures and gases mixtures;
- Determination of the polymer swelling at different temperatures and pressures;
- Investigate the change of the crystallinity fraction in the studied pressures and temperatures;
- Develop of a model that combines a SAFT model for solubility with a novel model for transport phenomena of gases in polymers integrating the work done before.

### Acknowledgements

The author gratefully acknowledges NOV Flexibles and DTU for funding the project.

### References

1. A. Rubin, C. Wang, Qualifications of Flexible Dynamic Risers for Supercritical CO<sub>2</sub>, Offshore Technology Conference, Houston, USA, 2012
2. S. Almeida, Measurement and Modeling of Supercritical CO<sub>2</sub> Solubility and Permeability in Polymers for Offshore Applications, M.Sc. thesis, DTU Chemical Engineering (2012).
3. REFPROP, NIST, version 8.
4. M. Klopffer, B. Flaconèche, Transport Properties of gases in polymers: Biographic Review, Oil & Gas Science and Technology, 56, (2001), 223-244.
5. J.S. Vrentas, J.L. Duda, Free-Volume Interpretation of Influence of Glass-Transition on Diffusion in Amorphous Polymers, J. Appl. Polym. Sci., 22, (1978), 2325.
6. J. K. Adewole, L. Jensen, U. A. Al-Mubaiyedh, N. von Solms, and I. A. Hussein, "Transport properties of natural gas through polyethylene nanocomposites at high temperature and pressure," J. Polym. Res., vol. 19, no. 2, p. 9814, Feb. 2012.
7. B. Flaconeche, J. Martin, and M. H. Klopffer, "Permeability, Diffusion and Solubility of Gases in Polyethylene, Polyamide 11 and Poly (Vinylidene Fluoride)," *Oil Gas Sci. Technol.*, vol. 56, no. 3, pp. 261–278, May 2001.
8. N. von Solms, M. L. Michelsen, G. M. Kontogeorgis, Prediction and Correlation of High-Pressure Gas Solubility in Polymers with Simplified PC-SAFT, Ind. Eng. Chem. Res. 44, (2005), 3330.
9. N. von Solms, M. L. Michelsen, and G. M. Kontogeorgis, Computational and Physical Performance of a Modified PC-SAFT Equation of State for Highly Asymmetric and Associating Mixtures, Ind. Eng. Chem. Res. 42, (2003), 1098.



**Amata Anantpinijwatna**

Phone: +45 4525 2912  
E-mail: amatana@kt.dtu.dk

Supervisors: Rafiqul Gani  
John M. Woodley

PhD Study  
Started: August 2013  
To be completed: July 2016

## Generic model-based tailor-made design and analysis of biphasic reaction systems

### Abstract

Biphasic reacting systems have a broad range of application in chemical, pharmaceutical, and agro-bio industries. The systems contain two immiscible liquid phases, in which reactants and catalysts (including also biocatalysts and enzymes) can exist in different liquid phases, allowing novel synthesis paths, higher yield, and faster reaction rate, as well as, making the separation tasks easier by manipulating process condition after reaction. A mathematical model which collectively describe reactions, mass transfer, and equilibrium of heterogeneous species can be a powerful tool for improve and innovative design of the systems. In this work, the predictive qualities of the model together with the improvements in the predicted design and operation of reaction with biphasic systems are highlighted. Also, applications of problem-specific models for selecting improved design alternatives based on different design targets are presented.

### Introduction

Biphasic reacting systems have a broad application range from organic reactions in pharmaceutical and agro-bio industries to CO<sub>2</sub> capture [1,2]. In these systems, phases are created by two immiscible liquids where reactants, catalysts (including biocatalysts and enzymes), and products can exist in different liquid phases, allowing novel synthesis path. As well as enhancing selectivity and conversion through regulating phases composition with solvent selection or operation conditions. Moreover, by manipulating reactor conditions, reactants, catalysts and products may end up in different phases, leading to lessening the separation tasks. In order to efficiently develop, design, and analysis the process, mathematical modelling which collectively describe physical and chemical equilibrium, reaction mechanism, and unit operation is generated with a framework for modelling of the biphasic reaction system [3].

A new predictive electrolyte model based on group contribution method (e-KT-UNIFAC) [4] has been incorporated into the framework. This new model has been successfully applied for alkali-halide salts in aqueous and mixed solvent systems and has the capability to predict the partitioning and equilibrium of electrolyte and non-electrolyte systems and also has the potential to accommodate a wide range of reaction systems and solvents.

### Objectives

General objectives of the project are listed as followed:

- To propose a framework for modeling biphasic reaction systems.
- To develop a model of interested biphasic reaction systems.
- To use developed models for designing, optimizing, and analyzing the system.

### Progress

#### *Framework and Generic Model*

The systematic framework for modelling of the biphasic reacting system consists of three modules of physical equilibrium, kinetic and mass transfer, and balance based on concept of extend of the reaction coupled with generic mathematical equations (Eqs. 1 - 5).

$$P_i = \frac{\gamma_i^\alpha}{\gamma_i^\beta} \quad 1$$

$$x_i^\alpha P_i = x_i^\beta \quad 2$$

$$R_j = k_j \left( \prod_i C_i^{\sigma_{ij}^>} - \frac{\prod_i C_i^{\sigma_{ij}^<}}{K_{Eq,j}} \right) \quad 3$$

$$\frac{d\xi_j}{dt} = R_j V \quad 4$$

$$N_i = N_i^0 + \sum_j \nu_{ij} \xi_j + F_i^0 - F_i \quad 5$$

Where, partition coefficient ( $P_i$ ) is defined as a distribution of each species between the two co-existing phases computed from activity coefficients ( $\gamma_i^\alpha, \gamma_i^\beta$ ) calculated with an appropriate thermodynamic model. Reaction kinetic ( $k_j$ ) and equilibrium ( $K_{Eq,j}$ ) are reaction specific parameters.

Problem-specific models are then generated from different combinations of the equations from the three modules.

#### Implementation of e-KT-UNIFAC for PTC

To apply the e-KT-UNIFAC for phase transfer catalyst (PTC) systems, 4 new ion groups for PTC have been defined. Figure 1 shows acceptable agreement between the measured experimental data and model predictions, with remarkable success in displaying the formation of micelle by the tetrabutylammonium chloride PTC.

#### Model-based PTC Process Design

In this section, the production of butyl bromide from butyl chloride with tetraalkylammonium as PTC cases study are presented. Results highlighting the application of problem-specific models for selecting the best combination of solvent-PTC with different design targets.

The model is used to estimate the effect of PTC partitioning toward the actual rate of reaction. In total, 13 solvents and 4 PTCs are analyzed. Half-life and equilibrium time of the reaction mainly depend on the activity coefficient of active PTC in organic phase as shown in Figure 2. The fastest reaction is almost 10 order of magnitude higher than the slowest one.

Also, to select the proper feed amount of PTC, the model is operated with varied concentration of PTC. As shown in Figure 3. At the optimum range, almost all fed PTC is converted to the active form in the organic phase, thereby allowing the reaction to take place. Below the optimum region, lower concentration of PTC makes its stay as active form in aqueous phase longer, causing slow organic phase reaction. While above the optimum region, PTC accumulates as inactive form in the organic phase, causing the loss of valuable catalyst.

#### Conclusion and Future Perspective

A biphasic reacting systems modelling framework has been extended with a predictive constitutive thermodynamic model (e-KT-UNIFAC), resulting in broadening the range of applicable systems, improving the predictive capability, as well as, reducing the need for experimental data. Coupled with the new thermodynamic model, a predictive reactor model with its sub-models has been developed for phase transfer catalyst systems for study of different operational scenarios. The model has been successfully applied for the design of a PTC system with the aim to improve

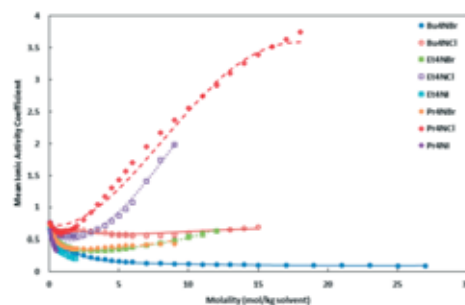


Figure 1: Comparisons of calculated mean ionic activity coefficients of Tetraalkylammonium PTC with data [5,6]

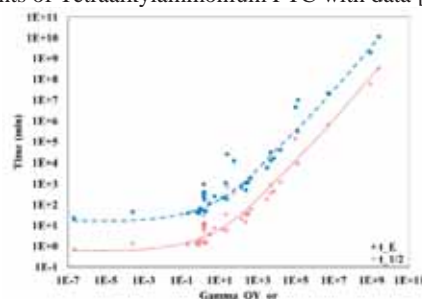


Figure 2: Relation between organic activity coefficient of PTC and reaction half-life ( $t_{1/2}$ ) and equilibrium time ( $t_E$ )

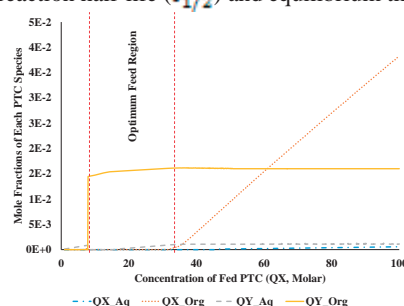


Figure 3: Relationship between amounts of PTC fed and the distribution of it into each form in both phases

production, reduce downstream separation, accelerate reaction, and/or optimize operation.

Though, the framework and the model are under constant further development and improvement, the current version has shown that very promising results can already be obtained for PTC based reacting systems.

#### Acknowledgement

I'd like to thank Professor Felipe Lopez-Isunza, Professor John P. O'Connell, and Professor Alfonso Mauricio Sales-Cruz for great advices. I'd also like to thanks Dr. Sun Hyung Kim for our collaboration. And I'd like to thank Thai's OCSC for a financial support.

#### References

1. E. Santacesaria, G. Vicente, M. Di Serio, R. Tesser, Catal. Today 195 (2012) 2–13.
2. H. Nowothnick, A. Rost, T. Hamerla, R. Schomäcker, C. Müller, D. Vogt, Catal. Sci. Technol. 3 (2013) 600.
3. A. Anantpinijwatna, G. Sin, J.P. O'Connell, R. Gani, Comput. Aided Chem. Eng. 34 (2014) 249–254.
4. S.H. Kim, A. Anantpinijwatna, J.W. Kang, M. Sales-Cruz, R. Gani, Comput. Aided Chem. Eng. 37 (2015) 701–706.
5. E. V. Dehmlow, Angew. Chemie Int. Ed. English 16 (1977) 493–505.
6. C.M. Starks, J. Am. Chem. Soc. 93 (1971) 195–199.



**Božidar Aničić**

Phone: +4525 2837  
E-mail: boza@kt.dtu.dk

Supervisors: Kim Dam Johansen  
Weigang Lin  
Hao Wu  
Wei Wang, Chinese Academy of Sciences

PhD Study  
Started: August 2015  
To be completed: July 2018

## Combustion of biomass in fluidized bed reactors

### Abstract

The PhD project focuses on biomass combustion in fluidized bed reactors. The major operational problems, NO<sub>x</sub> emission and bed agglomeration, will be studied in order to understand the fundamental mechanisms, and to develop modelling tools and countermeasures that can be applied to minimize the problems. Comprehensive experimental analysis will be performed to achieve a systematic understanding of the influences of fuel properties and operational parameters on NO<sub>x</sub> emission and bed agglomeration. Based on the experimental results, mathematical models will be developed to predict and evaluate NO<sub>x</sub> emission and bed agglomeration in fluidized bed reactors. Different countermeasures will be developed, tested and optimized through experiments and modelling.

### Introduction

Fluidized bed combustion is a promising technology for efficient and flexible utilization of biomass to produce heat and power [1]. On the other hand, there are several operational problems, such as NO<sub>x</sub> emission and bed agglomeration, that can hamper a continuous and high-efficient operation of biomass-fired fluidized bed boilers [2,3].

Bed agglomeration can cause instable combustion in biomass-fired fluidized bed boilers, and in extreme cases, result in defluidization and unscheduled plant shutdown [1]. Bed agglomeration can be induced by the reactions of alkali species from biomass and silica bed materials, which form a layer of molten potassium silicates on bed particle surface. Besides, bed particles can also attach to burning biomass particles due to the formation of molten ash phases at the high-temperature surface of burning particles [4]. In order to understand and minimize bed agglomeration problems, a systematical experimental analysis under different fuel and operation conditions is needed. On the other hand, it is desirable to develop modeling tools that can predict and evaluate the processes.

Emission of nitrogen oxides (NO<sub>2</sub>, NO, N<sub>2</sub>O) can result in severe environmental problems such as ozone depletion and acid rain. Thus strict legislation for NO<sub>x</sub> emission has been applied to biomass-fired fluidized bed boilers [5]. In fluidized bed combustion of biomass, NO<sub>x</sub> can be formed from the oxidation of fuel-bound nitrogen, and the reaction between N<sub>2</sub> and hydrocarbon radicals. The formation of NO<sub>x</sub> is influenced by many

factors, including the fuel chemical and physical characteristics as well as the temperature, mixing, and stoichiometric conditions in boilers [1]. An in-depth understanding of the effect of aforementioned factors through experiments and modelling is needed in order to minimize NO<sub>x</sub> emission.

Besides optimization of operation conditions in boilers, countermeasures for bed agglomeration and NO<sub>x</sub> emission problems in fluidized bed combustion of biomass have been explored and tested [6,7], such as pre-treatment of biomass, usage of additives, and co-combustion. In order to optimize the performance of countermeasures, extensive experimental and modeling analysis is needed.

### Specific Objectives

The PhD project focuses on fluidized bed combustion of biomass. The objectives are to:

- Achieve a systematical understanding of bed agglomeration and NO<sub>x</sub> emission mechanisms under different fuel and operation conditions.
- Develop reliable modeling tools to predict and analyze bed agglomeration and NO<sub>x</sub> emission.
- Evaluate and optimize countermeasures to reduce bed agglomeration and NO<sub>x</sub> emission.

### Approaches

The approaches of the project include experimental studies in a laboratory-scale fluidized bed reactor and other fixed bed/entrained flow reactors, and modeling

work using chemical engineer models and/or computational fluid dynamics models.

A laboratory-scale fluidized bed reactor will be established in DTU Chemical Engineering. The reactor will be applied to study the combustion of various biomass under well-defined experimental conditions (temperature, excess air ratio, superficial velocity etc.), with a focus on NO<sub>x</sub> emission and bed agglomeration behaviors. The influences of various additives, alternative bed materials, and fuel blending on combustion performance will be investigated. The experimental work will be supported by in-situ measurements of the gas, temperature and pressure distribution in the reactor, and by various ex-situ tools (e.g. scanning electron microscopy coupled with energy-dispersive x-ray spectroscopy, x-ray diffraction, thermogravimetric analysis, inductively coupled plasma optical emission spectroscopy) for characterization of bed materials and the fuel/char samples.

Fixed bed and entrained flow reactors in DTU Chemical Engineering will be used in the project to achieve quantitative understandings of the fundamental mechanisms of bed agglomeration, NO<sub>x</sub> formation, and countermeasures. Experiments on simple systems, e.g. NO<sub>x</sub> formation during different stages (pyrolysis and char oxidation) of biomass combustion and reaction between potassium salts and silica sand, will be carried out under fluidized bed conditions. The experiments will be supported by the aforementioned in-situ and ex-situ characterization tools.

Mathematic models that can describe bed agglomeration and NO<sub>x</sub> formation during fluidized bed combustion of biomass will be established based on the experimental results obtained from the fluidized bed, fixed bed, and entrained flow reactors. Currently, modelling of bed agglomeration is still to a large extent based on thermodynamic equilibrium models [8]. In this project, based on experimental input, an advanced chemical engineering model that consider transport processes and chemical reactions will be developed to describe reaction-induced bed agglomeration. In addition, simplified models for fuel conversion and NO<sub>x</sub> formation will be developed and implemented in a computational fluid dynamics model applicable for fluidized bed combustion of biomass. Moreover, models that can describe the effect of countermeasures (e.g. additives) may be developed. The aims of developing the aforementioned models are to facilitate the fundamental understanding of operational problems as well as sensitivity analysis and possible implementation of the models on industrial scale fluidized bed boilers.

#### **Acknowledgment**

This project is funded by Innovation Fund Denmark (DANCNGAS), Sino-Danish Center for Education and Research, and Technical University of Denmark.

#### **References**

1. A.A. Khan, W. de Jong, P.J. Jansens, H. Spliethoff, *Fuel Process Technology* 90 (2009) 21–50.
2. M. Bartels, J. Nijenhuis, J. Lensselink, M. Siedlecki, W. de Jong, F. Kapteijn, et al., *Energy Fuels*. 23 (2009) 157–169.
3. B. Gatternig, J. Karl, *Fuel*. (2015).
4. B. Gatternig, J. Karl, *Energy Fuels* 29 (2015) 931–941.
5. European, Directive 2010/75/EU on industrial emissions, Official journal of the European Union.
6. D. Vamvuka, D. Zografos, G. Alevizos, *Bioresource Technology* 99 (2008) 3534–3544.
7. J. Han, H. Kim, S. Cho, T. Shimizu, *Energy Sources* 30 (2008) 1820–1829.
8. Y. Niu, H. Tan, S. Hui, *Progress in Energy Combustion Science* (2015).

**Trine Marie Hartmann Arndal**

Phone: +45 4525 2809  
E-mail: trina@kt.dtu.dk  
Discipline: Catalysis and Reaction Engineering

Supervisors: Anker Degn Jensen  
Martin Høj  
Jan-Dierk Grunwaldt, KIT  
Jostein Gabrielsen, Haldor Topsøe A/S

PhD Study  
Started: April 2014  
To be completed: April 2017

## Catalytic hydrodeoxygenation of biomass pyrolysis oil for green fuels

### Abstract

Catalytic fast hydrolysis of biomass with downstream hydrodeoxygenation (HDO) of the pyrolysis vapors is a promising technique for sustainable production of green fuels. This study is focused on the experimental investigation of catalytic HDO. The scope of this project is to develop active and stable catalysts for hydrolysis and downstream HDO as well as optimizing operating conditions to minimize catalyst deactivation. The project is part of the project “H<sub>2</sub>CAP - Hydrogen Assisted Catalytic Biomass Pyrolysis for Green Fuels”.

### Introduction

The H<sub>2</sub>CAP process aims at converting solid biomass into fuel grade oil through continuous catalytic hydrolysis and downstream deep HDO (see also Magnus Zingler Stumm, pg. 165-166). Conventional pyrolysis of biomass produces a high yield of condensable bio-oil at moderate temperature and low pressure [1]. The produced bio-oil has a high content of oxygen which must be removed (down to <1 wt%) in order to enhance its fuel properties. The oxygen is present as water (15-30 wt%), carboxylic acids, aldehydes, ketones, alcohols, furans, phenols and more [1-3]. Depending on the biomass source, the higher heating value (HHV) of the produced oil is approximately 16-19 MJ/kg compared to approximately 44 MJ/kg of crude oil [2]. Additionally, the oxygenates present in bio-oil are responsible for a poor stability upon storage and heating, immiscibility with hydrocarbon fuels and a high acidity [1,2].

Bio-oil oxygenates can be converted to fuel grade hydrocarbons through HDO in the presence of hydrogen over a suitable catalyst. HDO of condensed bio-oil is challenged by severe coke formation upon heating. Hence, in the H<sub>2</sub>CAP process, catalytic HDO takes place both during pyrolysis of biomass and in a downstream fixed bed reactor, where the pyrolysis vapors are upgraded before condensation. The aim is to stabilize reactive oxygenates immediately when formed and to perform the downstream deep HDO before condensation of the product oil to minimize coke formation. Catalytic HDO is currently challenged by rapid catalyst deactivation. This deactivation is caused by coke deposition on the catalyst surface as well as

poisoning from e.g. water and sulfur present in bio-oil. It is therefore crucial to develop catalysts and optimize operating conditions that enable HDO with an appreciable activity, selectivity and stability.

### The objectives of the project cover:

- ❖ Preparation of HDO catalysts in the laboratory.
- ❖ Test of prepared catalysts in a high pressure experimental setup along with investigation of process conditions. Different bio-oil model compounds will be applied.
- ❖ Detailed characterization of prepared catalysts (fresh and spent).
- ❖ Selection of catalysts for hydrolysis and downstream deep HDO. Investigation of catalyst stability, reaction mechanisms and deactivation mechanisms.

Sulfide catalysts (supported CoMoS and NiMoS) are promising HDO catalysts due to their sulfur tolerance and known activity in the analogous hydrodesulfurization (HDS) reactions [2].

### Results and Discussion

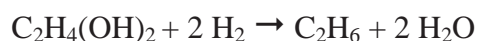
Experimental HDO is carried out in a Pyrolysis Oil Converter (POC) setup consisting of a fixed bed catalytic reactor with a typical bed volume in the range of 5-10 cm<sup>3</sup>. The setup is capable of operation up to 120 bar and 550 °C and the reactor is typically operated in trickle flow mode. It is possible to feed five unique

gasses and two unique liquids to the reactor feed. Liquids and gasses are separated downstream of the reactor and are analyzed by GC-MS (FID, liquids) and GC (FID/TCD, gasses).

The composition of bio-oil is very complex with more than 300 different compounds present [3]. Model compounds will thus be applied individually and in mixtures in order to investigate reaction mechanisms of individual compounds and interactions such as competitive inhibition. Special attention is paid to operating conditions (e.g. temperature, residence time and partial pressure of H<sub>2</sub>, H<sub>2</sub>O and H<sub>2</sub>S) and to tolerance against water and sulfur in bio-oil. Especially cellulose fragments (sugar polyols) are of interest as these are very reactive and contribute to undesired polymerization and coke formation reactions. Ethylene glycol (EG) has been chosen as a simple model polyol.

### HDO of ethylene glycol (EG) over NiMoS catalysts

The conversion of EG has been investigated at 50 bar (40 bar H<sub>2</sub>, 500 ppm H<sub>2</sub>S, balance N<sub>2</sub>), and 275-295 °C over various supported NiMoS catalysts in the POC setup. Full HDO of EG produces ethane and water with a heat of reaction, ΔH<sub>r</sub>, of -128 kJ/mol at 300 °C and 1 atm:



For steady state operation, carbon balances can be closed within 90-100 %.

Full conversion of EG and 90-100% yield of ethane has been obtained with a commercial NiMoS/γ-Al<sub>2</sub>O<sub>3</sub> catalyst (supplied by Haldor Topsøe A/S) at an EG liquid hourly space velocity (LHSV) of 1.5 h<sup>-1</sup> and 3 mol% EG in the feed. The activity remained stable with no deactivation for 47 h on stream. The temperature measured at the middle of the catalyst bed however increased during the run from a starting point of 274 °C (reactor oven setpoint 275 °C) to 283 °C after 0.5 h and 294 °C after 47 h on stream. This behavior illustrates a major challenge in HDO: controlling the heat development from the exothermal reaction.

In a similar experiment conducted with a higher LHSV of 6.75 h<sup>-1</sup> it has been possible to limit the HDO reaction and thereby control the temperature. A time on stream (TOS) profile is shown in Figure 1. Here it is seen how the conversion increases from ≈10% at 276 °C to ≈15% at 288 °C and ≈25% at 301 °C with the corresponding yield of ethane being 5.3-11.3%, 9.4-11.9% and 18.3-22.6%, respectively. Deactivation occurred for all three temperatures. In a similar experiment conducted at an initial temperature of 295 °C, it was seen that resulfidation could not fully regenerate the spent catalyst. This indicated that the catalyst was not only deactivated by surface S-O exchanges, but also by other mechanisms. Analysis on the spent catalyst has revealed a significant deposition of 11.8 wt% carbon.

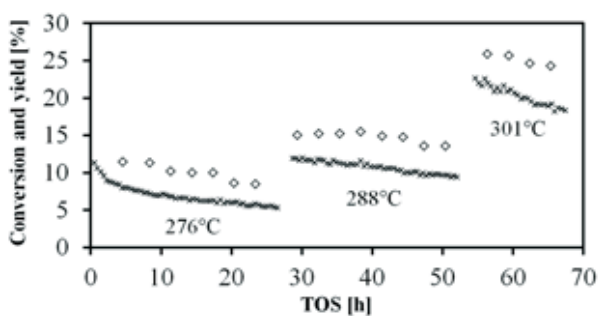


**Figure 1** Conversion of EG (◇) and yield of ethane (×) over NiMoS/γ-Al<sub>2</sub>O<sub>3</sub> at 50 bar (40 bar H<sub>2</sub>, 500 ppm H<sub>2</sub>S, balance N<sub>2</sub>) and LHSV = 6.75h<sup>-1</sup> (3 mol% EG in feed). The resulting temperature at the middle of the bed is noted in the figure (at reactor oven setpoints of 275, 285 and 295 °C). Main byproducts cover diethylene glycol, ethanol and ethylene (< 3% carbon based selectivity).

The influence of catalyst support will be investigated as γ-Al<sub>2</sub>O<sub>3</sub> is associated with a high propensity for coke formation due to its acidity. Instead, less acidic supports such as MgAl<sub>2</sub>O<sub>4</sub>, activated carbon and ZrO<sub>2</sub> will be tested. The role of H<sub>2</sub>S and H<sub>2</sub>O will be investigated in order to understand their influence on catalyst deactivation. In the future, other model compounds will be investigated as well. Density Functional Theory (DFT) calculations at Stanford University and advanced characterization such as X-ray Absorption Fine Structure (XAFS) at Karlsruhe Institute of Technology will aid the understanding of the investigated catalysts.

### Conclusions

HDO of bio-oil is a challenging process due to the complex nature of pyrolysis oil. Development of active and stable catalysts for the hydrolysis and downstream HDO requires a systematic investigation and understanding of the conversion of individual and mixed model compounds over selected catalysts at different operating conditions. Experiments on the conversion of ethylene glycol, a simple model polyol, have shown that sulfide catalysts are promising for HDO.

### Acknowledgements

This work is part of the Combustion and Harmful Emission Control (CHEC) research center at The Department of Chemical and Biochemical Engineering at DTU. The project is funded by The Danish Council for Strategic Research (Innovation Fund Denmark, project 1377-00025A), The Programme Commission on Sustainable Energy and Environment.

### References

1. A.V. Bridgwater, Biomass and Bioenergy 38 (2012) 68-94.
2. P. M. Mortensen, J.-D. Grunwaldt, P.A. Jensen, K.G. Knudsen, A.D. Jensen, Applied Catalysis A: General 407 (2011) 1-19.
3. A. M. Azeez, D. Meier, J. Odermatt, T. Willner, Energy Fuels 24 (2010) 2078-2085.

**Alay Arya**

Phone: +45 4525 2864  
E-mail: alaya@kt.dtu.dk  
Discipline: Centre for Energy Resources Engineering

Supervisors: Georgios Kontogeorgis  
Nicolas von Solms

**PhD Study**

Started: January 2014  
To be completed: December 2016

## Modeling of asphaltene system with association model

**Abstract**

Asphaltene precipitation is calculated using Cubic Plus Association (CPA) equation of state (EoS) following self-developed modeling approach and oil characterization. It is found that only ambient condition titrations of n-heptane with stock tank oil (STO) at different temperature of interest is required in order to calculate model parameters. Model is then used to predict asphaltene phase envelop for reservoir fluid with any type and amount of gas injection. Total 15 reservoir fluids are studied and 11 reservoir fluids out of 15 have two type of experimental data to validate model predictions. Model predictions are in agreement with experimental data. PVT properties is also calculated with the proposed modeling approach for 14 different reservoir fluids and the calculated results conform the experimental data.

**Introduction**

Asphaltene is normally present in the reservoir oil and for industry it is analogous to “cholesterol” since its precipitation stops the entire production and causes the loss of millions of dollars. It is an “ill defined” component of high molecular weight (around 500-4000 gm/mol), which is considered most polar part in the oil compared to the other components. This polar nature of asphaltene is believed to be imparted by heteroatoms (O, S, N, vanadium, nickel) present in its structure. Because of this polar nature asphaltenes associate with each other and precipitate at certain temperature, pressure and composition. However, prediction of these conditions, where asphaltene precipitates, is quite uncertain and detailed thermodynamic model and appropriate oil characterization is required. Asphaltenes can easily precipitates as pressure is reduced but also if the oil is diluted by light hydrocarbons eg. gas such as methane, CO<sub>2</sub> or nitrogen. Ever since the introduction of enhanced oil recovery (EOR) method with gas this problem has become even worse. Moreover, oil with little amount of asphaltene (say, 0.1 mol %) may show precipitation problem than the oil with moderate amount of it (say 1 mol %) and vice versa. Different EoSs with different modeling approach have been used to predict asphaltene phase equilibria; however, there is no single convincing model for industries to use.

Even though CPA EoS have been proposed earlier for asphaltene modeling, in this work we demonstrate how it can effectively be applied to calculate asphaltene

onset conditions considering asphaltene phase behavior as liquid-liquid equilibrium. We make the modeling approach less complex using a simple fluid characterization. This approach requires fewer experimental measurements, and can easily be used by industry. Modeling results are compared with different types of experimental data of several reservoir live oils in order to check the reliability of the model.

**Specific Objective**

The purpose of this project is to use EoS based on association theory and develop an approach to predict asphaltene precipitation at different conditions of temperature, pressure and composition. We plan to use CPA and Perturbed Chain Statistical Associating Fluid Theory (PC-SAFT) EoS models to compare the results.

**Discipline**

Engineering Thermodynamics.

**Modeling Approach**

In this work we assume the same modeling approach as presented by Arya et al [1,2]. Asphaltenes are considered as single self-associating compounds. The saturates, aromatics and resins are lumped into single component named as heavy component (HC), generally known as maltene fraction. This heavy component is cross associating with asphaltene. Asphaltene phase is modeled as liquid phase. For more information on the modeling approach, refer to Arya et al [1,2].

## Results and Discussion

### Asphaltene Phase Envelope

Ting et al [3] prepared a model oil by dissolving 1g of asphaltene in 100 ml of toluene. Titrating different n-alkanes with model oil, the volume fraction of each n-alkane was found at the onset of asphaltene precipitation. Methane was then injected isothermally and upper onset and bubble point pressures were found. We assumed cross-association between toluene and asphaltene and then calculated the cross-association energy ( $\epsilon^{AT}$ ) from the onset data with different n-alkanes. Figure 1a shows that CPA is able to correlate experimental data. We used the same parameters to check the effect of methane injection. Figure 1b shows that CPA is able to calculate results in agreement with experimental data. Since the difference between the two experimental temperatures is not large, we kept the  $\epsilon^{AT}$  as temperature independent parameter and this results to minor deviations in the upper onset pressure results at 339 K.

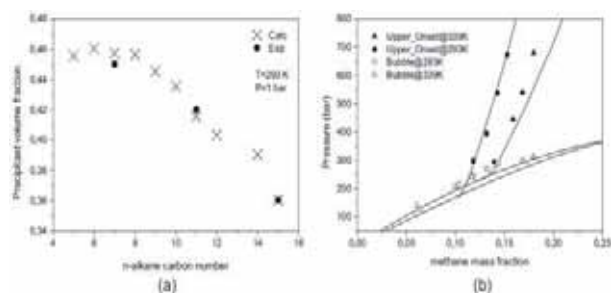


**Figure 1:** (a) Volume fraction of different n-alkane at the onset of asphaltene precipitation at 293 K and 1 bar vs carbon number of respective n-alkane. Circles represent experimental data from Ting et al [3] and cross marks represent the correlation by CPA. (b) Upper onset and bubble point pressures vs amount of methane injected in terms of mass fraction. Symbols represent experimental data and lines are the predictions with CPA.

### Effect of Gas Injection

Anadarko Petroleum Corporation and Schlumberger have jointly investigated the effects of gas addition on the Deepwater Gulf of Mexico reservoir fluid with respect to asphaltene precipitation and deposition. Three common EOR injection gases ( $N_2$ ,  $CO_2$  and  $CH_4$ ) have been studied experimentally. In this work, we use 0 mol% gas injection case to calculate model parameters using two cases and then the model is used to predict 10 mole%  $N_2$ ,  $CO_2$  and  $CH_4$  injection effect. In the first case, the value of  $\epsilon^{AA}/R$  and  $\epsilon^{AH}/R$  are calculated from the three upper onset pressures. In the second case, the value of  $\epsilon^{AA}/R$  is fixed to the default value of 3000K and  $\epsilon^{AH}/R$  is calculated from the two upper onset pressures. In both cases,  $P_c$  of HC is the same since it is calculated from the same single bubble point information. Both cases are able to predict the different types of gas injections effect in agreement with

experimental data as shown in Figure 2. We can also observe that the extrapolations beyond the experimental temperature range are different for the two cases.

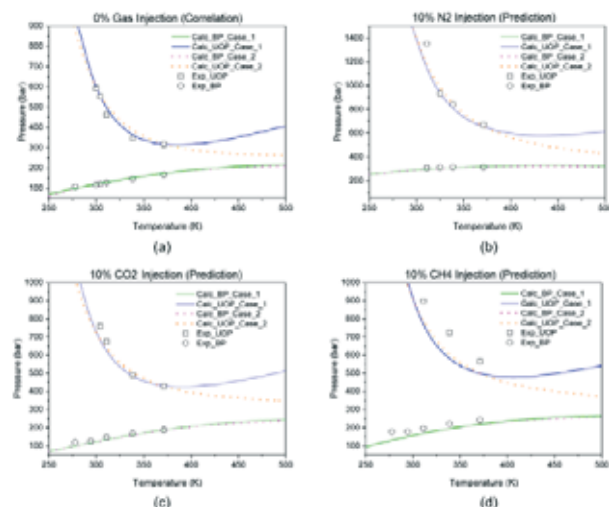


**Figure 2:** UOP and bubble points vs temperature for different types of gas injections. Symbols (squares for upper onset, circles for bubble points) represent experimental data from Gonzalez et al [4].

## Conclusion

From this work, it can be concluded that the applied modeling approach with the CPA EoS is able to predict the effect of different amounts and types of gas injections after the model parameters are calculated from a few experimental data. At least three asphaltene onset conditions at different temperatures, covering the temperature range of interest, and bubble point information should be available in order to calculate asphaltene phase envelope. Higher pressure measurements for the asphaltene upper onset boundary are not required with reservoir oil but relatively simple ambient or near ambient pressure measurements of STO with n-pentane/n-heptane precipitant are sufficient.

## Acknowledgments

The financial contribution to this project is partly from BP.

## References

1. Arya, A., von Solms, N., & Kontogeorgis, G. M. Fluid Phase Equilibria, 400 (2015), 8-19.
2. Arya, A., von Solms, N., & Kontogeorgis, G. M. Energy & Fuels (2015).
3. P.D. Ting, G.J. Hirasaki, W.G. Chapman, Modeling of asphaltene phase behavior with the SAFT equation of state, Petroleum Science and Technology 21-3&4 (2003) 647-661.A.K.M.
4. Gonzalez, D. L., Mahmoodaghdam, E., Lim, F. H., & Joshi, N. B. SPE (2012).

**Christian Bach**

Phone: +45 4525 2949  
E-mail: [chrba@kt.dtu.dk](mailto:chrba@kt.dtu.dk)

Supervisors: Krist V. Gernaey  
Ulrich Krühne  
Mads O. Albæk, Novozymes A/S

PhD Study  
Started: March 2015  
To be completed: February 2018

## Modeling of gradients in large scale bioreactors

### Abstract

The prediction and understanding of mixing and oxygen mass transfer in fermenters and bioreactors is useful for bioprocess improvement as these dynamics govern production rates of the biotransformation. Insufficient mixing or differences in mass transfer coefficient throughout fermenters have shown to form gradients in process conditions, which affect the performance of the bioreactor. These phenomena can be assessed using a combination of computational fluid dynamics and spatially distributed sensors. The purpose of this project is to develop methods which can quantify spatial differences in process conditions in pilot scale bioreactors using a combination of CFD and experiments.

### Introduction

A large range of industries use fermentation technology to produce products, such as pharmaceuticals and fine chemicals. These processes are usually carried out in aerated stirred bioreactors of volumes in the range of multiple hundred cubic meters. Variation in process conditions, such as pH, species concentration, temperature and pressure, are inevitable in these vessels due to the fact that feeding of substrate, agitation, aeration and cooling all take place at specific locations in the vessel [1]. The resulting variation in process conditions affects the performance of the given biotransformation occurring inside the vessel.

Substrate concentration heterogeneities arise from having one feeding position in large vessels, which induces consumption of the substrate before it is distributed in the vessel [2]. The rate of biotransformation in the bioreactor directly affects the severity of the heterogeneities resulting in different substrate concentration profiles throughout the duration of a fed-batch fermentation. The dynamic behavior of the substrate concentration profile requires adaptation of the process during a batch, and the success of such adaptations is based on information about the change in production rate and hence substrate consumption.

This information can be assessed by conducting exploratory experiments in production scale equipment at process relevant conditions, but such experiments are costly and reduce the capacity of the production facility. Alternatively simulations of the bioreactor can be

carried out to improve the understanding of the process response to changes in operating conditions without having to carry out costly industrial scale experiments. For such simulations computational fluid dynamic (CFD) investigations are suitable as they can incorporate spatial differences in industrially relevant conditions while determining production rates at different operating conditions. However CFD simulations require validation in order to be considered representative of the biological system, and such validation requires information of conditions at multiple locations in the vessel. The application of multiple sensors is suitable for this validation as they offer information about process conditions, such as pH or dissolved oxygen concentration, throughout the vessel.

### Specific Objective

The objective of this PhD project is to develop methods for describing heterogeneities in bioreactors using CFD. The methods will then be tested for different reactor technologies in pilot scale to compare heterogeneities and energy efficiency.

### Results and Discussion

The phenomena occurring in bioreactors can be divided into three categories: Interfacial mass transfer, convective transport and reaction. Each phenomenon has to be characterized independently in order to understand the complete system. This implies

conducting experiments to illustrate the impact of each separate phenomenon.

The convective transport of species in stirred bioreactors is directly influenced by the agitation caused by the impeller, and usually referred to as mixing. The mixing of a 700 l bioreactor was investigated as part of the methodology described above. The mixing characteristics were determined by pulse injection of sodium chloride into the vessel resulting in an increase in conductivity. The conductivity was simultaneously measured at four different locations in the vessel, which allowed the determination of the mixing time at different agitation velocities. This data was compared with CFD simulations using ANSYS® CFX 16. The results are shown in Figure 1.

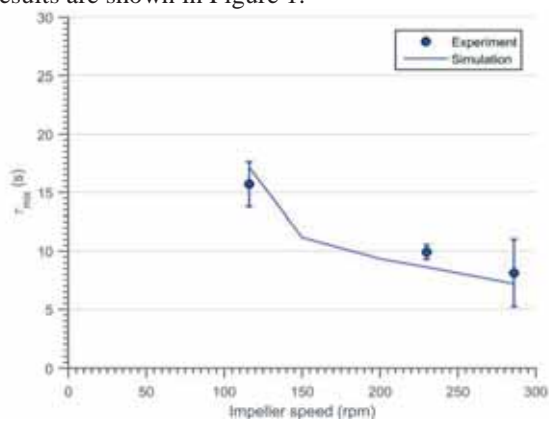


**Figure 1:** Comparison of experimental and simulated mixing time in a 700 l bioreactor containing water.

The representation of the mixing time indicates that the simulations are able to capture the dynamics of the convective transport of species, which can be utilized in the full analysis of the system.

In order to assess the presence of heterogeneities in substrate concentration throughout the vessel the conversion of hydrogen peroxide to water and oxygen using catalase was studied. The kinetics of the reaction was investigated in a 200 ml stirred reactor. The initial rate of reaction was determined through change in the dissolved oxygen concentration monitored by a PyroScience optical fiber. The kinetics of the reaction has previously been shown to follow Michaelis Menten kinetics [3], which can be represented mathematically as:

$$v = v_{max} \cdot \frac{[H_2O_2]}{K_m + [H_2O_2]} \quad (1)$$

where  $[H_2O_2]$  is the concentration of hydrogen peroxide,  $K_m$  is the half saturation concentration and  $v_{max}$  is the maximum reaction rate. The results of the kinetic study are presented in Figure 2 along with values for the kinetic parameters.

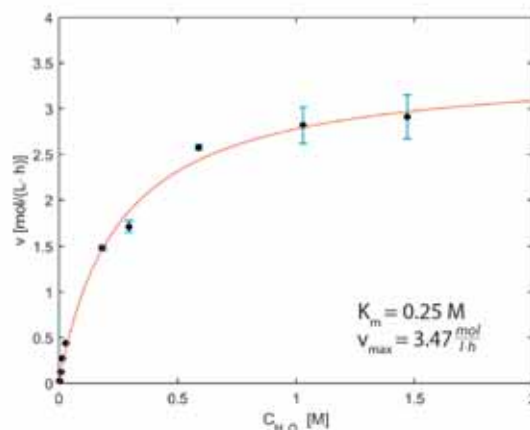


**Figure 2:** The initial rate of reaction at varying hydrogen peroxide concentration. The solid line represents the model prediction and the diamonds symbolize experimental values.

The reasonable fit to experimental data is shown in Figure 2, and forms a validation that the reaction can be represented by Michaelis Menten kinetics, which can be utilized to further investigate the complete system. The investigation of substrate gradients in pilot scale bioreactors is done by monitoring the dissolved oxygen concentration at multiple positions in the vessel while varying feed location and enzyme concentration.

## Conclusion

The use of spatially distributed sensors and computational fluid dynamics combined with a model system shows considerable potential as tools to characterize heterogeneities in bioreactors. The understanding and validation of each phenomenon in the system has to be established in order to take full advantage of the information available in large scale experiments.

## Acknowledgements

The PhD project of Christian Bach has received funding from the Technical University of Denmark (DTU), Novozymes A/S and Innovation Fund Denmark in the frame of the Strategic Research Center BIOPRO2 (BIO-based PROduction: TOwards the next generation of optimized and sustainable processes).

## References

1. Nienow, A. W. (1998). Hydrodynamics of Stirred Bioreactors. *Applied Mechanics Reviews*, 51(1), 3.
2. Larsson, G., Törnkvist, M., Ståhl Wernersson, E., Trägårdh, C., Noorman, H., & Enfors, S. O. (1996). Substrate gradients in bioreactors: Origin and consequences. *Bioprocess Engineering*, 14, 281–289
3. Jones, P., & Suggett, A. (1968). The catalase-hydrogen peroxide system. Kinetics of catalytic action at high substrate concentrations. *Biochemical Journal*, 110(4), 617-62



## Joseph Asankomah Bentil

Phone: +45 5032 5190

Email: [joben@kt.dtu.dk](mailto:joben@kt.dtu.dk)

Supervisors: Anne S. Meyer  
Lene Lange  
Anders Thygesen  
Moses Mensah

### PhD Study

Started: December 2014

To be completed: June 2017

## Local enzyme production in Ghana: biodiversity of multifunctional cellulases for lignocellulose deconstruction

### Abstract

This PhD study forms part of a general project dubbed ‘Second Generation Bioenergy (2GBIONRG)’ whose main goal is to generate ethanol from the bioconversion of lignocellulose materials through innovative technological applications. The present PhD project is focused on the production of cellulase enzymes from wild-type microbial strains that are capable of degrading cellulosic biomass effectively and efficiently to generate high yield of monomeric sugars for subsequent bioconversion to ethanol. The research would also explore enzymatic modification of recalcitrant lignin in order to maximize lignocellulose bioconversion by way of efficient enzymatic cellulose hydrolysis. The final part of the study involves development of process design for small scale enzyme production in Ghana.

### Introduction

Cellulose is the most abundant polymer forming 30-50% of plant cell wall composition. It is usually composed of two structurally different forms; the highly susceptible amorphous form and the recalcitrant crystalline form. The amorphous form which is normally small in composition is easily attacked by cellulases enzymes. On the other hand, crystalline cellulose is usually interlinked by lignin and xylans which makes it highly difficult for enzymatic attack. The heterogeneous nature of cellulose makes its enzymatic hydrolysis quite complicated. This is because three main enzymes are involved in cellulose hydrolysis namely; endo-1, 4-  $\beta$ -D-glucanase (EG) (EC 3.2.1.4), which cleaves internal bonds of the cellulose structure, exo-1, 4-  $\beta$ -D-glucanase or cellobiohydrolases (CBHs) (EC 3.2.1.91) which cleave the reducing and non-reducing ends of the cellulose yielding cellobiose units and  $\beta$ -glucosidase (BG) (EC 3.2.1.21) which

is responsible for producing glucose units from the dimers. For effective enzymatic hydrolysis of cellulose, these three enzymes work synergistically in proportional concentrations. Several attempts are made to produce these enzymes in the best proportions from single microbial strain using molecular engineering techniques but still a bottleneck. For instance, *Trichoderma reesei* has undergone several rounds of mutation/ selection starting from the QM6a strain to increase its capacity to produce and secrete cellulases in high yields (Le Crom *et al.*, 2009). As a result, the engineered *T. reesei* industrial CL847 strain is able to secrete more than 100 g of proteins per liter of culture and has been proposed to be one of the most promising strains for conversion of lignocellulose to fermentable sugars. However, conversion is still not optimal due to the heterogeneous composition of plant biomass. In addition, analysis of the *T.*

*reesei* genome has revealed a low number and low level of diversity of enzymes likely to be involved in biomass degradation compared with the number and diversity in other filamentous fungi (Martinez *et al.*, 2008). Thus, there is a need to develop at a significantly reduced cost more effective enzymatic cocktails with a range of properties complementary to current cellulase systems. The present study seeks to explore wild-type strains of fungi (Basidiomycetes) and bacteria (*Bacillus* sp.) and identify, characterize and produce cellulase enzymes preparations with highly thermostable and robust characteristics capable of effective cellulose hydrolysis. The study would also maximize cellulase enzymes action on lignocellulosic biomass by enzyme-assisted modification of the lignin.

## Methodology

The study will make use of certain strategies to screen for potential fungi and bacteria that can be explored for their enzymes produced in both submerged and solid state fermentations. The production of enzymes from these microorganisms would be performed at laboratory scale using micro-fermentors such as shake flasks, Erlenmeyer flasks and other improvised vessels. Enzyme yield and activity will be quantified using standard assays such as FPase activity assay, chromogenic assays and others. The degradation pattern of the microorganisms especially fungi, structural modification of substrates and enzyme secretion in the media will be monitored using certain microscopic applications such as Scanning Electron Microscopy, Transmission Electron Microscopy and Florescence Microscopy. The stability of the enzymes would be evaluated under optimized environmental conditions.

## Hypotheses

- (i) The multi-functional cellulases can be identified through explorative screening of indigenous (wild-type) microbes involving fungi and bacteria in combination with selective enzymes from culture banks
- (ii) Novel opportunities exist for producing enzymes from white-rot fungi using solid state fermentation in Ghana

- (iii) New multi-functional cellulases may be discovered for metagenomics studies
- (iv) Different cellulase enzymes may react differently to inhibitors produced by herbaceous biomass
- (v) Lignin-degrading enzymes produced may enhance cellulosic degradation of biomass in Ghana
- (vi) New multi-functional enzyme complexes may be identified for biomass pretreatment and degradation
- (vii) Enzyme preparations may be produced from different combinations of biomasses in Ghana

## Acknowledgement

I sincerely thank DANIDA for their financial support

## References

1. Le Crom, S., Schackwitz, W, Pennacchio, L, Magnuson, J. K., Culley, D. E. et al, 2009. Tracking the roots of cellulase hyper production by the fungus *Trichoderma reesei* using massively parallel DNA sequencing. *Proc. Natl. Acad. Sci. U. S. A.* **106**:16151–16156.
2. Martinez, D., Berka, R. M., Henrissat, B., Saloheimo, M., et al. 2008. Genome sequencing and analysis of the biomass degrading fungus *Trichoderma reesei* (syn. *Hypocrea jecorina*). *Nat. Biotechnol.* **26**:553–560.

**Maria-Ona Bertran**

Phone: +45 4525 6173  
E-mail: marber@kt.dtu.dk

Supervisors: Rafiqul Gani  
John Woodley  
Anker D. Jensen

PhD Study  
Started: September 2014  
To be completed: August 2017

## Modelling, synthesis and analysis of biorefinery networks

### Abstract

The production of fuels and chemicals is primarily based on crude oil. The use of biomass as raw material represents a sustainable alternative. In order to establish a new industrial system on the basis of biomass, a systematic approach to generating, evaluating and selecting biorefinery processing networks is needed. In this PhD study, a generic computer-aided methodology for synthesis and design of different processing networks, including biorefinery networks, is developed, along with the associated methods and tools.

### Introduction

Petroleum is currently the primary raw material for the production of fuels and chemicals. Consequently, our society is highly dependent on fossil non-renewable resources. Recently, renewable raw materials are receiving increasing interest for the production of chemicals and fuels, so a new industrial system based on biomass is being established with sustainability as the main driving force [1].

A biorefinery is a processing facility for the production of multiple products (including biofuels and chemicals) from biomass, an inexpensive, abundant and renewable raw material [2]. The optimal synthesis of biorefinery networks problem is defined as: *given* a set of biomass derived feedstock and a set of desired final products and specifications, *determine* a flexible, sustainable and innovative processing network with the targets of minimum cost and sustainable development taking into account the available technologies, geographical location, future technological developments and global market changes.

The synthesis and design of processing networks involves the selection of raw materials, processing technologies/configurations and product portfolio compositions among a number of alternatives. A common approach to the formulation and solution of this class of decision-making problems is mathematical programming, in which the problem is decomposed into: (i) representation of the superstructure of alternatives, (ii) formulation of the mathematical optimization problem, and (iii) solution of the optimization problem to determine the optimal design according to the defined criteria and constraints [3].

### Specific Objectives

The objective of this project is to develop a systematic method and associated tools to synthesize, design and analyze innovative biorefinery networks based on chemical and biological approaches to convert biomass feedstock into valuable chemicals and biofuels.

The project comprises two main tasks: (i) the development of a generic synthesis methodology for biorefinery networks and (ii) the establishment of generic methods and tools for synthesis, design and evaluation of biorefinery networks and their integration in a computer-aided framework. In the first task, the possible biorefinery networks is represented as a superstructure of alternatives. Each processing interval in the superstructure is modelled with a generic model. The complete biorefinery synthesis problem is solved to determine the optimal network for each considered scenario. In the second task, computer-aided methods and tools will be developed. A knowledge base of biorefinery raw material, processing technologies and products has been developed where all necessary data for the problem solution are to be stored. The developed method is able to identify the optimal route for a given set of biomass and products while satisfying the sustainability criteria and taking into account the geographical and supply chain constraints. The method will be applied to different case studies in order to show its application.

### Methodology and User Interface

The developed methodology for synthesis of processing networks represents the first stage (the synthesis stage) of the three-stage approach for sustainable process

synthesis, design and innovation [4]. The synthesis methodology consists of three steps: (1) problem formulation; (2) superstructure generation; and (3) solution of the optimization problem.

#### Step 1: Problem formulation

The problem formulation step consists of defining the problem characteristics, such as the objective function, the feedstocks that are to be converted, the products that are to be made, the geographical location and supply chain issues. Different types of network optimization problems can be formulated, some of them are given in Figure 1.

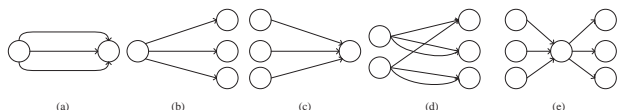


**Figure 1:** Problem types: (a) route selection; (b) product selection; (c) feedstock selection; (d) simultaneous feedstock, product and route selection; and (e) feedstock and product selection via an intermediate.

#### Step 2: Superstructure generation

To generate the superstructure, one or various databases are used to retrieve all the necessary information (alternatives, connections, and data for each alternative).

#### Step 3: Solution of the optimization problem

First, the mathematical representation of the superstructure is developed. Next, the optimization (MINLP or MILP) problem is solved. This problem includes the user-defined objective function, subject to a series of constraints, namely mass and energy balance constraints, flow model constraints, logic constraints, and other constraints [5]. The developed model is generic and data-independent.

#### User interface: Super-O

Super-O is a user interface for the synthesis of different processing networks based on the methodology.

It allows for the reduction of the time needed for the formulation and solution of network optimization problems. A schematic representation of the methodology as implemented in Super-O including the data flow and tools integration is shown in Figure 2.

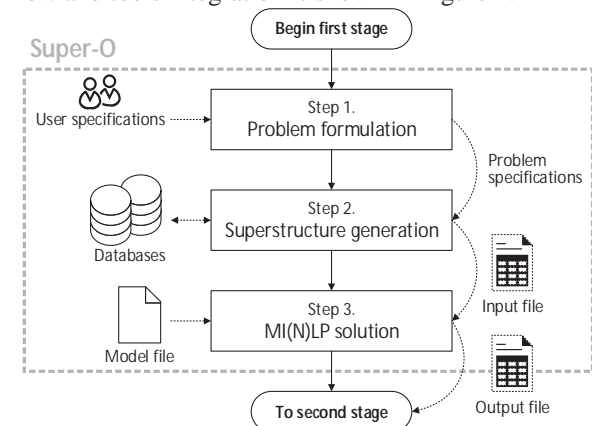


**Figure 2:** Schematic representation of the methodology, and its implementation in Super-O, the interface.

#### Case study: Sugarcane molasses

The objective of this case study is to determine which product(s) should be produced from sugarcane molasses, obtained as a by-product during the production of refined sugar from sugarcane in Mexico.

#### Step 1: Problem formulation

The problem has one feedstock (sugarcane molasses), three products (L-lysine, citric acid, and lactic acid), and one alternative production route per product, it is therefore a product selection problem. The problem location is Mexico. The selected objective function is the Gross Operating Income (GOI), defined in Eq. 1.

$$GOI = GREV - OPEX \quad (1)$$

Where GREV is the gross revenue obtained through the product sales and OPEX is the operating cost (including raw materials and utilities).

#### Step 2: Superstructure generation

The superstructure of alternatives is obtained from an academic collaboration and it has been included in the database of biorefinery-related processes. The problem superstructure is shown in Figure 3.

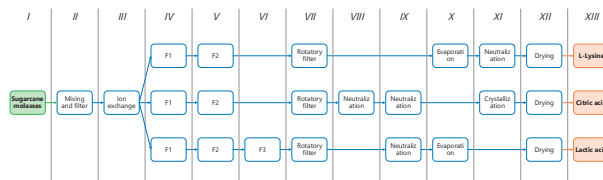


**Figure 3:** Superstructure of alternatives for the case study.

#### Step 3: Solution of the optimization problem

The selected product is L-lysine, with an objective function value of 19 M\$/y, which includes a product sales value of 30 M\$/y, cost of chemicals and utilities of 5M\$/y, and feedstock cost of 6 M\$/y.

#### Conclusion

A methodology for sustainable synthesis of biorefinery networks is developed. The methodology integrates the steps with the necessary models and tools, and is implemented in Super-O, a user-friendly software interface, which has been tested for various cases of varying type, size and complexity.

#### References

1. M. Hechinger, A. Voll, W. Marquardt, *Comput. Chem. Eng.* 34 (2010), 1909-1918.
2. B. Kamm, M. Kamm, *Appl. Microbiol. Biotechnol.* 64 (2) (2004), 137-145.
3. A. Quaglia, C. L. Gargalo, S. Chairawongsa, G. Sin, R. Gani, *Comput. Chem. Eng.* 72 (2015), 68-86.
4. A. Quaglia, B. Sarup, G. Sin, R. Gani, *Comput. Chem. Eng.* 38 (2012), 213-223.
5. D.K. Babi, J. Holtbruegge, P. Lutze, A. Gorak, J.M. Woodley, R. Gani, *Comput. Chem. Eng.* 81 (2015), 218-244.



**Thomas Bisgaard**

Phone:  
E-mail:

+45 4525 2811  
thbis@kt.dtu.dk

Supervisors:

Jens Abildskov  
Jakob Kjøbsted Huusom  
Nicolas von Solms  
Kim Pilegaard

PhD Study

Started: September 2012  
To be completed: February 2016

## Operation and design of diabatic processes

### Abstract

A systematic control structure design method is applied on the concentric Heat-Integrated Distillation Column (HIDiC) separating benzene and toluene. Optimal operation and active constraints are identified for constructing the supervisory control layer. Later, the fundamental problem of obtaining a stabilising control structure is addressed resulting in the regulatory control layer design, when combined, leading to a complete control structure for the given separation. Dynamic simulation illustrates an acceptable performance of the obtained control structure.

### Introduction

The heat-integrated distillation column (HIDiC) is considered a potential alternative to the conventional distillation column. In the HIDiC, gradual condensation occurs along the rectifying section and gradual boil-up occurs along the stripping section as heat is exchanged between the sections. This can be realised by operating the rectifying section at a higher pressure by introducing a compression step above the feed stage. One proposal for realisation of the HIDiC arrangement is a concentric HIDiC [1], in which the high-pressure rectifying section is surrounded by the low-pressure stripping section. An illustration of the concentric HIDiC is given in Fig. 1. Each stage in the same vertical position (e.g. #2 and #33) are heat-integrated such that heat is transferred from the inner rectifying section to the outer stripping section. Due to the gradual condensation and boil-up, the column sections changes diameter along their heights as indicated in the figure.

Most simulation studies consider only dual composition control schemes with dynamic models that assume constant pressures. Only few authors consider pressure dynamics for control [2], despite the large degree of interaction between column pressure and separation performance in the HIDiC. This contribution briefly outlines the design of a decentralised control structure using a systematic approach [3] for the separation of benzene/toluene.

### Specific Objectives

The overall aim of this PhD project is to shed light on the potential benefits of diabatic operation and to handle some of the barriers for industrial application and

acceptance of diabatic distillation columns. The project is divided in three phases concerning modelling/benchmarking, design, and operation. The latter phase is being outlined in this contribution.

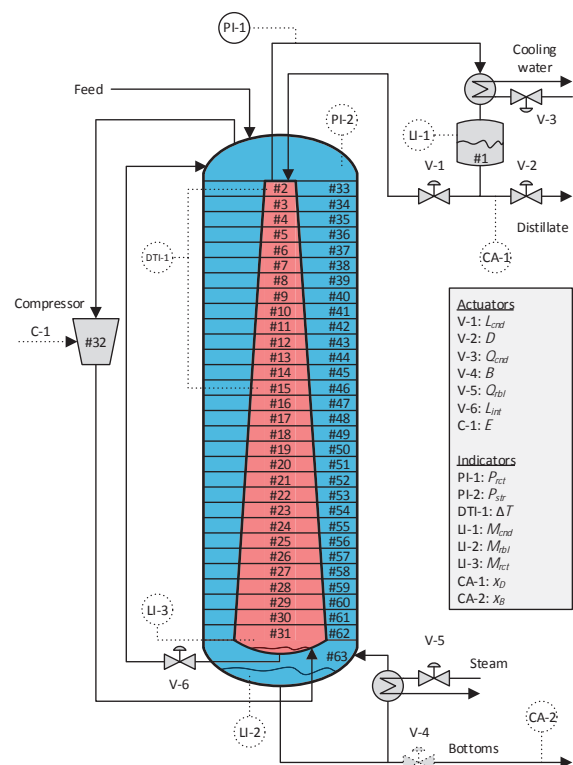


**Fig. 1.** Concentric heat-integrated distillation column for separating benzene/toluene.

Operability is investigated by deriving and simulating a control structure. The control structure design procedure is given by Skogestad [3]. Heuristic rules are collected in [4]. The procedure consists of systematic steps applied to the concentric HiDiC.

## Results and Discussion

Consider the separation of  $83.3 \text{ mol s}^{-1}$  of an equimolar, saturated liquid mixture of benzene/toluene by distillation. It is desired to obtain pure benzene (in distillate) and toluene (in bottoms) with purities of minimum 99%. A HiDiC design of 30 stages in both sections with all 30 stages in each section being heat integrated with a heat exchange area of  $15 \text{ m}^2$  per stage is used (see Fig. 1). A conservative overall heat transfer coefficient of  $0.60 \text{ kW m}^{-2} \text{ K}^{-1}$  is adopted. Conventional column sizing has been employed, leading to a gradually increasing rectifying section diameter when moving from top to bottom, while the stripping section diameter is gradually decreasing. As a result, the nominal tray, liquid hold-ups vary along the column. Ideal liquid and vapour phases were assumed for vapour-liquid equilibrium relations.

Seven operational degrees of freedom are listed in Fig. 1. Since three hold-ups  $M_{cnd}$ ,  $M_{rbl}$ , and  $M_{rct}$  have no impact on the steady-state operation (and on the cost function), four variables are available for optimisation. Optimal operation is defined as the solution to Eq. (1).

$$\begin{aligned} \min J &= 0.50m_F - 1.04m_D - 0.85m_B \\ &+ [1.99 + 20.4(P_{steam} - 1)^{0.05}]m_{steam} + 8.0 \cdot 10^{-5}m_{cw} \\ &+ 3.89 \cdot 10^{-5}E \\ \text{s.t. } &0.99 \leq x_D \\ &0.99 \leq 1 - x_B \\ &E \leq 500 \text{ kW} \\ &101.3 \text{ kPa} \leq P_i \leq 600 \text{ kPa} \\ &0.01F_0 \leq L_i \leq 200 \text{ mol s}^{-1} \\ &0.01F_0 \leq V_i \leq 150 \text{ mol s}^{-1} \end{aligned} \quad (1)$$

$L_i$  and  $V_i$  are the internal liquid and vapour flow rates at stage  $i$ ,  $E$  is the compressor duty and  $m$  is mass flow rate. The remaining nomenclature is provided in Fig. 1.

The nominal solution of the HiDiC has three active constraints for  $x_D = 0.99$ ,  $P_{str} = 101.3 \text{ kPa}$ , and  $L_{cnd} = 0.01F_0$ , hence (free) DOFs =  $4 - 3 = 1$ . In this case, one variable for self-optimising control can be used, since the active constraints must be controlled for optimum economic performance. By evaluating the loss of maintaining candidate self-optimising CVs constant, the bottom composition,  $x_B$ , is found to be the best candidate as the remaining primary controlled variable since the economic loss is the least when controlled (i.e. kept constant).

Using the identified optimum operating point, the supervisory control layer is derived. Design rules [4] are used to design the stabilising control layer, leading to the configuration:  $D \rightarrow M_{cnd}$ ,  $B \rightarrow M_{rbl}$ ,  $Q_{rbl} \rightarrow P_{str}$ ,  $Q_{cnd} \rightarrow \Delta T$ ,  $E \rightarrow P_{rct}$ ,  $\Delta T^{se t} \rightarrow x_D$ ,  $P_{str}^{se t} \rightarrow x_B$ ,  $P_{rct}^{set} \rightarrow P_{str}^{set}$  using simple cascade PI controllers. An example

simulation of five different step-changes in disturbance and set point variables is illustrated in Fig. 2.

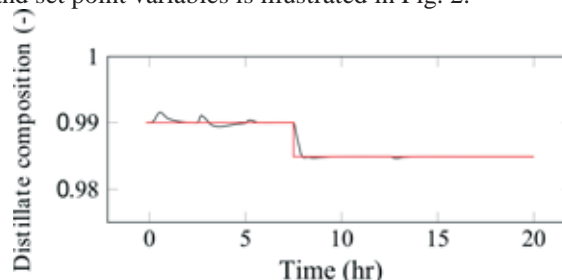


Fig. 2. Dynamic simulation to disturbance and set point changes.

## Conclusions

Based on rigorous distillation column simulations of the concentric Heat-Integrated Distillation Column (HiDiC) separating a binary mixture of benzene/toluene, the following main conclusions can be extracted: (i) Deriving a stabilising control system is challenging, however, in simulation we found that it can be operated steadily under realistic disturbance scenarios; (ii) In addition, under optimal operation under disturbances, weeping is predicted. Bubble-cap trays may be used to mitigate weeping; (iii) A control structure consisting of a regulatory and a supervisory layer has been systematically derived and evaluated for a separation with a more valuable distillate product, given an acceptable performance; (iv) There are significant interactions in all control loops, thereby encouraging the use of e.g. multi-variable pressure control; (v) The overall dynamics are complex giving evidence of non-linear behavior.

## References

1. R. Govind, 1987, US Patent 4,681,661.
2. T.-J. Ho, C.-T. Huang, J.-M. Lin, L.-S. Lee, Comput. Chem. Eng. 33 (6) (2009): 1187-1201.
3. S. Skogestad, Comput. Chem. Eng 28 (1-2) (2004): 219-234.
4. V. Minasidis, S. Skogestad, N. Kaistha, Proceedings of PSE2015/ESCAPE25, Denmark.

## List of Publications

1. T. Bisgaard, J.K. Huusom and J. Abildskov, AIChE Journal (accepted), doi: 10.1002/aic.14970.
2. T. Bisgaard, S. Skogestad, J.K. Huusom and J. Abildskov, Proceedings of DYCOPS 2016, Norway (Submitted)
3. T. Bisgaard, J.K. Huusom and J. Abildskov, Proceedings of ACD2012, 2012, Denmark.
4. T. Bisgaard, J.K. Huusom and J. Abildskov, Proceedings of ESCAPE, 2013, Finland.
5. T. Bisgaard, J.K. Huusom and J. Abildskov, Proceedings of DYCOPS 2013, India.
6. T. Bisgaard, J.K. Huusom, J. Abildskov, Proceedings of the 10th international conference on distillation & absorption 2014, Germany.



**Martin Gamél Bjørner**

Phone: +45 4525 2886

E-mail: [mgabj@kt.dtu.dk](mailto:mgabj@kt.dtu.dk)

Supervisors: Georgios Kontogeorgis

PhD

Started: June 2012

To be completed: February 2016

## CO<sub>2</sub>-hydrates - Challenges and possibilities

### Abstract

Modelling the phase equilibrium of mixtures containing carbon dioxide (CO<sub>2</sub>) is a challenge with most equations of state (EoS). One of the reasons for this is believed to be, that most models ignore the large quadrupolar moment of CO<sub>2</sub>. In this PhD project, in an attempt to obtain a more physically consistent model, a quadrupolar contribution is proposed and combined with the well-known cubic plus association (CPA) EoS. When the phase equilibria of binary mixtures are considered, the quadrupolar CPA (qCPA) appear to offer a systematic improvement as compared to the cases where quadrupolar interactions are ignored. When ternary mixtures containing CO<sub>2</sub> and hydrocarbons, water and/or alcohols are considered, however, the qCPA appear to give results similar to the best CPA approaches.

### Introduction

In recent years CO<sub>2</sub> has received a significant amount of negative attention due to its contribution to the global warming, and the fact that the amount of CO<sub>2</sub> in the atmosphere continues to rise. This is believed to be largely due to the combustion of fossil fuels. Alone in Denmark more than 40 million tons of CO<sub>2</sub> are emitted each year [1].

Technologies are thus needed, which can limit the emission of CO<sub>2</sub> to the atmosphere. For example a novel technique for CO<sub>2</sub> capture using gas hydrates has recently been patented [2]. The operation pressure of the technique, however, is currently too high to be economically profitable. It is believed that this pressure could be reduced by specific additives. Such a screening process, however, is expensive and time consuming, and accurate models for CO<sub>2</sub> in mixtures would greatly facilitate this process.

Despite the importance of CO<sub>2</sub> containing mixtures, modelling such mixtures is still a challenge for most equations of state. One reason for this may be that CO<sub>2</sub> has a large quadrupolar moment (i.e. a concentration of charges at four separate points in the molecule), which is ignored in most equations of state. The Soave-Redlich-Kwong (SRK) EoS, for instance, treats CO<sub>2</sub> as an inert. Even in modern equations of state such as the Statistical Association Fluid Theory (SAFT) only dispersive forces are usually considered. The continued use of these models may be attributed to the fact that the mixture behavior is (mostly) captured quite well when

the model is adjusted with a relatively large interaction parameter ( $k_{ij}$ ).

To model mixtures containing CO<sub>2</sub> more accurately with association models, pragmatic approaches which treat CO<sub>2</sub> as a self-associating (hydrogen bonding) or solvating molecule may be employed [3]. Such procedures often work well resulting in better correlations with smaller interaction parameters. Unfortunately the improvement is obtained at the cost of additional pure component parameters and, in some cases, an extra parameter for the binary mixtures.

Alternatively, to improve the physics behind the model, several quadrupolar terms have been proposed within the SAFT framework, e.g. the quadrupolar models suggested by Gross [4] and Karakatsani et al. [5]. These terms are mainly based on the statistical mechanical theories for quadrupolar fluids developed by Stell and coworkers [6-8].

Inspired by recent developments within SAFT, and in an effort to obtain a more physically correct cubic plus association (CPA) EoS (Kontogeorgis et al. [9]), Bjørner and Kontogeorgis [10] have recently developed a quadrupolar term which is directly applicable in the CPA EoS. The resulting quadrupolar CPA (qCPA) does not require any additional adjustable parameters compared to CPA.

In this contribution the performance of the new model is illustrated through predictions and correlations of selected binary and ternary vapor-liquid equilibria (VLE), liquid-liquid equilibria (LLE) and three-phase vapor-liquid-liquid equilibria (VLLE). The model is

compared to the performance of CPA without the addition of a quadrupolar term.

### Specific Objectives

A molecular thermodynamic model for CO<sub>2</sub> has been developed, based on CPA [10]. The model includes a quadrupolar term which is based on a modification of expressions developed from statistical thermodynamics [6].

To evaluate the quadrupolar model several pure compound bulk properties such as liquid densities, heat capacities, and the speed of sound have been predicted for CO<sub>2</sub>. The model has been evaluated for its ability to predict and correlate binary VLE and LLE of mixtures related to CO<sub>2</sub> hydrates such as mixtures containing CO<sub>2</sub> and hydrocarbons, water, alcohols, glycols as well as a few other quadrupolar compounds.

The model has furthermore been evaluated for its ability to predict the phase equilibria of multicomponent mixtures containing CO<sub>2</sub> and hydrocarbons, water and/or alcohols.

### Results and Discussion

The CPA is an equation of state, which combines the simplicity of the SRK EoS with the association term from Wertheim's theory. The quadrupolar CPA is set in the Helmholtz energy as a summation of independent contributions from the SRK term, the association term and the quadrupolar term respectively:

$$A^{res} = A^{SRK} + A^{Assoc} + A^{quad} \quad (1)$$

In the absence of any quadrupolar interactions, the equation reduces to the CPA.

In this contribution we compare three modelling approaches to CO<sub>2</sub> using either CPA or qCPA; namely when CO<sub>2</sub> is treated as either an inert species (only  $A^{SRK}$  in Eq. 1 is non-zero), a self-associating species using the 4C association scheme ( $A^{quad}=0$  in Eq. 1) or as a quadrupolar molecule employing the new quadrupolar term ( $A^{Assoc}=0$  in Eq. 1).

The CPA or qCPA has three adjustable parameters for non-associating compounds ( $\Gamma$ ,  $b_0$ ,  $c_1$ ) and two additional parameters for associating compounds ( $\beta$ ,  $\epsilon$ ). qCPA employs the same number of adjustable parameters as CPA. The experimental value of the quadrupolar moment of CO<sub>2</sub> (4.3D<sup>2</sup>) is employed in qCPA. The pure compound parameters are fitted to saturated liquid densities and saturated vapor pressures. Table 1 shows the regressed parameters of the three approaches, and Table 2 shows their deviation from experimental data.

It is clear from Table 2 that good agreement is obtained with all approaches. It is noteworthy that the deviations for CO<sub>2</sub> with qCPA are lower than CPA without association (n.a.), even though the same number of adjustable parameters are employed. However, good agreement between correlated and experimental pure compound properties is not a sufficient condition for a predictive model, although certainly a necessary one.

To evaluate the predictive capability of the quadrupolar term the VLE of a number of binary CO<sub>2</sub>-

hydrocarbon mixtures have been predicted based on the pure compound parameters only. That is, no binary interaction parameter has been fitted to the experimental data.

**Table 1:** Estimated pure compound parameters of the CPA using three different approaches for CO<sub>2</sub>. Reduced temperature range for the correlation:  $T_r=[0.7-0.9]$ .

Type	$\Gamma$ [K]	$b_0$ [mL /mol]	$c_1$	$\beta$	$\epsilon/R$ [K]	Ref
CPA, n.a.	1550	27.3	0.77	-	-	3
CPA, 4C	1329	28.4	0.66	25.7	513	3
qCPA	1284	27.9	0.68	-	-	10

**Table 2:** Percentage absolute average deviations (%AAD) from experimental data for CO<sub>2</sub> with the CPA using three different approaches for CO<sub>2</sub>.

Type	%AAD in $\rho^{liq}$	%AAD in $P^{sat}$	Ref
CPA, n.a.	0.95	0.18	3
CPA, 4C	0.10	0.07	3
qCPA	0.46	0.13	10

Using the three approaches for CO<sub>2</sub> Figure 1 and Figure 2 compares the predicted VLEs of the binary mixtures CO<sub>2</sub>-ethane and CO<sub>2</sub>-propane with experimental data.

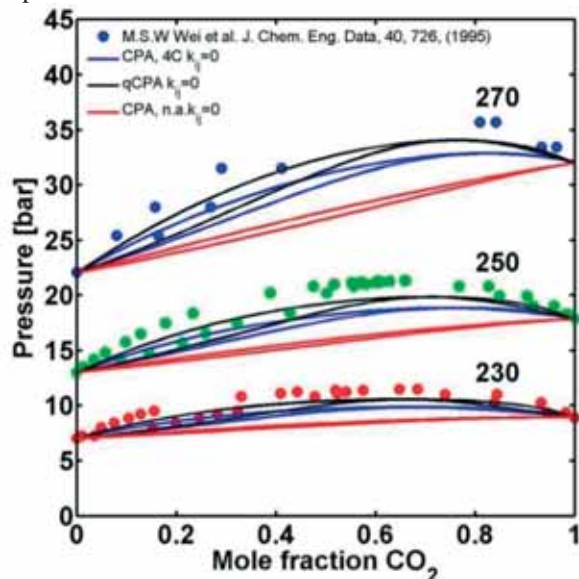


**Figure 1** - Predicted ( $k_{ij}=0$ ) VLE of CO<sub>2</sub>-ethane at three temperatures (in Kelvin). Circles are experimental data from [11].

It is clear from the figures that compared to CPA without association significant improvements can be obtained with a quadrupolar term, or by assuming that CO<sub>2</sub> can be modelled as an associating compound. That is, without the quadrupolar term an almost ideal Raoult's law type VLE is predicted in Figure 1, while both of the

other approaches predict the azeotrope, although at slightly lower pressures than experimentally observed.

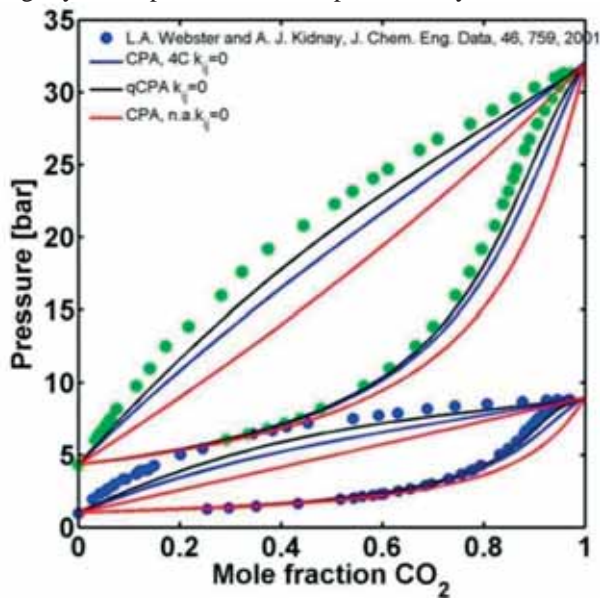


**Figure 2:** Predicted ( $k_{ij}=0$ ) VLE of CO<sub>2</sub>-propane at two different temperatures. Circles are experimental data from [12].

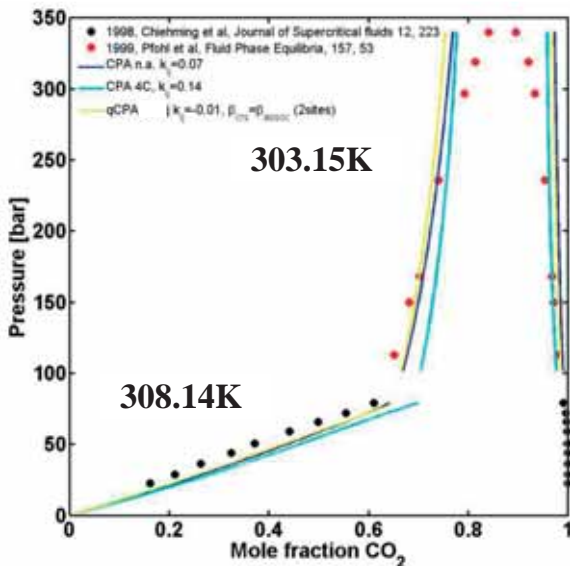


**Figure 3 -** Vapor liquid (308.14K) and liquid-liquid equilibrium (303.15K) of CO<sub>2</sub>-nonanol. Circles are experimental data from [13-14].

It is worth noting that in both cases qCPA results in slightly better predictions than CPA with association, even though qCPA only employ three pure compound parameters, compared to the five parameters in the associating case.

A rigorous test for any equation of state is how well it can correlate LLE. Figure 3 illustrate the vapor-liquid and liquid-liquid equilibrium of CO<sub>2</sub>-nonanol at two almost identical temperatures. A single interaction parameter has been correlated to the LLE data. It can be seen from the figure that all models correlate both the VLE and the LLE quite well; however, an interaction

parameter of almost zero is employed when CO<sub>2</sub> is correctly treated as a quadrupolar fluid, suggesting that the model can almost predict the equilibrium behavior of the system. When CO<sub>2</sub> is treated as an associating species, however, a very large interaction parameter is needed.

qCPA seems to perform very well for binary systems. On the other hand all models can accurately correlate the binary phase diagrams, if one or two binary interaction parameters are employed. As it is common practice to evaluate binary systems with at least one interaction parameter, conclusions may be affected by the adjustable parameters. That is, a more reliable comparison of the models should be based also on predicted multicomponent phase behavior.

Figure 4 shows the VLE predictions of the ternary CO<sub>2</sub>-methanol-water system. Interaction parameters from the binary subsystems have been employed, but no parameters have been correlated to the ternary experimental data. It is clear from the figure that of the three evaluated approaches the best predictions are obtained when qCPA is employed. Predictions are almost equally good if CO<sub>2</sub> is treated as an inert compound.

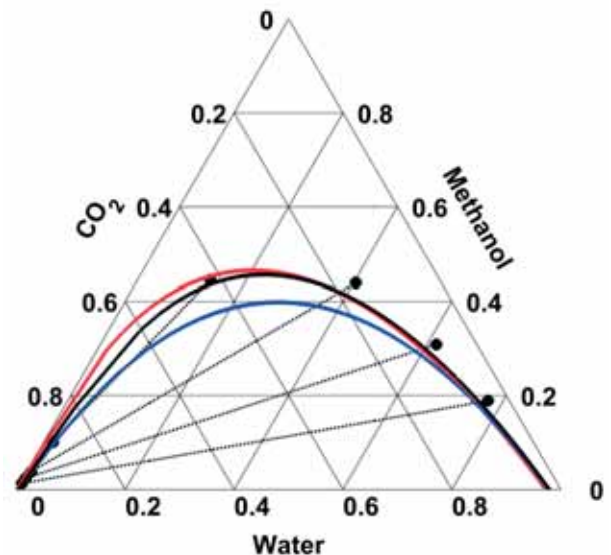


**Figure 4 –** Predictions compared to experimental data for the CO<sub>2</sub>-methanol-water VLE at 313.2 K and 100 bar. **Black line:** qCPA, **blue line:** CPA 4C, **red line:** CPA n.a. Circles are experimental data from [15].

Figure 5 shows the three-phase VLLE predictions for the lower liquid phase of the ternary CO<sub>2</sub>-methanol-ethane system compared to experimental data. Overall the predictions are rather similar when CO<sub>2</sub> is modelled either as a self-associating or quadrupolar compound.

Finally, consider the ternary system CO<sub>2</sub>-ethane-methane, which contain no self-associating compounds (except CO<sub>2</sub> in one of the approaches). This substantially simplifies the phase equilibria, and may allow us to better assess the effect of the quadrupole term. However, all models predict the VLE of the system quite accurately when binary interaction parameters are employed. For this reason we predict in

Figure 6 the VLE of the system without the use of any interaction parameters (all  $k_{ij} = 0$ ). It is clear that the best predictions are with qCPA followed by CPA with association. This corresponds well with the fact that qCPA needs smaller binary interaction parameters, which effectively work as a correction term.

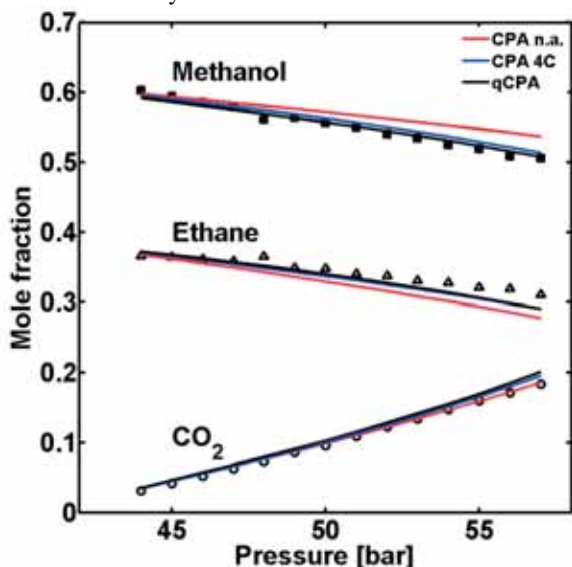


**Figure 5** – Predictions compared to experimental data for the lower liquid phase of the CO<sub>2</sub>-methanol-ethane VLE at 298 K. symbols are experimental data [16].

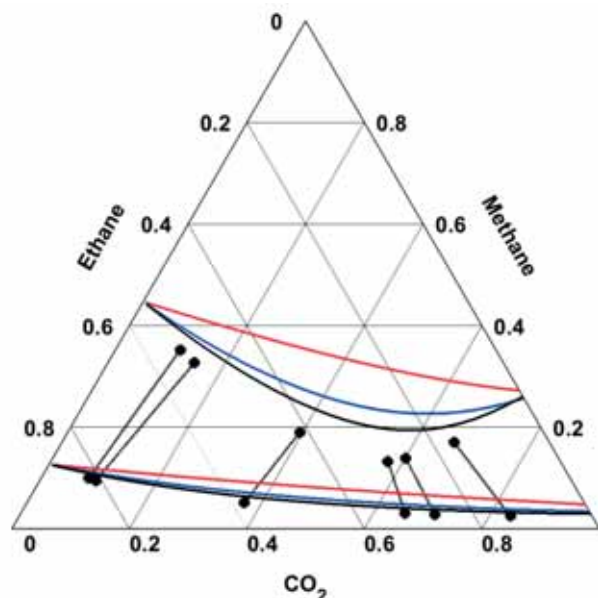


**Figure 6** – Pure predictions (all  $k_{ij} = 0$ ) compared to experimental data for the CO<sub>2</sub>-ethane-methane VLE at 250 K and 25 bar. **Black line: qCPA, blue line: CPA 4C, red line: CPA n.a.** Circles are experimental data from [17].

### Conclusions

In an effort to improve the predictive capabilities of classic thermodynamic models for mixtures containing CO<sub>2</sub> a novel quadrupolar term have been proposed and combined with CPA. It has been found that the model may significantly improve the prediction of binary VLE

for CO<sub>2</sub> containing mixtures. A very small interaction parameter may be employed to accurately correlate the phase equilibria of the binary mixtures.

For ternary mixtures it has been found that there is surprisingly little difference between predictions with the different model approaches when binary interaction parameters are employed. Without binary interaction parameters, however, the model seems to perform significantly better than the other models.

### Acknowledgements

The author is grateful to the Danish Research Council for Independent Research – Technology and Production Sciences and DTU for funding this project.

### References

1. O.-K. Nielsen, M.S Plejdrup, M. Winther, M. Nielsen, S. Gyldenkærne, M.H. Mikkelsen, R. Albrektsen, M. Thomsen, K. Hjelgaard, L. Hoffmann, P. Fauser, H.G. Bruun, V.K. Johannsen, T. Nord-Larsen, L. Vesterdal, I.S. Møller, O.H. Caspersen, E. Rasmussen, S.B. Petersen, L. Baunbæk, M.G. Hansen, Denmark's National Inventory Report 2014 No. 101 Aarhus University DCE – Danish Centre for Environment and Energy 2014.
2. D.F. Spencer, Methods of selectively separating CO<sub>2</sub> from a multicomponent gaseous stream, US Patent 5700311 (1997) and 6106595 (2000).
3. I. Tsivintzelis, G.M. Kontogeorgis, M.L. Michelsen, E.H. Stenby, Fluid Phase Equilibria 306 (1) (2011) 38-56.
4. J. Gross, AIChE Journal 51 (9) (2005) 2556-2568.
5. E.K. Karakatsani, T. Spyriouni, I.G. Economou, AIChE Journal 51 (8) (2005) 2328-2342.
6. B. Larsen, J. C. Rasaiah, G. Stell, Mol. Phys 33(4) (1977) 987-1027.
7. G. Stell, J.C. Rasaiah, H. Narang, Mol. Phys. 27 (5) (1974) 1393-1414.
8. G.S. Rushbrooke, G. Stell, J.S. Høye, Mol. Phys. 26 (5) (1973) 1199-1215.
9. Kontogeorgis, E.C. Voutsas, I.V. Yakoumis D.P. Tassios, Ind. Eng. Chem. Res 35(11) (1996) 4310-4318.
10. M.G. Bjørner, G.M. Kontogeorgis, Fluid Phase Equilibr 408 (2016) 151-169.
11. M.S. -W Wei, T.S. Brown, A.J. Kidnay, E.D. Sloan, J. Chem. Eng. Data 40 (1995) 726-731.
12. L.A. Webster, A.J. Kidnay, J. Chem. Eng. Data 46 (2001) 759-764.
13. C. Chiehming, C. Kou-Lung, D. Chang-Yih, J. Supercrit. Fluids 12 (1998) 223-237.
14. O. Pfohl, A. Pagel, G. Brunner, Fluid Phase Equilib 157 (1999) 53-79.
15. J.H. Yoon, M.K. Chun, W.H. Hong, H. Lee, Ind. Eng. Chem. Res 32 (11) (1993) 2881-2887.
16. T. Adrian, S. Oprescu, G. Maurer, Fluid Phase Equilib, 132 (12) (1997) 187-203.
17. J. Davalos, W.R. Anderson, R.E. Phelps, A.J. Kidnay, J. Chem. Eng. Data 21 (1) (1976) 81-84.



**Gerard Capellades Méndez**

Phone: +45 4525 2923  
E-mail: gcap@kt.dtu.dk

Supervisors: Søren Kiil  
Kim Dam-Johansen  
Michael J. Mealy, H. Lundbeck A/S  
Troels V. Christensen, H. Lundbeck A/S

PhD Study  
Started: September 2014  
To be completed: September 2017

## Continuous crystallization and filtration of active pharmaceutical ingredients and intermediates for pharmaceutical production

### Abstract

As a first step for the design of continuous crystallizers with improved control of the product crystal size distribution, a continuous Mixed Suspension Mixed Product Removal unit has been used to crystallize an Active Pharmaceutical Ingredient from ethanol solutions. Analysis of the solid phase shows that the obtained crystals have a needle-like morphology as well as negligible amorphous content. Furthermore, the solid product has the desired crystal structure, equivalent to that obtained from the industrial batch process.

### Introduction

Crystallization is one of the most important separation processes in pharmaceutical production, as most of the Active Pharmaceutical Ingredients (APIs) are crystals of organic molecules [1]. Properties of the final product such as crystal morphology and particle size distribution can have a significant effect on the drug's bioavailability. Consequently, requirements for crystallized APIs are usually very strict, and demand the use of controlled crystallization units.

Despite pharmaceutical production is traditionally taking place in batch processes, there is an increasing interest in transition to continuous production. When it comes to crystallization, Mixed Suspension Mixed Product Removal (MSMPR) crystallizers are the most common unit for small organic pharmaceuticals. This type of crystallizer is typically preferred for its simplicity, versatility and capacity for handling concentrated suspensions. Several studies have been published involving crystallization of pharmaceuticals in single stage or series of MSMPR units [2-6].

### Specific objectives

This PhD project involves the design of a versatile unit for continuous isolation of a given set of pharmaceuticals. Initial studies for each compound involve two steps:

- Solvent selection and determination of a solubility line.
- Crystallization experiments on an MSMPR unit, including quantification of nucleation and growth rates under different process conditions.

The next step will be to investigate methods for selective enhancement of nucleation kinetics. These methods should be applied to the design of a continuous crystallizer with improved control of the crystal size distribution. After evaluating both units, the optimal crystallizer will be coupled with a continuous filter.

The current contribution describes the setup and methodology for MSMPR crystallization of a given API. Results will later be used to study the advantages and limitations of this crystallizer, and will serve as a benchmark for the evaluation of future units.

### Results and discussion

An illustration of the designed crystallizer can be found in Figure 1.

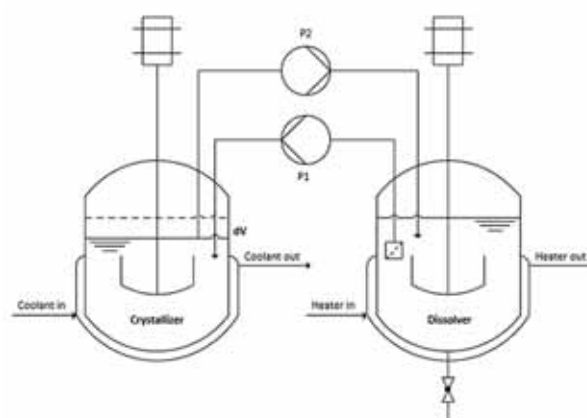


**Figure 1:** Schematic diagram of the crystallization unit.

The system consists of two vessels coupled with peristaltic pumps. P1 continuously delivers an undersaturated feed solution to the crystallizer, where it gets cooled to the studied temperature. To be able to operate the system for extended periods of time, the crystallization magma is recycled to the feed vessel, where it is re-dissolved. A 0.5  $\mu\text{m}$  in-line filter is placed at the outlet to ensure that the feed stream is free of crystals. P2 is programmed to work at full speed every 1/20<sup>th</sup> of a residence time. First, the pump removes part of the crystallization volume until the liquid level reaches the end of the dip pipe. Then, it pumps air for another 5 seconds to rinse the stream from any remaining suspension. This intermittent withdrawal system is used to minimize classification in the removed magma by applying high intermittent flows instead of a constant, lower flow rate.

Chord length distributions of the solid material are measured in-line by Focused Beam Reflectance Measurement (FBRM), and samples of the feed solution are taken every two residence times to ensure that no classification is occurring in the crystallizer.

Steady state samples are taken from the solid material, which is filtered, washed and dried. Samples of the mother liquor are taken through a 0.45  $\mu\text{m}$  syringe filter, and their concentrations are measured by HPLC. The solid's shape, morphology and crystallinity are assessed by optical microscopy and X-Ray Powder Diffraction.

Samples of a marketed API have been obtained from production in H. Lundbeck A/S, and the compound has been re-crystallized from ethanol according to the described methodology. As it can be seen from Figure 2, the obtained crystals have a uniform needle-like shape, as it is also found in the industrial batch process.

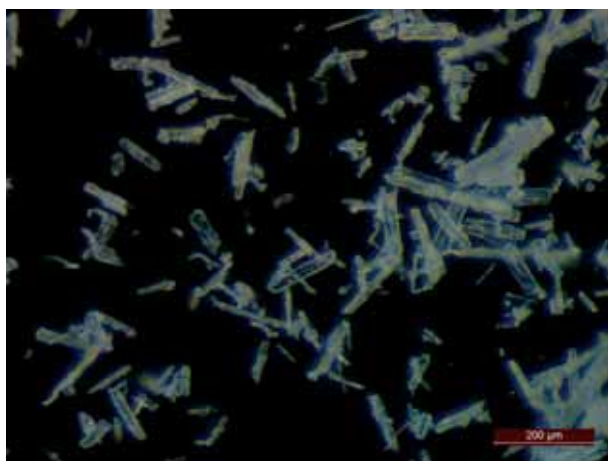


**Figure 2:** Optical microscope picture of the steady state crystals.

X-Ray Powder Diffraction results show that the obtained crystals give the same diffraction pattern as the product obtained from the industrial batch process. Therefore, the right crystal structure can be obtained from the continuous process. The strong baseline in the diffraction pattern is also an indication of the high crystallinity of the product.

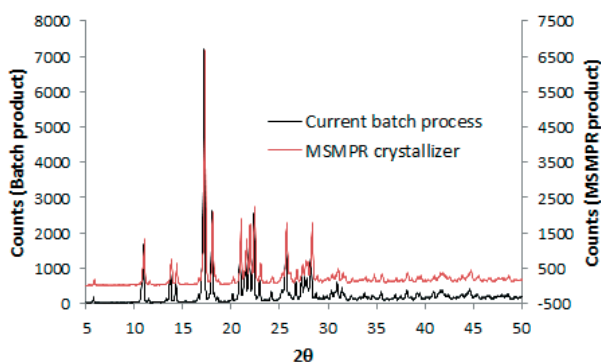


**Figure 3:** X-Ray Powder Diffraction patterns for the crystals obtained from the industrial batch process (black) and the designed MSMPR unit (red).

Experiments have been conducted for different crystallization temperatures, residence times, feed concentrations and agitation intensities. The effect of these process conditions on crystallization kinetics will be quantified to determine the critical parameters for process optimization.

### Conclusions

An MSMPR crystallizer has been designed and operated for continuous crystallization of a marketed API from ethanol solutions. Results show that the product meets the industrial demands regarding crystallinity, particle shape and morphology, indicating that this unit is a good alternative for continuous production of this compound. The unit's ability to control the product crystal size distribution will be compared to different crystallizer designs in future work.

### Acknowledgements

The author acknowledges H. Lundbeck A/S and the CHEC research center at DTU Chemical Engineering for their financial and professional support.

### References

1. A.J. Alvarez, A.S. Myerson, *Crystal Growth and Design* 10 (5) (2010) 2219-2228.
2. G. Hou, G. Power, M. Barrett, B. Glennon, G. Morris, Y. Zhao, *Crystal Growth and Design* 14 (4) (2014) 1782-1793.
3. H. Zhang, J. Quon, A.J. Alvarez, J. Evans, A.S. Myerson, B. Trout, *Organic Process Research and Development* 16 (5) (2012) 915-924.
4. A.J. Alvarez, A. Singh, A.S. Myerson, *Crystal Growth and Design* 11 (10) (2011) 4392-4400.
5. G. Power, G. Hou, V.K. Kamaraju, G. Morris, Y. Zhao, B. Glennon, *Chemical Engineering Science* 133 (2015) 125-139.
6. Y. Yang, Z.K. Nagy, *Industrial and Engineering Chemistry Research* 54 (21) (2015) 5673-5682.



## Ricardo Fernandes Caroço

Phone: +45 5270 3333  
E-mail: rcar@kt.dtu.dk

Supervisors: Jakob K. Huusom, DTU  
Jens Abildskov, DTU  
Paloma Santacoloma, CP Kelco

PhD Study  
Started: September 2015  
To be completed: August 2018

## Model-based monitoring of bioprocessing plants

### Abstract

The project focuses on the implementation of a monitoring strategy in industrial settings, exploring the development possibilities of a cross-(bio)industry framework. A case-study focusing on the performance monitoring of a pectin batch extraction process is conducted in a way to take advantage of the first principle dynamic models, which describe the reactions and transport phenomena of the pectin extraction, that were developed for the considered critical quality attributes: pectin bulk concentration, degree of esterification (%DE) and intrinsic viscosity (IV). An integrated procedure for a full-scale monitoring is envisioned, making use of state-of-the-art state estimation algorithms together with chemometric models, with the ultimate goal of providing the process operators with guidelines for process optimization and a decision making tool.

### Introduction

Monitoring and control strategies play a crucial role in the various stages of a product/process life-cycle, from process development to the optimization of an established process. These strategies are used to address a large number of objectives such as process understanding, statistical process control, real-time control actions, troubleshooting and continuous process optimization. Currently one of the major limitations in the biochemical industry is the multitude of disturbances that each process is subjected to, which can derive from processing biological feedstock or from working with living (micro) organisms. Nowadays the industry operates in a heuristic recipe-driven way, dependent on rule-of-thumb experience which results too often in batch-to-batch discrepancies. These difficulties can be mitigated by an appropriate monitoring strategy and model building comes as an integral part of such a strategy as models supply a representation of the underlying physical/chemical phenomena, allowing prediction and subsequent control decisions.[1]

Monitoring and control strategies applied in the biochemical industry have not reached the same level of maturity as the traditional bulk chemical industry, and the use of mathematical models and online optimization algorithms is still new. There is an opportunity to explore state feedback algorithms combined with process analytical technology (PAT) to develop model predictive control (MPC) as a way to reduce process

variations, improve product quality and lower the cost of operation.[2][3]

### Framework Formulation

The ultimate goal of the project is to develop a methodology/framework that provides a knowledgeable approach to bio-process operations monitoring in plants. The work intends to provide a detailed framework for entire monitoring implementation strategy: from objective definition and process risk assessment (identifications of critical quality attributes (CQAs) and critical process parameters (CPPs)) to modelling and corresponding monitoring strategies capable of meeting the process desired targets. The focus will be set on the models, which have to be complex enough to be able to accurately predict the dynamics of the system, but still usable to day-to-day application of the strategies in the plants.

Some of the major questions raised by this effort are:

1) Identifying what are currently the monitoring strategies employed in the industry. Is there currently any systematic logic behind the selection of a given approach?

2) Theory vs Industry reality. What is feasible to implement in a settled industry? What is needed from a current process to develop a monitoring strategy? What needs to be abdicated from a theoretical optimal strategy, to fit with the real process possibilities?

3) Relationship between type of process and monitoring strategy. Is there any correlation between the

type of process and a type of strategy, or is it a “case-by-case” scenario? Is it possible to construct a decision making tool based on the type of process, monitoring objective, available information, etc.

This effort will be done in an iterative way and taking into account the projected case studies. The final goal is set on the development of a methodology, critically re-visiting what was previously done in the case-studies and testing it on a variety of different scenario cases.

### Case Study – Pectin Extraction

Pectin is a polysaccharide, composed of different sub-structural entities that form a linear backbone (homogalacturonan - sequences of  $\alpha$  (1→4) linked D-galacturonic acid residues) and side-chain groups. The constituents of the backbone can be present in an esterified (as methylesters) and free acid form. They may be partly or fully neutralized with cations such as sodium, potassium, calcium, or ammonium. The ratio of esterified galacturonic acid groups to total galacturonic acid groups is termed the degree of esterification (%DE) and has a vital influence on the properties of pectin. Production comprises four core steps: extraction from the plant material, purification of the liquid extract, precipitation of pectin from the solution, and further de-esterification and/or amidation of the high methylester pectin with acid or alkali.[4]

The monitoring goals for this case-study are set in terms of the rate of extraction and the pectin quality in order to optimize the following batch runs. Figure 1 represents the extraction factors that impact the CQAs: pectin bulk concentration, degree of esterification (%DE) and intrinsic viscosity (IV).

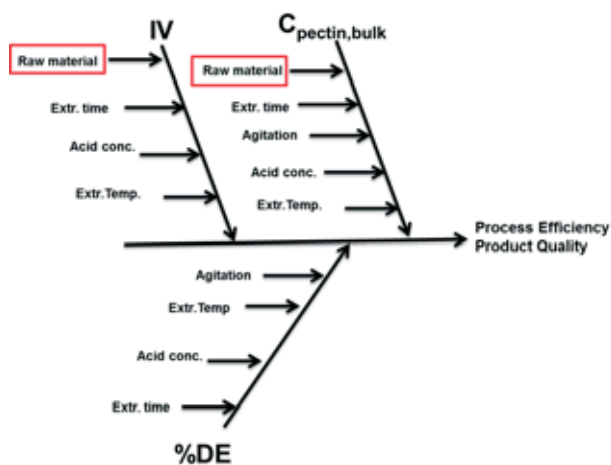


**Figure 1:** Ishikawa diagram for identification of cause-effect dynamics in process. Raw material variability is deemed as an important disturbance.

This project is the continuation of previous efforts to model this process, and will try to reach plant scale implementation of an adequate monitoring strategy. This model should be as such that describes the dynamics of the extraction that are immeasurable or that are not possible to measure, in a timely manner.

Work towards model robustness is key as the parameters that describe the models were tuned based pilot plant data and have now to be verified to describe production process behavior and validated to for a variety of different raw material and conditions, to ensure the which shows that the model is able to cope with the discrepancies in the raw material, allowing the product quality to hold consistently at the required standards despite variations. To take this into account the monitoring strategy has to be thought as whole and every step of that leads to the process (type of raw material, conditioning, handling, etc.) should be considered, as well as possible hybrid approaches, utilizing data obtained through empirical models.

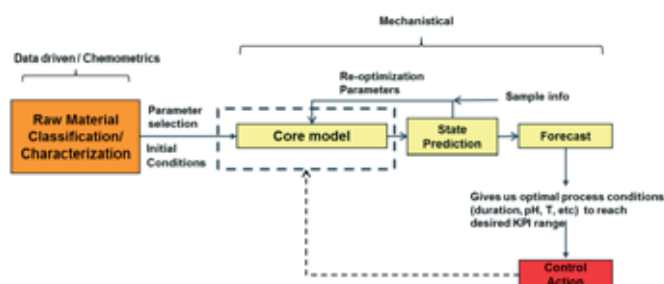


**Figure 2:** Possible representation of an integrated monitoring strategy approach.

The integrated monitoring strategy will involve a combination of first principle models with chemometric data-driven models, supplemented with online process measurements such as volume, temperature, pH as well as discrete sampling for NMR analysis at-line (Figure 2).

### Acknowledgements

The project is part of the Danish cluster in biotech manufacturing - BIOPRO. The financial and logistical support from the industry participants is acknowledged.

### References

1. D. Dochain (Ed.), Bioprocess Control, Control Systems, Robotics and Manufacturing Series, ISTE, London, UK., 2008, p. 11-16.
2. L. R. Formenti, A. Nørregaard, A. Bolic, D.Q. Hernandez, T. Hagemann, A.-L. Heins, L. Mears, M. Mauricio-Iglesias, U. Krühne, K. V. Gernaey. Challenges in industrial fermentation technology research. Biotechnology Journal, 9(6), 727–38.
3. J. K. Huusom. Challenges and opportunities in integration of design and control. Computers & Chemical Engineering, 81, 138–146.
4. CP Kelco. GENU® pectin Book. 2008.



**Carlos Eduardo Ramírez-Castelán**

Phone:

E-mail:

cara@kt.dtu.dk

Supervisors:

Jakob K. Huusom

Anker D. Jensen

Angélica Hidalgo-Vivas, Haldor Topsøe

Jacob Brix, Haldor Topsøe

PhD Study

Started:

November 2014

To be completed:

October 2017

## Optimal model-based monitoring of tubular reactors

### Abstract

Achieving high quality information online is a challenge for a large range of processes in the chemical and biochemical industry. Even if it is possible to implement online sensors on the process, it constitutes a cost which requires the companies to optimize the sensor selection. This is especially true for processes with spatial variations as for the concentration and temperature in tubular reactors. Such processes are examples of nonlinear processes which require that the operator can get information of the nonlinear transient and profile in the system. Real time information of the state of the process is paramount in terms of online optimization through control and for ensuring product quality as well as a safe and reliable process operation.

### Introduction

Modern refinery operations cover a wide and complex variety of processes, since the crude stills are the first major processing units, distillation processes are used to separate the crude oils by into fractions according to boiling point so that each of the processing units following will have feedstocks that meet their particular specifications. Higher efficiencies and lower costs are achieved if the crude oil separation is accomplished in two steps: first by fractionating the total crude oil at essentially atmospheric pressure; then by feeding the high-boiling bottoms fraction (topped or atmospheric reduced crude) from the atmospheric still to a second fractionator operated at a high vacuum.

Nevertheless, specific chemical reactions are vital for further refining stages such as hydrotreating, catalytic cracking, hydrocracking, hydroprocessing and hydrodesulfurization (Figure 1); terms that are used rather loosely in the industry because, in the processes hydrodesulfurization and hydrocracking, cracking and desulfurization operations occur simultaneously and it is relative as to which predominates.

Despite that, hydrotreating refers to a relatively mild operation whose primary purpose is either to saturate olefins, reduce the sulfur and nitrogen content of the feed, or both. It refers to a process in which petroleum products are catalytically stabilized and/or objectionable elements are removed from products or feedstocks by reacting them with hydrogen. Stabilization usually involves converting unsaturated hydrocarbons such as olefins and gum-forming unstable diolefins to paraffins.

Objectionable elements removed by hydrotreating include sulfur, nitrogen, oxygen, halides, and trace metals. Hydrotreating is applied to a wide range of feedstocks, from naphtha to reduced crude. When the process is employed specifically for sulfur removal it is usually called hydrodesulfurization. Catalytic hydrotreatment is essential to obtain fuels with improved quality and low polluting compounds content (sulfur, nitrogen, aromatics). Catalytic cracking is the most important and widely used refinery process for converting heavy oils into more valuable gasoline and lighter products over 1 million tons/day of oil processed in the world [1].

In the case hydrotreating, and other large scale processes, it is not always possible to directly measure the important state variables online which are needed by the operator to judge if the plant is behaving as planned or not. If these cannot be determined by indirect measurements, then the information can be constructed by means of a state estimator using a process model and the available measurements from the system. Examples of such systems are the spatial concentration and temperature profiles inside tubular reactors, more specifically trickle-bed reactors that play an important role in the overall refinery flow.

### Trickle bed reactors

A unique characteristic of trickle-bed reactors compared to other types of three-phase reactors is, in general, the catalyst particle is filled with liquid while the outer surface may not be completely wet or covered by the

flowing liquid which leads to a more direct contact between the gas phase and the catalyst [2].

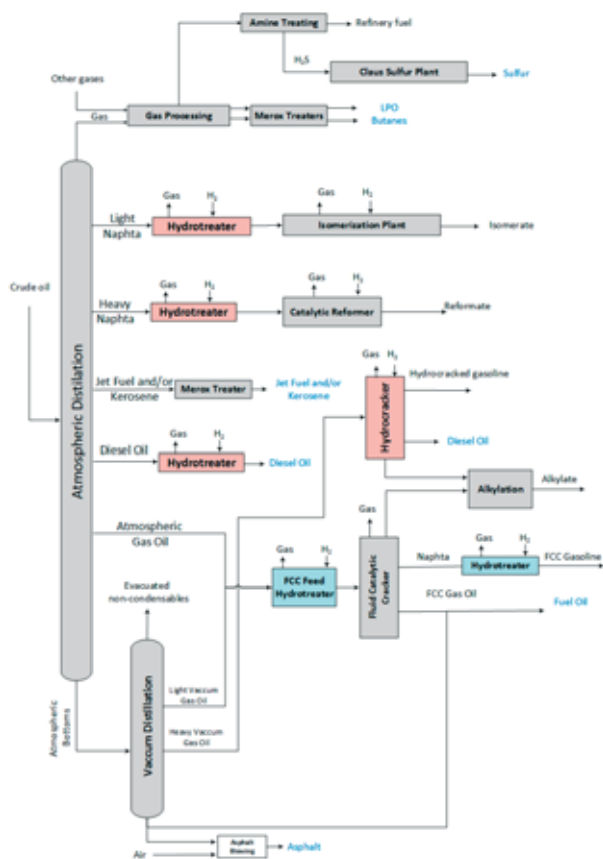


**Figure 1:** The overall refinery flow diagram

The operation conditions of trickle-bed reactors is too hostile or fouling for sensors to work. In such cases, the system measurements must be made whether by sampling and lab analysis, which results are issued with significant delay, or using state estimators that may also incorporate information of known disturbances from feed mixture analysis or upstream data. For these reasons, trickle-bed reactors are difficult to operate due to the coupling between transfer phenomena, non-linear kinetics and their distributed nature which can lead to temperature hot spots in the catalytic bed or formation of an undesired compound. In that sense, online information of the current state of the process is important for the operator or any model based control algorithm for process optimization. Especially when a system may be operated close to a process constraint or the operator needs to avoid an unstable region which may lead to run away or undesired reactions.

Given known process inputs the model can predict online what the state of the process is and what the sensors should measure. By comparison between actual and predicted measurements, corrections in the model predictions can be made through a systematic algorithm which utilizes the statistical uncertainty of the measurements. Linear state estimators such as the Kalman filter is in wide-spread use but advanced monitoring of nonlinear process behavior in tubular reactors by nonlinear state estimators could reduce the

risk of having a product that does not meet specifications significantly or conditions that reduce the performance of the catalytic bed.

For that reason, if the reaction rate depends on the liquid reactant, the wetting efficiency leads to reduced global reaction rates, on the other hand, if the reaction rate is controlled by the gas phase, the global reaction rate is higher since the resistance to mass transfer in the non-wetted surface is lower than in the covered surface [3]. Figure 2 shows the concept of trickle flow.

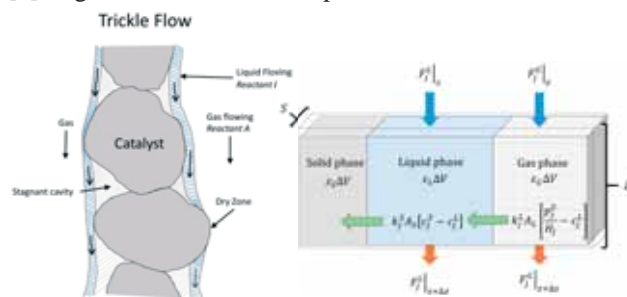


**Figure 2:** Trickle flow in fixed bed reactors

### Current status

A model of the trickle-bed reactor is derived from the mass and energy equations according to the law of conservation to a small element of volume. The focus of interest is the nonstationary volume element, fixed in space, through which a fluid and gas are flowing and chemical reactions taking place only in the solid phase. The model of a trickle-bed reactor can be validated with experimental data, and will allow to develop the state estimation of representative real case studies aiming towards the implementation of optimal model-based monitoring.

### Objectives

The aim of this project is to develop a generic optimal-model based monitoring framework suited for a wide range of tubular reactor applications of industrial relevance but the results may also be extended to other process system with similar characteristics.

### Acknowledgements

This project is being developed with the collaboration of Haldor Topsøe A/S and founded by Consejo Nacional de Ciencia y Tecnología (CONACyT), Mexico.

### References

1. James H. Gary, Glenn E. Handwerk, Mark J. Kaise Petroleum Refining: Technology and Economics, Fifth Edition, 2007.
2. AlDahhan, M. H.; Larachi, F.; Dudukovic, M. P.; Laurent, A. High-Pressure Trickle-Bed Reactors: A Review. Ind. Eng. Chem. Res. 1997, 36 (8), 3292-3314.
3. Herskowitz, M. Trickle-Bed Reactors: A Review. AIChE Journal (Vol. 29, No. 1) January, 1983



**Steen Müller Christensen**

Phone: +45 2666 1700  
E-mail: stmuch@kt.dtu.dk

Supervisors: Anker D. Jensen  
Brian B. Hansen  
Joakim R. Thøgersen, Haldor Topsøe A/S

PhD Study  
Started: September 2015  
To be completed: September 2018

## Selective catalytic reduction of NO<sub>x</sub> on ships

### Abstract

The introduction of MARPOL Annex VI requires a high degree of NO<sub>x</sub> reduction for shipping within NECAs and a global SO<sub>x</sub> reduction. Since Denmark is one of the world's foremost shipping nations, this creates a need for new technologies and engineering solutions that can comply with the new regulations. SCR of NO<sub>x</sub> is a well-known technology for reducing NO<sub>x</sub> and has been applied to both stationary and mobile applications. The technology also holds a great potential for application on-board ships, but performance is not yet optimized with respect to use in combination with marine equipment such as waste heat boilers and sulfur scrubbers (see fig. 1). Important considerations include optimal performance of the SCR reaction (including minimal N<sub>2</sub>O by-product formation) at the maritime conditions (incl. elevated pressures) and the potential of flue gas SO<sub>2</sub> and SO<sub>3</sub> to react with ammonia and form ammonium bisulfate and ammonium sulfate. The sulfates may foul heat transfer surfaces (ship boiler), and plug the catalysts flow channels and surfaces.

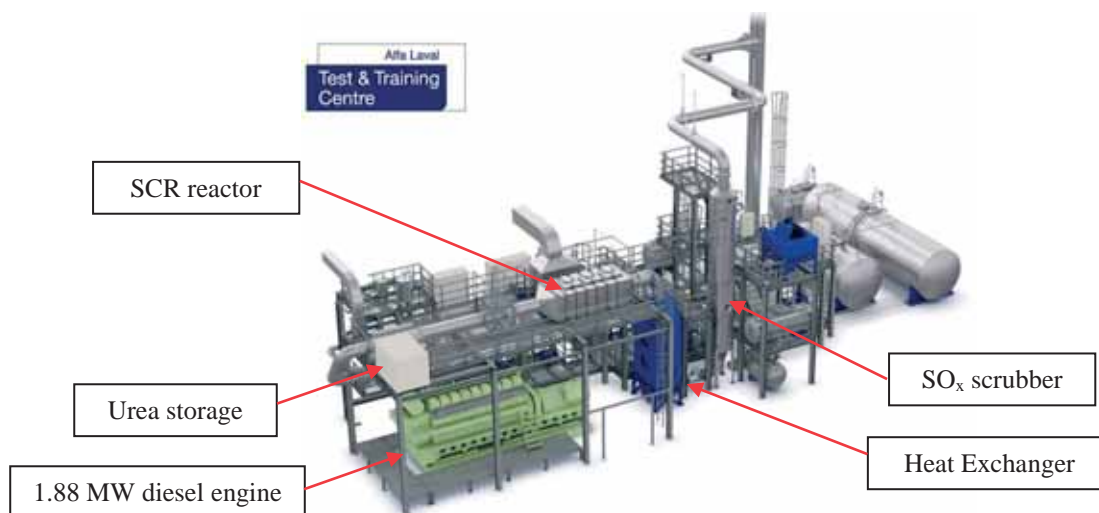


**Figure 1:** Alfa Laval's test facility, at which full scale measurements will be performed. Courtesy of Alfa Laval.

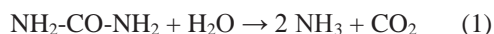
### Introduction

Denmark is one of the world's foremost shipping nations, leading in cargo transport, tanker shipping, refrigerated cargo, and offshore. Maritime transport and shipping benefits from low CO<sub>2</sub> emissions and low noise levels but emissions of SO<sub>x</sub>, NO<sub>x</sub> and particles are generated. The issues related to NO<sub>x</sub>/SO<sub>x</sub> emissions are being targeted by the introduction of NO<sub>x</sub> emission control areas (NECAs) for new ships and global SO<sub>x</sub> regulations, both of which are introduced through the

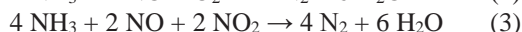
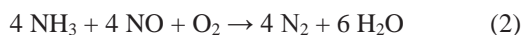
MARPOL 73/78 Annex VI[1] which generates a need for new technologies and engineering solutions on the matter.

Selective Catalytic Reduction (SCR) of NO<sub>x</sub> using ammonia (NH<sub>3</sub>) as reductant is a well-known abatement technology and was first used to remove NO<sub>x</sub> on stationary sources such as power plants, waste incinerators and in the cement industry[2]. Later, SCR has been introduced for mobile applications i.e. vehicles and ships for which urea is used as the reductant. The

injected urea spray decomposes into  $\text{NH}_3$  and isocyanic acid (HNCO), HNCO further decomposes at the SCR catalyst into a second molecule of  $\text{NH}_3$ . The overall decomposition of urea can be written according to Reaction (1)[3]:



The produced  $\text{NH}_3$  adsorbs on the SCR catalyst surface and reacts with gaseous NO. The most used catalyst is based on  $\text{V}_2\text{O}_5$ , doped with  $\text{WO}_3$ , washcoated on a carrier of anatase, the high surface area form of  $\text{TiO}_2$ . The SCR of  $\text{NO}_x$  consists of three reactions as shown below.



Reaction (2) is known as the standard SCR reaction, since 90% of engine out  $\text{NO}_x$  is comprised of NO. Reaction (3) is known as the fast SCR and Reaction (4) is known as the slow SCR reaction and they are generally of low importance for ships.

The highly unwanted oxidation of  $\text{SO}_2$  into  $\text{SO}_3$  is also catalyzed by the  $\text{V}_2\text{O}_5$  present in the SCR catalyst. This oxidation is especially unwanted due to reaction of  $\text{SO}_3$  with water forming sulfuric acid aerosol, which can further react with  $\text{NH}_3$  and produce solid products such as ammonium sulfate (AS) and ammonium bisulfate (ABS). The presence of AS and ABS poses an operational problem since they may condense and block the SCR pores or stick on cold surfaces such as the heat recovery systems reducing the heat transfer and hence the overall efficiency of such systems, potentially causing regular cleaning shutdowns.

Beside the unwanted oxidation of  $\text{SO}_2$  other unwanted reactions such as the oxidation of  $\text{NH}_3$  and formation of emissions such as  $\text{N}_2\text{O}$  are also possible and should be avoided.

The highest activity of a SCR catalyst is achieved around 300-400 °C[4] but depending on the load of the engine the exhaust temperature can be fairly low (<200°C). Therefore, for highly efficient 2-stroke engines, which usually have low temperatures after the turbocharger, it has been considered to place the SCR reactor before the turbocharger. Placing the SCR reactor before the turbocharger would both increase the temperature and the pressure within the reactor. The influence of pressure on both the SCR reactions and the  $\text{SO}_2$  oxidation is poorly known and hence before introducing the SCR technology within this part of the maritime sector a thorough investigation must therefore be conducted to ensure stable, efficient, and competitive SCR technology.

### Specific Objectives

The first part of this project will consist of a thorough literature survey within the use of vanadium based SCR catalyst for  $\text{NO}_x$  abatement both on stationary and

marine application. Thereafter a literature survey within  $\text{SO}_2$  oxidation across an SCR catalyst followed by the formation, reaction and modeling of AS and ABS will be conducted.

The second part of this project involves full scale experiments at Alfa Laval's test facility which includes a 1.8 MW diesel engine equipped with an SCR reactor, a heat recovery unit, and a wet  $\text{SO}_2$  scrubber as shown in Fig. 1. The experiments will focus on the formation of AS and ABS at various ammonia to  $\text{NO}_x$  ratios (ANR). These experiments are performed to test whether it is favorable to operate the plant under conditions where AS, a non-sticky by-product, is formed instead of ABS, a sticky by-product.

Based on the experimental results a model will be made which will be used to determine the amount of AS and ABS formed, and furthermore, the amount that condenses and blocks the SCR reactor and/or heat recovery system. The model should therefore include both the  $\text{NO}_x$  reduction efficiency and the  $\text{SO}_2$  oxidation across the SCR catalyst.

The fourth part of this project is to measure the kinetics of  $\text{SO}_2$  oxidation which lead to the formation of AS and ABS. For this, experiments will be conducted at laboratory scale to investigate the  $\text{SO}_2$  to  $\text{SO}_3$  oxidation under ship conditions i.e. at high concentrations of  $\text{SO}_2$  and at elevated pressures. The effects of elevated pressure on both the  $\text{SO}_2$  oxidation and the SCR reactions are unknown and hence are an essential part of the thesis.

### Acknowledgements

This project is part of the private-public society partnership named Blue INNOShip. This project is a collaboration between the CHEC research center at DTU Chemical and Biochemical Engineering, Haldor Topsøe A/S, Alfa Laval Aalborg and Maersk Maritime Technology.

### References

1. "Marpol 73/78 Annex VI." [Online]. Available: [http://www.dnv.com/binaries/marpol\\_brochure\\_tcm4-383718.pdf](http://www.dnv.com/binaries/marpol_brochure_tcm4-383718.pdf).
2. P. Forzatti and L. Lietti, *Heterog. Chem. Rev.* 3 (1) (1996) 33–51.
3. M. Koebel, M. Elsener, and M. Kleemann, *Catal. Today* 59 (3–4) (2000) 335–345.
4. S. Amanatidis, L. Ntziachristos, B. Giechaskiel, A. Bergmann, and Z. Samaras, *Environ. Sci. & Technol.* 48 (19) (2014) 11527–11534.



## Stefano Cignitti

Phone: +45 5250 6039  
E-mail: [steci@kt.dtu.dk](mailto:steci@kt.dtu.dk)

Supervisors: Rafiqul Gani  
Krist V. Gernaey  
John M. Woodley

PhD Study  
Started: September 2014  
To be completed: September 2017

## Computer-aided molecular, mixture and blend design

### Abstract

Design of chemical products is a multidisciplinary task and is a growing interest in the industry and academia. Regulations, consumer and sustainability needs push the necessity for finding novel chemical products that can meet these needs. In this research work, a computer-aided framework for chemical product design of molecular, mixed and blended products is developed. The framework utilizes a mathematical programming formulation and solution approach. New in this proposed framework, is the ability to integrate the process/application design and sustainability of the chemical product through mathematical programming using two proposed solution algorithms.

### Introduction

In chemical product design, molecular structures and formulation of mixtures and blends are designed based on desired product specifications [1]. The product specifications are selected based on the needs and target properties and can include several types of specifications, such as cost, physicochemical and thermophysical properties, environmental and safety properties, and consumer-oriented specifications, such as look, feel and smell. Types of chemical products that are single molecules (and therefore require the design of the molecular structure) include chemical products such as solvents, refrigerants, active ingredients and surfactants [1]. If the pure molecular chemical products are not able to satisfy the product specifications, it is necessary to design mixed or blended products. These chemical products are designed by the formulation of ingredients and their compositions to match target product specifications. For mixed and blended products, product specifications can be met by fine-tuning the composition of the ingredients, as well as matching the phase behavior at specific temperature ranges, such as homogeneity of emulsions. Blended products differ from mixtures in that there is a structural homogenous mixture obtained by use of chemical additives and/or various mixing techniques. The ingredients can be selected based the product specifications met by pure molecules, but may require additional ingredients to reach the desired chemical product formulation (blends). These additional ingredients, or additives, can be detergents, emulsifiers and foaming agents.

Several challenges exist in chemical products design:

1. How to well-define needs and translate these into target specifications.
2. How to tackle growing need for more sustainable chemical products.
3. How to integrate the process and application specifications into target chemical product specifications.
4. How to efficiently and systematically design optimal chemical products.

In this work, a computer-aided chemical product design framework is developed for the design of pure, mixed and blended chemical products through a mathematical programming approach.

### General mathematical program

Mathematical programming approaches set-up the chemical product design problem into a set of linear and non-linear constraints and specifications into a set of equality and non-equality constraints. A general mathematical program is given below [1].

$$\begin{aligned} F_{obj} &= \max [C^T y + f(x)] \\ h_1(x) &= 0 \\ h_2(x) &= 0 \\ h_3(x, y) &= 0 \\ l_1 &\leq g_1(x) \leq u_1 \\ l_2 &\leq g_2(x, y) \leq u_2 \\ l_3 &\leq By + Cx \leq u_3 \end{aligned}$$

The variable  $x$  is a continuous variable, such as mixture composition;  $y$  is binary variable for selection, such as selection of compounds or unit operation. The equality constraint  $h_1(x)$ , is process design based constraint, such as process operating pressure;  $h_2(x)$ , represents model equations, such as mass balances;  $h_3(x,y)$ , represents structural constraints for generated molecules, such as maximum number of functional groups or property models. Inequality constraint  $g_1(x,y)$ , is related to process design constraints;  $g_2(x,y)$ , is related to environmental constraints or chemical product design constraints, such as ozone depletion potential or solubility. The last constraint enforces logical conditions on binary and continuous variables that appear in the objective function, which is an optimization function for process or application related target of the desired product.

### Computer-aided chemical product design framework

In this work, a generic computer-aided framework for chemical product design (CAPD) is presented through a systematic framework. A CAPD problem for the generation of novel pure, mixed and blended chemical products is formulated and solved through the application of four sequential steps.

In step (1), the product design problem is defined together with the process and/or application boundaries.

In step (2), the CAPD problem is formulated through property constraints for pure, mixed and blended products, process/application constraints and objective function. The property constraints are carefully selected for the thermo-physical property needs and the process/application needs. Process/application and property needs are connected through an analysis of the property influence on the process/application models

and thermodynamic relations. The sustainability is considered through product and process/application performance, economics and environmental impact.

In step (3), the CAPD formulation is converted into a mixed-integer nonlinear program (MINLP) by set-up of constraints, objective and boundaries defined in step (2).

In step (4), the MINLP is solved through a decomposed approach [2]. The decomposed approach breaks down the MINLP problem into a sub-set of programs to manage the complexity: mixed-integer linear program (MILP) for molecular generation, linear program (LP) for property constraints, non-linear program (NLP) for mixture/blend property constraints, and NLP for process constraints and objective function. This approach ensures that the optimal chemical product can be found through systematic generation and screening of alternatives based on the problem definition.

### Conclusion

The current developments in computer-aided framework for design of molecular, mixed and blended products have been presented. Current solved case studies include solvents, surfactants, polymers, working fluids and lubricants [2-3]. More info can be given regarding framework and case studies by contacting the student.

### References:

1. Gani, R., Ng, K.M., 2015, *Comput. Chem. Eng.* 81(4), 70-79.
2. Cignitti, S., Zhang, L., Gani, R., 2015, *Comput. Aided Chem. Eng.* 37, 2093–2098.
3. Zhang, L., Cignitti, S., Gani, R., 2015, *Comput. Chem. Eng.* 78, 79-84.

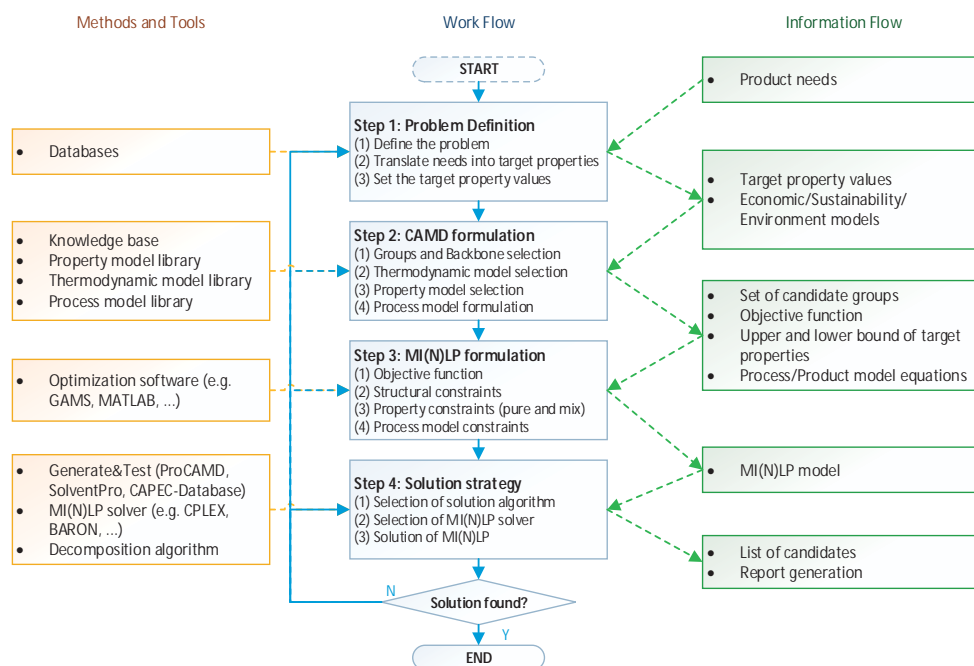


**Figure 1:** Computer-aided molecular, mixture and blend design framework



**Mafalda Dias**

Phone: +45 4525 2886  
E-mail: macoad@kt.dtu.dk

Supervisors: John M Woodley  
Mathias Nordblad

PhD Study  
Started: September 2015  
To be completed: August 2015

## Oxygen supply methods for processes using oxidases

### Abstract

Selective oxidation reactions are difficult to carry out in conventional process chemistry and it requires the use of protection and de-protection steps to guide the addition of oxygen. In contrast, biocatalytic oxidation can be carried out using molecular oxygen and offers high selectivity. However, implementing biocatalysis for oxidation reactions has quite some challenges for a feasible process to scale-up since it is limited by oxygen transfer and stability of the enzymes. This project is focused on the investigation of oxygen supply methods for oxidase-base reactions in order to analyze and select the most efficient method for a sustainable process design, regarding the characteristics of these type of reactions.

### Introduction

Oxidation represents a significant transformation in organic chemistry. Conventionally, oxidation reactions are conducted with stoichiometric toxic reagents like chromates. However, these processes are becoming less relevant in fine chemistry comparing with catalytic processes using environmentally favorable oxidants such as molecular oxygen ( $O_2$ ) or hydrogen peroxide ( $H_2O_2$ ). Remarkable advances in transition metal-catalyzed reactions, organocatalytic oxidations and oxyfunctionalizations utilizing those oxidants have been achieved. Simultaneously, biocatalysis is rising as an additional pillar for environmentally favorable oxidation catalysis [1].

Biocatalysis has several arguments for its application in organic synthesis over chemical processes such as mild reaction conditions (in terms of temperature and pressure) and use of non-problematic solvents. However, the major advantage consists in its exquisite regioselectivity and stereoselectivity properties [1], [2]. Oxidases are a notable subclass of oxidizing enzymes, which use oxygen either as oxidant or as electron acceptor. This property make them highly attractive for the production of chemicals. Alcohol oxidase (AOX) converts alcohols to aldehydes or ketones (Figure 1A). During this reaction, molecular oxygen is reduced to hydrogen peroxide. In order to avoid enzyme deactivation,  $H_2O_2$  is scavenged by addition of a catalase that converts it to  $H_2O$  and  $O_2$ .

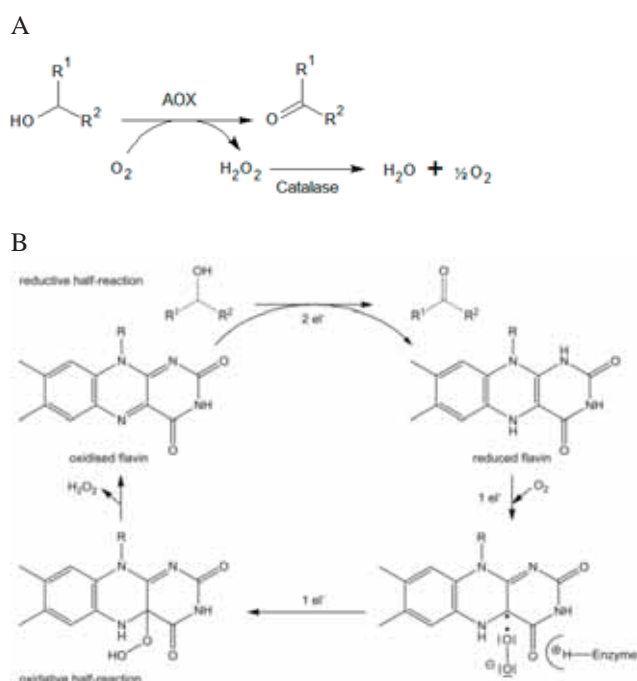


**Figure 1:** Biooxidation of alcohols using an AOX (A). Catalytic cycle of flavin-containing AOX (B) [3].

Flavin-dependent AOXs are enzymes where flavin adenine dinucleotide (FAD) or flavin mononucleotide (FMN) function as primary hydride acceptor. The stored reducing equivalents are then transferred to  $O_2$  yielding the catalytic active flavin and  $H_2O_2$  (Figure 1B) [1], [3]. The outstanding property of flavin is the chemical

versatility that enables flavoenzymes to catalyze a large variety of reactions with no need of adding a cofactor [4].

ROBOX European project aims to develop and demonstrate robust oxidative biocatalysis in the pharma, nutrition, fine chemicals and materials markets. Oxidative biocatalysis for industrial biotransformations requires enzymes able to transforming non-natural substrates and to operate in conditions they have not been designed for by nature. Therefore, this can compromise enzymes activity and stability. In order to introduce more biocatalytic process in industry, there is a demand for developing robust and effective enzymes capable of dealing with different conditions from its natural environment. Simultaneously, there is a growing need to design efficient biocatalytic processes and technology able to optimize the performance of these enzymes during reactions of commercial interest.

Oxidases such glucose oxidase are fast enzymes on their natural substrates, when high activity is achieved in ROBOX target substrates, oxygen supply will become a rate-limiting factor together with enzyme stability, since it is known that oxygen supplied by air bubbles may decrease enzyme stability. Thus, studying, analyzing and evaluating efficient oxygen supply methods for this type of reactions need to be investigated [5]. These challenges are considered and explored in this PhD project, which is integrated within ROBOX.

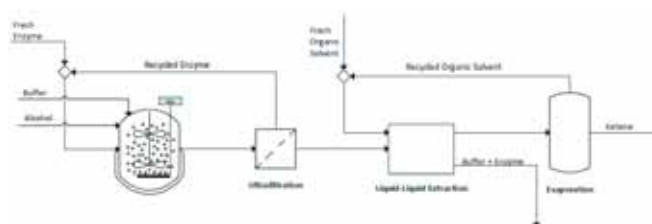
### Specific Objectives

The purpose of this PhD project is to investigate oxygen supply methods for oxidase-base reactions with the intention of analyze and select the most efficient method for a feasible process to scale-up. The reaction system of main interest is catalyzed by a modified sugar oxidase.

Therefore, the research is focused on reaction systems thermodynamically favorable, where the substrate and product are water soluble and non-volatile compounds. The oxidation is going to be catalyzed by a soluble and isolated enzyme with high reaction rate. The main challenge of these type of systems is to guarantee that the reaction rate is not limited by the oxygen supply rate, which depends on the oxygen concentration in the reaction medium. In this way, at the first stage of the project, different oxygen supply methods as (1) supply of  $H_2O_2$  that is degraded by a catalase to  $O_2$  and  $H_2O$ , (2) bubbling air or  $O_2$  and (3) membrane aeration are going to be experimentally studied and characterized based on the oxygen transfer rate and compared with industry requirements for designing a feasible process.

Furthermore, the enzyme stability will be studied regarding that the presence of  $H_2O_2$  or a gas phase in the reaction have strong influence on enzyme deactivation. The enzymatic rate of oxygen consumption will be experimentally studied to understand the oxygen requirements of the reaction and the biocatalytic system will be experimentally characterized.

A



B

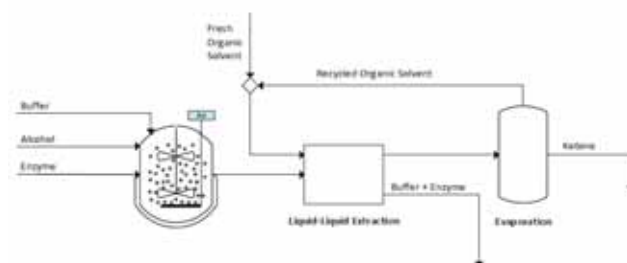


**Figure 2:** Possible downstream process flowsheets with (A) and without (B) enzyme recycling,

Additionally, a basic concept for the process flowsheet will be developed and bottlenecks identified (**Figure 2**). In the last part of the project, the designed process will be benchmarked against existing oxidation reactions using a computational framework that will be developed in the ROBOX project.

### Acknowledgements

The research for this work has received funding from the European Union (EU) project ROBOX (grant agreement n° 635734) under EU's Horizon 2020 Programme Research and Innovation actions H2020-LEIT BIO-2014-1.

### References

1. F. Hollmann, I. W. C. E. Arends, K. Buehler, A. Schallmeyer, B. Bühler. *Green Chem.* 13 (2) (2011) 226–265.
2. D. J. Pollard, J. M. Woodley. *Trends Biotechnol.* 25 (2) (2007) 66–73.
3. M. Pickl, M. Fuchs, S. M. Glueck, K. Faber. *Appl. Microbiol. Biotechnol.* (2015) 6617–6642.
4. A. Mattevi. *Trends Biochem. Sci.* 31 (5) (2006) 276–283.
5. <http://www.h2020robox.eu/>.



## **Demi Tristan Djajadi**

Phone: +45 4525 2612  
E-mail: dtdj@kt.dtu.dk

Supervisors: Henning Jørgensen, DTU  
Manuel Pinelo, DTU

### **PhD Study**

Started: February 2015  
To be completed: January 2018

## **Fractionation and enzymatic processing of biomass for biorefinery application**

### **Abstract**

In the face of diminishing fossil-based resources and the unwanted impacts of their utilization, biorefineries utilizing lignocellulosic biomass are being established. Lignin, a major component in lignocellulosic biomass is a barrier as well as underutilized material in most current bioprocessing setups dedicated for fuel ethanol production. This research project aims to gain better understanding of cellulases-lignin interaction, one of the rate-limiting factors in the saccharification of lignocellulosic biomass. Furthermore, modification of lignin is also aimed at the target of reduced interaction and better lignin separation. The interaction of cellulases and lignin will be studied by isolating lignin-rich residue from several biomass feedstocks pretreated at different levels. Various esterases and laccase treatment will be used for modification of lignin.

### **Introduction**

The prolonged use of fossil-based resources, mostly for fuels and chemicals, has been thought to create pollution, climate change and economic instability due to limited reserves and uneven geographical distribution [1]. Therefore numerous efforts have been directed to use renewable plant biomass as the new source of fuels and an array of chemical products, performing equivalent function as oil refinery, thus termed biorefinery. In light of answering the energy demand, several large scale demonstration and/or commercial ethanol plants utilizing agricultural waste have begun their operation in Europe and America [2].

Currently established advanced ethanol plants are mostly using biotechnological approach. Initially the biomass is pretreated mechanically and then thermo-chemically, with water steam-based treatment being predominant method used. Subsequently, the pretreated biomass is enzymatically hydrolyzed using commercial enzyme preparation to produce platform sugars. In this case, cellulases are the main components of the enzyme cocktail which degrade cellulose, producing glucose. These sugars are then fermented by microorganisms to produce for example ethanol. In this current setup, which is used for example in Denmark at the Inbicon demonstration plant, lignin-rich residue is produced. The residue is burnt to power up most of, if not the entire plant operations [3].

The occurrence of lignin in the lignocellulosic biomass, which makes it the second most abundant

organic polymer after cellulose, presents both opportunities and difficulties. On one side lignin can be used as a source of valuable aromatic chemicals and polymers such as vanillin, methanol, phenols, benzenes, toluenes, resins and adhesives [4]. However this potential is overlooked when lignin is burnt for energy. This is of importance since many of the newly established second generation biorefineries have been focusing mostly on fuel ethanol production [2]. On the other hand, lignin is also considered a barrier for efficient enzymatic hydrolysis of cellulose. This is due to the fact that lignin blocks the access of cellulose to cellulases and also promotes non-productive adsorption of cellulases [5].

### **Specific objectives**

The research project aims to gain further understanding in cellulases-lignin interaction which has been thought to be dictated by hydrophobic effect [6]. Afterwards, the lignin is targeted for modification in order to both reduce the interaction between cellulases and lignin as well as to enable better separation of lignin for use as source of valuable products. The detailed specific aims are as follow:

1. To understand the effect of botanical origin and pretreatment severity towards the surface properties of lignin
2. To understand the effect of removing residual carbohydrates in the lignin-carbohydrate

- complexes (LCCs) and laccase treatment towards the surface properties of lignin
3. To design and evaluate an overall biorefinery process using the previous findings to improve hydrolysis yield and lignin separation

#### **Outline of the research methods and goals**

Several biomass feedstocks that will be used for the study are corn stover, *Miscanthus* and wheat straw. Each biomass feedstock was hydrothermally pretreated at three different severity levels: 3.65 (190°C, 10 min), 3.83 (190°C, 15 min) and 3.97 (195°C, 15 min), thus yielding nine materials in total. In order to study the interaction of lignin with cellulases, the lignin has to be isolated in order to exclude other potentially affecting factors (e.g. carbohydrates which will also adsorb cellulases). Isolation of lignin-rich residue is performed by extensively hydrolyzing the pretreated biomass feedstocks using commercial cellulase preparation for 72 hours. The resulting residue is then treated with commercial protease preparation to remove the adsorbed enzymes that still remain in the substrate. CHN-S analysis will be performed in order to confirm protein removal through the reduction of the nitrogen content. Additionally composition analysis is performed for the pretreated biomass feedstocks and the isolated lignin-rich materials. The latter are then studied for surface properties.

The surface properties to be studied include surface hydrophobicity, surface charge and the adsorption of cellulases. The latter will be studied using two methods. Firstly, classical adsorption experiments to establish adsorption isotherms will be performed by measuring the concentration of free protein in the supernatant. Secondly, a more sensitive and on-line method of measuring adsorption will be used. This method is relying on measuring adsorption into thin film using a Quartz Crystal Microbalance with Dissipation Monitoring (QCM-D). These surface properties will be studied again after the isolated lignin-rich materials have been treated with esterases to remove residual carbohydrate in the form of LCCs and laccase to potentially modify the structure of the lignin.

Eventually, an entire process is envisioned where additional enzymes will be included in the initial hydrolysis of pretreated biomass. It is expected that the addition of esterase(s) will aid in the removal of carbohydrate residues that play role to the structural integrity of the biomass, allowing further separation between lignin and the carbohydrates. Addition of laccase is expected to further enhance hydrolysis yield by lowering the interaction between cellulases and lignin. In the end, an increase in hydrolysis yield and better separation of lignin is expected.

#### **Acknowledgements**

This work is supported by the Bio-Value Strategic Platform for Innovation and Research, co-funded by The Danish Council for Strategic Research and The

Danish Council for Technology and Innovation, Grant Case no.: 0603-00522B.

#### **References**

1. C. N. Hamelinck, G. van Hooijdonk, A. P. C. Faaij, *Biomass Bioenerg.* 28 (2005) 384-410.
2. R. Janssen, A. F. Turhollow, D. Rutz, R. Mergner, *Biofuels, Bioprod. Bioref.* 7 (2013) 647-665.
3. J. Larsen, M. Ø. Haven, L. Thirup, Inbicon makes lignocellulosic ethanol a commercial reality. *Biomass Bioenerg.* 46 (2012) 36-45.
4. J. Zakzeski, P. C. Bruijninx, A. L. Jongerijs, B. M. Weckhuysen, *Chem. Rev.* 110 (6) (2010) 3552-3599.
5. J. L. Rahikainen, R. Martin-Sampedro, H. Heikkinen, S. Rovio, K. Marjamaa, T. Tamminen, O. J. Rojas, K. Kruus, *Bioresour. Technol.* 133 (2013) 270-278.
6. D. W. Sammond, J. M. Yarbrough, E. Mansfield, Y. J. Bomble, S. E. Hobdey, S. R. Decker, L. E. Taylor, M. G. Resch, J. J. Bozell, M. E. Himmel, T. B. Vinzant, M. F. Crowley, *J Biol Chem.* 289 (30) (2014) 20960-20969.



## Jakob Dragsbæk Duhn

Phone: +45 22476700  
 E-mail: jadu@kt.dtu.dk  
 Discipline: Catalysis

Supervisors: Anker Degn Jensen  
 Stig Wedel  
 Christian Wix, Haldor Topsøe A/S

### Industrial PhD Study

Started: December 2013  
 To be completed: Marts 2017

## Development of highly efficient solid oxide electrolyzer cell systems

### Abstract

With the increasing amounts of renewable and fluctuating energy in the Danish energy system, efficient and high capacity storage solutions are necessary. A solution could be Solid Oxide Electrolyzer Cells (SOEC) systems capable of utilizing electrical energy to transform H<sub>2</sub>O and/or CO<sub>2</sub> to gas and liquid fuels. However, during operation solid carbon might be formed. If this happens, the cells will delaminate leading to a hard failure of the system. It is therefore of great importance to be able to predict the limits for carbon formation.

### Introduction

Solid oxide electrolyzer cells (SOEC) are electrochemical systems capable of converting H<sub>2</sub>O and CO<sub>2</sub> (H<sub>2</sub>O → H<sub>2</sub>+1/2 O<sub>2</sub>, CO<sub>2</sub> → CO+1/2 O<sub>2</sub>), see Figure 1. H<sub>2</sub>O and CO<sub>2</sub> can also be converted simultaneously to a syngas mixture which can be used eg to make fuels such as methanol and synthetic natural gas. The electrolysis of CO<sub>2</sub> and H<sub>2</sub>O is therefore interesting as a means to reduce the demand for fossil fuels.

Carbon formed from the Boudouard reaction (CO → CO<sub>2</sub> + C (s)) or the Heterogenous water-gas shift reaction (CO+H<sub>2</sub> → H<sub>2</sub>O + C(s)) can cause delamination of the electrode-electrolyte interface [1]. Thermodynamically the formation of C(s) is prohibited up to large CO/CO<sub>2</sub> ratios. However, in the literature carbon formation has been observed at ratios below the critical values and concentration and temperature gradients within the cell material (electrodes and electrolyte) is being suspected of being the reason [1,2].

### Specific Objectives

This PhD study focusing on investigating at which operating conditions carbon formation is taking place; if the carbon formation can be avoided and if not, whether the formed carbon can be removed without damaging the solid oxide electrolyzer cells.

In this contribution, the effect of gas diffusion limitations, as an explanation for the observed carbon formation in the literature, will be discussed.

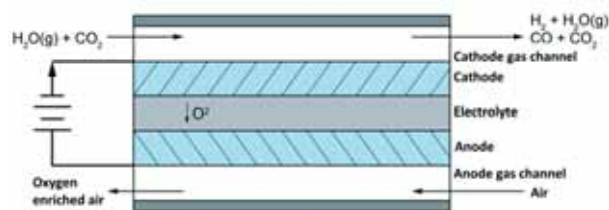


**Figure 1.** Schematic overview of an SOEC. H<sub>2</sub>O and/or CO<sub>2</sub> are entering the cathode gas channel and diffuse to the reaction zone located at the interface between the cathode and the electrolyte, where the gas is reduced. Formed H<sub>2</sub> and CO diffuses out of the cathode to the cathode gas channel and flows out of the system. The reverse water-gas shift reaction and methanation reaction take place in the cathode.

### Results and Discussion

Gas diffusion in solid oxide cells can be modelled by the dusty gas model. In order to investigate the diffusion limitations, a 2d model was created in COMSOL. The dusty gas model (DGM) is currently not implemented in COMSOL. However, it has been shown that Fick's law can be modified to simulate the DGM for different geometries and operating conditions with good accuracy [3,4]:

$$N_i = -D_i^{corr} \nabla c_i - \frac{c_i k_i \nabla P}{\mu} \quad (1)$$

$$D_{k,i}^{corr} = \frac{1}{D_{k,i}^{eff}} + \left( \sum_{j \neq i} \frac{x_j}{D_{ij}^{eff}} \right) \cdot \left( 1 + \frac{x_i \sqrt{M_i}}{\sum_{i \neq j} x_j \sqrt{M_j}} \right) \quad (2)$$

$$k_i = k + \frac{\mu}{P} D_i^{corr} \quad (3)$$

Where  $c$  is the concentration of  $i$ ,  $P$  is the pressure,  $\mu$  is the viscosity,  $D_k^{eff}$  is the effective Knudsen diffusion coefficient of  $i$ ,  $D_{ij}^{eff}$  is the effective binary diffusion coefficient between  $i$  and  $j$ ,  $x$  and  $M$  are the mole fraction and molar mass of  $i$ , respectively.

$D_k^{eff}$  and  $D_{ij}^{eff}$  is estimated as described in [5]. The electrolysis reaction and water-gas shift reaction is included in the model using kinetics from [6]. It is assumed that the temperature is constant through the electrode and that the methanation reaction is thermodynamically limited.

The simulations showed that in  $\text{CO}_2$ -electrolysis the concentration of  $\text{CO}$  increases significantly through the cathode (Figure 2) and, that there are situations where there is affinity for carbon at the reaction interface, but not at the channel ( $T_{\text{cell}} < T_B$ ). This result explains the observed carbon formation in [2].

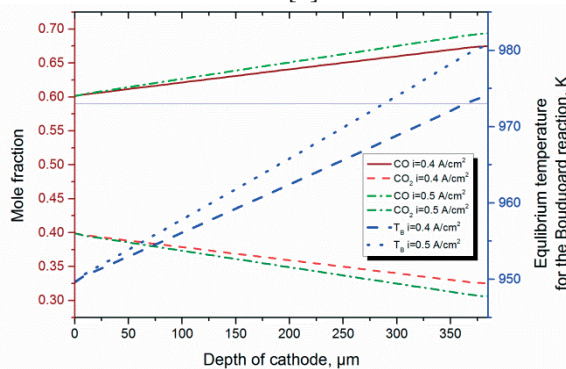


**Figure 2.** Concentration profiles of  $\text{CO}$  and  $\text{CO}_2$  through the cathode from the gas channel (left) to the cathode-electrolyte interface (right) with a current density of 0.4 (red) and 0.5 (green), respectively. The equilibrium temperature ( $T_B$ ) based on the reaction quotient is also shown (blue) for the two cases. When  $T_B$  is above the operating temperature of the cell (here 973 K), carbon will be formed. Simulation parameters:  $\epsilon = 0.3$ ,  $\tau = 3$ ,  $T_{\text{cell}} = 973$  K, Cathode depth = 385  $\mu\text{m}$  and a conversion of 60 %, corresponding to the operation parameters in [2].

In co-electrolysis diffusion limitations are also present (Figure 3). Here the high concentration of  $\text{CO}$  and  $\text{H}_2$  and low concentration of  $\text{H}_2\text{O}$  (close to zero), cause carbon to be formed via the Heterogenous water-gas shift reaction ( $T_{\text{HWGS}} > T_{\text{cell}}$ ). This result explains the observed carbon formation in [1].

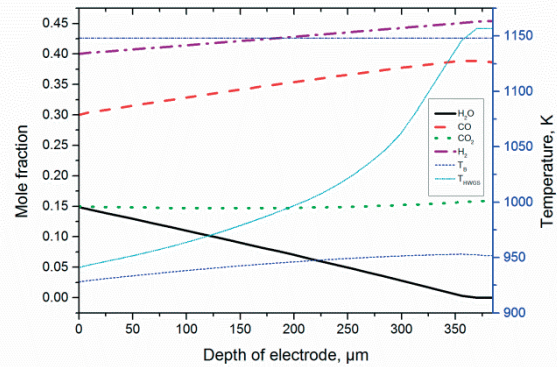


**Figure 3.** Concentration profile through the cathode from the gas channel (left) to the cathode-electrolyte interface (right). Modelling parameters:  $\epsilon = 0.3$ ,  $\tau = 3$ ,  $T_{\text{cell}} = 1148$  K, Cathode depth = 385  $\mu\text{m}$ , current density = 2.25  $\text{A}/\text{cm}^2$  and a conversion of 67 %, corresponding to the operation parameters in [1].

### Conclusions

The simulations have shown that diffusion limitation can explain the observed carbon formation in the literature. It is clear that the limitations cannot be ignored and must be included when selecting appropriate operating conditions, or designing new cells.

### Acknowledgements,

This project is a collaboration between the CHEC group at DTU Chemical Engineering and Haldor Topsoe A/S and is partially funded by the Danish Industrial Ph.D. Fellowship Programme administered by Innovation Fund Denmark.

### References

1. Y. Tao et al., J. Elec. Chem. Soc. 161 (2014) F337-F343
2. Skafta et al., ECS Trans. 68 (2015) 3429-3427
3. Kong et al., J. Power Sources 2006 (2012) 172-178
4. D.F Cheddie, Proceedings 2013 COMSOL conference, available on [https://www.comsol.com/paper/download/180879/cheddie\\_paper.pdf](https://www.comsol.com/paper/download/180879/cheddie_paper.pdf), accessed November 17, 2015
5. M. Ni, Int. J. Power Sources 202 (2012) 209-216
6. M. Ni, Int. J. Hydrogen Energy 37 (2012) 6389-6399

### List of Publications

J.D. Duhn, A.J. Degn. S. Wedel. C.F.F. Pedersen, Dansk Kemi 96 (10) (2015) 16-19.



## Francesco Cristino Falco

Phone: +45 4525 2992  
E-mail: [frac@kt.dtu.dk](mailto:frac@kt.dtu.dk)

Supervisors: Krist V. Gernaey  
Anna Eliasson Lantz

### PhD Study

Started: October 2014  
To be completed: September 2017

## Characterization of microbial consortia for keratin degradation processes

### Abstract

Especially in the last decade, the number of biofuels and biobased chemicals which can be obtained through microbial fermentation technologies has continuously increased. Nevertheless, a major step towards the sustainable and cost-effective production of such new biocommodities will certainly be the possibility to employ, to a larger extent, cheaper and widely available renewable feedstocks such as residual biomass and organic waste materials. This PhD project is part of a larger multi-partner research project, namely “Keratin2Protein”, where the potential of novel process technologies will be investigated in order to efficiently convert organic agro-industrial residual biomass into new alternative added-value products. Specifically, tailor-made microbial consortia, which can be cultivated in an industrial process for keratin degradation, will be employed to valorize slaughterhouse keratin-rich by-products for production of protein-enriched feed. In particular, the PhD project will focus, on the one hand, on the development and optimization of fermentation protocols to cultivate microbial consortia for efficient keratin biodegradation and, on the other hand, on the implementation of mathematical, deterministic, models describing microbial interactions within these synthetic ecological webs.

### Introduction

A large part of the research efforts for the production of fuels and chemicals from renewable resources have focused on the identification and engineering of single microbial cell factories in order to utilize complex substrate mixtures. Nevertheless, microbial species living in a large variety of naturally occurring environments have, after billions of years, evolved towards the formation of highly efficient consortia in which they perform multiple tasks in a synergistic manner. In particular, at the community level, this cooperation gives rise to higher-order properties such as improved stability, optimized use of the available nutritional and energetic resources, enhanced substrate degradation rates etc. Within this context, microbial communities can be defined as complex adaptive systems [1] which dynamically adjust their structure and function in response to external stimuli – that is to changes in the environmental conditions.

One of the major challenges in developing models capable to predict the structural and dynamic behavior of a microbial consortium is the complex relationship describing the inter-specific interactions that are established both in between community members and with respect to their local environment and the resulting

physiological phenotypes expressed by each individual species.

This PhD project will focus on the development of mechanistic models which will be used as simulation platforms to obtain a more clear insight into the interplay between different consortia members. In particular, these models will be employed to design and optimize synthetic microbial consortia for the efficient degradation of keratin-rich residual biomass.

### Methodology

Kinetic characterization of each possible consortium member will be performed at bench-top fermenter scale, and optimal conditions for efficient cultivation of these keratinolytic microorganisms will be determined. In particular, by means of pure culture experiments, the effect of keratin-rich substrates, medium composition and environmental conditions (i.e., temperature, pH, dissolved oxygen, agitation speed, etc.) on microbial growth and keratin degradation kinetics will be studied. In order to optimize both medium composition and cultivation parameters using a reduced number of experiments, statistical methods such as Plackett-Burman design and response surface methodology (RSM), or more specifically Box-Behnken design, will be employed [2].

Experimental information obtained in the fermenter for each keratinolytic strain tested will be employed to formulate and implement, in the MATLAB-Simulink programming environment, mathematical models capable to describe the effect of keratin-rich substrates, culture medium composition and selected environmental conditions on microbial growth and keratin degradation kinetics. In order to represent the biochemical transformations occurring in keratin-rich residual biomass degradation through some simplified process descriptions, mechanistic models, inspired by those typically used to represent microbial wastewater treatment processes [3], will be developed. Thereafter, kinetic models of pure cultures developed for optimal growth conditions will be adapted to suboptimal, common growth, conditions for co-cultures of interest.

To gain a better understanding about the interactions between different consortia members, the range of application of the deterministic models previously developed will be extended to the case of mixed microbial cultures. Subsequently it will be possible to apply these models in simulating keratin substrate degradation for a variety of consortia constellations in order to verify their potential as simplified tailor-made consortia that could be easily cultivated in a bioreactor. In more detail, the effect of medium formulation and environmental conditions on the behavior of the mixed population will be simulated, providing guidelines for further process design and optimization.

Cultivations in bioreactors of simplified consortia consisting of predicted optimal combinations of selected pure cultures will be established. Experimental information and model predictions will be used to evaluate dynamics between consortia members and the stability of the consortia itself. For some of the best performing co-cultures a more detailed quantitative characterization, involving enzyme profiling, analyses of substrates and microbial biomass will be performed in combination with omics profiles. Data from cultivation experiments will then iteratively be used for model validation and to improve model predictions. Finally the mathematical model will be used to support the design of the best reactor configuration: in particular a *Cell Recycle Membrane Fermenter (CRMF)* will be developed. With such a cultivation system the suspension containing nutrients, cells and products will be continuously filtered, and microbial mass, non-hydrolyzed keratin particles and keratinolytic enzymes will be repeatedly returned to the cultivation vessel while low-molecular weight products (that is, peptides and free amino-acids) will be constantly removed.

### Importance of the Mechanistic Model

In Figure 1 all the main steps involved in defining a quantitative description of a fermentation process are summarized. In particular, deterministic models used to describe fermentation processes involving microbial communities should be able to:

- describe, in a quantitative manner, fluxes through pathways for nutrient resources and energy,

- identify and quantify the effect of interactions of consortium members with each other and with the surrounding environment on the overall community performance,
- infer on the system's higher-order properties.

Therefore, during each phase of the PhD study, the model structure will be continuously and iteratively updated. First of all, the structured model will be fitted to experimental data collected during both pure and mixed culture experiments; if the model structure will not permit an accurate description of the data after parameter estimation, the model structure will need to be updated, and parameter estimation will be repeated. Model analysis tools, such as uncertainty and sensitivity analyses, will also be used to direct experimental efforts. In particular, ranking of parameters via sensitivity analysis will allow to direct experimental efforts only towards the most significant parameters [4].

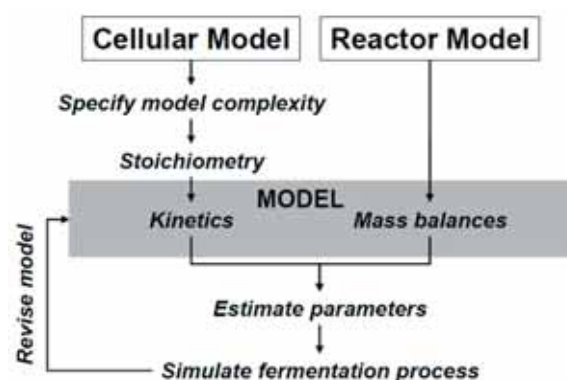


**Figure 1:** Main steps involved in the quantitative description of a fermentation process [5].

### Acknowledgments

The research project has received founding from the Danish Council for Strategic Research (Innovation Fund Denmark) (project Keratin2Protein: Novel approach to protein recovery from unutilized slaughterhouses waste through microbial conversion). The article represents only the author's view and Innovation Fund Denmark is not liable for any use of the information presented here.

### References

- H.-S. Song, W.R. Cannon, A.S. Beliaev, A. Konopka, *Process* 2 (4) (2014) 711-752.
- D.J. Daroit, A. Brandelli, *Crit. Rev. Biotechnol.* 34 (4) (2014) 372-384.
- H. Hauduc, L. Rieger, A. Oehmen, M.C.V. Loosdrecht, Y. Comeau, A. Héduit, P.A. Vanrolleghem, S. Gillot, *Biotechnol. Bioeng.* 110 (1) (2013) 24-46.
- K.V. Gernaey, A.E. Lantz, P. Tufvesson, J.M. Woodley, G. Sin, *Trends Biotechnol.* 28 (7) (2010) 346-354.
- C. Ratledge, B. Kristiansen, *Basic Biotechnology*, 3<sup>rd</sup> Ed., Cambridge University Press, New York, USA, 2006, p. 156.

**Hannah Feldman**

Phone: +45 4525 2811  
E-mail: hafe@kt.dtu.dk

Supervisors: Krist V. Gernaey  
Xavier Flores-Alsina  
Gürkan Sin  
Ulf Jeppsson (Lund University)  
Kasper Kjellberg (Novozymes A/S)

**PhD Study**

Started: April 2015  
To be completed: March 2018

## Model-based optimization of an industrial wastewater treatment plant combining a full-scale granular sludge reactor and autotrophic nitrogen removal

**Abstract**

This PhD project consists of two parts. In the first part, the IWA Anaerobic Digestion Model No. 1 (ADM1) is calibrated to the full-scale granular sludge reactor of Novozymes A/S in Kalundborg, Denmark, in order to use the model to investigate future optimization of the biogas production. In the second part, the applicability of Autotrophic Nitrogen Removal is studied, as a means to remove the nitrogen from the outflow of the anaerobic reactor.

**Introduction**

Biogas production is one of the methods to convert waste into energy, as biogas can be converted into electricity. The production is performed in an anaerobic reactor, where carbon rich wastewater enters the reactor, and micro-organisms degrade the organic carbon to hydrogen, carbon dioxide and methane (biogas). However, these types of reactors do not remove any nitrogen, which cannot remain in the wastewater if it is to return to the environment. The most common nitrogen removal process is via activated sludge reactors, where nitrification and denitrification take place in order to convert ammonium ( $\text{NH}_4^+$ ) to subsequently nitrite ( $\text{NO}_2^-$ ), nitrate ( $\text{NO}_3^-$ ), and nitrogen gas ( $\text{N}_2$ ) (Figure 1). This requires a high energy and oxygen consumption. Furthermore, organic carbon is needed for this process. Another possibility is to remove the nitrogen via autotrophic nitrogen removal, where partial nitrification and anaerobic ammonium oxidizers (anammox) convert the ammonium to nitrite and nitrogen gas (Figure 1). The anammox organisms consume inorganic carbon, and use nitrite as electron acceptor, to convert ammonium directly to nitrogen gas. This requires less energy, oxygen and organic carbon. The possible application of autotrophic nitrogen removal at industrial scale will mean that more organic carbon can be redirected to biogas production, and fewer costs will be associated with nitrogen removal. Two models will be used in this study; i) the Anaerobic Digestion Model No. 1 (ADM1) [1]; and, ii) The

Complete Autotrophic Nitrogen Removal (CANR) Model [2].

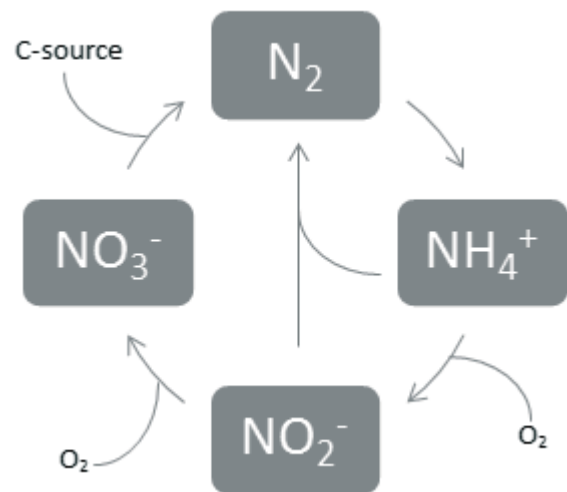


**Figure 1:** Schematic overview of the nitrogen cycle, where the reaction from  $\text{NH}_4^+$  to  $\text{NO}_2^-$  represents nitritation, the reaction from  $\text{NO}_2^-$  to  $\text{NO}_3^-$  represents nitratation and the reaction from  $\text{NO}_3^-$  to  $\text{N}_2$  represents denitrification. The anammox reaction is represented by the two interconnecting arrows from  $\text{NH}_4^+$  and  $\text{NO}_2^-$  to  $\text{N}_2$ .

### Specific objectives

The objective of this study is to develop a plant-wide wastewater treatment model of an industrial treatment facility (Novozymes A/S, Kalundborg, Denmark), combining a full-scale granular sludge (biogas) reactor and autotrophic nitrogen removal. This involves the following steps:

- 1) Calibration of the ADM1, which includes extensions to the full-scale granular sludge reactor. This step involves a sensitivity analysis, to find the parameters which need to be calibrated to the system, as well as an influent characterization.
- 2) Process optimization. Various scenarios will be tested to study the influence of specific operating variables on the biogas production.
- 3) Study the applicability of the Autotrophic Nitrogen removal through modelling and experimental work. To connect the ADM1 with the CANR model, a suitable interface will need to be developed.

### Modelling approach

As mentioned, two models will be used in this study. The first one, the Anaerobic Digestion Model No. 1 (ADM1) [1] is supplemented with several extensions, namely phosphorus [3], sulfur [4], and multiple mineral precipitation [5, 6]. The phosphorus extension describes the transformation of phosphorus into polyhydroxyalkanoates (PHA) by phosphate accumulating organisms (POA). The sulfur extension describes sulfate reduction through sulfate reducing bacteria. These bacteria compete with the bacteria that produce biogas. Furthermore, hydrogen sulfide (H<sub>2</sub>S) is produced, which inhibits bacteria at high concentrations [5]. Lastly, multiple mineral precipitation is important, as this process on the one hand can extract important minerals for growth from the water, and on the other hand can work as a means to remove high concentrations of ions, such as phosphorus.

The second model, the Complete Autotrophic Nitrogen Removal (CANR) model, has previously been published by Vangsgaard *et al.* (2012) [2]. It describes the removal of nitrogen from wastewater through partial nitrification and anammox, which take place in granules. The model contains both bulk liquid equations as well as biofilm equations.

The CANR model will be calibrated with experimental data from the lab, in which wastewater from the effluent of the full-scale granular sludge reactor will be used as influent. Model validation will then be done at pilot scale, on the site of Novozymes A/S.

### Conclusions

The goal of this project is to increase the biogas production from an industrial full-scale granular sludge reactor. In order to achieve this, the reactor will be modelled, and optimization strategies will be studied. Furthermore, the potential application of an autotrophic nitrogen removal reactor is researched, which can

further increase the sustainability of the wastewater treatment plant.

### Acknowledgements

The author would like to thank the Technical University of Denmark and Novozymes A/S for the financing of this PhD study.

### References

1. Batstone, D.J., Keller, J., Angelidaki, I., Kalyuzhnyi, S.V., Pavlostathis, S.G., Rozzi, A., Sanders, W.T., Siegrist, H. and Vavilin, V.A. (2002). *Water Science and Technology*, **45**(10) 65-73.
2. Vangsgaard, A. K., Mutlu, A. G., Gernaey, K. V., Smets, B. F., & Sin, G. (2013). Calibration and validation of a model describing complete autotrophic nitrogen removal in a granular SBR system. *Journal of Chemical Technology and Biotechnology*, **88**(11), 2007-2015.
3. Henze, M., Gujer, W., Mino, T., Matsuo, T., Wentzel, M. C., vR Marais, G., & Van Loosdrecht, M. C. (1999). Activated sludge model no. 2d, ASM2d. *Water Science and Technology*, **39**(1), 165-182.
4. Fedorovich, V., Lens, P., & Kalyuzhnyi, S. (2003). Extension of Anaerobic Digestion Model No. 1 with processes of sulfate reduction. *Applied biochemistry and biotechnology*, **109**(1-3), 33-45.
5. Flores-Alsina, X., Mbamba, C. K., Solon, K., Vrecko, D., Tait, S., Batstone, D. J., Jeppsson, U. & Gernaey, K. V. (2015). A plant-wide aqueous phase chemistry module describing pH variations and ion speciation/pairing in wastewater treatment process models. *Water research*, **85**, 255-265.
6. Mbamba, C. K., Tait, S., Flores-Alsina, X., & Batstone, D. J. (2015). A systematic study of multiple minerals precipitation modelling in wastewater treatment. *Water Research*, **85**, 359-370.



## Ana Carolina Fernandes

Phone: +45 4525 2958  
E-mail: ancafe@kt.dtu.dk  
Discipline: Biochemical engineering

Supervisors: Associate Professor Ulrich Krühne  
Professor Krist Gernaey  
Project Manager Adama Marie Sesay

PhD Study  
Started: July 2014  
To be completed: June 2017

## Micro scale reactor system development with integrated advanced sensor technology

### Abstract

Process development and optimization is a costly and time-consuming process involving the optimization of relevant process parameters tested at different process scales. Differences between phenomena across scales (e.g. mixing) often result in attaining less than optimum process parameters which may lead to a selection of suboptimal strains and/or process conditions, thus affecting process productivity. These differences are usually not detected due to insufficient process control at smaller scales [1],[2].

The main goal of this research project is to develop a commercially viable and interesting microbioreactor design, capable of performing multiple simultaneous biocatalytic reactions and/or fermentations in a highly controlled and automated manner. Different types of sensors (Optical, Electrochemical (EC), Near-Infra Red (NIR)) will be considered and evaluated in terms of applicability and design integration. The development of such new integrated device, with simultaneous monitoring, quantification and control of metabolites, besides physical parameters, will allow to decrease considerably the bioprocess development costs and time.

### Introduction

Bioprocess optimization and development requires the study of relevant process parameters, their influence and interaction, in a reliable and scalable way. This is, often due to a high number of variables, very expensive and time-consuming [1]. High-throughput (HTP) technology, in the form of parallelized controlled reactions, allows reducing the cost and duration of industrial bioprocess development and scale-up. This is achieved by enabling the simultaneous study of several process parameters, such as temperature, pH, oxygen transfer, mixing, culture mode, media composition, type of cell or strain, available vectors, among others [3],[4].

Microbioreactors (MBR) offer the potential to find a balance between process control and cultivation throughput in order to turn HTP cultivation economically and practically feasible [3]. Some recent commercial approaches integrate already sensors in cultivation chambers (e.g. Biolector system from m2p labs [4]; SensorDishes® from PreSens; ambr™ from TAP Biosystems [1]), with fluid handling equipment for automatic small volume sampling or inocula or medium addition. However, most of so far developed MBR systems lack online sensors for the most significant parameters (such as pH, O<sub>2</sub>, cell viability, product

concentration and quality, glucose, antibody, reaction metabolites, etc.) [6].

This PhD project, performed within the European Network for Innovative Microbioreactor Applications in Bioprocess Development (EUROMBR) project, aims to develop a HTP MBR setup with integrated sensors for relevant reaction constituents and physical parameters. Three types of sensors will be considered and evaluated in terms of applicability and design integration: Optical NIR luminescent polymer patches [7], amperometric electrochemical sensors [8] and miniaturization of a conventional NIR setup for MBR integration. Further, a new design for a MBR setup will be developed starting from an existing platform configuration with the intention to integrate the sensors in an easily operable, reliable and scalable way.

### Specific Objectives

1. Literature review of relevant metabolites in bioprocesses currently not monitored.
2. Development and optimization of sensors for desired application.
3. Design of a MBR setup for integration of chosen sensors. Pump assisted addition and sampling of fluids will be included, as well as, control of temperature, pH, mixing/DO and feeding.

4. Determination of the sensor's detection limits and sensitivity in the MBR setup for all chosen process applications.

5. Final validation (proof-of-concept) of the complete MBR setup and comparison with results from benchtop setup for all process applications.

## Results and Discussion

A microfluidic channel (received from iX-factory, Dortmund, Germany) was chosen as first approach since it simplifies the sensor integration for reaction monitoring and control. Near-Infrared (NIR) emitting indicator-based polymeric oxygen sensors (developed at TU Graz, Austria), were integrated in the microfluidic channel. A valve chip (from Microfluidic ChipShop, Jena, Germany) was coupled to the microfluidic channel to test further the sensors dynamic response. They have been applied for on-line monitoring of the glucose oxidase and catalase reactions (serving as a proof-of-principle).

NIR oxygen sensors present a fast response to changes in oxygen concentration (< 10s). This response was used to monitor a glucose solution pulse (introduced with the valve system) in the microfluidic channel. The obtained signal was similar to the one obtained for the same reaction parameters but static condition. With these sensors it was observed that inside the microfluidic platform, as expected, oxygen partial pressure decreases with increasing substrate (glucose) concentration and increasing reaction time. Also, using the relation between one of the sensors and the output residence time, as presented in Figure 1 (b), a correlation between oxygen concentration predicted from sensors' signal and HPLC measurements was found (Figure 1(a)). These sensors thus possess the ability to monitor more than one parameter simultaneously, as long as the reaction kinetics are known.

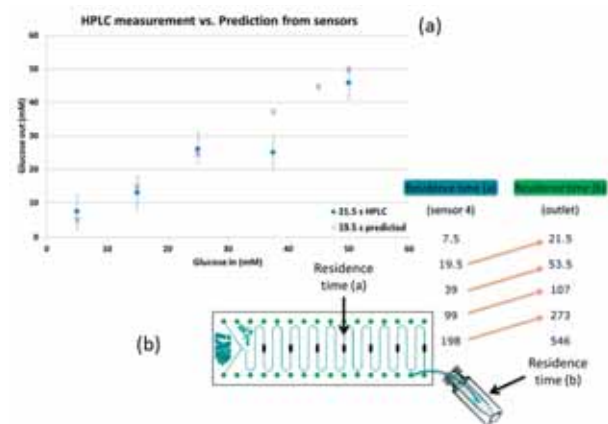


**Figure 1** - Comparison of sensor output and HPLC glucose measurement of reaction samples (a) Schematics of sampling and residence time comparison for correlation between oxygen sensors' output and HPLC glucose measurements (b).

Glucose and Pyruvate amperometric disposable sensors are under development in collaboration with

Oulu University, Finland. A microfluidic platform (Figure 2) for these sensors' integration has also been developed and the first test performed successfully. This platform will be connected to the previously used microfluidic platform in a modular form.

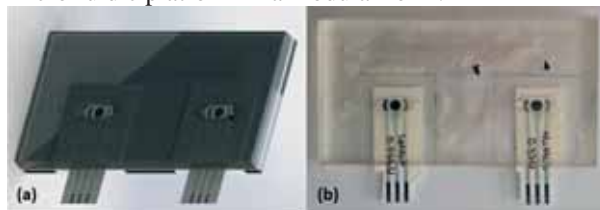


**Figure 2** – SolidWorks 3D design of microfluidic platform (a) and fabricated microfluidic platform with integrated electrochemical sensors.

## Conclusions

A microfluidic platform for biocatalytic reaction screening was used to characterize and monitor a glucose oxidation reaction using integrated oxygen sensors. Another microfluidic platform was developed for disposable electrochemical sensor integration. Both platforms can be coupled using a modular approach to each other, as well as, to micro-valve systems and other microfluidic channels.

## Acknowledgements

The research leading to these results has received funding from the People Programme (Marie Curie Actions) of the European Union's Seventh Framework Programme FP7/2007-2013/ under REA grant agreement n° 608104 (EUROMBR). The article reviews only the authors' views and European Union is not liable for any use of the information presented here.

## References

1. Rameez S, Mostafa SS, Miller C, Shukla AA.. *American Institute of Chemical Engineers* 30 (2014) 718-727.
2. Funke M, Buchenauer A, Schnakenberg U, *et al. Biotechnology and Bioengineering* 107(3) (2010) 497-505.
3. Long Q, Liua X, Yanga Y, *et al. Journal of Biotechnology* (2014).
4. Rohe P, Venkanna D, Kleine B, Freudl R, Oldiges M. *Microbial Cell Factories* 11(114) (2012).
5. Huber R, Roth S, Rahmen N, Büchs J. *BMC Biotechnology* 11(22) (2011).
6. Schäpper D, Alam, Muhd Nazrul Hisham Zainal, Szita N, Lantz AE, Gernaey KV. *Anal Bioanal Chem.* 39 (2009) 679-695.
7. Ungerböck B, Charwat V, Ertl P, Mayr T. *Lab on a Chip* 13(8) (2013) 1593-1601.
8. Arvinte A., Sesay A. M. Virtanen V., Bala C. *Electroanalysis* 20 (2008) 2355-2362.



**Diana Carolina Figueroa Murcia**

Phone: +45 4525 2978  
E-mail: difm@kt.dtu.dk

Supervisors: Kaj Thomsen  
Philip Loldrup Fosbøl

PhD Study  
Started: December 2013  
To be completed: December 2016

## Experimental determination of the solubility of exotic scales at high temperatures – zinc sulfide

### Abstract

“Exotic” scale materials, such as Zinc Sulfide (ZnS), Lead Sulfide (PbS) and Iron Sulfide (FeS), come as a new challenge in HP/HT reservoirs. This has led to the development of more advanced tools to predict their behavior at extreme conditions. Solubility data for ZnS are scarce in the open literature. In order to improve the available data, we study the experimental behavior of ZnS solubility at high temperatures (up to 100°C). The aqueous solution is analyzed using Inductively Coupled Optical Emission Spectrometry (ICP-OES) as analytical technique. The aim of this work is to develop a method for measuring the solubility of sulfides and measure the solubility at high temperatures. The experimental data are intended to be used for parameter estimation in the Extended UNIQUAC model.

### Introduction

The increasing need for fossil fuels has accelerated the process in search for new oil reservoirs. New explorations are focused now in reservoirs that are at deeper locations and at more extreme conditions (i.e. temperature and pressure) than the conventional ones. With these new characteristics the developing of new technologies is on the rise as the new reservoirs are characterized by high pressures and high temperatures. These reservoirs represent a challenge in terms of safety, drilling equipment, durability of materials and operating conditions, among others (Ahmad et al. 2014; Daniels et al. 2014).

Among those challenges the deposition of minerals is one of the most difficult to address. Scaling is mainly caused by changes in pressure and in temperature during the production of oil. Changes in pressure and temperature alter the equilibrium conditions of the formation water that contains different ions. When the equilibrium is altered this will cause the minerals to precipitate.

Initially the risk of calcium carbonate (CaCO<sub>3</sub>) and sodium chloride (NaCl) deposition was identified in HP/HT reservoirs, but later after years of production in the Elgin/Franklin field another type of obstruction was identified as zinc sulfide (ZnS) and lead sulfide (PbS) (Orski et al. 2006). These types of scaling materials have been also identified in wells in the Gulf of Mexico and in the North Sea fields and Norwegian sector (Berry et al. 2011; Orski et al. 2006)

### Methodology

The determination of the solubility of ZnS is carried out at temperatures up to 100°C. The set-up is shown in Figure 1. Zinc sulfide in powder form of purity 99.99% (from Sigma-Aldrich) and 10 μm as particle size. The sample is prepared at reduced oxygen concentration in a sealed box which is flushed with nitrogen (purity 99,999%) until reaching a value of 0% in an oxygen detector. The solid is equilibrated adding ultra-pure water (resistivity ~18.2 MΩ), degassed with nitrogen (purity 99,999%) until reaching a dissolved oxygen value less than 0.01 mg/L.

For runs above 40°C, a layer of silicon oil is added to the solution in order to avoid vapor formation of the solution. The solution is placed in a 30 mL polypropylene vial and stirred continuously using a magnetic stirring bar. The vial is immersed in a glass flask filled with glycerin and connected to a thermostatic bath until equilibrium is attained.

The suspension is filtered at the same process temperature and diluted immediately with ultra-pure water. The samples are acidified adding 1% of nitric acid (65%) for analysis using Inducted Coupled Plasma (ICP) as analytical technique.

### Results and analysis

The solubility data are presented in Table 1. The error presented in Table 1 corresponds to the error estimated of the equipment determined using a standard solution of zinc. The results of the equilibration time for ZnS are

presented as molality of the zinc ion ( $Zn^{2+}$ ) and total sulfur in Figure 2. The equilibration time reported in literature differs between authors.

hours and 410 hours (in which a “plateau” is observed). It can be said that the equilibration time for  $ZnS$  at  $70^{\circ}C$  is above 216 hours and the value of the solubility is  $2.8 \times 10^{-5}$  mol of  $Zn^{2+}/kg$  water (molality).

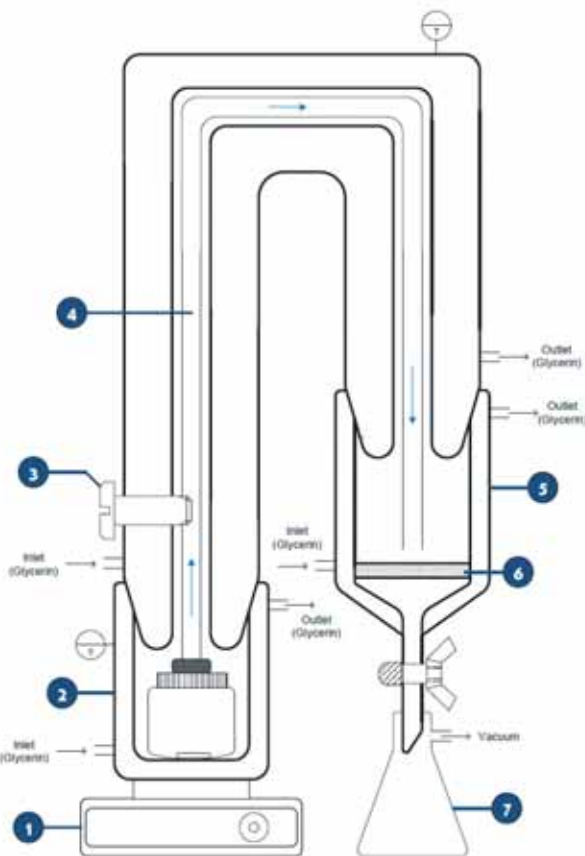


**Figure 1** Experimental set-up for measurements of solubility at temperatures up to  $100^{\circ}C$ . Stirring plate (1), equilibrium cell (2), screw (3), sampling hose (4), filter chamber (5), porous body (6), side-arm flask (7).

**Table 1** Solubility data of zinc ion ( $Zn^{2+}$ )

Time (h)	Runs	Points	Average (m)	SD	Error
46	2	4	1,0E-05	2E-07	-2,7%
96	2	3	1,0E-05	1E-07	-8,7%
143	2	4	1,7E-05	7E-06	-5,4%
166	2	4	7,1E-05	2E-05	-9,2%
192	2	4	2,0E-05	2E-06	-9,4%
216	2	4	2,6E-05	5E-06	-9,4%
238	2	4	4,1E-05	6E-06	-6,3%

According to Barret and Anderson (1982; 1988) the equilibrium is reached in less than 4 days. What we have observed in our experiment is different. The runs have been extended up to 407 hours (17 days) since changes in the concentration are observed at short times. No significant differences for the solubility of  $ZnS$  are observed at  $40^{\circ}C$  and  $70^{\circ}C$ . The equilibrium time is calculated based on the smallest value of the standard deviation obtained between runs at times between 216

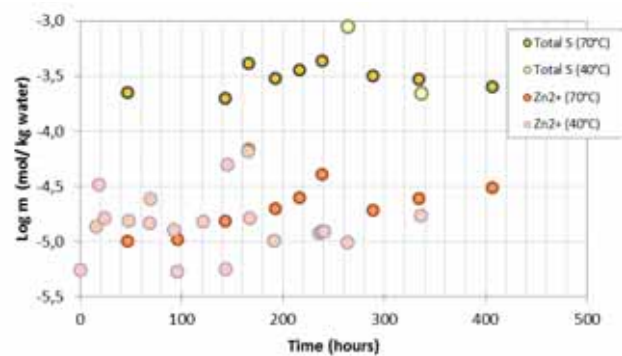


**Figure 2** Solubility of  $ZnS$  at  $70^{\circ}C$

### Conclusions

The results shown for the determination of the solubility of zinc sulfide using the set-up explained in this manuscript and using the ICP-OES as analytical technique to measure the concentration of zinc in aqueous solution have shown a promising combination to determine the solubility of sulfides or sparingly soluble salts. The error estimated for the experimental data varies from 3 to 10%. The standard deviation calculated for each run shows a very good precision of the methodology implemented.

### References

- Ahmad I, Akimov O, Bond P, Cairns P, Gregg T, Heimes T, Russell G, Wiese F. 2014. Drilling operations in HP/HT environment. Offshore Technology Conference. .
- Barrett T and Anderson G. 1988. The solubility of sphalerite and galena in 1–5 m NaCl solutions to 300 C. *Geochim Cosmochim Acta* 52(4):813-20.
- Barrett TJ and Anderson GM. 1982. The solubility of sphalerite and galena in NaCl brines. *Economic Geology and the Bulletin of the Society of Economic Geologists* 77(8):1923-33.
- Berry SL, Boles JL, Singh AK, Hashim I. 2011. Enhancing production by removing zinc sulfide scale from an offshore well: A case history. Society of Petroleum Engineers.
- Daniels JK, Littlehales IJ, Lau L, Linares-Samaniego S. 2014. Laboratory methods for scale inhibitor selection for HP/HT fields. Society of Petroleum Engineers.
- Orski K, Grimbert B, Menezes CA, Quin E. 2006. Fighting lead and zinc sulphide scales on a north sea HP/HT field. Society of Petroleum Engineers.



## Rebecca Frauzem

Phone: +45 4525 6173  
E-mail: rebfra@kt.dtu.dk  
Discipline: Process and Plant Design

Supervisors: Rafiqul Gani, DTU  
John M. Woodley, DTU

### PhD Study

Started: October 2014  
To be completed: September 2017

## Sustainable process design with process intensification

### Abstract

Increased need for sustainable practices has resulted in a push for research and development in emission reduction. This is particularly prevalent for carbon dioxide emissions. In order to help address this concern, a methodology has been developed to design sustainable carbon dioxide utilization processes with carbon capture. The methodology follows a three-stage approach: process synthesis, process design, and innovative and sustainable design. Within these stages, a detailed methodology that focuses on the first stage, process synthesis, is necessary. Here, the details of the methodology for the first stage, from problem formulation to solution, are described in detail. Then, the application of the entire three-stage methodology is illustrated for a small case study.

### Introduction

Growing concerns about the state of the environment are spurring efforts to develop sustainable practices, especially to address global warming. Global warming is attributed to the increasing amount of greenhouse gases in the atmosphere and carbon dioxide (CO<sub>2</sub>) is the largest constituent of these gases (IPCC 2007). Therefore, a large amount of research is focused on developing long-term CO<sub>2</sub> emission reduction techniques. Carbon capture and storage (CCS) and utilization by conversion are the primary methods being discussed and investigated. Carbon dioxide utilization is a unique opportunity for sustainable emission reduction as it takes the emissions, creates products for further use, and generates revenues. However, there is a need to evaluate developed technologies systematically in terms of CO<sub>2</sub> reduction and economic potentials.

As part of these efforts in CO<sub>2</sub> utilization, this paper presents an adopted methodology (Babi et al. 2015), containing three stages: process synthesis, process design, and innovative and sustainable design. This methodology implements process synthesis methods and tools to generate a network of CO<sub>2</sub> conversion pathways, which are analysed to determine the more sustainable alternatives. The sustainable solution is not just a CO<sub>2</sub> reducing process, but also a non-trade-off solution with respect to various performance criteria, including economic and other sustainability indicators.

### Methodology

The adopted methodology of Babi et al. (2015) involves three stages: process synthesis, process design, and innovative and sustainable design. This is illustrated in Figure 1. In addition, each of the sub-steps within the methodology incorporates methods and tools.

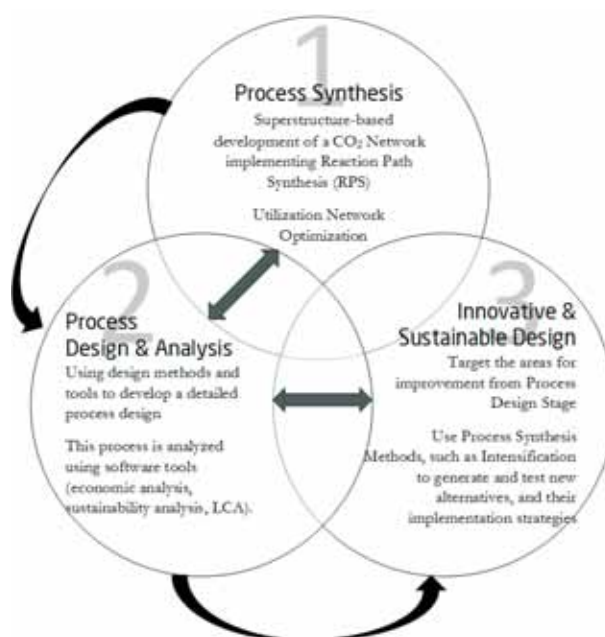


**Figure 1.** Illustration of the adopted methodology for sustainable synthesis-design of CO<sub>2</sub> utilization processes.

A systematic approach to the sustainable process synthesis problem has been developed to approach the first stage. In this methodology, a superstructure-based approach (Quaglia et al. 2015) is used to develop a network of CO<sub>2</sub> utilization processes. This task is performed using a series of steps: problem formulation, superstructure development and superstructure optimization. The problem formulation involves setting the objective function, raw materials and products, and any other additional elements of the problem. For CO<sub>2</sub> utilization via chemical conversion, it is first necessary to determine all the possible reactions for the problem formulated. For this, a network is developed using a reaction path synthesis method and software tool (Cignitti 2014). Then, a database created using a specific ontology is searched to obtain all the data for the network so that it can be formulated as a superstructure. For any data not available in the database, a literature search must be performed and the data added. From this formed network and the data from the database, the superstructure is generated, which enables the linkage of the raw material (CO<sub>2</sub>) and products via processing paths. Carbon capture can be included as a pre-processing step for the conversion process taking the raw material to the necessary composition for the reaction step. Finally, the superstructure is optimised using a mathematical model (Quaglia et al. 2015). The result of this stage is the generated processing path or a set of processing paths.

The processing path or set of processing paths that result from Stage 1 are then designed in detail, producing a detailed design of the process corresponding to the selected processing path (Stage 2: Process Design). In addition, the targets for the next stage (Stage 3: Innovative and more Sustainable Design) are set. These targets are set through analysis of the process in terms of economic and environmental factors, including net CO<sub>2</sub> emission. Where these factors indicate a poor performance, improvement targets are set. In the final stage, process alternatives that match the areas (targets) for improvement are identified. From this stage, the possibility for determining innovative and more sustainable process designs exist, because by definition, if the targets for improvement are met, the resulting process design alternatives also become more sustainable. In addition, how the new process design may be realised in an industrial setting is investigated here in terms of implementation strategies.

### Results and Discussion

The developed methodology has been applied to an illustrative case study. The objective is to highlight the application of the methodology including the necessary methods and tools. In addition, this case study shows the sustainability and innovative possibilities for CO<sub>2</sub> utilization.

First, a network is developed targeting smaller carbon, hydrogen and oxygen containing compounds. Using the reaction path synthesis tool, a network of over 50 reactions is generated. Then, data is required. For this, an ontology-based database has been developed. The necessary data is then retrieved so that the network is defined by a mathematical model. Using mathematical programming, this can be optimised. For a small superstructure for the production of dimethyl carbonate this has been performed. Additionally, logic-based screening has been used to narrow the list of alternatives for the case of methanol synthesis. Rather than perform mathematical optimization, this small list of alternatives is taken directly to Stage 2 for detailed design.

For the case of methanol synthesis, there are two promising processing paths from Stage 1: combined reforming of methane to syngas followed by methanol synthesis and direct hydrogenation to methanol. These two are taken to detailed design where analysis shows that these are competitive with existing methanol facilities and are able to reduce the CO<sub>2</sub> emissions. Then, innovative implementation strategies are described for each process: either replacement of existing methanol plant processes or new units to offset emissions with a product that can also produce revenue.

### Conclusions

While there is a need for further development of the network and database of utilization processes, there is great promise, as illustrated by the case studies, in CO<sub>2</sub> utilization. The methodology developed enables the systematic design of sustainable and innovative CO<sub>2</sub> utilization processes, inclusive of carbon capture. It has been applied to illustrative case studies, including for methanol synthesis and dimethyl carbonate production.

### References

1. IPCC, 2007. *Climate Change 2007: Mitigation of Climate Change* B. Metz et al., eds., New York: Cambridge University Press.
2. Babi, D.K. et al., 2015. Sustainable process synthesis-intensification. *Computers & Chemical Engineering*, 81, pp.218–244.
3. Cignitti, S., 2014. *Computer-Aided Reaction Path Synthesis*, Technical University of Denmark.
4. Quaglia, A. et al., 2015. Systematic network synthesis and design: Problem formulation, superstructure generation, data management and solution. *Computers & Chemical Engineering*, 72, pp.68–86. A

### List of Publications

1. R. Frauzem, P. Kongpanna, K. Roh, J. H. Lee, V. Pavarajarn, S. Assabumrungrat, R. Gani. Sustainable Process design: Sustainable Process Networks for Carbon Dioxide Conversion, in: F. You (Ed.), *Sustainability of Products, Processes and Supply Chains*, Elsevier Ltd., New York, 2015.



## Jerome Frutiger

Phone: +45 4525 2911  
E-mail: jfru@kt.dtu.dk  
Discipline:

Supervisors: Gürkan Sin  
Jens Abildskov

PhD Study  
Started: Jun 2014  
To be completed: May 2017

## Computer-aided molecular design and property prediction models for working fluids of thermodynamic cycles

### Abstract

The aim of the PhD project is the development of novel working fluids for thermodynamic cycles such as organic Rankine cycles. Through the use of Computer-aided molecular design (CAMD) novel candidates for both pure components and mixtures will be generated and evaluated. In this scope the development of new property prediction models is an important fundamental tool for the design.

### Introduction

The efficient use of heat sources is crucial in terms of resource efficiency and decreasing environmental impact of industrial application. Power cycles such as organic Rankine cycles (ORC) allow the conversion of heat into electric energy. The basic technology relies on thermodynamic cycles which consist of a compressor, an expansion valve and two heat exchangers (evaporator and condenser) (see Figure 1) [1].

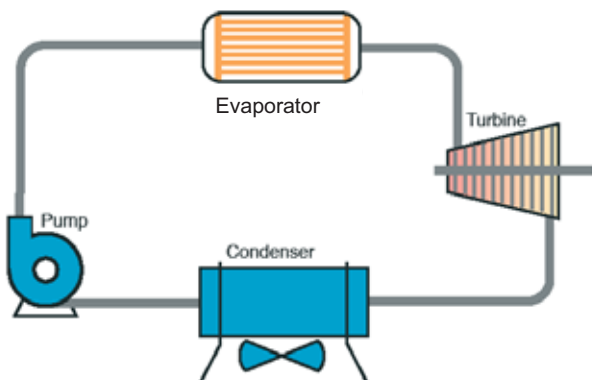


**Figure 1:** Scheme of an organic ranking cycle (ORC).

Currently this technology is known to be well established for high-temperature heat sources. However, in recent years there is a large availability of low-temperature heat sources in different applications such as waste heat from marine diesel engines, industries and refrigeration plants as well as renewable energy sources such as biomass combustion, geothermal and solar heat sources. So far the low-temperature heat cannot be

utilized efficiently for heat pump operation. This means, a large amount of moderate temperature heat is simply wasted [2].

In order to optimize industrial heat pump processes for adding and removing heat from the cycle, the influence of the working fluid, the cycle designs and the operating conditions can be vital.

The objective of this project is to develop new working fluids by the use of multi-criteria database search and Computer Aided Molecular Design (CAMD) principles [3] and is carried out in collaboration with DTU Mechanical Engineering.

In order to be able to design novel working fluids it is necessary to identify and develop property prediction models for estimating pure component as well as mixtures properties. Furthermore it is necessary to integrate the optimization of the working fluid and the cycle design, because the two key features influence each other strongly.

### Framework

The framework for the development of novel working fluids [4] looks as follows (see Figure 2).

1. Identification of needs of working fluids: The general requirements and desired behavior of a working fluid have to be identified and formulated in collaboration with DTU Mechanical Engineering.
2. Translation of needs into target properties: The target properties are specified from the needs. Examples of target properties are thermodynamic properties such as thermal conductivity or heat capacity, kinetic properties

such as viscosity and density, but also safety properties such as the lower flammability limit and environmental properties such as the ozone depletion potential.

- 2a) Development of pure component and mixture property models: Most of the specific properties have to be estimated and therefore novel property prediction models have to be developed.
- 2b) Database for experimentally measured properties: The estimated and experimental properties have to be stored for the use for specific thermodynamic cycle application
3. Generation candidates as working fluids: A CAMD algorithm is developed in order to generate new molecular candidates as well as mixtures as process fluids candidates. The optimization is subject to feasibility criteria and target application constraints.
4. Evaluation of candidates: The set of generated working fluids for a specific application is evaluated using a variety of assessment criteria such as heat transfer ability, safety and environmental constraints such as ozone depletion potential (ODP) and Global Warming Potential (QWP), chemical stability as well as efficiency and compatibility with compressor lubricants and equipment materials.

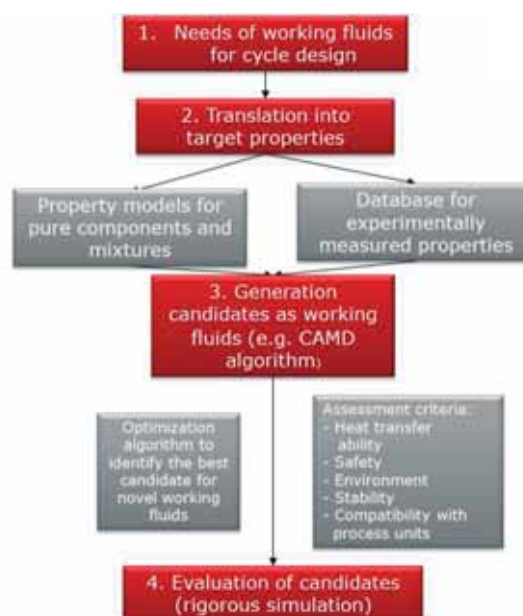


Figure 2: Framework of the project.

### Current and future work

We are developing a framework for group contribution property prediction models including algorithms, methodology development and uncertainty analysis. We are applying the model for the estimation of the upper and lower flammability limit of chemicals, which is important information to quantify the risk of working fluids for fire and explosion.

### References

1. C. M. Invernizzi, Closed Power Cycles, Springer-Verlag, London, UK, 2013.
2. H. Chen, D. Y. Goswami, E. K. Stefanakos, Renewable and Sustainable Energy Reviews, 14, (2010) 3059.
3. P. M. Harper, R. Gani, P. Kolar, T. Ishikawa, 1999. Fluid Phase Equilibria, 99, (1999) 158–160.
4. N. A. Yunus, K. G. Gernaey, J. M. Woodley, R. Gani, Computers and Chemical Engineering, 66, (2014), 201-213.



**Rasmus Østergaard Gadsbøll**

Phone: +45 6066 8815  
E-mail: [rgad@kt.dtu.dk](mailto:rgad@kt.dtu.dk)

Supervisors: Ulrik Birk Henriksen, CHEC, DTU  
Jesper Ahrenfeldt, CHEC, DTU  
Lasse Røngaard Clausen, MEK, DTU  
Jens Dall Bentzen, Dall Energy

PhD Study  
Started: December 2014  
To be completed: March 2018

## Investigation of oxygen-blown biomass gasification

### Abstract

This projects aim is to investigate oxygen-blown thermal biomass gasification and project larger scale gasifier plants using the concept of the Viking gasifier at DTU. Tests with oxygen-blown gasification will be carried out at Risø campus on a modified Viking gasifier, where efforts especially related to process optimization and gas analysis will be made. Tests with the gasifier coupled to a SOFC and a gas engine will be carried out as well. Studies will be carried out to investigate upscaling the Viking gasifier to 10-50 MW<sub>th</sub>, by analyzing different reactor designs, flow configurations, tar reducing measures, while still obtaining very high gas quality.

### Introduction

This project is a part of the Biomass Gasification Polygeneration (BGP) project under ForskVE. The projects aim is to design and optimize a flexible biomass gasification system, that in batch-operation can either: produce power through a solid oxide fuel cell (SOFC) when demand is high or consume power through at solid oxide electrolysis cell (SOEC) to produce Bio-SNG (synthetic natural gas) when the demand is low. Figure 1 displays the conceptual plant. While power production via biomass gasification and a SOFC stack has been done recently, conversion of biomass, oxygen and hydrogen into Bio-SNG is a very limited research subject.

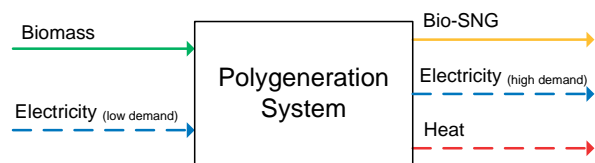


**Figure 1:** Flexible biomass gasification polygeneration concept. At high power demand, electricity is produced by a SOFC. At low demand, electricity is consumed in a SOEC to produce Bio-SNG.

This project is an applied research project that will research oxygen-blown biomass gasification, both experimentally and theoretically. The project will modify, test and operate the 75 kW<sub>th</sub> Viking gasifier located at Risø campus with an oxygen-steam mixture

(rather than its usual air-blown configuration) and investigate large-scale versions of the system at 10-50 MW<sub>th</sub>.

The Viking gasifier processes wood chips into high quality gas at high temperatures that can be utilized in combustion applications, engine operation, chemical synthesis etc. – see flow diagram of the gasifier in Figure 2. The gasifier is characterized by high efficiency and very good gas quality. The *product* gas consists mostly of CO, H<sub>2</sub>, CO<sub>2</sub> and N<sub>2</sub> and has a 5.6 MJ/Nm<sup>3</sup> lower heating value [1]. The gasifier uses partial combustion to convert the solid biomass to product gas, by injecting air into the reactor – producing a high-volume nitrogen containing gas (33 vol %).

It is desired to examine the potential for using the product gas in chemical synthesis and therefore the nitrogen content is unwanted, due to costly separation processes.

The Viking gasifier is constructed with a pyrolysis unit that features an externally heated conveyer screw and a fixed bed reactor for oxidation and char gasification. These reactors are however not easily scaled and new designs are needed to project larger plants of the gasifier.

Through extensive experimental work, this project will modify, operate and optimize oxygen-blown gasification on the Viking gasifier in order to investigate the potential for producing a nitrogen free product gas suited for chemical synthesis.

The reactors for pyrolysis and char gasification are not suited for significant upscaling, due to limited heat

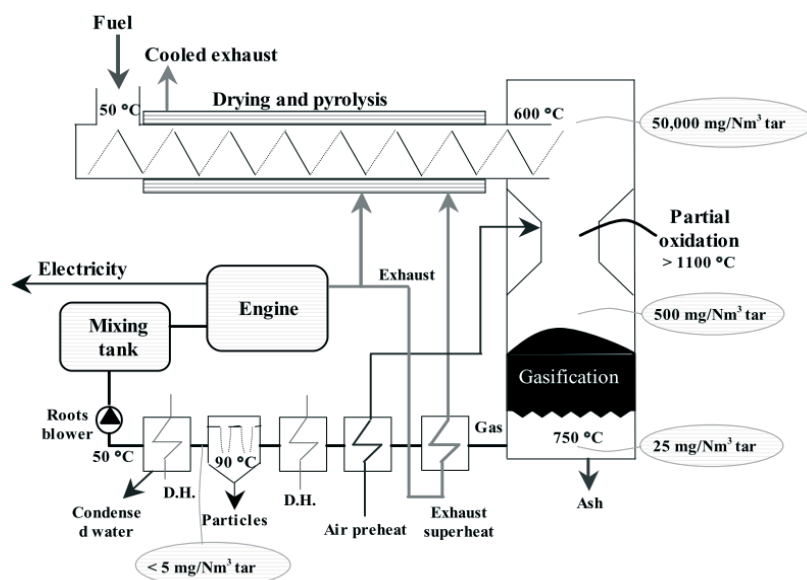


**Figure 2:** Flow diagram of the Viking gasifier

transfer capabilities among other aspects. The plant concept does however need to be upscaled if commercial operation shall be reached with chemical synthesis. Because of this, various versions of the concept will be investigated by analyzing reactors, flow configuration and tar reducing measures. Fluid bed, partial oxidation and fixed bed technologies will be assessed as an extension of a previous project [2].

### Experimental work

The project will investigate practical aspects of an oxygen-blown Viking plant (installation and operation). Oxygen is a troublesome chemical, as it is very corrosive and reactive and must be handled accordingly. Oxygen-steam mixtures are injected into the system at different ratios and performance is mapped. It is unknown to what extent the oxygen-injection will affect the tar and particle (e.g. soot) content of the product gas and therefore measurements and tests are made. Tar and particle levels are very important for downstream applications and advanced chemical tests are needed to clarify the mechanisms. Experimental efforts will be made to map the gas composition under different operational conditions.

The project will also operate a 0.8kW<sub>e</sub> SOFC stack on the product gas and take the necessary precautions to ensure sufficient gas quality into the sensitive cell. Very high electric efficiencies are expected [3]. The work will continue previous experimental work, that has shown promising results for coupling biomass gasification and SOFC. Tests with the product gas and a gas engine will be carried out as well, testing performance and emissions.

### Theoretical work

The project includes theoretical projections of upscaled versions of the oxygen-blown gasifier in medium and large scales in order to assess the plants scaling and fuel

potential. The aim is to maintain the very high gas quality, while getting the benefit of upscaling the system from e.g. fluid beds and achieving temperature control suited for various high-ash fuels (e.g. straw, wastes) to avoid ash sintering. Several reactor designs (e.g. moving bed, fluidized bed, fixed bed) will be investigated and analyzed in order to design a larger system and investigate fuel flexibility. Several design considerations have to be carried out for each sub-process including drying, pyrolysis, partial oxidation and gasification.

### Acknowledgements

This project is co-funded by ForskVE (project no. 12205) and is carried out in collaboration with DTU MEK, Dall Energy and Dansk Gasteknisk Center (DGC).

### References

1. B. Gøbel *et al.* Status - 200 Hours of Operation with The Viking Gasifier. 2003.
2. L. Andersen *et al.* Modeling the low-tar BIG gasification concept 2002.
3. C. Bang-Moeller. Design and Optimization of an Integrated Biomass Gasification and solid oxide fuel cell system. 2010.

**Jozsef Gaspar**

Phone: +45 4525 2876  
E-mail: joca@kt.dtu.dk  
Discipline: DTU Kemiteknik

Supervisors: Philip Loldrup Fosbøl  
Kaj Thomsen, Nicolas von Solms  
John Bagterp Jørgensen

**PhD Study**

Started: December, 2013  
To be completed: April, 2016

## Dynamic simulation and analysis of CO<sub>2</sub> post-combustion capture using piperazine and MEA

**Abstract**

Climate change as a result of anthropogenic activities is a key concern of our society. One of the main causes is the accelerated build-up of energy-related CO<sub>2</sub>. Immediate and large mitigation of CO<sub>2</sub> can be achieved by integrating CO<sub>2</sub> capture with fossil fuel fired power plants. CO<sub>2</sub> post-combustion capture is the most mature process which can be retrofitted to existing power plants. Although, several steady-state experimental and simulation studies proved its technology readiness, it has been recognized that dynamic studies are required to understand the dynamics of the capture process, to identify process bottlenecks and to assure continuous operation of power plants with integrated CO<sub>2</sub> capture in a dynamic energy market. In this work, we provide insight into the dynamics of the CO<sub>2</sub> capture process using PZ and MEA. We show how the system responds to disturbances in the flue gas flow rate, flue gas composition, and lean CO<sub>2</sub> loading. This analysis forms the basis for the design of the control structure.

**Introduction**

Although great efforts have been placed for the rapid growth and development of the renewable energy market, thermal power plants still represent the world's main energy supply and, especially in developing countries, they will dominate the market in the coming decades. Fossil-fuelled power plants produce almost one third of the global CO<sub>2</sub> emissions [1]; thus, CO<sub>2</sub> capture would greatly reduce the impact of power plants on the climate.

Post-combustion capture is one of the leading technologies in CO<sub>2</sub> capture. It is a mature concept, ready to be implemented on a large scale. However, plant-wide dynamic studies are needed to further demonstrate the feasibility and flexibility of thermal power plants with integrated CO<sub>2</sub> capture. Power plants need to handle fluctuations resulting from various sources, such as peak in energy demands, change in green energy production, raw material heterogeneity, malfunctioning of equipment, etc. As a consequence, CO<sub>2</sub> capture units need to accommodate large load changes or eventual shutdowns to become attractive. Recent efforts in the CO<sub>2</sub> capture field have focused on dynamic model development and flexibility evaluation of different operational scenarios [2-5]. The majority of these studies have used monoethanolamine (MEA) as solvent. Only a few studies present dynamic models using other solvents. Gaspar and Cormos presented an absorber model for MEA, DEA, AMP and MDEA [5].

They demonstrate that kinetics play a key role in the dynamic behaviour of the capture process. Thus, it is important to develop and validate dynamic models for innovative solvents.

The purpose of this paper is to explore the dynamic behaviour of an absorber using 30 wt% PZ and to compare the dynamics to the 30 wt% MEA for step changes in the flue gas flow rate, flue gas composition, and lean CO<sub>2</sub> loading. The dynamic CAPCO<sub>2</sub> (dCAPCO<sub>2</sub>) in-house DTU model was employed to describe the behaviour of the absorber. The present analysis provides a first insight into the dynamics of the absorber using the innovative PZ solvent.

**Validation of the absorber model**

We compare the model predictions to experimental measurements for CO<sub>2</sub> absorption against campaigns "Fall 2008" carried out at the J. J. Pickle Research Center, north of Austin, TX, USA [6].

Fig. 1 shows the good agreement between the model and pilot results using 4, 7 and 8 molal PZ. The deviations are less than 10%, within the accuracy of the measurements.

There is only one point visibly outside of the  $\pm 10\%$  range which is most probably an outlier. The flue gas inlet temperature for this point was  $-5^{\circ}\text{C}$ , which represents the lower limit of the experimental temperature range.

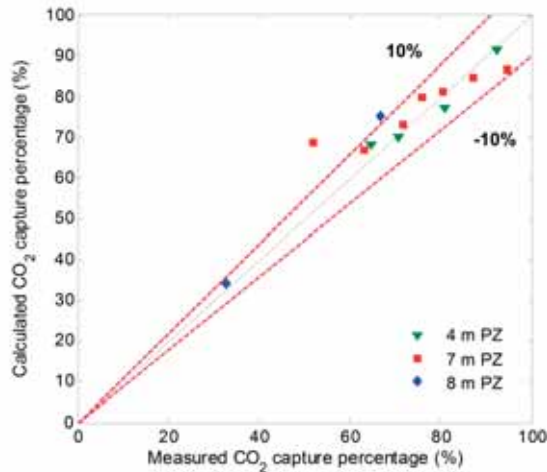


Fig. 1. Calculated versus measured CO<sub>2</sub> capture

### Dynamic simulation and analysis

This section shows the dynamic behaviour of the absorber for three scenarios:  $\pm 10\%$  step change in the flue gas CO<sub>2</sub> concentration (case 1),  $\pm 10\%$  step change in the lean CO<sub>2</sub> loading (case 2) and  $\pm 10\%$  step change in the flue gas flow rate (case 3). These steps are applied to the base case after 10 min of steady-state operation. Here, we show the results for both solvents: PZ and MEA.

In practice, case 1 resembles operational conditions when the output of the power plant changes due to the heterogeneity of the fuel. This case is common, especially for biomass co-fired power plants. Case 2 resembles a scenario when a disturbance occurs in the operation of the stripper, e.g. steam supply shortage. Case 3 corresponds to part load operation of the power plant and represents one of the most common scenarios observed during flexible operation. Case 1 and case 2 result in changes of the CO<sub>2</sub> concentration gradient between the gas phase and the liquid phase. This gradient represents the driving force for absorption. Case 3 results in varying contact time inside the column, which changes the L/G ratio between the gas and the liquid phases.

Fig. 2 shows the dynamic performance of the absorber for each case study using MEA and PZ. This figure illustrates how an increase of the flue gas CO<sub>2</sub> content, lean CO<sub>2</sub> loading, or the flue gas flow rate results in a reduction of the CO<sub>2</sub> capture efficiency and vice-versa (case 1 to 3). Furthermore, it highlights that the effect of a step change is greater using PZ compared to MEA. A 10% decrease of the shown variables results in a CO<sub>2</sub> capture percentage of approximately 92% and 96% for MEA and PZ, respectively. For a 10% increase, the CO<sub>2</sub> capture percentage reduces to 86% and 83% for MEA and PZ, respectively.

Fig. 2 also indicates that, for all the cases, the MEA system reaches steady-state faster than PZ. The CO<sub>2</sub> capture percentage stabilizes in about 10-15 minutes

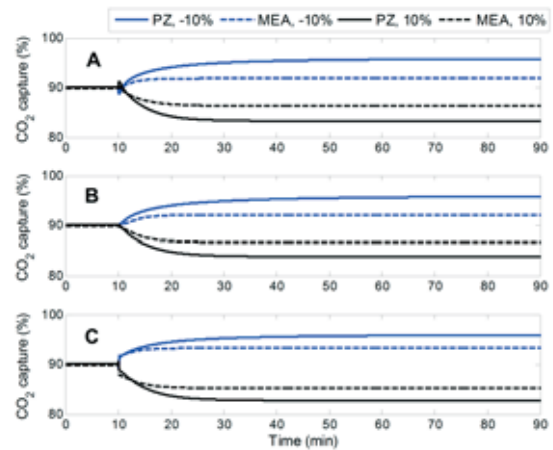


Fig. 2. CO<sub>2</sub> capture percentage versus time using MEA and PZ for (A) case 1, (B) case 2 and (C) case 3

using MEA and using PZ stabilizes in roughly 40 min for a 10% step increase and in about 1 hour for a -10% step change. This is contrary to expected since PZ has a faster kinetics than MEA.

This analysis reveals that piperazine responds slower to disturbances than MEA and the inlet parameters have a significant effect on the PZ process. Accordingly, feedback controllers with high gains and short time-integrals may be required in the case of PZ to maintain the dynamic operation of the absorber column within reasonable short closed-loop settling times in the presence of these disturbances.

### Conclusions

We have demonstrated that step changes in the flue gas and the lean flow rate have a significant impact on the absorber. The settling time is approximately 2–3 times slower in case of PZ compared to MEA. This behavior is related to the coupling between temperature and mass transfer rate.

### References

1. Pachauri RK, Reisinger A, on CC. Climate change 2007. Synthesis report. Contribution of Working Groups I, II and III to the fourth assessment report. IPCC, 2008.
2. Gaspar J, Jorgensen JB, Fosbol PL. Control of a post-combustion CO<sub>2</sub> capture plant during process start-up and load variations. IFAC-PapersOnLine 2015;48:580-5.
3. Nittaya T, Douglas PL, Croiset E, Ricardez-Sandoval LA. Dynamic modelling and control of MEA absorption processes for CO<sub>2</sub> capture from power plants. Fuel 2014;116:672-91.
4. Hossein Sahraei M, Ricardez-Sandoval LA. Controllability and optimal scheduling of a CO<sub>2</sub> capture plant using model predictive control. International Journal of Greenhouse Gas Control 2014;30:58-71.
5. Gaspar J, Cormos A. Dynamic modeling and absorption capacity assessment of CO<sub>2</sub> capture process. International Journal of Greenhouse Gas Control 2012;8:45-55.
6. Plaza JM, Rochelle GT. Modeling pilot plant results for CO<sub>2</sub> capture by aqueous piperazine. 10th International Conference on Greenhouse Gas Control Technologies 2011;4:1593-600.

**Soheila Ghafarnejad Parto**

Phone: +45 4525 2842  
E-mail: Sohg@kt.dtu.dk  
Discipline: Catalysis and Reaction Engineering

Supervisors: Anker Degn Jensen  
Jakob Munkholt Christensen  
Lars Saaby Pedersen, Haldor Tøpsoe

**PhD Study**

Started: November 2014  
To be completed: November 2017

## Catalytic hydro-liquefaction of lignin to value-added chemicals

**Abstract**

Solvolytical depolymerization of lignin followed by catalytic deoxygenation of the depolymerized compounds is a possible method for conversion of lignin to higher value products. In this project, catalytic conversion of lignins in solvents such as ethanol and ethylene glycol using heterogeneous catalysts is investigated and the yields and types of the products are determined.

**Introduction**

The growth of the global population and depletion of the fossil-based fuels, besides the environmental effects of the greenhouse gasses, drives interest towards sustainable and carbon-neutral resources for chemicals and energy supply. Lignin is the most abundant natural aromatic compound on Earth [1]. The annual production of technical lignin is around 50 million tones [2], though only 2 % is devoted for the commercial applications and the rest is burned as a low value material for the energy supply of the pulp and paper mills. Unclearly defined and highly cross-linked structure and high oxygen content are the major obstacles for exploitation of lignin as source of value-added chemical and fuels. Solvolytical depolymerization is one of the main approaches to break-down lignin and liquefy it to 'bio-oil'. The solvolytical conversion can be promoted by addition of a heterogeneous catalyst. Organic solvents such as ethanol and ethylene glycol are good candidates for liquefaction of lignin [3, 4].

**Specific Objectives**

Catalytic conversion of lignin to higher value products is the main objective of this project. Though this is exploratory research in terms of the target compounds, lower molecular weight and low oxygen content in products is the aim. The very first step for production of high-value chemicals from lignin is its liquefaction. The liquefied lignin will be further upgraded in the presence of hydrodeoxygenation (HDO) catalysts to lower oxygen containing compounds. Currently, sulfonated lignin or lignosulfonate is being investigated in this research. The lignosulfonate is provided by Borregaard, the Norwegian biorefinery company. Borregaard is

interested in expanding its product portfolio by introducing other products from lignosulfonate.

**Experimental**

Liquefaction of lignin is currently conducted using a 300 ml 4560 Parr reactor with temperature and pressure limit of 350 °C and 200 barg. Non-catalytic conversion of lignosulfonate in water, ethanol and water/ethanol mixtures as solvent at 200-340 °C and in 3 h reaction time in nitrogen atmosphere has been conducted. Moreover, catalytic conversion of lignin in ethanol and ethylene glycol over home-synthesized 5 wt% Ni/SiO<sub>2</sub> and 5 wt% Ni/AC catalysts in temperature range of 200-250 °C for 3 h and under 50 bar H<sub>2</sub> pressure is currently being investigated. The products of conversion of lignosulfonate in ethanol are obtained by evaporation of the light liquid products of the reaction and separation of ethanol, while the products of the conversion in ethylene glycol are separated by solvent extraction using cyclohexane.

**Results and Discussion**

Based on the preliminary results, non-catalytic experiments in water led to dissolution of lignosulfonate without any bond breakage; whereas with ethanolysis of lignin, bio-oil with maximal yield of 21.95 wt% was achieved at 340 °C. An increase in the oil yield is observed upon addition of catalyst as can be seen in Table 1: By addition of Ni/AC catalyst, with catalyst:lignin ratio of 0.1, the oil yield increases from 6.9 wt% to 21.1 wt% at 200 °C. Further increase of the temperature to 250 °C enhances the oil yield to 37 wt%. The non-liquefied lignin is converted to solid char.

**Table 1:** Results of the conversion of lignosulfonate in ethanol. Lignin: solvent ratio of 0.1 g/ml.

Exp No.	Catalyst	Temperature [°C]	Oil yield wt%	Char wt%
1	-	200	6.9	≈ 93
2	-	340	21.9	≈ 78
3	Ni/AC	200	21.1	≈ 78
4	Ni/AC	250	37.3	56.44

On the other hand and despite the high solubility of lignosulfonate in ethylene glycol, only 3.73 wt% oil yield is observed through conversion of lignosulfonate in this solvent. The oil is obtained in the cyclohexane soluble phase, while the size exclusion chromatography of cyclohexane insoluble phase (Fig. 1.) shows similar elution pattern to the original lignosulfonate. This shows that depolymerization is not taking place in this solvent. The superior performance of ethanol compared to ethylene glycol may be due to the *in-situ* hydrogen production, keeping the catalyst active despite the presence of sulfur in the lignin. The *in-situ* hydrogen by dissociation of ethanol is the atomic H form [5]. In the reaction with ethylene glycol, hydrogen gas must dissociate into reactive atomic H before participation in the depolymerization reaction. Furthermore, contact of the hydrogen gas to the catalyst surface for generation of active hydrogen is possible by its mass transfer from gas phase to the liquid phase followed by further transfer from liquid to the catalyst surface [6], whilst its transfer by ethanol decomposition is much easier.

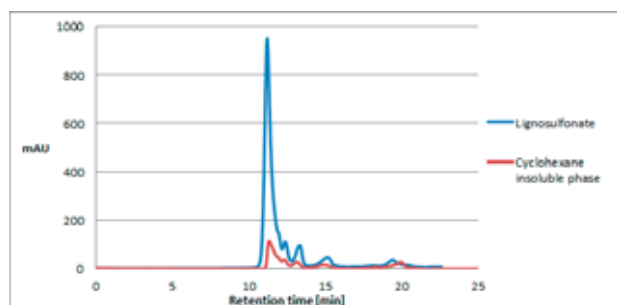


**Figure 1:** Chromatogram of the cyclohexane insoluble phase vs. lignosulfonate. Reaction at 200 °C. Catalyst: lignin: solvent ratio of 1 g: 10 g: 100 ml.

It should be noted that the solid residue remaining after conversion in ethanol is in solid char form with high yield (56-93 wt%), while the solid residue produced in ethylene glycol constitutes only 4.3 wt % of the reaction products, and the unreacted lignosulfonate is dissolved in ethylene glycol. This indicates that ethylene glycol could be a proper solvent for lignin conversion if a proper catalyst can be identified. Further work will among other involve testing of sulfur tolerant catalysts such as NiMoS<sub>2</sub> and CoMoS<sub>2</sub>.

## Conclusions

According to the preliminary results, catalytic conversion of lignosulfonate in the presence of Ni/AC catalyst and in ethanol medium, results in a higher oil

yield compared to using ethylene glycol. The superior performance of ethanol is maybe due to its *in-situ* atomic hydrogen production, which keeps the catalyst active. It should be noted that this conclusion is based on the initial results, and further experiments are required for a concrete conclusion.

## Acknowledgements

This project is part of Biovalue SPIR platform and in collaboration with Haldor Topsøe and Borregaard companies. The author would like to thank the companies for providing their support and expertise.

## References

1. M. Brebu, C. Vasile, *Cellul. Chem. Technol.*44 (9) (2010) 353–363.
2. S. Laurichesse, L. Avérous, *Prog. Polym. Sci.* 39 (7) (2014) 1266–1290.
3. X. Huang, T. I. Korányi, M. D. Boot, E. J. M. Hensen, *ChemSusChem* 7 (8) (2014) 2276–2288.
4. Q. Song, F. Wang, J. Xu, *Chem. Commun.*48 (56) (2012) 7019-7021
5. S. Huang, N. Mahmood, M. Tymchyshyn, Z. Yuan, C. (Charles) Xu, *Bioresour. Technol.*171 (2014) 95–102.
6. Q. Song, F. Wang, J. Cai, Y. Wang, J. Zhang, W. Yu, and J. Xu, *Energy Environ. Sci.* 6 (3) (2013) 994–1007



**Peter Sams Hammershøi**

Phone: +45 61926644

E-mail: [peha@topsoe.dk](mailto:peha@topsoe.dk)

Supervisors: Prof. Anker D. Jensen

Ton V. W. Janssens, Haldor Topsøe A/S

PhD Study

Started: May 2015

To be completed: May 2018

## Durable zeolite based catalyst systems for diesel emission control

### Abstract

Copper-zeolite based catalyst systems are considered to be the next generation catalysts for selective catalytic reduction (SCR) of nitrogen oxides ( $\text{NO}_x$ ) with  $\text{NH}_3$  in heavy duty diesel (HDD) applications. While issues such as activity and hydrothermal stability have been looked much into, and improved, during recent years, knowledge about  $\text{SO}_2$  poisoning remains relatively sparse. In order to assess the durability of Cu-zeolite catalysts, the extent of irreversible  $\text{SO}_2$  deactivation is to be quantified in this project, as well as operando/*in situ* spectroscopic methods will be employed to elucidate more fundamental aspects of the  $\text{SO}_2$  poisoning.

### Introduction

In diesel engines various environmentally harmful compounds are produced in the combustion process. Such compounds include unburnt hydrocarbons (HC), particulate matter and  $\text{NO}_x$  gasses. Legislation has been put into effect in order to limit emissions of said compounds [1]. For HDD exhaust systems, several components make up the entire after treatment system, including a diesel oxidation catalyst (DOC), diesel particulate filter (DPF),  $\text{NH}_3$ -SCR catalyst and ammonia slip catalyst (ASC). Figure 1 illustrates a typical exhaust treatment system complying with EURO VI regulations.

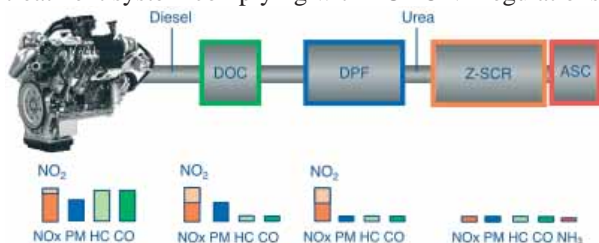


**Figure 1:** Schematic representation of diesel exhaust system to meet EURO VI emission standards.

Cu-zeolites are employed as catalysts in the  $\text{NH}_3$ -SCR, reducing  $\text{NO}_x$  into harmless  $\text{H}_2\text{O}$  and  $\text{N}_2$ . Depending on the location of the SCR catalyst in the exhaust system, different requirements apply. The compounds in exhaust gas and the after treatment conditions lead to high durability requirements of the catalysts – some of them being hydrothermal stability and resistance towards HCs. However, the use of small-pore zeolites of the CHA framework has highly improved the hydrothermal

stability [2] and HC resistance [3]. In modern ultra-low sulfur diesel, small amounts of sulfur are still present (<10 ppm), which leads to a few ppm of  $\text{SO}_2$  in the exhaust gas. Despite such low concentrations of  $\text{SO}_2$ , a severe negative impact on the performance of the Cu-zeolites in the  $\text{NH}_3$ -SCR reaction remains [4]. Although deactivation by  $\text{SO}_2$  is a recognized issue, the extent of the deactivation impact has still not been quantified. It is believed that the deactivation is due to formation of ammonium sulfates and copper sulfates, which may be removed by regeneration at 700 °C [5]. However, the precise mechanism(s) of the deactivation, and possible formation of  $\text{SO}_3$ , has not yet been unveiled.

### Specific Objectives

It is the objective of this project to find the optimal Cu-zeolite catalyst for a zeolite based SCR catalyst system to be implemented in a HDD exhaust after treatment system, with the restriction that the maximum achievable temperature is 550 °C. The optimal Cu-zeolite is to be assessed with respect to several performance indicators including  $\text{NH}_3$ -SCR activity, hydrothermal stability, HC resistance and particularly resistance towards  $\text{SO}_2$  poisoning. In order to identify the optimal Cu-zeolite catalyst, where deactivation by  $\text{SO}_2$  is the main concern, three approaches are applied:

1. Durability assessment by catalytic testing of state-of-the-art Cu-zeolite catalyst powders.
2. Improved fundamental understanding of  $\text{SO}_2$  deactivation by operando/*in situ* characterization with spectroscopic methods.

3. Development of up-scaling understanding and design of catalyst system that can accommodate SO<sub>2</sub> deactivation by catalytic evaluation of monolith samples.

### Results and Discussion

Catalytic testing of a state-of-the-art Cu-SAPO-34 catalyst with 1.9 wt% Cu loading and (P+Al)/Si ratio of 6.6, was carried out in a temperature controlled fixed bed quartz reactor with an inner diameter of 2 mm, using 5 mg catalyst powder of sieve fraction 150-300 μm. Steady-state NO<sub>x</sub> conversions were measured at different temperatures in the range 160-550 °C. For NH<sub>3</sub>-SCR activity measurements, the inlet SCR gas composition was 500 ppm NO, 530 ppm NH<sub>3</sub>, 10 % O<sub>2</sub>, 5 % H<sub>2</sub>O and N<sub>2</sub> as balance gas in a flow of 225 NmL/min at ambient pressure. The catalyst sample was afterwards exposed to 1.5 ppm SO<sub>2</sub> (which is comparable to the SO<sub>2</sub> concentration in an exhaust gas) in abovementioned SCR gas composition for 8 h at 200 °C. After exposure to SO<sub>2</sub>, the sulfated sample was regenerated in SCR gas for 1 h at 550 °C. Figure 2 displays the NO<sub>x</sub> conversion curves of the fresh, sulfated and regenerated sample as functions of the temperature.

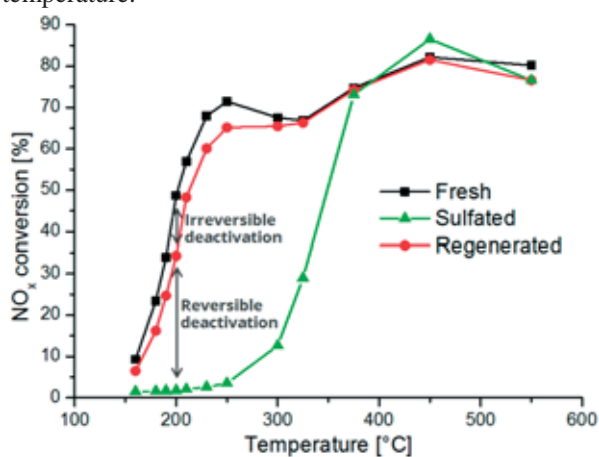


**Figure 2:** NO<sub>x</sub> conversions of fresh, sulfated and regenerated samples plotted as functions of temperature. Grey arrows show the drops in NO<sub>x</sub> conversion due to reversible and irreversible deactivation.

From Figure 2, it is obvious that the NO<sub>x</sub> conversion of the sulfated sample has been reduced significantly compared to that of the fresh sample, especially at temperatures below 350 °C. After regeneration at 550 °C a large fraction of the NO<sub>x</sub> conversion is restored. Due to its reversibility below 550 °C, this form of SO<sub>2</sub> deactivation is labelled “reversible deactivation”. The difference in NO<sub>x</sub> conversion between the fresh and regenerated sample shows that some of the catalyst remains deactivated even after regeneration, hence this form of deactivation is labelled “irreversible deactivation”. For commercial applications, both the reversible and irreversible deactivations are relevant, although the latter to a higher degree. This is because the reversible deactivation can be controlled to not

exceed a certain deactivation level by regeneration. The irreversible deactivation, on the other hand, will build up continuously throughout the lifetime of the catalyst. In order to assess how extensive the impact of the irreversible deactivation is, and ultimately the lifetime of the catalyst, it is, therefore, crucial to estimate the rate by which the irreversible deactivation develops. This will also be an important tool for designing a catalyst system that can accommodate SO<sub>2</sub> poisoning. Moreover, in a dynamic exhaust system, it is necessary to investigate how the deactivation rate is affected by various conditions, such as temperature and SO<sub>2</sub>/SO<sub>3</sub> ratio. Especially, the concentration of SO<sub>3</sub> may be important, since it has been proposed that the irreversible deactivation is due to formation of copper sulfates, which are formed at a higher rate when SO<sub>3</sub> is present at higher concentrations [5]. Lastly, in order to measure a realistic rate of the irreversible deactivation, it is also crucial to be able to separate the two forms of SO<sub>2</sub> deactivation correctly, since small increases of the deactivation rate will result in significantly higher degrees of deactivation when extrapolating over the 8000 h lifetime requirement of the catalyst.

### Conclusions

Despite the use of ultra-low sulfur diesel (<10 ppm), Cu-zeolite based NH<sub>3</sub>-SCR catalysts are still deactivated by exposure to such small concentrations of SO<sub>2</sub>. Two forms of SO<sub>2</sub> deactivation are observed; one that can be regenerated below 550 °C, and an irreversible one. In order to find the optimal Cu-zeolite based NH<sub>3</sub>-SCR catalyst, it is crucial to assess the development of the irreversible deactivation during the lifetime of the catalyst, by measuring the deactivation rate. Furthermore, it is important to assess the influence of factors such as temperature and SO<sub>3</sub> concentration, in order to obtain a realistic estimate of the deactivation rate.

### Acknowledgements

This project is carried out in collaboration between Haldor Topsøe A/S and the CHEC group at DTU Chemical Engineering. The project is sponsored by Innovation Fund Denmark and Haldor Topsøe A/S who are gratefully acknowledged.

### References

1. WHO Air quality guidelines - global update 2005, [http://whqlibdoc.who.int/hq/2006/WHO\\_SDE\\_PH\\_E\\_OEH\\_06.02\\_eng.pdf](http://whqlibdoc.who.int/hq/2006/WHO_SDE_PH_E_OEH_06.02_eng.pdf) (accessed 2015)
2. J.H. Kwak, D. Tran, S.D. Burton, J. Szanyi, J.H. Lee, C.H.F. Peden, *J. Catal.* 287 (2012) 203-209.
3. L. Ma, W. Su, Z. Li, J. Li, L. Fu, J. Hao, *Catal. Today* 245 (2015) 16-21.
4. Y. Cheng, C. Lambert, D.H. Kim, J.H. Kwak, S.J. Cho, C.H.F. Peden, *Catal. Today* 151 (2010) 266-270.
5. A. Kumar, M.A. Smith, K. Kamasamudram, N.W. Currier, H. An, A. Yezerets, *Catal. Today* 231 (2014) 75-82.



## **Zainatul Bahiyah Handani**

Phone: +45 4525 6136  
E-mail: zbha@kt.dtu.dk

Supervisors: Rafiqul Gani  
Gürkan Sin

PhD Study  
Started: May 2013  
To be completed: April 2016

## **Simultaneous synthesis of process and water networks with superstructure-based optimization technique**

### **Abstract**

This work presents a systematic framework for a simultaneous synthesis of process and wastewater treatment network using superstructure-based optimization method. The overall superstructure is composed of i) the process network ii) the wastewater treatment network that connected by converter intervals. In this approach, the problem is generally expressed as a mixed-integer nonlinear programming (MINLP), which is solved to identify the optimal configurations for the process and water network, among a set of feasible alternatives, according to selected performance criteria. A solution strategy to solve the multi-network problem accounts explicitly the interactions between the networks by selecting suitable technologies in order to transform raw materials into products and produce clean water to be reused in the process. The features of the developed synthesis method has been demonstrated using bioethanol production case study.

### **Introduction**

Process synthesis offers an attractive framework for undertaking various design problems through a systematic framework, either using sequential or simultaneous optimization approach. For the former, the overall process system is decomposed into different subsystems for ease of analysis. However, these subsystems (i.e., resource conservation network, heat exchanger network, water network etc.) may not guarantee a truly optimized system as they are synthesized separately after the process flowsheet is obtained. On the other hand, the simultaneous approach gives a better solution as all interactions and economics trade-offs are taken into consideration explicitly [1-3]. The solution strategies of an integrated network problem are able to find the optimal raw material, product portfolio, process and wastewater treatment technology by simultaneously screening various alternatives included in the search space, while minimizing fresh water intake and satisfying environmental regulations [4]. In addition, various water minimization strategies (i.e. reuse, recycle, regeneration and treatment-reuse) are considered in order to reduce the amount of freshwater intake.

### **Systematic Framework**

The framework is supplemented by a software infrastructure based on EXCEL for gathering required

input data and General Algebraic Modeling System (GAMS) for the solution of the formulated optimization problem. The framework has been developed in an earlier work and the details of the framework can be found in Handani et al. [4]. The systematic framework consists of four main steps as shown in Figure 1.

After defining the goal and scope of optimization problem as well as objective function in the first step, one can define a superstructure that consist of various alternatives for the process and wastewater treatment networks are specified with respect to raw materials, technologies and products. The treated wastewater in the treatment tasks can be either discharged into the environment and/or it can be recycled for use in the same processes or in neighboring processes. Then, generic models based on mass input-output describing each of the elements of the superstructure are developed. Generic model parameters require to represent the activity of each interval includes chemical and utility consumption, reaction conversion, split fraction and separation efficiency are collected from various sources i.e. open literature, simulation and technical report. Finally, the optimal process and wastewater treatment network are then formulated as MI(N)LP and solved under different process synthesis-design scenarios.

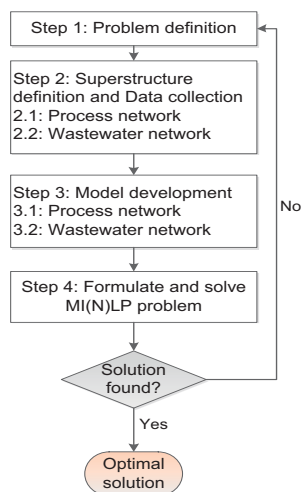


**Figure 1:** A systematic framework for synthesis and design process and wastewater networks

### Bioethanol Production Case Study

The production of bioethanol has been selected due to existing interest in the use of renewable resources. However, due to many possible technologies exist for pretreatment, hydrolysis and fermentation as well downstream separation process, it is important to select the best processing routes to convert the raw material to the desired product. In addition, one of the most main concerns in bioethanol production plant is consumptive use of water. Water consumption for bioethanol production varies significantly depending on the selection of processing technology and process configuration. In order to meet the water requirements and further reduce water consumption in the process plant, one of the alternatives considered here is by reusing water generated from the process or utility wastewater at acceptable limits.

The goal of this problem is to determine an optimal processing route to produce bioethanol from lignocellulosic biomass and optimal wastewater treatment configurations that minimize total annual cost. Hardwood chips are selected as a feedstock and the composition were obtained from Wooley et al. [5].

### Superstructure representation and data collection

In the bioethanol production network, different processes and treatment technologies are considered. The selection of technologies to be employed in the superstructure and the connections between the intervals are defined based on expert views. Because of the lack of publicly available data with hardwood biomass for different pretreatment process, some of the data are taken from different type of lignocellulosic biomass (e.g. softwood, corn stover etc.) by assuming the same conversions and reactions would also apply on hardwood biomass. A combined superstructure consists of 66 intervals which include 1 raw material, 63 intervals (25 process alternatives, 13 unit converters, 25 treatment alternatives, including bypass intervals) and 4 products and co-products from the bioethanol process and wastewater treatment plant as shown in Figure 2.

The selection of a wastewater treatment process depends on the characteristics of the wastewater. Two main contaminants are considered in the wastewater stream, organic compounds and total suspended solids (TSS). The organic compounds in the wastewater can be characterized in terms of chemical oxygen demand (COD). The COD values of the wastewater stream are determined by measuring the amount of oxygen based on the oxygen equivalent, which is determined from a specific organic matter component [6].

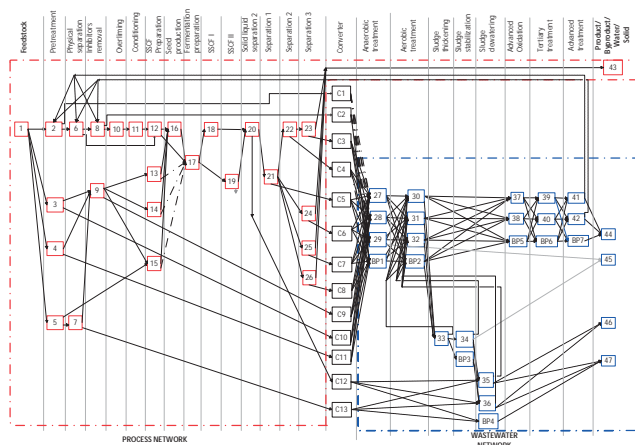


**Figure 2:** Process and wastewater network superstructure for bioethanol production case study

### Results and Discussion

The superstructure of the combined process and water network features 446,324 continuous variables, 459,046 equations and 52 binary variables. In this scenario, one possible recycled water alternative is considered to reduce fresh water consumption in the process. It should be noted that the effluent discharge of partially treated wastewater to the environment is one of the options. It is worth to note that by considering recycled water opportunity to be used in the process as raw material resulted in savings of up to 32% fresh water consumption. Conversely, the synthesis problem with recycled water option gives higher total annual cost (MM\$ 75.6/yr) since more treatment is required to generate higher quality of water to be reused in the process as a raw material.

### References

1. M.A. Duran, I.E. Grossmann, *AIChE J.*, 32 (1986) 123-138.
2. T. Yee, I.E. Grossmann, Z. Kravanja. *Computers & Chemical Engineering*, 14 (1990) 1151-1164.
3. L., Yang, I.E. Grossmann, *Industrial & Engineering Chemistry Research* 52(9) (2013) 3209-3224.
4. Z.B. Handani, A. Quaglia, R. Gani. *Computer Aided Chemical Engineering*, 37 (2015) 875-880.
5. R. Wooley, M. Ruth, J. Sheehan, K. Ibsen, H. Majdeski, A. Galvez.. *NREL/TP-580-26157*, National Renewable Energy Laboratory, 1999.
6. G. Tchobanoglous, F.L. Burton, H. D. Stensel, *Wastewater Engineering: Treatment and Reuse*, McGraw-Hill, NY, U.S.A, 2003.



## Thomas Klint Hansen

Phone: +45 4525 2920  
E-mail: tkli@kt.dtu.dk  
Discipline: Catalysis and Reaction Engineering

Supervisors: Anker D. Jensen  
Brian B. Hansen  
Ton V.W. Janssens, Haldor Topsøe A/S

### PhD Study

Started: April 2013  
To be completed: March 2016

## Development of new automotive diesel oxidation and NH<sub>3</sub> slip catalysts

### Abstract

Catalytic diesel exhaust aftertreatment systems are an essential part of emission control (NO<sub>x</sub>, PM, NH<sub>3</sub>, and HC) from heavy duty diesel vehicles. These systems are under constant development in order to meet the increasingly stringent emission limits, such as Euro VI. The focus of this project is the development of an efficient low noble metal content/low cost diesel oxidation catalyst (DOC) and a highly selective NH<sub>3</sub> slip catalyst (ASC). A more selective ASC will enable the use of higher NH<sub>3</sub> loads in the Selective Catalytic Reduction (SCR) unit and thereby ensure a higher NO<sub>x</sub> removal. The research and development of these units will include identification and screening of new catalyst formulations, as well as kinetic studies and mathematical modeling.

### Introduction

Heavy duty diesel (HDD) vehicles handle a substantial part of the world's transport and logistics. Harmful pollutants are however formed, such as nitrogen oxides (NO<sub>x</sub>), hydrocarbons (HC), particulate matter (PM), and carbon monoxide (CO). The diesel exhaust aftertreatment (DEA) system has been developed to treat the pollutants in the exhaust gas [1].

Figure 1 illustrates the current standard DEA system consisting of a series of four catalytic units. First, the Diesel Oxidation Catalyst (DOC) oxidizes CO and HC to CO<sub>2</sub> and H<sub>2</sub>O, as well as generates NO<sub>2</sub> from NO. Second, the Diesel Particulate Filter (DPF) is a wall-flow filter that traps PM in its monolith walls. The DPF can be regenerated actively by increasing the exhaust gas temperature by post-injection of fuel, or passively by using a catalyst. NO<sub>2</sub> generated by the DOC also significantly assists regeneration. Third, NO<sub>x</sub> is treated through Selective Catalytic Reduction (SCR) with NH<sub>3</sub> as the reducing agent. NH<sub>3</sub> is supplied to the system through urea dosing, regulated by the onboard Model Predictive Control (MPC) unit. Lastly, excess NH<sub>3</sub> is selectively oxidized to N<sub>2</sub> by the Ammonia Slip Catalyst (ASC). As a result, the treated exhaust gas exiting the DEA system meets the emissions restrictions imposed by regulations [1].

The DEA system is very complex, requiring efficient exhaust treatment for a wide range of highly transient operating conditions, corresponding to cold start, stop-and-start driving (inner city), and high speed driving (highways).

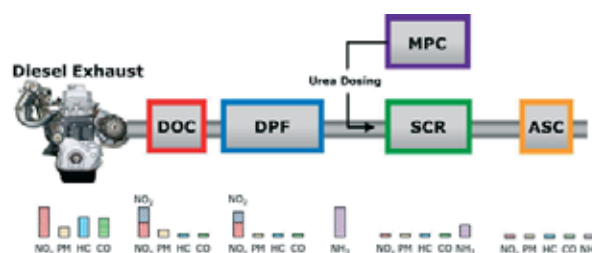


**Figure 1:** Example of a standard DEA system, consisting of a DOC, a DPF, an SCR component, a urea dosing MPC unit, and an ASC.

DTU Chemical Engineering and Haldor Topsøe A/S are collaborating on the development of the next generation DEA system to meet future regulations, with funding from Innovation Fund Denmark. The underlying PhD projects concern the development of new DOC and ASC formulations (Thomas Klint Hansen), the combination of the DPF and SCR components (Kasper Linde), the development of the control unit for efficient regulation of urea dosing (Andreas Åberg), and the detailed characterization of catalysts with pollutants using TEM (Ian Joseph Allen).

### Specific Objectives

The overall objective of this PhD study is to develop new DOC and ASC formulations for the next generation of DEA systems. New catalyst formulations will be identified and screened, and the kinetics investigated using a gas flow reactor with a catalyst bed.

Mathematical modeling will be used to help prepare optimal lab scale and full scale monolith samples based on the most promising formulations. The lab scale and full scale monoliths will be tested in a pilot setup at DTU Chemical Engineering and a full-scale engine testing unit at Haldor Topsøe A/S, respectively.

### Development of the Diesel Oxidation Catalyst

The DOC is commonly a Pd-Pt based catalyst and is therefore quite expensive [1]. The next generation DOC will be developed with the goal of reducing the component price, by reducing the dependency of the catalyst on noble metals. Pt based DOC formulations promoted with, amongst others, K and Fe will be prepared, based on their potential to decrease the light-off temperature of CO oxidation for conditions similar to those in a DEA system [2, 3]. A typical light-off curve for CO oxidation over the benchmark DOC (1 wt.% Pt/Al<sub>2</sub>O<sub>3</sub>) is shown in Figure 2.

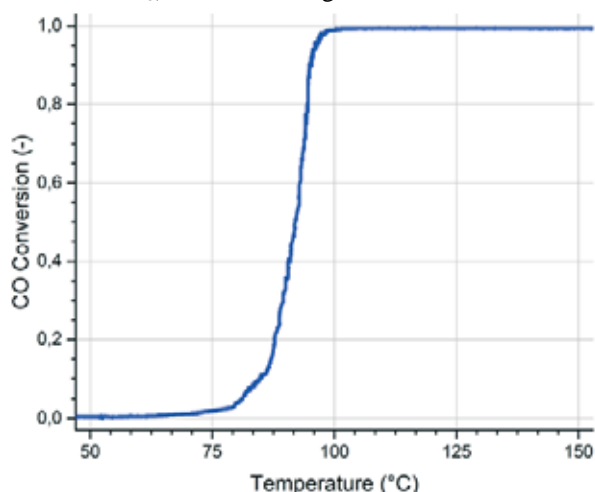


**Figure 2:** The light-off curve for CO oxidation over the benchmark DOC. Operating conditions: 10 mg 1 wt.% Pt/Al<sub>2</sub>O<sub>3</sub>, 300 NmL/min, 250 ppm CO, 10 vol.% O<sub>2</sub>, 3 vol.% H<sub>2</sub>O, and balance N<sub>2</sub>.

### Development of the Ammonia Slip Catalyst

Selective Catalytic Oxidation (SCO) of NH<sub>3</sub> to N<sub>2</sub> is the purpose of the ASC. Figure 3 illustrates the dual layer design used in the ASC. The upper layer is an SCR catalyst (Cu-beta zeolite) and the lower layer is an Ammonia Oxidation Catalyst (AMOX) (Pt/TiO<sub>2</sub>-SiO<sub>2</sub>).

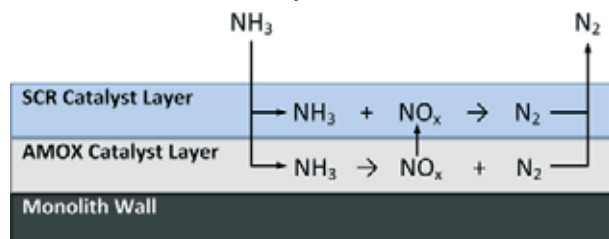


**Figure 3:** The dual layer design of the ASC. The lower layer oxidizes NH<sub>3</sub> to N<sub>2</sub> and NO<sub>x</sub>. The NO<sub>x</sub> produced in the lower layer reacts with NH<sub>3</sub> in the upper layer, over the SCR catalyst, increasing overall N<sub>2</sub> selectivity.

To further increase the N<sub>2</sub> selectivity, a model developed for the monolithic dual layer ASC has been used to optimize the catalyst design parameters. The optimized design will be the basis for catalyst preparation. Figure 4 shows a contour plot for the N<sub>2</sub> yield as a function of SCR layer thickness (catalyst loading) and temperature. The N<sub>2</sub> yield is a key performance indicator, since it is expressed using the NH<sub>3</sub> conversion and the N<sub>2</sub> selectivity. Depending on the operating temperature, Figure 4 suggests an optimal SCR catalyst loading between 20-50 g/L SCR. For lower operating temperatures, a thinner layer is better, while at higher temperatures, a thicker layer is better.

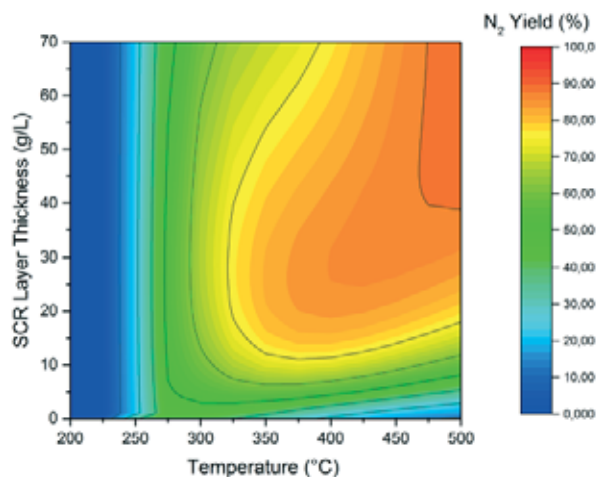


**Figure 4:** Contour plot of the N<sub>2</sub> yield for a DLASC with 26 g/L AMOX and varying SCR layer thickness for 200-500°C. Simulations consider a feed of 200 ppm NH<sub>3</sub>, 12.3 vol.% O<sub>2</sub>, 3.3 vol.% H<sub>2</sub>O, and balance N<sub>2</sub>.

### Conclusions

Improved DEA systems are needed to meet future emission regulations. Design of the next generation of DOC and ASC formulations is being performed through literature studies, mathematical modeling, and experimental investigations, including kinetic studies and activity screenings. The DOC will be improved by decreasing the noble metal content, resulting in a lower component price. The dual layer ASC design has been optimized through mathematical modelling. The next generation DOC and ASC will contribute to the overall improvement of the DEA system.

### Acknowledgements

This project is a collaboration between the CHEC research center at DTU Chemical Engineering and Haldor Topsøe A/S. The financial support from Innovation Fund Denmark under Grant number 103-2012-3 is gratefully acknowledged.

### References

1. W. A. Majewski, M. K. Khair, Diesel Emissions and Their Control, SAE International, 2006.
2. Y. Minemura, M. Kuriyama, S. Ito, Catal. Commun. 7 (9) (2006) 623-626.
3. H. Einaga, N. Urahama, A. Tou, Y. Teraoka, Catal. Lett. 144 (10) (2014) 1653-1660.



**Ludovica Hengeller**

Phone: +45 256813  
E-mail: luhe@kt.dtu.dk

Supervisors: Ole Hassager  
Anne Skov Ladegaard  
Kristoffer Almdal

PhD Study  
Started: April 2013  
To be completed: March 2016

## Relaxation mechanism and molecular structure study of polymer blends by rheological experiments

### Abstract

Industrial polymers are largely polydisperse systems. One step towards understanding polydisperse polymers is the characterization of bi-disperse blends. Even though linear viscoelastic properties of bi-disperse polystyrene blends have been investigated thoroughly both theoretically and experimentally in recent years [1], both nonlinear shear and extensional flow properties are lacking. The purpose of the present study is to investigate the nature of interactions, namely polymer-polymer, in strong elongational flow using a bi-disperse polystyrene blend of 95 K and 545 K Mw with 50% weight ratio. We present both uniaxial extension and stress relaxation experiments to determine if orientation and extension of long PS chains induce orientation and extension in shorter chains.

### Introduction

We present start-up of uniaxial extension followed by stress relaxation experiments of a bi-disperse 50% by weight blend of 95k and 545k molecular weight polystyrene. We also show, for comparison, stress relaxation measurements of the polystyrene melt with molecular weight 95k and 545k, which are the components of the bi-disperse melt. The stress decay data at short time show a faster relaxation of the blend at high strain rates, probably due to polymer-polymer interactions in strong elongational flow. At longer times in the relaxation process of the blend, the short components have relaxed their anisotropy, so the long components keep relaxing in a sea of relaxed shorter polymers, and regardless of the strain rate applied in the start-up of the elongational flow, approach to a Rouse-like relaxation process albeit with a modified exponent.

### Specific Objectives

The purpose is to investigate cooperative interactions between polymer chains and measure how the mechanism of the short chains is affected in presence of the long chains. Data for the blend are compared to data for the pure components.

### Materials

The polystyrene PS-545k melt used in this work has been previously described and characterized in both shear and extensional rheology by Huang et al. [3]. The polystyrene PS-95k has been synthesized by the means of living anionic polymerization according to the standard

procedure by Ndoni et al. [4]. The reaction was carried out for 4 hours at 35°C in freshly distilled cyclohexane, with the use of the titrated solution of sec-butyllithium in hexane as the initiator. The molar mass of PS-95k was determined with size exclusion chromatography (SEC) with non-stabilized tetrahydrofuran (THF) as the eluent and with the use of a column set consisting of a 5µm guard column and two 300 x 8 mm<sup>2</sup> columns (PLgel Mixed C and Mixed D). The system was equipped with a triple detector system including a combined Viscotek model 200 differential refractive index (DRI), a differential viscosity detector and a Viscotek model LD 600 right angle laser light scattering detector (RALLS). On the basis of calibration with narrow molar mass polystyrene standards and flow rate signal adjusting according to Irganox signals, the values of the weight-average molecular weight Mw and the polydispersity index PDI, defined as the ratio of the Mw over the number-average molecular weight Mn, were determined.

**Table 1:** Properties of the two monodisperse polystyrene components (the values for PS-545k are taken from Huang et al. [3]).

	Long Chains	Short Chains
Material	Linear PS	Linear PS
Mw	545 k	95 k
PDI	1.12	1.06
%wt	50	50

$\tau_m$	58700 s	170 s
$\tau_R$	700 s	20s

### Results: Shear Rheology

The linear viscoelasticity of the pure monodisperse polystyrene melts and the Blend 50L-50S have been measured on an ARES-G2 rheometer from TA Instruments, with an 8 mm parallel plate geometry. Small amplitude oscillatory shear flow measurements were performed for all three samples at 130, 150 and 170 °C in nitrogen atmosphere. The data were shifted to a single master curve at 130 °C, using the principle of time temperature superposition (TTS).

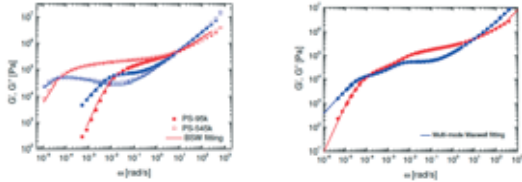


**Figure 1: Left.** LVE data fitted with the BSW spectrum for PS-545k and PS-95k at 130°C. **Right.** LVE data fitted with the Multi-mode Maxwell spectrum for Blend 50L-50S at 130°C.

The storage modulus  $G'$  and loss modulus  $G''$ , plotted as a function of the angular frequency  $\omega$ , are shown in Figure 1 (Left) for PS-95k and PS-545k, and in Figure 1 (Right) for the Blend 50L-50S. The LVE data for the two monodisperse melts have been fitted with a continuous Baumgaertel-Schausberger-Winter (BSW) relaxation spectrum [5].

### Results: Extensional Rheology

The molecular weight  $M_w$  of the two monodisperse components in Blend 50L-50S is selected such that their respective longest relaxation times are well separated from each other. We expect therefore that different mechanisms can be activated for each component independently. The Rouse time  $\tau_R$ , which indicates the stretch relaxation time, is defined as  $\tau_R = Z^2 \tau_c$ , where  $\tau_c$  is the relaxation time of the strand between two entanglements with molecular weight  $M_e$ , and  $Z = M_w/M_e$  is the number of entanglements per chain. We use  $M_e = 13300\text{g/mol}$  [6] to determine the value of  $Z$  for our monodisperse melts. The reptation time  $\tau_m$ , which indicates the maximum relaxation time of a whole chain, can be obtained from LVE measurements. The values of  $\tau_m$ ,  $\tau_R$  and  $Z$  for the two monodisperse polystyrenes are listed in Table 1.

To identify the regimes, we wish to interpret the dynamics in terms of time constants for the components. We estimate the Rouse times of the short and long constituents in the blend to be identical to those in the pure melts given in Table 1. Moreover since the long chains are essentially frozen at the relaxation time of the short component, we may roughly estimate the terminal relaxation time of the short chain to be approximately equal to that of the pure melt. However, the terminal

relaxation of the blend will be reptation of the long chains in a sea of fully relaxed short chains. As an estimate for this time we use the relaxation time obtained from the Maxwell spectrum. Hence we arrive at the relaxation times in Table 2.

**Table 2:** Time constants for short and long components in the blend.

Blend 50L-50S	Rouse time	Terminal time
Short comp.	$\tau_R^S=20.4\text{ s}$	$\tau_m^S=169\text{ s}$
Long comp.	$\tau_R^L=705\text{ s}$	$\tau_w^L=23000\text{ s}$

Figure 2 (Left) shows the measured corrected extensional stress growth coefficient  $\bar{\eta}^+$  plotted as a function of time at 130°C for the Blend 50L-50S. The sample was stretched at 5 different rates  $\dot{\epsilon}$ , which correspond to 5 different flow regions separated by the reptation time and Rouse time of the long and short chains. All the measurements were conducted at 130°C, except the ones at the slowest stretch rates  $\dot{\epsilon} = 1 \cdot 10^{-5}$  and  $=3 \cdot 10^{-4}\text{s}^{-1}$ . These two were performed at 160°C and shifted to 130°C according to the Time Temperature Superposition principle, with shift factors  $a_T=0.0038$  and  $b_T=0.91$ . The solid line in the plot is the LVE prediction. The elongational measurements show good agreement with the LVE at small strains. The measurement at  $\dot{\epsilon} = 1 \cdot 10^{-5}$  closely follows the LVE, except at high Hencky strains where the stress is slightly higher. At this strain rate we expect the system to be still close to the equilibrium configuration, which means that the flow is not fast enough to orient the polymer chains. As the  $\dot{\epsilon}$  increases, more and more deviation from the LVE envelope of the experimental curves is observed, meaning that the chains experience higher degree of stretching, which results in more strain hardening.

In Figure 2 (right) we show the same corrected extensional stress difference  $\sigma_{zz} - \sigma_{rr}$  plotted as a function of Hencky strain at 130°C for the Blend 50L-50S. From this plot it is clear that  $\sigma_{zz} - \sigma_{rr}$  reaches a steady-state value above  $\epsilon=3$  for each stretch rate. That allows the determination of a steady-state viscosity  $\bar{\eta}_s$ .

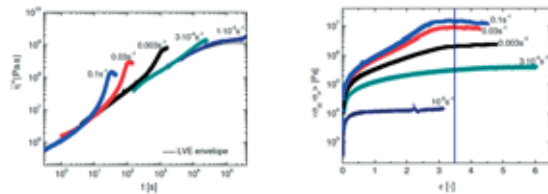


**Figure 2: Left.** Stress growth coefficient as function of time for the Blend 50L-50S measured at 130°C. The solid line is the LVE prediction. **Right.** The measured stress for the Blend 50L-50S at 130°C as function of Hencky strain.

### Stress Relaxation

Stress relaxation measurements present a special challenge, since merely halting the plates does not produce a true stress relaxation experiment, because typically the filament will be subjected to a progressive thinning on its own. A technique to perform a direct stress relaxation experiment following steady uniaxial extension on polymer melts has been introduced by [7] on the above-mentioned FSR. The novelty consists in the use of a closed loop controller that monitors the mid-filament diameter; in this way the necking is avoided by adjusting the position of the top plate. In a stress relaxation experiment, at the start-up of the elongation, a constant strain rate is applied on the sample. As soon as the stress relaxation starts at an arbitrarily given Hencky strain  $\varepsilon_0$ , the mid-filament radius is kept constant by the active control loop, giving  $\varepsilon_0$ . The extensional stress decay coefficient during the stress relaxation is defined as  $\overline{\eta}^- = \frac{(\sigma_{zz} - \sigma_{rr})}{\dot{\varepsilon}}$ , where  $\dot{\varepsilon}$  is the strain rate in the start-up of the uniaxial extensional flow.

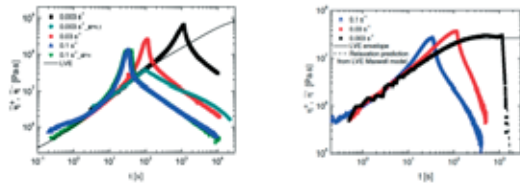


**Figure 3:** Left. Stress relaxation measurements of the Blend 50L-50S after fixed Hencky strain of 3.5. Right. Stress relaxation measurements of the pure short component after fixed Hencky strain of 3.5.

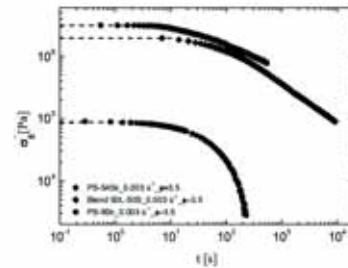
We performed stress relaxation measurements after a fixed Hencky strain of 3.5, where steady-state was reached.

Figure 3 (left and right) show the results for the Blend 50L-50S and PS-95k, respectively. We plot the extensional stress growth coefficient  $\overline{\eta}^+(t)$  followed by the stress decay coefficient  $\overline{\eta}^-(t)$  as a function of time for the Blend 50L-50S. All the measurements were performed at 130°C. We expected steady extensional flow to be established at  $\dot{\varepsilon}_0 = 3$ , see Fig. 2 (right). To confirm this hypothesis one additional experiment was performed with  $\dot{\varepsilon} = 0.1s^{-1}$  and  $\varepsilon_0 = 4$ . Indeed it appears that the relaxation process is independent of  $\varepsilon_0$  provided  $\varepsilon_0 > 3$ , confirming that once steady flow is reached, the following relaxation process is unaffected by the flow time. Also in the plot we show an experiment made at  $\dot{\varepsilon} = 0.003s^{-1}$  and stopped at  $\varepsilon_0 = 0.3$ , so that the relaxation spectrum is in the linear regime. The solid line in the figure is the LVE envelope for start-up. Figure 3 (right) shows the analogous results for the monodisperse melt PS-95k. At the stretch rate of  $\dot{\varepsilon} = 0.003s^{-1}$ , the measured data follow the LVE envelope and the relaxation prediction (dashed line) even at Hencky strain of 3.5.

### Discussions

Figure 3 compares the stress relaxation process of the Blend 50L-50S with the pure components PS-95k and

PS-545k at the same three strain rates and the same imposed macroscopic Hencky strain. Data points for  $t > 600s$  have not been reported because their reproducibility ends up at that time (Figure 3). The very high  $M_w$  of the sample prevented measurements at higher strain rates. Although the short components represent 50% in weight of the blend it is seen from Figure 3 that the stress in the Blend 50L-50S is much closer to the stress in the pure long component than the stress in the pure short component. It means that the short chains do not contribute significantly to the stress level (depicted by the dashed lines in the plot) in the bi-disperse melt. The stress reduction in the Blend 50L-50S relative to the pure long component is circa of a factor of 2.



**Figure 3:** Comparison of the stress relaxation process of the Blend 50L-50S with the pure components in the blend at the same strain rate and the same imposed macroscopic Hencky strain ( $\varepsilon = 3.5$ ).

Concerning the measurements of the Blend 50L-50S at different strain rates we refer to Figure 4. The stress relaxation curves can be approximately divided into two regimes: the fast modes covering time from start of relaxation to the terminal time of the short chains, and the slow modes covering time from the terminal time of the short chains to the end of the experiment, which is well before the terminal time of the long chain.

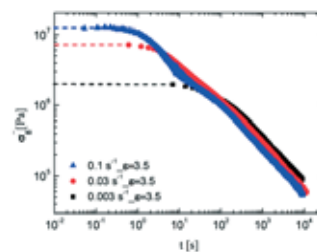


**Figure 4:** The stress decay for the Blend 50L-50S. The data are originally from the Fig. 3 (left). The dashed lines are guidelines meant to show the stress level right when relaxation starts.

### Short time dynamics

Initially we concentrate on the relaxation for time up to the estimated terminal relaxation time of the short chains, that is up to  $t = 200s$  as shown in Table 2.

To compare the data of Figure 7, measured at the three different stretch rates,  $\dot{\varepsilon} = 0.003, 0.03$  and  $0.1s^{-1}$ , we re-plot the stress relaxation phase after extensional flow in Figure 4.

The relaxation data starting at  $\varepsilon_0 = 3.5$  for three different strain rates show a considerable acceleration for the bi-disperse blend, this is similar to the acceleration pointed out by Yaoita and co-workers [8] for a monodisperse polystyrene with increasing strain rate. For a fixed  $\varepsilon_0$ , the flow time  $t_0$  decreases with increasing  $\dot{\varepsilon}$ . According to Eqs.16-17 keep in mind that this gives rise to faster relaxation even in the LVE limit. The observed behavior may also be compared by the fast stretch relaxation measured and analysed by Nielsen et al. [7]. Here the authors showed that the relaxation is faster with larger stretch ratio of the chain. Nevertheless molecular stress origin and configuration need further investigations that can be done with neutron scattering measurements on the nanoscale.

### Long time dynamics

Now we turn to the relaxation of slow modes that covers time from the terminal time of the short chains ( $t = 200s$  as shown in Table 2) until the end of the experiment, which is well before the terminal time of the long chains. It can be seen from Figure 4 that in this regime the relaxation curves of the blend show a similar slope in the log-log scale plots, corresponding to a power law behavior over approximately two decades in time. Also Figure 6 shows that the trend of the stress data at  $\dot{\varepsilon} = 0.1s^{-1}$  look quite different at long times compared with the other two data set at lower strain rates where the faster modes have not been activated.

### Acknowledgements

The research leading to these results has received funding from the Danish Council for Independent Research - Natural Sciences under EPMEF on Grant 0602-02179B, and Aage og Johanne Louis-Hansens Fond.

### Conclusions

Results are given for relaxation after steady flow. We observe that the rate of stress relaxation increases as the stretch rate in the prior flow is increased. This may be taken as an indication of the friction reduction caused by alignment of the chains as suggested by Yaoita et al. (2012) [8]. However it may also be simply because more fast relaxation modes are activated at high stretch rates. Especially the short component in the blend may not be activated in slow flow at all.

The measurements reveal two clearly separated relaxation regimes. A fast regime and a slow regime. In the fast regime we expect the long chains to be essentially frozen and the stress relaxation to be due to relaxation of the short chains primarily. Conversely in the slow regime we expect the long chains to be relaxing in a sea of essentially fully relaxed short chains that act as a solvent. The latter relaxation has a distinct power law behaviour that extends in one situation over more than two decades in time.

It is noted that the power law corresponds to the Rouse relaxation of the pure long chains, although this correspondence may be fortuitous. Comparison with the pure long and short components seems to indicate that the

stress in the blend is carried primarily by the long component even though it represents only 50% by weight.

We realize that our conclusions on the molecular dynamics of the two components are based on stress measurements alone. We hope in the future to present more direct evidence based on neutron scattering experiments performed on quenched PS samples.

### References

1. Nielsen J. K.; Rasmussen, H. K.; Hassager O., and McKinley G. H., "Elongational viscosity of monodisperse and bidisperse polystyrene melts", *J. Rheol.* 2006, 50, 453–476.
2. Huang, Q.; Alvarez, N. J.; Matsumiya Y.; Rasmussen, H. K.; Watanabe H. and Hassager O. "Extensional Rheology of Entangled Polystyrene Solutions Suggests Importance of Nematic Interactions", *ACS Macro Lett.* 2013, 2, 741–744.
3. Huang, Q., O. Mednova, H. K. Rasmussen, N. J. Alvarez, A. L. Skov, K. Almdal, and O. Hassager, "Concentrated polymer solutions are different from melts: role of entanglement molecular weight", *Macromolecules* 46, 5026-5035 (2013).
4. Ndoni, S., C. M. Papadakis, F. S. Bates, and K. Almdal, "Laboratory-scale setup for anionic polymerization under inert atmosphere", *Rev. Sci. Instrum.* 66, 1090-1095 (1995).
5. Baumgaertel, M., A. Schausberger, and H. H. Winter, "The relaxation of polymers with linear flexible chains of uniform length", *Rheol. Acta* 29, 400-408 (1990).
6. Bach, A., K. Almdal, H. K. Rasmussen, and O. Hassager, "Elongational viscosity of narrow molar mass distribution polystyrene", *Macromolecules* 36, 5174-5179 (2003).
7. Nielsen, J. K., H. K. Rasmussen, and O. Hassager, "Stress relaxation of narrow molar mass distribution polystyrene following uniaxial extension", *J. Rheol.* 52(4), 885-899 (2008).
8. Yaoita, T., I. Takeharu, Y. Masubuchi, H. Watanabe, G. Ianniruberto, and G. Marrucci, "Primitive chain network simulation of elongational flows of entangled linear chains: stretch/orientation-induced reduction of monomeric friction", *Macromolecules* 45, 2773-2782 (2012).



**Christian Hoffmann**

Phone: +45 4525 6195  
E-mail: chhof@kt.dtu.dk

Supervisors: Anders Egede Daugaard  
John Woodley  
Manuel Pinelo

PhD Study  
Started: August 2014  
To be completed: July 2017

## Heterogeneous surface functionalization of polysulfone membranes as a method for tailoring surface properties

### Abstract

In this study, a versatile surface functionalization method of commercially available polysulfone (PSf) membranes is presented, leading to tailored surface properties with simultaneously retained bulk integrity. These PSf membranes were surface modified in a direct two-step procedure by heterogeneous lithiation followed by functionalization with a range of various acid chlorides. Post-functionalization polymer grafting with hydrophilic monomers was illustrated through both a “grafting from” approach by surface initiated atom transfer radical polymerization (SI-ATRP) and by a “grafting to” approach exploiting Cu(I) catalyzed 1,3-cycloadditions of alkynes with azides (CuAAC). Both methods resulted in membranes with an increased hydrophilicity and a lowered permeability.

### Introduction

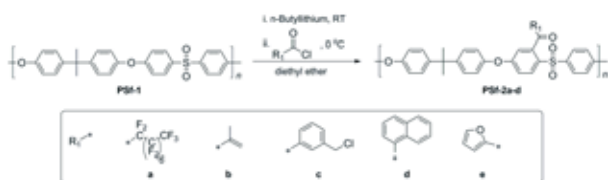
Polysulfone (PSf) and polyethersulfone (PES) are classes of polymers which, due to their chemical structure, are characterized by a broad spectrum of advantageous properties. Very good thermal and mechanical stability provide an outstanding operational spectrum in many different environments, such as organic solvents, a wide pH, and temperature range. This diversity leads to increased application possibilities within many different fields, such as membranes in fuel cells<sup>1</sup> and ion-exchange membranes<sup>2</sup>. Modification of PSf membranes has already been widely studied in order to further improve the materials properties and consequently to meet requirements for these different purposes. Dissolution of the PSf and homogeneous lithiation in solution is a widely used pathway. Initially, the dissolved polymer is activated with n-butyllithium to form a lithiated intermediate. In a subsequent substitution reaction, a diverse range of functionalities can be introduced, such as phosphonic acids<sup>3</sup>, azides<sup>4</sup>, carboxylates<sup>5</sup>, or halogens<sup>3</sup>. This procedure is followed by membrane casting of the functionalized polymer as a third step within the membrane preparation procedure. The introduced halogen functionality can act as a precursor for further polymer grafting by SI-ATRP in a “grafting from” approach. By carefully selecting vinyl-based monomers, this surface grafting approach can then be utilized to tailor surface properties according to application requirements. Alternatively, the use of “Click Chemistry” as a “grafting to” technique permits the introduction of a large range of different substituents

or fully characterized polymers.<sup>6</sup> As such, Cu(I)-catalyzed alkyne azide cycloaddition (CuAAC) between organic azides and terminal alkynes has been applied for polymer grafting, showing high selectivity and reaction yields in mild conditions.<sup>7</sup> As an alternative to the homogeneous bulk reaction mentioned above, a few cases of heterogeneous PSf functionalization have been reported. In the early 1990s Guiver et al. investigated the heterogeneous lithiation of PSf membranes followed by reactions with carbon dioxide and further reactions with acyl fluoride.<sup>4</sup> Inspired by this approach, the current study focuses on the heterogeneous activation of commercially available PSf ultrafiltration flat sheet membranes. Lithiation, followed by acylation using various acid chlorides, can be utilized to introduce a large variety of different functionalities. This heterogeneous functionalization with low molecular weight compounds then leads to the possibility of further surface modification through polymer grafting, using SI-ATRP or CuAAC. This process allows the introduction of new functionality on the prepared membrane without further membrane casting procedure.

### PSf surface activation by heterogeneous lithiation and acylation

Commercially available PSf membranes were submerged in diethyl ether and heterogeneously lithiated at room temperature, followed by acylation using various acid chlorides, as shown in Scheme 1, demonstrating the versatility of this activation procedure. For each of the modifications, a

concentration of 5 mmol<sub>n</sub>-BuLi / g<sub>membrane</sub> was utilized. Functionalization was confirmed by IR and XPS analysis and the appearance of new carbonyl stretch bands and characteristic bands of the different functionalities. The introduction of the various functional groups opens up for further derivatization methodologies through, for example, methacryl groups by thiol-ene reactions<sup>8</sup> or Aza Michael additions<sup>9</sup>, whereas furyl groups are known to react through a Diels-Alder cycloaddition.<sup>10</sup>



**Scheme 1** Heterogeneous activation of PSf membranes PSf-1 via lithiation (i) and subsequent acylation (ii) using various acid chlorides: a) pentadecafluorooctanoyl chloride, b) methacryloyl chloride, c) 3-(chloromethyl)benzoyl chloride, d) 1-naphthoyl chloride, and e) 2-furoyl chloride

### Polymer Grafted PSf membranes employing two strategies: “Grafting from” vs. “Grafting to”

Chloride functionalization opens up a range of possible post-functionalization modification reactions through both the “grafting from” and “grafting to” approaches. Therefore, PSf-2c was investigated as a platform for SI-ATRP “grafting from” polymerization reactions with various hydrophilic monomers, such as HEMA (PSf-5a), MPEGMA (PSf-5b), and PEGMA (PSf-5c). A significant increase in the hydrophilicity of the grafted surfaces was observed. The decrease in the water contact angle of the grafted surfaces compared to the substrate can be seen in Figure 1. Advancing as well as receding WCA decreased from 83.0° and 48.5° to values lower than 70° and 30°, respectively. An alternative strategy for modifying the PSf surface by introducing polymer grafts is through the so-called “grafting to” approach. The chloride functionality stemming from PSf-2c can be substituted easily by an azide, thus offering a pathway for CuAAC with alkyne-

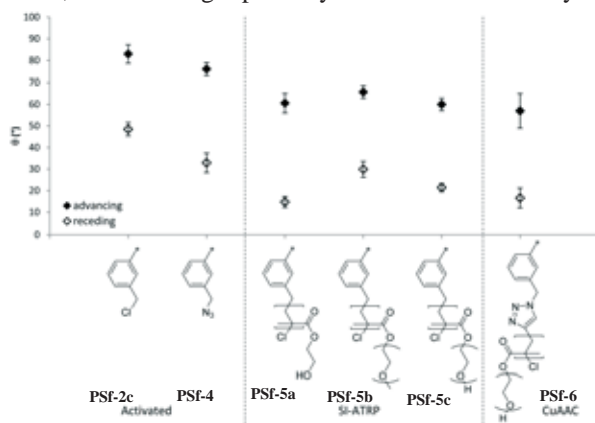


**Figure 1** Dynamic WCAs of PSf membranes activated via acylation and azidation, post-functionalization, via SI-ATRP and CuAAC

terminated polymers. A further reaction through the CuAAC with the alkyne-pPEGMA led to significantly lower advancing and receding WCAs, similar to those of the SI-ATRP products. Additionally, water permeability measurements showed a slightly decreased permeability after activation by acylation and by azidation of  $35.1 \pm 4.03$  and  $25.6 \pm 2.37$  L bar<sup>-1</sup> m<sup>2</sup> h<sup>-1</sup> compared to the virgin membrane ( $43.8 \pm 1.04$  L bar<sup>-1</sup> m<sup>2</sup> h<sup>-1</sup>). Further surface grafting by either SI-ATRP or CuAAC led to a further reduced permeability within a range of 4.8 to 8.4 L bar<sup>-1</sup> m<sup>2</sup> h<sup>-1</sup> as a result of a substantial decrease in pore size after polymer grafting.

### Conclusions

In this study, a facile and easily conductible methodology has been applied in order to covalently surface modify commercially available PSf membranes. For this purpose, off-the-shelf PSf flat sheet membranes were heterogeneously lithiated prior to acylation, using various acid chlorides. Surface modifications with methacryl-, furyl-, and halogen-containing functional groups open up a broad range of surface grafting reactions for tailoring the surface properties. Especially, the introduction of chloride functionality to the membrane surface opens up the possibility of post-derivatization reactions. SI-ATRP treatment of hydrophilic monomers such as HEMA, MPEGMA, and PEGMA in a “grafting from” approach was utilized and compared to CuAAC as a “grafting to” techniques. CuAAC was exploited to couple an alkyne-pPEGMA to the azide surface of the membrane. The grafted membranes prepared through either approach were found to have significantly improved hydrophilicity, though they also resulted in reduced water permeability.

### Acknowledgements

The author wants to thank Aage Louis-Hansens Legat for Teknisk Forskning for financial support.

### References

- Jannasch, P. *Fuel Cells* **2005**, *5*, 248.
- Wang, G.; Weng, Y.; Chu, D.; Chen, R.; Xie, D. *J. Memb. Sci.* **2009**, *332*, 63.
- Dimitrov, I.; Takamuku, S.; Jankova, K.; Jannasch, P.; Hvilsted, S. *Macromol. Chem. Phys.* **2012**, *33*, 1368.
- Guiver, M. D.; Robertson, G. P. *Macromolecules* **1995**, *28*, 294.
- Guiver, M. D.; Croteau, S.; Hazlett, J. D.; Kutowy, O. *Br. Polym. J.* **1990**, *23*, 29.
- Kolb, H. C.; Finn, M. G.; Sharpless, K. B. *Angew. Chemie* **2001**, *40*, 2004.
- Meldal, M. *Macromol. Rapid Commun.* **2008**, *29*, 1016.
- Lowe, A. B. *Polym. Chem.* **2010**, *1*, 17.
- Hoffmann, C.; Stuparu, M. C.; Daugaard, A.; Khan, A. *J. Polym. Sci. Part A Polym. Chem.* **2015**, *53*, 745.
- Tarducci, C.; Badyal, J. P. S.; Brewer, S. A.; Willis, C. *Chem. Commun.* **2005**, 406.

**Morten S e Jepsen**

Phone: +45 30924876  
E-mail: [mosje@kt.dtu.dk](mailto:mosje@kt.dtu.dk)  
Discipline: CHEC Research Center

Supervisors: Peter Glarborg  
Peter Arendt Jensen  
Thomas Norman, B&W V lund

**Industrial PhD Study**

Started: December 2014  
To be completed: December 2017

## NO<sub>x</sub> reduction in grate-firing solid waste power plants

**Abstract**

Combustion of solid fuels in Grate-firing waste-to-energy plants are one of the most competitive methods for conversion of solid fuels to electrical energy and heat. The emission of nitrogen oxides (NO<sub>x</sub>) from waste-to-energy plants is a major environmental concern and the use of CFD models to reduce the emission is of great interest. In this PhD-project a CFD model of NO<sub>x</sub> formation and reduction in a MSW waste-to-energy plant will be developed. The model will be used to develop a set of guidelines for low NO<sub>x</sub> emission from combustion of MSW in grate-firing waste-to-energy plants.

**Introduction**

Managing the large amounts of municipal solid waste that is produced daily has become a significant challenge, and R&D efforts to resolve the problems are increasing. Traditionally, the municipal solid waste has been disposed at landfills due to the low cost. In many regions this is no longer possible as an increase in municipal solid waste generation is experienced. Furthermore, according to the European Landfill Directive the use of Landfills has to be avoided whenever possible [1]. This has generated a shift in municipal solid waste handling, from disposal at landfills to extraction of energy through combustion. One of the main combustion technologies for solid waste is grate-firing [2]. This technology is widely regarded as one of the most competitive, as it enables the use of a wide range of fuels, both biomass and solid waste, with varying moisture content, and the fuel preparation and handling requirements are limited [3]. Combustion of solid waste, similar to combustion of other solid fuels, emits nitrogen oxides (NO<sub>x</sub>). The emission of NO<sub>x</sub> continues to be a major environmental concern [4] as it is an acid rain precursor and participates in formation of photochemical smog, which is problematic in urban areas [4,5]. Nitrogen oxides are formed either from oxidation of the N<sub>2</sub> in the combustion air (thermal NO<sub>x</sub> formation), from reaction between hydrocarbon radicals and nitrogen from the combustion air [4] or from oxidation of organically bound nitrogen in the fuel (fuel-NO<sub>x</sub> formation) [4]. For solid fuels such as waste, which has a significant content of organic nitrogen, the fuel-NO<sub>x</sub> mechanism is

the dominating source of NO<sub>x</sub> [4]. In grate combustion of waste, most of the nitrogen bound in the fuel is released during devolatilisation of the fuel in the fuel-bed, mostly as ammonia (NH<sub>3</sub>), hydrogen cyanide (HCN) and aromatic N-compounds [3]. It has been shown that the formation and partitioning of these NO<sub>x</sub> precursors depends strongly on fuel characteristics (i.e., biomass type, fuel nitrogen content, particle sizes, and moisture content [4,6,7]) and on process conditions (devolatilisation temperature and stoichiometric air ratio [4,8]). The reactive nitrogen species released from the fuel-bed are subsequently oxidized to either NO or N<sub>2</sub> in the freeboard. The selectivity for forming NO, rather than N<sub>2</sub>, depends strongly on the process in the freeboard, mainly temperature and stoichiometry [4].

**Specific Objectives**

The project aims to develop a suitable CFD model describing the formation and reduction of NO<sub>x</sub> in grate-firing waste-to-energy plants, which can be used commercially by B&W V lund. The main focus will be on the development of the chemical model. Due to limited simulation time in the industry the chemical model needs to be restricted to a certain number of reactions.

A large emphasis has been put on the development of an in-house SNCR system at B&W V lund. In connection with this it is of great interest to be able to simulate the SNCR system using CFD. A CFD model of a SNCR system for NO<sub>x</sub> reduction is developed for this purpose.

The main objectives are:

- Determining the maximum number of reactions for the chemical model that complies with the computer resources set up by B&W Vølund.
- Developing a chemical model for formation and degradation of NO<sub>x</sub>.
- Evaluate the chemical model through simulations in CHEMKIN.
- Determine an appropriate bed model to simulate the release of combustibles to the computational domain.
- Evaluate the CFD model through pilot- and full scale waste-to-energy plant measurements.
- Set up a set of guidelines for low NO<sub>x</sub> emission from grate-firing waste-to-energy plants through CFD simulations using the developed model.

### Preliminary Results

In the preliminary part of the project the focus has been on identifying readily available NO<sub>x</sub> mechanisms, identifying CFD modeling methods and identifying gaps in the literature. Furthermore, initial simulations of combustion of waste in incineration plants have been performed in Fluent, and methods for reduction of the computational expenses have been identified.

After identification of NO<sub>x</sub> mechanisms, the most promising has been tested upon computational time. An important criterion for a NO<sub>x</sub> mechanism is that the size is limited to a size at which the formation of NO<sub>x</sub> can be simulated within a certain time limit. Three skeleton mechanisms consisting of 92, 198 [9] and 214 reactions [10] were used to simulate the formation of NO<sub>x</sub> in the furnace of a waste-to-energy plant. The computational time for the three mechanisms was measured and is shown in Figure 1.

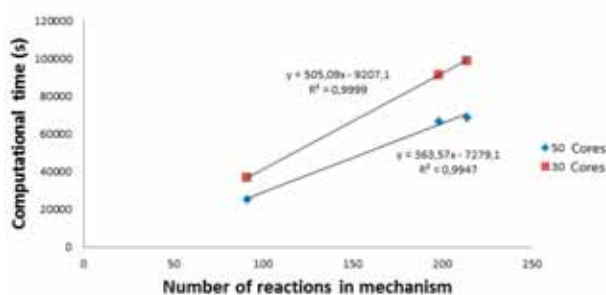


**Figure 1:** The simulation time of NO<sub>x</sub> formation in a waste-to-energy plant using three mechanisms [10,11] with varying size. The NO<sub>x</sub> is simulated using a post-processing procedure.

It was identified that the maximum size of the mechanism is 220 reactions, as this complies with the limitations set up by B&W Vølund. The readily available mechanisms were tested against a well-validated Detailed Chemical Kinetic Mechanism [11] in

ideal-reactor calculations using CHEMKin as shown in Figure 2, where a gas composition, similar to that of a gas from devolatilization of waste, is used as inlet gas composition.

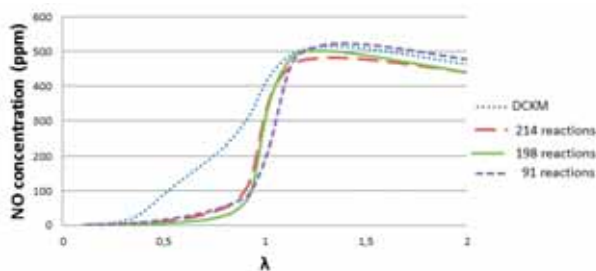


**Figure 2:** Ideal reactor simulations of the formation of NO from a devolatilization gas containing NH<sub>3</sub>. The temperature and pressure has constant values of T=1200K and P=1atm.

Readily available mechanisms [9,10] have difficulty describing the formation of NO at lower temperatures and reducing conditions as shown in Figure 2. The development of an improved mechanism describing the formation of NO<sub>x</sub> is therefore crucial. The mechanism must describe the formation of NO<sub>x</sub> better than the readily available mechanisms. At the same time the mechanism must be limited to a certain size, the mechanism can not exceed 230 reactions, in order to limit the computational resources.

### Acknowledgements

This project is a collaboration between B&W Vølund and the CHEC group at DTU Chemical and Biochemical Engineering. The project is funded by Innovation Fund Denmark and B&W Vølund.

### References

1. Diverting waste from landfill, EEA Report No 7/2009
2. E. Ranzi, S. Pier. Pierucci, P.C. Aliprandi, S. Stringa, *Energy Fuels* 25 (2011) 4195–4205.
3. C. Yin, L. A. Rosendahl, S. K. Kær, Grate-firing of biomass for heat and power production, *Powder Technol.* 193 (2009) 266–273.
4. P. Glarborg, A. D. Jensen and J. E. Johnsson, *Prog. Energy Combust. Sci.* 29 (2003) 89–113.
5. Frank and M. J. Castaldi, *Waste Management Res* (2014).
6. R. Bassilakis, R. Carangelo, M. Wójtowicz, *Fuel* 80 (2001) 1765–1786.
7. G. Stubenberger, R. Scharler, S. Zahirovic, I. Obernberger, *Fuel* 87 (2008) 793–806
8. K. Hansson, J. Samuelsson, C. Tullin, L. Åmand, *Combust. Flame* 137 (2004) 265–77
9. E. Houshfar, Ø. Skreiberg, P. Glarborg and T. Løvås, *Int. Joul. Chem. Kin.* 44 (2012) 219–231
10. T. Løvås, E. Houshfar, M. Bugge and Ø. Skreiberg, *Energy & Fuels* 27 (2013) 6979–6991
11. T. Mendiara and P. Glarborg, *Combustion and Flame* 156 (2009) 1937–1949



## Stavros Kalafatakis

Phone: +45 4525 6184  
E-mail: skal@kt.dtu.dk

Supervisors: Hariklia N. Gavala  
Ioannis V. Skiadas

PhD Study  
Started: November 2013  
To be completed: October 2016

## Improving fermentation processes for production of bio-based chemicals and fuels

### Abstract

Biorefineries can potentially provide a sustainable way for production of biofuels and bio-based chemicals. However, developing economically viable and competitive bioprocesses compared to already existing alternatives is the key challenge that biorefineries face and there is a need and space for a better understanding and further improvement in this respect. The current study investigates methods to improve fermentation processes by two different approaches. The first is the development of a novel concept targeting the use of forward osmosis membrane technology to recover water during the fermentation processes and up-concentrate the products. The second is dealing with the deeper understanding of the pure and mixed culture fermentations and the factors controlling the products distribution.

### Introduction

Biorefineries utilizing 2<sup>nd</sup> generation feedstocks are becoming a great candidate for sustainable production of bio-based chemicals and fuels. Whereas demonstrating substantial potential, some hurdles are yet to be overcome in order to achieve an environmentally and financially attractive solution. Among others, substrate and product inhibition are commonly occurring challenges in biological conversion processes. Hence, it is a general practice to dilute the feedstock in order to reduce potential inhibition effects during the bioconversion process [1].

The latter results in low product yields which in turn increases the downstream processing costs. Hence, the introduction of an intermediate, forward osmosis (FO) Aquaporin Inside<sup>TM</sup> membrane system [2] step targeting water separation and recycling may improve the economy of the process. This separation technology is based on membranes containing naturally occurring water-transport proteins, called aquaporins [3].

Furthermore the factors affecting the metabolic product distribution in pure and mixed microbial consortia (MMC) fermentation are poorly understood. Especially for MMC, it has been attempted to model the product distribution under different operational conditions [4]. Nevertheless, the experimental verification was particularly challenging [5].

### Objectives

The project focuses on investigating the potential to improve biorefinery processes with two different approaches. The first is the coupling of Aquaporin A/S biomimetic membranes with fermentation systems. The second is the investigation of the factors affecting the distribution of the metabolic products in fermentations, based on mixed microbial consortia, with the ultimate goal of controlling and directing the final formation of products.

In short the objectives can be summarised as follows:

- I. Investigating and testing the potential of the Aquaporin Inside<sup>TM</sup> membranes for water recirculation in fermentation processes.
- II. Developing an improved process for production of butanol by *C. pasteurianum* with the use of Aquaporin Inside<sup>TM</sup> membranes.
- III. Finding a direct link between the operating conditions and products formation during fermentations based on pure microbial cultures and mixed microbial consortia.

The overall objective is to develop a cost efficient concept for water recovery, dilution of feedstock and up-concentration of the targeted products that could be implemented in a number of industrial activities.

## Results and discussion

### Membrane separation with crude glycerol as feedstock

The experimental set-up comprised a low osmotic pressure feed solution (fermentation effluent), an Aquaporin Inside™ membrane, and a high osmotic pressure draw solution (concentrated feedstock) (Figure 1). Crude glycerol coming from 2<sup>nd</sup> generation, based on animal fat, biodiesel production was used as the concentrated feedstock and fermentation with *Clostridium pasteurianum* targeted the production mainly of butanol and 1,3 propanediol. Further investigation of important variables was conducted. Osmolality difference and pump cross-flow velocity were assumed as the most important parameters to be optimized through a Central Composite Design.



**Figure 1:** Off-line testing of wheat straw hydrolysate.

### Design of Experiments

Experimental Design has been applied with the use of the statistical optimization software Unscrambler® x 10.3 (CAMO, Norway). Pump cross-flow velocity ( $\text{ml s}^{-1}$ ) and osmotic pressure difference (expressed as draw dilution factor) between the feed and the draw solution were considered as the key factors. Water flux was set as the response of the model. The off-line optimization experiments were conducted with the use of fermentation effluent as the feed solution and crude glycerol as the draw solution. The optimization was carried out by applying a 2<sup>3</sup> Inscribed Central Composite (ICC) design with 3 central point replications. The range of the design variables is presented at the table below (Table 1).

**Table 1:** Range of design variables for optimization of forward osmosis separation.

Parameter	Coded factor levels				
	-a	-1	0	1	a
Pump cross-flow velocity ( $\text{ml s}^{-1}$ )	4.5	6.5	11.5	16.5	18.5
Dilution factor	70	60	35.5	11.1	1

The optimization experiments have shown that the membrane performance, in terms of water flux, ranged between 0.93 and 9.76  $\text{l/m}^2/\text{h}$ . Furthermore high glycerol and butanol rejection has been recorded. The ANOVA analysis has demonstrated that only osmolality

difference can be considered as a statistical significant factor while the pump cross-flow velocity exhibited not any statistically significant effect on the water flux (Figure 2). Finally, there was no interaction of the pump cross-flow velocity and the osmolality difference.

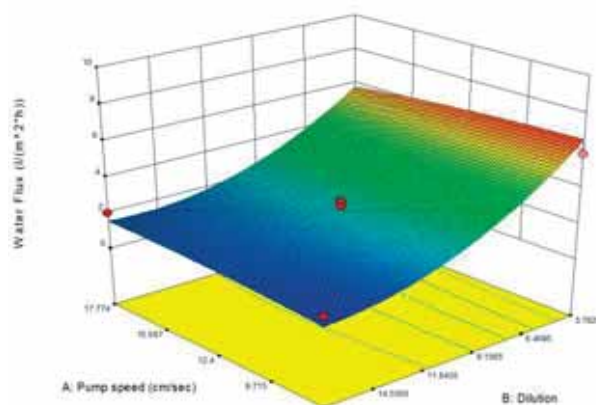


**Figure 2:** Response surface of the experimental design. (Water flux:  $\text{Ln}_{\text{Waterflux}} = 2.11 - 0.103 * \text{Dilution}$ ).

### Future work

The use of Aquaporin Inside™ membrane system has demonstrated significant potential for water recovery during bioconversion processes (off-line testing). A mathematical model simulating the fermentation process and the water recovery in a combined process is under development. A FO membrane module will be designed and tested in-line with a 2 liter bioreactor for verification purposes and an extensive technical-economic analysis will be performed. Furthermore, the variation trend of products yields with the operating conditions during glycerol fermentation by *Clostridium pasteurianum* and mixed microbial consortia will be investigated as well.

### Acknowledgement

The author would like to thank Innovationsfonden for the financial support of the IBISS project and the collaborators from Aquaporin A/S.

### References

1. S. Nicolaou, S. Gaida, E. Papoutsakis, *Metab. Eng.* (12) (2010) 307–331.
2. Y. Zhao, C. Qiu, X. Li, A. Vararattanavech, W. Shen, J. Torres, C. Hélix-Nielsen, R. Wang, X. Hu, A. G. Fane, and C. Y. Tang, *J. Memb. Sci.* (423–424) (2012) 422–428.
3. G. M. Preston, T. P. Carroll, W. B. Guggino, P. Agre, *Science* (256) (1992) 385–387.
4. J. Rodríguez, R. Kleerebezem, J. M. Lema, M. C. M. van Loosdrecht, *Biotechnol. Bioeng.* (93) (2006) 592–606.
5. S. de Kok, J. Meijer, M. C. M. Van Loosdrecht, R. Kleerebezem, *Appl. Microbiol. Biotechnol.* (97) (2013) 2617–2625.

**Sawitree Kalakul**

Phone: +45 50186588  
E-mail: sawit@kt.dtu.dk

Supervisors: Rafiqul Gani  
Georgios Kontogeorgis  
Sponsors: QNRF-Qatar, Alfa Laval Copenhagen,

PhD Study  
Started: June 2013  
To be completed: May 2016

## Property modeling and tailor-made mixture design involving complex chemical systems

**Abstract**

This work proposes an integrated model-based framework for chemical product design and evaluation based on which the software, VPPD-Lab (The Virtual Product-Process Design Laboratory) has been developed. The framework allows the following options: (1) design a product using design templates, such as, single molecule products, formulated products, blended products, emulsified products and devices; (2) analyze the product by performing virtual experiments (product property and performance calculations); (3) create and add new product property and product performance models; (4) create new product design templates when the desired template is not available. The product design templates follow the same common steps in the workflow for a product type but have options to employ product specific property models, data and calculation routines, if necessary. This paper highlights the application of the templates for a tailor-made product design of jet-fuels (blended chemical products).

**Introduction**

In chemical product design, one tries to determine chemical products that exhibit certain desirable properties and improves the product performances. While this procedure is still based on experimental-based trial and error approaches, it is now generally accepted that application of model-based methodologies helps to design/improve products to reach the market faster by reducing costly and time-consuming experiments [1] and experiments are only performed during the last stage as a verification stage. Recent efforts have been concerned with developing model-based methodologies that can handle a large range of chemical product design problems such as a mathematical programming for the design of novel pure, mixed and blended products, a systematic model-based methodology applied to the design of homogeneous formulated products [2], blended products [3] and emulsified products [4]. However, within the currently available methods and tools can only solve a small percentage of product design problems due to lack of needed property models, data and the multidisciplinary nature of many chemical product design problems. This is challenging task requiring data acquisition, data testing, model development, multi-scale modeling that needs to be integrated in a computer-aided framework. The objective is to design, analyse and verify chemical based products in a fast, efficient and systematic

manner. A new and extended version of the product design simulator is presented here [5].

**Objectives of the project**

- (i) Propose a systematic framework for chemical product design and evaluation
- (ii) Implement the framework into a computer aided model-based tool (VPPD-Lab)
- (iii) Apply the framework with several product design case studies (such as tailor made design of jet-fuels, gasoline, emulsion, etc.)

**Framework of VPPD-Lab**

The framework for property modeling and extension of VPPD-Lab is illustrated in Figure 1. The user interface gives 4 main options. Each option is composed of stages: sub-options, algorithms, and tools for a specific task according to the specific problem requirements. The framework allows the use of a suite of tools, such as: (1) property toolbox, the main recurrent toolbox that comprises (i) databases for a very wide range of chemicals, (ii) property models and parameters, (iii) search engine, (iv) property calculation algorithms, and (v) consistency test for pure and mixture data-model parameters; (2) template generator toolbox, (3) experiment toolbox for product verification and guidelines for design of experiments. Furthermore, the framework allows the link and integration with other tools, such as: ModDev (model development

algorithms); ModTem (model template algorithms); MoT (modeling tool); ProCAMD (computer aided molecular design tool); GAMS (The general algebraic modeling system); SolventPro (solvent selection tool); ProPred (pure compound property prediction tool); and TML (Thermodynamic model parameter estimation tool) (ICAS Documentation, 2003).

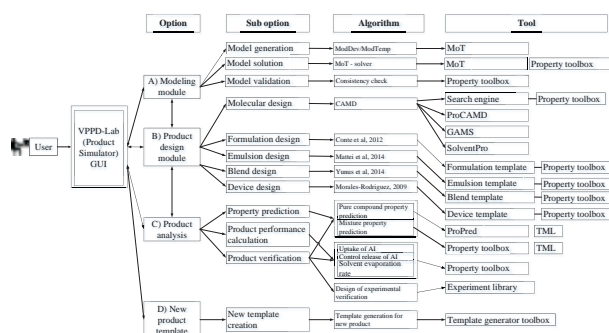


**Figure 1:** Architecture (framework) of the VPPD-Lab software

### Case Study: Tailor-made jet-fuels design

The aim of this case study is the design of a blend containing a main ingredient (MI), which is the conventional A1 jet-fuel and additives to obtain a tailor-made jet-fuel that has properties better than MI.

(1) *Problem Definition:* The new formulation of jet-fuel blends should have good fuel performance and meet or exceed stringent requirements for worldwide fuel handling and products standards as listed in Table 1.

(2) *Problem formulation:* A set of feasible additives is generated using CAMD. Thousands of chemicals are screened through the pure component constraint of molecular weight, which is reduced to 209 chemicals based on the knowledge base and existing products as a benchmark; pure component properties listed in Table 1.

**Table 1:** Standard specification of jet fuel

Need	Target Property	Target Value
Ability to be burned	- Reid vapor pressure (kPa)	RVP < 1
Flammability	- Flash point (K)	$T_f > 311.15$
Engine efficiency	- Higher heating value (MJ/gal)	- HHV > 131.32 - $2.93 < \rho < 3.17$
Consistency of fuel flow	- Density (kg/gallon)	- $V < 8$
Stability	- Kinematic viscosity at -20 °C (cSt)	- $T_m < 226.15$
	- Melting point (K)	-
Environmental impacts	- Gibbs energy of mixing	-
	- CO <sub>2</sub> emission (kg CO <sub>2</sub> /mile)	- $\frac{d}{dx} (G_{mix}/RT) > 0$ - CO <sub>2</sub> < 24.69
	- -logLC <sub>50</sub> (mol/L)	- -log(LC <sub>50</sub> ) < 4.726

(3) *MI(N)LP formulation:* The product design problem is formulated as a Mixed Integer Non-Linear Programming (MINLP) problem, where the fuel composition is to be optimized, subject to target properties. Finally, the most promising ternary blends with the minimum conventional jet-fuels composition are obtained with target properties values. Blending MI

(42% vol) with decane (26% vol) and 4-methylnonane (32% vol) helps to reduce to consumption of MI and help to improve properties (HHV and  $\rho$ ). Furthermore, it reduces CO<sub>2</sub> emission (3.2% compared to MI and 5.78% compared to average jet-fuels) and toxicity (-logLC<sub>50</sub>).

(3) *Model-based/Experimental verification:* Flash point ( $T_f$ ) property model requires an iteration to obtain the flash point of the mixture, thus it is only used for the blends from Step-3.  $T_f$  of all blends are higher than MI and satisfy aviation Jet-A1 standard. Furthermore, experimental toolbox suggests experimental tests to verify V,  $\rho$ , RVP, distillation profiles and JFTOT  $\Delta P$  at 260 °C to ensure that the final blends meet the aviation fuel standards based on these properties.

### Conclusions

A computer-aided framework for design of chemical products has been developed and used as the architecture for the VPPD-Lab software. Blend product design template has been applied for the case study of tailor-made jet fuels design. The product design template is able to handle the large mixed-integer non-linear problem formulated to design the products. It helps to reduce the search space and provides promising chemical candidates that are competitive and are economic and environmentally feasible, making it more flexible and capable of solving a wide range of product design problems.

### Future Work

More Property models for fuels related chemicals, formulated liquid products-processes involving lipids will be developed in order to predict their primary and functional properties. Also, the models will be extended to the specific design procedures. The chemical databases and calculation models for each type of product will be revised and managed through the system information and integrated in order to design a wide range of chemicals based liquid products.

### References

1. R. Gani. Computers and Chemical Engineering (28) (2004) 2441-2457.
2. E. Conte, R. Gani, K.M. Ng. AIChE J. (57) (2011) 2431.
3. M. Mattei, M. Hill, G.M. Kontogeorgis, R. Gani. Computer Aided Chemical Engineering (32) (2013) 817-822.
4. N.A. Yunus, K.V. Gernaey, J.M. Woodley, R. Gani. Computer Aided Chemical Engineering (32) (2013) 835-840.
5. S. Kalakul, R. Hussain, N. Elbashir, R. Gani. Computer Aided Chemical Engineering (37) (2015) 1415-1420.

**Andreas Kamp**

Phone:

+45 21 33 05 17

E-mail:

[ankam@kt.dtu.dk](mailto:ankam@kt.dtu.dk)

Supervisors:

Hanne Østergård

Simon Bolwig

PhD Study

Started:

August 2011

To be completed:

March 2016

## A biophysical perspective on integrated food & bioenergy systems in Ghana

### Abstract

Simple biomass-based fuels such as wood fuels and biogas will continue to be important energy carriers. Emery Assessment (EmA) is a useful tool to evaluate central characteristics of bioenergy, e.g. the biophysical value and renewability of inputs required for their production. Procedures for assessing integrated food and bioenergy systems have been developed in EmA and the special role of human labour inputs has been highlighted. In a case study of integrated versus separated food and bioenergy production, biogas and agroforestry technologies were shown to reduce the need for synthetic fertiliser and soil loss without compromising biophysical efficiency.

### Introduction to PhD project

Challenges of resource scarcity, climate change and energy poverty are partly addressed through the development and implementation of improved energy technologies [1]. Bioenergy carriers are based on biological material. Since biomass is extensively available and relatively simple technologies for converting biomass into useful energy exist, bioenergy remains important, including in a development context.

In a biophysical perspective, a key feature of any energy carrier is the balance between energy output and the energy required to make that energy available. Efficient energy conversions are less wasteful and thus reduce resource use. Nature shows us that higher efficiency can be reached through co-production, and we simulate this in integrated food and bioenergy production. When technologies are assessed in a life-cycle perspective, the accumulated energy dissipation associated with all inputs required for the provision of useful energy in the resulting outputs can be estimated with EmA. This provides us with indications of energy efficiency in a biophysical perspective. This PhD project applies EmA to study integrated food and energy systems (IFES) in Ghana.

### Specific Objectives

Relevant biofuel feedstock in Ghana are identified and quantified, and the useful energy potential is estimated [3]. The EmA methodology is developed by establishing the calculation procedure for assessing IFES [4,5] and elaboration of the importance of and procedures for accounting for human labour inputs [6]. Appropriate

technologies for different scales and end-uses are selected and assessed using the developed methods [7,8,9]. The ability to model results while assuming alternative societal contexts is investigated in scenario modelling based on future narratives [10,11].

### Materials and methods

EmA estimates the accumulated, direct and indirect exergy use (the emergy) in provision of a product or service, in solar equivalent joules (seJ). EmA includes work by natural and human systems alike. The emergy-to-available energy ratio indicates the (biophysical) efficiency of a process in converting scattered solar energy to concentrated available energy [2].

Physical units of input are converted to seJ with unit emery values. Information about the fraction of renewable emery of every input makes it possible to conclude on the renewability of the final output(s).

EmA is particularly useful in the study of integrated systems because of its intrinsic emphasis on system perspective vis-a-vis product perspective. This is important in studies of bioenergy systems where outputs in one subsystem, farming, is considered 'waste' but are then considered 'resources' in another subsystem, bioenergy production. A 'full system' perspective [4] avoids this confusion and eliminates the need for allocation.

EmA accounts for (human) labour inputs alongside material and energy inputs. Labour constitutes the process control function without which little would happen. With no human control, there is no application of information and there is no organisation of material

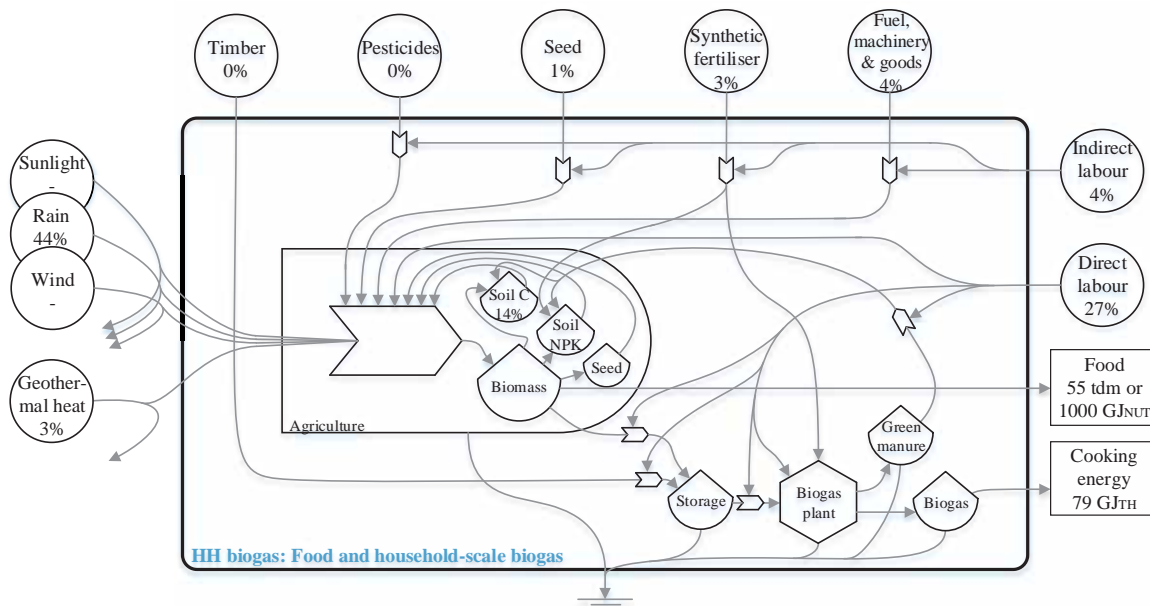


**Figure 1:** An IFES diagram. Percentages refer to the total input of  $2.6 \cdot 10^{17}$  seJ per year on an area of 45 hectares required to yield 55 tdm food and 79 GJ<sub>TH</sub> of cooking energy. Sources on the left are entirely renewable, while other sources are partly renewable (timber, labour) or entirely non-renewable (pesticides, soil).

and energy inputs [6]. Labour is distinguished as directly applied in the assessed process or as embodied labour, accompanying purchased products and services.

#### Assessment example

Four technologies for provision of food and cooking energy in a village in Ghana are evaluated (for an example, see Figure 1). The biophysical efficiency and renewability of each technology is assessed [8].

#### Results and Discussion

Results show that the technologies of integrated food and household-scale biogas, integrated food and village-scale biogas, and agroforestry are equally or more efficient and renewable than the typical technology of separate food and wood fuel production. Interestingly, reductions in fertiliser requirement and soil loss in integrated approaches were almost balanced by increased labour requirements. Labour, mainly direct labour, is shown to be a significant input.

#### Conclusions

A method that accounts for nature's work and human labour inputs, with a scientific definition of renewability, that can manage co-production systems without allocation and adjust for the quality of inputs is a strong analytical tool in assessments of biofuel production. Emergy Assessment has these features, providing valuable insights into highly relevant aspects of environmental sustainability.

Integrated food and bioenergy production appears competitive in terms of efficient resource use and dependence on renewable flows. Emphasis on integrated production may reduce dependence on non-renewable inputs and relieve pressure on soil and forest reserves in Ghana and similar places.

#### Acknowledgements

The work is made possible through the support of 'Biofuel production from lignocellulosic materials – 2GBIONRG' DFC no. 10-018RISØ.

#### References & List of Publications

1. H. Østergård et al., *Journal of the Science of Food and Agriculture* 89 (2009) 1439–1445.
2. H.T. Odum, *Environmental Accounting: Emergy and Environmental Decision Making*. John Wiley and Sons, New York, 1996.
3. F. Kemausuor, A. Kamp, S.T. Thomsen, E.C. Bensah, H. Østergård, *Conservation and Recycling* 86 (2014) 28–37.
4. A. Kamp, H. Østergård. *Emergy Synthesis 7: Theory and Applications of the Emergy Methodology* (2012). University of Florida, Gainesville, USA, 2013, p. 503–511.
5. A. Kamp, H. Østergård, *Ecological Modelling* 253 (2013) 70–78.
6. A. Kamp, F. Morandi, H. Østergård, *Ecological Indicators* 60 (2016) 884–892.
7. A. Kamp, H. Østergård. *Emergy Synthesis 8: Theory and Applications of the Emergy Methodology* (2014). University of Florida, Gainesville, USA, submitted.
8. A. Kamp, H. Østergård, S. Bolwig, submitted to *Emergy for Sustainable Development*.
9. A. Kamp, H. Østergård, *Journal of Cleaner Production*, in preparation.
10. A. Kamp, H. Østergård. *Emergy Synthesis 8: Theory and Applications of the Emergy Methodology* (2016). University of Florida, Gainesville, USA, in preparation.
11. A. Kamp, H. Østergård, *Ecological Economics*, in preparation.



**Malgorzata Kostrzewska**

Phone: +45 4525 2959  
E-mail: malko@kt.dtu.dk

Supervisors: Anne Ladegaard Skov  
Søren Hvilsted

PhD Study  
Started: September 2013  
To be completed: September 2016

## Magnetically activated microcapsules – Preparation and characterization

### Abstract

The scope of the project is to design remotely activated microcapsules. Magnetic nanoparticles (MNPs), which generate heat upon application of an alternating magnetic field, have been incorporated into the microcapsules structure. Properties such as morphology, composition, and encapsulation efficiency were investigated. It was found that microcapsules with relatively high concentration of MNPs could be prepared easily by phase separation technique since a high amount of nanoparticles did not influence negatively on encapsulation efficiency.

### Introduction

The usage of magnetic nanoparticles (MNPs) in hyperthermia for cancer treatment, based on heat dissipation mechanism of MNPs in an alternating magnetic field [1], has inspired us to design magnetically activated microcapsules with the purpose of remotely controlling poly(dimethylsiloxane) (PDMS) cross-linking reaction.

Cross-linking reaction between hydride functional cross-linker and vinyl terminated PDMS occurs at room temperature resulting in formation of a three dimensional network. Enclosing of the cross-linker within a polymeric shell (in this case PMMA) leads to separation of the two compounds [2]. As the release of the cross-linker starts due to externally applied stimulus, the encapsulation technique enables control over the reaction. From a wide range of triggering stimuli [3], only remotely applicable signals were considered, which are capable to activate the microcapsules in hard-to-access places. As the alternating magnetic field (AMF) passes through materials easily, it is a good candidate as an activating stimulus. Moreover, when the magnetic microcapsules are subjected to AMF, their temperature increases due to heat dissipation phenomenon of MNPs. When the temperature inside the microcapsules becomes higher than the glass transition temperature ( $T_g$ ) of the shell, the cross-linker is released.

Influence of concentration of MNPs on microcapsules' properties has been examined. Microcapsules with various types of MNPs were prepared using phase separation technique. Scanning

electron microscopy (SEM), thermogravimetric analysis (TGA) and nuclear magnetic resonance (NMR) were employed to investigate the morphology and the composition of the microcapsules. Reactivity of the microcapsules at temperatures lower and higher than the glass transition temperature ( $T_g$ ) of the shell was investigated by a controlled strain rheological experiments.

### Specific objectives

The aim of this work is to design a method that enables the controlled formation of PDMS networks. It can be done through encapsulation of PDMS cross-linker. Microcapsules should be stable at 50°C and release encapsulated cross-linker in a controlled manner. The release should occur in response to an external stimulus, preferably remotely applied. This approach allows for application of silicone elastomers in traditionally unreachable places.

### Results and Discussion

Magnetic microcapsules containing 20% of the MNPs ( $MnFe_2O_4$ ) were successfully prepared without compromising the impermeable nature of the shell. The nanoparticles are mainly located in the core of the capsule facilitating intact shell structure (Figure 1). Composition of the magnetic microcapsules was investigated by TGA and NMR methods. The residue difference at 700°C for the magnetic and non-magnetic microcapsules, is the amount of inorganic nanoparticles. From Figure 2 it can be seen that mass content of MNP is approximately 20%. The content of the cross-linker

and the polymeric shell was determined by NMR. Due to inherent magnetic properties of MNPs signals coming from PMMA and the cross-linker were undetectable [4]. Therefore, microcapsules were first dissolved in chloroform-d, and the solution was decanted in order to

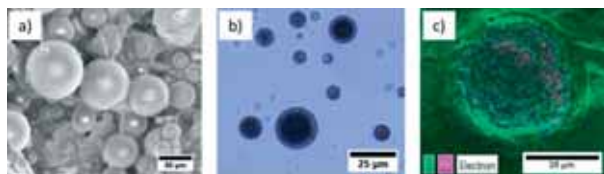


**Figure 1.** Microscopic images of the microcapsules with magnetic nanoparticles. Figure 1a presents SEM images of dried microcapsules, whereas Figure 1b shows microcapsules in a water solution. Distribution of the magnetic nanoparticles (Figure 1c) was investigated by EDS analysis. Purple color represents iron atoms.

remove the MNPs. Peak integration method allowed for determination the ratio between the shell and core materials. It was found that the shell represents 45% of the two compounds. Therefore, 1g of the magnetic microcapsules consists of 0.2g of MNPs, 0.36g of PMMA and 0.44g of HMS-301.

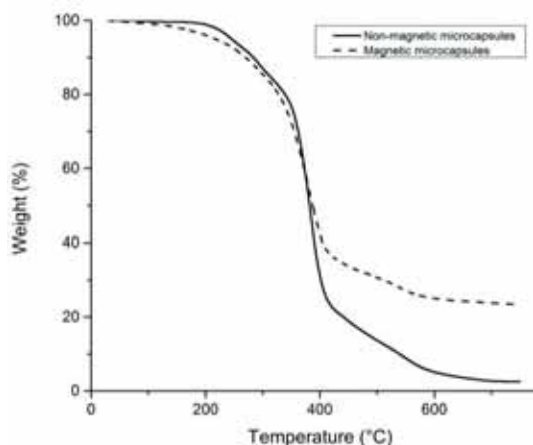


**Figure 2.** Thermogravimetric (TGA) graph showing thermal decomposition of non-magnetic and magnetic microcapsules. The residue difference at 700C is the mass content of the inorganic MNPs.

Encapsulation efficiency was examined by mixing the capsules with a reactive (vinyl-terminated) PDMS. Rheological measurement showed that at 120°C the gel point was achieved after 5 minutes as the storage modulus  $G'$  became higher than loss modulus  $G''$ . While at 50°C the mixture stayed liquid ( $G'' > G'$ ) proving good encapsulation of the cross-linker. Next step is to activate the capsules applying the alternating magnetic field and monitor the temperature of the mixture in order to find out optimal conditions for releasing the cross-linker.

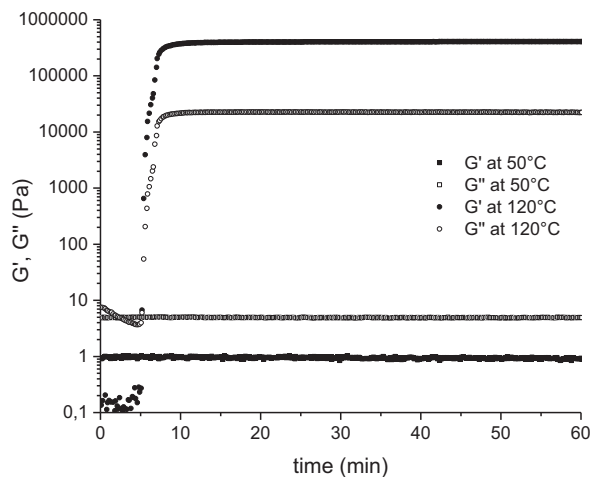


**Figure 3.** Storage and loss moduli of the magnetic microcapsules and vinyl terminated PDMS mixture at different temperatures. The gel point at 120°C was achieved after approximately 5 minutes, whereas the mixture remained stable at 50°C.

## Conclusions

Microcapsules containing magnetic nanoparticles have been successfully prepared using the phase separation technique, which was found to be an universal method for encapsulating the MNPs. Impermeability of the microcapsules has not been reduced although the concentration of encapsulated nanoparticles is 20wt%. Moreover, the capsules are stable at 50°C and the cross-linker is efficiently released at 120°C. Further work will be conducted in order to find optimal magnetic field parameters (frequency, field strength etc.), which will ensure fast response of the system.

## Acknowledgments

I would like to acknowledge Ramona Valentina Mateiu from DTU Center for Electron Nanoscopy for help with EDS analysis. The author is also grateful to the Mærsk Oil & Gas Research, Qatar for founding this project.

## References

1. A. Hervault, K. Nguyen, *Nanoscale*, 6, (2014), 11553-11573
2. L. Gonzalez, M. Kostrzewska, M. Baoguang, L.Li, J. H. Hansen, S. Hvilsted, A. L. Skov, *Macromolecular Materials and Engineering*, 299, (2014), 1259-1267
3. M. Kostrzewska, B. Ma, I. Javakhishvili, J. H. Hansen, S. Hvilsted, A. L. Skov, *Polymers for Advanced Technologies*, 26, (2015), 1059-1064
4. P. Kanhakeaw, B. Rutnakornpituk, U. Wichai, M. Rutnakornpituk, *Journal of Nanomaterials*, 2015, (2015), 121369-79



## Carina Lira Gargalo

E-mail: carlour@kt.dtu.dk  
Discipline: Process Systems Engineering  
Supervisors: Gürkan Sin  
Krist V. Gernaey

### PhD Study

Started: November 2013  
To be completed: May 2017

## Sustainable design of biorefinery systems for biorenewables

### Abstract

The design assessment and design of sustainable chemical/biochemical processes is shown to be a complex multi-criteria/objective decision-making process, not only regarding the multi-level evaluation, but also due to the significant amount of uncertain input data [1]. As a guide through this process, sustainability indicators [2] have been being proposed along the years as a performance measurement tool.

Furthermore, replacing oil in all applications (including plastics, chemicals and other value-added products) by biobased products could be the key to achieve this goal [3]. Therefore, the objective of this project is to develop a framework that allows the user to systematically generate competing solutions and optimal biorefinery options. The framework will be validated through several case studies on the integrated biorefinery concept, such as the production of biodiesel and value-added derivatives from vegetable oil or lignocellulosic biomass.

### Introduction

One of the biorefineries biggest challenges is to develop the ability to sustainably convert different biorenewables into high value-added chemicals and fuels as efficiently as the current petrochemical industry. Moreover, it is important to note that there are significant sources of uncertainty that biorefineries are subject to. Among others, these uncertainties may include market price fluctuations, technical performance variations and environmental model predictions. Several studies have developed methods to create new designs or improve an already existing design by retrofit techniques with the objective of decreasing for instance the energy, water or raw material consumption. Among them, Uerdingen *et al.* (2003), El-halwagi (1998), Rapoport *et al.* (1994), Carvalho *et al.* (2008) and Cheali *et al.* (2013).

However, there is still a need to systematically collect and manage the overwhelming amount of data required for analysis, and to efficiently identify the sources of uncertainty and their propagation into the decision-making procedure. The objective of the present project is to propose a systematic multi-level framework under uncertainty analysis which uses superstructure optimization to obtain a base-case design subject to design constraints and a set of performance criteria. The base-case design will be evaluated through sustainability

analysis in order to logically identify the process hot spots. The obtained information is then used to set design targets for achieving a more sustainable design through retrofitting techniques.

### Discipline

The research is mainly conducted within the field of process systems engineering and sustainable design.

### Research Methodology & Tasks

The objective of this work is achieved by developing a systematic step-by-step methodology. The workflow is presented in Figure 1, and a brief description follows. Part 1 & Part 2: to actively and efficiently manage the data collection by a superstructure generation technique, Part 3: to perform economic analysis under deterministic and uncertainty analysis. Part 4: to perform environmental impact analysis by applying life-cycle assessment models under uncertainty and sensitivity analysis. Part 5: multi-criteria decision making.

Integrating parts 1 to 5, the user will be able to (i) comprehensively collect all the alternatives, (ii) identify the process's critical points, (iii) propose alternatives to overcome them and, (iv) to evaluate the system through a full sustainability set of metrics, under uncertainty and sensitivity analysis.

The framework will be validated by applying it to biorefinery case studies, such as, the lignocellulosic and vegetable oil conversion to biofuels and value-added

chemicals, identifying the respective optimal solutions with respect to the selected set of constraints.

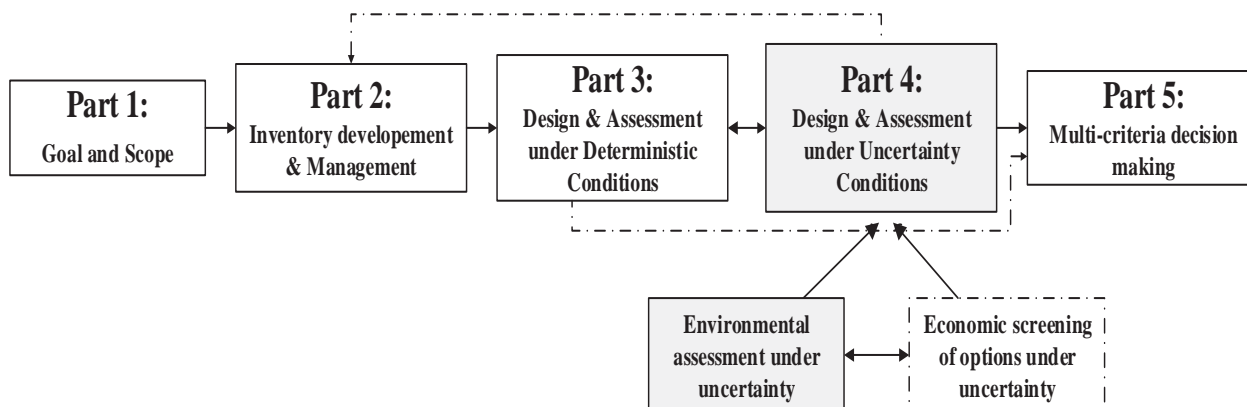


**Figure 1:** Workflow for sustainable process design under uncertainty. Adapted from [9].

### Conclusions

The integrated use of detailed sustainability analysis and life cycle assessment models in selecting the best design has not yet been proposed. Therefore, the framework objective is to systematically generate and identify the optimal flowsheet alternative(s) with respect to the objective function subject to a set of performance criteria given by sustainability metrics involving economic and environmental indicators. The framework, it will be applied to several case studies, such as the production of biofuels and high value added chemicals from vegetable oil and lignocellulosic feedstocks.

### References

1. A. E. Björklund, "Survey of Approaches to Improve Reliability in LCA," *Int. J. Life Cycle Assess.*, vol. 7, no. 2, pp. 64–72, 2002.
2. A. Azapagic, A. Howard, A. Parfitt, B. Tallis, C. Duff, and C. Hadfield, "Sustainable Development Progress Metrics," *ICHEME*, 2002.
3. E. de Jong, R. van Ree, and I. K. Kwant, "Biorefineries: Adding Value to the Sustainable Utilisation of Biomass.," *IEA Bioenergy*, 2009. [Online]. Available: [www.ieabioenergy.com/LibItem.aspx?id=6420](http://www.ieabioenergy.com/LibItem.aspx?id=6420).
4. E. Uerdingen, U. Fischer, K. Hungerbühler, and R. Gani, "Screening for Profitable Retrofit Options of Chemical Processes: A New Method," *AIChE J.*, vol. 49, no. 9, pp. 2400 – 2418, 2003.
5. [5] M. M. El-Halwagi, "Pollution Prevention Through Process Integration: Systematic Design Tools," in *Academic Press, CA., San Diego*, 1997.
6. H. Rapoport and R. Lavie, "Retrofit Design of New Units into an Existing Plant," *Comput. Chem. Eng.*, vol. 18, pp. 743–753, 1994.
7. A. Carvalho, R. Gani, and H. Matos, "Design of sustainable chemical processes: Systematic retrofit analysis generation and evaluation of alternatives," *Process Saf. Environ. Prot.*, vol. 86, no. 5, pp. 328–346, Sep. 2008.
8. P. Cheali, K. V. Gernaey, and G. Sin, "Towards a computer-aided synthesis and design of biorefinery networks – data collection and management using a generic modeling approach," *ACS, Am. Chem. Soc.*, 2013.
9. C. L. Gargalo, K. V. Gernaey, and G. Sin, "Sustainable Process Design under uncertainty analysis: targeting environmental indicators," in *ESCAPE/PSE2015*, 2015.

**Morten Jesper Greisen Larsen**

Phone:  
E-mail:

+45 31 77 45 67  
morjgl@kt.dtu.dk

Supervisors:

Jens Abildskov  
Jakob Kjøbsted Huusom

PhD Study

Started: August 2015  
To be completed: August 2018

## Diabatic separation of fermentation liquids

### Abstract

This PhD project aims to model, simulate, design, and optimize a novel type of diabatic distillation unit operation specifically developed for improving the economics of downstream processing in the bioprocess field. Bioprocesses often involve difficult liquids that are viscous or have solids; a horizontal, tray-less design will improve the processing of such liquids while a mechanical vapor recompression heat integration system will make the unit diabatic, thus less dependent on the steam and cooling water supplies that large scale productions enjoy. As such, the unit will be very suitable for small scale biofuel productions, adding versatility to the use of difficult biomass.

### Introduction

This PhD is part of the project SYNFERON [1], which stands for Optimized SYNgas FERmentation for biofuels production. The overall aim of SYNFERON is to create a complete technological platform for versatile production of synthetic natural gas and alcohols – whichever is favorable at a given time – from biomass of the second generation type, such as straw, wood chips, and similar difficult material. It is important that the platform be relevant in small scale.

SYNFERON is divided into four work packages: Biomass gasification, in which new gasification processes are explored, microbial fermentation of syngas, examining fermentation of the produced natural gas to produce alcohols, concentrating and separation of liquid alcohols will seek new methods within membrane filtration and advanced distillation technology to remove the vast amounts of water present in fermentations processes, and lastly the engineering analysis of proposed platform will combine the packages and analyze and optimize them as a whole, making sure to connect the ends and produce a coherent technology platform as mature for implementation as possible.

This PhD is dedicated to the concentrating and separation of liquid alcohols package and the focus is on advanced distillation technology. A novel constellation for diabatic distillation that is horizontal, tray-less (making it rate-based as opposed to equilibrium-based), and heat integrated with itself, will be defined, modelled, and simulated with the purpose of developing

design methods, control structures, start-up procedures, and economic evaluation.

### Process Description

Based on a recent patent by Biosystemer [2] a horizontal design will be examined. This distillation unit operation employs a stripping section operated at decreased pressure to which the feed is introduced. The feed flows horizontally through the stripper, counter current with a vapor that is being developed in the stripper and carried to the rectifier, which surrounds the stripper, heating it. The horizontal orientation of the unit facilitates better processing of viscous fluids and fluids with solids which are often encountered in the bioprocess industry. Heavy components that cause high viscosity, or solids, will only be present in the stripper, because the rectifier contains only the light components evaporated from the stripper. Different interiors are possible, providing an avenue of optimization.

The developed distillation system will not have trays like a conventional column, which means the separation is rate-based rather than equilibrium based. The liquid flows horizontally in one direction, while the vapor flows counter current to the liquid. This makes the modelling more complicated than that of columns with trays, since transport kinetics from between the phases need to be included.

The internal heat integration is known from the heat-integrated distillation column (HIDiC) design. In the HIDiC design, the rectifier is operated at elevated pressure compared to the stripper making the rectifier hotter than the stripper. This enables heat transfer from

the rectifier, which needs to be cooled, to the stripper, which needs to be heated [3].

### **Modelling and Analysis**

Dynamical models of increasing geometrical complexity will be developed, and a fitting degree of complexity will be chosen for further analysis. Algorithms will be determined and programmed, allowing the simulation of the developed models. Key process parameters will be identified and methods for their estimation will be developed, for each of the different models if necessary. System sensitivity to process parameters and operational variables will be analyzed. System stability will be examined, including bifurcation analysis.

Several aspects of the developed model will pose high requirements of the solution methods. The transport kinetics introduce nonlinearities, the counter current flow pattern leads to inhomogeneous boundary conditions, and two phases in two chambers produces either discontinuities or splitting of variables into phase specific variables, increasing the number of equations. Furthermore, the geometry of the system may call for some mesh generation.

The model needs to be solved using quick algorithms to facilitate design and optimization and integration with the other SYNFERON work packages. To achieve this, high order methods should be applied to get good accuracy with low computation time.

### **Control and Operation**

Based on the studied dynamics, different control paradigms will be developed and simulated. Simple and advanced control systems will be examined and a final control scheme will be proposed. The expected performance of the control structure will be evaluated based on expected fluctuations or disturbances upstream in the process and requirement of providing steady product flow to the downstream. Plant-wide control considerations will also be addressed because versatility is at the heart of the SYNFERON project.

The desired controlled variables are product purity and production rate, and an obvious manipulated variable is the work of the compressor performing the mechanical vapor recompression. To ensure both desired controlled variables can be controlled, it may be necessary to install an additional heater either as a reboiler type heater or a pre-heater.

Start-up and shut-down procedures will also be developed. In the start-up phase, where little vapor is available in the rectifier to heat the stripper, it may also be beneficial with a reboiler before the heat integration gets going properly. Start-up and shut-down are important aspects in a versatile process where gaseous fuel is sometimes preferred of liquid fuel and vice versa.

### **Economic Evaluation**

Based on simulations, the operating costs for utilities will be assessed. The overall cost in terms of pr. unit purified biofuel will be determined. A simplified

economic model, separate from the rate-based model will be developed enabling quick economic evaluation of different implementation scenarios.

The ambition of the SYNFERON project is to reduce the costs of the downstream processing, including membrane and distillation, by 30-60% compared to current methods [1]. The diabatic distillation itself is expected to have a reduction of 40-60% compared to conventional adiabatic distillation.

### **Conclusion**

The project will provide the entire toolbox required for design and optimization of a novel type of distillation, capable of cutting downstream processing costs of biofuel productions in small scale.

The distillation unit will be modelled with high accuracy and fast convergence of high order solution methods for systems of partial differential equations. Fast solution makes the system compatible with future optimization and process design.

Control options will be examined and the need for added utility will be determined. The control structure will fit into the SYNFERON concept and as such needs to be versatile, being able to aptly turn from one product to another.

The economic evaluation must result in a cost reduction of 30-60%, compared to current methods, to be considered successful. The diabatic distillation should do its part with an expected cost reduction of 40-60% compared to conventional distillation.

### **References**

1. G. Kontogeorgis, SYNFERON-Optimised syngas fermentation for biofuels production, Project Application, 2014.
2. E. Jensen, US Patent 7972423 B2, Rectification apparatus using a heat pump.
3. A. A. Kiss, J. Chem. Tech. & Biotech. 89 (4) (2014) 479-498.



**Hilde Larsson**

Phone: + 45 4525 2993  
E-mail: hila@kt.dtu.dk

Supervisors: Ulrich Krühne  
Krist Gernaey  
Anne Ladegaard Skov

PhD Study  
Started: December 2012  
To be completed: November 2015

## Modeling of oxygen transfer in a 1 ml microbioreactor and a 8 ml magnetically stirred reactor

### Abstract

The aim of this PhD project is to use computational fluid dynamics (CFD) to increase the understanding of mass transfer phenomena in chemical and biochemical reactors. The case studies presented here describe the CFD modeling of oxygen transfer in a 1 ml microbioreactor and an 8 ml magnetically stirred reactor using the eddy cell model and the simulated specific interfacial areas. The simulated data is compared to experimental results.

### Introduction

The most common way to describe oxygen transfer in bioreactors is via the oxygen transfer coefficient,  $k_L a$ , which describes the dynamic relationship between the oxygen concentration ( $C$ ) and the oxygen saturation concentration ( $C_{sat}$ ) assuming a perfectly mixed liquid according to the following:

$$\frac{dC}{dt} = k_L a (C_{sat} - C) \quad 1$$

In CFD simulations  $k_L a$  is often calculated as the product of the simulated mass transfer coefficient  $k_L$  and the simulated specific interfacial area. The eddy cell model [1] displayed in Equation 2 is often used to model  $k_L$ .

$$k_L = \sqrt{D_\phi \epsilon} \quad 2$$

In Equation 2 is  $D_\phi$  the mass diffusion coefficient,  $\nu$  the kinematic viscosity,  $\epsilon$  the turbulent energy dissipation rate and  $C_p$  an often used case-specific constant.

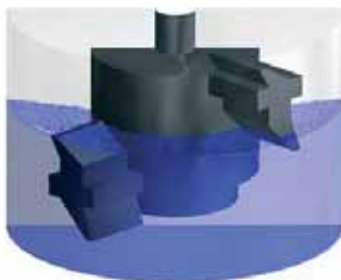


**Figure 1.** The microbioreactor filled with 1 ml liquid.

### Specific objectives

The specific objective of this PhD project is to explore mass transfer phenomena in chemical and biochemical reactor systems using CFD. The here presented case studies describe the simulation of oxygen transfer in a microbioreactor developed for fermentation purposes previously presented at [2] and in a magnetically stirred reactor.



**Figure 2.** The magnetically stirred reactor filled with 8 ml liquid.

### Method

The CFD software ANSYS CFX 15.0 was used to simulate both the microbioreactor and the magnetically stirred reactor displayed in Figure 1 and 2. The  $k$ - $\epsilon$  turbulence model was used and the two-phase flow (air and water) was simulated with the free-surface interfacial model. The gas-liquid interface was defined as where the volume fraction of water was 0.5, and the area of this interface was calculated with help of the

software. These areas were used to calculate the simulated specific interfacial areas.

The values of  $\epsilon$  were calculated as the liquid phase averages, the liquid phase maximal and the gas-liquid interface averages. The values of  $\epsilon$  in the reactors were directly simulated by the applied turbulence model. The values of  $\epsilon$  were inserted into Equation 2 for the simulation of  $k_L$ , and the case specific proportionality constants  $C_P$  were found by correlating the simulated and experimental  $k_{L,A}$  values.

The experimental  $k_{L,A}$  values for the microbio reactor were previously published in [2]. The oxygen transfer rates for the magnetically stirred reactor were experimentally determined by recording the dissolved oxygen recovery profiles in the liquid phase with an optical sensor from PyroScience GmbH, Germany.

### Results and Discussion

The appearances of the gas-liquid interfaces and the specific interfacial areas for the microbio reactor are displayed in Figure 3. The rotational speed has a large impact both the location of the (turquoise) liquid phase and on the appearance of the gas-liquid interface (green). The effect of the rotational speed on the specific interfacial areas in the magnetically stirred reactor was not as large (data not shown).

The simulated and experimental  $k_{L,A}$  values are displayed in Figure 4 for the microbio reactor and in Figure 5 for the magnetically stirred reactor. The interface averaged data is not displayed in Figure 3 since it was very close to the volume averaged value. The varying proportionality constants  $C_P$  are described in the legends.

The experimental  $k_{L,A}$  values are higher for the microbio reactor than for the magnetically stirred reactor, which is mainly explained by larger specific interfacial areas.

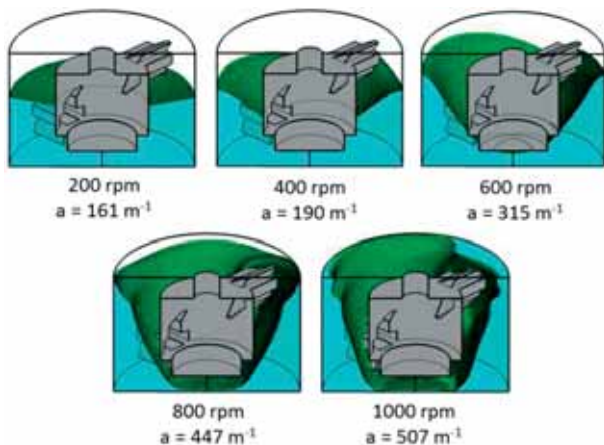


**Figure 3.** The appearances of the gas-liquid interfacial areas and the specific interfacial areas in the microbio reactor.

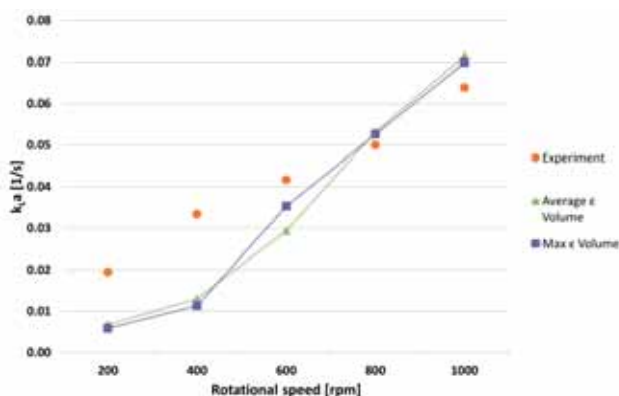


**Figure 4.** The simulated and experimental  $k_{L,A}$  values for the microbio reactor.  $C_P$  was set to 0.13 for the volume averaged  $\epsilon$  and to 0.07 for the maximal values.

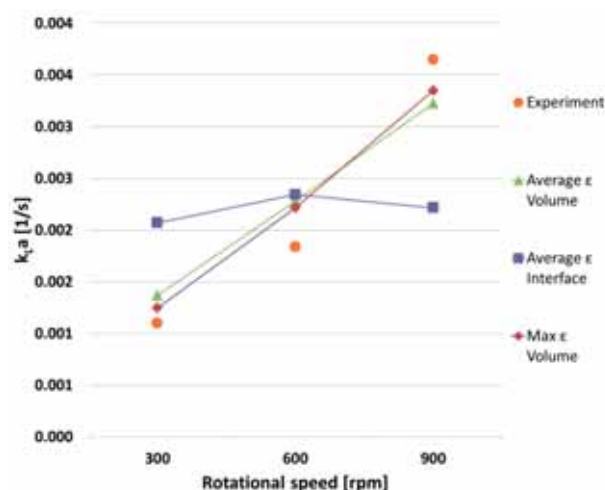


**Figure 5.** The simulated and experimental  $k_{L,A}$  values for the magnetically stirred reactor.  $C_P$  was set to 0.11 for the volume averaged data, 0.04 for the maximal values and 0.07 for the interface averaged values.

### Conclusions

By applying the eddy cell model in combination with CFD it was possible to achieve simulated data close to experimental results for the two case studies. The proportionality constants  $C_P$  varied however between the cases and for the different methods to quantify  $\epsilon$ .

### Acknowledgements

This PhD project is funded by Novo Nordisk Foundation.

### References

- Lamont, J.C. & Scott, D.S., 1970. An eddy cell model of mass transfer into the surface of a turbulent liquid. *AIChE Journal*, 16(4), pp.513–519.
- Bolić, A., Krühne, U., Prior, R. A., Vilby, T., Hugelier, S., Lantz, A. E., Gernaey, K. V., 2012. One-Millilitre Microbio reactor with Impeller for Improved Mixing, Poster presented at IMRET12.



## **Yashasvi Laxminarayan**

Phone: +45 4525 2853  
E-mail: ylax@kt.dtu.dk

Supervisors: Peter Glarborg  
Peter Arendt Jensen  
Flemming Frandsen  
Martin Bøjer, DONG Energy

PhD Study  
Started: October 2014  
To be completed: October 2017

## **Adhesion strength of biomass ash deposits**

### **Abstract**

This study investigates the shear adhesion strength of biomass ash deposits on superheater tubes. Artificial biomass ash deposits were prepared on superheater tubes and sintered in an oven at temperatures up to 1000°C. Subsequently, the deposits were sheared off by an electrically controlled arm, with the corresponding force measured by a load cell. Higher sintering temperatures resulted in greater adhesion strengths, with a sharp increase observed near the deformation temperature of the ash. Repetition of the experiments revealed considerable variation in the obtained adhesion strengths, portraying the stochastic nature of the debonding process.

### **Introduction**

One of the major operational problems encountered during biomass combustion in boilers is the formation of ash deposits on boiler surfaces, especially on convective pass tubes, thereby hindering heat transfer to the steam cycle. Ash deposition adversely influences the boiler efficiency and may completely block flue gas channels in severe cases, causing expensive unscheduled boiler shutdowns. Furthermore, ash deposits may cause severe corrosion of boiler surfaces. Therefore, timely removal of ash deposits is essential for optimal boiler operation.

Natural as well as artificially induced shedding of ash deposits may be caused by several mechanisms including erosion, debonding, molten slag flow, and thermal and mechanical stresses in the deposits [1]. Debonding is the dominant mechanism for shedding of dense and hard deposits in biomass boilers, occurring when the generated stress (e.g. by soot-blowing or due to the inherent weight of the deposit) exceeds the adhesion strength at the tube-deposit interface [2]. Hence, quantification of the adhesion strength of ash deposits is crucial for the understanding of deposit shedding as well as the estimation of required soot-blower pressures.

### **Specific Objectives**

The objective of the present work is to quantify the shear adhesion strength of biomass ash deposits on superheater tubes under different boiler conditions to determine the effect of boiler and steel surface temperature, sintering duration, ash particle size and

steel type. Moreover, the study aims to develop a model in order to optimize soot-blowing in boilers based on the obtained experimental data.

### **Experimental Approach**

An attempt to replicate boiler deposits has been made in this experimental analysis, by preparing artificial deposits using fly ash particles on superheater tubes, and allowing them to heat up and sinter inside an oven at a specified temperature. Higher sintering temperatures are used to simulate the deposit formation process (since the fly ash is at a much higher temperature before condensing on the tubes) as well as longer sintering times. In order to obtain tightly packed and adherent deposits, the fly ash particles were mixed with a water-isopropanol solution (50 vol%) to prepare a thick slurry, and moulded into a cubical shape using a Teflon mould, on the surface of the tube.

Experimental analysis was carried out using pure KCl (Sigma Aldrich), as well as fly ash obtained from a straw-fired grate boiler, a wood-fired suspension boiler, and a wood+straw co-fired suspension boiler. TP347HFG steel tubes (Salzgitter Mannesmann) were used for the experiments. Pre-oxidation of the steel tubes prior to strength measurements is beneficial for replicating operational boiler tubes. Based on inferences drawn from thermogravimetric analysis of the steel, the steel tubes were pre-oxidized for 24 hours at 600°C prior to conducting strength measurements.

The artificial deposits were allowed to sinter inside the oven for a fixed duration, followed by shear strength measurements at a specified temperature, where an

electrically controlled arm was used to de-bond the artificial deposit from the superheater tube, as shown in Fig. 1. The arm was controlled using a linear actuator and the corresponding force applied on the ash deposit was measured using a load cell. In order to estimate the reproducibility of the measurements, strength measurements were conducted on 4 artificial deposit samples for each instance of experimental conditions.

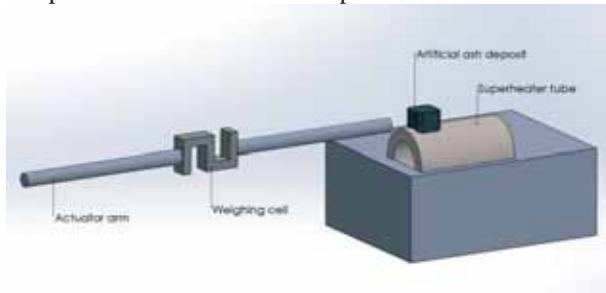


**Figure 1:** Experimental setup for adhesion strength measurements.

### Results and Discussion

The primary results obtained from this study outline the effect of sintering temperature on shear adhesion strength for pure KCl as well as the aforementioned fly ashes. As shown in Fig. 2, the shear adhesion strength usually increases with increasing sintering temperature. However, a sharp increase in the adhesion strength is observed for temperatures close to the ash deformation temperature (point of initiation of melting [3]) or melting point, 640°C for straw fly ash and 770°C for KCl. This is due to the formation of a partially molten film at the interface, with increased surface wetting leading to higher surface adhesion. For example, straw fly ash, which is predominantly a mixture of KCl and  $K_2SO_4$ , forms a eutectic system. Above its deformation temperature of 640°C, a molten, KCl-rich phase is formed, which adheres to the tube surface, firmly solidifying when the temperature is reduced to 600°C for strength measurements. This scenario is similar to the actual deposit formation process, where the initial deposits at the interface are formed by the condensation and subsequent solidification of fly ash [1]. Similar results have been observed in the literature with molten coal ash particles, where the presence of a liquid film at the interface resulted in the formation of strong deposits [4]. The sharp increase in adhesion strengths for wood fly ash and the straw+wood co-fired fly ash has not been observed in this study due their high ash deformation temperatures, 1220°C and 1240°C respectively.

Furthermore, it should be noted that the standard deviation for the obtained data is considerably high, particularly for high adhesion strengths. This represents the stochasticity of the debonding process, as seen in real-life scenarios. For large-scale boiler soot-blowing probe measurements, it has been observed that deposits are removed over a wide range of soot-blowing peak impact pressures (PIP) [5]. Other studies have also identified the considerable scatter present in the adhesion strength of boiler deposits [6].

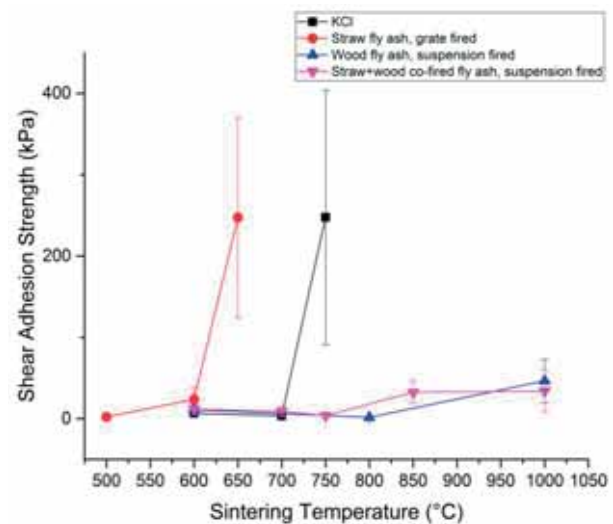


**Figure 2:** Effect of sintering temperature on shear adhesion strength for KCl and different fly ashes. Measurement temperature- 600°C, sintering time- 4 hours, steel tubes pre-oxidized for 24 hours.

### Conclusions

In this study, the shear adhesion strength of KCl and artificial fly ash deposits has been investigated at different sintering temperatures. Higher sintering temperatures lead to greater adhesion strengths, with a sharp increase observed near the melting point of the ash. Furthermore, a relatively large variation in the deposit adhesion strengths was observed, portraying the stochastic nature of the debonding process.

Future work is being directed towards the determination of adhesion strength of model fly ash deposits, containing pre-determined mixtures of KCl,  $K_2SO_4$ ,  $K_2CO_3$ , CaO and  $SiO_2$ . Furthermore, the effect of particle size, sintering duration and measurement temperature will be investigated. Finally, strength investigations will be conducted using different superheater steel samples. Based on the obtained experimental data, a model is being developed in ANSYS-Fluent to optimize soot-blowing in boilers. Apart from investigating the shear strength of ash deposits, a setup is being designed and constructed to measure the tensile strength of the ash deposits to superheater steel surfaces.

### References

1. F. Frandsen, Ash formation, deposition and corrosion when utilizing straw for heat and power production, Lyngby, Denmark, 2011.
2. A. Zbogor, F. Frandsen, P.A. Jensen, P. Glarborg, Prog. Energy Combust. Sci. 35 (2009) 31-56.
3. European Standards on Solid Biofuels. CEN/TS 15370-1:2006.
4. A.K. Moza, L.G. Austin, Fuel 60 (1981) 1057-1064
5. M.S. Bashir, P.A. Jensen, F. Frandsen, S. Wedel, K. Dam-Johansen, J. Wadenback, Energy & Fuels 26 (2012) 5241-5255.
6. A. Kaliazine, D. Cormack, A. Ebrahimi-Sabet, H. Tran, J. Pulp Paper Sci. 25 (1999) 418-424.

**Kasper Hartvig Lejre**

Phone: +45 4525 2957  
E-mail: kasphal@kt.dtu.dk

Supervisors: Søren Kiil  
Peter Glarborg  
Philip Fosbøl  
Henrik Christensen, MAN Diesel & Turbo

PhD Study  
Started: October 2015  
To be completed: October 2018

## Mathematical modelling of sulfuric acid accumulation in lube oil in diesel engines

### Abstract

In recent years, large ships have started to operate at reduced load in order to decrease the fuel consumption. As a consequence, “cold corrosion” has turned out to be a serious problem in the engines. The scope of this project is to investigate how  $\text{H}_2\text{SO}_4$  is formed, transported, and neutralized in the lubricant oil film on the cylinder walls. The conditions inside the cylinders will be reproduced in laboratory experimental setups, where the different subprocesses can be studied separately.

### Introduction

Focus on optimizing the operation of marine engines, with respect to reducing the fuel oil consumption, has always been of great importance. Some years ago, ship operators have taken to run engines at reduced speeds (so-called “slow-steaming”) as a means of reducing fuel oil consumption, which leads to colder cylinder liners. Since the shipping sector currently suffers from over-capacity on the world market, the slow-steaming approach is possible to implement. On new engines, engine designers have reduced the fuel oil consumption by increasing the pressure in the combustion chamber among others. This and the decrease of the temperature on the cylinder liners allow sulfuric acid and water to condense to a greater extent on the cylinder liners in the engines which promotes “cold corrosion”. The phenomenon is a mixture of chemical corrosion from the acid and mechanical wear. Expensive lubrication oil with limestone is continuously added to the cylinders to neutralize the sulfuric acid generated, but the efficiency of this procedure is not always optimal. A certain degree of corrosion is, however, beneficial on the cylinder liners, making the liner surface a little rough. This means that the cylinder liner surface can better maintain a protective oil film. However, uncontrolled cold corrosion destroys the liners and piston rings [1].

### Specific Objectives

This PhD project is a part of a large research project (SULCOR) in corporation with MAN Diesel & Turbo A/S, DTU Chemical Engineering (KT), and DTU Mechanical Engineering (MEK), where the combined

output from the different projects should lead to new engine designs and/or new operational engine procedures, which will consume less lubrication oil. The main core of this PhD project is to develop a mathematical model that can predict conditions prevailing at the oil-cylinder liner interface, where corrosion takes place. The cast iron tribo-corrosion process is handled in another PhD project at KT, where this PhD project provides the boundary condition data required. Other PhD/Post doc projects at MEK will provide valuable information on e.g. oil flow pattern, gas phase composition, and the actual formation and condensation of  $\text{H}_2\text{SO}_4$  on an oil film under laboratory conditions (lube oil test rig). The project objectives cover the following:

- A literature study on diesel engines, lube oils, and the chemistry of a selected running engine.
- Collection and analysis of spent lube oil from selected full-scale diesel engines.
- Development of the analysis technique.
- Design and construction of mixed flow reactor setup for  $\text{H}_2\text{SO}_4/\text{SO}_2$ -lubrication oil experiments.
- Mapping and quantification of acid generation, transport, and neutralization mechanisms in a running diesel engine.
- Mathematical modelling of sulfuric acid accumulation in lube oil in diesel engines.
- Recommendations for practical use of the results from the different subprojects.

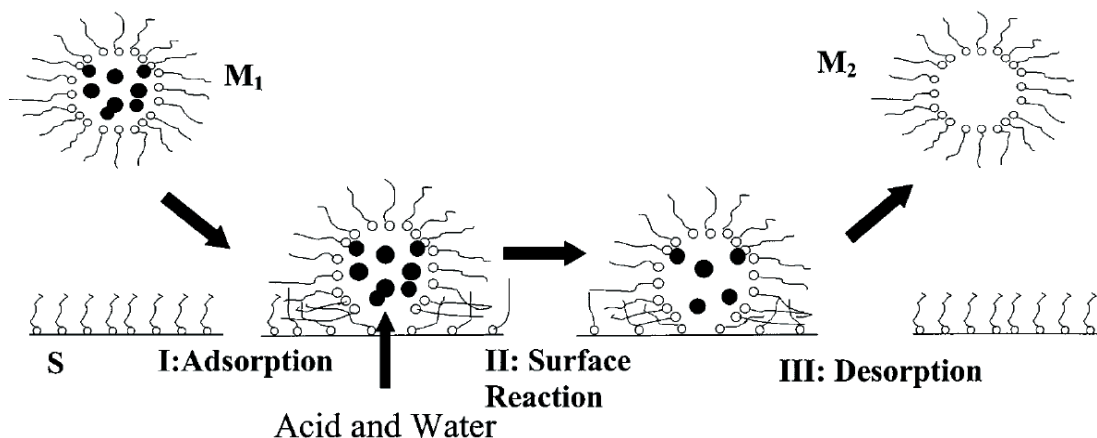


**Figure 1:** Proposed neutralization mechanism between an overbased detergent reverse micelle ( $M_1$ ) and an oil-acid interface (S).

### Results and Discussion

The ability of lubrication cylinder oil to neutralize  $H_2SO_4$  is essential for preventing the uncontrolled cold corrosion of the cylinder liners [2]. This ability is quantified by the cylinder oils base number (BN), which is defined as ‘the quantity of acid – expressed in terms of the equivalent number of milligrams of the alkaline potassium hydroxide – that is required to neutralize all alkaline constituents in one gram of cylinder oil’ [3]. The BN of cylinder oil is equal to the amount of overbased detergents added, e.g. calcium carbonates ( $CaCO_3$ ). These overbased detergents exist as reverse micelles which provide  $CaCO_3$  to react with the formed  $H_2SO_4$  through the proposed reaction mechanism presented in Figure 1 [4]. The first step of the reaction mechanism is the adsorption (I) of the reverse micelle ( $M_1$ ) on the acid-oil interface (S) followed by the neutralization reaction (II) between  $CaCO_3$  and  $H_2SO_4$ . Following the neutralization reaction, the reverse micelle becomes  $M_2$ , where  $H_2O$  and reaction products are solubilized. Finally, the  $M_2$  is desorbed from the interface (III) [4]. It is observed that the adsorption step (I) of the overbased reverse micelles is the rate-limited step [4]–[6]. This suggests that the neutralization reaction between  $CaCO_3$  and  $H_2SO_4$  is diffusion-controlled. This neutralization mechanism is based on experiments, where a drop of  $H_2SO_4$  is introduced into a lube oil phase. The fate of the acid drop and the surrounding oil phase is then monitored visually [4]–[6].

It is, however, unknown whether this proposed mechanism can be used to describe the neutralization reaction mechanism in a working oil film in a marine diesel engine. While currently in the initial steps of the project, a laboratory setup is planned to investigate this. Other possible important parameters will also be investigated in these measurements, such as the impact of  $SO_2$ ,  $O_2$ , temperature, etc., on the oil-acid mechanism. The marine cylinder lubrication oils are analyzed by an automated titration procedure following the standard test method D2896 [7].

### Conclusion

The cold corrosion problem is a significant problem in the marine industry, where the cylinder liners and piston rings corrode; if not a proper lubrication system is used. Since this procedure is not always optimal and very expensive, it is desirable to understand the underlying processes in the oil-acid system inside the engines with the purpose of constructing new engine designs and/or new operational engine procedures, which will consume less lubrication oil. This is done by gaining knowledge about how  $H_2SO_4$  is formed, transported, and neutralized in diesel engines.

### Acknowledgements

This work is part of the Combustion and Harmful Emission Control (CHEC) research center at the Department of Chemical and Biochemical Engineering at Technical University of Denmark. The project is funded by the Innovation Fund Denmark and co-sponsored by MAN Diesel & Turbo A/S and Technical University of Denmark.

### References

1. D. Atkinson, 11th Int. Conf. Cond. Monit. Mach. Fail. Prev. Technol. C. 5 (2) (2014) 17-22.
2. A. K. van Helden, M. C. Valentijn, H. M. J. van Doorn, Tribol. Int. 22 (3) (1989) 189-193.
3. Chevron, Marine Lubricants Information Bulletin 4: Base number (2013) 1-2.
4. R. C. Wu, K. D. Papadopoulos, C. B. Campbell, AIChE J. 46 (7) (2000) 1471-1477.
5. R. C. Wu, C. B. Campbell, K. D. Papadopoulos, Ind. Eng. Chem. Res. 39 (10) (2000) 3926-3931.
6. R. C. Wu, K. D. Papadopoulos, C. B. Campbell, AIChE J. 45 (9) (1999) 2011-2017.
7. ASTM International, ASTM 2896-11: Standard test method for base number of petroleum products by potentiometric perchloric acid titration (2011) 1-9.



## Kasper Linde

Phone: +45 2249 6663  
E-mail: kaspli@kt.dtu.dk  
Discipline: Catalysis and Reaction Engineering

Supervisors: Anker D. Jensen  
Brian B. Hansen  
Peter A. Jensen  
Pär L.T. Gabrielsson, Haldor Topsoe A/S

### Industrial PhD Study

Started: July 2013  
To be completed: June 2016

## New catalytic materials for combined particulate and NO<sub>x</sub> removal from diesel vehicles

### Abstract

A combined particulate filter and selective catalytic reduction unit for NO<sub>x</sub> removal holds a great potential with respect to reducing the overall size and cost of the automotive diesel exhaust aftertreatment system. This project will develop and test catalytic systems with the required combination of soot oxidation and selective catalytic reduction properties without unwanted side reactions such as NH<sub>3</sub> oxidation. The main focus is now on mechanically mixed systems of a soot oxidation catalyst and a NH<sub>3</sub>-SCR catalyst, and identifying and taking advantage of the potential synergies of such a system.

### Introduction

Heavy duty diesel (HDD) vehicles handle a substantial part of the global transport and logistics. Harmful pollutants, such as nitrogen oxides (NO<sub>x</sub>), hydrocarbons (HC), particulate matter (PM), and carbon monoxide (CO), are however formed. The diesel exhaust aftertreatment (DEA) system has been developed to treat the pollutants in the exhaust gas.

Figure 1 illustrates the current standard DEA system consisting of a series of catalytic units. The Diesel Oxidation Catalyst (DOC) oxidizes CO and HC to CO<sub>2</sub> and H<sub>2</sub>O, and generates NO<sub>2</sub> from NO as well. The Diesel Particulate Filter (DPF) is a wall-flow filter, entraining PM in its monolith walls. The DPF can be regenerated actively by increasing the exhaust gas temperature using post-injection of fuel, or passively using a catalyst. NO<sub>2</sub> generated by the DOC also assists regeneration. NO<sub>x</sub> is targeted through Selective Catalytic Reduction (SCR) using NH<sub>3</sub> as the reducing agent. NH<sub>3</sub> is supplied to the system through urea dosing, regulated by the onboard Model Predictive Control (MPC) unit. Excess NH<sub>3</sub> is controlled with the Ammonia Slip Catalyst (ASC). Upon exiting the DEA system, the emissions should meet the restrictions imposed by the Euro VI, US LEV III or similar regulations.

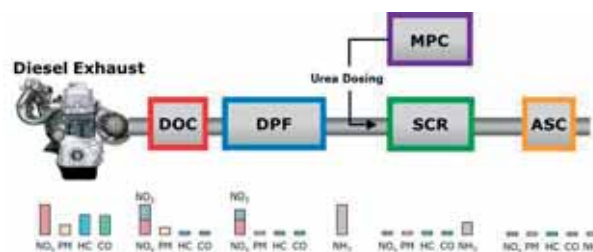


**Figure 1:** Example of a standard design of the DEA system, consisting of the DOC, DPF, SCR component, urea dosing MPC unit, and the ASC.

The DEA system is very complex, requiring efficient exhaust treatment for a wide range of transient operating conditions, corresponding to cold start, stop-and-start driving (inner city), and high speed driving (highways). As a result, DTU Chemical Engineering and Haldor Topsoe A/S are collaborating on the development of the next generation DEA system, with funding from The National Danish Advanced Technology Foundation. The underlying PhD projects concerns the development of new DOC and ASC formulations (Thomas Klint Hansen at CHEC); the combination of the DPF and SCR components (present project); model development of the control unit for efficient urea dosing system (Andreas Åberg at CAPEC-PROCESS); and advanced characterization of diesel exhaust catalysts (Ian Joseph Allen at CHEC and Haldor Topsoe A/S).

### Specific Objectives

The two largest components of the DEA system are the DPF and the SCR. A combination of these could therefore result in a considerable reduction in cost, size, and warmup time of the overall system. In order to achieve this, the present project will develop catalytic materials for combined particulate and NO<sub>x</sub> removal. This will be done by applying catalyst synthesis, characterization, kinetic lab-scale studies and pilot scale tests.

In order to develop such a unit with catalytic activities for combined soot and NO<sub>x</sub> removal, two overall coating approaches may be used: Zone coating of the filter, allowing deposition of different catalytic formulations in different zones of the filter (e.g. entrance or exit); or a multi-function catalyst coating, which has activities for both reactions simultaneously. Both approaches have advantages and disadvantages, but a major benefit of the multi-function coating is a potentially simpler production.

### Multi-function Coatings

The multi-function coatings can be further divided into subtypes, distinguished by the degree of mixing between the catalytic systems or activities, see Figure 2:

Layered coatings (Figure 2a) consist of independent systems, washcoated onto the substrate separately, resulting in minimal mixing of the catalysts. Hence, the layered coatings consist of 2 systems in 2 washcoats.

Mechanically mixed coatings (Figure 2b) are prepared by mixing already prepared catalytic systems, before they are washcoated in a single layer onto the substrate. This results in a washcoat with 2 systems in close contact with each other, but minimal chemical contact between the catalytic components.

The chemically mixed coatings (Figure 2c) consist of a single catalytic system, with catalytic activities for both reactions. The benefit of this system is that the production procedure is very simple, as it only contains 1 system in 1 layer. However, a major disadvantage of the chemically mixed coatings is to find a catalytic system with multiple activities, especially when these activities include both oxidizing and reducing reactions.

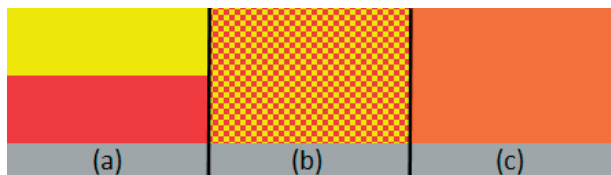


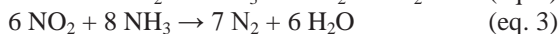
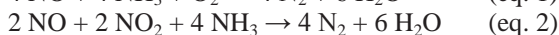
**Figure 2:** Three different types of multifunction coatings on a substrate (grey): Layered coatings (a); mechanically mixed coatings (b); and chemically mixed coatings (c).

### NO<sub>2</sub> Challenges of Combined Filters

One of the major challenges for a combined filter is maintaining sufficient NO<sub>2</sub> for both passive soot oxidation and increased SCR activity.

NH<sub>3</sub>-SCR consists primarily of three reactions: standard SCR (eq. 1), fast SCR (eq. 2), and slow SCR

(eq. 3). It can be seen from the equations that they are dependent on the NO<sub>2</sub>/NO<sub>x</sub> ratio with standard SCR occurring with excess NO, slow SCR with excess NO<sub>2</sub> and fast SCR with equimolar amounts of NO and NO<sub>2</sub>.



In Figure 3 it can be seen that equimolar amounts of NO and NO<sub>2</sub> results in the highest SCR activity (DeNO<sub>x</sub> activity), especially at lower temperatures. Furthermore it is seen that slow SCR (excess NO<sub>2</sub> in the feed) results in less DeNO<sub>x</sub> activity than the other reactions. The SCR catalyst will therefore be most efficient if the NO<sub>2</sub>/NO<sub>x</sub> ratio at the catalyst is close to 50%, less rather than more. [1]

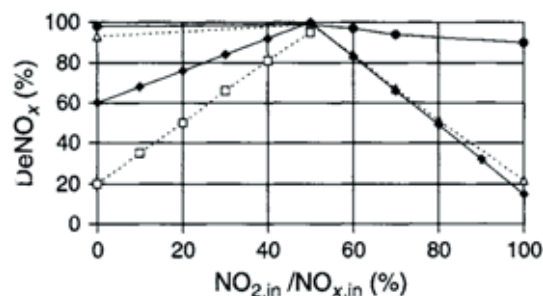


**Figure 3:** Influence of the NO/NO<sub>2</sub> ratio on the DeNO<sub>x</sub> activity of a coated V<sub>2</sub>O<sub>5</sub>/WO<sub>3</sub>-TiO<sub>2</sub> SCR catalyst. (□) 200°C, (◆) 250°C, (Δ) 300°C, (●) 350°C. 1000ppm NO<sub>x</sub>, NH<sub>3</sub> (10 ppm slip), 5% H<sub>2</sub>O, 10% O<sub>2</sub>, balance N<sub>2</sub>. [1,2]

NO<sub>2</sub> is also important for the soot oxidation. As can be seen from Figure 4, NO<sub>2</sub> is a better oxidant of soot, and allows for soot oxidation at lower temperatures, than O<sub>2</sub>. Preliminary results from experiments at DTU Chemical Engineering indicates that soot, under realistic fast SCR conditions (300ppm NO, 300ppm NO<sub>2</sub>, 600ppm NH<sub>3</sub>, 10% O<sub>2</sub>, 5% H<sub>2</sub>O, 675 mL/min, 400°C, and 100 mg Printex U model soot) will react with NO<sub>2</sub> yielding NO.

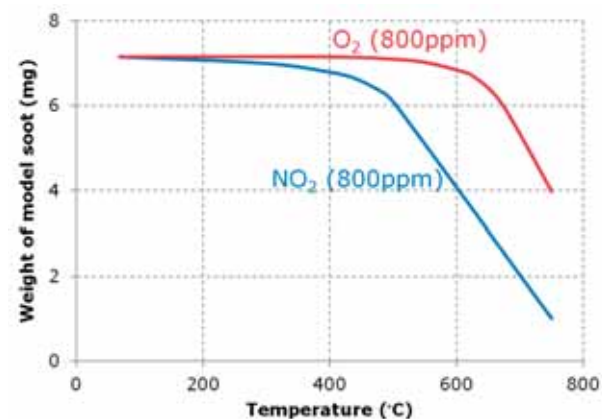


**Figure 4:** Oxidation of model soot (Printex U) in 800ppm O<sub>2</sub>/N<sub>2</sub> and 800ppm NO<sub>2</sub>/N<sub>2</sub>. Heating rate 100°C/hr with 18L/min. [3]

As seen from the concept drawing of a catalyzed filter (Figure 5), the exhaust gas will first pass the soot

layer, before meeting the SCR catalyst embedded in the filter wall. As a result,  $\text{NO}_2$  is consumed in the soot layer, leaving less for the fast SCR reaction at the catalyst, resulting in decreasing  $\text{NO}_x$  conversion.

It is therefore of interest to design systems to provide  $\text{NO}_2$  for the SCR catalyst, for instance by generating  $\text{NO}_2$  after the soot layer and before or in the vicinity of the SCR catalyst.



**Figure 5:** The concept of a catalyzed filter: The flow through the filter is forced across a catalyzed filter wall (yellow) while the soot in the exhaust gas becomes entrained in the inlet channel, forming a layer (grey).

### Synergy of Combined Catalyst Systems

One way to facilitate  $\text{NO}_2$  regeneration in the vicinity of the SCR catalyst is to introduce an oxidation catalyst.

This can be done by mechanically mixing (see Figure 2b) the oxidation component with the SCR component, thereby making a combined system. However, this could theoretically result in unwanted oxidation of the  $\text{NH}_3$  in the inlet gas, worsening the SCR activity.

In order to investigate this, Stakheev et al. [4] prepared such a system, using a commercial Fe-beta (zeolite) SCR catalyst and a commercial  $\text{CeO}_2$ -ZrO<sub>2</sub> soot oxidation catalyst. They found that it was possible to replace three quarters (by volume) of the SCR catalyst with the oxidation component without losing any overall SCR activity, see Figure 6. [4]

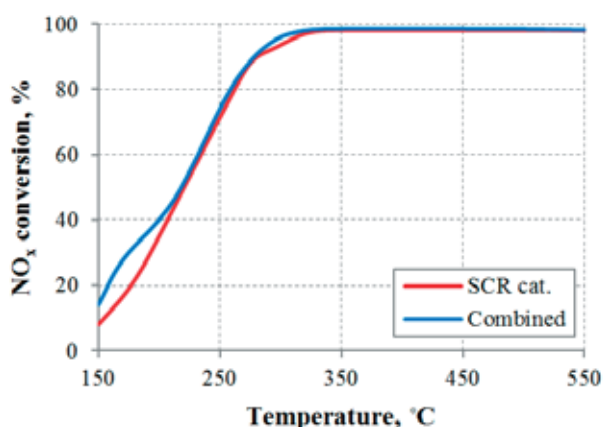


**Figure 6:**  $\text{NO}_x$  conversion over a SCR catalyst and a combined catalyst. SCR: 0.7% wt Fe-beta; Combined: [ $\text{Ce}_{0.67}\text{Zr}_{0.33}\text{O}_2$  + 0.7% wt Fe-beta], 3:1 vol. ratio. Conditions: 500ppm NO, 550ppm  $\text{NH}_3$ , 10vol%  $\text{O}_2$ , 6vol%  $\text{H}_2\text{O}$ ,  $\text{N}_2$  balance, GHSV: 270,000 1/h. Flow-through reactor. [4]

Stakheev et al. looked further into the individual components in the system, see Figure 7. By comparing the conversion of the combined system with the individual components, two synergetic areas between

the curves can be seen: One at 150-350°C and one for  $T > 450^\circ\text{C}$ .

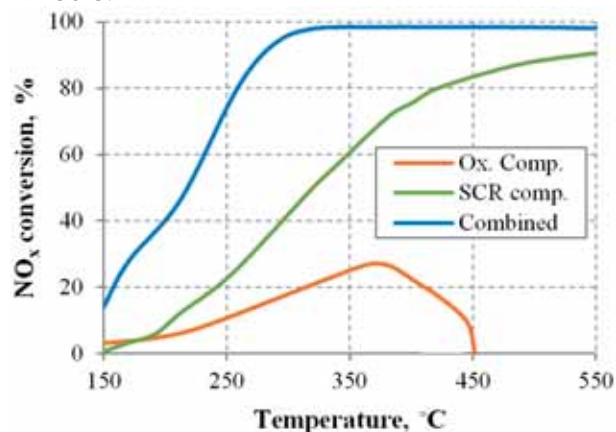


**Figure 7:**  $\text{NO}_x$  conversion over the individual components and the combined catalyst. Ox. Comp.:  $\text{Ce}_{0.67}\text{Zr}_{0.33}\text{O}_2$  (GHSV: 360,000 1/h); SCR: 0.7% wt Fe-beta (GHSV: 1,080,000 1/h); Combined: [ $\text{Ce}_{0.67}\text{Zr}_{0.33}\text{O}_2$  + 0.7% wt Fe-beta], 3:1 vol. ratio (GHSV: 270,000 1/h). Conditions: 500ppm NO, 550ppm  $\text{NH}_3$ , 10vol%  $\text{O}_2$ , 6vol%  $\text{H}_2\text{O}$ ,  $\text{N}_2$  balance. Flow-through reactor. [4]

The low temperature synergy arises from fast SCR as a result of the  $\text{NO}_2$  regeneration over the oxidation component. The high temperature synergy is a result of the competing reactions: SCR reactions over one component and  $\text{NH}_3$  oxidation over the oxidation component. The data suggests that the SCR activity is faster than the  $\text{NH}_3$  oxidation activity, thereby maintaining the overall SCR activity. [4]

### Results and Discussion

Inspired by the work of Stakheev et al., the present project has looked more into the mixed catalyst systems and their synergies.

First, three different mechanically mixed catalyst systems were tested for  $\text{NH}_3$ -SCR. The systems used a similar oxidation component, a mixed CeZrLa-oxide, and the same volumetric ratio between the two components as Stakheev et al. found optimal for their system. The difference between the systems was the SCR components, which were 0.8% wt Fe-beta, 3.5% wt Cu-beta and 1% wt  $\text{V}_2\text{O}_5$ - $\text{WO}_3$ - $\text{TiO}_2$ .

The results from the  $\text{NH}_3$ -SCR experiments can be seen in Figure 8 where the results from both mixed systems and the individual SCR component are shown. It is seen that all mixed systems achieve a boost from the synergetic effect at lower temperatures, while the oxidation component is more active towards  $\text{NH}_3$  oxidation as compared to the results of Stakheev et al., as seen from the decreasing  $\text{NO}_x$  conversion at higher temperatures.

In order to reflect on the synergetic effect, Table 1 lists the conversions for the individual SCR catalysts and the combined catalysts at 250°C. It is seen that the vanadia based catalyst obtains the largest relative increase in activity, while the beta zeolites also show great benefits of mixing the systems. To put the numbers into context, it was shown experimentally that

the individual CeZrLa-oxide produce 6.2% NO<sub>2</sub>/NO<sub>x</sub> under standard SCR conditions (NO<sub>2</sub>/NO<sub>x</sub>=0 in feed). Comparing this to Figure 3, it doesn't seem likely that the improved conversions were obtained as a result of 6.2% NO<sub>2</sub>/NO<sub>x</sub>. It was therefore speculated, that some product inhibition of the NO oxidation occurs on the CeZrLa-oxide which is absent in the presence of the SCR catalyst.

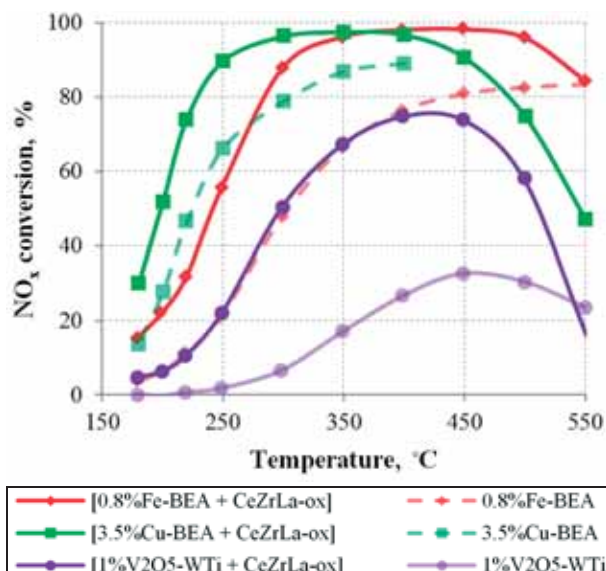


**Figure 8:** NO<sub>x</sub> conversion over the combined catalysts and the individual SCR components. GHSVs: 270,000 1/h (mixed); 1,080,000 1/h (SCR comp.). Conditions: 500ppm NO, 530ppm NH<sub>3</sub>, 10vol% O<sub>2</sub>, 5vol% H<sub>2</sub>O, N<sub>2</sub> balance. Flow-through reactor. BEA: Beta zeolite. WTi: WO<sub>3</sub>-TiO<sub>2</sub>.

**Table 1:** NO<sub>x</sub> conversions of the individual components and the mixed systems at 250°C. GHSVs: 270,000 1/h (mixed); 1,080,000 1/h (SCR comp.). Conditions: 500ppm NO, 530ppm NH<sub>3</sub>, 10vol% O<sub>2</sub>, 5vol% H<sub>2</sub>O, N<sub>2</sub> balance. Flow-through reactor. BEA: Beta zeolite.

	0.8%Fe-BEA	3.5%Cu-BEA	1%V <sub>2</sub> O <sub>5</sub> -WO <sub>3</sub> -TiO <sub>2</sub>
<b>SCR</b>	22%	66%	2%
<b>Mixed</b>	56%	90%	22%

To show the suspected inhibition, CeZrLa-oxide was tested for NO oxidation with varying NO<sub>2</sub> in the feed, see Figure 9. It is clearly seen that at lower temperatures, for increasing amounts of inlet NO<sub>2</sub>, the conversion of NO decreases significantly, even though we are far from equilibrium, which indicates product inhibition.

With this in mind it is speculated that the synergy shown by Stakheev et al. [4] can be beneficial for both catalysts in the mechanically mixed system: The oxidation component oxidizes NO to NO<sub>2</sub> and promotes fast SCR, freeing oxidation sites on the oxidation catalyst by consuming the NO<sub>2</sub> in close proximity of the latter, promoting increased NO oxidation.

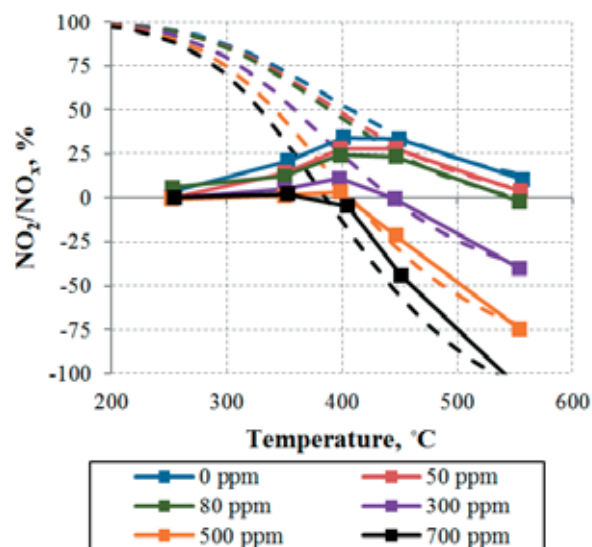


**Figure 9:** NO oxidation over CeZrLa-oxide at varying amounts NO<sub>2</sub> in the feed. Dotted lines indicate the thermodynamic equilibria. Conditions: 500ppm NO, varying NO<sub>2</sub>, 10vol% O<sub>2</sub>, 5vol% H<sub>2</sub>O, N<sub>2</sub> balance. Flow-through reactor.

## Conclusions

The development of a combined filter and SCR unit holds a great potential for reducing the overall cost and size of the automotive diesel aftertreatment system. Mechanically mixed systems have the potential of meeting some of the challenges arising when combining these units, as synergetic effects are seen.

Future work will focus on optimizing such a mechanically mixed system, using a Vanadia based SCR catalyst and a CeZr based soot oxidation component.

## Acknowledgements

This project is carried out in collaboration between Haldor Topsoe A/S, the CHEC group at DTU Chemical Engineering and Innovation Fund Denmark. The financial support from Innovation Fund Denmark under Grant number 103-2012-3 is gratefully acknowledged.

## References

1. O. Kröcher, *Stud. Surf. Sci. Catal.* 171 (2007) 261-289.
2. G. Madia, M. Koebel, M. Elsener, A. Wokaun, *Ind. Eng. Chem. Res.* 41 (2002) 3512-3517
3. K. Y. Choi, N. W. Cant, D. L. Trimm, *J. Chem. Technol. Biotechnol.* 71 (1998) 57-60.
4. A. Y. Stakheev, G. N. Baeva, G. O. Bragina, N. S. Teleguina, A. L. Kustov, M. Grill, J. R. Thøgersen, *Top. Catal.* 56 (2013) 427-433.

**Ming Liu**

Phone: +45 4525 6184  
E-mail: miliu@kt.dtu.dk

Supervisors: Anne S. Meyer  
Anders Thygesen

PhD Study  
Started: Sep 2013  
To be completed: Sep 2016

## Characterization and biological depectinization of hemp fibers originating from different stem sections

### Abstract

The wide variation of mechanical properties of natural fibers limits their applications in matrix composites. The aim of this study is to evaluate the properties of hemp fibers from different stem sections (top, middle and bottom) and to assess fungal retting pretreatment of hemp fibers from different stem sections with white rot fungi, *Phlebia radiata* Cel 26 and *Ceriporiopsis subvermispota*. For the untreated hemp fibers, the fiber strength and stiffness were highest for the fibers from the top and middle stem sections, and lowest for the fibers from the bottom sections of the stem. These properties were related to the compositional make up and morphological properties of hemp fibers, notably the secondary fiber cell contents, in the different stem sections. In fungal retting treatment, there was a strong dependence of depectinization selectivity on stem section. The depectinization selectivity decreased from bottom to the top of the stem presumably due to the significantly higher lignin content in bottom section than in the top section (middle section is in between).

### Introduction

Natural cellulosic fibers, such as hemp and flax, are increasingly considered important raw materials for the production of high quality textiles and potential reinforcement agents in composite materials due to their environmental sustainability and biodegradability. Replacing synthetic glass fibers with natural cellulosic fibers offer advantages including low cost, low density and desirable mechanical properties in the resulting composite materials [1].

The mechanical properties of bast fibers vary greatly, rendering them unsuitable for use in high grade composite materials where high reliability and stability are required. Hemp fibers from different parts of the stem may have different chemical composition and lignification due to varied ripeness. Consequently, fibers from different parts of the stem exhibit variations in mechanical performances. The differences in chemical composition and structure of hemp fibers will affect depectinization efficiency of adapted microorganisms, resulting in more scattered mechanical properties during controlled microbiological retting.

In the present study, two species of white rot fungi, *P. radiata* Cel 26 and *C. subvermispota*, were incubated with fibers from different stem sections (i.e. top, middle, and bottom) under controlled conditions to evaluate the

effect of stem section on the performance of depectinization [2].

### Results and discussion

The chemical components of the bast fibers from different stem sections are shown in Table 1. Notably, fibers from top of stem have the lowest cellulose content (indicated by a glucose content of 55%), while these from the bottom and middle sections exhibit a statistically higher cellulose content of 61% and 62%, respectively. Furthermore, the lignin content decreased significantly from 4.8 to 3.6% from bottom to the top section and wax content decreased significantly from 3.3 to 2.4%. A highly significant ( $P < 0.01$ ) increase in pectin deposition indicated by a significant increase in galacturonic acid (GalA) content from bottom to top section was noted.

It has been reported that the accumulation of wax on the cuticle forms a protective barrier against entry of infection agents into the plant. Additionally, the high lignin concentration in the middle lamellae between individual fibers in the hemp bast was found to be an effective barrier to enzymatic retting. Therefore, a higher content of waxy substances and lignin can inhibit depectinization of hemp stems with microorganisms during the retting process.

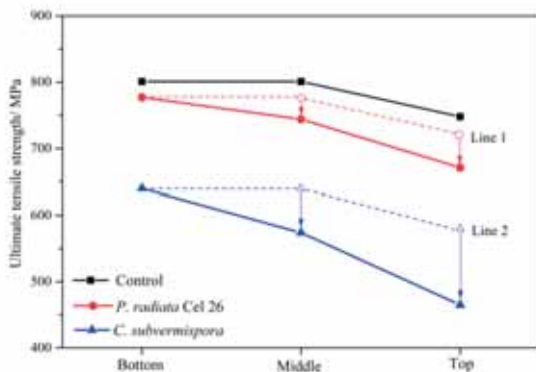
**Table 1:** Chemical composition of hemp fibers from different stem sections after different treatments.

Pretreatment <sup>1</sup>	Stem section	Amount (g/100 g dry matter)					
		Glu	GalA	Man	Xyl	Lignin	Wax
Untreated	Bot	61.3 <sup>aGH</sup> (0.4)	6.3 <sup>bBCD</sup> (0.3)	3.0 <sup>ab</sup> (0.3)	1.1 <sup>b</sup> (0.1)	4.8 <sup>a</sup> (0.5)	3.3 <sup>a</sup> (0.2)
	Mid	62.1 <sup>aFG</sup> (3.9)	7.3 <sup>bB</sup> (0.5)	3.4 <sup>a</sup> (0.4)	1.4 <sup>a</sup> (0.1)	4.4 <sup>ab</sup> (0.1)	2.9 <sup>ab</sup> (0.1)
	Top	54.8 <sup>bH</sup> (2.6)	9.0 <sup>aA</sup> (0.6)	2.5 <sup>b</sup> (0.2)	1.0 <sup>b</sup> (0)	3.6 <sup>b</sup> (0.3)	2.4 <sup>b</sup> (0.1)
Control	Bot	68.1 <sup>abDEF</sup> (2.8)	5.1 <sup>bD</sup> (0.6)	3.5 (0.6)	1.3 (0.2)	5.3 <sup>a</sup> (0.2)	/
	Mid	69.5 <sup>aCDE</sup> (2.7)	5.4 <sup>abCD</sup> (0.7)	3.4 (0.3)	1.5 (0.2)	4.9 <sup>ab</sup> (0.3)	/
	Top	65.3 <sup>bEFG</sup> (2.8)	6.5 <sup>aBC</sup> (1.3)	3.5 (0.3)	1.5 (0.3)	4.6 <sup>b</sup> (0.3)	/
<i>Pr</i> -treated	Bot	76.5 <sup>bAB</sup> (2.8)	1.7 <sup>bF</sup> (0.2)	4.4 (0.4)	0.9 <sup>b</sup> (0.2)	5.9 <sup>a</sup> (0.2)	/
	Mid	80.5 <sup>aA</sup> (2.8)	1.7 <sup>bF</sup> (0.2)	4.1 (0.3)	1.0 <sup>b</sup> (0.1)	5.1 <sup>b</sup> (0.2)	/
	Top	74.1 <sup>bBC</sup> (2.4)	2.0 <sup>aEF</sup> (0.2)	4.3 (0.9)	1.3 <sup>a</sup> (0.2)	4.5 <sup>c</sup> (0.2)	/
<i>Cs</i> -treated	Bot	70.9 <sup>CD</sup> (2.4)	3.0 <sup>aE</sup> (0.2)	3.8 (0.7)	1.1 (0.2)	6.0 <sup>a</sup> (0.1)	/
	Mid	72.4 <sup>BCD</sup> (2.8)	2.8 <sup>abE</sup> (0.2)	3.8 (0.2)	1.0 (0.2)	5.6 <sup>b</sup> (0.1)	/
	Top	70.7 <sup>CD</sup> (2.4)	2.7 <sup>bEF</sup> (0.1)	4.2 (0.4)	1.1 (0.3)	5.0 <sup>c</sup> (0.1)	/

<sup>1</sup> For one pretreatment, values for the same monosaccharide with different lowercase are significantly different at a confidence of 5%. In addition, values in the whole column for the same monosaccharide with different capital letters are significantly different at a confidence of 5%. (Glu-glucan, GalA-galacturonan, Man-mannan, Xyl-xylan, Lignin: Klason lignin, *Pr*-treated: samples treated with *P. radiata* Cel 26, *Cs*-treated: samples treated with *C. subvermispora*)

**Table 2:** Component losses, fiber yield and depectinization selectivity at different sections after cultivation with white rot fungi for 14 days

Pretreatment	Stem section	Selectivity value	Yield %	Weight loss (%)			
				Glu	GalA	Ara	Lignin
<i>P. radiata</i> Cel 26	bottom	36.1	88(5)	2(11)	71(5)	64(9)	3(8)
	middle	18.1	83(2)	4(10)	74(6)	63(25)	14(8)
	top	10.0	82(4)	7(9)	75(5)	69(11)	19(8)
<i>C. subvermispora</i>	bottom	8.2	92(1)	4(9)	46(8)	30(22)	-4(-3)
	middle	3.2	83(1)	14(9)	57(9)	46(24)	7(7)
	top	3.1	74(5)	20(9)	69(4)	70(10)	18(9)

**Figure 1:** Ultimate tensile strength of hemp fibers from the bottom, middle and top stem sections pretreated with *P. radiata* Cel 26 and *C. subvermispora* for 14 days. (Line 1: trend line showing changes in tensile strength for fibers treated with *P. radiata* Cel 26 if same decrease happened to middle and top sections as bottom section; Line 2: similar trend line showing changes for fibers treated with *C. subvermispora*).

The results in Fig. 1 suggested that fibers from different stem sections responded differently to fungal pretreatment with either *P. radiata* Cel 26 or *C. subvermispora* causing a variable change in mechanical

properties. The strong dependence of responses of fibers to fungal pretreatment with respect to mechanical properties on stem section was consistent with the stem section dependence of fungal selectivity of depectinization (Table 2). A high fungal selectivity of depectinization (e.g. at bottom section) resulting in less cellulose loss (Table 2) caused UTS of fibers to be decreased slightly (Fig. 1 for bottom stem section). In contrast, a lower fungal selectivity (e.g. at top section) resulting in a higher amount of cellulose loss (Table 2) consequently caused UTS of fibers to be reduced a lot (Fig. 1 for top stem section).

## References

1. M. Fan, D. Dai, and A. Yang, High strength natural fiber composite: defibrillation and its mechanisms of nanocellulose hemp fibers, *Int. J. Polym. Mater. Polym. Biomater.*, 2011, 60: 1026–1040.
2. M. Liu, D. Fernando, A. S. Meyer, B. Madsen, G. Daniel, and A. Thygesen, Characterization and biological depectinization of hemp fibers originating from different stem sections, *Ind. Crops Prod.*, 2015, 76: 880–891.



**Anna Lymperatou**  
Phone: +45 4525 6187  
E-mail: alym@kt.dtu.dk

Supervisors: Ioannis V. Skiadas  
Hariklia N. Gavala

PhD Study  
Started: October 2013  
To be completed: September 2016

## Improving the manure-based anaerobic digestion by means of ammonia

### Abstract

The anaerobic digestion of livestock manure usually results to be a financially non-feasible process due to the low degradability rate of its solid fraction (fibers) that presents the highest biogas potential. In order to improve the efficiency of this process, a sustainable pretreatment of the manure fibers that could increase the methane yield without prejudicing the economy of the biogas plant is of interest. In this study Aqueous Ammonia Soaking has significantly increased the methane yield of manure fibers (by more than 200%), while the ammonia used can be easily removed and recycled for covering the chemical requirements of the process.

### Introduction

Livestock manure is a nutrient-rich waste stream that constitutes a major source of diffuse agricultural pollution when not handled properly. Anaerobic digestion is an attractive solution for handling manure as it stabilizes the nutrients and at the same time produces energy in the form of biogas that can substitute natural gas, summing up to the renewable energy resources. In Denmark, where the annual production of manure is very high and the whole country is characterized as a Nitrogen Vulnerable Zone [1], the government has set the goal to increase the amount of manure used for green energy up to 50% until 2020 [2].

Nevertheless biogas production from digesting anaerobically only manure is currently a financially non-feasible process. This is due to the low degradation rate of the lignocellulosic fibers it contains. Instead of co-digesting livestock manure with easily digestible organic residues that become scarce and make the economy of biogas plants dependent on extra materials, technologies should be developed that will allow the anaerobic digestion of solely manure to be a self-sustained process [3]. This could lead to a significant increase of manure treated anaerobically.

In light of this, many alternative pretreatments of manure fibers have been proposed, aiming at increasing the methane ( $\text{CH}_4$ ) yield. The highest increase of  $\text{CH}_4$  yield achieved up to now has resulted from pretreating manure fibers with Aqueous Ammonia Soaking (AAS)

corresponding to a 178% increase compared to non-treated fibers [4]. Apart from the improved energy output AAS achieved, this pretreatment presents extra advantages as it can be applied at ambient temperatures resulting thus in low energy requirements. Moreover, due to the volatile nature of ammonia it can be easily removed and possibly recycled, resulting thus in minimum chemical consumption.

### Specific Objectives

This dissertation focuses on investigating the conditions and configuration under which AAS can be applied to manure fibers for rendering manure-based anaerobic digestion a profitable and sustainable process.

More specifically the objectives are to:

- Optimize the conditions under which AAS of manure fibers is applied for maximizing the  $\text{CH}_4$  yield. For this purpose Design of Experiments (DoE) will be applied and the results will be analyzed by Response Surface Methodology (RSM)
- Assess the applicability of ammonia ( $\text{NH}_3$ ) removal technologies that will allow recovering the chemical used for the pretreatment, as well as recovering an excess of  $\text{NH}_3$  from the N-rich effluent. The surplus of  $\text{NH}_3$  can be used for the catalytic reduction of emissions of nitrogen oxides from gas engines that convert biogas to electricity. The comparison of different  $\text{NH}_3$

technologies will be assessed based on mass balances and techno-economic analysis.

- Study the behavior of AAS-treated fibers and manure in bench-scale continuous digesters.
- Evaluate the agronomic properties of the digestate after the proposed process. Focus will be given in the N content and availability for plant uptake and risk of losses to the environment.
- Optimize the conditions of AAS of an additional agricultural residue (e.g. straw) for providing flexibility to biogas plant operation.

## Results and Discussion

In order to understand better how the conditions of the AAS treatment of manure fibers affect the CH<sub>4</sub> produced, a series of batch anaerobic digestion experiments were performed with manure fibers treated under different AAS conditions. The varying factors of the AAS treatment were the NH<sub>3</sub> concentration of the reagent (NH<sub>3</sub>), the duration of the treatment (D) and the solid-to liquid ratio (S:L). The response of the experiments was the CH<sub>4</sub> yield obtained from the AAS-treated fibers after 17 days of digestion. The different combinations tested were based on a Central Composite Design (Table 1) and the results were assessed by RSM.

**Table 1:** Coded values of the independent variables of AAS treatment based on a Central Composite Design

Independent Variable	-a	-1	0	1	a
NH <sub>3</sub> (% w/w)	0,9	7	16	25	31,1
D (hours)	4,8	28	62	96	119,1
S:L ratio (g fibers/ml solution)	0,12	0,16	0,22	0,28	0,32

The obtained increases of CH<sub>4</sub> yield after 17 days of digestion of AAS-treated fibers varied from 96% to 230% compared to the CH<sub>4</sub> yield of non-treated fibers, demonstrating thus that the conditions of AAS applied can have a major effect on the success of the treatment.

The most influencing variable of AAS affecting the CH<sub>4</sub> yield was found to be the duration D of the treatment as well as the interaction between NH<sub>3</sub> and D. Generally, medium to low concentrations of NH<sub>3</sub> and S:L ratios seem to be more favorable for maximizing the CH<sub>4</sub> yield, in combination to high durations, as shown in Figure 1. The low S:L ratio would be translated to a larger pretreatment vessel increasing thus the cost of construction, although in combination to the low NH<sub>3</sub> levels the NH<sub>3</sub> recovery is expected to be facilitated.

## Conclusions

Aqueous Ammonia Soaking has been identified as a promising pretreatment as it can significantly enhance

the CH<sub>4</sub> yield of treated manure fibers, while minimizing the consumption of extra energy and chemicals. In the present study even higher increases of CH<sub>4</sub> yield (230%) were obtained than observed until recently (178%), hence making this pretreatment even more attractive for industrial-scale application.

The above experiments will result to the construction of an empirical model that can predict the CH<sub>4</sub> yield of AAS-treated fibers under different NH<sub>3</sub> concentrations, durations of AAS and S:L ratios that will be used for assessing the techno-economic viability of the whole process.

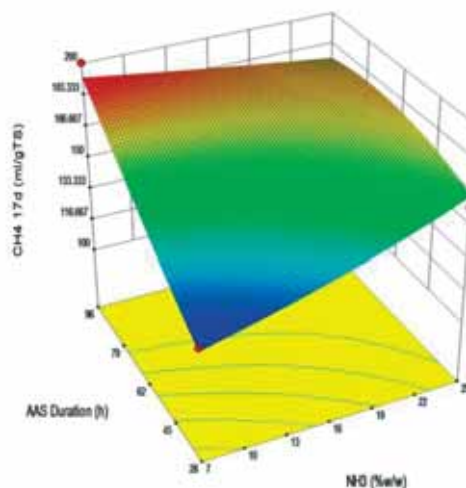


**Figure 1:** Response Surface of the CH<sub>4</sub> yield resulting from pretreated manure fibers according to the NH<sub>3</sub> concentration and duration of AAS (at a S:L of 0,22g/ml).

## Acknowledgements

The author would like to thank Energinet.dk for the financial support of the AMMONOX project (ID: 12069).

## References

1. Danish Environmental Protection Agency, Ministry of the Environment, Status and trends of aquatic environment and agricultural practice, 25 May 2009
2. Danish Environmental Protection Agency, Ministry of Environment and Food, Agreement on Green Growth, 16 June 2009
3. I. Angelidaki, B.K. Ahring, *Water Sci Technol* 41 (3) (2000) 189-194
4. E. Jurado, I.V. Skiadas H.N. Gavala, *Appl. Energy* 109 (2013) 104-111.

## List of Publications

1. A. Lymperatou, H.N. Gavala, K.H. Esbensen, I.V. Skiadas, *Waste Biomass Valor* 6(4), 449-457 (2015)

**Seyed Soheil Mansouri**

Phone: +45 4525 2907  
E-mail: seso@kt.dtu.dk

Supervisors: Rafiqul Gani  
Jakob Kjøbsted Huusom  
John M. Woodley

PhD Study  
Started: September 2013  
To be completed: August 2016

## Integrated design, control and analysis of intensified processes

### Abstract

Integrated process design and control of an intensified process (reactive distillation) is presented. Simple graphical design methods that are similar in concept to non-reactive distillation processes are used, such as reactive McCabe-Thiele method and driving force approach. The methods are based on the element concept, which is used to translate a system of compounds into elements. The operation of the reactive distillation column at the highest driving force and other candidate points is analyzed through analytical solution as well as rigorous open-loop and closed-loop simulations. By application of this approach, it is shown that designing the reactive distillation process at the maximum driving force results in an optimal design in terms of controllability and operability. It is verified that the reactive distillation design option is less sensitive to the disturbances in the feed at the highest driving force and has the inherent ability to reject disturbances.

### Introduction

Conventionally, process design and process control have been considered as independent problems. In this context, a sequential approach is used where the process is designed first, followed by the design of process control. However, as it is well-known, this sequential approach has limitations related to dynamic constraint violations, for example, infeasible operating points, process overdesign or under-performance. Therefore, a robust performance may not always be guaranteed as process design decisions can influence process control and operation [1]. To overcome these limitations, alternatives to tackle process design and controllability issues simultaneously, in the early stages of process design have been proposed. In control design, operability addresses stability and reliability of the process using a priori operational conditions and controllability addresses maintenance of process at desired operating points subject to disturbances [7]. This simultaneous synthesis approach provides optimal/near optimal operation and more efficient control of chemical processes [8]. Most importantly, it is possible to identify and eliminate potentially promising design alternatives that may have controllability problems. To date, a number of methodologies have been proposed and applied on various problems to address the interactions between process design and control, and they range from mathematical programming

optimization-based approaches to model-based decomposition methods.

### 1. Reactive Distillation Column

Reactive distillation column (RDC) is a multifunctional unit operation, which incorporates separation and reaction in a single operation, attracting considerable interest in research from academia and industry. Reactive distillation provides more sustainability, safer environmental performance as well as better energy management [13]. However, as a result of integration of functions/operations into one system the controllability region of reactive distillation processes may become smaller due to the loss in degrees of freedom; thereby making the process becomes non-linear with highly interacting dynamics.

Various studies have addressed the design-control of reactive distillation processes. Al-Arfaj and Luyben [3] explored six alternative control structures for an ideal two-product reactive distillation column. They illustrated the interaction between design and control by the impact of holdup in the reactive zone. Georgiadis et al. [4] investigated the design and control of a RDC via two different optimization approaches. In the first approach, the steady-state process design and the control system were optimized sequentially. They confirmed that operability is strongly influenced by the process design. In the second approach, the process

design and the control system were optimized simultaneously using mixed integer dynamic optimization leading to a more economically beneficial and better controlled system than that obtained using the sequential approach. Therefore, the objective (or target) for the integrated process design and control is to overcome the bottlenecks associated with the sequential approach and to obtain optimal/near optimal design of a reactive distillation column which is also the easiest to control and operate.

## 2. Integrated Design-Control Solution

From a process design point of view, a set of process design objectives (specifications) are determined at the maximum reactive driving force for a RDC that satisfy for specified inputs,  $u$ , and disturbances,  $d$ , values for states,  $x$ , and outputs,  $y$ . Here,  $x$  and  $y$  also represent some of the operational conditions for the process. From a controller design point of view, for any changes in  $d$  and/or set point values in  $y$ , values of  $u$  that recovers the process to its optimal designed condition at the maximum driving force are determined. Note that the solution for  $x$  and  $y$  is directly influenced by  $\theta$  (the constitutive variables such as reaction rate or equilibrium constant). This concept is illustrated through representation of a dynamic process system in Fig. 1. The optimal solution for  $x$  (states) and  $y$  (outputs) can be obtained at the maximum point of the driving force which are based on  $\theta$  (the constitutive variables)). By using model analysis, the corresponding derivative information with respect to  $x$ ,  $y$ ,  $u$ ,  $d$  and  $\theta$  are obtained (to satisfy controller design objectives).

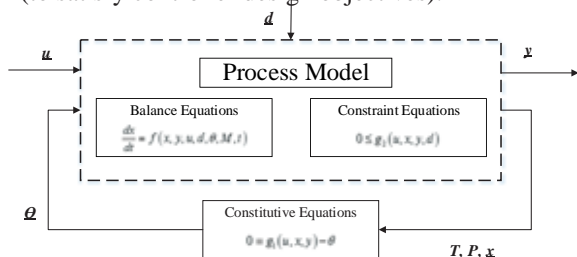


Fig. 1. Dynamic process system representation

Selecting the design targets at the maximum driving force for designing the RDC, the optimal design objectives are obtained. Furthermore, at these design targets, from a controller point of view, the controllability and operability of the process is best achieved. This means that, the value of the derivative of controlled variables  $y$  with respect to disturbances in the feed,  $d$ ,  $dy/dd$  and manipulated variables,  $u$ ,  $dy/du$  will determine the process sensitivity and influence the controller structure selection. Accordingly,  $dy/dd$  and  $dy/du$  are defined as Russel et al. [5]:

$$\frac{dy}{dd} = \left( \frac{dy}{d\theta} \right) \left( \frac{d\theta}{dx} \right) \left( \frac{dx}{dd} \right) \quad (1)$$

$$\frac{dy}{du} = \left( \frac{dy}{d\theta} \right) \left( \frac{d\theta}{dx} \right) \left( \frac{dx}{du} \right) \quad (2)$$

The values for  $d\theta/dx$  can be obtained from the process (dynamic and/or steady state) constraints:

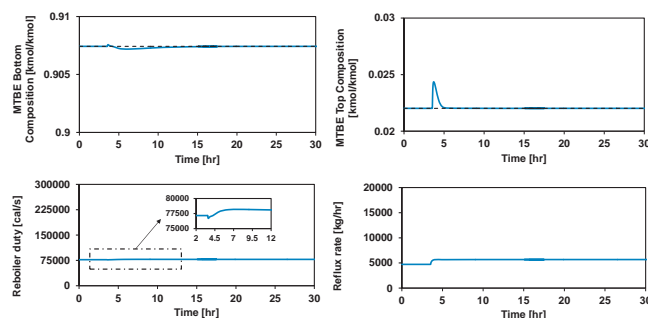
$$\frac{dx}{dt} = f(x, y, u, d, \theta, Y, t) \quad (3)$$

and values for  $dy/d\theta$ ,  $dx/dd$  and  $dx/du$  can be obtained from constitutive (thermodynamic) constraints:

$$0 = g(u, x, y) - \theta \quad (4)$$

## 3. Closed-Loop Verification

Fig. 2 shows the closed-loop performance of the MTBE multi-element reactive distillation process operating at the maximum driving force (optimal design) in the presence of a disturbance force in the feed. The disturbance scenario is a +16.5% step change in the methanol flowrate in the feed after 3.4 hrs.



## Conclusions

Integrated process design and control of RDC system was presented. It is verified through steady-state and dynamic analysis that designing RDC at the maximum driving force results in least energy consumption and carbon footprint as well as the best controllability and disturbance rejection. It was also demonstrated that using the equivalent binary element concept is advantageous in designing multi-component reaction-separation operations. To read more details please refer to [5].

## Acknowledgements

The collaboration with Prof. Mauricio Sales-Cruz at Universidad Aut3noma Metropolitana-Cuajimalpa (Mexico) is greatly acknowledged.

## References

- Seferlis P, Georgiadis MC. The Integration of Process Design and Control. *Comput Aided Chem Eng.* 2004;17:1-639.
- Al-Arfaj M, Luyben WL. Comparison of Alternative Control Structures for an Ideal Two-Product Reactive Distillation Column. *Ind Eng Chem Res.* 2000;39(9):3298-3307.
- Georgiadis MC, Schenk M, Pistikopoulos EN, Gani R. The interactions of design, control and operability in reactive distillation systems. *Comput Chem Eng.* 2002;26(4-5):735-746.
- Russel BM, Henriksen JP, J3rgensen SB, Gani R. Integration of design and control through model analysis. *Comput Chem Eng.* 2002;26(2):213-225.
- Mansouri S.S., Sales-Cruz M., Huusom J.K., Woodley J.M., Gani R. Integrated Process Design and Control of Reactive Distillation Processes. *IFAC PapersOnLine.* 2015; 48(8):1120-1125.



**Fauziah Marpani**

Phone: +45 4525 6184  
E-mail: fama@kt.dtu.dk

Supervisors: Professor Anne S. Meyer  
Assoc. Prof. Manuel Pinelo

PhD Study  
Started: November 2012  
To be completed: April 2016

## Biocatalytic alginate membrane by enhanced concentration polarization

### Abstract

A thin alginate layer induced on the surface of a commercial polysulfone membrane was used as a matrix for non-covalent immobilization of enzymes. Despite the expected decrease of flux across the membrane resulting from the coating, the initial hypothesis was that such a system should allow high immobilized enzyme loadings, which would benefit from the decreased flux in terms of increased enzyme/substrate contact time. The study was performed in a sequential fashion: first, the most suitable types of alginate able to induce a very thin, sustainable gel layer by pressure-driven membrane filtration were selected and evaluated. Then, an efficient method to make the gel layer adhere to the surface of the membrane was developed. Finally, and after confirming that the enzyme loading could remarkably be enhanced by using this method, several strategies to increase the permeate flux were evaluated. Alcohol dehydrogenase (EC 1.1.1.1), able to catalyze the conversion of formaldehyde into methanol, was selected as the model enzyme. An enzyme loading of 71.4% ( $44.8 \mu\text{g}/\text{cm}^2$ ) was attained under the optimal immobilization conditions, which resulted in a 40% conversion to methanol as compared to the control setup (without alginate) where only 10.8% ( $6.9 \mu\text{g}/\text{cm}^2$ ) enzyme was loaded, with less than 5% conversion. Such conversion increased to 60% when polyethylene glycol (PEG) was added during the construction of the gel layer, as a strategy to increase flux. No enzyme leakage was observed for both cases (with/without PEG addition). Modeling results showed that the dominant fouling mechanism during gel layer induction (involving enzyme entrapment) was cake layer formation in the initial and intermediate phases, whilst pore blocking was the dominant mechanism in the final phase. Such mechanisms had a direct consequence on the type of immobilization promoted in each phase. The results suggested that the strategy proposed could be efficiently used to enhance the enzyme loading on polymer membranes [1].

### Introduction

Fouling is always seen as undesirable effect in membrane technology. Given the similarities between the mechanisms promoting enzyme immobilization and membrane fouling, it can be exploited in a positive manner [2]. Non-covalent enzyme entrapment in hydrophilic gel layer, which was induced on polymeric membrane surface based on concentration polarization (CP) phenomenon, was evaluated. The initial hypothesis was that such a system should allow high enzyme loadings to be immobilized without compromising the flux through the membrane significantly. A sequence of works has been executed to evaluate this concept (**Figure 1**): (i) selection of different types of alginate that could induced a very thin, sustainable gel layer by pressure-driven membrane filtration; (ii) method to make the gel layer adhered to the surface of the

membrane and (iii) strategies to increase the permeate flux. Alcohol dehydrogenase (EC 1.1.1.1), able to catalyze the conversion of formaldehyde into methanol, was selected as the model enzyme.

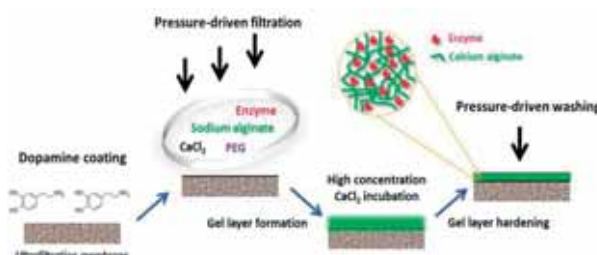


**Figure 1:** Schematic diagram of in-situ formation of biocatalytic alginate membrane by enhanced concentration polarization.

## Experimental Method

Experiments were conducted in Amicon 8050 cell (50 ml) with 44.5 mm diameter membrane disc. A constant applied pressure comes from a nitrogen gas source. Permeate was collected in a beaker on an electronic scale or in a precise cylinder to monitor the flux reading. New membrane was used for each experiment. Virgin membrane was cleaned with 70% ethanol for 30 minutes. Water permeability was measured at 1 and 2 bars. For certain experiments, membrane was coated with dopamine, where 0.5 g/l dopamine hydrochloride in 10 mM Tris buffer (pH 8.5) was stirred at 100 rpm and exposed to the air for 1 hour.

## Results and Discussion

An enzyme loading of 71.4% ( $44.8 \mu\text{g}/\text{cm}^2$ ) was attained at the optimal immobilization conditions (Table 1), which resulted in a 40% conversion to methanol as compared to the control setup where only 10.8% ( $6.9 \mu\text{g}/\text{cm}^2$ ) enzyme was loaded with less than 5% conversion (Figure 2). Such conversion increased to 60% when polyethylene glycol (PEG) was added during the construction of gel layer, as a strategy to increase flux (Figure 2). No enzyme leakage was observed for both cases (with/without PEG1500 addition). PEG molecules are believed to prevent/interrupt the cross linking of intra-cluster association of alginate dimers and would be expected to diffuse out from the network during pressurized washing stage, resulting in some micro channels/voids in the gel layer. Such channels could increase the exposure of enzyme active sites and thus improve the biocatalytic conversion. Modeling results from Hermia's [3] showed that the dominant fouling mechanism during gel layer induction with enzyme entrapment was cake layer formation in the initial and intermediate phases (I & II), whilst pore blocking was the dominant mechanism in the final phase (III) (Figure 3).

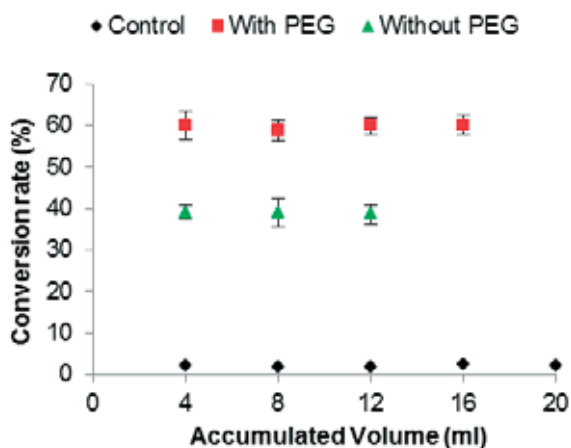


**Figure 2:** Conversion rate of NADH with ALG3000G67 induced on dopamine coated reactive membranes during the reaction (TMP = 2 bar).

**Table 1:** Enzyme loading for the reactive membranes induced by different types of alginate with dopamine coating.

Alginate type	Enzyme Loading ( $\mu\text{g}/\text{cm}^2$ )	Loading rate (%)
ALG3000G39	44.8	71.4
ALG2000G67	36.9	58.9
Control	6.9	10.8

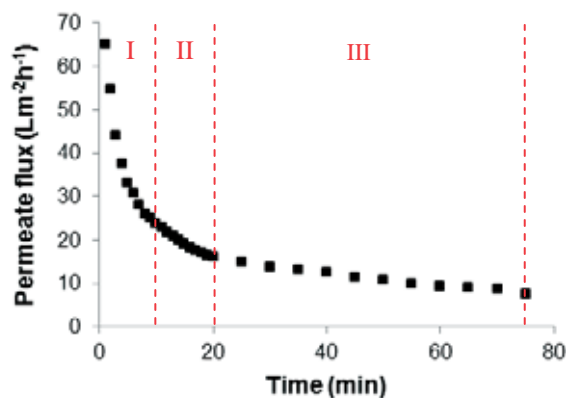


**Figure 3:** Sample of region analysis of fouling behavior during immobilization by fitting to Hermia's model for ALG3000G39.

## Conclusions

Inevitable fouling associated with membrane separation processes could be exploited as a strategy to immobilize enzyme on the surface of an ultrafiltration membrane by entrapment of the enzyme in a stable, thin calcium alginate gel layer. Technically, concentration polarization was the dominant effect that governs the induction of thin calcium alginate layer and immobilization of enzyme. It was confirmed that the composition of mannuronic and guluronic acid in alginate determined the features and properties of the gel layer induced on the surface of the membrane. A higher viscosity type of alginate with low guluronic acid fraction was the suitable type of alginate in this application. The results suggested that the strategy proposed could be efficiently used to enhance the enzyme loading on polymer membranes.

## References

1. F. Marpani, J. Luo, R.V. Mateiu, A.S. Meyer, M. Pinelo, ACS Appl. Mater. Interfaces, 7 (32) (2015) 17682-17691.
2. J. Luo, F. Marpani, R. Brites, L. Frederiksen, A.S. Meyer, G. Jonsson, M. Pinelo, J. Memb. Sci. 459 (2014) 1-11.
3. J. Hermia, Trans. Inst. Chem. Eng. 60 (1982) 183-187.

**Lisa Mears**

Phone: +45 42 26 06 15  
E-mail: lmea@kt.dtu.dk

Supervisors: Prof. Krist V. Gernaey, DTU  
Assoc. Prof. Gürkan Sin, DTU  
Dr. Stuart M. Stocks, Novozymes

**PhD Study**

Started: December 2013  
To be completed: December 2016

## Novel strategies for control of fermentation processes

**Abstract**

Industrial fermentation processes are typically operated in fed batch mode, which poses specific challenges for process modelling, monitoring and control. This is due to many reasons including non-linear behaviour, and a relatively poor understanding of the system dynamics. It is therefore challenging for the process engineer to optimise the operation conditions, due to a lack of available process models, and complex interactions between variables which are not easy to define, especially across scales and equipment. The aim of this work is to develop a control strategy which is applicable to industrial scale fermentation processes. The scope of this project is to consider modelling approaches in order to characterise fermentation batches, including both mechanistic and data driven strategies. Utilising the model as a tool for process monitoring, can then aid control strategy development. This work is completed in collaboration with Novozymes A/S and considers an industrially relevant fermentation process.

**Introduction**

Bioprocesses are inherently sensitive to fluctuations in processing conditions and must be tightly regulated to maintain cellular productivity. Industrial fermentations are often difficult to replicate across production sites or between facilities as the small operating differences in the equipment affect the way the batches should be optimally run. In addition, batches run in the same facility can also be affected by batch variations in the growth characteristics of a specific cultivation. For these reasons it is important to have optimal control of the process to achieve the desired product quality and yields. It is especially important to regulate feed rates and achieve the highest productivity without over feeding the system.

Over feeding increases production cost, due to expensive raw materials [1], and also produces unwanted metabolites. There is demand therefore to research strategies to continually monitor the performance of a fermentation which is universal across equipment, and to design control systems which quickly and accurately respond to maintain the process within tightly controlled conditions.

**Discipline**

This research project focusses on the discipline of Industrial fermentation technology and is conducted in collaboration with Novozymes A/S.

**Specific Objectives**

The overall objective for this work is to develop a control strategy which is applicable to an industrial scale fermentation process. In order to achieve this goal, the following objectives are described:

- Literature review of control strategies applied to fermentation systems to assess the state of the art. This is focused on feed strategy development.
- A study of fermentation modelling to include both black box modelling and mechanistic modelling approaches.
- Development of a process model which characterises the process of interest operating at Novozymes A/S.
- Development of a control strategy which utilizes the model developed in the previous stage of the work to control the feed rate in the fed batch operation.

## Results and Discussion

Mechanistic models are valuable tools for process monitoring. A limitation for fermentation monitoring is a lack of available measurements for key process parameters [2]. This includes substrate concentration, biomass concentration and product concentration. State estimators may then be applied utilizing on-line measured variables to predict the unknown states in real-time [3], [4]. There is limited application of soft sensors in the fermentation industry despite the advantages of real-time process understanding, and no need for investment in additional hardware [4].

A state estimator is developed for pilot scale fermentations operating at Novozymes A/S based on a stoichiometric balance [5]. This utilises online measured parameters of carbon dioxide evolution, oxygen uptake and ammonia addition. The rates obtained by the stoichiometric balance are coupled to a dynamic process model in order to predict the concentration of biomass and product, based also on the changing mass in the system. These state predictions are also incorporated in the dynamic model to calculate physical process parameters, including viscosity and the oxygen mass transfer coefficient,  $k_{La}$ , which are calculated as described by Albaek (2011) [6].

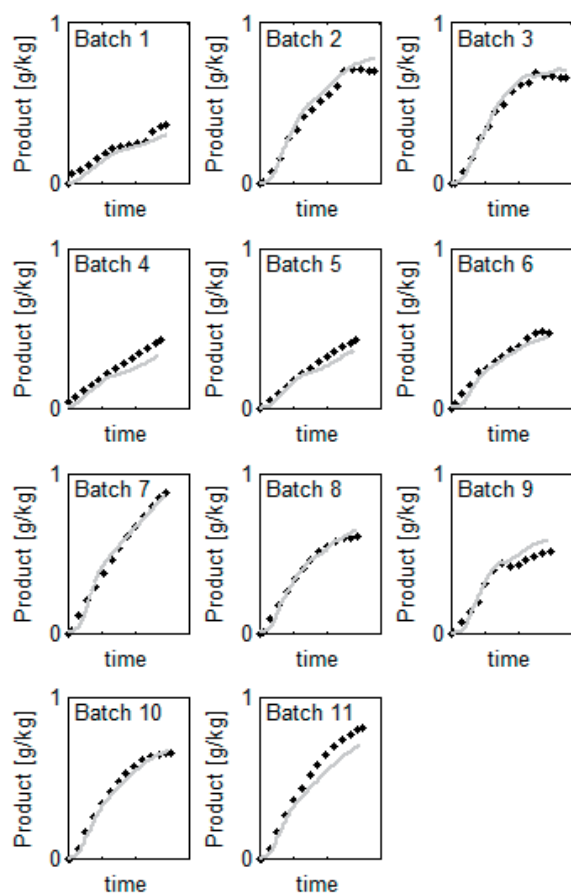


**Figure 1:** Scaled data: product prediction from the state estimator applied offline to 11 batches operated at Novozymes A/S pilot scale facility, as described by Albaek et al (2011) [6]. Scaled axis for confidentiality.

The results of the product concentration prediction for 11 batches of pilot scale data are shown in Figure 1. The results show that a good prediction is achieved over the 11 batches, which were operated at very different operating conditions, which shows that the prediction is robust across batches.

## Conclusions

A state estimator is developed for pilot scale filamentous fungus fermentations, which is able to predict the product and biomass concentration using only standard online measured variables. This model is also extended to include other parameters of interest for process optimisation including viscosity and  $k_{La}$  (results not shown). The future work for this project is then incorporation of the online state estimator into a model-based control strategy. In reference to the specific aims of the project as previously described, the first three aims are achieved, and the focus is now on controller strategy development.

## Acknowledgements

The author would like to thank the Technical University of Denmark and Novozymes A/S for the financing of this PhD study.

## References

1. M. O. Albaek, K. V Gernaey, M. S. Hansen, and S. M. Stocks, "Evaluation of the energy efficiency of enzyme fermentation by mechanistic modeling.," *Biotechnol. Bioeng.*, vol. 109, no. 4, pp. 950–61, Apr. 2012.
2. A. Chéry, "Software sensors in bioprocess engineering," *J. Biotechnol.*, vol. 52, no. 3, pp. 193–199, Jan. 1997.
3. P. Sagmeister, P. Wechselberger, M. Jazini, A. Meitz, T. Langemann, and C. Herwig, "Soft sensor assisted dynamic bioprocess control: Efficient tools for bioprocess development," *Chem. Eng. Sci.*, vol. 96, pp. 190–198, Jun. 2013.
4. R. Luttmann, D. G. Bracewell, G. Cornelissen, K. V Gernaey, J. Glassey, V. C. Hass, C. Kaiser, C. Preusse, G. Striedner, and C.-F. Mandenius, "Soft sensors in bioprocessing: a status report and recommendations.," *Biotechnol. J.*, vol. 7, no. 8, pp. 1040–8, Aug. 2012.
5. R. T. J. M. Van Der Heijden, B. Romein, H. Jj., H. C., and L. Kcam, "Linear Constraint Relations in Biochemical Reaction Systems: II Diagnosis and estimation of gross errors," *Biotechnol. Bioeng.*, vol. 43, pp. 3–20, 1994.
6. M. O. Albaek, K. V Gernaey, M. S. Hansen, and S. M. Stocks, "Modeling enzyme production with *Aspergillus oryzae* in pilot scale vessels with different agitation, aeration, and agitator types.," *Biotechnol. Bioeng.*, vol. 108, no. 8, pp. 1828–40, Aug. 2011.



**Murray P. Meissner**

Phone: +45 5029 9315  
E-mail: mmeiss@kt.dtu.dk

Supervisors: Prof. John Woodley  
Dr. Gustav Rehn

PhD Study  
Started: July 2015  
To be completed: July 2018

## Biocatalytic Baeyer-Villiger oxidations

### Abstract

Baeyer-Villiger oxidations catalysed by Baeyer-Villiger monooxygenases (BVMOs) have become industrially relevant in light of their superior selectivity, use of molecular oxygen, and ability to satisfy new ‘green chemistry’ legislations when compared to conventional chemical oxidants. This project aims to produce a laboratory-scale reaction module that is able to demonstrate and evaluate BVMO-based processes. The target reactions, which are the oxygenation of cyclic ketones to lactones, present a number of challenges in the form of low aqueous solubility, volatility and inhibitory nature of both substrates and products. These challenges will be addressed by process engineering solutions, with a particular focus on *in situ* substrate supply and product removal.

### Introduction

The broadening of the industrial scope of biooxidation processes beyond pharma applications to new fine chemicals, nutrition, feed and materials markets has been targeted in light of the EU 2020 goal for industrial biotechnology. One such group of flavin-dependent monooxygenases presents a promising route of performing Baeyer-Villiger type oxidation reactions to yield numerous products from non-native substrates [1]. The biocatalytic route allows the substitution of conventional, unsafe and unstable oxidants and affords superior region-, chemo-, and enantioselectivities [2]. The requirement of NADPH cofactor necessitates the consideration of either an ancillary cofactor regeneration system for isolated enzymes [3] or the use of metabolically active whole-cells [4]. Primary considerations for the biocatalyst concern enzyme stability and cofactor recycling. In whole-cell systems, substrate uptake, product secretion, byproduct formation, product metabolism, and oxygen demand may require further consideration. Furthermore, the toxicity of substrates and products in these processes may warrant the use of *in situ* substrate supply (ISSS) and *in situ* product removal (ISPR) [5].

The target reactions for a BVMO-based process in this project are the conversions of a macrocyclic ketone (exaltone: *cyclopentadecanone*) and smaller cyclic ketone (jasmatone: *hexylcyclopentanone*) to their respective lactones, which correspond to musk and jasmine fragrances respectively.

The challenge and novelty of such reactions lies in the low aqueous solubility, volatility, and potential inhibitory properties of both substrates and products. In order to address these challenges, a special reactor system will need to be devised to function as a demonstration platform for BVMO reactions. More specifically, the ability of ISSS and ISPR to satisfy these challenges will be a particular focus of this project. One such reactor system that will inspire those used in this project is shown in Figure 1. Hilker et al. (2008) [6] used this bubble column reactor for similar gram-scale Baeyer-Villiger oxidations carried out by whole-cell *Escherichia coli* (*E. coli*). A resin-based ISPR and ISSS allowed the reaction to proceed at high substrate and product loadings via the mechanism shown in Figure 2.

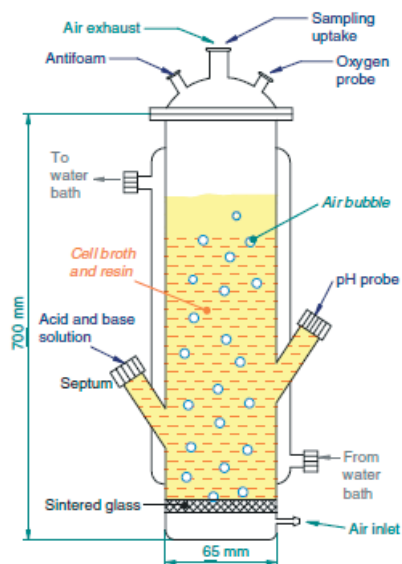


**Figure 1:** Schematic of the bubble column reactor used by Hilker et al. (2008) [6] for gram-scale Baeyer-Villiger biooxidation using *Escherichia coli* whole-cells and a resin-based ISPR/ISSS method. The reactor features a pH probe, pH control (via acid/base inlets), dissolved oxygen tension probe, and glycerol feeding system, which are controlled by a fermenter base unit (reproduced from [6], with permission from Nature Publishing Group).

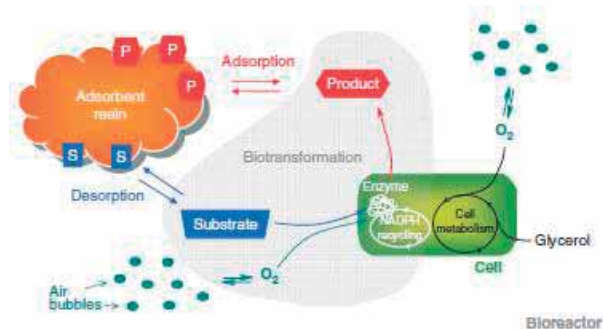


**Figure 2:** Mechanism of biocatalytic whole-cell Baeyer-Villiger oxidation using adsorption for ISSS and ISPR (reproduced from [6], with permission from Nature Publishing group).

### Future Work

The objective of this project is to establish a laboratory-scale demonstration platform for the Baeyer-Villiger biooxidation of poorly soluble, volatile and inhibitory compounds. Whole-cell *E. coli* expressing cyclopentadecanone monooxygenase (CPDMO) and cyclohexanone monooxygenase (CHMO) will be used as the biocatalyst for each reaction respectively. Specific research focus will involve:

- Characterising ISSS and ISPR by adsorption, absorption, and liquid-liquid extraction
- Addressing the oxygen supply mechanism for reaction
- Determining the extent of inhibition
- Establishing the necessity and means of immobilisation

### Acknowledgements

This project falls under EU ROBOX (grant agreement n° 635734): “Expanding the industrial use of robust oxidative biocatalysts for the conversion and production of alcohols.” Givaudan S.A. are acknowledged for their contributions of providing materials and helpful discussions.

### References

1. G. de Gonzalo, M.D. Miholovic, M.W. Fraaije, *ChemBiochem* 11 (2010) 2208-2231.
2. M.D. Miholovic, B. Müller, P. Stanetty, *Eur. J. Org. Chem.* 22 (2002) 3711-3730.
3. F. Zambianchi, P. Pasta, G. Carrea, S. Colonna, N. Gaggero, J.M. Woodley, *Biotechnol. Bioeng.* 78 (5) (2002) 489-496.
4. A.Z. Walton, J.D. Stewart, *Biotechnol. Progr.* 20 (2004) 403-411.
5. V. Alphand, G. Carrea, R. Wohlgemuth, R. Furstoss, J.M. Woodley, *Trends Biotechnol.* 7 (2003) 318-323.
6. I. Hilker, M.C. Gutiérrez, R. Furstoss, J. Ward, R. Wohlgemuth, V. Alphand, *Nat. Protoc.* 3 (3) (2008) 546-554.

### List of Publications

M.P. Meissner, Z. Xu, G.C. Jones, S.H. Minnaar, S.T.L. Harrison, *Miner. Eng.* 60 (2014) 8-13.



## **Mohd Shafiq Mohd Sueb**

Phone: +45 4525 2705  
E-mail: mosh@kt.dtu.dk  
Discipline: Reaction Separation Technology

Supervisors: Manuel Pinelo  
Anne S. Meyer

### **PhD Study**

Started: December 2013  
To be completed: December 2016

## **Detoxification of a liquid stream from biomass pretreatment by nanofiltration: key role of the interaction membrane material-inhibitors on flux and retention**

### **Abstract**

The liquid stream from biomass pretreatment requires detoxification (removal of inhibitors) to make feasible the subsequent enzymatic treatment and/or fermentation. Nanofiltration can be an efficient, inexpensive alternative for detoxification as compared to the traditional methods. The study was performed in a sequential fashion. First, the performance of three commercial NF membranes (NTR 7450, NF 270 and NP 030) were evaluated. The NF 270 membrane provided the highest permeate flux and largest difference in retention between carbohydrates (mono- and oligosaccharides) and inhibitors (furans, acids) and salts. Secondly, the influence of key operational variables i.e. pressure, and temperature was tested. A maximal pressure of 4 bars and a temperature of 20 °C were found to be optimal, as the higher pressure or temperature levels tested (10/20 bars and 50 °C) resulted in significant increases of retention of inhibitors. The results suggested that the interactions between the membrane material and the functional groups of the different species contained in the pretreated liquid are the key factor to consider in order to obtain a high permeate flux and a proper separation factor.

### **Introduction**

Generation of inhibitors from sugar and lignin degradation during pretreatment has negative consequences on the fermentation, as they are harmful for fermentative microorganisms and inhibit their metabolism [1], [2]. The inhibitory compounds that can be released from lignocellulosic biomass can be classified into three groups: 1. furans which mainly consists of furfural and 5-hydroxymethylfurfural (HMF), 2. aliphatic acids that includes formic acid, acetic acid, propionic acid, and lactic acid 3. phenolic compounds [2], [1].

The use of membrane technology -particularly for separation and purification of mono-/ oligosaccharides from the lignocellulosic hydrolysate- is attracting increasing interest as an alternative to the costly traditional methods, due to several advantages like low energy consumption, cost competitiveness, facile sustainable processing and easy scale-up [3]. Membrane separation processes have indeed become the main focus of studies within the last decades for removing acids via different operations such as pervaporation, electrodialysis, reverse osmosis and nanofiltration [4]. Besides that, previous studies have reported that other inhibitors such furans, carboxylic acids and phenolic

compounds were effectively removed by reverse osmosis and nanofiltration [5], [6].

### **Specific Objectives**

The overall objective of the present work was to obtain a pure stream of carbohydrates (mono- and oligosaccharides) from the liquid obtained from pretreatment of wheat straw. This was achieved in sequential steps:

1. Selection of the best nanofiltration membrane from three common commercial ones (NF 270, NTR 7450 and NP 030) with regards to a high retention for carbohydrates and low retention for inhibitors and salts, that would pass to the permeate.
2. Evaluation of the most relevant operational variables which affecting retention i.e. temperature, pressure, and feed concentration, in order to define the value of such variables enabling the highest performance.

The experiments were carried out in model solutions –using the same concentrations of the main components of the real solution.

## Results and Discussion

### Membrane selection

Considering the highest flux (over 50 L/m<sup>2</sup>h), the low retention of salts, acids and furans (less than 15%) and the high retention of monosaccharides (higher than 70%) and oligosaccharides, the NF 270 was selected as the membrane for removal of inhibitors and salts.

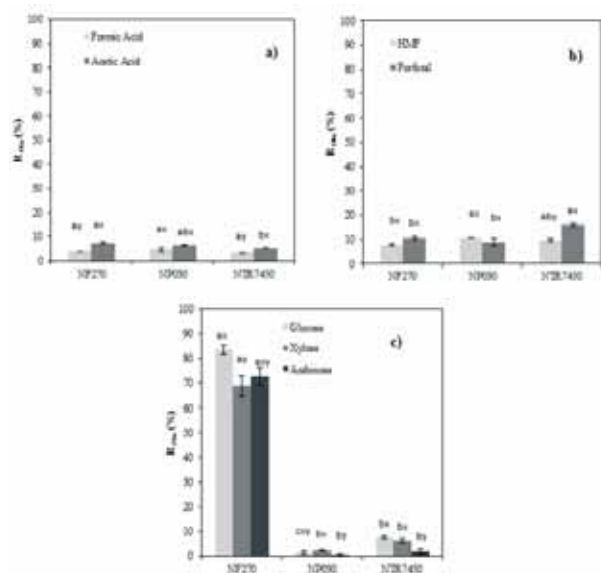


**Fig. 1.** Effect of the used membrane (NF 270, NP 030, NTR 7450) on the retention of **a)** acids (formic acid 0.4 g/L and acetic acid 1.2 g/L), **b)** furans (furfural 0.5 g/L, and HMF 0.1 g/L), **c)** monosaccharides (xylose 0.8 g/L, arabinose 0.3 g/L and glucose 0.1 g/L) at room temperature, pressure = 4 bar and agitation = 200 rpm.

### Influence of operational conditions on permeate retention: pressure and temperature

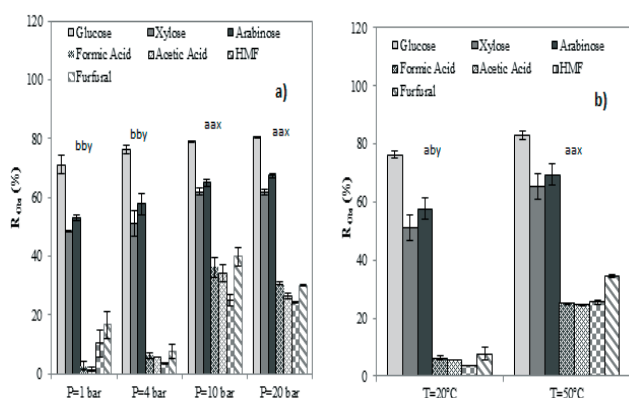


**Fig. 2.** Observed retention at different **a)** Pressure (P = 1 bar, P = 4 bar, P = 10 bar and P = 20 bar); **b)** Temperature (T = 20 °C and T = 50 °C) on the model solution for membrane NF 270.

Increasing pressures did not have any significant effect on the retention of monosaccharides. Pressure increases did however have a very significant effect on the retention of inhibitors, which increased four times when pressure was enhanced from 4 to 10 bars. No

further increases of retention were observed when pressure was changed from 10 to 20 bars though.

Retention also increased at high temperature. It was found that the retention of monosaccharides increased 10–20% when the temperature was increased, and the retention of inhibitors increased four times at 50 °C compared with room temperature.

### Conclusion

Results suggest that the material of the membrane is crucial in the efficiency of the nanofiltration of this type of compounds. High pressures and temperatures, even if promote higher fluxes, are not necessarily convenient for this type of separations, as they result in significant increases of retention of furans and acids. Lastly, and in order to obtain a stream with an acceptable purity of carbohydrates, an additional step of diafiltration was found to be required.

### References

1. J.-W. Lee, L. T. P. Trinh, and H.-J. Lee, "Removal of inhibitors from a hydrolysate of lignocellulosic biomass using electrodialysis," *Sep. Purif. Technol.*, vol. 122, pp. 242–247, Feb. 2014.
2. J. Luo, B. Zeuner, S. T. Morthensen, A. S. Meyer, and M. Pinelo, "Separation of phenolic acids from monosaccharides by low-pressure nanofiltration integrated with laccase pre-treatments," *J. Memb. Sci.*, vol. 482, pp. 83–91, 2015.
3. M. Pinelo, G. Jonsson, and A. S. Meyer, "Membrane technology for purification of enzymatically produced oligosaccharides: Molecular and operational features affecting performance," *Sep. Purif. Technol.*, vol. 70, no. 1, pp. 1–11, Nov. 2009.
4. M. D. Afonso, "Assessment of NF and RO for the potential concentration of acetic acid and furfural from the condensate of eucalyptus spent sulphite liquor," *Sep. Purif. Technol.*, vol. 99, pp. 86–90, 2012.
5. B. Qi, J. Luo, X. Chen, X. Hang, and Y. Wan, "Separation of furfural from monosaccharides by nanofiltration," *Bioresour. Technol.*, vol. 102, no. 14, pp. 7111–8, Jul. 2011.
6. Y.-H. Weng, H.-J. Wei, T.-Y. Tsai, W.-H. Chen, T.-Y. Wei, W.-S. Hwang, C.-P. Wang, and C.-P. Huang, "Separation of acetic acid from xylose by nanofiltration," *Sep. Purif. Technol.*, vol. 67, no. 1, pp. 95–102, May 2009.



## Sofie Thage Morthensen

Phone: +45 4525 2612  
E-mail: soth@kt.dtu.dk

Supervisors: Manuel Pinelo  
Henning Jørgensen

PhD Study  
Started: May 2014  
To be completed: April 2017

## High performance separation of xylose and glucose using an integrated membrane system

### Abstract

Membrane technologies for biorefining applications are receiving growing attention due to their low chemical consumption and reduced energy requirements compared to traditional separation processes. In the first part of this PhD project, an integrated membrane system was studied for the purification of xylose from glucose. Glucose was first oxidized to gluconic acid, an important building block chemical, and then xylose was separated from gluconic acid by nanofiltration due to charge effects. A production rate of 0.61 mg gluconic acid/mg enzyme/min was achieved in the membrane bioreactor allowing for >98% xylose purity in the nanofiltration.

### Introduction

The increasing world population consuming high value products puts a huge pressure on resources both environmentally and economically. Lignocellulosic biomass offers an abundant and renewable resource, which can be used for production of fuels and chemicals in the future bio-based society. However, in order to realize the visions of biorefining, there is a need for designing sustainable conversion and separation processes. Among the various separation strategies used, membrane technology has shown great potential in process intensification and product purification due to excellent fractionation and separation capability, low chemical consumption and reduced energy demands [1]. The purpose of this PhD project is to develop novel reactive membrane-based separation techniques for purification of monosaccharides in biorefinery applications.

### Specific objectives

The specific objective of this work was to enhance purification of xylose from glucose. The strategy was to convert glucose to gluconic acid in an ultrafiltration (UF) membrane reactor followed by separation of xylose from gluconic acid by nanofiltration (NF). The separation mechanism was based on negative charge repulsions – rather than sieving effects – between gluconate and the surface of the NF membrane, thus allowing only xylose to pass through the membrane (Fig. 1).

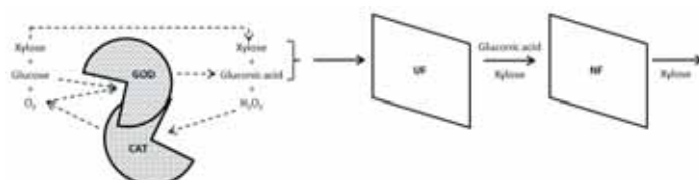
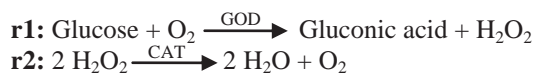


**Figure 1:** Separation of xylose from glucose in an integrated membrane system.

Besides being a flavoring agent in the food industry, gluconic acid is also an important building block chemical for higher value products. The oxidation of glucose to gluconic acid was obtained by two coupled reactions (r1-r2) catalyzed by glucose oxidase (GOD) and catalase (CAT).



Oxygen for r1 was provided via r2 by initially adding hydrogen peroxide according to the reaction stoichiometry. Two different enzyme-membrane configurations (UF1 and UF2) were investigated with respect to maximizing the biocatalytic productivity of the process. In UF1, both enzymes were entrapped inside the support layer of the UF membrane by fouling-induced enzyme immobilization and subsequent polydopamine coating, while in UF2 both enzymes were free in solution so the membrane merely served as a barrier for the enzymes (Fig. 2).

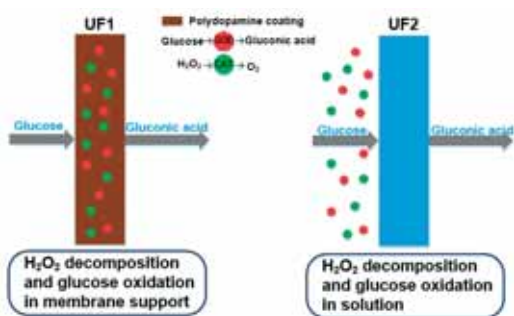


**Figure 2:** Enzyme-membrane configurations.

## Results and Discussion

The membrane bioreactor performance was found to be highly related to the robustness against  $H_2O_2$ , an inactivator of GOD. When the enzymes were confined in the membrane, the robustness severely decreased compared to when they were free in solution (Fig. 3). On a molecular level, the CAT to GOD ratio in both UF1 and UF2 was 1:18 (bovine liver CAT) and 1:29 (*Aspergillus niger* CAT), respectively. As a result, there was a serious risk of  $H_2O_2$  inactivating GOD before being decomposed by CAT when the enzymes were confined in the membrane. However, full conversion of glucose to gluconic acid could still only be achieved in the first three cycles of UF2 (with CAT from bovine liver) thus indicating that there was also a serious risk of CAT inactivation by  $H_2O_2$ . This was verified by enzyme stability studies, which showed a severe drop in activity after three reaction cycles (6% residual bovine liver CAT activity). When changing the catalase origin to *Aspergillus Niger*, full conversion was achieved in all cycles with UF2 corresponding to a biocatalytic productivity rate of 0.61 mg gluconic acid/mg enzyme/min in each cycle. The improved robustness of *Aspergillus Niger* catalase was further verified by enzyme stability studies showing unaffected activity after five cycles. The performance of UF1 similarly improved when changing the catalase origin, however, the unfavorable diffusion of  $H_2O_2$  inside the membrane still did not allow the biocatalytic productivity rate to exceed 0.26 mg gluconic acid/mg enzyme/min in the first cycle.

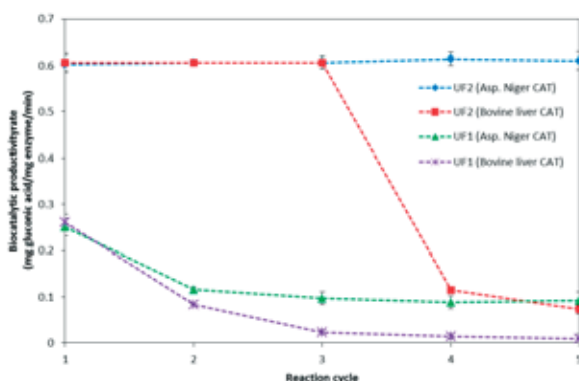


**Figure 3:** Biocatalytic performance of UF1 and UF2 with GOD from *Aspergillus niger* and CAT from *Aspergillus niger* and bovine liver, respectively.

Following the enzymatic conversion, separation of xylose from gluconic acid could be achieved by NF due to significant difference in retention of the two molecules. The retention of the membrane was 98 % with respect to gluconic acid and 42 % with respect to xylose. Since the molecular weights of xylose and gluconic acid only differ by a factor 1.3, the difference in the observed retentions was not explained by sieving effects but rather by the more significant charge effect on gluconic acid. When the NF membrane was immersed in aqueous solution at pH 9.5, the dissociation of its carboxyl groups caused the membrane surface (polyamide) to become negatively charged [2]. Since gluconic acid also deprotonates in solution at this pH, significant charge repulsions occurred between gluconic acid (gluconate) and the surface of the membrane which led to almost full retention of gluconic acid. Since significant amounts of xylose were still retained by the membrane, consecutive diafiltration cycles were further conducted. The recovery of xylose in the permeate was found to increase from 41.2 to 97.9 % after ten diafiltration cycles without remarkably compromising the xylose purity, which in turn only decreased from 99.2 to 98.1 %.

## Conclusions

An integrated membrane system was investigated for the purification of xylose from glucose. Glucose was converted to gluconic acid in an UF membrane bioreactor at a constant biocatalytic productivity rate of 0.61 mg gluconic acid/mg enzyme/min. Subsequently, xylose separation from gluconic acid was achieved by NF due to high retention of gluconic acid (98 %) resulting from significant charge effects. Integrating reaction and NF to enhance separation, while obtaining another value-added stream, presented new options for separating two compounds with similar molecular weights by membrane technology.

## Acknowledgements

This work was supported by the Bio-Value Strategic Platform for Innovation and Research, co-funded by The Danish Council for Strategic Research and The Danish Council for Technology and Innovation, case no: 0603-00522B.

## References

1. Y. He, D.M. Bagley, K.T. Leung, S.N. Liss, B.-Q. Liao, *Biotechnol. Adv.* 30 (2012) 817–858.
2. J.-H. Choi, K. Fukushi, K. Yamamoto, *Sep. Purif. Technol.* 59 (2008) 17-25.

## List of Publications

1. S.T. Morthensen, J. Luo, A.S. Meyer, H. Jørgensen, M. Pinelo, *J. Membrane Sci.* 492 (2015) 107-115.



## Victor Buhl Møller

Phone: +45 4525 2923  
 E-mail: Vibum@kt.dtu.dk  
 Discipline: Coating and polymer technology

Supervisors: Søren Kiil  
 Kim Dam-Johansen  
 Sarah Maria Frankær, Hempel

PhD Study  
 Started: August 2014  
 To be completed: August 2017

## Acid and abrasive resistant coatings for the heavy duty industry

### Abstract

Acid and abrasive resistant organic coatings have found their uses as cheap alternatives to ceramics and metal alloys as protective measures in the heavy duty industry. Despite the use of these coatings, there are still knowledge gaps when it comes to chemical interactions in the polymer matrix with aggressive species, as well as the combined erosion/corrosion mechanism that occurs when acidic chemicals are combined with erosive particles. The construction of test equipment capable of exposing coatings to simultaneous erosive and corrosive environments is completed, and investigations on effects of process and formulation variables and possible synergistic degradation mechanisms has commenced.

### Introduction

The heavy duty industry displays a large variety of corrosive and environmentally damaging compounds in need of proper containment. With the added effects of hostile environments such as elevated temperatures and erosive particles, structural material is put to the test. The use of protective coating technology provides a chemical barrier between the process environment and the structural substrate, thus giving a desired chemical inertness while retaining physical properties.

Organic coatings are polymeric materials similar to plastics, commonly seen as decorative paints. They are capable of adhering to a surface or a substrate to create a continuous film, and thermoset coatings are chemically cured.

Protective coating technology has found its uses in flue gas desulphurization plants, rail car tanks and copper mineral leaching, among others. The coatings are often based on the chemical resistant epoxy technology, with the front runner being a styrene-cured epoxy vinyl ester, see Fig. 1, often reinforced with glass mats. Organic coatings are cheap alternatives to installing ceramic linings or using high grade acid resistant alloys, though they are considered more risky and are not as durable with regard to wear resistance [1][2].

### Objectives

Having recently completed a test set-up capable of simulating the environment inside an agitated copper leach reactor, the current focus is on proving

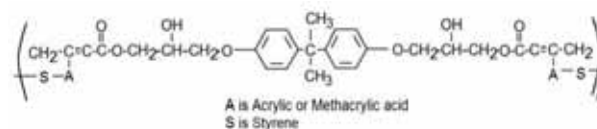


**Figure 1:** Structure of a repeating unit of bisphenol A epoxy vinyl ester cured with styrene.

reproducibility of results, followed by the actual research experiments.

The project has emphasis on practical application as well as developing the research field academically, focus points include:

- Investigating physical and chemical degradation mechanisms and establishing predictive models
- Studying the effects of process and coating formulation variables. Parameter study.
- Developing and constructing tests equipment capable of simulating abrasive slurry or/and combined acidic exposure. (completed)

### Results and Discussion

The construction of the miniature leaching reactor is finished and has required a plethora of custom made equipment as well as infrastructural work to complete. The set-up is placed in a laboratory where special acid resistant ventilation is available, the set-up can be seen in Fig. 2. No experiments have yet been completed on the set-up, but I will give an appetizer of what to come, from screening experiments I have performed.



**Figure 2:** Reactor, dump tanks and frame of the set-up during construction in the DTU workshop.

By coating the inside of a metal can, filling it with water and 20 wt% particle load and using a pigment disperser to stir at 500 rpm, it was possible to perform erosion tests. The main eroded areas was a circular pattern on the can bottom, see Fig. 3, while the reactor sides remained unharmed.



**Figure 3:** Circular erosion pattern observed on can bottom. 0h (left), 34h (middle) and 180h (right) exposure time.

The erosion rate was determined by observing changes in film thickness, using a non-destructive Elcometer 355. Fig. 4 shows these changes over time at 2 set positions from the can center. The trend shows an initial increase in film thickness, caused by swelling, followed by a steady decrease, measuring around 0.055 to 0.081  $\mu\text{m}/\text{h}$ .

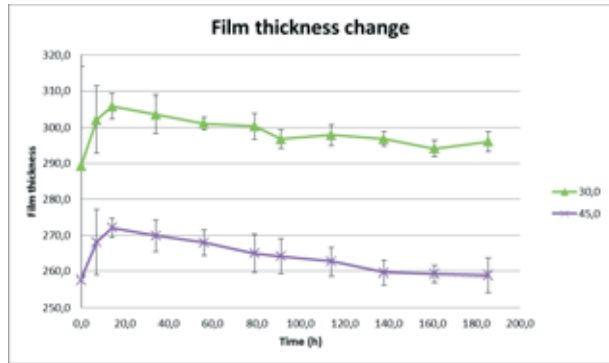


**Figure 4:** The change in mean film thickness of the coating. Measurements taken in a circular pattern 30 and 45 mm away from the center position.

### Conclusion

Preliminary investigations suggest that the change in film thickness is a function of swelling and erosion. The film thickness is dominated by an initial swelling due to rapid diffusion of solution into the film, followed by a seemingly linear decrease caused by the action of erosive particles, chipping away at the coating.

The erosion pattern is symmetric around the center axis, thus it is expected that wear severity is a function of distance from the center.

The experiments with the new set-up following these preliminary investigations will seek to prove the above statements, show reproducibility of results, and determine the exposure time required for determining coating lifetime.

### Acknowledgements

This work is part of the research platform ‘Minerals and Cement Process Technology – MiCeTech’ funded by Innovation Fund Denmark, FLSmidth A/S, Hempel A/S, and DTU.

### References

1. P. Hag, N. Harrison, *Anti-Corrosion Methods and Materials*, 43 (2) (1996) 15-19.
2. C. Compère, J. Hechler, and K. Cole, *Progress in Organic Coatings*, 20 (2) (1992) 187-198.



## **Kasper Skov Mørk**

Phone: +45 4525 2837  
E-mail: kaskm@kt.dtu.dk

Supervisors: Ass. Prof., Søren Kiil, DTU Chem. Eng.,  
Prof., Kim Dam-Johansen DTU Chem. Eng.,  
Ass. Prof., Ion Marius Sivebæk DTU Mech.,  
Sarah Maria Frankær, Hempel A/S R&D,  
Jesper Lebæk, FLSmidth A/S R&D

PhD Study  
Started: March 2015  
To be completed: March 2018

## **Tribological studies of anti-stick coatings for adhesive raw material build-ups in the cement industry**

### **Abstract**

The content of this PhD study is to quantify and predict the unwanted raw material build-up on handling equipment surfaces in the cement industry. A possible solution to the raw material build-up in lower abrasive environments is to modify the exposed surface by an organic coating that shows anti-stick properties. The raw material handling problem is significant when the raw material is wet due to e.g. rainfall. The surface tension effects from the water is dominating the adhesion force, but the dynamics of the raw material handling can also develop friction forces in the wet raw material – exposed surface interface. Hydrophobic organic coatings show promising anti-stick results. However, these coatings have limitations in terms of their low wear resistance, thus the appropriate coating parameters need to be identified in this PhD study in order to solve the raw material handling problem in the cement industry.

### **Introduction**

The understanding of adhesion, friction and wear between wet granular materials and various solid surfaces are still remains unclear. Adhesive raw materials (clay and limestone) in the cement industry tend to “stick” on equipment surfaces, when it is transported through chutes and casings from a conveyor belt. This can cause blockage of outlets, unpredictable raw material flow and even sudden production shutdowns. The exposed surfaces are modified by low friction linings that decrease the raw material build-up. However, the raw material build-ups are also observed in lower abrasive environment where cheaper organic coatings may be used. The use of coatings in the cement industry are new, hence in-situ tests of organic coating performance in terms of anti-stick and wear properties need to be investigated. The quantification of adhesion and friction is not straightforward, hence new experimental designs will be constructed in order to have a set-up that imitate the in-situ process conditions at a cement plant that observes the raw material handling problem.

Tribology is in general the science that describes the adhesion, friction and wear of surfaces in relative motion. Thus tribology is identified when the raw material impacts on the equipment wall and is deposited due to high adhesion/friction forces. Inevitably, wear

will be an issue when dealing with organic coatings even for the low abrasive environment. The adhesive build-up is often observed when the raw material is wet, thus wet adhesion (surface tension effect) is believed to be the main adhesion contribution [1]. However, the dynamics from the impact between the raw material leaving the conveyor belt and hitting the equipment can have other contributing adhesive forces as viscous forces. This strongly depends on the water content of the raw material and the impact speed [2]. In terms of frictional forces, the particles have the ability to interlock in-between the grooves of the exposed surface, which will increase the friction during shearing of the raw material – exposed surface interface [3]. Similar interlocking trends can be confirmed from experimental work conducted in the master thesis from the PhD student. The development of capillary forces in the wet raw material – exposed surface interface can also have an influence on the shear strength of the interface, thus friction forces may be related to the wet adhesion phenomenon. This again depends on the surface roughness profile of the exposed solid surface [4].

### **Specific Objectives**

The process design of raw material handling equipment at FLSmidth A/S is expected to be enhanced in terms of supervision to their customers. DTU Chemical

Engineering will investigate how models based on experimental findings can be developed in order to predict and decrease the raw material build-up. This model will have relevant coating parameters from Hempel A/S implemented, which makes it easier for FLSmith A/S to select the appropriate coating system from Hempel A/S that can decrease the handling problem.

### Results & Discussion

The adhesive raw material is investigated tribologically by impacting it towards surfaces of different treatments from Hempel A/S. The free-fall experiment can be used to assess the impact dynamics of a raw material lump that possible will stick to the

**First drop raw material lump ... then vertical placement**

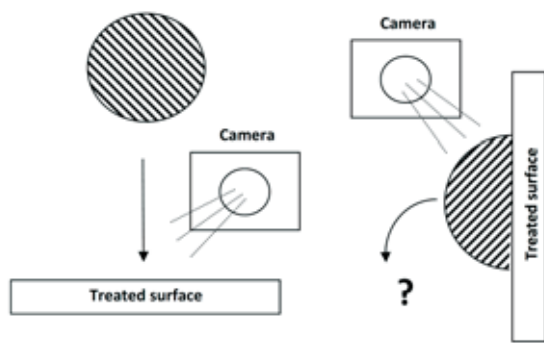


**Figure 1:** Sketch of the principles of the free-fall experiment. The camera can record the impact dynamics in terms of deformation and possible rebound.

impact plate as seen in Figure 1. The free-fall experiment is fairly simple, but can be analyzed by the use of a camera that can record the impact dynamics in greater detail than the naked eye. Additionally, the vertical placed surface can be rotated in the vertical axis and the friction between the deposited lump and the surface can be analyzed from centrifugal forces.

Preliminary free-fall tests show differences in performance from selected coatings from Hempel A/S.

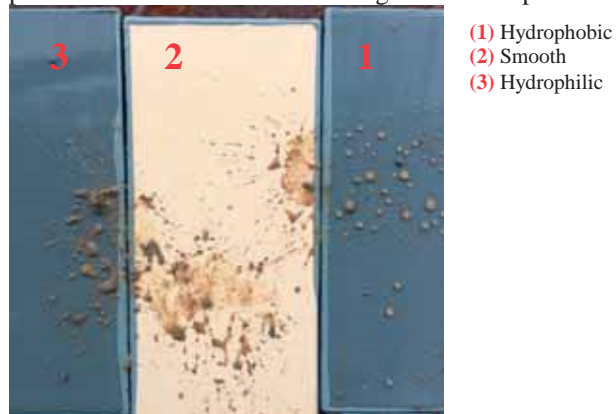


**Figure 2:** Hempel A/S coating performance from preliminary free-fall test. Different coating properties were investigated in terms of hydrophobicity and roughness.

The results from the preliminary free-fall test are shown in Figure 2, where three different coating properties are tested. Hydrophobic action is observed due to the formation of drops (high water contact angle) on the hydrophobic coating. However, the preliminary tests did also show that there exists a certain water content threshold for the hydrophobic action to occur. At certain water contents of the raw material, the hydrophilic and hydrophobic coating will show the same performance in order to decrease the adhesive build-up. By further designing (see Figure 1) of the free-fall test it is believed to be possible to identify and quantify the tribological phenomena that appear in the raw material – exposed solid surface interface.

### Conclusion

The adhesion and friction mechanisms behind the adhesive raw material build-up will be investigated through more advanced and scientific experimental design than previously seen in the published literature. This will be used to map the most essential coating parameters in terms of developing an anti-stick coating that can decrease the deposition of raw materials on exposed handling equipment. Surface tension effects between the wet raw material and the equipment surface are argued to be important in the literature, thus hydrophobic coatings are to be tested. The development of frictional forces is inevitable in tribological system, where the particles of the raw material tend to interlock into the grooves of the exposed surface. Experiments from the literature show that this interlocking of particles is prone to appear for sheared and compressed raw material. These literature findings are to be related to the dynamics and impacts of raw material towards equipment walls in the cement industry due to processing.

From initial tests it can be concluded that organic hydrophobic coatings have to ability to ease the cleaning of surfaces exposed to impacting raw material. Uncertainties still remain to be discussed regarding the in-situ coating performance.

### Acknowledgement

This work is part of the research platform ‘Minerals and Cement Process Technology – MiCeTech’ funded by Innovation Fund Denmark, FLSmith A/S, Hempel A/S, and DTU.

### References

1. E.R. Fountaine, Journal of Soil Science 5 (2) (1954) 251-263.
2. F.R. Eirich and D. Tabor, Mathematical Proceedings of the Cambridge Philosophical Society 44 (1948) 566-580
3. A.W. Roberts, L.A Sollie and S.R. de Silva, Tribology International 26 (5) (1993) 335-343
4. T.B. Hamid and G.A. Miller, Canadian Geotechnical Journal 46, (2009) 595-606

**Mohammadhadi Nakhaei**

Phone: +45 4525 2853  
E-mail: mnak@kt.dtu.dk

Supervisors: Kim Dam-Johansen  
Peter Glarborg  
Hao Wu  
Linda Kaare Nørskov, FLSmidth

PhD Study  
Started: May 2015  
To be completed: May 2018

## Multiphase flow and fuel conversion in cement calciner

### Abstract

The main focus of this PhD project is the development of a Computational Fluid Dynamics (CFD) model for simulation of cement calciners firing Refuse Derived Fuels (RDF). RDF particles are composed of different waste materials with diverse physical and chemical properties. In order to develop a CFD model that can describe the aerodynamic and conversion of RDF in cement calciners, advanced characterizations of the chemical, physical, aerodynamic and combustion properties of RDF will be carried out. The developed CFD model will be validated and compared with pilot-scale and full-scale measurements. The validated CFD model will be applied to evaluate the influences of fuel properties and operation conditions on calciner performance, and to optimize the operation and design of cement calciners.

### Introduction

Driven by the demand of reducing fuel price and CO<sub>2</sub> emission in cement production, there are growing interests in utilizing alternative fuels, such as Refuse Derived Fuels (RDF), in cement plant calciners. Compared to the conventional calciner fuels such as coal and petroleum coke, the characteristics of RDF are very different in both physical and chemical aspects. They also have large variations depending on their source and processing technology. In order to design and operate RDF-based calciners with high fuel conversion and low pollutant emissions, in-depth knowledge on the multiphase flows and conversion of RDF under calciner conditions is required. This could be obtained by conducting experiments and developing cost-efficient modelling tools, such as Computational Fluid Dynamics (CFD) models. The model could be used to support the process design, trouble shooting, and performance optimization in industrial calciners.

### Objectives

The main objective of this project is to achieve new and improved knowledge about aerodynamics of gas-solid flows, calcination, and conversion of RDF (i.e. drying, pyrolysis, and char oxidation) in cement plant calciners. A CFD model will be developed and validated for this purpose. This CFD model can support the design and operation of RDF-fired cement plant calciners to achieve a high fuel conversion and low pollutant emissions.

### Approaches

#### *RDF characterization*

RDF is produced from combustible fraction of municipal solid waste or industrial waste using various techniques such as sorting, screening, shredding, and so on [1]. Despite the production processes help RDF to become more uniform in content compared to its original source, there are still a large number of material types in RDF which makes it a heterogeneous fuel. Additionally, RDF composition varies depending on its source and production techniques [2]. Thus, in order to support the development of a CFD model for RDF combustion, detailed characterizations of the physical, chemical, aerodynamic and combustion properties of RDF are needed.

In this project, a method will be developed and tested to characterize the physical, chemical and aerodynamic properties of RDF, and to identify the correlations between these properties. The method will combine several novel/conventional characterization tools, such as wind sieve, image-based tool for particle size and shape analysis, video-based tool for drag analysis, a wet-chemical/thermochemical tool for analyzing plastic fractions, fuel proximate and ultimate analysis etc. It is expected that the method developed can separate RDF into several fractions each having similar physical, chemical and aerodynamic properties. The method will support both the development of a CFD model for RDF combustion, and the assessment of RDF quality for cement calciners.

The combustion behaviors of RDF will be studied experimentally in a single particle combustor and/or an entrained flow reactor simulating cement calciner conditions, and a thermogravimetric analyzer (TGA). The influences of fuel properties and operation conditions on RDF conversion will be investigated systematically. The experimental results will be utilized to develop sub-models (drying, pyrolysis, and char oxidation/gasification) that are needed to describe RDF conversion in CFD modeling.

#### *Pilot-scale and full-scale measurements*

Experiments will be carried out in a pilot-scale cold calciner located at FLSmidth Research Centre Dania. The pilot-scale setup is composed of a vertical vessel, where air can be injected from the bottom and raw meal particles can be fed from the side by a spreader box. Besides, a feeding system for RDF particles will be established in order to assess their aerodynamic behaviors inside the calciner. Qualitative and quantitative measurements of the particle concentration and velocity distributions in the calciner will be carried out. The obtained experimental data will be used for CFD validation under cold conditions.

Besides pilot-scale measurements, it is expected that full-scale measurements will be carried out in a RDF-fired cement calciner. The raw meal distribution inside the calciner, especially near the spreader box, will be assessed using video-imaging methods. Moreover, probing measurements will be carried out to reveal the gas temperature and composition distribution in the calciner. The data from these measurements will be used for validating the CFD model under reacting conditions.

#### *CFD simulation and validation*

One of the commonly used methods for CFD simulation of dilute gas-solid flows is Eulerian-Lagrangian approach. In this method, Navier-Stokes equations are solved for the fluid in an Eulerian platform while individual particles are tracked in time. This method requires less empirical modelling compared to the Eulerian-Eulerian method in which both phases are solved as fluids. This matter becomes more important when there are irregular-shaped RDF particles in the flow of interest. The main CFD program to be used in this project is Barracuda CFPD software along with comparison with other commercial CFD software such as ANSYS FLUENT and ANSYS CFX.

The first step is to simulate a full-scale coal fired calciner based on the current computational practice of research and development center of cement division, FLSmidth. It is then possible to evaluate the limitations of this practice and make new suggestions for improvements. The modeling methods and boundary conditions for the raw meal spreader box and its dispersion inside the calciner can be improved using aforementioned full-scale and pilot-scale camera-based measurements.

In order to simulate a RDF-fired calciner, sub-models should be developed for aerodynamic and conversion of large non-spherical RDF particles, based on the RDF characterization experiments. Pilot-scale and full-scale measurements will be used for comparison and validation of the CFD model under cold and reaction conditions.

Once the CFD model is validated with pilot-scale and full-scale measurements, parametric studies will be performed in the following areas:

- The number, position, and alignment of inlets for raw meal, fuel, and tertiary air.
- The flow rate of each inlet mentioned above.
- RDF properties such as heating value, moisture content, size and shape distribution, etc.

It should be noted that the most important target functions in these parametric studies are fuel burnout and NO<sub>x</sub> reduction capability of the calciner.

#### **Acknowledgement**

This work is part of the research platform ‘Minerals and Cement Process Technology – MiCeTech’ funded by Innovation Fund Denmark, FLSmidth A/S, Hempel A/S, and DTU.

#### **References**

1. D. Lechtenberg, *Alternative Fuels and Raw Materials Handbook for the Cement and Lime Industry*, Vol. 1. Verlag Bau and Technik, 2012.
2. C.A. Velis, P.J. Longhurst, G.H. Drew, R. Smith, S.J.T. Pollard, *Production and quality assurance of solid recovered fuels using mechanical-biological treatment (MBT) of waste: A comprehensive assessment*, *Critical Reviews in Environmental Science and Technology*, 40 (12) (2010) 979-1105.



**Henrik Lund Nielsen**

Phone: +45 4525 2886  
 E-mail: hluni@kt.dtu.dk

Supervisors: Philip Fosbøl  
 Peter Glarborg  
 Søren Kiil  
 Kaj Thomsen

PhD Study  
 Started: July 2015  
 To be completed: June 2018

**Measuring and modelling of chemical sulfur corrosion mechanisms in marine diesel engines**

**Abstract**

When large ships engines are run at reduced load, “cold corrosion” has turned out to be a considerable problem. Cold corrosion occurs from mechanical wear in combination with acidic flue gas species condensing at the liner surface inside of the engine cylinder. The purpose of this project is to investigate the electrochemical mechanisms that are taking place at the surface. Experiments and measurements of the current densities at relevant conditions are to be performed. The results will be the basis for a model that are able to describe the rate of corrosion and allows limiting conditions and mechanisms to be identified.

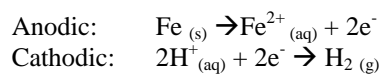
**Introduction**

In the next 5-10 years stricter regulations on ships’ fuel sulfur content and pollution are coming into force. A consequence is that ships engines, and in particular their operation will change due to alteration of the market requirements. With regard to this, prevention of "cold corrosion" in the engines is a major challenge. This phenomenon happens mainly when “slow-steaming” (i.e. sailing at reduced speeds). "Cold corrosion" is a mixture of acid attack and mechanical wear in the engine that occurs because the sulfur components like sulfuric acid (H<sub>2</sub>SO<sub>4</sub>), SO<sub>2</sub>, and SO<sub>3</sub> to a greater extent condense on the cylinder walls in the engines at conditions of slow-steaming where the engine runs at a reduced load. Expensive lube oil which has a specific high content of dissolved limestone is continuously added to the cylinders to neutralize the acid generated, but the efficiency of this procedure is not always optimal. The life time of certain components is reduced by a factor 5-10.

This PhD project is a part of a large project, SULCOR, involving DTU Chemical Engineering, DTU Mechanical Engineering, and MAN Diesel and Turbo A/S. The overall objective is to develop a multi-zone model that can identify and predict the corrosion occurring from combustion of Sulphur-containing fuels. This PhD project addresses the corrosion mechanisms taking place right at the cylinder liner surface. Other PhD/Post doc projects in the SULCOR framework provide data/models for other “zones”, serving as boundary conditions for this work. These are mainly the

cylinder bulk gas and the lube oil film that covers the cylinder wall.

The objective of this work is to develop a mathematical model describing the corrosion from flue gas components. Several possible electrochemical reactions can be expected to occur in this multi-component environment. The typical reactions of acid corrosion of steel are as follows:



A number of species are suspected to contribute to the corrosion mechanism: H<sup>+</sup>, CO<sub>2</sub>, SO<sub>2</sub>, SO<sub>3</sub>, O<sub>2</sub> and Fe<sup>3+</sup>. The molecules accept electrons transferred at the metal surface resulting in formation of Fe<sup>+2</sup> ions and thereby dissolution of iron.

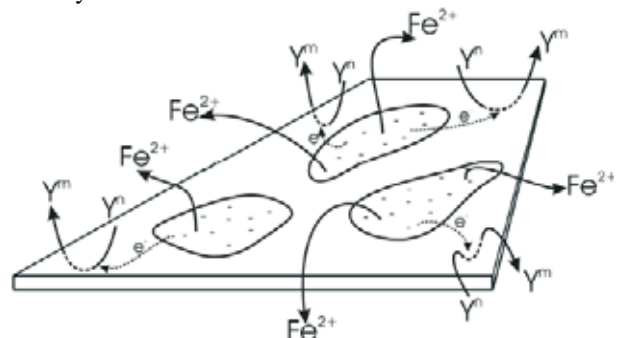


**Figure 1:** Graphical representation of the electron exchange taking place at the metal surface [1]. Y<sup>n</sup> represents electron accepting species.

The main corrosion products are likely  $\text{FeSO}_4$  (s) and  $\text{Fe}_2(\text{SO}_4)_3$  (s). These products can potentially have a shielding effect on the surface but when diluted and dissolved in water they can hydrolyze to acid and contribute further to the corrosion phenomena [2]. Furthermore, the movements of the piston are continuously removing the shielding surface layer. Thereby the wear inflicted by the piston movements causes the surface to be more exposed to contact with the corrosive flue gas components, and even more iron is dissolved. Experience shows that chemical corrosion alone or mechanical wear alone are not a major problem. A combination of both, however, significantly accelerates the overall corrosion process.



**Figure 2:** View of a large ships engine cylinder at the container ship, Matz Maersk. The internal liner surface is exposed to corrosive flue gas components, wear from piston movements as well as high temperatures and pressures.

### Specific objectives

1. The first part of the work is a comprehensive literature study covering diesel engines, flue gas corrosion and the mechanisms and reactions behind. Not much literature and data exists on this specific topic, but relevant theory from other strategic fields will be included.
2. The next step is to design and conduct experiments that reveal the nature of the corrosion phenomena. The conditions investigated should reflect those in diesel engines as much as possible. The experiments are aimed at measuring the current densities that are governing the corrosion processes. These data can be used for estimating the rate and extent of metal dissolution from the cylinder liner at given engine operation conditions. Experimental electrochemical techniques to consider are e.g. linear polarization resistance, rotating disc electrode, and electrochemical impedance

spectroscopy. Key variables to consider are temperature, pressure, concentrations, oil film properties as well as steel type/structure, piston movements and wear. Measuring solubility of Fe-precipitates at surface conditions is also a point to consider. To the extent possible the different sub-processes, e.g. the reactions of different substances contributing to the overall corrosion phenomena, should be investigated separately.

3. The experiments conducted as well as literature and results from the other SULCOR PhD/Post-doc projects are used for basis of creating a mathematical model describing the corrosion process. This should be valid at temperatures ranging from 70-200 °C and pressures at 50-200 bars. Expressing the current densities at various relevant conditions will likely be a basis for the model.

### Results

A valuable output of the work would be identifying the limiting mechanisms of the corrosion process. In this way, focus can be put on the conditions that lead to further limiting of the corrosion rate. Limitations could be thermodynamic, kinetic or related to diffusion (e.g. protective films or precipitate).

The aim of the developed model is to fit into the large multi-zone model of the SULCOR project. In this way it serves to provide valuable information about the core corrosion mechanism.

### References

1. P.L. Fosbøl, Carbon Dioxide Corrosion: Modelling and Experimental Work Applied to Natural Gas Pipelines, PhD Thesis, Technical University of Denmark, 2008, p. 29.
2. A. Groysman, Corrosion for Everybody, Springer, 2010, p. 128.



## Joachim Bachmann Nielsen

Phone: +45 4525 2922  
E-mail: jobni@kt.dtu.dk

Supervisors: Prof. Anker Degn Jensen  
Prof. John Nielsen, KU

PhD Study  
Started: September 2012  
To be completed: September 2016

## Lignin ethanolysis: a non-catalytic route to a green diesel

### Abstract

The process of converting solid biomass in a solvent under high pressure in order to obtain a liquid product is called direct liquefaction. It is desired to develop a process for direct liquefaction of lignin to obtain a low oxygen content liquid diesel product. A parameter study of lignin ethanolysis has been carried out in a high pressure batch autoclave. Lignin ethanolysis at 400°C has yielded an oil that is stable, non-corrosive and ash and sulfur free. The oil had an oxygen content of less than 10 wt% and therefore blends with fossil diesel with a solubility of at least 75%. It is proven that exhaustive deoxygenation may not be necessary in order to convert lignin into a green diesel that can directly substitute fossil diesel.

### Introduction

There is an increasing pressure on the transport sector to blend fossil fuels with biofuels. Over the recent years there has been an increased focus on liquid fuel production from lignin. Lignin is of particular interest as it is found in quantities up to 30wt% in lignocellulosic biomass and the majority is burned as a low value fuel [1]. In order to transform solid lignin to a liquid fuel the lignin polymer needs to be depolymerized and the oxygen content lowered. Depolymerization can be obtained by direct liquefaction where lignin is dissolved in a solvent at elevated temperatures. Subsequent upgrading by hydrodeoxygenation (HDO) may be required in order to sufficiently lower the oxygen content and improve fuel quality [2].

At the CHEC research center at DTU experiments are carried out to investigate solvolysis at high temperature using ethanol. In collaboration with Copenhagen University (KU) the results obtained from non-catalyzed lignin ethanolysis without the addition of hydrogen have been thoroughly analyzed.

### Specific Objectives

It is desired to transform solid lignin from a low value fuel to a higher value liquid transport fuel. It will be sufficient to obtain a product that can satisfy a 10vol% blend with a marine diesel. This requires depolymerization of the lignin polymer and lowering of the oxygen content from 34wt% to a level where blending with a nonpolar diesel is possible. Furthermore it is important to ensure a low ash content of the

obtained liquid product as ash particles can cause excessive wear to internal combustion engines.

### Experimental Setup

A 500ml stirred HT 4575 Parr batch autoclave capable of handling temperatures up to 500°C and pressures up to 345bar has been used for lignin ethanolysis experiments. The lignin used is a hydrothermally extracted lignin from a 2G bioethanol plant. Experiments have been carried out by mixing a weighed amount lignin with ethanol. The reactor is sealed and an inert N<sub>2</sub> atmosphere inside the vessel is ensured prior to heat up. Reaction time was 0 – 8 hours. After the reaction the vessel is rapidly cooled in an ice bath. The product mixture is filtered and the filtrate is subjected to centrifugation (3min at 11.000 rpm) prior to removal of solvent by rotary evaporation. The remaining heavy fraction is the obtained liquid oil which is subjected to a series of analyses such as elemental analysis to determine the oxygen content of the oil and size exclusion chromatography and NMR. GC-MS/FID analyses on the solvent and light fractions were carried out as well as Karl Fischer titration to determine the amount of water produced.

### Results and Discussion

#### 1. Temperature Effects

In order to identify a suitable process for lignin to liquid conversion it is necessary to obtain a high liquid yield. Oil yields obtained from treating lignin at temperatures

ranging from 250-450°C in ethanol are shown in Figure 1. The final gas pressure is also shown. The plot clearly shows that an optimum oil yield can be obtained at around 400°C and if the temperature is increased further the lignin is increasingly gasified. It is widely reported in literature [1] that the alcohol solvent needs to be supercritical to ensure the highest liquefaction yield. Ethanol becomes supercritical at 241°C so for all of the data represented the solvent is supercritical but parameters such as solvent density, polarity and reactivity may change considerably as a function of different temperatures. Furthermore as the temperature is increased to above 400°C the pathway for lignin depolymerization and decomposition may be dominated by simple thermal breakage of lignin interlinkages.

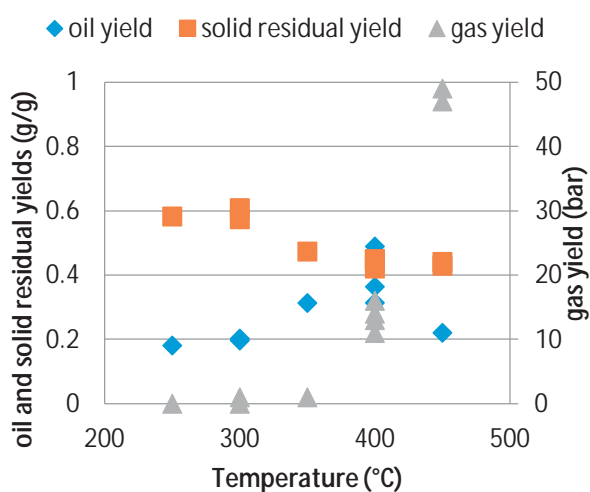


**Figure 1** Yields of lignin-oil and residual solid per lignin is represented as a function of reaction temperature. Furthermore the final pressure of the autoclave is also shown. 100ml of ethanol and 10g lignin was heated for 4 hours at autogenous pressure starting with a non-pressurized inert N<sub>2</sub> atmosphere.

In Figure 2 the molar O/C ratios of the obtained lignin oils is plotted as a function of reaction temperature. The lignin feedstock has an O/C of 0.5 so for all of the different reaction temperatures a reduction of oxygen content in the oils is obtained. Seemingly an increase in temperature increases the degree of deoxygenation as one would also expect as the most reactive functionalities and linkages in the lignin molecule are those containing oxygen.

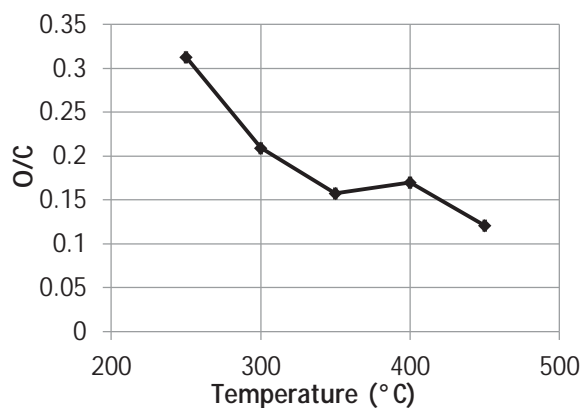


**Figure 2** Molar O/C ratios of the lignin-oils obtained at different reaction temperatures. Lignin oils were obtained by treatment of 10g lignin in 100ml of ethanol for 4 hours at autogenous pressure starting with a non-pressurized inert N<sub>2</sub> atmosphere.

Incorporation of ethanol into the lignin structure could also yield a lowering of the O/C ratio in the resulting oil but a removal of oxygen atoms would be a necessity as ethanol has an O/C ratio of 0.5 and the resulting oils have an O/C of less than 0.3.

There are typically two routes by which deoxygenation can occur:

1. Hydrogenation and dehydration resulting in the formation of water
2. Removal of light oxygen containing functionalities typically through decarboxylation/decarbonylation resulting in oxygen containing gaseous species such as CO and CO<sub>2</sub>.

Ethanol is not believed to have hydrogen donating abilities without the presence of a catalyst and therefore water formation from the non-catalyzed ethanolsis carried out in his study is not believed to be attributed to this effect. The formation of water is therefore mainly assumed to be due to condensation reactions where ethanol takes part. That may be by reaction of the solvent with itself or by reaction with lignin directly facilitating bond cleavage or by reaction with already cleaved oxygen-containing lignin species. CO and CO<sub>2</sub> have been detected in the gas formed from the ethanolsis of lignin but it is not possible to accurately determine if these species come from the lignin or the ethanol. Lignin does however have a large presence of carboxyl groups and decarboxylation could be a pathway for oxygen removal that will lead to a gas phase containing CO/CO<sub>2</sub>.

In order to get a better idea of which route oxygen removal is achieved an oxygen mass balance is shown in Figure 3 where the amount of oxygen found in the different products such as gas (CO/CO<sub>2</sub>), water, char (residual solid lignin) and the lignin-oil relative to the amount of oxygen initially present in the lignin

feedstock has been plotted as a function of reaction temperature.

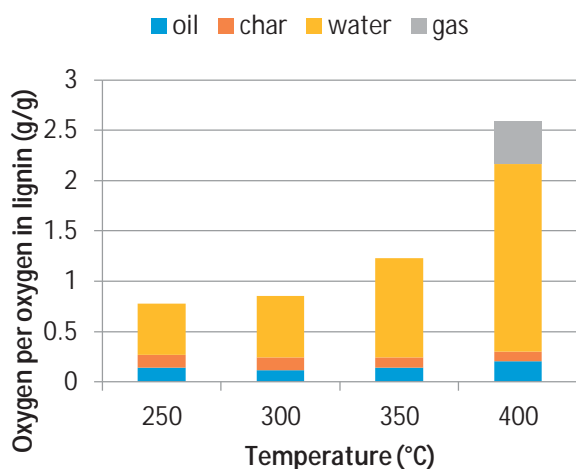


**Figure 3** Oxygen mass balance represented as mass of oxygen present in gas phase ( $\text{CO}/\text{CO}_2$ ), water, char (residual solids) and oil product relative to the mass of oxygen initially present in the lignin feed. Data is represented as a function of reaction temperature. Reaction conditions: 10g lignin, 100ml ethanol, 4 hour reaction time, inert non-pressurized atmosphere prior to heat-up and autogenous pressure.

From the oxygen mass balance it is clear that at reaction temperatures 250°C and 300°C the oxygen found in the gas and water phase could account for all of the oxygen removed from the lignin as the oxygen found in all four fraction represented does not add up to more than the amount of oxygen initially present in the lignin. Reliable gas data was however only obtained for the experiment carried out at 400°C but at lower temperatures the amount of gas formed was also very low (see Figure 1). At 350°C and higher temperatures the amount of oxygen found in water accounts for up to twice the initial oxygen content present in the lignin hence indicating that at higher temperatures an increase in water formation will come mainly from condensation reactions with ethanol. At 400°C the oxygen found in the gas phase would account for 40% of the oxygen initially present in the lignin. Based on this data alone it is however not possible to conclude that the  $\text{CO}/\text{CO}_2$  formed did in fact come from the lignin as significant quantities of ethane and ethane were also detected at these conditions indicating a gasification of the ethanol.

Solvent consumption is highly undesired as the price of ethanol is comparable to the value of the produced oil product. For the ethanolysis reaction at 400°C a solvent consumption between 25-30 wt% was obtained. Even when neglecting the possible loss of solvent when the loss of solvent from handling the reaction products during filtering and evaporation has been taken into account a solvent consumption of around 20wt% was still achieved. A significant portion of the solvent consumption is believed to be attributed to condensation

reactions with ethanol where water is one of the main products but also other light products as one would typically expect to see when ethanol undergoes condensations with itself have been registered. In Figure 4 below the GC-MS spectrum of the solvent fraction is shown for the reaction at 400°C both with and without lignin present. Without any lignin present a solvent consumption of 13 wt% was still obtained. This would seem to indicate that at 400°C there is an inevitable solvent loss due to undesired reactions of ethanol with itself. The light reaction products found in the solvent phase after reaction at 400°C both with and without the presence of lignin are very similar which also highlights this fact.

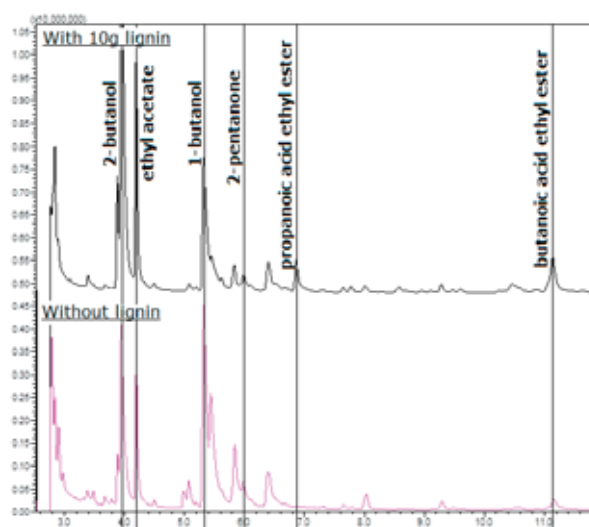


**Figure 4** GC-MS spectra of the solvent fraction after reaction at 400°C for 4 hours at autogenous pressure with and without the presence of lignin. Some of the identified species have been highlighted.

The reaction products include alcohols of different chain lengths and different light oxygenated products. Some of the identified species are ethyl esters but various chain length esters exist. Many of the light reaction products are similar to those typically found from higher alcohol synthesis but in this case any reaction where ethanol is a reactant is undesired.

## II. Product Quality

It is desired to reduce the oxygen content as much as possible as low oxygen content will yield a higher heating value of the lignin-oil. A low oxygen content also has other benefits which typically include reduced reactivity and thus higher stability of the oil product. A clear advantage of low oxygen content is the reduced polarity and thus increased miscible with a non-polar fossil diesel. The target of this study is to not only produce a lignin oil that will satisfy fuel standards but also successfully blend with a fossil diesel. The molar O/C ratio which was highlighted in the previous section as a measure of the degree of deoxygenation also serves as a benchmark for the oil quality as can be seen in

Figure 5 below where the solubility in heptane as a function of O/C for select oils is represented. Heptane was used as a substitute for fossil diesel possibly representing an even more non-polar substance due to the lack of aromatics. Still the representation in Figure 5 clearly shows that with O/C approaching lower values near 0.1 the solubility is increased to near 80% thus indicating that exhaustive deoxygenation is not necessary.

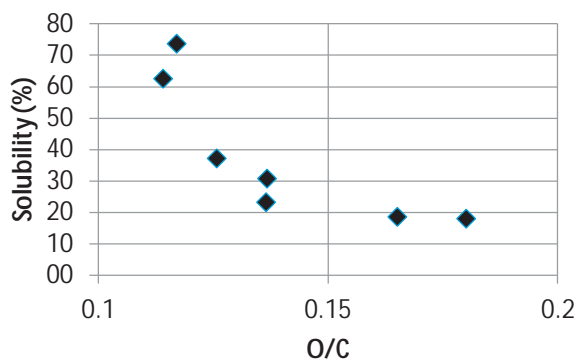


**Figure 5** Solubility of lignin-oils in heptane as a function of molar O/C-ratio. Target blend of oil in heptane was 10vol%.

In these studies the residence time for the lignin ethanolysis was also varied as well as the amount lignin relative to solvent used. Extensive parameter studies in batch mode operation have shown that without the addition of hydrogen and without a catalyst a lignin-oil with an oxygen content of less than 10 wt% can be obtained. The resulting oil is non-corrosive, ash and sulfur free and has been proven to be stable after a period of 12 month shelf storage. Size exclusion chromatography and NMR has highlighted that the molecular structure and size of the lignin oil is a mixture of mono- and dimeric partially oxygenated and alkyl substituted aromatics bearing strong resemblance to the original lignin structure.

Below in Table 1 an elemental analysis of one of the lignin-oils is shown for comparison with the lignin feed. It is evident that simple non-catalyzed ethanolysis can yield an oil product of comparable quality to a fossil fuel despite not having undergone exhaustive deoxygenation. The resulting lignin oil has a heating value of 38 MJ/kg which is similar to that of a fossil diesel which is typically 40-45 MJ/kg.

**Table 1** Elemental composition of lignin and lignin-oil obtained from a single experiment. The oil was obtained by treatment of 40g lignin in 100ml for 4 hours at autogenous pressure. Oxygen is determined by difference.

Sample	C	H	N	S	O	Ash	HHV
Lignin	47	4.9	1.5	0	34	13	18M J/kg
Oil	79	9.6	1.8	0	9.7	0	38 MJ/kg

## Conclusions

Non-catalyzed lignin ethanolysis has shown to yield an oil product comparable in quality to that of fossil diesel. The resulting oil is stable, non-corrosive and ash and sulfur free. An oxygen content of less than 10 wt% has been achieved by treatment in ethanol at 400°C and the resulting oil can blend with fossil diesel with a solubility of at least 75%. This shows that exhaustive deoxygenation is not necessary which typically requires use of expensive catalyst and hydrogen. The ethanol solvent may however be consumed as products of ethanol to gas and undesired condensation reactions have been verified.

## References

1. Zakzeski, J., Bruijninx, P.C.A., Jongerius, A.L. and Weckhuysen, B.M., *Chem. Rev.*110 (2010) 3552-3599.
2. Pandey, M.P, Kim, C.S., *Chem. Eng. & Technol.*34 (2011) 29-41.



**Mads Willemoes Nordby**

Phone: +45 4525 2809  
E-mail: mwnor@kt.dtu.dk

Supervisors: Kim Dam-Johansen  
Weigang Lin  
Peter Arendt Jensen

PhD Study  
Started: December 2012  
To be completed: April 2016

## Release behaviour of alkali species in different atmospheres

### Abstract

Biofuels high in potassium and silica content, such as wheat straw, are problematic when used for combustion or gasification in fluidized bed reactors as there is a high risk of bed agglomeration. The fundamental mechanisms for agglomeration are still not fully understood, and this is especially true for gasification conditions. Therefore the purposes of this project are to gain a better understanding of alkali release and the ash chemistry observed during biomass gasification and how this might affect agglomeration tendencies.

### Introduction

The utilization of biomass with high alkali metal content in fluidized bed combustors has proven to be problematic due to agglomeration. The agglomeration occurs due to the presence of melt-phases containing mixtures of reacting silica and potassium. However, the mechanisms at gasification conditions are not completely revealed. It is therefore important to know the behaviour of these problematic species during gasification. The release of elements during gasification can be separated into two steps: Release during pyrolysis and release during char gasification.

The release characteristics of alkali metals during pyrolysis and subsequent char gasification have shown that 53-76 % of the alkali metals were volatilized during the pyrolysis step, while during the char gasification it was 12-34 %. Expanding upon these results showed that during pyrolysis the evaporation was partly with the decomposition of lignin, hemicellulose and cellulose, and partly due to char-volatile interactions [1].

Research has also shown that during gasification the majority of the released alkaline species are combined with tar, primarily in the water-soluble fraction. At a temperature of 873 K 65 % of sodium and 63 % of potassium were released and present in the tar. Increasing the gasification temperature lead to secondary decomposition of the water-soluble tar, where the resulting released alkali species, could not be captured by quartz glass filter, which indicated that the alkaline species were released as very fine particles during secondary decomposition of the water-soluble

tar. The yield of condensed alkaline species also increased significantly along with increasing gasification temperature [2].

Char reactivity has also been seen to drastically reduce during contact with steam. This was due to changes in the char structure, and was found to have no connection to the volatilization of the catalytically active alkali metals [3].

Increasing the amount of phosphor present in biomass, either by additives or by co-combustion with fuels high in phosphor such as sewage sludge, could potentially be used as a means of reducing agglomeration tendency, as during combustion phosphor has been shown to react with potassium, reducing the amount available to volatilize or react with the bed material. However some of the phosphate rich ash particles were found to form low-temperature – melting alkali-rich phosphates promoting agglomeration behaviour. A general observation is that phosphor plays a controlling role in ash transformation reactions during biomass combustion, due to the high stability of phosphate compounds [4, 5].

### Specific Objectives

As the effects of gasification conditions on alkali release and ash chemistry in biomass are not currently well understood, this PhD project aims to investigate some of the release characteristics in differing atmospheres, and how it might affect the ash chemistry and agglomeration behaviour. The goals are:

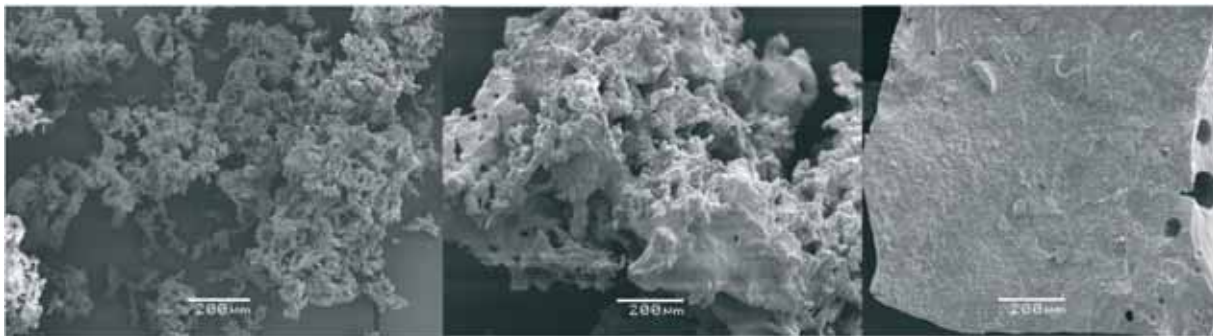


**Figure 1:** SEM images of ash particles from CO<sub>2</sub> gasification of wheat straw. (left) Gasified at 750°C. (middle) Gasified at 900°C(right) Gasified at 1000°C.

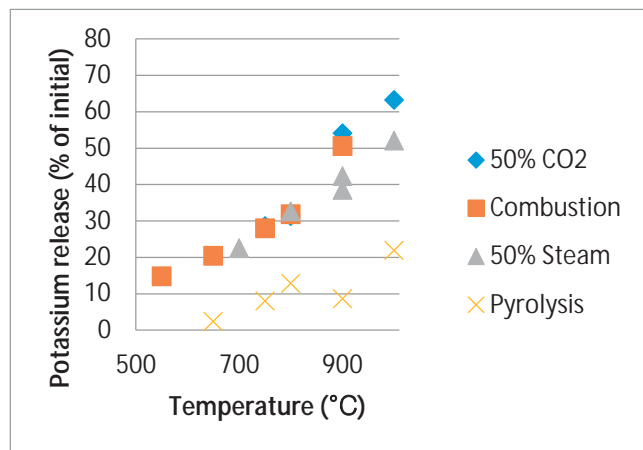


**Figure 2:** Potassium release from wheat straw during combustion, pyrolysis and gasification at different temperatures.

- Investigate how the transformation of alkali metals is affected under gasification conditions.
- Determine the effects of various operating conditions such as temperature, gas flow, fuel composition, etc., have on the agglomeration tendency as well as the effect on the physical properties of ash.

### Results and Discussion

Wheat straw samples have been combusted, pyrolysed or gasified using 50% CO<sub>2</sub> or steam in a fixed bed reactor at temperatures ranging from 550 to 1000 °C.

A slight decline in ash content as temperature increases has been observed in experiments, although not much difference is seen when distinguishing between the different atmospheres used as the ash content generally appear similar to each other at the same temperature.

The ash samples have also been analysed using SEM/EDS and ICP-OES. Based on the general morphology and pore size changes observed, the SEM results indicated increasing sintering/melting of the ash with increasing temperature as seen in Figure 1. This is expected behaviour as the biomass ash containing high amount of potassium and silica would gradually begin melting at temperatures above around 750°C.

In Figure 2 the release of potassium at different temperatures is shown for wheat straw is shown. Changing from between oxidizing and reducing conditions seems to have little effects for the overall release of potassium with mostly uniform release showing at the different temperatures.

The release during pyrolysis suggests that for wheat straw the potassium is captured by the char matrix, as the release is significantly lower during this process.

### Conclusion

Initial results indicate that wheat straw ash across the entire temperature interval and in all atmospheres is comprised mainly of K<sub>2</sub>O, which is the main constituent causing agglomeration. Additionally no significant difference was observed for potassium release when using different atmospheres.

### Future Work

Pilot scale experiments in a fluidized bed reactor will test the effects of atmosphere on agglomeration tendency.

Using the results from these experiments, a release mechanism for the potassium under gasifying conditions is to be proposed.

### Acknowledgements

This project is part of DANCNGAS and is funded by the Innovation Fund Denmark and the Sino-Danish Center for Education and Research, and I would like to thank the Chinese Academy of Sciences for their hospitality and support.

### References

1. L. Jiang, S. Hu, J. Xiang, S. Su, L.-S. Sun, K. Xu, Y. Yao, *Bioresour. Technol.* 116 (2012) 278-284.
2. O. Hirohata, T. Wakabayashi, K. Tasaka, C. Fushimi, T. Furusawa, P. Kuchonthara, A. Tsutsumi, *Energy Fuels* 22 (6) (2008) 4235-4239.
3. D. M. Keown, J.-I. Hayashi, C.-Z. Li, *Fuel* 87 (2008) 1127-1132.
4. A. Grimm, N. Skoglund, D. Boström, M. Öhman, *Energy Fuels* 25 (2011) 937-947.
5. A. Grimm, N. Skoglund, D. Boström, C. Boman, M. Öhman, *Energy Fuels* 26 (2012) 3012-3023.



## Anders Nørregaard

Phone: +45 4525 2990  
E-mail: [andno@kt.dtu.dk](mailto:andno@kt.dtu.dk)

Supervisors: Krist V. Gernaey  
Brian Madsen, Novo Nordisk  
Stuart M. Stocks, Novozymes  
John M. Woodley

### PhD Study

Started: January 2013  
To be completed: April 2016

## Mixing and oxygen transfer processes in bioreactors

### Abstract

Biotechnological production in stirred tank reactors suffers from limited available knowledge about the oxygen mass transfer properties and flow patterns in the fermentation broth. This knowledge could be valuable in order to design and optimize the fermentation processes that account for production of a large variety of products. This project investigates the concentration gradients that emerge in the fermentors, and more specifically the focus will be on characterizing the oxygen concentration in the broth. New experimental techniques with minimal impact on the process together with mathematical modeling are necessary in order to investigate this problem in more detail. Experiments will be performed in pilot scale and industrial scale fermentors.

### Introduction

Biochemical production by suspended aerobic fermentation processes is nowadays used to produce most industrial enzymes, many pharmaceuticals and chemical precursors. The processes are based on the conversion of a carbon substrate by a microorganism, in the presence of oxygen, to form biomass, products and carbon dioxide. During production, mass transfer of oxygen to the fermentation broth is the rate-limiting factor which has considerable importance for the process. [1] Due to the large size of the industrial-scale fermentation vessels, concentration gradients inside the reactor will occur, and thereby the often made assumption of perfect mixing in the reactor - usually applied in process models - does not apply. Differences in pressure, agitation intensity and viscosity together with organism growth differentiation make this heterogeneity difficult to predict. The purpose of this project is therefore to investigate the properties of mixing and oxygen transfer in large scale bioreactors in order to better understand the processes and phenomena that take place in these vessels.

Modelling large-scale bioreactor systems is challenging because only a limited experimental basis in large scale vessels exists, and significant differences between laboratory scale and production scale are often observed. Since the processes take place inside a sealed stainless steel vessel, sampling from the vessel is limited to probes that can tolerate the high temperature of the initial heat sterilization of the vessel together with

surface growth of the production organism. A limited number of ports are available for these kinds of probes, often limited to ports in one location in the bottom of the fermentor. The fermentation broth is also opaque which limits the applicability of many optical methods. Getting access to large scale bioreactors is difficult, since the industries operating such bioreactors usually do not reveal any details related to the dimensions of the reactors. Furthermore, they are normally part of existing industrial processes which means that they cannot be modified for academic reasons to avoid taking any risks of disturbing the production.

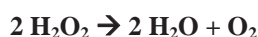
The time scale of oxygen consumption in a bioreactor is measured in seconds. That is, if the oxygen supply to the fermentor is shut off it will be starved for oxygen within seconds. That makes oxygen a good process parameter for the bioprocess, but it also requires equipment that can detect this parameter fast enough in order to detect the changes. This is not the case for the existing oxygen probes that are built more rugged for the reasons mentioned above.

### Specific Objectives

The first part of the project is focused on finding a suitable method to establish informative measurements in the bioreactor with the lowest degree of disruption of the cultivation. The first processes to be investigated are the production of cellulase enzyme from cultivation of the filamentous fungus *Trichoderma reesei*, and insulin production with the yeast *Saccharomyces cerevisiae*.

These production methods both utilize pure cultures of fungi to produce a secreted protein, but differ significantly in the morphology of the production strain and in regards to the product purity requirements and value.

The bioreactor environment is highly dynamic and phenomena like mixing, substrate gradients, reaction and mass transfer are correlated. In the second part of the project the oxygen mass transfer coefficient ( $k_L a$ ) is investigated with a pilot scale experimental model system. The model system is based on the one presented by Vasconcelos et al. [2] and utilizes a stirred tank with a working volume of 750 L. Hydrogen peroxide is continuously added to the vessel and oxygen is produced in the liquid phase by enzymatic reaction with catalase, with the following reaction stoichiometry:



Four optical oxygen sensors are attached to the baffle and oxygen values can be measured throughout the vessel. Oxygen mass transfer can be modelled from the system using the expression for oxygen transfer rate (OTR):

$$\text{OTR} = k_L a \cdot (c_{\text{O}_2} - c^*_{\text{O}_2})$$

Where  $k_L a$  is the oxygen mass transfer coefficient [ $\text{s}^{-1}$ ],  $c_{\text{O}_2}$  is the experimentally determined oxygen concentration [ $\text{mol}/\text{m}^3$ ] and  $c^*_{\text{O}_2}$  is the saturation oxygen concentration.

The OTR in the model system can be controlled by the addition rate of hydrogen peroxide and the reaction rate can be modelled using Michaelis-Menten kinetics. Experiments are carried out with constant feed of peroxide until a steady state is achieved.

Knowledge about the spatial heterogeneity in the bioreactor can be put into a compartmentalized model that is described in principle in figure 2 for a 4 compartment model.

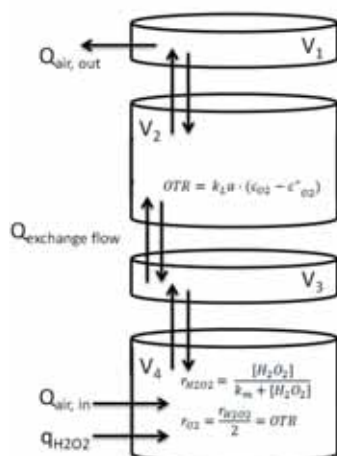


**Figure 2:** Compartment model with 4 separated well mixed compartments.

Liquid flow is determined using tracer experiments with either pH or saline tracer solution. By fitting the compartment model to experimental values for steady state oxygen concentrations from the model system, the  $k_L a$  for each compartment can be calculated.

Combining the experimental knowledge from dedicated mixing and mass transfer experiments can be used to estimate the model parameters in a compartmentalized fermentation model.

## Results and Discussion

An experimental method for oxygen measurements in large scale fermentation vessels has been proposed; equipment has been acquired and tested in lab and pilot scale. From these learnings an improved and sturdier setup has been proposed, which will be used for further cultivation experiments in large and pilot scale vessels. Experimental data from dedicated mixing and mass transfer experiments have been collected in order to determine model parameters in the compartment model.

## Conclusions

The issue concerning characterization of the spatial heterogeneity in fermentors has long been known and several studies to investigate the problem by means of mathematical modeling supported with pilot scale experiments have been carried out. These experiments often suffer from being highly dynamic and are difficult to extrapolate to full-scale due to the issue of scalability of the processes. In this project, a new method for characterization of the spatial heterogeneity in a production scale fermentor has been proposed, and will be utilized in order to determine the extent of bioreactor oxygen heterogeneity.

## Acknowledgements

The project is carried out in collaboration with Novo Nordisk A/S and Novozymes A/S. The project is financed by the BIOPRO project, and by the Technical University of Denmark

## References

1. Alvaro R.L., Enrique G., Octavio T.R., Laura A.P. (2006) Living With Heterogeneities in Bioreactors. *Mol. Biotech.* 34:355-381
2. Vasconcelos, J. M. T., Alves, S. S., Bujalski, W., & Nienow, A. W. (1997). Spatial characteristics of oxygen transfer in a dual impeller agitated aerated tank. In *Bioreactor & Bioprocess Fluid Dynamics* (pp. 361–377).

## List of Publications

A. Nørregaard, S.M. Stocks, K.V. Gernaey, J. Woodley, Filamentous fungi fermentation. In Meyer, H.P. & Schmidhalter, D. (eds.) *Industrial scale suspension culture of living cells*, Wiley-VCH, 2014.  
L.R. Formenti, A. Nørregaard, A. Bolic, D. Q. Hernandez et al. (2014) Challenges in industrial fermentation technology research. *Biotechnol. J.* 9,727-738

**Stylianos Pachitsas**

Phone: +45 4525 2830  
Email:

Supervisors: Kim Dam-Johansen  
Jytte Boll Illerup  
Stig Wedel  
Martin Hagsted Rasmussen (FLSmidth)

PhD Study  
Started: May 2015  
To be completed: May 2018

## Hydrogen chloride (HCl) emission from cement plants

### Abstract

Environmental regulations and cement plant maintenance issues require further decrease of HCl emissions and accurate prediction of HCl levels during the cement manufacturing process. The aim of this project is the development of a model for the prediction of HCl concentration at cement plant units and in stack gases as function of the operating conditions and raw materials. This project aspires to contribute to the identification of the species and mechanisms that are involved in HCl release, optimization of the applied HCl reduction methods, and the reliable prediction of HCl emissions from cement plant units.

### Introduction

HCl is a common industrial pollutant with significant environment impact and one of the major acid gases emitted from cement plants [1]. The newly legislated EU and US environmental regulations in combination with maintenance issues require further decrease of HCl emissions from cement plant and effective control of HCl levels at cement plant units (Figure 1). Unfortunately, in some cases the applied HCl reduction systems provide partial solution to the HCl emissions problem. Additionally, the structural modification of cement plant units for further reducing HCl emissions has high cost.

Generally, the reduction of HCl emissions from cement plants is very complex due to limited knowledge of the identity of HCl source species and the release mechanisms involved. Furthermore, the high water solubility of HCl in combination with its strong acidic nature results in many issues in relation to HCl detection and measurement in dusty industrial conditions where water vapor, fine reactant particles (CaCO<sub>3</sub>, CaO, etc.), and condensation spots co-exist. However, industrial measurements indicate that the HCl content in stack gases is mainly related to the HCl release in cement preheater upper cyclones (300-500°C)(Figure 2). The measured HCl profiles in cement

preheaters imply that the released HCl is unaffected by the HCl formation in kiln and fuel types (when the bypass system is off). It is believed that HCl release in preheaters is associated with raw material chlorine content, but—unfortunately—the involved species-mechanisms are unidentified.

The successful handling of HCl emissions from cement plant units is related to the identification quantification of HCl release sources, evaluation of their HCl release capacity at different conditions (temperature, moisture etc.), and the prediction of HCl absorption at cement plant units as function of the operating conditions.

### Objectives

The main objective of this project is the implementation of an effective model for the prediction of HCl content at cement plant units and in stack gases as function of the operating conditions. The basic requirements for that are: (i) identification of the raw material species and mechanisms that govern the HCl release in cement preheaters, (ii) modelling of cement plant unit based on industrial measurements, (iii) experimental evaluation of HCl absorption at cement plant units for different operating conditions, and (iv) evaluation of the HCl prediction model with industrial scale tests.

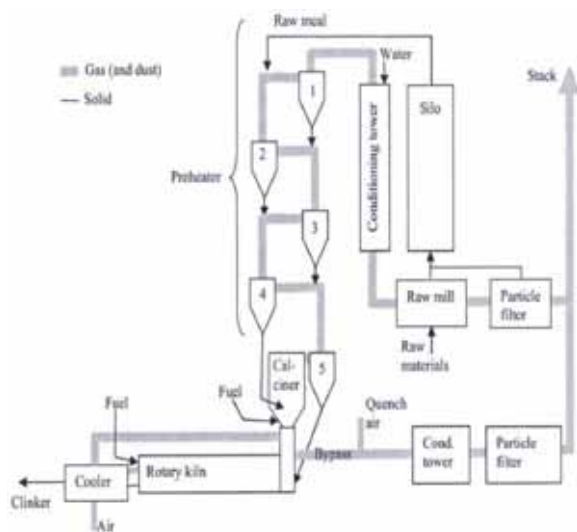


**Figure 1 :** Typical cement plant schematic presentation (dry method) [2].

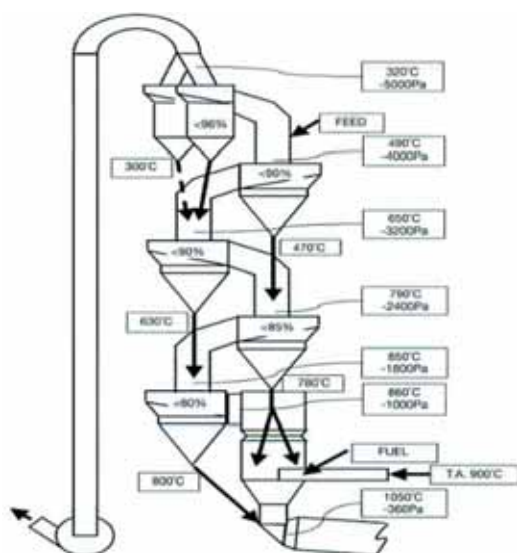


**Figure 2:** Typical cement preheater schematic presentation [3].

The first priorities in this project are the identification of the species-mechanisms related to HCl release in preheaters and the determination of a cement plant unit model which will effectively simulate cement plant structures. The selection of cement plant units and operating conditions-input parameters (temperature, moisture, gas flow etc.) will be based on the analysis of HCl industrial measurements.

The HCl absorption in different cement plant units and the effect of operating conditions on it will be investigated extensively. Special experimental set-ups and methods will be applied for the simulation of

cement plant unit conditions. The experimental results will form the backbone of the HCl prediction model.

HCl industrial measurements are planned for the familiarization with cement plant unit facilities, evaluation of HCl emissions, effective parameters, construction of operating conditions database, and test of lab experimental results on industrial scale. It is obvious that the industrial measurements play a crucial role in this project due to their contribution on the model design and evaluation.

### Experimental activities

Experimental activities for the evaluation of HCl absorption by cement raw meal and raw meal components were conducted using TGA-FTIR and fixed bed -FTIR systems. In practice, two different experimental approaches were used: (i) TGA-FTIR experiments investigated the HCl absorption in ramping temperatures with use of a solid HCl source and (ii) fixed-bed tests at constant temperature and gas phase composition similar to that in cement preheaters.

### Conclusions

This study will address the insufficient prediction of HCl emissions from cement plant units and the control of HCl during cement manufacturing processes. The implementation of this project requires the combination of industrial measurement campaigns, advanced experimental activities, and modelling work. The development of a model which predicts HCl levels in different cement plant units will contribute significantly to the utilization of the applied HCl reduction methods and production cost reductions.

### Acknowledgments

This project is part of the research platform 'Minerals and Cement Process Technology—MiCeTech' funded by Innovation Fund Denmark, FLSmidth A/S, Hempel A/S, and DTU.

### References

1. Javed I. Bhatti, F. MacGregor Miller and Steven H. Kosmatka, Innovations in Portland Cement Manufacturing, CPA, Illinois, 2004, p.660.
2. J. P. Hansen. SO<sub>2</sub> emissions from cement production. PhD thesis, DTU, 2003.
3. Philip A. Alsop. The Cement Plant Operations Handbook. David Hargreaves, International Cement Review, 5th edition, 2007. p.41

**Emmanouil Papadakis**

Phone: +45 4525 2808  
E-mail: empap@kt.dtu.dk  
Discipline: CAPEC-PROCESS

Supervisors: Professor Rafiqul Gani  
Professor Krist V. Gernaey  
Associate Prof. Gürkan Sin

**PhD Study**

Started: October 2013  
To be completed: September 2016

## **Modeling and synthesis of pharmaceutical processes: Moving from batch to continuous manufacturing**

**Abstract**

The majority of the pharmaceutical production systems involve batch processes which offer the equipment flexibility and the product quality control that is desired in multipurpose production lines as the pharmaceutical ones. However, the batch processes are not very good for the product quality assurances and have some drawbacks such as low productivity, high operational cost and big amounts of generated waste. Therefore, the objective of this study is to develop a framework to enhance the pharmaceutical process understanding in order to improve the pharmaceutical processes development and evaluate opportunities for continuous manufacturing. The framework is applicable in the multipurpose pharmaceutical production line and it aims to the development of safer and more sustainable processes using model-based methods and tools. The developed framework has been applied in three case studies (1) BHC ibuprofen synthesis and (2) glucose isomerization and (3) 6-hydrobuspirone synthesis and purification.

**Introduction**

The delay with the introduction of innovative systems into pharmaceutical manufacturing can be attributed to the regulatory uncertainty. Generally, the batch processes are not good for product quality assurance and possess a number of drawbacks such as poor process understanding, low productivity, high energy consumption, high capital cost, low product purity, scalability and waste production [1].

Process Systems Engineering (PSE) methods and tools can have important roles to play, for example: (a) apply computer aided-methods and tools that are mature for other industries (such as chemical and petrochemical) also in solving problems in pharmaceutical industries, (b) in the evaluation and implementation of alternative solutions and/or design and (c) to evaluate opportunities for continuous manufacturing [2, 3, 4, 5, 6].

The objective of this project is to develop a systematic integrated methodology which its objective is to improve pharmaceutical process operation/design and to evaluate opportunities for continuous manufacturing through better understanding of pharmaceutical processes. The integrated systematic framework needs to be applicable in the multipurpose pharmaceutical industry in order to achieve greener and safer processes with higher product quality by using systematic model-based methods. One of the main objective the opportunities investigation for continuous manufacturing (CPM) which naturally

eliminates some of the batch process drawbacks and enhances the process understanding. The reaction and separation improvement which lead in increased process efficiency. Solvent selection/optimization to improve processes and reduced energy and mass consumption. Process optimization and intensification necessary in order to improve the reaction and the separation efficiency. The final objective is the process evaluation, integration and optimization.

**Integrated Systematic Methodology**

The systematic integrated framework (Figure 1) is developed with the specific aim to assist the multipurpose pharma/biochemical industry to systematically solve the multiple complex problems, to enhance the process understanding and to exploiting potential improvements of the pharmaceutical processes. The framework starts with a problem definition where the objectives of the study are defined. The subsequent reaction pathway identification section (Section A) aims at identifying the number and the type of necessary reaction steps to produce a pharma/bio-product of interest. Section B is the reaction analysis, and aims at collecting data for each reaction, to perform kinetic analysis, to identify reaction limitations, to evaluate the reaction variables, and to make a decision on whether the reaction can be operated in continuous or batch mode, to design the reactor, and finally to define the objectives of

the separation if needed [6]. Section C (Separation Synthesis and Design) is performed in case separation of a specific compound is needed. Section C starts with the mixture analysis to identify separation limitations, and generates the binary ratio mixtures in order to identify the most feasible separation task. Based on the driving force principles, the separation alternatives can be generated and evaluated in order to select the most feasible ones. Once a flowsheet has been obtained, a process simulation (Section D) needs to be performed in order to evaluate the process and identify the process hotspots. Based on the process evaluation, process optimization and process operation can be performed.

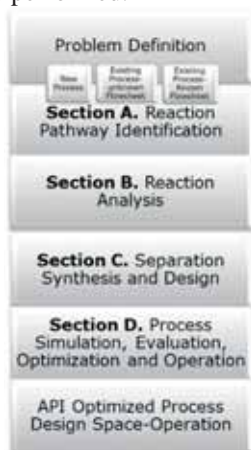


**Figure 1.** Integrated Systematic Framework.

### Methods and Tools

In order to collect the information for each section of the framework, the use of model-based methods and tools are necessary. Such methods and tools are knowledge databases, model libraries, solvent selection tools, mathematical solvents and evaluation tools. Knowledge databases need to provide information for the reactions (APIs Synthesis database), for the unit operations (Unit Operation database), pure compound property database (CAPEC database) and monitoring-control (ICAS-PAT) database. Model libraries need to provide information for different unit operation models, property prediction models, and reaction kinetics models. Solvent selection tools for proper solvent selection and evaluation tools for economics, sustainability and LCA analysis.

A new addition to the solvent selection methods and tools is the solvent swap methodology. The solvent swap process is used to remove and replace solvents between unit operations in the production line. A new solvent swap method, a database and a computer-aided tool have been created to address the solvent swap processes by batch distillation.

### Case Study 1-BHC ibuprofen Synthesis

The objective of this case study is to apply and verify the developed framework in order to generate the batch process to produce high purity ibuprofen crystals. Also, process alternatives need to be generated to achieve the objectives and finally, to identify possible process hotspots to improve the process such as possibilities of

CPM, solvent selection and optimization, reaction improvement and separation improvement.

### Case Study 2-Glucose Isomerization

In this study, the use of model-based methods within the systematic framework is illustrated through a glucose isomerization (GI) reactor case study. The objective of this study is the use of a multi-scale reactor model which includes the reaction kinetics and the enzyme activity decay as a function of temperature with and without the diffusion term, to simulate the reactor and to investigate opportunities for improving the productivity of a typical reactor plant.

### Case Study 3 – 6-hydroxybuspirone synthesis and purification

The objective of this case study solvent selection and analysis to purify the pharmaceutical intermediate. The state task network is known for this case study and it involves a reactor, liquid-liquid extraction, and distillation to remove/replace the reaction solvent with the crystallization solvent. The solvent swap method was utilized for solvent selection and evaluation.

### Conclusions-Future work

A systematic integrated framework to enhanced process understanding and exploiting potential improvements of the pharma/biochemical processes has been developed and applied. The framework is going to be applied in other cases studies, to be extended and include bioprocesses. The knowledge databases (APIs database, unit operation database and solvent swap database) and the model libraries are going to be extended. Finally, the framework will be integrated with reaction pathway synthesis.

### References

1. K. Plumb, Chem. Eng. Res. Des., 83 (6), (2005), 730-738.
2. C. Jiménez-González, P. Poehlauer, Q. B. Broxterman, B.-S. Yang, D. am Ende, J. Baird, C. Bertsch, R. E. Hannah, P. Dell'Orco, H. Noorman, S. Yee, R. Reintjens, A. Wells, V. Massonneau, and J. Manley, Org. Procces Res. Dev. 15(4), (2011), 900-911.
3. S.D. Schaber, D.I. Gerogiorgis, R. Ramachabdran, J.M. Evans, P.I. Barton, B. L. Trout., Ind. Eng. Chem. Res. 50 (17), (2010), 10083-10092
4. K.V. Gernay, A. E. Cervera- Pardell, J. M. Woodley, Comput. Chem. Eng., 42, (2012) 30-47
5. A. Rogers, A. Hashemi, M. Ierapetritou, 1, (2013), 67-127
6. A. E. Cervera- Pardell, T. Skovby, S. Kiil, R. Gani, K.V. Gernay, Eur. J. Pharm. Biopharm., 82 (2), (2012), 437-456



## **Morten Nedergaard Pedersen**

Phone: +45 4525 2843  
E-mail: monepe@kt.dtu.dk

Supervisors: Kim Dam-Johansen  
Peter Arendt Jensen  
Sønnik Clausen  
Lars Skaarup Jensen, FLSmidth A/S

PhD Study  
Started: March 2015  
To be completed: February 2018

## **Burners for cement kilns**

### **Abstract**

Waste derived fuels are increasingly being used in the cement industry as a way to reduce cost. However, the shift from traditional fossil fuels is difficult, due to the widely different physical and chemical properties of the alternative fuels. New burners are therefore required in the cement industry, in order to best deal with the challenges imposed by the use of alternative fuels. This project aims to increase the knowledge of the combustion process in the cement rotary kiln by video imaging at large scale cement plants firing high amounts of alternative fuels. Another goal is to model the rotary kiln flame with various fuels in order to assess the influence of a high degree of alternative fuels and propose guidelines for how the use can be increased.

### **Introduction**

Alternative fuels are increasingly being used in the cement industry, primarily as a method to reduce the cost of the energy intensive manufacturing process [1]. If the fuels are partly biogenic and substitute fossil fuels, net CO<sub>2</sub> emissions from the industry can also be reduced [1]. Solid Recovered Fuel (SRF), which is produced by sorting the combustible fraction of municipal solid waste [2], is one type of fuel receiving much interest.

The use of alternative fuels introduces various challenges, since the fuels are very different from the fossil fuels. Compared to coal or petcoke, SRF is difficult to mill [3] and has a larger particle size. Full conversion in the suspension fired rotary kiln flame is thus difficult to achieve. The water content is also higher and the heating value is lower [2], which makes it difficult to obtain the high temperatures required for efficient heat transfer in the cement rotary kiln [4].

To overcome these challenges a new development in kiln burners is required. FLSmidth A/S is currently developing a new burner, which has the capability to control the air flow in the near burner region of the cement kiln and obtain a good dispersion of the SRF in the flame.

### **Specific Objectives**

The project considers two parts

- 1) Video imaging at a full scale cement plant

- 2) Mathematical model development of a rotary kiln flame

The objective of part 1 is to gain increased knowledge of the combustion process in the near burner region of the rotary kiln and support the development of FLSmidth's new burner.

The objective of part 2 is to formulate a model that can predict the temperature and heat transfer in the rotary cement kiln using fossil fuel or SRF. The model can then be used to create guidelines on how to increase the share of alternative fuels at a given cement plant.

### **Results and Discussion**

Only the results of the initial measurement campaigns will be covered here. Video imaging of the burner in a full scale cement plant was performed. The plant is a dry kiln with a 5 stage preheater and has a daily production capacity of approx. 3,500 ton clinker. The plant fires a mix of SRF and petcoke in the kiln burner, with the SRF contributing up to 70 % of the energy.

The camera equipment is protected in a water cooled probe, which has been specially developed to withstand the high temperatures (1000 °C) and dusty environment in the cement rotary kiln hood. Imaging has been performed both in the visual and infrared spectrums.

The images in Figure 1 and 2 show the situation with the burner currently installed at the cement plant.

The images in Figure 1 have been recorded in the visual spectrum during co-firing of petcoke and SRF.

The images show a lack of mixing of petcoke and SRF in the kiln. The SRF is mainly located at the bottom of the fuel plume and can be seen as the larger particles. The petcoke is more dispersed, but still only covers the upper half of the kiln. The ignition point lies approx. 10 meters into the kiln resulting in a relatively cold zone near the burner.

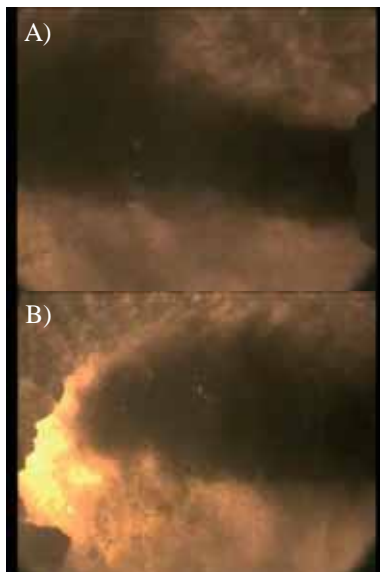


**Figure 1:** The kiln flame recorded in visual spectrum during co-firing of petcoke and SRF. A) View from burner tip and approximately 3 m into kiln. B) View up to approximately 10 m into kiln.

The infrared images in Figure 2 have been recorded during 100 % SRF firing. The lack of mixing of the SRF is clear. The SRF enters in a dense rope, which is difficult to disperse. The result is a small contact between the SRF and oxygen, which results in a low burnout of the fuel. A downwards motion of the particles can be seen approx. 10 meters into the kiln, which suggests that the SRF drops to the clinker bed largely unconverted.

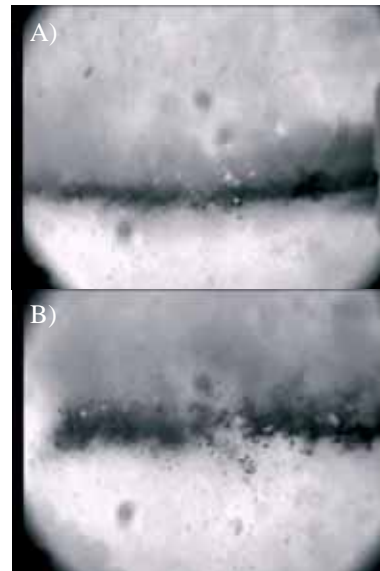


**Figure 1:** The kiln flame recorded in infrared spectrum during 100 % SRF firing. A) View from burner tip and approximately 3 m into kiln. B) View up to approximately 10 m into kiln.

### Conclusions

The images show a lack of mixing of the Solid Recovered Fuel (SRF) in the rotary kiln flame. This results in a long ignition delay and low conversion of the SRF that likely drops to the clinker bed largely unconverted. The implications can be reduced clinker quality and process stability caused by reducing conditions in the clinker bed or caused by the low temperature near the kiln exit [4].

It is expected that the new burner from FLSmidth A/S will be able to create a better mixing of the SRF and hot secondary air, which will move the ignition point closer to the burner and increase the burnout of the SRF. This will be tested during a future measurement campaign.

### Acknowledgments

This work is part of the research platform ‘Minerals and Cement Process Technology – MiCeTech’ funded by Innovation Fund Denmark, FLSmidth A/S, Hempel A/S, and DTU.

### References

1. A. A. Usón, A. M. López-Sabirón, G. Ferreira, E. Llera Sastresa, *Renewable and Sustainable Energy Reviews*, 23 (2013) 242–260.
2. L. F. Diaz, G. M. Savage, L. L. Eggerth, *Solid Waste Management*, United Nations Environment Program (UNEP), 2005, pp. 295–302.
3. J. Maier, A. Gerhardt, G. Dunnu, in: P. Grammelis (Ed.), *Solid Biofuels for Energy*, Springer-Verlag, London, 2011, pp. 75–94
4. L.K. Nørskov, *Combustion of solid alternative fuels in cement kiln burners*, PhD thesis, Technical University of Denmark, 2012

**Olivia Ana Perederic**

Phone: +45 42725918  
E-mail: oper@kt.dtu.dk

Supervisors: John M. Woodley  
Rafiqul Gani  
Bent Sarup, Alfa-Laval

PhD Study  
Started: September 2015  
To be completed: September 2018

## Systematic computer aided methods and tools for lipids process technology

### Abstract

Lipid process technology could not exploit available computer aided methods and tools till recently because lack of property models, physical and thermodynamic data, which are the basic requirements to perform process design, simulation and optimization, as well as product design. Recent work within lipid property modelling and property data base development, allows improved studies regarding lipid process design and analysis. Main objectives of this PhD project are to further extent available lipids data base with emphasis on some specific systems, to develop a framework for fats and oil technology able to guide the user to achieve its specific target, and to perform several case studies analysis by applying proposed framework.

### Introduction

Lipid processing covers several oil and fats technologies such as: edible oil production, biodiesel production, oleochemicals (e.g.: food additives, detergents) and pharmaceutical product manufacturing. Lipids are naturally occurring compounds classified according to chemical complexity and structure (e.g.: simple – triacylglycerides, esters; compound – phospholipids, sulpholipids, lipoproteins; derived – saturated and unsaturated fatty acids, monoacylglycerides, diacylglycerides, alcohols) [1]. New challenges regarding design and development of better products and more sustainable processes related to lipids technology, emerge according to consumers increased quality requirements and new legislation regarding environmental safety. [2].

The demand of oils and fats has grown from 40.8 million tons in 1980 to more than 200 million tons in September 2015 [3–5] and it is correlated to the world growing needs of renewable fuels and oleochemical products. In the last decade, the production growth rates of 17 major oil and fats increased considerably (e.g.: palm oil – 95%, palm kernel oil – 86%, soybean oil-42%, rapeseed oil - 78%, sunflower – 62%) and over 50% of oil and fats production is accounted for palm and soybean oil [6].

The main drawback for lipid industry to apply the available computer aided methods and tools for process synthesis, modelling and simulation, is the lack of available property data and models within commercial

software applications [7]. In the last years, new methods and models for predicting single properties and temperature dependent properties (e.g.: critical properties [8], viscosity [9], heat capacity [10], heat of vaporisation [10-11], vapour pressure [11]) were reported. Another important modelling task is phase equilibria prediction which is directly related to designing and optimisation of separation processes. An important aspect in phase equilibria prediction is represented by quality of the data used for regression of model parameters. Cunico et al. applied several consistency test for VLE lipids data sets available in literature and their results show that only 3% of the analysed data sets have quality factors over 0.5 (where the quality factor varies between 0 – minimum, and 1 – maximum) [12]. Considering quality data sets, new original UNIFAC parameters values were reported, allowing better prediction of the lipids properties and phase equilibria [1].

Several studies regarding oils and fats are reported within the literature, but a systematic approach to cover all the aspects starting from property modelling and finishing with process optimisation and intensification is not yet reported. Existence of framework for oil and fats, which integrate state-of-the-art methods, tools and solution strategies [13] and which is designed to guide the user step by step, allows a systematic study by using efficient problem formulations and solutions. Such a framework can have a great potential for results quality and workflow productivity [13-14].

## Specific objectives

Oils and fats increasing production, along with limited physical and thermodynamic property data and models available within commercial process simulator lead to a necessity for a framework existence. This PhD project will focus on the following topics:

1. Property modelling and lipids data base maintenance and extension.
2. Generation of a framework for fats and oils industry
3. Case studies analysis by applying proposed framework.

Property modelling main task will be to study phase equilibria for two specific mixtures (e.g: Vapor-liquid equilibrium related to water – glycerin in terms of manufacture of glycerin pharma grade, 99.5 - 99.9+% purity, from 5 - 7% aqueous solution; liquid-liquid equilibrium for fat splitting processes involving water - fat or fatty acid distillate at 40 - 60 bar and 220 - 260°C).

Lipids data base, Figure 1, maintenance is done by adding and testing data for new compounds and mixture. Extension of the data base is done by adding new features to it.

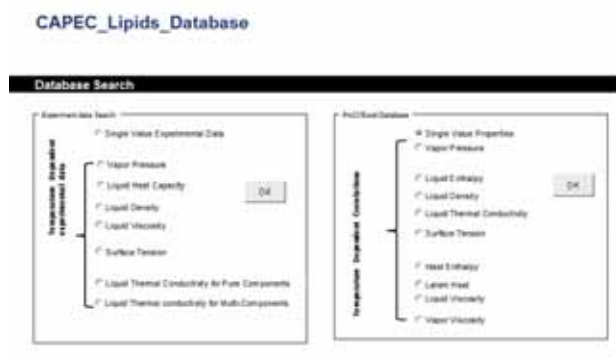


**Figure 1:** Lipids database user interface.

The framework main objective is to guide the user through several steps for achieving propose target. Several aspects should be covered by the framework: operation guide, required data to achieve the target, description of applied tools and methodologies, solutions pathways for troubleshooting the problems that may emerge.

## Conclusions and future work

Development of lipids property modelling with emphasis on process simulation, presents a big evolution in the last years. However, there are still a lot of research areas to cover within the lipids modelling and technology development. The future steps of this project will try to cover some of these aspects: extension of available lipids data base, study of several VLE and LLE systems, generation of a systematic framework for oils and fats able to improve the research within lipids area.

## References

1. Cunico LP. [PhD Thesis] Modelling of Phase Equilibria and Related Properties of Mixtures Involving Lipids. Lyngby, Denmark: Technical University of Denmark; 2015. ISBN 978-87-93054-69-1
2. Diaz-Tovar C, Mustaffa A., Hukkerikar, A., Quaglia A, Sin G, Kontogeorgis G, Sarup B, Gani R. Lipid Processing Technology: Building a Multilevel Modeling Network. . In: Pistikopoulos EN, Georgiadis MC, Kokossis A, editors. Proceedings of the 21th European Symposium on Computer Aided Process Engineering 2011, 29:256–260.
3. Food And Agriculture Organization Of The United Nations Statistics Division. Edible oil. [Online] faostat3.fao.org/home/E [accessed 20.10.2015].
4. R. E. A. Holdings PLC. World Consumption Of Oils & Fats. [Online] www.rea.co.uk/rea/en/markets/oilsandfats/worldconsumption [accessed 20.10.2015].
5. OIL World statistics 25 September 2015 [Online] http://www.oilworld.biz/app.php [accesses 25.09.2015].
6. IHS. Fats and Oils Industry Overview. [Online] www.ihs.com/products/fats-and-oils-industry-chemical-economics-handbook [accessed 20.10.2015].
7. Sarup B. Advances and Challenges in Modelling of Processing of Lipids. In: Gernaey KV, Huusom JK, Gani R editors. Proceedings of 12th International Symposium on Process Systems Engineering and 25th European Symposium on Computer Aided Process Engineering, 2015, 37:117-122.
8. Marrero, J, Gani R. Group-contribution based estimation of pure component properties. Fluid Phase Equilibria 2001, 183-184:183–208.
9. Ceriani R, Gonçalves CB, Coutinho J. Prediction of viscosities of fatty compounds and biodiesel by group contribution. Energy and Fuels 2011, 25:3712–3717.
10. Ceriani R, Gani R, Meirelles AJA. Prediction of heat capacities and heats of vaporization of organic liquids by group contribution methods. Fluid Phase Equilibria 2009, 283:49–55.
11. Ceriani R, Gani R, Liu Y. Prediction of vapor pressure and heats of vaporization of edible oil/fat compounds by group contribution. Fluid Phase Equilibria 2013, 337:53–59.
12. Cunico LP, Ceriani R, Sarup B, O’Connell JP, Gani R. Data, analysis and modeling of physical properties for process design of systems involving lipids. Fluid Phase Equilibria 2014, 362:318–327.
13. Quaglia A, Sarup B, Sin G, Gani R. A systematic framework for enterprise-wide optimization: Synthesis and design of processing networks under uncertainty. Computers and Chemical Engineering 2013, 59:47–62.
14. Carvalho A, Mimoso AF, Mendes AN, Matos H. From a literature review to a framework for environmental process impact assessment index. Journal of Cleaner Production 2014, 64:36–62.



## Christine Malmos Perfeldt

Phone: +45 4525 2892  
E-mail: mmos@kt.dtu.dk

Supervisors: Nicolas von Solms  
John M. Woodley

PhD Study  
Started: August 2011  
To be completed: August 2015

## Antifreeze proteins and a hydrophobic surface on oil and gas pipelines can better handle flow assurance issues

### Abstract

Gas hydrate deposition can cause plugging in oil and gas pipelines which leads to flow assurance challenges. Recently, antifreeze proteins (AFPs) have been studied as an environmentally friendly kinetic hydrate inhibitor and promising results have shown that AFPs may have potential as gas hydrate inhibitors. Here we show the effect of a hydrophobically coated surface and the presence of only 0.014 wt% AFP that reduce the hydrate formation significantly in contrast to a steel surface. This shows that the use of hydrophobic surface could serve as a potential approach to inhibit hydrate formation.

### Introduction

Gas hydrates are non-stoichiometric crystalline compounds of hydrogen bonded water molecules with enclathrated gas molecules such as methane, ethane, propane and carbon dioxide.[1] Natural gas hydrate formation conditions are frequently encountered in the oil and gas industry, potentially leading to blockage of pipelines causing production losses and safety issues.

The energy industry uses chemicals such as thermodynamic inhibitors (THIs) e.g. methanol or glycols in substantial amounts (up to 50 wt%) in order to shift the hydrate formation boundary towards lower temperatures.[2] However, the large amounts of THI required can cause safety and environmental issues as well as resulting in higher expenses. These issues encouraged the industry to search for low dosage hydrate inhibitors as the kinetic hydrate inhibitors (KHIs). KHIs are often water soluble polymeric compounds that prevent or delay hydrate formation for a certain period of time. Nevertheless, due to environmental restrictions and the poor biodegradability of KHIs, the use has been limited.[3]

Antifreeze proteins (AFPs) found in certain plants, fish and insects can prevent ice from growing when cooling below the freezing temperature. Promising results for AFPs as an environmentally friendly kinetic hydrate inhibitor have been obtained for THF, methane and multi-component systems indicating that AFPs may have potential as a gas hydrate inhibitor.[4, 5]

Deposition and plugging of gas hydrates in pipelines are still not completely understood phenomena. Several experimental studies and field trials suggest that hydrate deposition occurs on the pipeline wall. Hence, the wetting conditions of the pipeline wall were believed to be important for determining the stickiness of hydrates to the wall. As hydrate particles are very hydrophilic, a hydrophobic surface (Figure 1) should be able to reduce water bridging to the pipeline wall and thereby have an influence on gas hydrate nucleation.[6]



**Figure 1:** Water droplet on a hydrophobic surface to the left and on a hydrophilic surface to the right.

### Specific Objectives

The objective of this PhD project was to investigate if AFPs can be applied in field conditions to control the formation of gas hydrates.

The focus was to setup laboratory scale experiments to simulate realistic hydrate formation scenarios using four different experimental apparatus: high pressure

micro-Differential Scanning Calorimeter (HP- $\mu$ DSC), Rocking Cells, a pressurized stirred cell and two high pressure crystallizers (one coated inside with a hydrophobic coating). Using these high pressure equipments, different types of commercial kinetic hydrate inhibitors were evaluated and the performance was compared to AFPs. Finally, synergy effects between other production chemicals were studied.

### Experimental method

Systems with deionized water (with or without KHI) and pure methane under high pressure and flowing circumstances were studied in order to mimic actual pipeline conditions. The objective was to assess the influence of the hydrophobic surface on hydrate growth. A high pressure setup (Figure 2) that consists of two stirred crystallizers (one of stainless steel and one coated with PFA) was used to examine the performance of both AFP I from the fish winter flounder and LuvicapBio (modified PVCap) using the constant cooling method.



**Figure 2:** High pressure crystallizer setup.

### Results and Discussion

The coated crystallizer was observed to have an impact on the hydrate growth (Figure 3). In the presence of the control, the hydrate growth was reduced by two times in the coated crystallizer compared to the stainless steel crystallizer.

Addition of 0.20 wt % LuvicapBio reduced the growth, although the growth reduction was similar in both crystallizers. This indicates that at 0.20 wt% LuvicapBio the surface effect of the hydrophobic coating disappears. Furthermore, in the presence of 0.02 wt% of LuvicapBio or 0.014 wt% AFP I in the hydrophobic coated crystallizer; the hydrate growth was reduced to almost the same level as obtained with 0.20 wt% of LuvicapBio in a stainless steel crystallizer. This indicates that 10 to 14 times less KHI was needed in the presence of a hydrophobically coated surface.

The relation between the experimental observed hydrate growth and the change in surface chemistry was investigated by using the theory by Owens and Wendt.[7] Based on measured contact angles and the surface tension parameters for the reference liquids (water and diiodomethane), the solid surface tension and the work of adhesion between water and solid surface were estimated (Table 1).

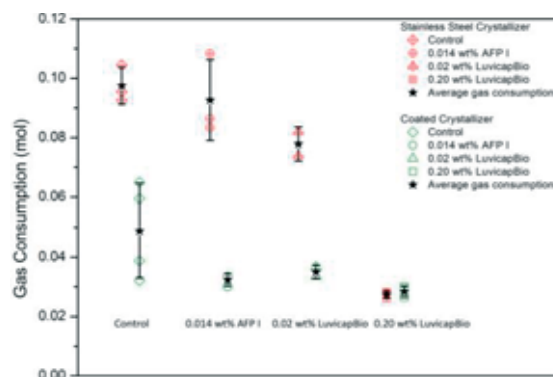


**Figure 3:** Hydrate formation (consumed gas) in the stainless steel and coated crystallizer with and without KHIs. Error bars represent the standard deviation.

**Table 1:** Solid surface tension and the work of adhesion between the surface and water for the stainless steel surface and the coated surface.

Surface	$\gamma_s$ (mN/m)	$W_{st}$ (mN/m)
Stainless steel	41.7	84.4
Coated	21.3	57.3

It was found that the stainless steel surface had 2 times higher solid surface tension and 1.5 times higher work of adhesion between water and the solid surface.

### Conclusions

Based on the experimental work and the estimates from Owens and Wendt showed clearly that the lower the solid surface tension was, the lower the work of adhesion between water and solid surface which lead to less hydrate growth. These experimental studies suggest that the use of hydrophobic surfaces or pipelines could serve as an alternative or additional flow assurance approach for gas hydration mitigation and management.

### Acknowledgements

The project was a part of the ‘Biotechnology in Oil Recovery’ program, funded by the Innovation Fund Denmark, the Technical University of Denmark, Maersk Oil A/S, Dong Energy A/S, Novozymes A/S, Danish Technological Institute and Roskilde University.

### References

1. E.D. Sloan, Nature 426 (2003) 353-363.
2. M.A. Kelland, Energy Fuels 20 (2006) 825-847.
3. L.D. Villano, R. Kommedal, M.A. Kelland, Energy Fuels 22 (2008) 3143-3149.
4. V.K. Walker, H. Zeng, H. Ohno, N. Daraboina, H. Sharifi, S.A. Bagherzadeh, S. Alavi, P. Englezos, Canadian Journal of Chemistry 93 (2015) 1-11.
5. C.M. Perfeldt, P.C. Chua, N. Daraboina, D.S. Friis, E. Kristiansen, H. Ramløv, J. Woodley, M.A. Kelland, N. von Solms, Energy Fuels 28 (2014) 3666-3672.
6. T. Austvik, X. Li, L.H. Gjertsen, Ann. N. Y. Acad. Sci. 912 (2000) 294-303.
7. D.K. Owens, R. Wendt, J. App. Polym. Sci. 13 (1969) 1741-1747.

**Daniela Quintanilla**

Phone: +45 4525 2990  
E-mail: danaquh@kt.dtu.dk

Supervisors: Krist V. Gernaey  
Ole Hassager  
Anna Eliasson Lantz  
Kim Hansen, Novozymes

PhD Study  
Started: November 2013  
To be completed: October 2016

## Morphology, rheology and mass transfer in fermentation processes

### Abstract

It is believed that the morphology of filamentous fungi is closely associated with productivity in fermentation processes. However, until now there is no clear evidence of this relation and there is an ongoing discussion around the topic, due to the poor understanding of fungal morphogenesis. Therefore, fungal morphology is usually a bottleneck for productivity in industrial production, and will be extensively studied in this work. This will allow us to determine whether a certain microorganism's phenotype has an influence on process performance, and how this performance can be influenced actively by manipulating different process variables or by genetic engineering, as a means of improving the design and operation of filamentous fungi fermentations.

### Introduction

Production of industrial enzymes is usually carried out as submerged aerobic fermentation, a process that is performed with a substrate, which is either dissolved or remains suspended in an aqueous medium in a closed fermentation vessel where the production microorganism is grown. Filamentous microorganisms are widely used as hosts in these processes due to diverse advantages. Nevertheless, they also present major drawbacks, due to the unavoidable oxygen transfer limitations as a consequence of the high viscosity of the medium that they develop, which is believed to be related to the biomass concentration, growth rate and morphology [1]. This last variable is one of the most outstanding characteristics of the filamentous fungi due to its great complexity and it is extensively studied in this project.

### Further Background

In submerged cultivations one can recognize different types of morphology, which are usually classified as dispersed and pelletized. Depending on the desired product, the optimal morphology for a given bioprocess varies and cannot be generalized; in some cases both types of morphology are even combined in one process, as illustrated in Figure 1.

A pellet type morphology is preferred since it allows for simplified downstream processing and yields a Newtonian fluid behavior of the medium, which results in low agitation power input. However, the pelleted morphology results in nutrient concentration gradients

within the pellet. This situation is obviously not observed in freely dispersed mycelia allowing for enhanced growth and production, which has been attributed to the fact that at the microscopic level the morphology has an influence on the production kinetics, e.g. on the secretion of enzymes [3]. Therefore, dispersed morphology is the preferred morphology for industrial enzyme production, even though on the macroscopic level this type of morphology greatly affects the rheology of the fermentation broth, resulting in very high apparent viscosities and a non-Newtonian fluid behavior. This leads to oxygen mass transfer limitations and poor mixing [4]. An obvious choice to overcome these problems is to increase the agitation speed. However, then the question about potential damage of the microorganisms' due to the high shear forces arises [5].

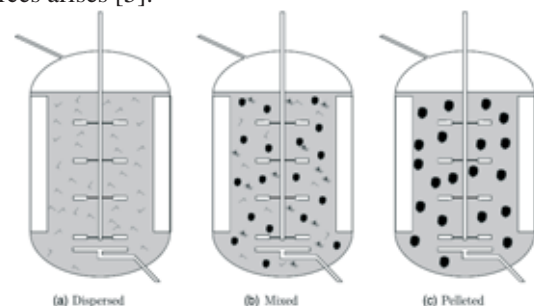


**Figure 1:** The morphology of filamentous microbes cultivated in bioreactors can range from dispersed hyphal elements to distinct pellets. Adapted from [2].

### Influence of agitation intensity in the morphology, rheology and productivity of *T. reesei*

Four fed-batch fermentations were conducted at two different agitation speeds and two enzyme induction levels in 2L bioreactors. The induction level was manipulated in order to determine whether hyphal fragmentation is favored by the stresses caused by the high enzyme expression. The expressed enzymes were cellulases. The fermentations were started with an identical batch phase and glucose was used as a carbon source. After the carbon source was consumed, the feeding was added at a constant feed rate and the agitation speed was increased for two fermentations. Lactose was used to feed the induced fermentations and glucose was used for the control experiments. Samples were taken every 24h and dry weight, extracellular protein, and enzyme activity were determined. Rheology and laser diffraction measurements were also conducted. The latter method has been proven to give a particle size distribution which is very similar to those obtained using image analysis [6].

The results from the dry weight determination, extracellular protein and enzyme activity can be found in Figure 2. The results show that the agitation speed has no influence on enzyme production under conditions without oxygen limitation. For the non-induced processes, there is also no influence of agitation intensity on the biomass growth, which was confirmed by the oxygen uptake rate trends (data not shown). However, significant effects are observed in the viscosity of the fermentation broths, Figure 3. At a higher agitation speed the viscosity is reduced due to changes in morphology, i.e. a higher fragmentation occurs for increased agitation intensity, Figure 4.

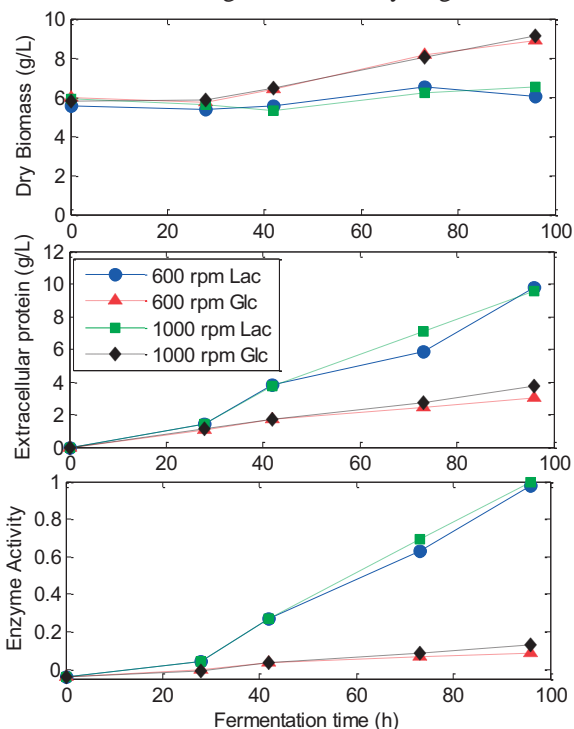


**Figure 2:** Off-line measurements for the four different fermentations.

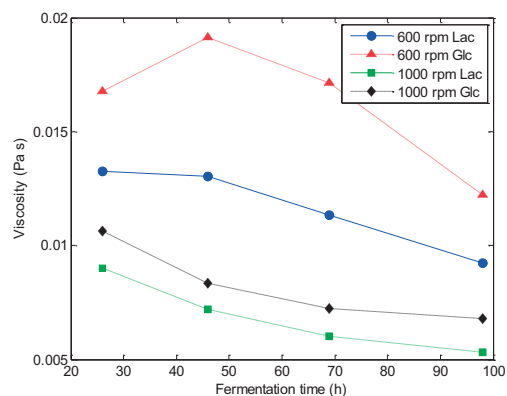


**Figure 3:** Viscosity measurements for the four different fermentations.

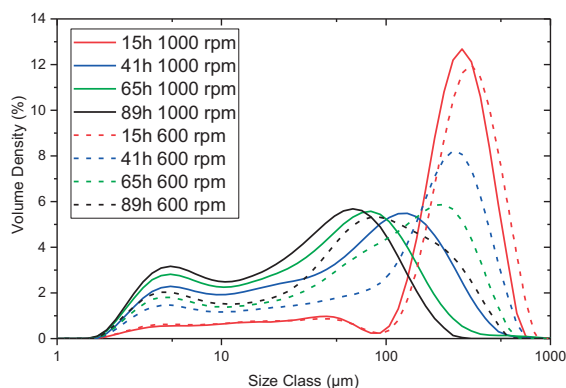


**Figure 4:** Particle size distributions for the induced fermentations at different fermentation times.

This study has allowed us to conclude that agitation intensity can be manipulated in order to reduce oxygen transfer limitations and improve bulk mixing. It can also be used to reduce viscosity by affecting the morphology without affecting enzyme production. This is in agreement with the results from [4].

### Acknowledgements

The project is funded by the Novo Nordisk Foundation, Novozymes A/S and the Technical University of Denmark.

### References

- J.J. Smith, M.D. Lilly & R.I. Fox. *Biotechnol. Bioeng.* 35 (1990) 1011-1023.
- D.J. Barry & G.A. Williams. *J. Microscopy* 244 (2011) 1-20
- A. Spohr, C. Dam-Mikkelsen, M. Carlsen, J. Nielsen & J. Villadsen. *Biotechnol. Bioeng.* 58 (5) (1998) 542-553.
- A. Amanullah, L.H. Christensen, K. Hansen, A. W. Nienow & C. R. Thomas. *Biotechnol. Bioeng.* 77(7)(2002)815-826
- Z.J. Li, V. Shukla, A. P. Fordyce, A. G. Pedersen, K.S. Wenger & M. R. Marten. *Biotechnol. Bioeng.* 70 (3) (2000) 300-312
- N.P. Rønneest, S. M. Stocks, A. E. Lantz & K. V. Gernaey. *Biotechnol. Lett.* 34(8)(2012)1465-1473



**Helena Rasmussen**

Phone: +45 99516262  
E-mail: heras@dongenergy.dk

Supervisors: Anne S. Meyer  
Hanne R. Sørensen, DONG Energy

Industrial PhD Study

Started: October 2012  
To be completed: March 2016

## Degradation products from pretreated biomass

### Abstract

The degradation compounds formed during pretreatment when lignocellulosic biomass is processed to ethanol or other biorefinery products include furans, phenolics, organic acids, as well as mono- and oligomeric pentoses and hexoses. Depending on the reaction conditions glucose can be converted to 5-(hydroxymethyl)-2-furaldehyde (HMF) and/or levulinic acid, formic acid, and different phenolics at elevated temperatures. The reactions are of interest because the very same compounds that are possible inhibitors for biomass processing enzymes and microorganisms may be valuable biobased chemicals. Hence a new potential for industrial scale synthesis of chemicals has emerged. A better understanding of the reactions and the impact of the reaction conditions on the product formation is thus a prerequisite for designing better biomass processing strategies and forms an important basis for development of new biorefinery products from lignocellulosic biomass as well.

### Introduction

When lignocellulosic biomass is processed into biofuels - and potentially other biorefinery products - the biomass is usually pretreated in order to make the cellulose and hemicellulose amenable to enzymatic depolymerization. The biomass pretreatment, particularly pretreatment regimes involving acid and/or temperatures above 160-180 °C, induces formation of degradation products that may inhibit the cellulolytic enzymes and/or the ethanol producing microorganisms (notably yeast, *Saccharomyces cerevisiae*) that are required for the subsequent sugar conversion.

The advances in the recent two years have also revealed that the chemistry of formation of the putative inhibitors during thermal biomass pretreatment for biofuel production have many features overlapping with the discipline of industrial scale synthesis of biobased platform chemicals from glucose and potentially from other biomass monosaccharides [1]. The deliberate production of this type of products from biomass carbohydrates for industrial uses currently only appears feasible via targeted catalytic or biocatalytic technologies [1].

### Biomass Degradation during Hydrothermal Pretreatment

A summary overview of cellulose, hemicellulose and lignin degradation is shown in Figure 1.

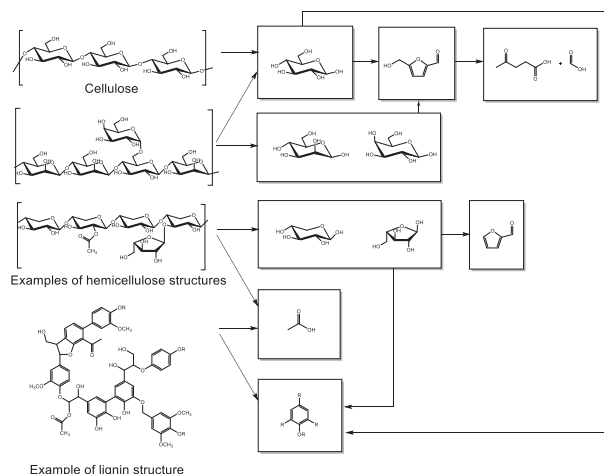


**Figure 1:** Biomass degradation summary overview.

The degradation products include furans, phenolics, organic acids, as well as mono- and oligomeric pentoses and hexoses. These compounds are moreover able to undergo various reactions with each other. Such intermolecular reactions can lead to several new products and polymerization reactions as pseudo lignin and humins.

Pseudo lignin is an aromatic material containing hydroxyl and carbonyl functional groups. In this way pseudo lignin resembles native lignin but is not derived thereof. Recent progress has confirmed that pseudo-lignin can form solely via carbohydrate degradation [2]. Humins are dark colored substances that are formed during thermal hydrolysis of glucose. Formation of humins has been shown to arise from reaction of HMF with glucose [3] and/or via reaction of HMF with 2,5-dioxo-6-hydroxy-hexanal (hydrated HMF) [4] and subsequent polymerization. The formation of humins via HMF reactions have been reported relatively recently [3][4], and whether, and to which extent, humins impact cellulolytic enzymes and/or yeast during cellulosic ethanol production is at present uncertain.

### Mechanistic Considerations regarding Degradation

Via ab initio molecular dynamics simulations it has been shown that the rate limiting step in the reaction of glucose is protonation of hydroxyl groups on the glucose or direct protonation of the pyranose oxygen. Different protonation sites can lead to different reaction mechanisms and hence different subsequent degradation products [5] as illustrated for glucose in Figure 2.

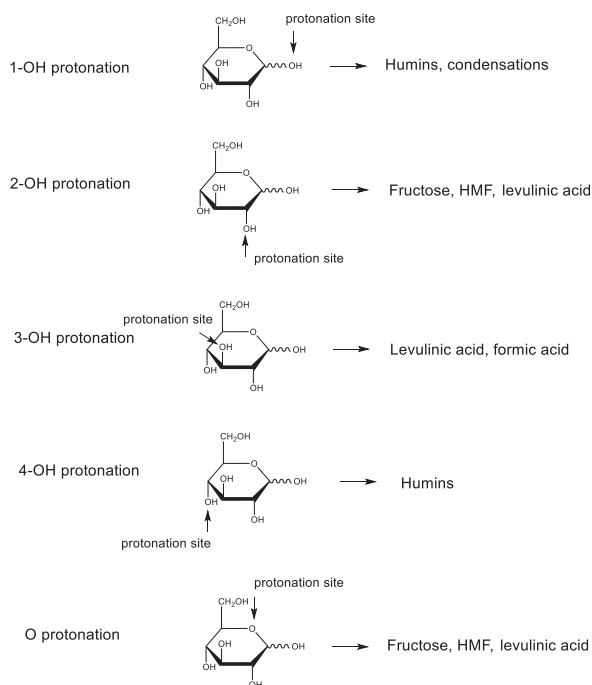


**Figure 2:** Site of protonation and subsequent degradation products from glucose determined by ab initio molecular dynamics in water and quantum mechanics modelling with solvent water.

Solvent water structure is crucial for the protonation site since water molecules compete for protons and hydrogen bond to the hydroxyl groups. In addition, reaction conditions (pH, solvent, salts etc.) can easily alter the water molecule surroundings and hence the

hydroxyl protonation site and the reaction mechanism and the following reaction.

In the literature it has long been discussed which degradation mechanisms and products that are correct [6][7][8] and the key point is that they may all be correct depending on reaction conditions.

It is still to be revealed how actual reaction conditions can be coupled to degradation mechanisms and routes in order to control the degradation product profile. Detailed knowledge about the impact of process conditions is important with respect to cost reduction of biofuel processes, but is also highly relevant for industrial scale synthesis of biomass derived chemicals where the aim is to increase the yield of one or more particular compounds of interest.

### Conclusions

Whether the goal is to reduce or increase degradation/synthesis compounds from lignocellulosic biomass, it is important to understand the chemistry of the degradation or synthesis of compounds.

It has long been discussed which exact reaction routes and mechanisms that lie behind monosaccharide degradation during hydrothermal pretreatment of lignocellulosic biomass. In fact the different reaction routes proposed in the literature may all be correct and may even occur side by side. The site of protonation initiating the monosaccharide degradation determines the mechanism and degradation route and hence the biomass degradation products. Protonation site is depending on solvent water structure surroundings, which in turn depend on the reaction conditions. The key point is thus that degradation product profile is depending on reaction conditions and may potentially be controlled by controlling the process parameters

### References

1. P. Gallezot, *Chem. Soc. Rev.* (41) (2012) 1538-1558.
2. R. Kumar, F. Hu, P. Sannigrahi, S. Jung, A.J. Ragauskas, C. Wyman, *Biotechnol. Bioeng.* (110) (2013) 737-753.
3. J. S. Dee, A. T. Bell, *Chemsuschem* (4) (2011) 1166-1173.
4. R. K. S. Patil, C. R. F. Lund, *Energy Fuels* (25) (2011) 4745-4755.
5. X. Quian, M. Nimlos, M. Davis, D. Johnson, M. Himmel, *Carbohydr. Res.* (340) (2005) 2319-2327.
6. G. Yang, E. A. Pidko, E. J. M. Hensen, *J. Catal* (295) (2012) 122-132.
7. H. Kimura, M. Nakahara, N. Matabayasi, *J. Phys. Chem* (115) (2011) 14013-14021.
8. X. Qian, *Top Catal.* (55) (2012) 218-226.

### Publications

1. H. Rasmussen, H. R. Sørensen, A. S. Meyer, *Carbohydr. Res* (2013) DOI <http://dx.doi.org/10.1016/j.carres.2013.08.029>



## Kristian Viegard Raun

E-mail: [krvie@kt.dtu.dk](mailto:krvie@kt.dtu.dk)

Supervisors: Anker Degn Jensen  
Martin Høj  
Bjarke T. Dalslet, Haldor Topsøe A/S

### PhD Study

Started: September 2015

To be completed: August 2018

## Next generation methanol to formaldehyde selective oxidation catalyst

### Abstract

Formaldehyde (CH<sub>2</sub>O) is one of the most important industrial intermediate chemicals, with an approximate production of 42 million ton in 2013 [1]. Formaldehyde is synthesized industrially by selective oxidation of methanol over an iron-molybdate (Fe-Mo) oxide catalyst. The average lifetime of the industrial catalyst is only 6 - 12 months depending on the operating conditions [2]. The focus of this project is to investigate novel catalyst preparation methods, determine the catalyzed reaction mechanism and kinetics, and develop an understanding of the catalyst deactivation and find solutions to extend the catalyst lifetime.

### Introduction

The first attempt to synthesis of formaldehyde was in 1859 by Butlerov, who tried to prepare formaldehyde by hydrolyzing methylene acetate. However, formaldehyde was first truly synthesized in 1867, when Hoffman oxidized methanol vapor with air over a heated platinum spiral. In 1882 industrial production became possible, due to Kekulé describing the preparation of pure formaldehyde and Tollens discovery of a method to regulate the methanol-air ratio and affecting the yield. Today all industrial production of formaldehyde is still based on conversion of methanol, now using modern heterogeneous catalyst [3].

Formaldehyde is produced from methanol by two major reactions. The first reaction is partial oxidation of methanol (Eq. 1) and the second is methanol dehydrogenation (Eq. 2) [4]:



In the industry, the reactions are catalyzed by silver or metal oxide catalysts. Silver catalyze both reactions and metal oxides catalyze only the partial oxidation reaction (Eq. 1). The following three catalytic processes are employed industrially [4]:

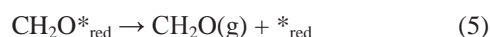
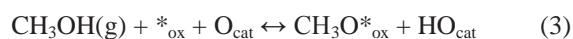
1. Partial oxidation and dehydrogenation of methanol over silver crystals in presence of air, steam and excess of methanol at 680 – 720 °C. (Conversion = 97 – 98 %)
2. Partial oxidation and dehydrogenation of methanol over crystalline silver or silver gauze with presence of air, steam and excess of methanol at 600 – 650 °C. (Single pass conversion = 77 – 87 %, unconverted methanol is recovered by distillation and recycled.)
3. Selective oxidation of methanol over iron/vanadium – molybdenum oxide catalyst with excess of air at 250 – 400 °C. (Conversion = 98 – 99 %)

The third process is known as the Formox process [4]. The catalyst can either be modified iron – molybdenum oxide or modified vanadium – molybdenum oxide. The third process using iron – molybdenum oxide catalyst is dominant in the industrial production of formaldehyde due to high single pass conversion and selectivity.

The Formox process will be the one studied in this PhD project.

The iron-molybdate catalyst consist of two phases of primarily  $\text{Fe}_2(\text{MoO}_4)_3$  and  $\text{MoO}_3$ . The core of the catalyst particles consist of  $\text{Fe}_2(\text{MoO}_4)_3$  with a layer at the surface mainly consisting of  $\text{MoO}_3$ . The molybdenum atoms at the surface are forming the active sites of the catalyst and are selective towards formaldehyde.

Pernicone et al. [5] proposed that the lattice oxygen of the catalyst participates in the selective oxidation of methanol as follows:



Where  $*_{\text{ox}}$  is the oxidized active site (Mo) and  $*_{\text{red}}$  is the reduced active site.  $\text{O}_{\text{cat}}$  is an oxygen atom in the catalyst lattice. The rate limiting step is the dehydrogenation of the methoxy group (Eq. 4), however the re-oxidation of the active site is also a slow reaction. Eq. 3-7 is a so called Mars van Krevelen mechanism.

Eq. 3: Methanol adsorbs by forming a methoxy and hydroxyl group on the active site and the lattice oxygen respectively.

Eq. 4: The methoxy group dehydrogenate by reaction with the lattice oxygen.

Eq. 5: Formaldehyde desorbs to the gas phase.

Eq. 6: The hydroxyl groups forms water that desorbs to the gas phase. The oxygen atom in the water molecule is originally from the catalyst lattice.

Eq. 7: The catalyst is re-oxidized by oxygen from the gas phase.

The average lifetime of an industrial iron molybdate catalyst is only 6-12 months depending on the operating conditions. The major reason for the deactivation is the loss of molybdenum from the catalyst, due to formation of volatile compounds of molybdenum.

Ivanov and Dimitrov [6] performed an experiment at industrial conditions over several months to investigate the deactivation of iron-molybdate catalyst. Over time they observed axial changes in the composition of the catalyst through the test-reactor. The molybdenum content was decreased significantly in the initial zone of the reactor and slightly increased in the subsequent zone. This shows that during operation of the catalyst molybdenum species migrate along the catalyst bed.

As the molybdenum migrate away from the initial zone of the reactor, the molybdenum rich phase of the catalyst surface changes. The loss of molybdenum at the catalyst surface decreases the selectivity towards formaldehyde due to formation of side products such as CO and  $\text{CO}_2$ .

### Specific Objectives

The objectives of the project are to:

- Develop improved iron molybdate catalyst synthesis, by exploring novel catalyst preparation methods and by addition of promoters.
- Obtain a complete understanding of the reaction mechanism and kinetics of methanol selective oxidation over iron molybdate catalyst.
- Understand catalyst deactivation and molybdenum transport through the catalyst bed.

### Acknowledgements

This project is a collaboration between the CHEC research center at DTU Chemical Engineering and Haldor Topsøe A/S. Financial support from The Independent Research Council (DFF – 4184-00336) is gratefully acknowledged.

### References

1. IHS Chemical, IHS analysis report Forecast: global formaldehyde market demand after five years, (2013).
2. C. Brookes, P. P. Wells, G. Cibin, N. Dimitratos, W. Jones, D. J. Morgan, M. Bowker, ACS Catal. 4 (2014) 243-250.
3. G. Reuss, W. Disteldorf, A. O. Gamer, A. Hilt, Ullmann's Encyclopedia of Industrial Chemistry, Wiley-VCH Verlag GmbH & Co. KGaA. (2000).
4. A. M. Bahmanpour, A. Hoadley, A. Tanksale, Rev. Chem. Eng. 30 (6) (2014).
5. N. Pernicone, F. Lazzarin, G. Liberti, G. Lanzavecchia. J. Catal. 14 (4) (1969) 293-302.
6. K. I. Ivanov and D. Y. Dimitrov. Catal. Today. 154 (3-4) (2010) 250-255.



**Nanna Rhein-Knudsen**

Phone: +45 4525 6892  
E-mail: nark@kt.dtu.dk

Supervisors: Anne S. Meyer  
Marcel Tutor Ale

PhD Study  
Started: Dec. 2014  
To be completed: Dec. 2017

## Seaweed polysaccharides production using enzymes technology

### Abstract

Agar and carrageenans are high-value seaweed hydrocolloids, which are used as gelation and thickening agents in different food, pharmaceutical, and biotechnological applications. The techno-functional properties of these polysaccharides depend strictly on their unique structural make-up, notably degree and position of sulfation and presence of anhydro-bridges. Classical extraction techniques include hot alkali treatments, but there is a need for a more selective and mild extraction methods that maintains specific functionalities and avoids the destructible effects the classical extraction method has on both the hydrocolloids and the environment.

### Introduction

Agar and carrageenans are hydrocolloids found in selected red seaweed species. They have significant importance, both technologically and economically, since they are used in the food, pharmaceutical, medicinal, and biotechnological industries due to their distinct physicochemical properties [1].

Carrageenans are hydrophilic sulfated linear galactans that mainly consist of D-galactopyranose units bound together with alternating  $\alpha$ -1,3 and  $\beta$ -1,4 linkages. This base structure is consistent in the three main commercially used carrageenans,  $\kappa$ -,  $\iota$ -, and  $\lambda$ -carrageenan, figure 1. The presence of 4-linked 3,6-anhydro- $\alpha$ -D-galactopyranose varies among the different carrageenans, as do the substitutions of sulfates, which are ester-linked to C2, C4, or C6 of the galactopyranose units, depending on the specific carrageenan [2]. Carrageenans are soluble in water, but the solubility depends on the content of hydrophilic sulfates, which lowers the solubility temperature, and on the presence of potential associated cations such as potassium, calcium, and magnesium, which promote cation-dependent aggregation between carrageenan helices. Another factor affecting the physico-chemical properties in relation to viscosity and gelation, is the presence of anhydro-galactose, which allow the polysaccharide to undergo conformational transitions. The thermo-reversible gel formation is proposed to occur in a two-step mechanism, dependent on temperature and gel-inducing agents. At high temperatures, i.e. above 75-80 °C, the carrageenans exist as random coil structures as a result of electrostatic repulsions between adjacent polymer chains. Upon

cooling, the polymeric chains change conformation to helix structure. Further cooling and presence of cations lead to aggregation of the helical dimers and formation of a stable three dimensional network, which forms through intermolecular interactions between the carrageenan chains [3].

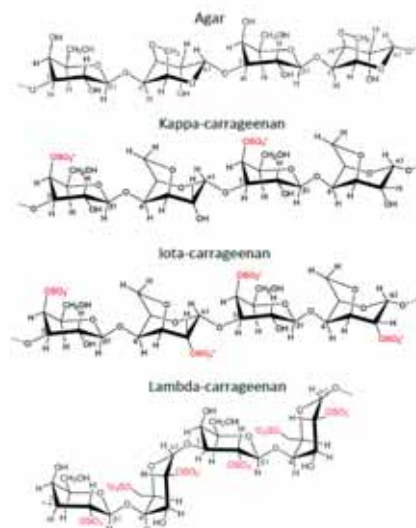


**Figure 1:** Chemical structures of the seaweed hydrocolloids: Agar and kappa-, iota-, and lambda-carrageenan.

The cations, typically potassium for  $\kappa$ -carrageenan, function to stabilize the junction zones between the two helices by binding to the negatively charged sulfate groups without hindering cross-linking of the two helices, figure 2 [1].

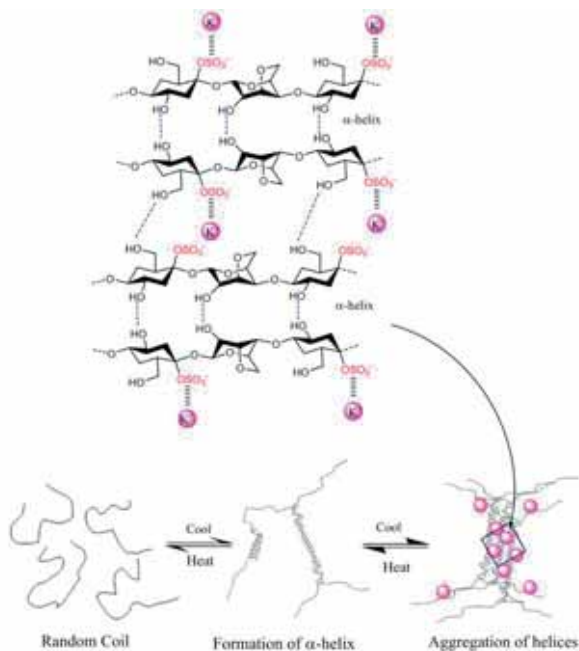


**Figure 2:** The gelation mechanism of  $\kappa$ -carrageenan in the presence of potassium ions.

Calcium, typically for  $\iota$ -carrageenan, functions to cross-link the two helices through ionic salt bridges. The charged sulfate esters on the other side of the monomer though, present on  $\iota$ -carrageenan, encourage an extensive conformation via a repulsion effect of the negative  $\text{SO}_3^-$  groups and inhibit gelation while promoting viscosity in the solution. The differences in sulfate position, their proportion, and the presence of anhydro-bridges thus give the carrageenans distinctive gel profiles:  $\kappa$ -carrageenan forming strong and rigid gels,  $\iota$ -carrageenan forming soft gels, and  $\lambda$ -carrageenan that does not gel, but still provides elevated viscosity in solution, due to a structure that does not allow helix formation [1].

Like carrageenans, agars are hydrophilic galactans consisting of galactopyranose units with alternating  $\alpha$ -1,3 and  $\beta$ -1,4 linkages, but whereas the  $\alpha$ -linked galactopyranose is in the D-configuration in carrageenans, agar is made up of L-galactopyranose units. The gelling and solubility properties of agar polysaccharides are outstanding among the hydrocolloid polysaccharides because of their relative hydrophobicity that allows agar to form helical dimers according to a mechanism similar to that of the carrageenans as described above [1].

The extraction procedures for these two seaweed hydrocolloids are dependent on the specific seaweed species, but generally consist of an alkali treatment followed by a hot-water extraction. The alkali treatment causes a chemical change in the hydrocolloids: the formation of 3,6-anhydro-galactopyranose that increases the gel strength. The hot-water extraction is usually done at temperatures around 100 °C for 2-4 hrs, sometimes under pressure. The hydrocolloids are dissolved in the water, seaweed residuals are removed

by filtration and the hydrocolloids are recovered by alcohol precipitation and freeze-drying [4].

For extraction of these seaweed polysaccharides, there is a need for a mild extraction technique, which can promote solubility and gel strength and avoid the severe conditions like pressure extraction, high temperatures, and high alkali concentrations that has both harmful effects on the valuable hydrocolloids and the environment. In addition, it is of interest to develop a more selective extraction method that allows for tailor-made modifications in order to obtain specific functional properties, depending on the use of the hydrocolloid. [1].

### Specific Objectives

The first part of the project will be devoted to a characterization of seaweeds and hydrocolloids from seaweed species collected along the coastline of Ghana. This will be done by estimation of carbohydrate content and a characterization of extracted hydrocolloids that will include yield determination, chemical composition, sulfate content determination and determination of rheological parameters such as gelling and melting temperatures.

The second part of the project will concern a more selective and sustainable extraction of these seaweed hydrocolloids. As a first attempt, different commercial enzyme cocktails will be considered for the extractions. Secondly, new enzymes and designed mixtures of monoactive microbial enzymes will be assessed in order to, hopefully, develop more selective and sustainable extraction methods for these high-value seaweed carbohydrates.

### Acknowledgement

This PhD project is part of the Seaweed Biorefinery Research Project in Ghana (SeaBioGha) supported by Denmark's development cooperation (Grant DANIDA-14-01DTU), The Ministry of Foreign Affairs of Denmark.

### References

1. N. Rhein-Knudsen, M. T. Ale, A. S. Meyer, Marine Drugs 13 (2015) 3340-3359
2. A. I. Usov, Polysaccharides of the red algae (2011)
3. S. Genicot-Joncour, A. Poinas, O. Richard, P. Potin, B. Rudolph, B. Kloareg, W. Helbert, Plant Physiol (2009) 1609-1616
4. D. Renn, Trends Biotechnol (1997) 9-14

### List of Publications

N. Rhein-Knudsen, M. T. Ale, A. Meyer, Marine Drugs, 13 (2015) 3340–3359.

**Anders Schlaikjer**

Phone: +45 4525 2869  
E-mail: andsh@kt.dtu.dk

Supervisors: Georgios Kontogeorgis  
Kaj Thomsen

PhD Study  
Started: June 2014  
To be completed: June 2017

## Development of the electrolyte Cubic-Plus-Association equation of state

### Abstract

Electrolytes have a significant effect in many industrial processes. In the oil and gas industry salts have many either beneficial or harmful effects, while electrolytes have many applications in the chemical industry. The objectives of this project are to parameterize an electrolyte extension to the Cubic-Plus-Association Equation of State, as well as test the capabilities of the model on a range of industrially relevant systems. Estimating a three-parameter temperature dependence to osmotic and mean ionic activity coefficients as well as solubility data yields excellent descriptions of the solubility, while having acceptable deviations for the osmotic and activity coefficients. The parameters are tested on multicomponent systems with great representation of mixed salt solubility and low deviations to mixed salt osmotic coefficients.

### Introduction

Electrolytes have a significant effect in many industrial processes. In the oil and gas industry salts can increase the inhibitory effect of methanol, ethanol and glycols on the formation of gas hydrates, and have an effect of the gas solubility in water-hydrocarbon mixtures. Salts may enhance corrosion of pipelines and also precipitation of salts (scaling) may occur, due to the change in temperature, pressure and composition from reservoir to surface[1].

Salts also play a role in many chemical industries, for instance for separation purposes as salts may induce liquid-liquid separation for some otherwise miscible liquids. Water-Acetone is such a system which is miscible under normal conditions, but when adding specific salts a phase separation occurs. Also electrolytes are important in the energy industry, both with regard to energy storage, as well as flue gas cleaning.

Accurate prediction of thermodynamic properties is important in the design and operation of processes, especially for complex mixtures. For many complex mixtures there are typically very little to none experimental data, and therefore it is needed to use trusted thermodynamic models.

Electrolyte systems are typically modeled with activity coefficient models such as the e-NRTL, and extended-UNIQUAC, however such models have difficulty handling high pressures, in which case there is a need for an Equation of State.

Several Equations of State for electrolytes have been developed over the year, but relatively few have been proposed that can handle mixtures of both hydrogen bonding compounds as well as electrolytes. Also virtually none of them have been developed to a stage where it can be considered ready for implementation in industry.

### Specific Objectives

The overall objective of the e-CPA project is to develop an electrolyte Equation of State (EoS), such that the model in absence of electrolytes reduces to the Cubic Plus Association (CPA) EoS. The initial focus for this model is implementation in the Oil and Gas industry, and is developed with engineering problems in mind.

The Current PhD study directly succeeds a completed PhD study, from which a model equation has already been proposed [2,3]. This provides a strong baseline to work from, and thus the focus of the study has and will, at least for now, be on validation and parameterization.

Different Approaches to parameterizations have and will be tested, both with regards to the method of parameter estimation, and with regards to the type of data used.

Finally the model, with optimized parameter, will be test on a wide range of industrially relevant systems, in order to evaluate the performance of the model. Based on this evaluation the model equation will be revisited if necessary.

### Electrolyte-CPA Equation of State.

A new model for electrolytes has been proposed as an extension to the CPA EoS. The electrolyte-CPA (e-CPA) reduces to the CPA in the absence of electrolytes, while the CPA in turn reduces to the Soave-Redlich-Kwong (SRK) cubic EoS in the absence of associating compounds. [2]

A major difference between electrolytes and most other compounds is the long-range electrostatic interactions. The CPA EoS cannot account for such interactions and therefore extra terms must be added to the model to account for these interactions. For electrostatic interactions the Debye-Hückel term is added to the model, while a Born term is added to the model to account for ion-solvation [2, 3]. With these additions, the contributions to the model will be as showed in Figure 1, where the first three contributions are what the CPA EoS covers. The full model equation can be viewed in [2,3].



**Figure 1:** Contributions to the Electrolyte CPA EoS. [3]

The typical parameters of the CPA EoS is the co-volume,  $b_0$ , and the two energy parameters,  $\Gamma$  and  $c_1$ , which together can be viewed as a temperature dependent energy parameter  $a(T)$ , for the physical part (SRK) and the association volume,  $\beta$ , and the association energy,  $\epsilon$ , for the associating part. In the e-CPA extension, a few additional parameters are introduced, however none of them is considered adjustable, as they are predicted from physical properties. This includes the volume parameter in the Debye-Hückel, which is set equal to the co-volume and the volume parameter in the Born term, which is interpreted as the radius of the Born cavity.

A key property for the accuracy of the electrostatic contributions is the static permittivity of the solvent. Therefore a need for accurate estimation of this was needed, and a model for the static permittivity of associating fluids has been proposed and further extended to fluids containing electrolytes. A more detailed description of this can be found in the graduate year book of 2013 by Bjørn Maribo-Mogensen and in [4, 5].

While the CPA EoS is typically implemented with the van der Waals one fluid mixing rule (vdW1f) mixing rule for the co-volume and energy parameters, for the electrolyte-solvent interaction the Huron-Vidal mixing rule is used instead as the classical mixing rules is not suitable for these systems. The Huron-Vidal mixing rule is shown in eq. 1.

$$\frac{a}{b} = \sum x_i \frac{a_i}{b_i} - \frac{g^{E,\infty}}{\ln 2} \quad (1)$$

The excess Gibbs energy is found from the modified Huron Vidal/NRTL equation. By simplifying the expression by stating that no interaction between ions should be taken in to account and by setting the NRTL non-randomness parameter,  $\alpha$ , to zero, the relation will look as in eq. 2.

$$\frac{g^{E,\infty}}{RT} = \frac{1}{b} \sum_i \sum_j x_i x_j b_j \frac{\Delta U_{ji}}{RT} \quad (2)$$

By setting the CPA energy parameter,  $a(T)$  to 1 by default for all ions, prediction the co-volume from eq. 3, and by assuming that no association between ions occurs, the number of adjustable parameters pr. ion-solvent mixture is reduced to one, being the  $\Delta U_{ji}$  parameter.

$$b = \frac{2}{3} \pi N_A \sigma^3 \quad (3)$$

This single parameter does however not capture temperature dependence very well and a temperature dependence of parameter is introduced as seen in eq. 4.

$$\frac{\Delta U_{ij}}{R} = \frac{\Delta U_{ij}^{ref}}{R} + \alpha_i \left[ \left( 1 - \frac{T}{T_\alpha} \right)^2 - \left( 1 - \frac{T_{ref}}{T_\alpha} \right)^2 \right] \quad (4)$$

Here the  $\Delta U_{ij}^{ref}$  is a parameter estimated at a reference temperature  $T_{ref}$  typically 298.15K, while  $T_\alpha$  and  $\alpha$  are additional parameters.

Finally instead of considering the parameters as ion specific it is chosen to have salt specific parameters by adding that both ions in a salt must have the same parameter values as a constrain.

### Results and Discussion

Model parameters have been estimate for a range of salts consistent of alkali and alkaline-earth cations and halogen, nitrate or sulfate anions, with water as a solvent. Thus for each salt three parameters are estimated for the interaction between the salt and water. The parameters are estimated by regression to osmotic – and mean ionic activity coefficient data as well as salt solubility data, all available from [6]. Initially only the reference interaction parameter was fitted to data at 298.15K in order to obtain a suitable initial guess for  $\Delta U_{ij}^{ref}$ . Following this, data at all temperatures was included and all three parameters were estimated. In addition to the model parameters several standard state properties of the solids were also used as adjustable parameters in order to obtain accurate solubility description.

The deviations from osmotic and activity coefficients for the 11 salts investigated are found in table 1, and the mean ionic activity coefficient for NaCl is presented graphically in figure 2 where the performance of the parameters are compared to the parameters of Maribo-Mogesen[2] and the extended UNIQUAC model [7] .

**Table 1:** Relative average deviation (RAD) for osmotic and mean ionic activity coefficients the investigated 11 salts, with the parameters of this work. The number in brackets are the deviations with the parameters from [2].

	RAD $\Phi$ %	RAD $\gamma$ %
<b>NaCl</b>	1.40% (1.45%)	3.35% (2.38%)
<b>NaBr</b>	2.58% (2.37%)	10.47% (7.57%)
<b>Na<sub>2</sub>SO<sub>4</sub></b>	2.94% (1.98%)	5.53% (4.91%)
<b>NaNO<sub>3</sub></b>	5.64% (2.12%)	6.24% (3.71%)
<b>KCl</b>	1.82% (1.57%)	3.27% (3.34%)
<b>KBr</b>	1.93% (1.73%)	10.20% (4.93%)
<b>K<sub>2</sub>SO<sub>4</sub></b>	2.39% (2.46%)	3.27% (3.60%)
<b>KNO<sub>3</sub></b>	4.47% (2.90%)	1.75% (0.43%)
<b>MgCl<sub>2</sub></b>	5.93% (4.99%)	9.54% (13.40%)
<b>MgBr<sub>2</sub></b>	5.37% (4.50%)	10.16% (10.86%)
<b>MgSO<sub>4</sub></b>	5.76% (7.23%)	8.76% (8.00%)
<b>Average</b>	3.66 % (3.03%)	6.59% (5.74%)

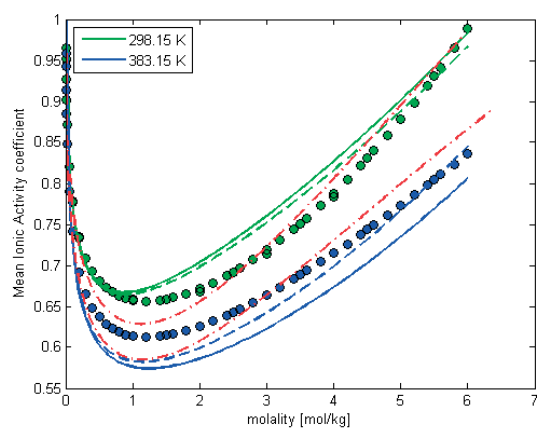


**Figure 2:** Mean Ionic activity coefficients of NaCl at different temperatures modelled with e-CPA and extended UNIQUAC. Dots are experimental data, solid line is e-CPA with parameters of this work, dashed lines are e-CPA with parameters of [2] and dot-dash lines are extended UNIQUAC [7]. Data from [6].

The goal of including the solubility in the parameter estimation was to obtain better solubility descriptions. For MgCl<sub>2</sub> for instance the model with the original parameter of Maribo-Mogensen [2] completely fails to describe the solubility, but by introducing the data to the solubility in to the estimation it is possible to describe the solubility of MgCl<sub>2</sub> very satisfyingly as can be seen

in figure 3. From table 1 it can be seen that including the solubility data to the parameter estimation affect the accuracy in osmotic and activity coefficient slightly when looking at the overall picture. The largest effect is seen in the activity coefficient where for a few of the salts the deviation doubles while for others it is almost unchanged. A qualitative comparison between the e-CPA and the extended UNIQUAC shows that e-CPA can model the solubility just as well as extended UNIQUAC and actually better at higher temperatures. The extended UNIQUAC description of the osmotic and activity coefficients are found to be similar to e-CPA, however as can be seen from figure 2, the shape of the curve differs between e-CPA and extended UNIQUAC.

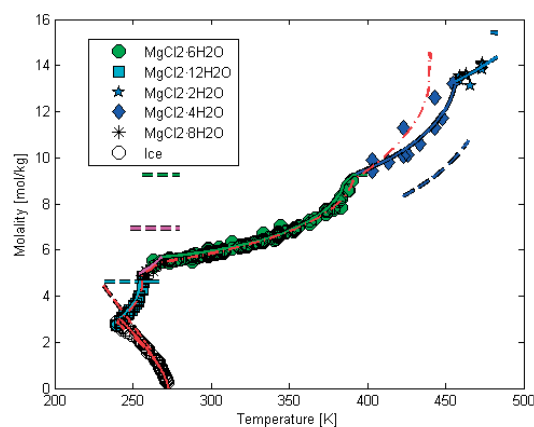


**Figure 3:** Solubility of MgCl<sub>2</sub> as a function of temperature, modelled with e-CPA and extended UNIQUAC. Dots are experimental data, solid line is e-CPA with parameters of this work, dashed lines are e-CPA with parameters of [2] and dot-dash lines are extended UNIQUAC [7]. Data from [6].

The model, with the new parameters, has been employed to mixed salt systems for prediction of solubility and the osmotic coefficient. In figure 4 the solubility of the NaCl, Na<sub>2</sub>SO<sub>4</sub> system is shown at 298.15 K and 473.15 K respectively. This shows similar performance between the new parameters and the original parameter of Maribo-Mogensen [2] at 25°C, but significantly better accuracy at 200°C with the new parameters.

For the same system the osmotic coefficient are investigated at 25 °C as can be seen in figure 5. The Relative average deviation for this mixed salt system is found to be 1.04% with the new parameters compared to 0.87% with the original parameters. For other mixed salt systems deviations are also found to be low and very similar between the two e-CPA parameter sets.

Finally the parameters have also been tested for a system of the three salts NaCl, KCl and Na<sub>2</sub>SO<sub>4</sub>. For this system the average deviation for the osmotic coefficient with the new parameters are 7.94% while

with the parameters of Maribo-Mogensen the deviation is 5.24%

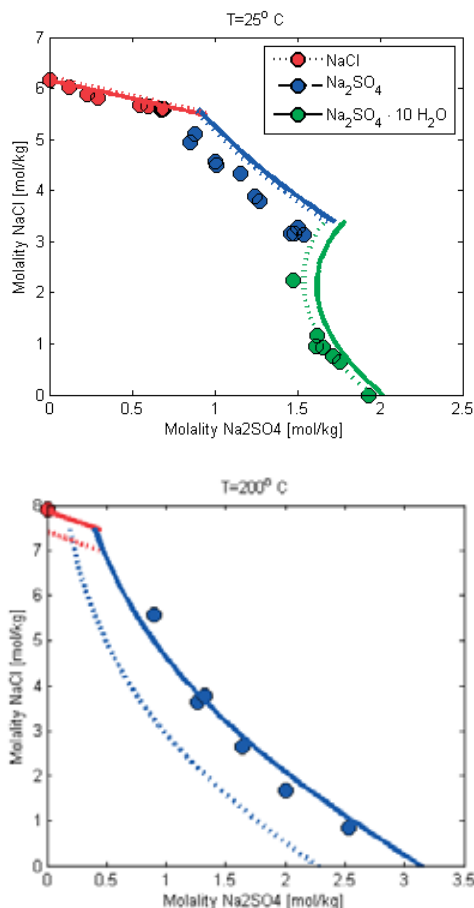


**Figure 4:** Solubility of the NaCl + Na<sub>2</sub>SO<sub>4</sub> system at 25°C and 200°C, 1 atm. Solid lines are e-CPA with the parameters of this work, and dashed lines are e-CPA with parameters from [2]. Data from [6]

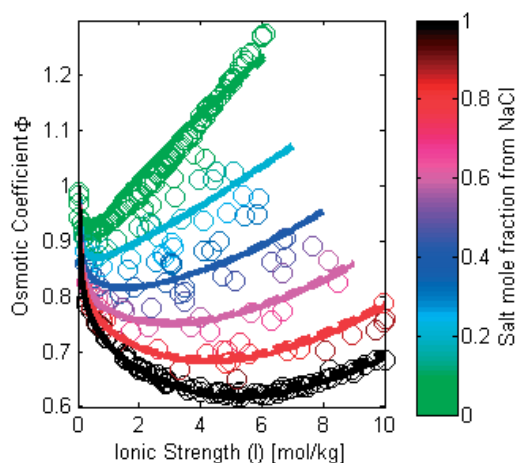


**Figure 5:** Osmotic coefficient of NaCl + Na<sub>2</sub>SO<sub>4</sub> in water at 25°C modelled with e-CPA. Solid lines are with the parameters of this work, dashed lines are with parameters from [2]. Data from [6]

## Conclusions

The e-CPA model has been parameterized with a three parameter, non-linear temperature dependence. It is fitted to osmotic and activity coefficient data as well as solubility data.

It was found that including the solubility data in the parameter estimation significantly increases the accuracy in description of solubility, however, when doing so the deviations for especially the activity coefficients, but also for the osmotic coefficients increase. When estimating parameters to solubility data it was necessary to use the solid standard state properties as adjustable parameters.

When compared to the extended UNIQUAC model it is clear that the e-CPA yields similar deviations, and have better accuracy in high temperature solubility. It is, however, interesting to notice that while deviations are very similar the shape of the osmotic or activity coefficient curves is different between the two models.

## Future Work

The future work of the project includes investigation in to an ion specific parameterization, with individual interaction parameters between each ion-solvent mixture. Also application to industrially relevant systems will be emphasized.

## Acknowledgements

The author wishes to thank the industrial partners in the CHIGP (Chemicals in Gas Processing) consortium and DTU for financial support.

## References

1. G. M. Kontogeorgis, G. K. Folas. Thermodynamic Models For Industrial Applications : From Classical and Advanced Mixing Rules To Association Theories. John Wiley & SonsLtd, 2010.
2. B. Maribo-Mogensen, K. Thomsen, G. M. Kontogeorgis. AIChE Journal 61(9) 2933-2950 (2015)
3. B. Maribo-Mogensen, (2014). Development of an Electrolyte CPA Equation of state for Applications in the Petroleum and Chemical Industries. PhD thesis, Department of chemical and Biochemical Engineering Technical University of Denmark
4. B. Maribo-Mogensen, G. M. Kontogeorgis, and K. Thomsen, Journal of Physical Chemistry B 117(12) (2013): 3389-3397
5. B. Maribo-Mogensen, G. Kontogeorgis, and K. Thomsen, Journal of Physical Chemistry B 117(36)(2013): 10523-10533.
6. K. Thomsen, Cere electrolyte database, [www.cere.dtu.dk/Expertise/Data\\_bank/Search](http://www.cere.dtu.dk/Expertise/Data_bank/Search)
7. K. Thomsen, P. Rasmussen, Chemical Engineering Science, 54(12):1787–1802, 1999



**Rasmus Seerup**  
Phone: +45 45 25 28 53  
E-mail: [rasee@kt.dtu.dk](mailto:rasee@kt.dtu.dk)  
CHEC Research Center

Supervisors: Kim Dam-Johansen  
Weigang Lin

PhD Study  
Started: November 2013  
To be completed: October 2016

## Modelling of gasification of biomass in dual fluidized beds

### Abstract

In fluidized bed gasification of biomass, tar may be problematic for downstream processing. Controlling the tar properties may make the gas cleaning process easier, and help to run the apparatus at optimal conditions. This project investigates the formations of tars from biomass under gasification conditions in the dual fluidised bed, by modelling the development of tar in a particle scale and reactor scale.

### Introduction

There is an increasing interest on the utilization of biomass as a renewable source for energy. Gasification of biomass in dual fluidised beds provides the possibility of producing synthetic gas with high hydrogen content and a high heating value. Biomass ash may cause a high tendency of agglomeration at elevated temperature. Consequently, biomass is usually gasified at relatively low temperatures, which lead to a high content of tars. Understanding tar formation and properties is important for optimizing the downstream cleaning or separation.

Tar produced at gasification conditions is mainly originating from monolignols released from lignin in the pyrolysis process before actual gasification proceed [1]. Many observations have shown that torrefaction and slow heating rate increases the fixed carbon (char) in the residual biomass from pyrolysis [2]. The increase in char is caused by a radical reaction between the monolignols. Thus, a pretreatment of the biomass by torrefaction may affect the amount of tar released.

### Specific Objective

The objective of the project is to understand the tar development in dual fluidized beds gasification of biomass, by experimental and modelling studies at both particle and reactor scale.

### Previous work

A model has been set up for cellulose, hemicellulose and lignin to predict tar release. The major problem was the lumped treatment of tars from biomass, because the tar reactivity is very different. Furthermore, the low heating rates used, diminished the release of tars. The combination of GC/MS and TGA gives a more detailed

understanding of which tars are released at which temperatures, and may thus be used to assembly a better reaction scheme to represent the release of tars. Under gasification the primary tars from cellulose and hemicellulose is easily decomposed and thus of less interest.

### Experimental

Pyrolysis and torrefaction is performed using a pyroprope 5200. A sample of approximate 1-2 mg pulp lignin is placed in a quartz tube that is placed in a heating coil with helium as carrier gas. The tar released is analyzed by a GC/MS.

Torrefaction is done at desired temperature and time before pyrolysis started at a high heating rate of 20°K/ms. The fast cooling and the low end-temperature minimize the secondary reactions.

### Results and discussion

#### *Torrefaction effect on tar release*

Figure 1 shows the accumulated absorption from the GC/MS analysis. The absorption of the individual compounds are grouped according to the functional groups on the aromatic ring. Aliphatic phenols include ethyl, methyl, ethanyl or propenyl as functional groups. Methoxy phenols vary in the amount and placement of methoxy groups. Aliphatic methoxy phenol has both methoxy and aliphatic groups. Toluene include toluene with any functional groups except hydroxyl.

The reduction in the methoxy phenols and aliphatic methoxy phenols fits well with lower bounding energy for the methoxy groups [3], [4]. The removal of methoxy groups from the aliphatic methoxy phenols may explain the increase in aliphatic phenols.

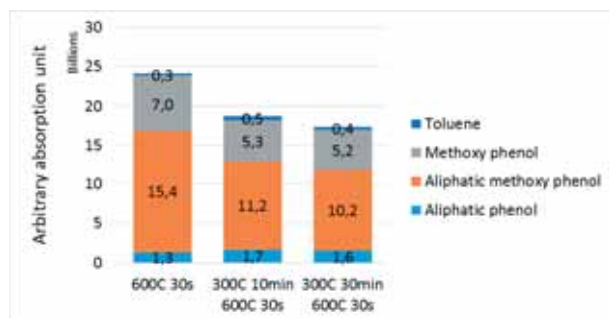


**Figure 1:** Accumulated tar detection grouped according to functional groups available (phenol with methoxy or aliphatic groups or both).

### Temperature at the release of tar

**Error! Reference source not found.** shows two temperatures at which tar is mainly released, 200°C and 400°C-450°C. Phenol has been independently shown, as this is a primary precursor for higher tar species. The main aliphatic methoxy phenol at 200°C is Vanillin. While other aliphatic methoxy compounds are released at higher temperatures. O-m-p-methoxy phenol is released over 200°C-500°C. The early release of a very specific tar compound at low temperature is very surprising.

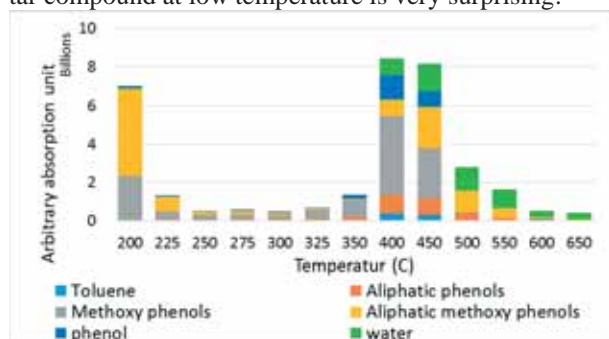


**Figure 2:** Tar release with temperature from pulp lignin.

Figure 3 shows the STA (TGA+DSC) of pulp lignin under N<sub>2</sub> atmosphere at a heating rate of 10°C/min.

The result of the TGA show a small endothermal weight loss at the beginning up to about 100°C. This is often attributed to the evaporation of water. However, GC/MS did not detect considerable water. Further weight loss is seen from about 200°C up to around 600°C which seem mostly exothermal. This is attributed to the release of tars and gases. At about 750°C a third peak in mass loss (6.92% from 70°C to 80°C) is observed, with a highly endothermal peak (DSC curve), which is attributed to the evaporation of inorganics.

The TGA curve indicate three overlapping peaks in the range of 150°C-600°C. The results, combined with knowledge on the release of tar, indicate that Vanillin may be controlled by the first peak. The o-m-p-methoxy phenol may be controlled by the second peak. A low amplitude peak seem to control the rest of the species resulting in the slope of the mass lose from around 400°C. Endothermic processes are often attributed to pyrolysis and the exothermic processes to condensation reaction [5]. The torrefaction in this case is happening in an endothermic range of the biomass, which may explain that no change in residual fixed carbon is observed.

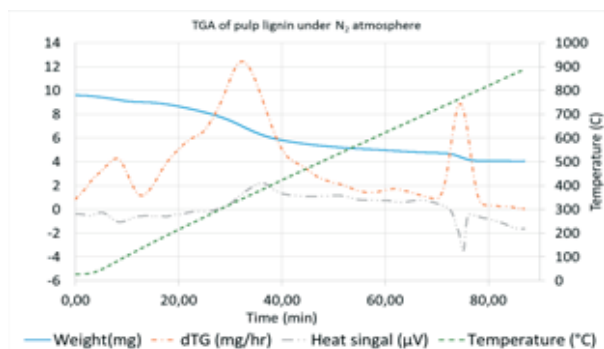


**Figure 3:** TGA and DSC of 9,586mg pulp lignin under N<sub>2</sub> atmosphere at 10°C/min.

Setting up a three-reaction-rate-scheme based on the TGA may be possible to generate a rather complex release rate of the tars, if more detailed quantitative determination for the tar can be obtained.

### Conclusion

- Torrefaction primary affect the methoxy groups which fits well with the lower bonding energy.
- Two major tars can be related to the TGA peaks giving possibilities for a simple tar release calculation with details of the tar composition.
- The reduction in tar is related to the formation of gases rather than formation char. The variance in mass lose is insufficient to reveal any formation of fixed carbon

The combined information of TGA and GC/MS shows that dominant tar release may be modelled as three reactions, and possibly by their substituent groups.

### Future work

Further work will focus on modeling of tar development in the gas phase under gasification environment of the dual fluidized bed. Changes in the gas phase composition is of interest as it may change the tar development.

### Acknowledgements

This project is part of DANCONGAS. Financial support provided by Sino-Danish Centre for education and research and the Technical University of Denmark are gratefully acknowledged.

### Reference

1. T. Hosoya, H. Kawamoto, and S. Saka, *J. Anal. Appl. Pyrolysis*, vol. 80, no. 1, pp. 118–125, Aug. 2007.
2. M. Adam, R. Ocone, J. Mohammad, F. Berruti, and C. Briens, *Ind. Eng. Chem. Res.*, vol. 52, no. 26, pp. 8645–8654, Jul. 2013.
3. S. Kim, S. C. Chmely, M. R. Nimlos, Y. J. Bomble, T. D. Foust, R. S. Paton, and G. T. Beckham, *J. Phys. Chem. Lett.*, vol. 2, no. 22, pp. 2846–2852, Nov. 2011.
4. R. Parthasarathi, R. a. Romero, A. Redondo, and S. Gnanakaran, *J. Phys. Chem. Lett.*, vol. 2, no. 20, pp. 2660–2666, Oct. 2011.
5. C. Gomez, E. Velo, F. Barontini, and V. Cozzani, *Ind. Eng. Chem. Res.*, vol. 48, no. 23, pp. 10222–10233, Dec. 2009.



### Catarina Seita

Phone: +45 4525 2926  
E-mail: casse@kt.dtu.dk

Supervisors: John Woodley, DTU  
Mathias Nordblad, DTU  
Jessica Rehdorf, BRAIN AG

### PhD Study

Started: December 2013  
To be completed: November 2016

## Bioprocess evaluation tools

### Abstract

Many biocatalytic processes at an early-stage of development require redesign to meet the necessary economic constraints at full industrial scale. That is not surprising since bioprocesses for industrial production of chemicals are usually pushed way beyond their natural limits to produce for example high concentrations of product. This project aims to develop a strategy to assist an early-stage process development for biocatalytic processes that can ultimately facilitate the scale-up. Such approach is illustrated with a representative case-study – the synthesis of *R*-perillic acid by a wild type strain of *Pseudomonas putida*. A simple economic model of the bioprocess was developed and a sensitivity analysis was made to understand how simple process metrics, such as space-time yield ( $g_{\text{product}}/L_{\text{reactor}}/h$ ) or reaction yield, are affected by process variables. This analysis allowed the identification of the main bottlenecks of the bioprocess, highlighting where research and development efforts should be focused on.

### Introduction

Currently, the implementation of scalable biocatalytic processes often requires the introduction of process and/or biocatalyst enhancements to ensure effective scale-up.

This project aims to develop an approach for evaluating biocatalytic processes in an early-stage of development in order to provide guidance on process and biocatalyst modification.

This approach is illustrated with a case-study – the biocatalytic synthesis of *R*-perillic acid using a whole-cell catalyst (Figure 1).

*R*-perillic acid is an antimicrobial chemical that shows a broad growth-inhibitory effect on bacteria, yeast and moulds, which makes it an attractive candidate to be used in substitution of conventional preservatives, particularly in cosmetic industry [1].

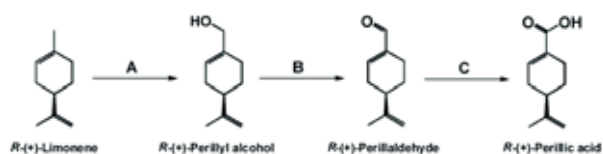


**Figure 1:** Bioconversion of *R*-limonene to *R*-perillic acid by *P. putida* GS1: (A) monooxygenase; (B) alcohol dehydrogenase; (C) aldehyde dehydrogenase [1].

This bioprocess faces numerous bottlenecks, which are summarized in Table 1.

**Table 1:** Summary of bottlenecks for the biocatalytic reaction being studied.

Bottleneck	Possible strategies to solve the bottleneck
Product inhibition	<ul style="list-style-type: none"> <li>• <i>In situ</i> product removal (ISPR);</li> </ul>
High volatility of the substrate	<ul style="list-style-type: none"> <li>• Fermentation with a two-phase liquid medium;</li> <li>• Pressurized reactor;</li> <li>• Reduced aeration;</li> <li>• Alternative methods for oxygen supply.</li> </ul>
Low space-time yield ( $g_{\text{product}}/L_{\text{reactor}}/h$ )	<ul style="list-style-type: none"> <li>• High cell density fermentation;</li> <li>• Overexpression of the enzymes involved in the reaction in the whole-cell biocatalyst.</li> </ul>
Low solubility of the substrate in aqueous phase	<ul style="list-style-type: none"> <li>• Fermentation with a two-phase liquid medium.</li> </ul>

## Results and Discussion

A process model was developed in the commercial process simulation software SuperPro Designer®. The model is based on experimental data collected at laboratory scale and scalability to industrial scale was assumed. In Figure 2 is shown a simplified process flowsheet for *R*-perillic acid production.

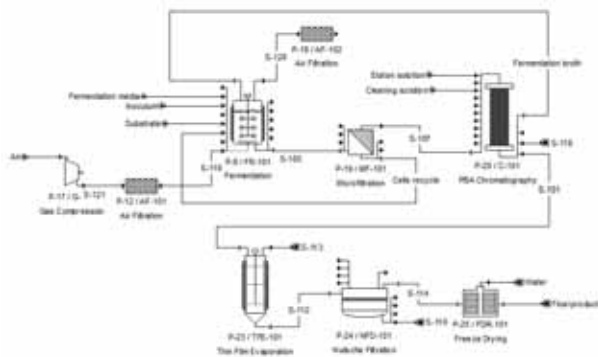


**Figure 2:** Simplified process flowsheet for *R*-perillic acid production.

The impact of single input variables (*e.g.* reaction yield or reaction time) was studied by sensitivity analysis, which allowed the identification of key parameters for process development. In Figure 3 is shown the influence of space-time yield ( $g_{\text{product}}/L_{\text{reactor}}/h$ ) on the production costs (excluding depreciation of equipment).

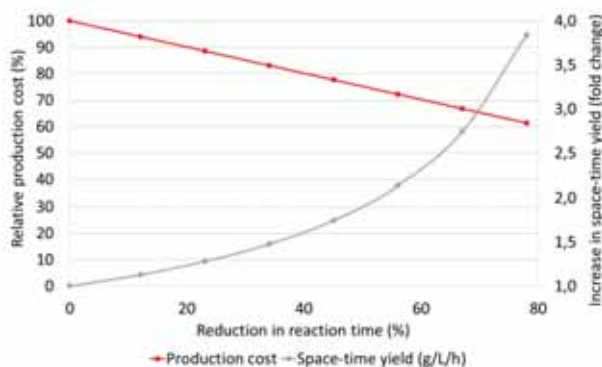


**Figure 3:** Relative production cost and increase in space-time yield as a function of reduction in reaction time.

The sensitivity analysis showed that production costs are very sensitive to space-time yield ( $g_{\text{product}}/L/h$ ). Other parameters such as reaction yield do not affect production cost in a significant way.

Therefore, the focus of biocatalyst and process development should be on increasing space-time yield by decreasing the reaction time. There are several strategies to increase space-time yield. One option is the overexpression of the enzymes responsible for the

reaction in the cell. Another option is running a high cell density fermentation, since starting the reaction with a higher concentration of the whole-cell biocatalyst should lead to the formation of product in a shorter period of time.

A combination of both strategies would potentially yield a higher reduction in reaction time and should also be investigated.

## Conclusions and Outlook

The approach followed to analyze this process in an early-stage of development allowed the identification of the main bottleneck without the need of running time-consuming experiments.

This tool can provide guidelines for biocatalyst and process development, assist research and support decision-making, which ultimately can lead to a reduced process development time.

Currently, some of the strategies to solve the bottlenecks of the process are being experimentally tested in laboratory scale.

## Acknowledgements

The project is part of the strategic alliance NatLife 2020 coordinated by BRAIN Aktiengesellschaft. The financial support from BMBF (grant no. 031A206-B) is acknowledged.

## References

- 1 M. A. Mirata, D. Heerd, J. Schrader, Integrated bioprocess for the oxidation of limonene to perillic acid with *Pseudomonas putida* DSM 12264, *Process Biochemistry* 44 (2009) 764-771.



**Daria Semenova**

Phone: +45 4525 2958  
E-mail: dsem@kt.dtu.dk

Supervisors: Krist V. Gernaey  
Ulrich Krühne

PhD Study  
Started: August 2014  
To be completed: August 2017

## **Development of advanced mathematical data interpretation methods for the description of bioprocesses in microbioreactors**

### **Abstract**

The interest in downscaling within industrial biotechnology has increased significantly in the last decade. It has resulted in the development and further implementation of small scale reactors such as microbioreactors (MBRs). The design and development of MBRs with integrated sensors and parallel operation is an adequate solution for rapid, high-throughput, and cost-effective screening, with considerably reduced reagent usage and waste generation [1]. However, the successful application of MBR technology will only be possible if it can rely on appropriate software and automated data interpretation of the MBR experiments. Thus, the software and data interpretation tools should allow maximizing the exploitation of the flexibility and the capabilities of the MBR platform to deliver information-rich experiments on the one hand, and on extracting as much information as possible from the obtained experimental data on the other hand. This can be achieved by designing the model-based state and parameter estimators that can provide reliable on-line information about the biological variables and model parameters.

### **Introduction**

Industrial biotechnology processes rely on screening programs for achieving high yields and volumetric productivities, which are crucial to economic viability. High-throughput screening is a feasible approach to identify interesting, refined production strain candidates. However, a significant problem – both in screening and in large scale biotechnological processes – is state estimation. The design of model-based state and parameters estimators that could provide reliable on-line information on the biological variables and model parameters has always been a popular discussion topic. Thus, there is a clear need for systems that enable rapid testing, optimization, control and bioprocess development in low sample volumes, allowing parallel cultivations with limited setup and run-time efforts, both in terms of time and resource consumption, that remain nearly independent of the number of bioreactors. MBR technology with integrated sensors is an adequate solution for rapid, high-throughput, and cost-effective screening. It allows, in principle, continuous measurement and control of various biological parameters, despite the low volumes.

### **Methodology**

Performing experiments at microscale will generate a considerable amount of data, and in the end operating

such a microscale system with multiple functions in parallel will cause difficulties to interpret all generated data using traditional tools such as a spreadsheet program. Therefore, this project will be focused on streamlining the data interpretation. The first part of the work will be based on describing cultivations and biocatalytic processes at microscale by mechanistic models of reactor systems, either based on ordinary differential equations (ODEs) or partial differential equations (PDEs), and will specifically work on the modeling of the enzymatic oxidation of glucose for different operation modes of the reactor model.

Based on an existing Matlab<sup>TM</sup> toolbox developed at DTU, the work will be continued for the further application of uncertainty and sensitivity analysis for this model with the aim to use the analysis results for proposing targeted new experiments in order to collect informative experiments with the experimental microbioreactor set-up using as few experiments as possible.

Furthermore, software sensors have to be developed to extend the number of variables for which on-line information is available. The two chemometric methods principal component analysis (PCA) and partial least squares (PLS) regression are commonly applied together with spectroscopic data and process data, and will be used to predict variables such as biomass

concentration and substrate concentration which are usually difficult to measure on-line.

The last part of the project will be focused on automating experiments, coupling simulations with a model with techniques like Design of Experiments (DoE), Monte Carlo simulation or optimization methods on the one hand, and then transforming results into new experiments that can be performed in a MBR platform.

### Mechanistic model

Modelling of biocatalytic processes has resulted in the development of models with different levels of details such as catalyst, reaction, reactor and process models [2]. In this project the reaction and reactor models have been developed for further implementation in the process model. The operation of the reactor model can be batch, fed-batch or continuous.

The enzymatic reaction of glucose oxidase has been chosen as an initial bioprocess for development of a mechanistic model in the MBR platform. In Figure 1, the transformation of glucose (1) into gluconic acid (2) is shown. The monitoring of the reaction will be possible by the catalyzed decomposition of hydrogen peroxide (3).

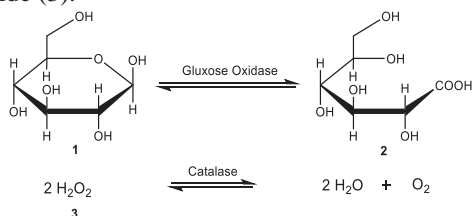
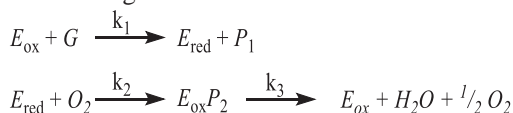


**Figure 1:** Enzymatic reaction of glucose oxidase and catalase.

The specific reaction mechanism forms the basis for the reaction model (mechanistic models). Linek et al. [3] proposed the following sequence of reactions (Scheme 1) for developing a model of the system presented in Figure 1.



*E* - enzyme, *G* - glucose, *P*<sub>1</sub> - gluconolactone, *P*<sub>2</sub> - hydrogen pyroxide

**Scheme 1:** Schematic representation of the enzymatic reaction of glucose oxidase and catalase.

### Simulation data analysis

The kinetic data estimated by Linek et al. [3] was used for the development of the initial model. The following equation represents the overall reaction rate for the majority of proposed glucose oxidase/catalase reaction mechanisms:

$$v = \frac{C_E k_3}{1 + \frac{K_m^O}{C_{O_2}} + \frac{K_m^G}{C_G}}$$

$$C_E = C_{E_{ox}} + C_{E_{red}} + C_{E_{ox}P_2},$$

$$K_m^O = k_3/k_2, \quad K_m^G = k_3/k_1$$

Figure 2 demonstrates the simulation results of the mechanistic model corresponding to the mechanism of Scheme 1.

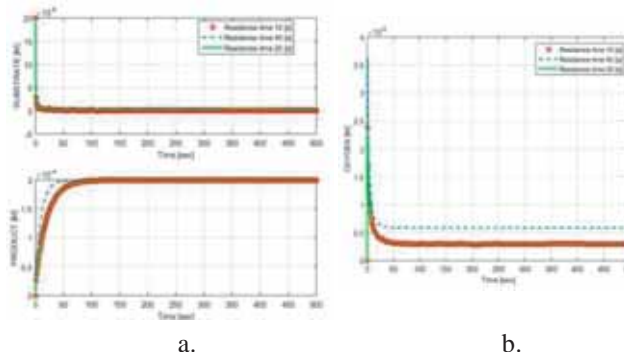


**Figure 2:** Continuous reactor, establishment of substrate, product (a) and oxygen (b) steady state for different residence times.

### Software sensors

The concept ‘software sensor’ associates two terms: a sensor and a software part that could be defined as a hardware and an estimation algorithm respectively (Figure 3). Integration of reliable sensors for relevant bioprocess parameters leads to on-line estimation of the unmeasurable variables and kinetic parameters.

**Figure 3:** Representation of a ‘software sensor’ principle.

The key tools in software sensor design are mathematical models. The model properties settle an appropriate estimation algorithm, and the quality and validity of the model affects the performance of the resulting ‘software sensor’. Usually, mechanistic bioprocess models are based on mass balance equations, which can be used as software sensors [4]. The developed mechanistic model has been implemented for further modelling of bioprocesses in a microfluidic platform with different types of integrated biosensors.

### Acknowledgements

The research project has received funding from the People Programme (Marie Curie Actions) of the European Union's Seventh Framework Programme FP7/2007-2013/ under REA grant agreement n° 608104 (EUROMBR). The article represents only the authors' views and European Union is not liable for any use of the information presented here.

### References

1. Z. Zhang et al., JALA 12 (2007), 143-151.
2. R. L. Fernandes et al., Adv. Biochem. Eng. Biotechnol. 132 (2013), 137-166.
3. V. Linek et al., Biotechnol. Bioeng. 22 (1980), 2515-2527.
4. A. Chéry, J. Biotechnol. 52 (1997), 193-199.

**Aamir Shabbir**

Phone: +45 45256195  
E-mail: aash@kt.dtu.dk  
Discipline: Chemical and Biochemical engineering

Supervisors: Ole Hassager  
Anne Ladegaard Skov

PhD Study  
Started: October 2013  
To be completed: September 2016

## The influence of hydrogen bonding on linear and nonlinear rheology of polymer melts

**Abstract**

Supramolecular polymers are used in many fields as adhesives, coatings, cosmetics and in printing. They indicate that they are very promising for tailoring the appearance of strain hardening. On the other hand, such data is also needed to develop sophisticated multi-scale models that can later be used for predicting the flow behavior and molecular dynamics of supramolecular networks. We investigate rheological properties of well-defined linear supramolecular polymers based on Poly (n-butyl acrylate) (PBA). Systems with varying hydrogen bonding made via hydrolysis of PBA were studied. While systems with moderate degree of hydrolyzation exhibit pure reptation based relaxation in the linear regime, they exhibit significant strain hardening behavior compared to the untreated PBA. Furthermore, at a critical percentage of hydrolyzation, the supramolecular PBA exhibits rubber like characteristics. The extensional rheology experiments were performed on an updated filament stretching rheometer

**Introduction**

Hydrogen bonding is the most employed non-covalent reversible interaction to create supramolecular polymeric assemblies [1]. The dynamics of hydrogen bonded transient networks can be significantly altered by changing the exchange rate between two hydrogen bonding motifs via external stimuli such as temperature. At high temperatures molecular chains can release stress at a fast rate because of decrease of hydrogen bond life time which can lead to low viscosity melts. This remarkable property thus allows easy processing of such materials for various applications [2]. Alternatively, at low temperatures the hydrogen bond life can be significantly larger than the experimental time scales leading to transient networks [3].

Majority of work in the field of hydrogen bonded supramolecular networks exists for small deformations or linear viscoelasticity (LVE) [3,4]. To the best of our knowledge, mostly un-entangled systems have been investigated to study the linear rheological response of hydrogen bonded supramolecular polymers primarily due to the ease of practicality involved with them and importantly such systems offer isolating the dynamics of entanglements from the dynamics of association/disassociation. This however, still leaves out room for the study of entangled hydrogen bonded supramolecular polymer, albeit the complexity

involved. Surprisingly, no literature exists on the non-linear elongational behaviour of such hydrogen bonded supramolecular polymers which provided us the incentive for this research.

**Experimental Details****Materials**

We used pure Polybutyl-n-acrylate (PnBA) and three of its hydrolyzed variants mentioned here in increasing amount of hydrogen bonding content. These include samples: AA6, AA12, AA38. The numbers used in this nomenclature denote the percentage of acrylic acid groups. Pure PnBA was obtained from Polymer source, Inc. and had a polydispersity index, PDI, of 1.38. Hence polydispersity may have an effect on the data reported hereafter, albeit small.

**Non-linear viscoelasticity**

The extensional stress growth coefficient as a function of time was measured by a filament stretching rheometer (DTU-FSR). Measurements were performed at a constant Hencky strain rate imposed at the mid-filament diameter using an online control scheme [5]. All experiments were performed at 21.5°C. The imposed strain rates were varied from  $0.0006\text{s}^{-1}$  to  $1\text{s}^{-1}$ .

## Results

Linear rheology results indicate deviation of terminal power law slopes from 1 and 2 to a slope of 0.5 with the increase of hydrogen bonding.

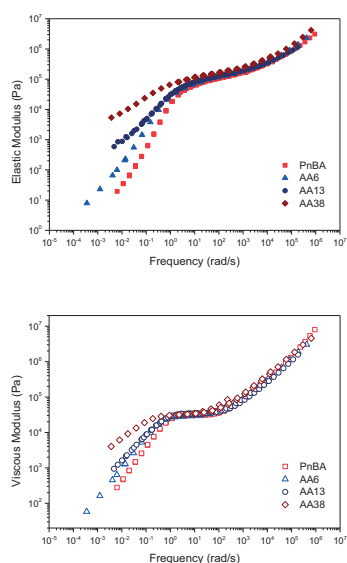


**Figure 1:** LVE master curves for PnBA and its hydrolyzed derivatives.

The non-linear rheology measured using the DTU-FSR is shown in Figure 1. The strain rates increase from right to left in Figure 1. The solid lines represent the LVE envelop obtained from a multi-mode Maxwell fit to the linear rheology data.

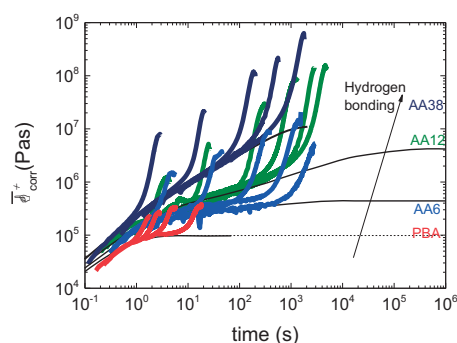


**Figure 2:** Stress growth coefficients at various strain rates for PnBA and its hydrolyzed derivatives as a function of time.

Typically for monodisperse entangled linear melts no deviation from the LVE envelop (often termed as strain hardening) is observed for imposed strain rates less than the inverse of longest relaxation time. However, strain hardening is observed for our samples as evident from Figure 2 despite the fact that the strain rates were well less than the inverse of longest relaxation time. This deviation is attributed to the presence of acrylic acid groups in the hydrolyzed samples thus representing hydrogen bonding. When the stress is plotted as a function of Hencky strain, the curves show a tendency to come closer as opposed to what one

would expect for a pure monodisperse linear melt where each curve is distinct and separated. This is shown in Figure 3. The black line represents the stress prediction of Neo-hookean model.

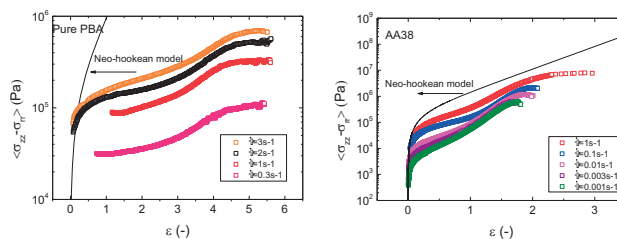


**Figure 3:** Extensional stress as function of Hencky strain at different strain rates for pure PnBA and 38% hydrolyzed PnBA.

## Discussion

We interpret the increase of strain hardening behaviour with increasing acrylic acid group density, as an increase of life time of hydrogen bonds causing more extension of sticky rouse modes thus resulting in an increased strain hardening. This reasoning correlates well to the slope of 0.5 observed in the linear rheology data for AA38. Deviation from Neo-hookean prediction becomes relatively less for hydrolyzed PnBA suggesting that the hydrogen bonds are relatively long lived yet still transient because of absence of a unique stress-strain curve.

## Conclusions

The incorporation of acrylic acid groups resulted in significant increase in strain hardening behaviour of hydrolyzed PnBA melts indicating that the life of hydrogen bonds increases with increasing concentration. These results suggest a potential in utilizing hydrogen bond transient networks in melt rheology to tailor strain hardening behaviour.

## References

1. Nair, Kamlesh P. and Breedveld, Victor and Weck, Marcus 41 (10) (2008) 3429-3438.
2. Yan, Xuzhou and Wang, Feng and Zheng, Bo and Huang, Feihe 41 (18) (2012) 6042-65.
3. Lewis, Christopher L and Stewart, Kathleen and Anthamatten, Mitchell 47 (2014) 729-740.
4. Feldman, Kathleen E. and Kade, Matthew J. and Meijer, E. W. and Hawker, Craig J. and Kramer, Edward J. 42 (22) (2009) 9072-9081.
5. Roman Marin, Jose Manuel and Huusom, Jakob Kj\o bsted and Alvarez, Nicolas Javier and Huang, Qian and Rasmussen, Henrik Koblitz and Bach, Anders and Skov, Anne Ladegaard and Hassager, Ole. 194 (2013) 14-22.

## Acknowledgments

This project is a part of SUPOLEN, funded under the Initial Training Network in the Seventh Framework Marie Curie Program.

**Robert Spann**

Phone: +45 4525 6194  
E-mail: rosp@kt.dtu.dk

Supervisors: Gürkan Sin, DTU  
Krist V. Gernaey, DTU  
Anna Eliasson Lantz, DTU

PhD Study  
Started: August 2015  
To be completed: July 2018

## Bioprocess risk assessment using a mechanistic modelling framework

### Abstract

Process system engineering methods relying on mechanistic models are increasingly applied to control biotechnology manufacturing processes. In this context, it is substantial to quantify the impact of input uncertainties of the model in order to determine e.g. the risk of not achieving the desired product quality. The aim of this PhD project is to develop, apply, and validate a risk assessment method using a mechanistic modelling approach. In particular it will account for uncertainties and non-ideal sensor behavior during a bioprocess. This methodology will feed into a toolbox that will enable effective and rapid development of novel bioactive molecules.

### Introduction

Process system engineering methods relying on mechanistic models are increasingly applied to biotechnology manufacturing processes since process understanding has reached an advanced level. This counts for processes producing small molecules as well as complex biomolecular drugs, e.g. monoclonal antibodies nowadays. However, proof of reliability of the models by using tools like identifiability, uncertainty, and sensitivity analysis are often missing [1]. Instead, it is assumed that model parameter values are known exactly, although these are estimated from experimental data, which include considerable measurement errors. Mechanistic models consequently contain a certain degree of subjective uncertainties in input and kinetic parameters that directly affect output uncertainties. Bioprocess risk assessment takes uncertainties into account in order to predict a probability distribution function of the output parameters, e.g. product concentration. It provides proof of the quality of the model prediction and allows risk-based decision making for bioprocess development, optimization, and control [2]. In addition, sensitivity analysis provides important information about which input parameters are most responsible for output uncertainties and is therefore used to optimize analytical effort and to apply sensor equipment purposefully. Hence risk assessment is an essential method for bioprocess modelling.

### Specific Objectives

The objective of this PhD study is a risk based methodology based on mechanistic, first principle modelling for the evaluation of product attributes, which is validated on an industrial case study.

In principle, the PhD project include several tasks of a model-based approach for PAT system design from problem definition, model development, PAT system design, and evaluation using uncertainty analysis to validation in industrial scale [3, 4]. This general methodology will be transferred to a biological process. Providing more details, the PhD project will perform the following steps systematically (see figure 1): Once a bioprocess and target attributes are determined, a model-based computer-aided framework for a monitoring and analysis system (PAT system) including a control strategy will be designed. Here, the objective of the process control system and the available measurements of the production scale process are taken into account. Most likely a first principle kinetic models is developed and applied. Nevertheless, available metabolic models are taken into account and applied, especially if they lead to a reduction of the degree of freedom. Second, the designed process control system is evaluated using uncertainty and sensitivity analyses. Variations in the most important model parameters will be evaluated on the basis of a series of experimental data and experts' opinions. Likewise, detailed characterization of sensors and actuators in lab- as well as pilot-scale fermentations will be performed. Moreover, non-ideal behavior will be incorporated in the model library. These variations will then be

implemented in the design and evaluated using uncertainty and sensitivity analyses, resulting in a distribution of the outputs, e.g. product concentration. The engineering standard Monte Carlo procedure will be applied for uncertainty analysis because it is computationally effective and reliable [5]. Sensitivity analysis is crucial since it reveals which input parameters explain most of the variance in model predictions [2, 6]. Such acquired distribution will then be evaluated and interpreted to calculate the risk of not obtaining the required product quality. Finally, the designed and robust process control system, which takes the uncertainties into account, will be validated on an industrial case study. The outcome will be a validated model-based process control system.

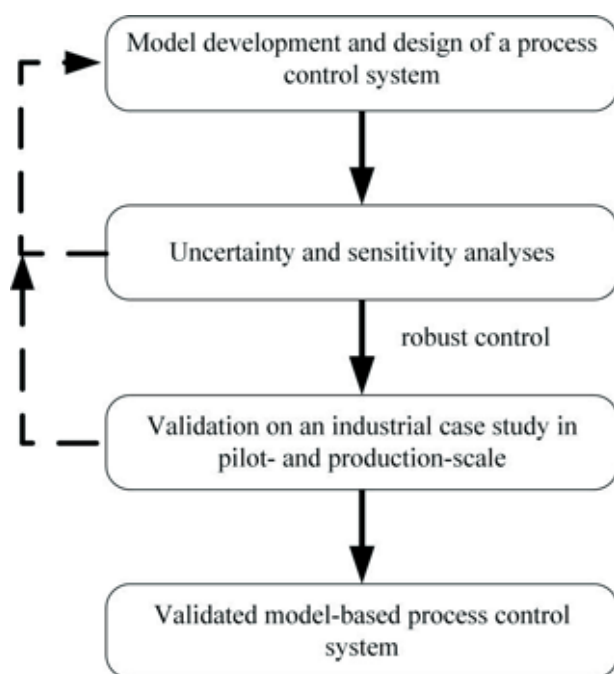


**Figure 1:** Tasks of the project. First, the bioprocess model including the process control system is designed. Then uncertainty and sensitivity analyses are performed. Finally, the robust system is validated on an industrial case study.

Demonstration on industrial scale is challenging due to a greater complexity of the system and the fact that less data is available compared to lab- and pilot-scale. However, it is indispensable in order to rise knowledge to the level of market production. Results from this systematic approach will have significant influence on decision-making because they provide reliable and robust data even in large scale.

### Conclusion

This PhD project will provide a risk based methodology based on mechanistic, first principle modelling for the evaluation of product attributes in bioprocess engineering. It is part of the Marie Skłodowska-Curie Innovative Training Network “BioRapid” in the Horizon 2020 programme of the European Commission.

The network will create screening, development, scale-up, monitoring, and modelling methods, which will be applicable to bioprocess development as demonstrated by validation on a range of relevant bioactive molecules. The presented PhD project will feed the bioprocess risk assessment approach into the BioRapid methodology toolbox that will enable effective and rapid bioprocess development.

### Acknowledgement

This project has received funding from the European Union’s Horizon 2020 research and innovation programme under the Marie Skłodowska-Curie grant agreement No 643056.

Web-link: <http://www.bio-rapid.com/>



### References

1. R. L. Fernandes, V. K. Bodla, M. Carlquist, A.-L. Heins, A. E. Lantz, G. Sin, K. V. Gernaey, *Adv. Biochem. Eng. Biotechnol.* 123 (2012) 137-166.
2. G. Sin, K. V. Gernaey, A. E. Lantz, *Biotechnol. Prog.* 25 (4) (2009) 1043-1053.
3. R. Singh, K. V. Gernaey, R. Gani, *Comput. Chem. Eng.* 33(1) (2009) 22-42.
4. N. A. F. A. Samad, G. Sin, K. V. Gernaey, R. Gani, *Comput. Chem. Eng.* 54 (2013) 8-23.
5. J. C. Helton, F. J. Davis, *Reliab. Eng. Syst. Saf.* 81 (1) (2003) 23-69.
6. A. Saltelli, M. Ratto, S. Tarantola, F. Campolongo, *Reliab. Eng. Syst. Saf.* 91 (10–11) (2006) 1109-1125.



## Magnus Zingler Stummann

Phone: +45 4525 2957  
E-mail: mazi@kt.dtu.dk  
Discipline: Catalysis and Reaction Engineering

Supervisors: Anker Degn Jensen, DTU-KT  
Martin Høj, DTU-KT  
Peter Arendt Jensen, DTU-KT  
Jostein Gabrielsen, Haldor Topsøe A/S

PhD Study  
Started: October 2015  
To be completed: October 2018

## Hydrogen assisted catalytic biomass pyrolysis for green fuels

### Abstract

Catalytic hydropyrolysis of biomass is a promising technology for production of sustainable liquid fuels. This project targets the development of new catalysts and improved understanding of the process. A catalytic hydropyrolysis pilot plant is currently under construction and will soon be used for screening of suitable catalysts and operating conditions. The project is part of the project “H<sub>2</sub>CAP – Hydrogen assisted catalytic biomass pyrolysis for green fuels”.

### Introduction

The world’s energy consumption continues to increase because of our way of living and the increasing world population [1,2]. The transportation sector consumes one fifth of the total energy consumption [3]. Currently transportation fuels are mainly produced from crude oil, however, these reserves are depleting and the need for alternative fuels increases [4]. In order to decrease the CO<sub>2</sub> emission future fuels must come from renewable energy sources [5].

During the last years there has been an increasing interest in converting biomass to liquid fuels. Biomass can be converted to bio-oil by rapidly heating the biomass to 400-500 °C in an inert atmosphere [6]. Unfortunately, the properties of bio-oil are very different from crude oil, due to high oxygen and water content in the bio-oil. The bio-oil is unstable and has a heating value approximately half the heating value of crude oil and further hydroprocessing of the bio-oil is necessary, if it shall be used as a transportation fuel [7]. However, since the bio-oil is very reactive, rapid catalyst deactivation, because of coking, is common [7]. Recent research has shown that conducting the pyrolysis in a hydrogen atmosphere at elevated pressure instead of using an inert atmosphere can significantly improve the properties of the bio-oil, thus making the further upgrading much easier [8]. Despite the fact that catalytic hydropyrolysis is a promising technology, only few articles have been published within this field and further research is needed.

As a result, DTU Chemical Engineering, DTU Mechanical Engineering, Karlsruhe Institute of Technology, Stanford, and Haldor Topsøe A/S are collaborating on the development of hydrogen assisted

catalytic biomass pyrolysis followed by hydrodeoxygenation (HDO). The PhD projects within this project concerns improved understanding of HDO by using model components, development of new HDO catalysts (Trine Marie Hartmann Arndal at CHEC, pg. 15-16), and catalytic hydropyrolysis of real biomass in a new pressurized set up (present project).

### Specific Objectives

The main objective is to prove that it is possible to produce a high quality liquid fuel through catalytic hydropyrolysis. Furthermore it is desired to develop new sustainable catalysts for fluid bed hydropyrolysis, determine the optimal conditions for this process, and improve our understanding of the process. This will be done through mainly experimental investigations of the catalytic hydropyrolysis using well-defined condition and real biomass. A considerable part of the project will also be to investigate further upgrading of the produced bio-oil in a fixed bed reactor. The project objectives cover:

- Literature survey of pyrolysis and catalytic hydropyrolysis of biomass. Since further upgrading of the produced bio-oil is a part of the project, literature regarding HDO of bio-oil will also be studied.
- Starting up and commissioning of bench scale equipment for catalytic hydropyrolysis in a fluid bed reactor with a downstream fixed bed HDO reactor, currently under construction.
- Synthesis and characterization of hydropyrolysis catalysts suitable for fluid bed operation.

- Performing an experimental investigation of hydrolysis of different biomass sources with systematic variation of process parameters.
- Performing detailed physical and chemical analysis of bio-oil products using e.g. elemental analyzer and GC-MS.

## Results and Discussion

The experimental work will be conducted on the new H<sub>2</sub>CAP unit. The process diagram for the pilot plant is very similar to the desired process diagram for the industrial process, shown in Figure 1. Biomass is shredded and fed to a fluid bed reactor (hydrolysis reactor), where it is degraded to gas, vapor, and char. The reactive oxygen-containing hydrocarbons are hydrogenated in the fluid bed reactor, while the more stable oxygen containing hydrocarbons, such as dibenzofuran, are hydrogenated in the HDO reactor. In the H<sub>2</sub>CAP setup the char is removed by a filter, but in the final process it is desired to remove it by cyclones. H<sub>2</sub> will be supplied by reforming of light gases followed by water gas shift (WGS), and/or water electrolysis in the final process. With this process it will be possible to save more than 90 % on the greenhouse gas emission compared to when using crude oil [9].

The H<sub>2</sub>CAP unit is planned to be ready at the end of February 2016 at which the commissioning phase will begin. There is only limited information in the open literature regarding catalysts for the catalytic hydrolysis. Since biomass contains sulfur a sulfide based catalyst would be ideal for the hydrolysis, because it otherwise might be poisoned by sulfur. The catalyst should also have a high mechanical strength in order to limit attrition in the fluid bed and it should have a low acidity, which will avoid undesirable cracking of the vapors. It is therefore very likely that NiS, NiMoS, or CoMoS will be used as the active phase and a strong carrier such as MgAl<sub>2</sub>O<sub>3</sub> spinel will be used in the initial tests.

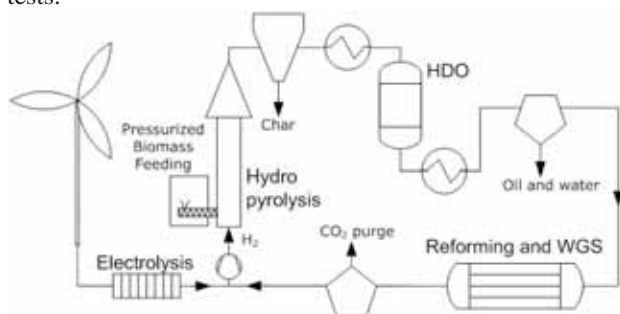


**Figure 1:** H<sub>2</sub>CAP process diagram including catalytic hydrolysis, char separation, temperature adjustment, deep HDO, liquid separation, pyrolysis gas reforming, and water gas shift. Additional hydrogen is obtained from water electrolysis.

## Conclusion

Biomass conversion to liquid fuel by pyrolysis and HDO is a challenging process, and catalytic hydrolysis can be a sustainable alternative, which will make it possible to significantly lower the greenhouse gas emission. More research regarding catalytic hydrolysis is needed and the H<sub>2</sub>CAP unit can be used to find new catalysts and more optimal process conditions. Future work will include the startup of the H<sub>2</sub>CAP unit and testing several different sulfide catalysts in the fluid bed reactor.

## Acknowledgements

This work is part of the Combustion and Harmful Emission Control (CHEC) research center at the Department of Chemical and Biochemical Engineering at DTU. The project is funded by the Danish Council for Strategic Research (project 1305-00015B), The Programme Commission on Sustainable Energy and Environment.

## References

1. U. S. Energy Information Administration, Annual Energy Outlook 2015 with projections to 2040, 2015.
2. ESA, World Population Prospects, The 2015 Revision, 2015.
3. B. van Ruijven and D. P. van Vuuren, *Energ Policy* 37 (11) (2009) 4797–4808.
4. S. Sorrell, J. Speirs, R. Bentley, A. Brandt, R. Miller, *Energ Policy* 38 (9) (2010) 5290–5295.
5. R. K. Pachauri, L. Meyer, J.-P. Van Ypersele, S. Brinkman, L. Van Kesteren, N. Leprince-Ringuet, and F. Van Boxmeer, *Climate Change 2014 Synthesis Report*. 2014.
6. A. V. Bridgwater, *Biomass Bioenerg* 38 (2012) 68–94.
7. P. M. Mortensen, J.-D. Grunwaldt, P. A. Jensen, K. G. Knudsen, A. D. Jensen, *Appl. Catal. A Gen.* 407 (1–2) (2011) 1–19.
8. M. Linck, L. Felix, T. Marker, M. Roberts, *Wiley Interdiscip. Rev. Energy Environ.* 3 (2014) 575–581.
9. E. Maleche, R. Glaser, T. Marker, *Environ. Prog. Sustain. Energy* 33 (1) (2013) 322–329.

**Tannaz Tajssoleiman**

Phone: +45 4525 2986  
E-mail: tantaj@kt.dtu.dk

Supervisors: Ulrich Krühne  
Krist V. Gernaey  
Jakob Kjøbsted Huusom

PhD Study  
Started: August 2015  
To be completed: August 2018

## Automating experimentation in miniaturized reactors

### Abstract

In the present agile society, pharmaceutical and biotech industries face growing pressure to reduce development costs and accelerate process development. This is a major challenge, especially in view of the need for increasing upstream experimentations to support the quality of final products and the necessity of having predictive models from biological systems. Microscale bioreactors, which can be applied as high throughput processes, not only provide the possibility of studying multiple reactions in parallel but also bring great improvement in functionality and performance. This project aims at developing the next generation of high throughput screening methodologies which can be applied in biological processes. Subsequently, optimal experimental design (OED), mainly based on mechanistic models and automated experimentation in microscale, will be developed on a recombinant yeast model system and then validated on industrial case studies.

### Introduction

During the last decade, the application of commercial scale biotechnological production processes has seen a significant growth, for example in the pharmaceutical industry. In this perspective, competitive forces drive companies to design robust, efficient and economic processes in order to reach high quality products within the shortest possible process time. The focus on cost control applies not only to manufacturing but also to the process development phase where significant numbers of costly experiments are needed. The development of several different types of micro-bioreactors (MBR) has delivered a promising response to the need for developing low cost experimental techniques suitable for high-throughput application. Moreover, MBR technology with integrated sensors can offer a high level of control of reaction conditions during high throughput screening (HTS) processes [1].

The goal of this project is to develop the next generation of HTS methodologies based on optimal experimental design (OED). Therewith, the focus is mainly on the development and use of miniaturized reactor systems that allow running a fermentation process by consistent use of batch or fed-batch principles in micro to milliliter scale. Accordingly, the project is divided into three general phases: (1) investigation of a common type of enzymatic biosensor and finding its optimum design; (2) automation and optimization of the target process in lab

scale; (3) scale up of the model and apply the optimization routine in an industrial case study.

### 1. Enzymatic biosensor:

Biosensor technology is a developing area of innovative approaches to analyze and monitor various bio-based production processes. A biosensor converts the physical or chemical properties of a system, such as the analyte concentration, into an electrical signal. In biosensors, a bioactive substance (typically an enzyme, multi-enzyme system, antibody, membrane component, or microorganism) plays often the main role for recognizing the desired species by contact with a suitable transducing system [2]. The substrate specificity of enzymes can increase the selectivity of sensors, especially in the case low ranges of substrates concentration [3]. The selectivity potential of glucose oxidase (GOx) was initially shown by Clark and Lyons in their enzyme electrodes biosensor [4].

In view of the growing biotechnology sector and the increasing need of screening processes, developing more accurate and sensitive biosensors has been a main concern for researchers, and has resulted in three generations of glucose biosensors. The first generation of glucose biosensors relies on oxygen consumption in the biocatalytic reaction 1 and detection of hydrogen peroxide through the second reaction:





The amperometric (anodic) measurements of peroxide formation can then be used as a measure of the glucose concentration in the electrolyte [5]. Further improvements were obtained in the second generation by replacing the use of oxygen with a non-physiological electron acceptor (mediator) capable of shuttling electrons from the redox center of the enzyme to the surface of the electrode, which is illustrated in Figure 1.

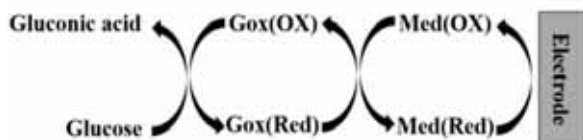


**Figure 1:** Sequence of events that occur in mediator-based glucose biosensors.

The reduced mediator is reoxidized at the electrode to its oxidized form which gives a current signal proportional to the glucose concentration. In this generation, measurements become largely independent of oxygen partial pressure and the needed potential at electrodes is decreased [6]. In the latest generation, shown in Figure 2, direct electron transfer between enzyme and electrodes happens within a low operating potential, close to the redox potential of the enzyme [7].

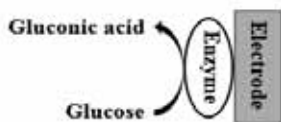


**Figure 2:** Sequence of events that occur in the third generation of glucose biosensors.

The aim of this part of the project is to find the optimum design of the biosensor that is illustrated in Figure 3, by using mathematical modelling and computational fluid dynamics (CFD) simulation of the glucose oxidase reaction in this device.

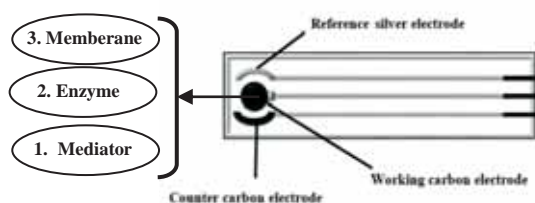


**Figure 3.** Sequence of layers in the glucose oxidase biosensor with membrane of Nafion 117 and Prussian blue as the mediator.

Afterwards, the developed model and the related simulation can be used for other types of enzymatic biosensors such as pyruvate oxidase in order to predict the process state in the biosensor and subsequently, the response of it at different conditions.

## 2. Lab scale automation and optimization

The main focus of this phase is to find a robust OED methodology, based on a mechanistic model of a biological system, and enabling to automate the experimentation in microscale by using the presented biosensors. For this purpose, initially a standard Design of Experiments (DoE) will be carried out and tested in a

miniaturized reactor system, where a proposed series of experiments will be analyzed with automated data interpretation before the next experiment is carried out. Finally, the experimental data will be used to support model calibration and validation which is included in the optimization routine.

## 3. Scale up and industrial scale validation

The final step in this project is to scale up the model and apply the optimization routine for an industrial case study to investigate the accuracy of the results and robustness of the methodology at large scale. Furthermore, in this phase the capability of the biosensor resulting from the 1<sup>st</sup> project phase can be examined to reach the optimum design for a reliable industrial biosensor.

## Acknowledgements

The research project has received funding from the People Program (Marie Curie Actions) of the European Union's Seventh Framework under grant agreement n°643056.

## References

- Battersby, B.J. and M. Trau, Novel miniaturized systems in high-throughput screening. *Trends in biotechnology*, 2002. **20**(4): p. 167-173.
- Frew, J.E. and H.A.O. Hill, Electrochemical biosensors. *Analytical chemistry*, 1987. **59**(15): p. 933A-944A.
- Carr, P.W. and L.D. Bowers, Immobilized enzymes in analytical and clinical chemistry. 1980: Wiley.
- Clark, L.C. and C. Lyons, Electrode systems for continuous monitoring in cardiovascular surgery. *Annals of the New York Academy of sciences*, 1962. **102**(1): p. 29-45.
- Wang, J., Electrochemical glucose biosensors. *Chemical reviews*, 2008. **108**(2): p. 814-825.
- Cass, A.E., Davis, G., Francis, G.D., Hill, H.A., Aston, W.J, Higgins, I.J., Plotkin, E.V., Scott, L.D., Turner, A.P., Ferrocene-mediated enzyme electrode for amperometric determination of glucose. *Analytical chemistry*, 1984. **56**(4): p. 667-671.
- Ghindilis, A.L., P. Atanasov, and E. Wilkins, Enzyme-catalyzed direct electron transfer: Fundamentals and analytical applications. *Electroanalysis*, 1997. **9**(9): p. 661-674.



**Tobias Pape Thomsen**

Phone: +45 2235 4425  
 E-mail: ttho@kt.dtu.dk

Supervisors: Jesper Ahrenfeldt, DTU KT  
 Ulrik B. Henriksen, DTU KT  
 Henrik Hauggaard-Nielsen, RUC  
 Jens Kai Holm, DONG Energy

PhD Study  
 Started: September 2013  
 To be completed: December 2016

## Low Temperature Thermal Gasification of marginal biomass and waste resources – coproduction of energy and fertilizer

### Abstract

This work involves identification and characterization of new fuels for low temperature gasification and examines the potential for combined energy and fertilizer production in such systems. The project includes development of a procedure for screening of new fuels as well as investigations of the influence of fuel characteristics and the design of the thermal conversion platform on ash and char quality in relation to its use as fertilizer and soil enhancer.

### Introduction

The global biomass resources are limited, and especially the high quality biomass resources – i.e. woody biomasses, are stressed by increased utilization in small and large scale energy and material systems around the world. This limits substitution of fossil fuels with renewable biomass, and to increase the substitution further new conversion systems need to be introduced that converts biomass resources of lower quality.

The Low Temperature Circulating Fluidized Bed (LT-CFB) Gasifier is such a system. A simple process diagram of the process is provided in Figure 1 below.

based co-firing systems. After treatment in the LT-CFB gasifier, more than 95% of the energy potential and below 5% of the inorganics of the fuel are present in a hot, combustible gas product. The remaining 5% of the energy potential is left as residual carbon along with 95% of the inorganics in the solid fraction extracted from the bottom of the secondary cyclone. The gas product is used to substitute coal in large scale utility boilers and the solid product is applicable as ash fertilizer and soil enhancer [1]–[3]. An illustration of integration of LT-CFB gasification and existing coal based power plant infrastructure is provided in Figure 2.

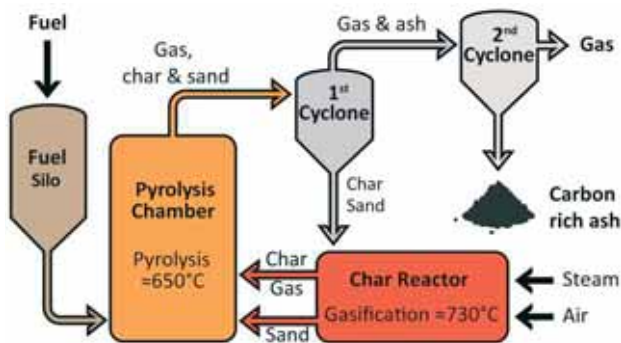


**Figure 1:** Process diagram of the LT-CFB gasification process.

The LT-CFB technology is highly fuel flexible, robust and relatively inexpensive [1].

The current commercial application of the LT-CFB gasification technology is as pretreatment and thermal separation unit for biomass and waste fuels in coal-

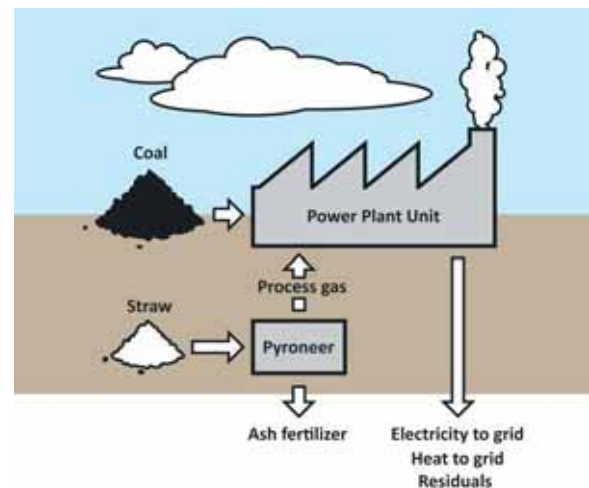


**Figure 2:** Illustration of the integration of LT-CFB gasifiers and existing coal-based power plant infrastructure.

### Specific Objectives

A pilot LT-CFB facility with a thermal feed capacity of 100 kW is used within the project to produce ashes for subsequent characterization. Experimental campaigns have also included incineration and pyrolysis platforms, and it is a goal of the project to determine key correlations between fuel characteristics and plant design on one hand and ash quality and overall system performance on the other. The project consists of the following stages:

- An initial fuel screening and selection process involving an assessment of key fuel and ash characteristics in LT-CFB systems
- An investigation into correlations between fuel ash composition and key ash and char characteristics in LT-CFB systems
- An assessment of the influence of the design of the thermal system on char and ash phosphorous characteristics. Fuel: Dry sewage sludge
- An assessment of the influence of the design of the thermal system on system performance and overall level of long-term sustainability. Fuel: Dry sewage sludge

### Results and Discussion

So far, the published results from the project are related to the findings of the fuel screening process. The focus of this part of the work was on development of a suitable, fast and easy-to-apply screening method and the subsequent identification and characterization of multiple new marginal biomass resources. The assessment included 4 references, 9 residues from vegetable production, 4 residues from animal production and 5 sludge- and waste fractions. The technical assessment was conducted by comparing the results from a series of physical-mechanical and thermochemical experiments to those of already proven references, and the results were supplemented by an evaluation of practical application and overall energy balance.

The assessment yielded a long list of results including the following:

- Bulk energy density per weight and volume
- Energy use for transport, drying and grinding
- Fuel proximate composition
- Char reactivity in reducing atmosphere, 750 °C
- The ratio between energy content in char and volatiles from pyrolysis
- Agglomeration/char-sticking issues in pyrolysis at 650 °C
- Ash sintering issues in steam/air at 750 °C
- Ash volatilization at 750 °C
- Char and ash densities
- Potential production of electricity and heat from the thermal conversion system (including power plant block)

Based on the screening, many fuels were identified as suitable potential candidates for LT-CFB conversion, and sewage sludge from municipal waste water treatment was selected for subsequent conversion in a Cross Platform Sludge Experiment (CPSE). This fuel was selected for its global perspective within three important selection criteria - energy potential, fertilizer potential and waste issues/price. CPSE involved pilot scale conversion of a well-defined municipal sewage sludge sample in a range of different low-temperature thermal systems involving two different gasifiers, an incineration facility and two pyrolysis processes. The next part of this campaign involves identification of relations between process ash phosphorous plant-availability (fertilizer quality) and the process design.

In addition to the already published results and the work conducted on the CPSE campaign, focus has been on the assessment of potential correlations between fuel ash composition and key fuel characteristics in LT-CFB systems.

### Conclusions

Low temperature gasification has a strong potential to co-produce electricity, heat and fertilizer from marginal biomass resources unsuitable for conversion in most other thermal conversion systems. An initial fuel screening process has identified numerous promising new fuels for the platform, and municipal sewage sludge has been selected for subsequent cross platform pilot scale testing, product characterization and system assessment.

### Acknowledgements

I would like to acknowledge Energistyrelsen and the EUDP project funding as well as all project partners for realizing the project. I would also like to thank everyone contributing to the work with the fuel screening, ash and char characterization and cross platform sludge experiment.

### References

1. J. Ahrenfeldt, T. P. Thomsen, U. Henriksen, and L. R. Clausen, *Appl. Therm. Eng.*, 50 (2) (2013) 1407–1417.
2. R. G. Nielsen, *Optimering af Lav Temperatur Cirkulerende Fluid Bed forgasningsprocessen til biomasse med højt askeindhold*, DTU, 2007.
3. K. Kuligowski, *Utilization of ash from thermal gasification of pig manure as p-fertilizer and soil amendment*, Aalborg University, 2009.

### List of Publications

1. T. P. Thomsen, G. Ravenni, J. K. Holm, J. Ahrenfeldt, H. Hauggaard-Nielsen, U. B. Henriksen, *Screening New Marginal Biomass and Waste Resources for Low Temperature Gasification – Method Development and Application*, *Biomass Bioenerg* 79 (2015) pp. 128-144



## Asbjørn Toftgaard Pedersen

Phone: +45 4525 2992  
E-mail: [astp@kt.dtu.dk](mailto:astp@kt.dtu.dk)

Supervisors: John M. Woodley  
Ulrich Krühne  
Gustav Rehn

PhD Study  
Started: April 2014  
To be completed: March 2017

## Biooxidation – Reactor and process design

### Abstract

Oxidation reactions are a cornerstone in the fine chemical industry, but the reactions often suffer from low selectivity and excessive waste generation. Biocatalysis can potentially solve these problems, however, it requires that the technology is developed further to ensure industrially relevant product concentration, yield and productivity. This PhD project investigates how process and reaction engineering principles can help to solve the challenges encountered in oxidative biocatalysis.

### Introduction

Oxidation reactions are a key part of organic chemistry, and perhaps the most frequently employed reaction type in the chemical industry. Oxidation reactions enable the formation of important functional groups such as alcohols, aldehydes, epoxides and carboxylic acids, from which various other functionalities can be incorporated to produce the compound of interest. Traditionally the oxidation chemistry is conducted with stoichiometric amounts of transition metal based oxidants (e.g. permanganate and dichromate) in the fine chemical industry. These processes often generate large amounts of waste, and most often require chlorinated organic solvents. Much work have been carried out to develop metal catalysts that enable highly selective oxidation using simple oxidants such as  $O_2$  or  $H_2O_2$ , however, there are still significant requirements for improvements in order to develop processes complying with the principles of green chemistry [1].

Biocatalytic oxidation (biooxidation) can potentially solve many of the problems encountered with traditional oxidation methods, as enzymes offer high regio- and stereoselectivity and high turnover rates at mild reaction conditions using simple oxidants [2]. Industrial applications of biooxidation do exist, but are limited to few specialty chemicals employing mainly whole-cell biocatalysis (growing or resting cells) [3]. A reason for the low level of industrial implementation is the complexity of biooxidation reactions, which primarily arise from the requirement to molecular oxygen. Traditionally, bioreactors are aerated by sparging the reactor with air. However, oxygen is poorly soluble in

water, which results in a low driving force for mass transfer from the gas to liquid. The productivity of reactions requiring available oxygen in the liquid phase is therefore typically limited by the amount of oxygen that can be transferred to the liquid phase. A further complication created by the requirements to oxygen is enzyme deactivation accelerated by the presence of a gas-liquid interfaces. Not all enzymes experience such deactivation, but many industrially relevant enzymes do [4]. The stability is further challenged by the need for processing unnatural substrates, which typically are both inhibitory to the enzymes and increase deactivation. In addition to the above mentioned drawbacks, aeration also can cause significant substrate and/or product losses due to stripping, depending on the solubility of the compounds in the reaction media.

This PhD project investigates how process and reaction engineering principles can improve the productivity of alcohol synthesis and transformation using oxygen dependent enzymes. This is done via two case studies (Figure 1); galactose oxidase catalyzed oxidation of benzyl alcohol to benzaldehyde[5] and P450 catalyzed  $\omega$ -hydroxylation of myristic acid.

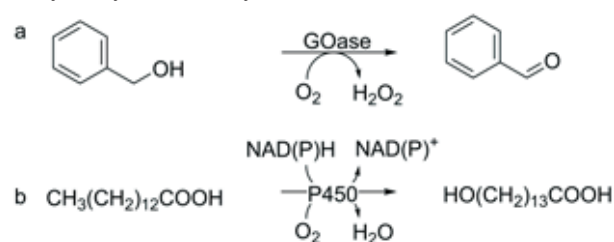


**Figure 1:** Case studies using two enzymes galactose oxidase (a) and cytochrome P450 (b).

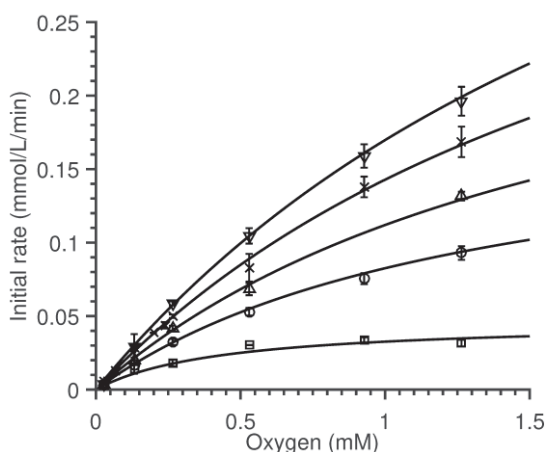


**Figure 2:** Initial rate data at five different alcohol substrate concentrations: ( $\square$ ) 5 mM, ( $\circ$ ) 25 mM, ( $\Delta$ ) 50 mM, ( $\times$ ) 100 mM, ( $\nabla$ ) 200 mM. Line: For of model for ping-pong mechanism with substrate activation.  $K_{mO} = 2.7$  mM.

### Oxygen transfer in relation to kinetic requirements

Transfer of oxygen to the reaction media is essential for developing a successful biooxidation process, since the transfer of oxygen often becomes the bottleneck when intensifying reactions to industrially relevant space-time yields. The oxygen transfer rate is determined by the volumetric mass transfer coefficient ( $k_L a$ ), the oxygen solubility in the reaction media and the concentration of oxygen in solution. The lower the concentration in solution the higher oxygen transfer rate. However, the enzymes requires oxygen as electron acceptor, and as for other substrates the rate of reaction is determined by the concentration experienced by the enzyme up to a certain point at which the active site of the enzyme is saturated. The concentration at which the enzyme is 50% saturated is called the Michaelis-Menten constant,  $K_m$ , for the given substrate.  $K_m$  for oxygen ( $K_{mO}$ ) varies significantly from enzyme to enzyme, and can most likely be ascribed to the origin of the enzyme. If an enzyme is of intra-cellular origin, the  $K_{mO}$  is relatively low due to the evolutionary pressure caused by the competition for oxygen with other enzymes combined with low oxygen availability. Whereas an extra-cellular enzyme, such as many oxidases, typically has a higher  $K_{mO}$  due to the evolution in an environment with excess oxygen and hence lower evolutionary pressure.

Determination of two-substrate enzyme kinetics is typically done by recording initial rate data keeping one substrate constant, and varying the other, as seen in Figure 2 for the case of galactose oxidase catalyzed oxidation of benzyl alcohol to benzaldehyde. The  $K_{mO}$  for galactose oxidase was determined to 2.7 mM. This is 10 times the solubility of oxygen in water, which is 0.268 mM when applying air for aeration at 25 °C. In other words, this means that reaction rate is almost linearly dependent on the oxygen concentration at normal operating conditions. Furthermore, this implies that the process should be designed to operate with as high an oxygen concentration as possible in order to

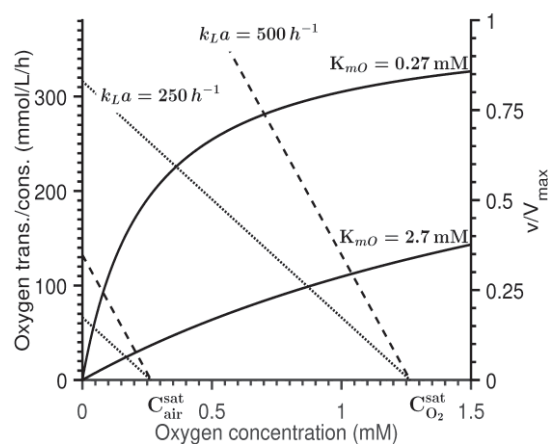


**Figure 3:** Illustration of the importance of  $K_{mO}$  to the rate of reaction as a function of dissolved oxygen concentration (solid lines), and the influence of dissolved oxygen concentration on the oxygen transfer rate (dashed lines) when using air or pure oxygen for aeration.

reduce the amount of the enzyme required. However, a high oxygen concentration will limit the amount of oxygen that can be transferred, and hence the maximum volumetric productivity. This is illustrated in Figure 3, where the oxygen transfer/consumption rate is plotted as a function of oxygen concentration. It is clearly seen that an enzyme with a high  $K_{mO}$  (e.g. 2.7 mM) will be significantly slower and operate at a much lower efficiency (percentage of maximum rate if saturated with oxygen,  $v/V_{max}$ ), than an enzyme with a medium  $K_{mO}$  (e.g. 0.27 mM), and even if pure air is used for aeration the enzyme efficiency will be low.

The importance of  $K_{mO}$  encourages further evolution of galactose oxidase in order to reduce the  $K_{mO}$ . This requires novel screening techniques under reduced oxygen concentrations, which will be pursued through collaboration with partners within the EU project BIOOX [6]. Additionally, evaluation of other oxygen transfer methods, such as sparging with oxygen enriched air, must be performed in order to assess when such options are feasible.

### Acknowledgements

The research leading to these results has received funding from the European Union's Seventh Framework Programme for research, technological development and demonstration under grant agreement n° 613849.

### References

1. T. Punniyamurthy, S. Velusamy, J. Iqbal, Chem. Rev. 105 (2005) 2329-2363.
2. N. Turner, Chem. Rev. 111 (2011) 4073-4087.
3. A. Liese, K. Seelbach, A. Buchholz, J. Haberland, in: A. Liese, K. Seelbach, C. Wandrey (Eds.), Industrial Biotransformations, Wiley-VCH Verlag, Weinheim, 2006, p. 148.
4. A. Bommarius, A. Karau, Biotechnol. Prog. 21 (2005) 1663-1672.
5. A. Toftgaard Pedersen, W. Birmingham, G. Rehn, S.J. Charnock, N.J. Turner, J.M. Woodley, Org. Process Res. Dev. (2015)
6. www.BIOOX.eu

**Anjan Kumar Tula**

Phone: +45 4525 2817  
E-mail: antu@kt.dtu.dk

Supervisors: Prof. Rafiqul Gani  
Gurkan Sin

PhD Study  
Started: December 2013  
To be completed: December 2016

## Process synthesis and design using process group contribution methodology

### Abstract

Process synthesis can be considered as the cornerstone of the process design activity which involves investigation of chemical reactions needed to produce the desired product, selection of the separation techniques needed for downstream processing, as well as making decisions on sequencing the involved reaction and separation operations. This work highlights the development of computer aided methodology for fast, reliable and consistent generation of process flowsheets and rank them based on various flowsheet performance indices. The methodology is based on the group contribution principles to solve the synthesis-design problem of chemical processes, where, chemical process flowsheets could be synthesized in the same way as atoms or groups of atoms are synthesized to form molecules in computer aided molecular design (CAMD) techniques. As in CAMD the generated molecules are quickly evaluated with respect to target molecular properties using GC property models, the generated flowsheet alternatives are also evaluated for properties like energy consumption, atom efficiency, environmental impact, etc.

### Introduction

In a group contribution method [1] for estimating pure component/mixture properties of a molecule, the molecular identity is described by means of a set of functional groups of atoms bonded together to form a molecular structure. Once the molecular chemical structure is uniquely represented by the functional groups, the specific properties can be estimated from regressed contributions of the functional groups representing the molecule. Having the groups, their contributions and their interactions together with governing rules to combine the groups into a molecule, allows us to synthesize molecules and/or mixtures. This is known as CAMD, computer aided molecular design. Let us now imagine that each group used to represent a fraction of a molecule could also be used to represent a chemical process operation or a set of operations in a chemical process flowsheet. A functional process-group would represent either a unit operation (such as a reactor, or a distillation column), or a set of unit operations (such as, two distillation columns in extractive distillation). The bonds among the process-groups represent the streams connecting the unit operations, similar to the bonds combining (molecular) functional groups. In the same way as CAMD method applies connectivity rules to combine the molecular functional groups to form feasible molecular structures, functional process-groups would have connectivity rules

to combine process-groups to form structurally feasible process alternatives. Finally with flowsheet property model and corresponding process-group contributions it would be possible to predict various flowsheet properties which can be used as performance indicators for screening of alternatives.

### Objective

The research conducted in this field is primarily within the field of process systems engineering (PSE). The main objective of this work is to develop generic framework and its corresponding computer-aided tool to systematically solve process synthesis and design problems. The framework should be able to

- Generate all feasible process flow-sheets for a given problem so as to identify novel/innovative solutions.
- To rapidly, efficiently and reliably evaluate the generated alternatives.
- To perform detailed design and analysis of promising alternatives.
- Perform the above steps with collection of models where model complexity increases as the number of alternatives decrease.

## Computer Aided Flowsheet Design (CAFD) Methodology

The computer aided flowsheet design methodology [2,3] as shown in figure 1 has 6 main steps: the synthesis problem definition; the selection of the matching process group building blocks; the generation of flowsheet alternatives; the ranking of the alternatives and selection of the most promising alternatives; the design & analysis of the selected alternatives; and the final verification & selection.

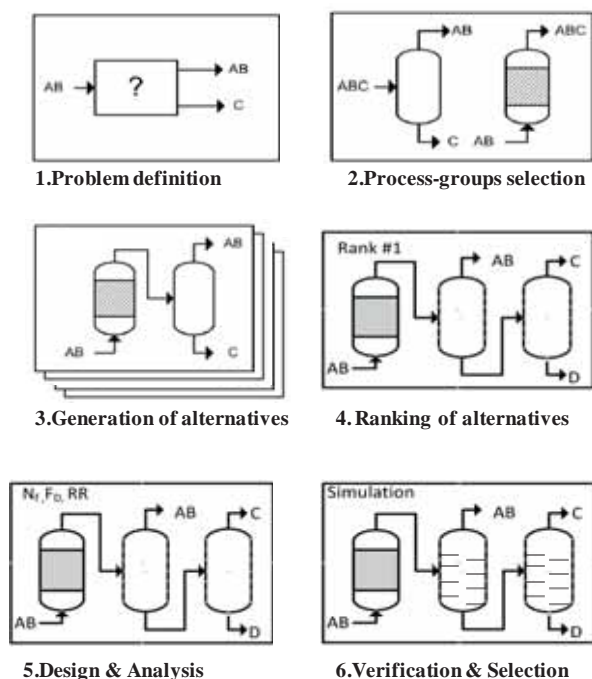


**Figure 1:** Computer Aided Flowsheet Design (CAFD) Methodology

### Step 1: Problem Definition

In this step the user defines the synthesis problem by selecting the necessary raw material, the desired products streams and performance criteria based upon which the alternatives are evaluated. Along with the stream properties, if the synthesis problem requires reaction to produce the product then this data is also provided in this step.

### Step 2: Process-groups selection

The objective of this step is to select the process-group building blocks that are applicable for the given synthesis problem which is achieved through further analysis of the process synthesis problem. First the pure component analysis is performed by retrieving a list of 22 pure component properties from the ICAS database. For compounds missing data/new compounds, the properties are calculated using ProPred (property prediction tool box) which is part ICAS [4]. Second the mixture property analysis is made in terms of the binary pairs of all the chemical species identified in the problem. This analysis information is used for

identification of feasible separation techniques using Jaksland and Gani's [5] method. Based upon the identified separation techniques, process groups representing all the combinations possible for each of the separation technique are selected and initialized.

### Step 3: Generation of Alternatives

The objective in this step is to combine the process-groups selected in step 2 according to a set of connectivity rules and specifications to generate feasible flowsheet structures.

- *Superstructure generation:* In this task a combinatorial algorithm is employed to generate the superstructure of all flowsheet alternatives from the initialized process-groups. The combinatorial algorithm generates new flowsheet alternatives by combining process-groups according to a set of connectivity rules.
- *Generation of SFILES:* Having a process flowsheet represented by process groups provides the possibility to employ simple notation systems for efficient storage of structural information of all the process alternatives generated. The SFILES method for flowsheets is similar to SMILES (Simplified Molecular Input Line Entry System) developed by David Weininger [6].

### Step 4: Ranking of Alternatives

In this step, the generated alternatives are evaluated and ranked using flowsheet property models based on group contribution principles. The main objective of the process flowsheet property model is to calculate the impact generated by the whole process as a sum of contributions of the process-groups present in the flowsheet. General equation for a flowsheet group contribution based property model can be derived as shown by equation (1).

$$f(P) = \sum_{k=1}^{NG} pos_k * a_k \quad (1)$$

Where  $f(P)$  is the flowsheet property function,  $NG$ : number of process groups,  $a_k$ : regressed contribution of group  $k$ , and  $pos_k$ : topology factor.

### Step 5: Design & Analysis

This step of the framework has two tasks: i) calculation of flowsheet design parameters of the process unit operations in the flowsheet structure through reverse simulation using driving force concept [7], and ii) Analysis of the selected alternatives to further benchmark the alternatives based on various indicators related to environmental impact, process safety and efficiency.

### Step 6: Verification & Selection

At this step of the methodology, all the necessary information to perform the final verification through rigorous simulation is available. Rigorous simulators like PROII or ICASSim are used to further refine the

most promising process flowsheet and to perform optimization of the design parameters.

### Case Study

The application of the methodology is highlighted through a case study involving production of benzene through hydrodealkylation of toluene.

#### Step 1:

The synthesis problem is defined as to find the best processing alternative to produce benzene from toluene and hydrogen with minimum energy consumption. The structural definition of the problem has 2 inlet streams for toluene and hydrogen (methane as impurity) and 2 outlet streams representing main product benzene and byproduct biphenyl. Reaction data for toluene hydrodealkylation is as follows:

Temperature: 700-850 k

Pressure: 40 bar



#### Step 2:

Based upon the pure component analysis and mixture analysis, feasible process operation tasks to separate each of all the binary pairs present in the system are identified. This feasible separation techniques information is used to select the corresponding process-groups from the database and initialize with corresponding compound configurations. Table 1 gives information on the selected process-groups for the synthesis problem.

**Table 1:** Process-groups initialized

Operation type	Gas membrane separation	Molecular-sieve separation	Distillation	Crystallization	Liquid membrane separation
Process groups	gmemE/DCAB	msE/DCAB	ABCD/E	crsE/C	lmemE/C
	gmemD/CAB	msD/CAB	ABC/D	crsE/D	lmemD/C
	gmemC/AB	msC/AB	AB/C	crsE/CD	lmemE/D
	gmemED/CAB	msE/D	ABC/DE	crsEC/D	lmemE/D
	gmemE/D	msED/C	AB/CDE	crsC/D	lmemE/DC
	gmemDC/AB	msDC/AB	C/D		
	gmemED/C	msED/CAB	AB/CD	Inlet/Outlet	Reactor
	gmemD/C	msD/C	C/DE	iAB	rABD/ABCDE
	gmemE/C	msE/DC	D/E	iD	
	gmemEDC/AB	msE/C	C/E	oC	
	gmemE/DC	msEDC/AB		oE	

Along with separation process-groups, separate process groups are initialized for two inlet streams representing, hydrogen along with methane and pure toluene streams and reactor. Two outlet process groups are also initialized for the benzene and biphenyl product streams, respectively.

#### Step 3:

In this step superstructure of all feasible alternatives are generated from 47 initialized process-groups using a combinatorial algorithm. Total of 74,046 alternatives are possible from different combinations of selected process-groups. But using the combinatorial algorithm along with logical decision rules, only 272 feasible

flowsheet alternatives are generated for production of benzene from toluene hydrodealkylation.

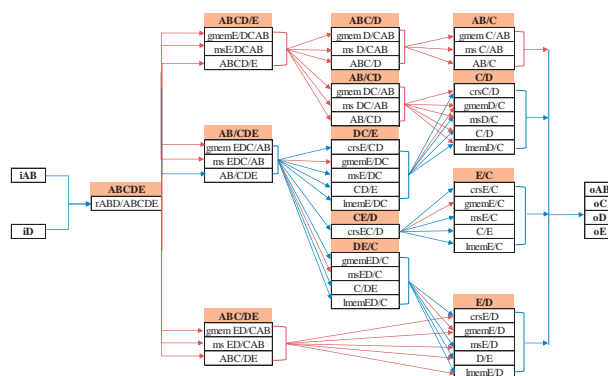


**Figure 2:** Superstructure of generated alternatives

All the identified process alternatives are converted into SFILES, which stores the structural information of the alternatives.

#### Step 4:

All the alternatives generated are evaluated using flowsheet property model for calculating energy consumption of the process alternative. Table 2 represents the top five alternatives for the synthesis problem. The first two designs reported in Table 2 has same energy index. This is explained by the fact that the energy consumption index (Ex) is only calculated for the distillation process groups, so the contribution of the other process groups is considered as 0.

**Table 2:** Process-groups initialized

Design No	Initial Screening			Analysis			
	Energy Index	Benzene Purity	Biphenyl Purity	Energy (MkJ/hr)	Atom efficiency	Purity	Benzene (kmol/hr)
1	0.0539	99.5	99.9	27.87	81.57	99.8	127.8
2	0.0539	99.5	99	27.71	81.52	99.8	127.5
3	0.0641	99.5	99.5	28.57	79.9	99.8	127.3
4	0.067	99.5	99.9	28.58	81.61	99.8	127.8
5	0.0772	99.5	99.5	29.03	81.52	99.8	127.5

#### Step 5:

Design parameters (number of stages for distillation, feed location, reflux ratio etc) for the selected alternatives are calculated using reverse simulation approach. Table 3 gives the design parameters of distillation columns (calculated using driving force method) for the selected alternative.

**Table 3:** Design parameters for distillation columns

Distillation column design (driving force method)	Stabilizer	Benzene		Toluene
		column	column	column
Given a NC component process group	5	3	2	
Order the components with respect to relative volatility	AB/CDE	C/DE	D/E	
Driving force between the key components $FD_{i,max} \cdot Di$	>0.75	0.22	0.4	0.6, 0.25
Recovery of light key	0.999	0.995	0.995	
Recovery of heavy key	0.999	0.995	0.995	
$N_{i,ideal} = 1.5$	5	31	15	
$N_i$ Feed location	2	19	12	

Also in this step, mass balance is resolved for selected alternatives using simple models to calculate overall benzene production, purity and atom efficiency. Along with mass balance results and process-groups definition, it is possible to estimate the energy required by each unit operation of the flowsheet and the corresponding energy requirements for the whole flowsheet as shown in table 2. Apart from these, various environmental and safety factors are evaluated for the alternatives to further analyze them as shown in table 4.

3. L. d' Anterrosches, R. Gani, Fluid Phase Equilib, 228-229 (2005) 141–146.
4. R. Gani, 2002, ICAS documentation. CAPEC, Technical University Of Denmark
5. C. Jaksland, PhD Thesis, Department of Chemical and Biochemical Engineering, DTU, Denmark, 1996.
6. D. Weininger, Journal of Chemical Information and Computer Sciences, 1988
7. E. Bek-Pedersen, R. Gani, Chem. Eng. Process. 43 (2004) 251.

**Table 4:** Design parameters for distillation columns

Process Alternative	Environmental Impact Factors								Process Safety	
	HTPI	HTPE	ATP	TTP	GWP	ODP	PCOP	AP	IT	IP
1	81.95	349.59	44.02	81.95	3.12	0	-3801.48	0	3	2
2	81.91	349.41	44	81.91	3.12	0	-3799.48	0	3	2
3	80.29	342.42	43.11	80.29	3.06	0	-3723.1	0	3	2
4	81.95	349.59	44.02	81.95	3.12	0	-3801.48	0	3	2
5	81.91	349.41	44	81.91	3.12	0	-3799.48	0	3	2

#### Step 6:

For this case study, the top 2 alternatives are selected for verification using rigorous models. Commercial process simulator (Pro- II) was used to verify the selected designs. The top process alternative obtained from the framework has slightly improved heating energy efficiency with respect to the alternative (2<sup>nd</sup> design) proposed in the literature. Table 5 gives the energy comparison between the selected designs.

**Table 5:** Energy requirements comparison

	Heating	Cooling	Benzene	Biphenyl
	M KJ/hr	M KJ/hr	kg-mol/hr	kg-mol/hr
Process alternative 1	34.57	-43.67	126.3	3.48
Process alternative 2	34.78	-39.98	126.41	3.49

#### Conclusions:

A novel approach based on the computer-aided molecular design principles has been developed to systematically solve the complex process synthesis and design problem, which facilitates more efficient and innovative solutions. Since rigorous simulation is done only in the last step of the method and feasible alternatives are generated by combining process groups, numerous process alternatives are quickly generated for a given synthesis problem. Also Introduction of flowsheet property models based on group contribution approach made it possible to quickly & efficiently evaluate and systematically screen generated alternatives.

#### References

1. Marrero, J., Gani. R. Fluid Phase Equilibria 2001; 183-184: 183-208
2. Tula, A.K., Eden, M.R., Gani, R. Computers and Chemical Engineering. 2015, 81. 245-259.

**Fragkiskos Tzirakis**

Phone: +45 4525 2821

E-mail: frtz@kt.dtu.dk

Supervisors: Georgios Kontogeorgis  
Nicolas von Solms  
Christophe Coquelet, MINES ParisTech  
Paolo Stringari, MINES ParisTech

**PhD Study**

Started: June 2013

To be completed: June 2016

## An experimental and theoretical study of CO<sub>2</sub> hydrate formation systems

**Abstract**

CO<sub>2</sub> capture and sequestration (CCS) is nowadays an important area of research for alleviating CO<sub>2</sub> emissions worldwide. According to literature, CO<sub>2</sub> is globally the largest pollutant to which the global warming is attributed. Consequently, hydrate technology may become an alternative post combustion solution of CO<sub>2</sub> capture from flue gases (hydrate crystallisation). A main disadvantage of hydrate process is the high pressure it needs and, therefore, several chemicals (promoters) are currently under examination. The promoters reduce the hydrate equilibrium pressure. In this study hydrate experimental results with several promoters are presented which were produced in MINES ParisTech. Different CO<sub>2</sub> and N<sub>2</sub> gas mixtures were used with presence of promoters such as tetra butyl ammonium bromide (TBAB), tetra butyl ammonium fluoride (TBAF), cyclopentane (CP) and mixtures of TBAB/F with CP.

**Introduction**

The capture of CO<sub>2</sub> and sequestration (CCS) has become an important area of research for treating CO<sub>2</sub> emissions. The effort is to develop energy efficient and environmental friendly technologies to capture the CO<sub>2</sub> produced in large scale power-plants, where flue gas typically contains mostly CO<sub>2</sub> and N<sub>2</sub> [1]. One novel approach to separate CO<sub>2</sub> from combustion flue gas is via gas hydrate crystallization technique [2], [1]. This technique allows hydrate crystals to be formed from a mixture of CO<sub>2</sub>+gases and CO<sub>2</sub> is captured. Then the hydrate crystals dissolve through imposition of increased temperature and CO<sub>2</sub> is concentrated in one stream. [2]

**Project objectives**

This project aims to close the gap of experimental and theoretical knowledge on CO<sub>2</sub> hydrates concentrating mainly on promoters. Two research groups, one from DTU and one from MINES ParisTech, are working on closely, developing a new theory for the thermodynamic treatment of CO<sub>2</sub> hydrates (DTU) as well as producing new experimental data (France) for enhancing hydrate formation literature. More particularly, the project core is the execution of equilibrium experiments on gas hydrate-formation systems e.g. for mixtures of CO<sub>2</sub>+N<sub>2</sub>+H<sub>2</sub>O+promoter. The chosen promoters were tetra butyl ammonium bromide (TBAB), tetra butyl ammonium fluoride (TBAF), cyclopentane (CP) and mixtures TBAB/F with CP. The combination of TBA

halides with CP was inspired by [3] as it was revealed synergetic effect between TBAB and CP. This work was conducted in collaboration with the Center of Thermodynamic of Processes in MINES ParisTech, where the experimental work was undertaken.

**Carbon dioxide hydrates**

CO<sub>2</sub> hydrates are solid non-stoichiometric inclusion compounds formed by a lattice structure, composed of water molecules (named *host* molecules) linked together by hydrogen bonding, and stabilized by encapsulating CO<sub>2</sub> molecules (named *guest* molecules). The most common gas hydrates belong to the three crystal structures: cubic structure I (sI), cubic structure II (sII) and hexagonal structure H (sH). CO<sub>2</sub> forms sI structure.

**Hydrate promoters**

Currently various promoters (or formers) and mixtures of them are under examination. Thermodynamic promoters extend the hydrate formation region in a  $P,T$  diagram. Thermodynamic promoters are considered as kinds of ionic liquids (ILs). Some tetra-alkylammonium halides, which are water-soluble, such as tetrabutyl ammonium bromide (TBAB), of fluoride (TBAF), of chloride (TBAC) and some tetra-alkylphosphonium halides like tetra-butylphosphonium bromide (TBPB) have also been proposed as promoters of gas hydrates as well as water immiscible cyclic hydrocarbon such as cyclopentane

(CP). Especially, the TBAB is generally considered as promising material for various innovating processes. The literature study showed lack of results in this system while many results indeed exist for  $\text{CO}_2+\text{CH}_4+\text{TBAB}$ ,  $\text{CO}_2+\text{H}_2+\text{TBAB}$  and  $\text{CO}_2+\text{TBAB}$ .

### Equipment description

A brief sketch of the experimental equipment as used in Mines ParisTech is presented in Figure 1. At first, two cylinders one of nitrogen and one of  $\text{CO}_2$  and  $\text{N}_2$  are used. The first is used for cleaning the cell and the last for providing the gas mixture in desirable pressure. Then there is a vacuum pump in order to avoid contamination of the tube and also to help cleaning the cell. The procedure was as follows. The cell was immersed in a water bath for controlling the temperature and three transducers were attached to it; two of temperature (on the top and bottom of the cell) and one of pressure on the top. All of them were connected after acquisition units to personal computer. The acquisition results were obtained by the temperature transducer of the top and pressure transducer of the bottom.

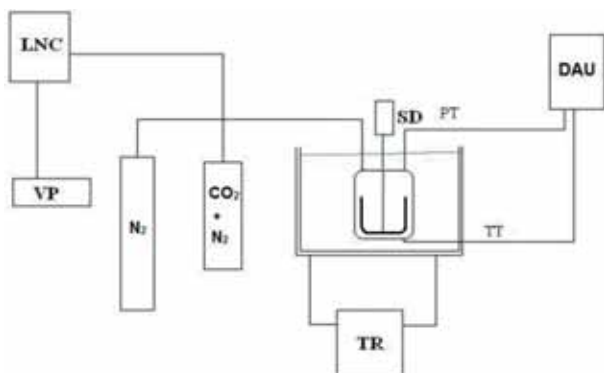


**Figure 1** Simplified schematic diagram of equipment of gas hydrate dissociation point measurement. LNC: liquid nitrogen container. VP: vacuum pump. SD: stirring device. TR: temperature regulator. TT: temperature transducer. PT: pressure transducer. DAU: data acquisition unit.

Temperature of the cell was controlled using a thermostatic water bath (LAUDA PROLine RP3530). One platinum temperature probe (Pt100) inserted in the cell interior was used to measure the temperature inside the cell within measurement uncertainties, which are estimated to be less than 0.02K with a second order polynomial calibration equation. The data acquisition units (Agilent 34970A, HP 34970A) were coupled with a personal computer to measure -and automatically record- pressure, temperature and time data. The data acquisition software also allowed adjusting the rate of data acquisition. Continuous recording of pressures and temperatures allowed detecting any subtle changes in the system and true equilibrium conditions. A motor-driven turbine agitation system (Top Industrie, France) enabled to stir the cell contents at a speed up to 1100 rpm to increase the fluids contact and enhance water conversion into hydrate.

### Experimental part

The four gas mixtures used in this work were produced with the use of a cylinder in which different concentrations of  $\text{CO}_2$  and  $\text{N}_2$  were mixed. The  $\text{CO}_2$  and  $\text{N}_2$  gas bottles used in this work were supplied by Air Liquide. The molar fractions of  $\text{CO}_2$  gas mixture were app. 0.15, 0.11, 0.07 and 0.005. The exact concentrations were measured by a gas chromatograph. TBAB solutions with mass fractions of (0.05, 0.10 and 0.20) and TBAF solutions with mass fractions of (0.03, 0.05 and 0.10) were prepared by gravimetric method using an accurate analytical balance (Mettler, AT200), with mass uncertainty of  $\pm 0.0001\text{g}$ . Double-distilled and deionized water from Direct-Q5 Ultrapure Water Systems (MilliporeTM), was used in all experiments. When needed, cyclopentane was added in TBAB and TBAF solutions with use of proper syringes. The results for different  $\text{CO}_2/\text{N}_2$  mixture concentration for TBAB promoter are summarised in Fig. 2. In general, it is observed very good agreement with the literature for similar systems of 5, 10 and 20 wt % TBAB solutions which correspond to 0.29, 0.62 and 1.38 mol % respectively.

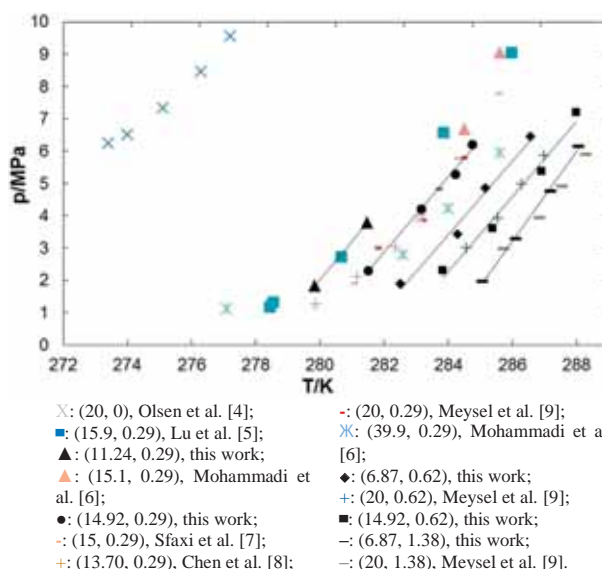


**Figure 2** Hydrate dissociation points for different systems using TBAB as promoter. The figure contains systems of this work and systems of  $\text{CO}_2+\text{N}_2+\text{TBAB}+\text{H}_2\text{O}$  from literature. For clarity reasons, the systems are presented by two numbers in brackets. The first number denotes the mol fraction of  $\text{CO}_2$  in  $\text{N}_2$  gas mixture cylinder and the second one denotes the promoter concentration. Black markers connected with trendlines correspond to results of this work. References are presented according to diagram from left to right.

The results of similar promoter and gas mixture concentrations are in excellent agreement, e.g. with (14.92, 0.29) from this work, with (13.70, 0.29) from Chen et al. [8], with (20, 0.29) from Meysel et al. [9] and with (15, 0.29) from Sfahi et al. [7]. Another observation is that the system of (6.87, 0.62) of this work is approximately placed on the left of (20, 0.62) of Meysel et al. [9] which shows that  $\text{CO}_2$  hydrates are formed at lower pressures than  $\text{N}_2$  hydrates.

Similarly for higher TBAB concentrations, the results of similar promoter and gas mixture concentrations are in good agreement, e.g. with (6.87, 1.38) from this work, with (20, 1.38) from Meysel et al. [9]. According to the literature, there is mismatch of (13.70, 0.29) of Chen et al. [8] with the system (15.9, 0.29) of Lu et al. [5] respectively as shown in Fig. 2.

Similar procedure was followed for the system  $\text{CO}_2 + \text{N}_2 + \text{CP} + \text{H}_2\text{O}$ . For  $\text{CO}_2/\text{N}_2$  mixture (6.87/93.13), 15 ml and 25 ml of CP aqueous solution of 20 wt % (6.03 mol %) and 52.57 wt % (22.15 mol %) were prepared respectively. The stoichiometric concentration of CP in the solution for structure II hydrates is 18.65 wt % (5.56 mol %) [10]. For CP concentrations >27.80 wt %, according to Galfrè et al. [11], emulsion system is produced. For P-T measurements, stirring velocity is not of importance. We have used relatively high stirring velocity (1070 rpm). It came out that our results were similar for both CP concentrations used. Fig. 3 summarizes the results.

In Fig. 3, there is a region in which  $\text{CO}_2 + \text{N}_2$  mixture dissociation points should exist according to experimental results [12,13,14]. These are the boundaries of pure  $\text{CO}_2$  and pure  $\text{N}_2$  with CP +  $\text{H}_2\text{O}$  systems respectively. Our results are included in these boundaries. Another observation is that CP does not "sense" the small mol fraction of  $\text{CO}_2$  (e.g. 6.87 mol %) of  $\text{CO}_2$  in  $\text{CO}_2 + \text{N}_2$  gas mixture. In other words, most probably  $\text{N}_2$  is predominantly captured -higher  $\text{N}_2$  selectivity- rather than  $\text{CO}_2$  since the results between pure  $\text{N}_2$  and  $\text{CO}_2 + \text{N}_2$  are identical. According to our results, the CP concentration does not have any significant impact on the thermodynamic equilibrium in contrast with TBAB due to water insolubility in cyclopentane. This occurs for both the emulsion and the non emulsion CP case. In other words, the two systems of different CP concentrations match each other excellently.

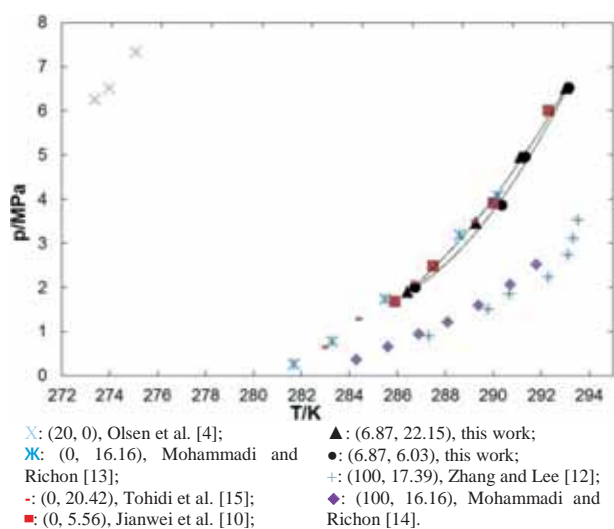


**Figure 3** Hydrate equilibrium points for different systems using CP promoter. References are presented according to diagram from left to right. The systems of this work are in excellent agreement with systems of pure  $\text{N}_2$  indicating that cyclopentane

at high concentrations favors  $\text{N}_2$  hydrates instead of  $\text{CO}_2$  hydrates in  $\text{CO}_2+\text{N}_2$  gas mixtures. Moreover, the high difference of CP concentrations used in this study is not thermodynamically important and this is shown by the fact that both systems of this study are in very good agreement with each other.

For  $\text{CO}_2/\text{N}_2$  mixture (0.48/99.52), 30 ml of TBAF promoter were used, purchased by Sigma-Aldrich (75% wt in  $\text{H}_2\text{O}$ ). In Figure 4 the results of this work are presented.

The results for 3.2%, 5% and 10 wt % TBAF, which correspond to 0.23, 0.36 and 0.76 mol % respectively, seem well placed in the Figure 1. The gas mixture, which is 99.52mol %  $\text{N}_2$ , produced steeper results than with higher  $\text{CO}_2$  concentration. In addition it is observed that for 0.68 mol % TBAF the addition of CP is not inducing promotion while for 0.36 mol % TBAF and at higher pressure of 4 MPa the promotion is enhanced.

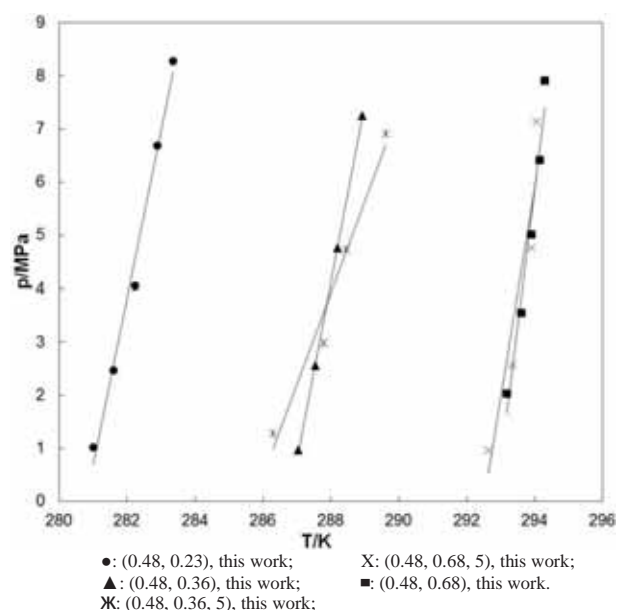


**Figure 4** Hydrate dissociation points for different systems using TBAF as promoter. The figure contains only systems of this work for the system  $\text{CO}_2+\text{N}_2+\text{TBAF} (+\text{CP})+\text{H}_2\text{O}$ . For clarity reasons, the systems are presented by two numbers in brackets. The first number denotes the mol fraction of  $\text{CO}_2$  in  $\text{N}_2$  gas mixture cylinder, the second one denotes the promoter concentration and the third is the 5 vol % cyclopentane. Black markers connected with trendlines correspond to results of this work. References are presented according to diagram from left to right.

### Consistency analysis

For data treatment, Clausius –Clapeyron method is applied, eq. 1.

$$\frac{d \ln(P)}{d\left(\frac{1}{T}\right)} = \frac{-\Delta H_{dis}}{Z \cdot R} \quad (1)$$

where  $\Delta H_{dis}$  is the apparent dissociation enthalpy of the hydrate phase,  $Z$  is the compressibility factor and  $R$  is the gas constant. Lee-Kesler-Plöcker (LKP) Equation of State (EoS) [16] is applied for estimation of  $Z$  as a function of  $T$  and  $P$  using binary interaction parameter

$\kappa_{ij}=1.11$ . It is assumed very low solubility and, thus, no changes in the gas composition. The  $\Delta H_{diss}$  as a function of dissociation temperature shows the goodness of fit. The table 1 presents the data treatment for results of this work.

**Table 1** Coefficient of determination of  $\Delta H_{diss}$  in terms of temperature for results of this work

Promoter concentration (mol %)	CO <sub>2</sub> in CO <sub>2</sub> +N <sub>2</sub> gas mixture concentration (mol %)	Coefficient of determination (R <sup>2</sup> )
<b>TBAB+CP</b>		
0.29	6.87	1.000
0.62	6.87	0.999
1.38	6.87	0.822
<b>TBAB</b>		
0.29	14.92	0.988
0.62	6.87	0.979
0.62	14.92	0.997
1.38	6.87	0.990
<b>CP</b>		
6.03	6.87	0.983
22.15	6.87	0.977
<b>TBAF+CP</b>		
0.36	0.05	0.995
0.72	0.05	0.864
<b>TBAF</b>		
0.23	0.05	0.997
0.36	0.05	0.991
0.72	0.05	0.993

The analysis shows that the results of this work are very good ( $R^2 > 0.90$ ). There are, nonetheless, two exceptions: the system 1.38 mol % TBAB+CP and 0.72 mol % TBAF+CP.

### Conclusions

The simultaneous use of TBAB (0.29 mol %) with CP (5 vol %) induced inhibition effect. For the system, TBAB (0.62 mol %) with CP (5 vol %) the results are virtually identical. On the contrary, the use of higher TBAB concentration (1.38 mol %) and CP (5 vol %) revealed promotion effect and also as the pressure rises, this phenomenon becomes more intense. In addition, the higher the CO<sub>2</sub> concentration, the stronger the promotion is for every TBAB solution. However, this fact is not easily observable for low CO<sub>2</sub> concentration differences in mixtures. Consequently, it came out that the factor of gas mixture concentration has moderate impact on hydrate equilibrium compared to promoter's concentration.

The use of CP solution (even though virtually water insoluble) proved to be stronger promoter than TBAB maybe because of the different hydrate structure it induces. According to the promotion trend of TBAB, for

42 wt % TBAB, above of which it acts as inhibitor, the promotion results may become similar to CP results. In addition, there is slightly inhibition effect when higher CP concentration is used, e.g. 22.15 mol %.

Finally, TBAF proves to be by far much stronger promoter than TBAB and CP, especially for lower pressures. This is not easily observable because of the almost pure N<sub>2</sub> mixture it was used. The use of TBAF concentration (10 wt %) with CP (5 vol %) revealed promotion effect above 30bar and also as the pressure raises it becomes more intense.

Finally, the data consistency analysis carried out using Clausius-Clapeyron method revealed that measurements of this work are satisfactory.

### Acknowledgments

The project is part of "CO<sub>2</sub> Hydrates – Challenges and possibilities" (Project ID: 50868) and is financed by 2/3 through Danish Research Council for Independent Research and by 1/3 through DTU.

### Reference

1. Belandria V., Eslamimanesh A., Mohammadi A.H., Richon D., *Ind. Eng. Chem. Res.* 50 (2011) 4722–4730.
2. Mohammadi A.H., Eslamimanesh A., Belandria V., Richon D., *J. Chem. Eng. Data* 56 (2011) 3855–3865.
3. Li X.-S., Xia Z.-M., Chen Z.-Y., Wu H.-J., *Energy Fuels* 25 (2011) 1302–1309.
4. Olsen M.B., Majumdar A. and Bishnoi P.R., *Int. J. of The Soc. of Mat. Eng. For Resources* 7 (1999) 17-23.
5. Lu T., Zhang Y., Li X.-S., Chen Z.-Y., Yan K.-F., *The Chinese J. of P. Eng.* 9 (2009) 541-544. (in chinese).
6. Mohammadi A.H., Eslamimanesh A., Belandria V., Richon D., Naidoo P., Ramjugernath D., *J. Chem. Thermodyn.* 46 (2012) 57–61.
7. Sfaxi I., Durand I., Lugo R., Mohammadi A., Richon D., *Int. J. of Greenh. Gas Control* 26 (2014) 185–192.
8. Chen C., Li X.-S., Chen Z.-Y., Xia Z.-M., Yan K.-F., Cai J., *J. Chem. Eng. Data* 59 (2014) 103–109.
9. Meysel P., Oellrich L., Bishnoi P.R., Clarke M.A., *J. Chem. Thermodyn.* 43 (2011) 1475–1479.
10. Jianwei D., Deqing L., Dongliang L., Xinjun L., *Ind. Eng. Chem. Res.* 49 (2010) 11797–11800.
11. Galfré A., Kwaterski M., Brântuas P., Cameirao A., Herri J.-M., *J. Chem. Eng. Data* 59 (2014) 592–602.
12. Zhang J., Lee J.W., *J. Chem. Eng. Data* 54 (2009) 659–661.
13. Mohammadi A.H., Richon D., *Chem. Eng. Sci.* 66 (2011) 4936–4940.
14. Mohammadi A.H., Richon D., *Chem. Eng. Sci.* 64 (2009) 5319–5322.
15. Tohidi B., Danesh A., Todd A.C., Burgass R.W., Østergaard K.K., *Fluid Phase Equilib.* 138 (1997) 241–250.
16. Plöcker U., Knapp H., Prausnitz J. M., *Int. Chem. Proc.* 17 (1978) 324-334.



**Andre Vinhal**

Phone: +45 4525 2876  
E-mail: anpi@kt.dtu.dk

Supervisors: Georgios Kontogeorgis  
Wei Yan

PhD Study  
Started: May 2015  
To be completed: April 2018

## Application of an association equation of state in compositional reservoir simulation

### Abstract

Due to the increasing demand for fossil fuel, unconventional hydrocarbon resources are becoming more important each day. In spite of its relevance, producing from such sources is challenging, thus broad knowledge of the reservoir fluids is required. The properties of reservoir fluids are usually estimated by cubic Equations of State (EoS). Although accurate for hydrocarbon systems, high deviations from experimental data are found when used to describe complex fluids. One way to precisely predict the properties of non-ideal fluids is to use non-cubic EoS, such as Cubic-Plus-Association (CPA). In this work the performance of the CPA was compared with different cubic models for several properties of pure fluids. Though the association model was superior in the prediction of saturated properties, an over estimation of the critical properties was observed. To improve the performance of CPA a new parametrization method was applied with a volume correction method to correlate liquid density data.

### Introduction

Exploitation of unconventional hydrocarbon resources, like ultra-deep reservoirs, are very challenging, but owing to the crescent demand for fossil fuels this sources are becoming more relevant for the oil and gas industry. Many problems arise from the production of such reservoirs, because of high pressure and also the complexity of reservoir fluids and rock [1].

Due to the intricacy of implementing projects in ultra-deep waters, broad knowledge of the reservoir fluids is required. On the other hand, most of the commercial reservoir simulators use cubic EoS to predict the properties of these fluids. The reason that traditional models are widely used in such software is their precision for conventional polar systems. However, when these equations are applied for describing complex fluids high deviations are observed.

In order to precisely estimate the properties of complex fluids, non-cubic EoS like CPA should be applied. Association EoS are known to correctly describe the phase behavior of non-ideal mixtures, but at the same time over predict the critical properties of the pure components. The over prediction of the critical properties is a consequence of the parametrization, done by the fitting of the pure species' vapor pressure and liquid density curves. With the view to improve the critical point estimation and keep the model's performance for phase equilibrium calculations, a

different parametrization procedure was tested and the predictions for the saturated and critical properties were compared for each approach.

### Objectives

The first goal is to compare the performance of different EoS in the description of saturated and critical properties of pure components. The second objective is to test a new parametrization procedure, for the purpose of reducing the critical properties deviations. In the next stage this methodology will be applied in binary and multicomponent complex mixtures.

### Equations of State

The precision of the phase behavior calculations are direct related to the choice of the EoS. Cubic models usually have the following form:

$$P = \frac{RT}{v-b} - \frac{a(T)}{v(v+b)} \quad (1)$$

For complex systems cubic EoS are not reliable. In such cases, it is important to employ advanced equations. The CPA EoS [2] is given by:

$$P = \frac{RT}{v-b} - \frac{a(T)}{v(v+b)} - \frac{RT}{2v} \left( 1 + \rho \frac{\partial \ln(g)}{\partial \rho} \right) \sum x_i \sum (1 - X_{A_i}) \quad (2)$$

where the third term accounts for non-physical interactions, e.g. hydrogen bonding.

### Parametrization Procedure

Unlike cubic EoS that use the critical properties as input parameters, CPA's parameters are usually estimated by the fitting of the vapor pressure and liquid phase volume curves. In this approach no information of the critical properties is used, thus a different parametrization procedure is suggested, with the following object function for the optimization process:

$$OF = \sum \left| \frac{P_{exp}^{vap} - P_{calc}^{vap}}{P_{exp}^{vap}} \right| + \sum \left| \frac{v_{exp}^{liq} - v_{calc}^{liq}}{v_{exp}^{liq}} \right| + \left| \frac{P_{c,exp} - P_{c,calc}}{P_{c,exp}} \right| + \left| \frac{T_{c,exp} - T_{c,calc}}{T_{c,exp}} \right| \quad (3)$$

### Results and Discussion

Equations 1 and 2 were applied in the prediction of the vapor pressure and liquid phase volume of several alkanes (methane to eicosane), polar (methanol to octanol, water and hydrogen sulfide) and non-polar (nitrogen, carbon dioxide) compounds.

Table 1 shows the absolute average percentage deviations for Soave-Redlich-Kwong (SRK), Patel-Teja (PT), and CPA EoS. CPA is superior to other models for both properties, in special for the polar compounds.

**Table 1:** Average absolute percentage deviation of the vapor pressure and liquid phase density using three EoS.

Group	AAD P <sub>vap</sub> (%)			AAD v <sub>liq</sub> (%)		
	SRK	PT	CPA	SRK	PT	CPA
HC	1.74	2.95	1.53	26.3	3.36	2.13
Polar	9.88	12.1	2.15	19.9	7.29	1.74
Non-Polar	0.91	0.84	0.44	8.60	3.83	2.02

Table 2 shows the deviations for the critical properties calculated using CPA with the parameters found in the literature [3]. Particularly high deviations are found for the critical pressure.

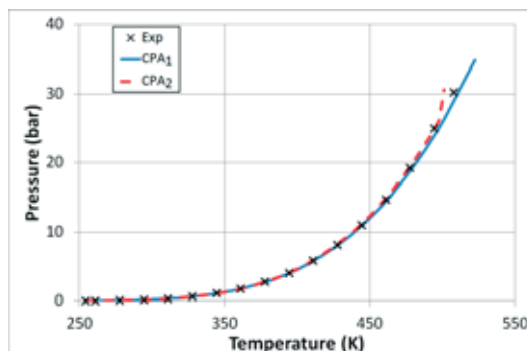
**Table 2:** Average absolute percentage deviation of the critical temperature and pressure from CPA.

Group	AAD P <sub>c</sub> (%)	AAD T <sub>c</sub> (%)
HC	16.2	2.42
Polar	24.3	3.24
Non-Polar	7.54	1.55

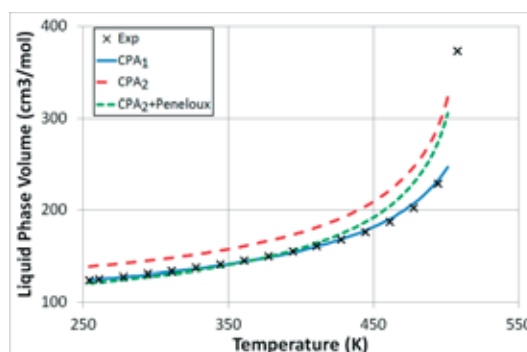
Eq. 3 was applied to estimate new parameters for n-hexane. Figure 1 shows the vapor pressure curves with original (CPA<sub>1</sub>) and new parameters (CPA<sub>2</sub>), indicating that the new set precisely describes the critical point.

Figure 2 presents the experimental curves of liquid phase volume for n-hexane and the calculated values with CPA<sub>1</sub> and CPA<sub>2</sub>. For this first property a large deviation is found for CPA<sub>2</sub>, thus the Peneloux volume

translation method was employed, enhancing the correlation capacity of the model.



**Figure 1:** Vapor pressure of n-hexane from CPA using two sets of parameters.



**Figure 2:** Liquid phase volume curves from CPA using two sets of parameters and the volume correction.

### Conclusions

CPA is superior to the two cubic EoS in the estimation of the saturated properties of fluids. However, it over predicts the critical properties of the components.

A different parametrization procedure for CPA was tested for n-hexane. A better description of the critical point was achieved, nevertheless the liquid phase volume deviation increased. To reduce the error in the liquid density a volume translation technique was applied.

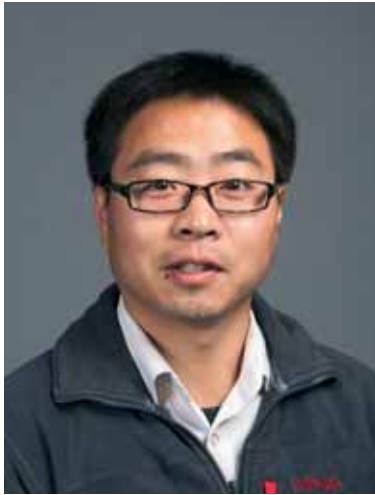
Based on the results for n-hexane this procedure can be extended for other components and in future works complex mixtures will be tested.

### Acknowledgment

The author wishes to thank the Brazilian Education Ministry for the PhD Scholarship.

### References

1. J.O.d.S. Pizarro, C.C.M. Branco, Challenges in Implementing an EOR Project in the Pre-Salt Province in Deep Offshore Brasil, Society of Petroleum Engineers, Muscat, Oman, 2012, SPE-155665-MS.
2. G.M. Kontogeorgis, et. al., Ind. Eng. Chem. Res. 35 (1996) 4310-4318.
3. I. Tsvintzelis, et. al., The cubic-plus-association EoS parameters for pure compounds and interaction parameters, CERE DTU, Lyngby, DK, 2012.

**Guoliang Wang**

Phone:

+45 4525 2890

E-mail:

guow@kt.dtu.dk

Supervisors:

Peter Glarborg

Peter Arendt Jensen

Flemming Jappe Frandsen

Hao Wu

Martin Bøjer, DONG Energy

PhD Study

Started:

October 2014

To be completed:

September 2017

## Experimental study of KCl capture by kaolin in an entrained flow reactor

### Abstract

A method to simulate the reaction between gaseous KCl and solid additives at suspension fired conditions has been developed in a pilot-scale Entrained Flow Reactor (EFR). A water slurry containing kaolin and KCl is injected into the EFR, and the extent of the reaction between kaolin and KCl is quantified by determining the amount of water-insoluble K formed at different conditions. The amount of K captured by per gram of kaolin increased upon increasing the molar ratio of  $K / (Al + Si)$  in the water slurry. A change in the reaction temperature, from 1100 °C to 1300 °C, did not significantly influence the extent of the reaction, which is different from the trend observed in fixed-bed reactors. This is probably related to the shorter residence time and the smaller kaolin particle size used in the EFR compared to that in fixed bed reactors.

### Introduction

Using biomass in suspension-fired boilers leads to relatively high concentrations of vapor phase K-species such as KCl,  $K_2SO_4$  and KOH which tend to condense on heat transfer surfaces, leading to increased deposition and corrosion. Upon flue gas cooling the K-species condense as aerosols that may lead to deactivation of SCR (Selective Catalytic Reduction) catalysts. An option for abating these problems is the introduction of additives into boilers for transforming harmful gaseous alkali compounds (e.g. KCl) into less corrosive ash species with a higher melting point [1]. Kaolin and coal fly ash react with gaseous KCl and form K-aluminasilicates with HCl released to the gas phase. K-aluminasilicates have higher melting point and can be more easily removed in deposits than KCl. The capture reaction by kaolin and coal ash has been extensively studied for decades. However, most of the previous studies were carried out in fixed-bed reactors where the reaction conditions are different from that in suspension fired boilers [2-4]. Detailed knowledge of the reaction between KCl vapor and solid additives under suspension-fired conditions is still limited.

The objective of the present work is to develop a method using a pilot-scale Entrained Flow Reactor (EFR) to simulate the KCl capture reaction by different additives under suspension-fired conditions. The impact of the type and amount of additives, reaction temperature and particle size is investigated. The developed method will be used for further study on

other additives. The experimental results obtained from this study will be used for developing a mathematical model describing the KCl capture process by solid additives. And recommendations for optimal use of additives in biomass suspension-fired boilers will be provided.

### Experimental Section

A water slurry, consisting of KCl and kaolin was fed into the EFR shown in Figure 1. Solid samples collected from the cyclone and filter of the EFR were analyzed by inductively coupled plasma optical emission spectrometry (ICP-OES), for elemental composition. The concentrations of water-soluble K, total-K and total-Cl in the products were quantified. The extent of the reaction between additives and KCl under different conditions (Table.1) was evaluated and compared by the amount of water-insoluble K formed in the EFR.

### Results and Discussion

In order to quantify the extent of the KCl binding reaction, K-capturing capacity of additives ( $C_K$ ) is defined as the mass of K captured by per gram of additives during the reaction, and the conversion of KCl is defined as the percentage of KCl transferred into water-insoluble K-species. Figure 2 (a) shows that with the increase of the molar ratio of  $K / (Al + Si)$  from 0.22 to 0.66 in the reactants, the conversion of KCl decreased from 64% to 33%, implying that more KCl stayed

unreacted. The  $C_K$  was in a range of 0.08 - 0.13 g K/ 1 g kaolin under the investigated conditions, which is obviously lower than the maximum theoretical value of 0.30 g K/ 1 g kaolin. The results of experiments conducted at 1100°C and 1300°C are shown in Figure 2 (b). There is no obvious impact of changing the temperature on the extent of the reaction, which is significantly different from previous fixed-bed results [1], where less KCl was captured at 1300 °C than at 1100 °C, due to sintering and the formation of less active mullite at 1300 °C. A possible reason for this difference is the much shorter residence time (0.78 - 0.89 s) in the EFR compared to that in a fixed bed reactor (1 hour). Another thing should be note in Figure 2(b) is that the  $C_K$  in the EFR is much higher than that in fixed bed although the residence time in the EFR is much shorter. In the fixed bed large kaolin pellets are employed for KCl capturing, and the reaction is largely influenced by the pore diffusion of KCl into the pellets. In the EFR the controlling mechanism is expected to be very different.

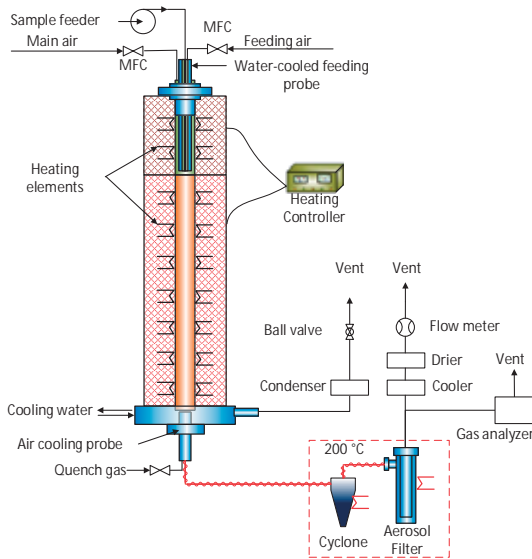


**Figure 1:** Schematic drawing of the entrained flow reactor (EFR).

**Table 1:** Experimental matrix and conditions.

Run no.	Temp./°C	KCl/ppmv	K/(Al + Si) molar ratio	Gas Residence time /s
1	1300	1021	0.44	0.78
2	1100	1019	0.22	0.89
3	1300	500	0.66	0.78
4	1300	1551	0.66	0.78

## Conclusions

A method of simulating the reaction of gaseous KCl capture by solid additives under suspension-fired conditions was developed using an Entrained Flow Reactor (EFR). The method makes it possible to investigate the influence of residence time, reaction temperature, particle size and alkali concentration on the K-capturing reaction by different additives. Kaolin was employed in the preliminary tests of this method. The results showed that under suspension-fired conditions,

kaolin can effectively capture corrosive gaseous KCl. The K-capturing capacity of kaolin increased upon increasing molar ratio of K / (Al + Si) in the reactant. The KCl-capturing behavior of kaolin in the EFR differed from that in a fixed-bed reactor when changing the reaction temperature. This is probably because of the much shorter residence time in the EFR compared to that in fixed bed reactors and the controlling mechanism in the EFR is expected to be very different from that in fixed bed reactor. A detailed explanation of these observations needs further experimental investigation and analysis. The developed method using the EFR in this study will be used for future investigation of different solid additives. The experimental data will be used for developing a mathematical model describing the KCl capture and for providing recommendations for the optimal use of solid additives in suspension-fired boilers.

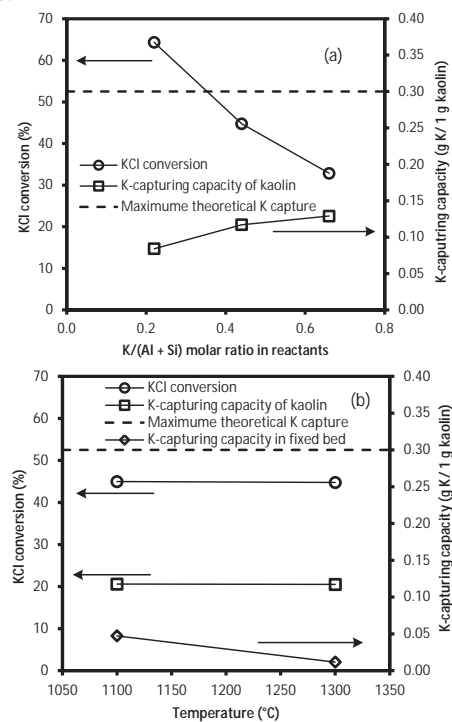


**Figure 2.** (a) Effect of K/(Al + Si) molar ratio in the reactants on the KCl conversion and the K-capturing capacity of kaolin ( $C_K$ ); reaction temperature = 1300 °C, (b) Influence of temperature on the KCl conversion and K-capturing capacity of kaolin ( $C_K$ ), K/(Al + Si) = 0.44; the fixed bed data is from [1], using large kaolin pellets ( $\Phi = 1.56$  mm).

## References

1. B.M. Steenari, O. Lindqvist, Biomass and Bioenergy 14 (1) (1998) 67-76.
2. Y. Zheng, P.A. Jensen, A.D. Jensen, Fuel 87 (15-16) (2008) 3304-3312.
3. W.A. Punjak, M. Uberoi, F. Shadman, AIChE Journal 35 (7) (1989) 1186-1194.
4. S. Q. Turn, C. M. Kinoshita, D. M. Ishimura, J. Zhou, T. T. Hiraki, Journal of the Institute of Energy 71 (1999) 163-177.



**Xueting Wang**

Phone: +45 4525 2890  
E-mail: xewa@kt.dtu.dk

Supervisors: Søren Kiil  
Marcus Tullberg, Hempel A/S  
Stefan Møller Olsen, Hempel A/S  
Kenneth Nørager Olsen, Maersk Maritime  
Technology  
Kim Dam-Johansen

PhD Study  
Started: August 2015  
To be completed: July 2018

## Low friction non-fouling coatings for high fuel efficiency at low speed

### Abstract

Slow steaming has been applied as an approach to save fuel by ship owners. The majority of the overall cost for ship owners is attributed to fuel consumption which is directly related to frictional resistance for slow steaming vessels. Therefore, decreasing the frictional resistance for slow steaming vessels is significant to achieve high fuel efficiency. The increased frictional resistance can be attributed to not only biofouling but also the applied rough coating surface when the ship hull is still free of fouling. Noticeably, they are interrelated since the rougher the coating surface, the more likely the biofouling occurs. Consequently, the roughness of the antifouling coating surface is a crucial parameter related to biofouling and frictional resistance, which should be reduced for high fuel efficiency.

### Introduction

Biofouling, defined as the accumulation of micro- and macro-organisms on ship hulls, is undesired because it increases the roughness and frictional resistance, decreases the speed or increases fuel consumption, increases the emissions of harmful gases and the frequency of dry dockings and translocate invasive species [1]. The heavily fouled ships may need to increase up to 86% shaft power to compensate for the speed loss due to the increased drag [2].

Slow steaming, in which the operation speed is below its design speed in order to decrease fuel consumption, is typically defined as no more than 16 knots. During sailing, ships spend a lot of time in slow steaming, especially for container vessels, tankers and bulkers. However, when a ship is slow steaming, it is more likely to be fouled since it is easier for biofouling to attach to the hull surface, especially during idle period.

Antifouling coatings applied on ship hulls can help to decrease or limit biofouling over the course of its lifetime (usually 3-5 years). Currently, there are two kinds of commercialized antifouling coatings, the conventional biocide-based antifouling coatings and fouling release coatings. The conventional antifouling coatings release biocides to combat biofouling and polish the outer-most layer to ensure the stability of biocides release rate. However, the biocide release rate

is proportional to the water flow velocity along the hull. When the ship is slow steaming, the polishing rate is lower, which will lead to the build-up of leached layer (the coating layer left behind after the biocides release into the seawater) and thereby the biocide release efficiency at the very surface will be lower. Consequently, the possibility of biofouling will be higher. For the fouling release coating, when the ship is slow steaming the hydrodynamic forces of seawater is not sufficiently strong to wash biofouling away according to its working mechanism. Therefore, slow steaming has created a particular challenge for the current antifouling coating systems.

There are two types of drag: one is viscous drag determined by frictional resistance caused by roughness of a ship hull, which dominates at low speed (around 80-85%), one is wave-making drag determined by the length of the ship and the ratio of width to the vertical distance between the bottom of the hull to the waterline, which dominates at high speed (around 50%) [3]. Furthermore, the frictional resistance on some hull types can account for as much as 90% of the total drag resistance even when the hull is still free of fouling [4]. Consequently, the fuel consumption and cost due to frictional resistance are in great amounts. Therefore, the coating surface condition of the ship hull is of primary importance in the performance of marine vessels from economic point of view. Overall, to decrease the coating

surface roughness and thereby decrease the frictional resistance is essential to achieve high fuel efficiency for slow steaming vessels.

### Specific Objectives

The overall aim is to find ways to decrease the coating surface roughness and thereby remove or limit biofouling and decrease the frictional resistance and increase the fuel efficiency for slow steaming vessels.

According to previous published results, the drag performance between different newly applied coatings is almost same, which is in conflict with the fact that in real life ship owners do observe some differences (drag and fuel consumption) between newly applied coatings after few weeks out docking period. Therefore, the first objective is to find ways to detect the initial drag differences for different newly applied coatings using the pilot-scale rotary setup as shown in Figure 1.

The pilot-scale setup is used to measure the surface frictional resistance. It consists of two concentric cylinders where the inner one is applied with coating samples and rotates. Both of them are immersed into a tank containing around 500 l of artificial seawater where the temperature is controlled by a heat exchanger. A static cylinder is placed outside of the rotating cylinder to obtain Couette flow. The rotating speed can be adjusted and monitored by a tachometer. A torque sensor is used to measure the torque of the bearings and cylinder. The surface frictional resistance can be calculated from the measured torque.

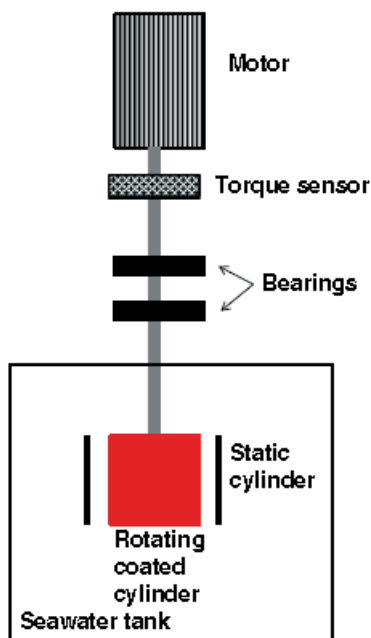


**Figure 1:** The schematic map of the pilot-scale rotary setup [5]

Roughness caused by large surface irregularities (such as welding seams and mechanical damage) affected the frictional resistance in a larger extent compared to roughness caused by the conditions of coating itself, for instance, the leveling out behaviors of the coatings during drying [6]. Therefore, the second

objective is to build CFD model as a tool to investigate the effect of different coating surface profiles on frictional resistance. The model can be verified based on both experimental data and real-life data from Maersk Maritime Technology.

To decrease the frictional resistance, the coating surface roughness should be decreased. In the third objective, the principles behind the coating systems will be scrutinized with the aim to identify how a smooth hull can best be obtained. The impact of coating rheology on the coating surface roughness and initial drag forces will be investigated. Meanwhile, novel formulation principles which will contribute to better coating surface smoothness are aimed at.

### Conclusions

Decreasing the frictional resistance of the ship hull is a remarkable step for both coating industries and ship owners according to the lower fuel consumption and the reduced emissions of harmful gases.

Overall, there are three main objectives for this project. The main efforts of this project will be focused on decreasing the coating surface roughness. Besides, large quantities of initial frictional resistance measurements will also be involved. Finally, building a CFD model to predict drag resistance of various coating surface profiles will also be highlighted.

### Acknowledgements

This project is part of a work-package that involves DTU, Hempel A/S and Maersk Maritime Technology. Financial support from Blue Innoship, a research collaboration between leading Danish Maritime institutions, the Innovation Fund Denmark and the Danish Maritime Fund, is gratefully acknowledged.

### References

1. D.M. Yebra, S. Kiil, K. Dam-Johansen, *Prog. Org. Coatings* 50 (2004) 75–104.
2. M.P. Schultz, *Biofouling* 23 (2007) 331–341.
3. J.H. Todd, in: J. Comstock (Ed.), *Princ. Nav. Archit.*, The society of naval architects and marine engineers, New York, 1980, pp. 288–462.
4. M.P. Schultz, J.A. Bendick, E.R. Holm, W.M. Hertel, *Biofouling* 27 (2011) 87–98.
5. A. Lindholdt, K. Dam-Johansen, D.M. Yebra, S.M. Olsen, S. Kiil, *J. Coatings Technol. Res.* (2015).
6. C.E. Weinell, K.N. Olsen, M.W. Christoffersen, S. Kiil, *Biofouling* 19 Suppl (2003) 45–51.



**Sara Lindeblad Wingstrand**

Phone: +45 2890 5680  
E-mail: [saliwi@kt.dtu.dk](mailto:saliwi@kt.dtu.dk)

Supervisors: Ole Hassager  
Peter Szabo

PhD Study  
Started: Month 2014  
To be completed: Month 2017

## On the correlation between Young's modulus and melt flow in fiber spinning operations

### Abstract

Polymer fibers are known to have extraordinary strength. The outstanding properties are believed to be tied to molecular orientation in the solid fibers. This work aims to study the correlation between molecular orientation in polymers induced during uniaxial extensional flow and the final solid properties of the material. Here the initial results are presented along with a method on how to perform tensile testing on specimen with a non-homogeneous diameter. It is found that the solid properties of a well characterized low density polyethylene (LDPE) are reproduced very well confirming the validity of the presented method. In addition it is found that the stress at quench determines the solid properties of the material rather than the strain at quench.

### Introduction

Polymers in extensional flow is encountered in a wide range of polymer processing techniques, among others fiber spinning. Here we investigate the correlation between parameters of controlled uniaxial extensional flows and the final mechanical properties of the quenched samples. This has, until very recently, proved very challenging due to difficulties in obtaining a constant strain rate throughout the entire course of elongation. Consequently only very few studies report results on how flow induced molecular orientation of polymers in controlled uniaxial extension, influences the crystallinity and final mechanical properties of the fiber [1]. With the invention and optimization of the filament stretching rheometer (FSR) it is now possible to perform extensional nonlinear rheological experiments at a controlled strain rate and subsequently quench the sample [2]. Subsequently a wide range of solid characterization can be performed e.g. scattering, microscopy, differential scanning calorimetry as well as standard mechanical testing as will be presented here.

The FSR enables the response of viscous fluids (e.g. polymers) in uniaxial extension to be studied. It consists of a moving top plate and a stationary bottom plate (see fig. 1A). A molten sample between the two plates can thus be subjected to a uniaxial extensional flow by moving the upper plate while the response of the fluid is monitored using a force transducer mounted on the bottom plate. The deformation is measured in the mid-

filament plane using a laser sheet. Hence one can extract following quantities from one stretch experiment force ( $F$ ), top plate position ( $h$ ) and mid-filament plane diameter ( $D$ ), this also holds for solid samples.

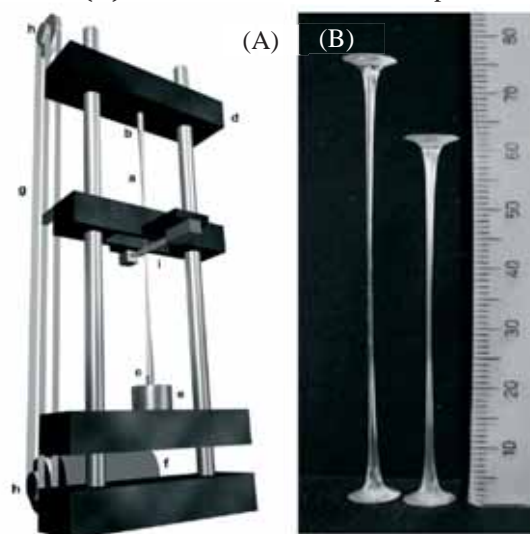


**Figure 1:** (A) Sketch of the FSR at DPC. (a) filament, (b) top plate, (c) stationary bottom plate, (d) movable support for top plate, (e) weighing cell (f) motor, (g) timing belts, (h) gearing and (i) laser [3]. (B) Example of quenched samples after deformation. In this case the samples are poly styrene [4].

In this study the deformation rate ( $\dot{\epsilon}$ ) in the melt is constant throughout the entire experiment hence the deformation ( $\epsilon$ ) increases linearly in time. In order to satisfy this condition the diameter ( $D$ ) must decrease exponentially in time as seen from eq. (1)

$$\epsilon(t) = -2 \ln\left(\frac{D(t)}{D_0}\right) \quad (1)$$

The final diameter profiles of quenched filaments created on a filament stretching rheometer vary with axial position ( $z$ ) (see fig. 1B). It is not possible to properly characterize the mechanical properties of such specimen in a regular “Instron”-type tensile machine as the deformation of the filament will vary axially.

Discretizing over the height of the sample enables the sample to be regarded as a stack of  $i$  discs with height  $h_i$  and diameter  $D_i$ , in doing so the Young’s modulus ( $E$ ) can be found just from the position of the top plate:

$$E = \frac{4F}{\pi(h - h_0)} \sum_i \frac{h_{i,0}}{D_{i,0}^2} \quad (2)$$

Here the lower case “0” indicate initial properties of the solid sample. This relationship between  $h$  and  $E$  rely on several assumptions. Most importantly the deformation is assumed to be small. Also the Young’s modulus is assumed to be independent of axial position.

## Experimental

The test material is LDPE Lupolen 3020D. Its rheology is well characterized [3] and tensile properties at quiescent conditions are known. LDPE discs of various height and diameter were placed in the FSR, melted and stretched at 130 °C and then quenched. The strain at quench  $\epsilon_q$  was varied among the samples. Subsequently solid tensile properties of the quenched filaments were measured using the FSR as well.

## Results and Discussion

In fig. 2, stress-strain curves across the mid-filament plane are shown for three different samples. It is seen that the quiescent sample shows clear sign of necking. The tensile properties of the quiescent sample are in fairly good agreement with values obtained in the literature (see Table 1). This is a good indication that the solid characterization of non-homogeneous specimen indeed is possible using the FSR.

The two remaining samples have been elongated in the melt state at  $\dot{\epsilon} = 0.03 \text{ s}^{-1}$ . At this rate the Lupolen 3020D shows a stress overshoot at  $\epsilon \approx 3.6$  before reaching steady state at  $\epsilon \approx 4.8$  [6]. Hence these two

**Table 1:** Solid properties of samples quenched at various  $\epsilon_q$ . A quiescent sample and literature values are presented as well.

$\epsilon_q$	$E$ [GPa]	$\epsilon_y$ [-]	$\sigma_y$ [MPa]
Ref.[7]	0.300	0.127	13.0
Quiescent	$0.35 \pm 0.01$	$0.09 \pm 0.03$	$10.0 \pm 0.9$
3.6	$0.38 \pm 0.02$	$0.093 \pm 0.008$	$11.9 \pm 0.9$
4.8	$0.37 \pm 0.03$	$0.081 \pm 0.009$	$11.7 \pm 0.8$

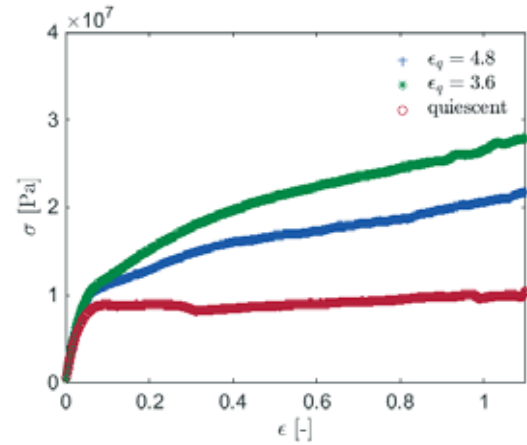


**Figure 2:** Stress strain curves for LDPE samples extended at a rate of  $\dot{\epsilon} = 0.03 \text{ s}^{-1}$  and quenched at various  $\epsilon_q$  along with sample at quiescent conditions.

values were chosen as  $\epsilon_q$ . It is seen that these two samples are stiffer than the quiescent sample and they do not show any sign of necking. This trend is expected as the uniaxial flow orients the molecules, thereby increasing the crystallinity of the sample. The really interesting point, though, is that the sample with  $\epsilon_q = 3.6$  is stiffer than the sample with  $\epsilon_q = 4.8$  suggesting that stress at quench determines the solid mechanical properties rather than the strain which is the general perception. These results need further validation before anything certain can be concluded.

## Conclusion

Tensile testing of samples with non-homogeneous diameter in the FSR was successful. In relation to the correlation between melt flow and solid properties of the LDPE, it was found that necking was suppressed in samples that had been subjected to a nonlinear uniaxial elongation prior to quenching. Furthermore results suggest that the stress at quench determines the solid properties rather than the strain at quench.

## References

1. B. E. White, H.H. Winter, J. P. Rothstein, *Rheologica Acta*, 51(4) (2011), 303–314.
2. Román Marín, J.M., J.K. Huusom, N.J. Alvarez, Q. Huang, H.K. Rasmussen, A. Bach, A.L. Skov, and O. Hassager, *J. Nonnewton. Fluid Mech* 194 (14) (2013).
3. A. Bach, H. Koblitz, P. Longin, and O. Hassager, *Journal of Non-Newtonian Fluid Mechanics* 108 (2002) 163–186.
4. Nielsen, J.K., H.K. Rasmussen, and O. Hassager, *J. Rheol.* 52 (4) , 885 (2008).
5. Nielsen, J.K., H.K. Rasmussen, and O. Hassager, *J. Rheol.* 52 (4) , 885 (2008).
6. Rasmussen, H.K., J.K. Nielsen, A. Bach, and O. Hassager, *J. Rheol.* 49 (2) , 369 (2005).
7. BASF, LyondellBasell Lupolen® 3020 D LDPE, url: <http://www.matweb.com/>, 22/04/2015



**Mengzhe Wu**

Phone: +45 4525 2802  
E-mail: mewu@kt.dtu.dk

Supervisors: Krist V. Gernaey  
Ulrich Krühne  
Jakob Kjøbsted Huusom

PhD Study  
Started: December 15 2014  
To be completed: December 14 2017

## Development of optimal operating conditions for producing single cell protein

### Abstract

Unlike many other bio-chemicals, Single Cell Protein is a commodity product. Therefore, it is essential that the production of SCP is energy and nutrient efficient and can be produced at a high yield. One of the main problems facing the production of Single Cell Protein fermentation is the mass transfer of oxygen from the supplied gas to the liquid media as well as the efficient recovery of the biomass. An attractive future alternative to classical fermentation systems is the cultivation of the organism in a continuous U-loop fermentor to enhance the mass transfer.

### Introduction

Proteins and amino acids are essential food ingredients for humans and animals. Soya beans and fish are important sources of protein for animal feed; in turn, the animals serve as protein sources in human nutrition. With the increasing world population, the demand for proteins increases. One of the important non-conventional protein sources is single cell protein (SCP), which is protein obtained from microbial sources. Currently, agricultural products such as soybean are outcompeting SCP due to their lower price. Therefore, optimizing the efficiency in SCP production and reducing operation cost without reducing the protein yield is required to achieve an economically viable SCP production process.

Rose (1979) has shown that continuous operation is advantageous in economic terms for microbial SCP production. The cultivation normally involves several basic process engineering unit operations, such as stirring and mixing of a multi-phase system (gas-liquid-solid), transport of oxygen from the gas bubbles through the liquid phase to the microorganisms, and heat removal from the liquid phase. One of the main problems related to the SCP production via fermentation is the mass transfer of oxygen from the supplied gas to the liquid media as well as the efficient recovery of the biomass. An attractive future alternative to classical stirred tank reactors is the cultivation of the organism in a continuous U-loop fermenter (Figure 1) to enhance the mass transfer.

Modelling, simulation and optimization of such a U-loop reactor requires dynamic models. In the literature,

some basic approaches to dynamic flow simulation of the gas-liquid system in a U-loop reactor have been discussed. Prado-Rubio *et al.* (2010) have modelled the U-loop reactor as a Tanks-in-Series system. Olsen *et al.* (2010) have treated the U-loop reactor as an integrated system consisting of a mixer, a PFR and a CSTR. To date, both approaches considered liquid and gas phase motion in a homogeneous way, or in other words, few studies have dealt with the detailed fluid flow pattern within the reactor.

### Specific Objectives

The scientific objective of the project is to model, simulate and control the operation of a pilot-scale (100L) continuous fermentation process for production of single cell protein (SCP). The first stage of the project aims at modelling the SCP production in the U-loop. Using Computational Fluid Dynamics (CFD), a three-dimensional two-phase model is set up to obtain a better understanding of the phenomena occurring in the U-Loop reactor and to investigate the implication of design changes on process performance. Parallel to the simulation work, the lab experiments will start up. Whenever the pilot data is available, it will be compared with the simulation results, such that model simulations can be validated. To the extent possible, the model will indeed be calibrated to the data and validated. Based on the validated simulation model, design concepts such as the geometry and placement of gas spargers and static mixers will be optimized so these solutions can be tested in the pilot-scale facilities afterwards.

At the end of this stage, the model, parameterized using data obtained from the pilot plant, will facilitate the prediction of the effect of changes in fermentation operation conditions, such as feed composition, gas flow rate, position of gas injection and recirculation flow rate, and even the scale-up of the production. After the validation, an optimal and feasible operational strategy for the fermentor will be explored. This will lead to the synthesis of a low level control design for regulatory control and possibly a high level coordination control strategy for optimization.

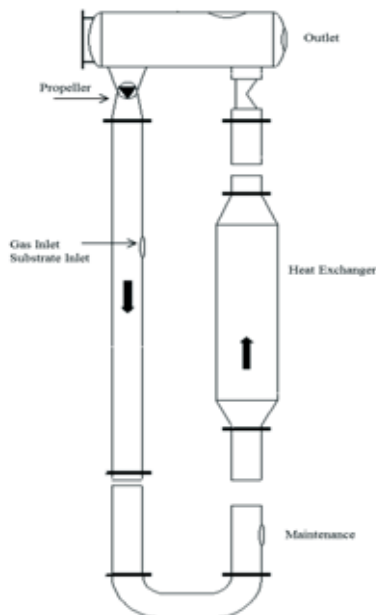


**Figure 1.** The U-loop Reactor pilot plant at the Technical University of Denmark. (Technical details are not provided for confidentiality reasons)

### Current Results and Discussion

A simple CSTR one-phase dynamic model and a three-dimensional one-phase model using Computational Fluid Dynamics (CFD) have been developed to make a comparison for the available experimental data. And the main assumptions different from Olsen *et al.* (2010) are:

1. There is only a liquid phase in the model.
2. The reactor is assumed well-mixed.
3. Oxygen supply in the liquid phase is assumed to have a constant  $k_{LA}$  and saturation oxygen concentration.

For the three-dimensional one-phase model using Computational Fluid Dynamics (CFD). The main assumptions are:

1. The recirculation pump is not modelled; instead an impulse source is introduced to simulate the pump impact.
2. A standard  $k-\epsilon$  model is applied for the turbulence model.

The comparison is based on the following operating conditions: the dilution rate is 0.04 1/h and the gas pressure is 1 atm. The start-up conditions are 1 kg/m<sup>3</sup>

biomass on the left, and 16 kg/m<sup>3</sup> biomass on the right in Figure 2.

The lower initial biomass concentration (Figure 2, left) shows a wash out situation for the biomass for both models. The biomass starts to grow when the concentration at the start is 4 kg/m<sup>3</sup> or more. In general, both CSTR and CFD simulations show the same trends under different operation conditions. However, biomass grows slower in the U-loop reactor simulated by CFD than in the CSTR. This reflects the effect of the real mixing situation in the U-loop reactor compared with an ideal mixing assumption of the CSTR reactor.

### Conclusion and Future work

The CFD model considers the hydrodynamic information by introducing the fluid dynamic equations, and generally predicts lower biomass growth compared to the CSTR model. On the other hand, the CFD applies the fluid model treating the gas and liquid effectively in predicting the performance of the reactor.

The future work includes the development of a two-phase CFD model that should allow a description of differences between gas and liquid flow velocity. A reliable prediction of the flow pattern is a necessary prerequisite for the oxygen mass transfer investigation and the selection of the correct value of  $k_{LA}$ , but also for the prediction of the scale up of the SCP production. This knowledge of the process behaviour gained from the simulation work will then lead to the optimal operation conditions and control strategy set-up.

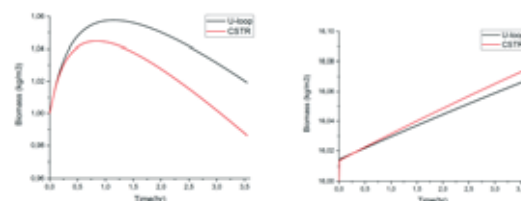


**Figure 2.** Biomass growth predicted by CSTR and CFD models

### Acknowledgements

The PhD project is funded by Innovation Fund Denmark (project “Environmentally Friendly Protein Production (EFPro2)”) and the Technical University of Denmark (DTU).

### References

1. D. F. Olsen, J. B. Jørgensen, J. Villadsen, and S. B. Jørgensen. Modeling and simulation of single cell protein production. Computer Applications In Biotechnology, 2010.
2. O. Prado-Rubio, J. B. Jørgensen, and S. B. Jørgensen. Systematic model analysis for single cell protein production in a U-loop reactor. 20th European Symposium on Computer Aided Process Engineering (ESCAPE20). 2010
3. A.H. Rose. Microbial Biomass in Economic Microbiology. Academic Press. London, 2. edition, 1979.

**Shamsul Zakaria**

Phone: +45 4525 6817  
E-mail: shaza@kt.dtu.dk  
Discipline: Chemical Engineering

Supervisors: Anne Ladegaard Skov

**PhD Study**

Started: January 2013  
To be completed: January 2016

## The influence of static pre-stretching on the mechanical ageing of filled silicone rubbers for dielectric elastomer applications

**Abstract**

Dielectric elastomer (DE) pre-stretching is a key aspect of attaining better actuation performance, as it helps prevent electromechanical instability (EMI) and usually lowers the Young's modulus, thus leading to easier deformation. The pre-stretched DE is not only susceptible to a high risk of tearing and the formation of mechanical defects, but films with sustained and substantial strain may also experience mechanical degradation. In this study a long-term mechanical reliability study of DE is performed. Young's moduli and dielectric breakdown strengths of commercial silica(SiO<sub>2</sub>)-reinforced silicone elastomers, with and without an additional 35% (35 phr) of titanium dioxide (TiO<sub>2</sub>), were investigated after being subjected to pre-stretching for various timespans at pre-stretches to strains of 60 and 120%, respectively. The study shows that mechanical stability when pre-stretching is difficult to achieve with highly filled elastomers. However, despite the negative outlook for metal oxide-filled silicone elastomers, the study paves the way for reliable dielectric elastomers by indicating that simply post-curing silicone elastomers before use may increase reliability.

**Introduction**

Incorporating rigid fillers, such as titanium dioxide, into the cross-linked PDMS matrix increases the dielectric permittivity of the resulting composite elastomer. Mechanical properties are also affected, with results varying according to particle size and surface treatment, from reinforcing to softening<sup>1</sup>. On the other hand, a thinly filled elastic film that maintains high strain for a given period of time will, to some extent, suffer mechanical ageing at the microscopic level. The Payne and Mullins effects explain hysteresis in the mechanical properties of filled elastomers. The Payne effect refers to the effect of the strain dependence of the dynamic viscoelastic properties of filled elastomers above their glass transition temperature<sup>2</sup>. Clement et al.<sup>3</sup> investigated the Payne effect in SiO<sub>2</sub>-filled PDMS elastomers, and they posited it as the existence of a gradient in elastomeric chain mobility from the PDMS filler interface to the bulk, leading to a stress-softening effect at low strains upon "initial activation" of the elastomer.

Generally, silicone elastomers are commercially synthesized through the equilibration polymerization of cyclic oligomers and end groups in the presence of acid or basic catalysts<sup>4</sup>. One of the disadvantages of this process is the production of by-products as a result of the reaction, consisting of unreacted cyclic oligomers<sup>5</sup>.

These residues are mobile within the silicone, and they can also migrate to a device interface. This migration during post-manufacture changes the elastomer surface as well as its mechanical properties such as tensile strength, tear strength, maximum elongation, etc.<sup>6</sup>. As reported by Brook et al.<sup>7</sup>, these volatile siloxanes from commercial silicones usually remain within the elastomer when post-curing has been omitted. Post-curing is usually conducted by heating the elastomer far above its curing temperature but below its degradation temperature for some time. Brook et al.<sup>7</sup> showed that the mechanical properties of the elastomer were enhanced (a larger Young's modulus, greater tensile strength and lower maximum extensibility) upon post-curing.

As reported by Meunier et al.<sup>8</sup>, unfilled PDMS lacks the Mullins effect, hysteresis and strain rate dependency. However, for DE applications filled, reinforced silicones are required to obtain acceptable performance. This study was performed in order to understand the intrinsic mechanical behavior of pre-stretched PDMS elastomers, with and without additional permittivity enhancing fillers, over time. Furthermore, the study aims at elaborating how mechanical ageing affects other parameters relevant to the DE being used, namely the Young's modulus, breakdown strength and dielectric permittivity.

## Methodology

### Materials

Four different compositions from two commercial silicone elastomers, without and with one type of permittivity enhancing filler ( $\text{TiO}_2$ ), were investigated. The elastomers were POWERSIL® LR 3043/30 A/B and ELASTOSIL® RT625 A/B. POWERSIL® LR3043/30 A/B is a high-viscosity LSR and is supplied as a two-part system. The mixing ratio of parts A and B is 1:1. ELASTOSIL® RT625 A/B is an RTV elastomer, which is also supplied as a two-part system. The mixing ratio for parts A and B is 9:1. The permittivity-enhancing filler added is alumina-silica-zirconia surface-treated hydrophobic rutile titanium dioxide ( $\text{TiO}_2$ ) Sachtleben® R420® from Sachtleben Chemie, Duisburg, Germany, while the average primary particle size is 250 nm. The filler is added in a weight percentage of the original elastomer (i.e. phr) of 35%. Solvent (OS-20) is added to all elastomers, to reduce the viscosity of the formulations and thereby ease the coating of thin films.

### Sample preparation

Thin films were carefully prepared based on the procedures described in Zakaria et al.<sup>9</sup> For this study, two sample thicknesses were targeted by using different blade gaps, namely 150  $\mu\text{m}$  (relatively thinner films) and 200  $\mu\text{m}$  (relatively thicker films). Film thicknesses were approximately 34-88  $\mu\text{m}$  and 52-119  $\mu\text{m}$  for the thin and thick samples, respectively. Film details can be seen in Table 1.

### Pre-stretching of the samples

The samples were pre-stretched on an in-house-built frame. The films were 130 mm in width and 350 mm in length. In order to pre-stretch the films successfully, both ends were rolled with metal rods to prevent slippage. Then the metal rods, together with the stretched films, were attached to the frame, as shown in Figure 1. The films were then covered by 50  $\mu\text{m}$ -thick ETFE foils to prevent them from contamination. Finally, they were stored for different timespans: one day, one week, one month and three months, before they were released for further characterization.

**Table 1:** Details of prepared  $\text{SiO}_2$ -filled (commercial) and  $\text{SiO}_2$ - $\text{TiO}_2$ -filled (composite) PDMS films.

Sample ID	Material	Thickness	Pre-stretch (%)
A1	RT625	Thin	60
A2	RT625	Thin	120
A3	RT625	Thick	60
A4	RT625	Thick	120
B1	LR304330	Thin	60
B2	LR304330	Thin	120
B3	LR304330	Thick	60
B4	LR304330	Thick	120
C1	RT625+35%R420	Thin	60
C2	RT625+35%R420	Thin	120
C3	RT625+35%R420	Thick	60
C4	RT625+35%R420	Thick	120
D1	LR304330+35%R420	Thin	60
D2	LR304330+35%R420	Thin	120
D3	LR304330+35%R420	Thick	60
D4	LR304330+35%R420	Thick	120



**Figure 1:** The device used to pre-stretch the thin filled PDMS elastomer films. The pre-strains were adjusted by changing the position of the metal rods.

## Results and discussions

In Figure 2, the Young's moduli at  $s=120\%$  have been plotted as functions of time for both thin and thick films. The most significant observable mechanical degradation was obtained for composite D2, as the Young's modulus at  $s=120\%$  of the non-aged reference sample declines by a factor of approximately four after three months of pre-stretching (2.55 MPa and down to 0.66 MPa). However, only slight changes to the Young's moduli at  $s=120\%$  were obtained for A2 samples (0.70-0.45 MPa). This indicates a longer term of mechanical reliability for  $\text{SiO}_2$ -filled elastomers compared to composite elastomers. This is also expected, as commercial elastomers are formulated to high standards. As reported by Dorfmann and Ogden<sup>10</sup>, the effect of stress softening is only present to a small extent in unfilled compounds and elastomers with low filler content.

It is clear that the Young's moduli for different PDMS materials and conditions at  $s=120\%$  vary significantly over time. The effect of pre-stretching on the mechanical degradation of filled PDMS films can be seen clearly in Figure 2. The samples that had larger pre-stretches ( $s=120\%$ ) reveal severe mechanical ageing (red circle and violet downward triangle) compared to the samples that were subjected to smaller pre-stretching ( $s=60\%$ ) (black square and blue upward triangle), due to stress-softening increasing progressively in line with the increasing strain<sup>11</sup>. Even though the dependency of mechanical ageing on thickness was not clearly noticeable in Figure 2, nevertheless the coupling of the thin film and a larger strain demonstrates the most severe effect on the mechanical ageing of filled PDMS films. Thick samples will experience delayed ageing, because the constructive evaporation of cyclic silicones and destructive structure changes appear simultaneously at the timescales investigated within this study.

For the two composite formulations, the composite RTV (C2) shows the severest loss of tension on the one month time scale, but it continues to lose tension over time. The composite LSR formulation obviously loses significant tension, with a drop in Young's moduli greater than 50% for all strains investigated following three months of ageing at a pre-stretch of 120%.

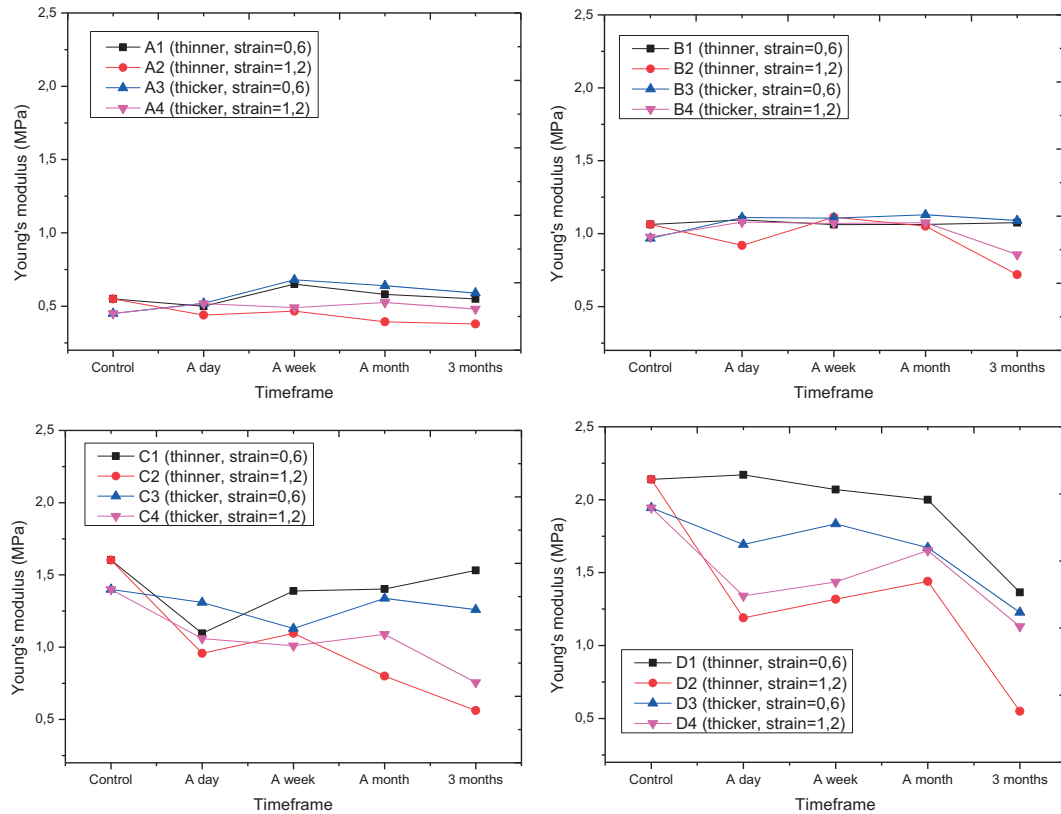


**Figure 2:** Young's moduli of different samples measured at  $s = 120\%$  after pre-stretching from time=0–control to 3 months. A= RT625, B= RT625+35% TiO<sub>2</sub>, C= LR3043/30 and D= LR3043/30+35% TiO<sub>2</sub>. Conditions for A1, B1, C1 and D1= the films were coated with a 150  $\mu\text{m}$  blade (thin films) and  $s = 60\%$ , A2, B2, C2 and D2= the films were coated with a 150  $\mu\text{m}$  blade (thin films) and  $s = 120\%$ , A3, B3, C3 and D3= the films were coated with a 200  $\mu\text{m}$  blade (thick films) and  $s = 60\%$  and A4, B4, C4 and D4= the films were coated with a 200  $\mu\text{m}$  blade (thick films) and  $s = 120\%$ .

To illustrate the loss of tension in the elastomers over time, stress-strain diagrams under cyclic loading conditions are shown in Figure 3. The cyclic deformation diagrams are shown for two representative samples (lowest (A) and highest (D) total filler content, respectively). Initially before ageing, the control sample strongly exhibits Mullins softening, as the area of

hysteresis loop for the first deformation is approximately three times that of the second deformation for both the A2 and D2 samples. After constant pre-stretching, the Mullins effect becomes less pronounced for the aged sample, since the area of the initial hysteresis loop decreases significantly.

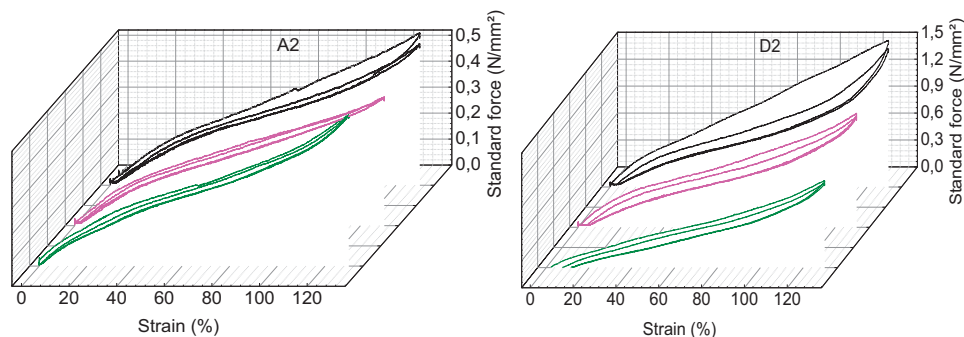


**Figure 3:** Stress-strain diagrams of control (black), 1 month (violet) and 3 months (green) of RTV elastomer (A2) and composite LSR (D2) sample (pre-stretching 120%).

### Breakdown strength

Since the mechanical properties of pre-stretched PDMS films change over time, it can be argued that the breakdown strengths of filled PDMS films are also likely to change. The thicknesses of the investigated

films cannot be controlled precisely due to different PDMS formulation viscosities, and the variation in thicknesses. Simultaneously, as mechanical properties change, breakdown strengths will also change<sup>12</sup>, and as discussed previously the Young's moduli do not change

monotonically. For better comparison –without complications aligned with thickness variations – the breakdown strengths of several samples with minimal thicknesses deviations ( $\pm 3 \mu\text{m}$ ) in relation to the control samples were compared, as shown in Table 2. The breakdown results for the one- and three-month samples were chosen, as they show greatest effect of volatile siloxanes diffusion. The standard deviations were considerably greater for several samples, due to the non-

uniformity of film thicknesses and defects contained in the prepared samples, while the major uncertainty of the breakdown data may also indicate bimodal distributions of breakdown strengths for several samples. Nonetheless, the data in Table 2 confirm that the breakdown strengths lower in line with mechanical ageing, due to the decrease in the Young's modulus of the aged samples<sup>12</sup>.

**Table 1:** Breakdown strengths of several samples that have thickness differences at  $\pm 3 \mu\text{m}$  in relation to the thicknesses of the control films

Sample ID	Control			1 Month		3 Month			
	Sample thickness ( $\mu\text{m}$ )	Breakdown strength ( $\text{V}/\mu\text{m}$ ) (Un-stretched)	Breakdown strength ( $\text{V}/\mu\text{m}$ ) (stretched)	Sample thickness ( $\mu\text{m}$ )	Breakdown strength ( $\text{V}/\mu\text{m}$ ) (Un-stretched)	Breakdown strength ( $\text{V}/\mu\text{m}$ ) (stretched)	Sample thickness ( $\mu\text{m}$ )	Breakdown strength ( $\text{V}/\mu\text{m}$ ) (Un-stretched)	Breakdown strength ( $\text{V}/\mu\text{m}$ ) (stretched)
A3	106	98 $\pm$ 4	160 $\pm$ 3	108	90 $\pm$ 8	125 $\pm$ 6			
B4	63	101 $\pm$ 5	169 $\pm$ 3	66	95 $\pm$ 6	161 $\pm$ 3			
C1	67	113 $\pm$ 3	159 $\pm$ 7	67	111 $\pm$ 4	151 $\pm$ 3			
C2	67	113 $\pm$ 3	194 $\pm$ 5	64	97 $\pm$ 3	166 $\pm$ 5			
A2	73	97 $\pm$ 4	160 $\pm$ 2				76	89 $\pm$ 4	146 $\pm$ 3
C3	89	114 $\pm$ 5	144 $\pm$ 4				88	98 $\pm$ 8	142 $\pm$ 5
C4	89	114 $\pm$ 5	190 $\pm$ 2				88	77 $\pm$ 5	126 $\pm$ 4
D2	41	141 $\pm$ 4	266 $\pm$ 6				41	133 $\pm$ 6	249 $\pm$ 6

## Conclusion

Dielectric elastomers with enhanced permittivity are heavily sought after for enhanced actuation, and so many approaches in this respect are being currently developed. The addition of high-permittivity metal oxide fillers to silicone elastomers is a facile method for such an enhancement, but studies so far have focused solely on how the metal oxides affect instant mechanical behavior. In this study we show that titanium dioxide cannot be added unlimitedly when pre-stretching the elastomer, since the composites lose their tension very quickly. If such high loadings of fillers are required, it is important to further functionalize the particles for better compatibility and integrity. Another important finding is that even commercial silicone elastomers require post-curing for mechanical stability, which is an overlooked feature for silicone elastomers utilized in dielectric elastomers. The two commercial elastomers in this research (RT625 and LR3043/30) both showed improved strength over a time scale of weeks, and thus a decrease in actuation will take place. This phenomenon can be ascribed to the evaporation of volatile cyclic silicones and other residues from elastomers which have had their protective surface broken during pre-stretching. Over a timescale of months, a slight reduction in elasticity takes place due to ageing. In other words, the elastomer will not provide constant actuation over time if it is not ensured beforehand that all volatiles have been removed. The removal of volatiles is additionally favorable, as it increases breakdown strength and thus enhances the reliability of the elastomer.

## Acknowledgement

The authors gratefully acknowledge the financial support from the Ministry of Education of Malaysia and Universiti Malaysia Pahang. Danfoss PolyPower A/S is also acknowledged for financial support to Z. Shamsul.

## References

1. S. Vudayagiri, S. Zakaria, L. Yu, S. S. Hassouneh, M. Benslimane, and A. L. Skov, "High breakdown-strength composites from liquid silicone rubbers," *Smart Materials and Structures* **23**(10), p. 105017 (2014).
2. A. R. Payne and G. Kraus, "Reinforcement of elastomers," in *Interscience, New York* **69**, p. 69–123, Interscience publication, New York, USA (1965).
3. F. Clément, L. Bokobza, and L. Monnerie, "Investigation of the Payne Effect and its Temperature Dependence on Silica-Filled Polydimethylsiloxane Networks. Part II: Test of Quantitative Models," *Rubber Chemistry and Technology* **78**(2), p. 232–244 (2005).
4. J. Chojnowski, *Polymerization in Siloxane Polymers*, PTR Prentice Hall, Englewood Cliffs, New Jersey (1993).
5. W. Noll, *Chemistry and Technology of Silicones*, Academic, New York (1968).
6. A. Ghosh, R. S. Rajeev, A. K. Bhattacharya, A. K. Bhowmick, and S. K. De, "Recycling of silicone rubber waste: Effect of ground silicone rubber vulcanizate powder on the properties of silicone rubber," *Polymer Engineering & Science* **43**(2), p. 279–296 (2003).
7. M. A. Brook, H.-U. Saier, J. Schnabel, K. Town, and M. Maloney, "Pretreatment of Liquid Silicone Rubbers to Remove Volatile Siloxanes," *Industrial & Engineering Chemistry Research* **46**(25), p. 8796–8805, American Chemical Society (2007).
8. L. Meunier, G. Chagnon, D. Favier, L. Orgéas, and P. Vacher, "Mechanical experimental characterisation and numerical modelling of an unfilled silicone rubber," *Polymer Testing* **27**(6), p. 765–777 (2008).
9. A. L. Skov, S. Vudayagiri, and M. Benslimane, "Novel silicone elastomer formulations for DEAPs," in *Proceeding of SPIE: 8687I*, p. 86871I – 86871I – 8, International Society for Optics and Photonics (2013).
10. A. Dorfmann and R. W. Ogden, "A constitutive model for the Mullins effect with permanent set in particle-reinforced rubber," *International Journal of Solids and Structures* **41**(7), p. 1855–1878 (2004).
11. J. Diani, B. Fayolle, and P. Gilormini, "A review on the Mullins effect," *European Polymer Journal* **45**(3), p. 601–612 (2009).
12. M. Kollosche, H. Stoyanov, H. Ragusch, S. Risse, A. Becker, and G. Kofod, "Electrical breakdown in soft elastomers: Stiffness dependence in un-pre-stretched elastomers," in *Proceedings of the IEEE International Conference on Solid Dielectrics, ICSD*, p. 1–4, IEEE (2010).

**Guofeng Zhou**

Phone: +45 4525 2853  
E-mail: guzho@xx.dtu.dk

Supervisors: Anker Degn Jensen  
Peter Arendt Jensen  
Niels Ole Knudsen, DONG Energy

PhD Study  
Started: October 2012  
To be completed: September 2015

## Atmospheric hydrodeoxygenation of lignin fast pyrolysis vapor by MoO<sub>3</sub> catalyst

### Abstract

Lignin fast pyrolysis and direct upgrading of pyrolysis vapor over MoO<sub>3</sub> under H<sub>2</sub> was studied using a Pyrolysis Centrifuge Reactor. Direct upgrading of lignin pyrolysis vapor can be done to achieve a yield of 17 wt.%<sub>daf</sub> organic liquid, while achieving 47 % of deoxygenation at 450 °C catalyst temperature under 85 % mole concentration of H<sub>2</sub> estimated in the gas phase. The corresponding energy recovery is 24 %. Compared to untreated bio-oil the upgraded lignin organic liquid showed improved compatibility with hydrocarbons, for instance it is miscible with a toluene/heptane mixture.

### Introduction

Fast pyrolysis technology has been developed for more than 40 years. By this process, biomass is heated to 450°C – 600°C in the absence of oxygen, whereby it is converted into a liquid product, known as bio-oil, as well as a solid char and gases. The oxygen content of the bio-oil is typically similar to its biomass precursor. For example, the oxygen content of lignin derived bio-oil is 25 wt.%, compared to 24 wt.% oxygen in the lignin.[1] A subsequent catalytic upgrading step can be used to remove the oxygen and transform the bio-oil into a liquid product which is compatible with engine fuels.

Hydrodeoxygenation of bio-oil model compounds and real lignin in a micro scale batch pyrolyzer by MoO<sub>3</sub> under low H<sub>2</sub> pressure have been proved possible.[2,3] We investigated such an upgrading technique in a bench scale continuous pyrolysis centrifuge reactor to pyrolyze the biomass and a close coupled catalytic reactor for in-situ hydrodeoxygenation of the pyrolysis vapor using MoO<sub>3</sub> catalyst.

### Materials and Methods

The lignin particles are fed tangentially to the horizontally oriented reactor cylinder where the centrally mounted arch-shaped rotor pushes the particles against the reactor wall. The reactor is kept at 500°C. While circulating on the wall, the particles simultaneously move axially towards the tangential reactor outlet. External to the reactor, the flow of gas and particles are first directed to a simple change-in

flow-direction separator (460°C), a cyclone (440 °C) and then a hot gas filter (300°C) to remove solid chars. The char free gas then passes through a catalytic reactor. The liquid product is condensed in a series of condensers placed in a cooling bath (-20°C) and a dry ice/ethanol bath (-70°C). A carrier gas, 4 NI/min H<sub>2</sub> preheated to 450 °C is introduced to the reactor, which provides a gas residence time inside the reactor of 1.8 seconds and about 85 mole% of H<sub>2</sub> in the gas phase. A typical run lasts 25 minutes with 1.7–2.1 g/min feeding rate of lignin. For each experiment, 40 g MoO<sub>3</sub> (500 – 850 μm; ≥ 99.5 %; Sigma-Aldrich) and 60 g sand (350 – 450 μm) were used.

### Results and Discussion

The effect of catalyst temperature on MoO<sub>3</sub> hydrodeoxygenation of lignin derived pyrolysis vapor was conducted from 350°C to 550°C. The product yields are shown in Figure 1. The organic liquid yield decreased with increasing catalyst temperature. The oxygen in the organic liquid was rejected in the form of water, as the yield of reaction water increased with increasing catalyst temperature until 500 °C and then decreased again. The lower yield of reaction water at the highest catalyst temperature of 550 °C is probably due to fast reduction of MoO<sub>3</sub> to MoO<sub>2</sub> and MoO<sub>2</sub> is not an active catalyst. The total gas formation increased with increasing catalyst temperature. As shown in Figure 2, the yields of CO and C<sub>2+</sub> increased with catalyst temperature and the yields of CO<sub>2</sub> and CH<sub>4</sub> peaked at 450°C and 500°C, respectively. Hence oxygen was also

rejected in the form of CO<sub>2</sub> and CO. At 350°C catalyst temperature, the coke yield was negligible, but at temperatures higher than 350 °C, the coke yield was significant, in the range of 3-4 wt.% daf.

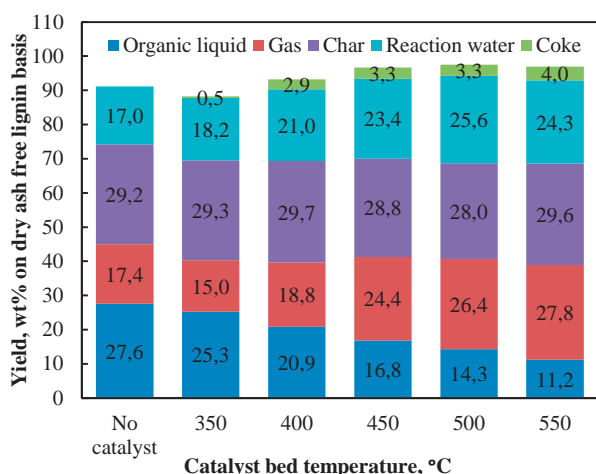


**Figure 1:** Product yields from lignin fast pyrolysis and MoO<sub>3</sub> atmospheric hydrodeoxygenation at different catalyst temperature.

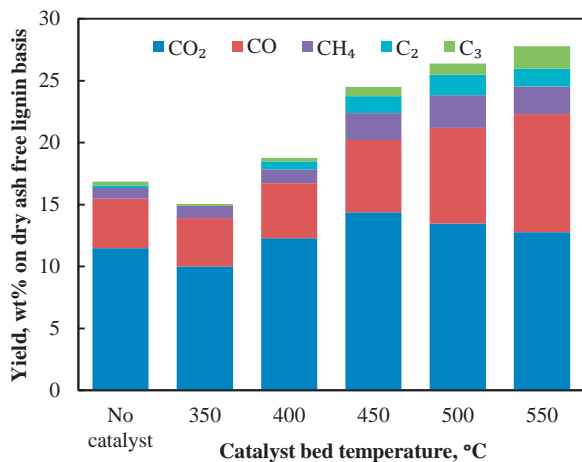


**Figure 2:** The yield of individual gas components from MoO<sub>3</sub> hydrodeoxygenation of lignin derived pyrolysis vapor at different catalyst temperature.

Few aromatic hydrocarbons were identified in the upgraded organic liquid, among which the experiment conducted at 500°C gave the highest yield of aromatic hydrocarbons of 1.87 wt.% daf. Most of the organic liquid species were not identified. The unidentified fraction had lower oxygen content than the non-catalytic upgraded bio-oil (23.4 wt.%). The oxygen content of the total upgraded organic liquid can be found in Figure 3. The best temperature was found to be 450°C, which achieved the highest deoxygenation level with only 12 wt.% oxygen in the total organic liquid. Ideally, the MoO<sub>3</sub> hydrodeoxygenation step should operate at temperatures lower than 400°C to avoid quick reduction of MoO<sub>3</sub> to MoO<sub>2</sub>. However, temperatures lower than 450°C did not result in significant level of deoxygenation for the lignin fast pyrolysis vapor. At

higher temperatures than 450°C, the oxygen content increased again. This is because that MoO<sub>3</sub> was reduced to MoO<sub>2</sub>. The energy recovery of the total organic liquid decreased from 33% for the non-catalytic run to 24%, when the catalyst is operated at 450°C. One improved property of the upgraded organic liquid is better miscibility with, for instance aromatics. A simple compatibility test of untreated organic liquid (unidentified heavy fraction) and the upgraded organic liquid (unidentified heavy fraction) with toluene/heptane (1:1 on weight basis) was performed. The test was simply conducted by adding toluene/heptane mixture into the unidentified heavy organic liquids, which were not evaporated during rotary evaporation. The upgraded heavy organic liquid is miscible with the toluene/heptane mixture, but this is not the case for the non-upgraded organic liquid.

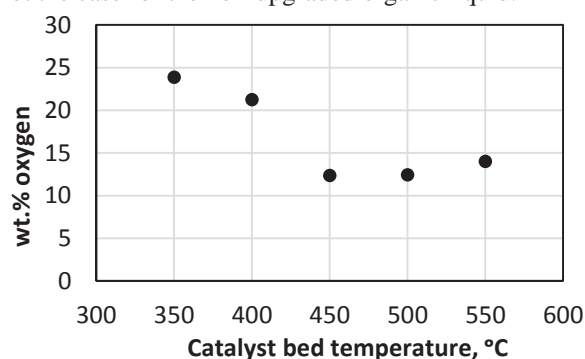


**Figure 3:** Oxygen contents of the total organic liquids from MoO<sub>3</sub> hydrodeoxygenation of lignin derived pyrolysis vapor at different catalyst temperatures.

## Conclusion

Lignin was pyrolyzed in a continuous pyrolysis reactor and the pyrolysis vapor was subsequently upgraded directly over a downstream, close coupled, fixed bed reactor containing the MoO<sub>3</sub> catalyst. Temperatures > 400°C were needed to obtain a decent degree of hydrodeoxygenation. The yield of organic liquid was 17 wt.% and achieved a 47 % degree of deoxygenation. The energy recovery was 24%. When operating the catalyst at high temperature (≥450 °C), a severe reduction of MoO<sub>3</sub> to MoO<sub>2</sub>, which is not a hydrodeoxygenation catalyst, was observed. There is thus a delicate tradeoff between catalyst activity and deactivation at the optimum temperature. The improved compatibility of the final liquid product with hydrocarbons however, is expected to make the product easy to be integrated into refinery streams.

## References

1. T.N. Trinh, P.A. Jensen, Z. Sárossy, K. Dam-Johansen, N.O. Knudsen, H.R. Sørensen, H. Egsgaard, *Energy Fuels* 27 (2013) 3802-3810.
2. D.A. Ruddy, J.A. Schaidle, J.R. Ferrell III, J. Wang, L. Moens, J.E. Hensley, *Green Chem.* 16 (2014) 454-490.
3. M.W. Nolte, J. Zhang, B.H. Shanks, B. H. Green Chem. 2015.



**Andreas Åberg**

Phone: +45 4525 2912  
E-mail: aben@kt.dtu.dk

Supervisors: Jens Abildskov  
Jakob Kjøbsted Huusom  
Anders Widd, Haldor Topsøe A/S

PhD Study  
Started: August 2013  
To be completed: October 2016

## Modeling the automotive SCR system

### Abstract

Diesel engine exhaust gases contain amongst other things nitrous gases such as NO and NO<sub>2</sub>. Reducing the amount of these gases is of great importance due to new legislation, and because of the effect they have on urban air quality. A promising and widely used technology for this is based on selective catalytic reduction (SCR) of the gases, with ammonia as a reducing agent. A model for the SCR catalyst was derived based on first principles. The kinetic model was calibrated with bench-scale equipment and validated using full-scale equipment. The project is in collaboration with Haldor Topsøe A/S.

### Introduction

Heavy duty diesel (HDD) vehicles handle a substantial part of the world's transport and logistics. Harmful pollutants are however formed, such as nitrogen oxides (NO<sub>x</sub>), hydrocarbons (HC), particulate matter (PM), and carbon monoxide (CO) [1]. The diesel exhaust after treatment (DEA) system has been developed to treat the pollutants in the exhaust gas. Figure 1 illustrates the current standard DEA system consisting of a series of catalytic units. The Diesel Oxidation Catalyst (DOC) oxidizes CO and HC to CO<sub>2</sub> and H<sub>2</sub>O, as well as generates NO<sub>2</sub> from NO. The Diesel Particulate Filter (DPF) is a wall-flow filter, entraining PM in its monolith walls. The DPF can be regenerated actively by increasing the exhaust gas temperature using post-injection of fuel, or passively using a catalyst. NO<sub>2</sub> generated by the DOC also assists regeneration. NO<sub>x</sub> is treated through Selective Catalytic Reduction (SCR) using ammonia (NH<sub>3</sub>) as the reducing agent. NH<sub>3</sub> is supplied to the system through urea dosing, regulated by the onboard control unit. Excess NH<sub>3</sub> is controlled with the Ammonia Slip Catalyst (ASC). Upon exiting the DEA system, the emissions should meet the restrictions imposed by the Euro VI regulations [2].

The DEA system is very complex, requiring efficient exhaust treatment for a wide range of operating conditions, corresponding to cold start, stop-and-start driving (inner city), and high speed driving (highways). As a result, DTU Chemical Engineering and Haldor Topsøe A/S are collaborating on the development of the next generation DEA system, with funding from Innovation Fund Denmark. The underlying PhD

projects concern the development of new DOC and ASC formulations (Thomas Klint Hansen), the combination of the DPF and SCR components (Kasper Linde), and the development of the control unit for efficient regulation of urea dosing in this project.

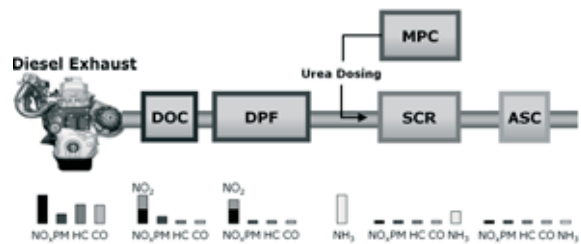


**Figure 1:** Example of a standard design of the DEA system, consisting of the DOC, DPF, SCR component, urea dosing control unit, and the ASC.

### Specific Objectives

The overall objective of this project is to develop models and model based control structures to control the urea injection to the catalyst demanded by enhanced legislation. Since a new catalyst design most likely will be developed by the other PhD-students in the overall project, it is important that the results in this project are generic and can be used for a new system as well. Therefore, the project will focus on developing a methodology on a currently used catalyst, to be able to tackle similar problems. Developing the methodology will involve several steps:

- Develop high fidelity simulation model based on first principles, parameter estimation and validation of the model
- Develop lower accuracy models, parameter estimation and validation of the models
- Quantify information loss in different models to understand the needed model complexity
- Develop and investigate several model based control schemes
- Validate the chosen control structure with full-scale engine tests using standardized test driving cycles.

## Results and Discussion

The physical phenomena inside the catalyst resulted in the model described by Eqs. (1) through (4). The equations describe the concentration of the relevant species and temperature in the bulk phase and the washcoat phase of the catalyst. It is assumed that no diffusion occur in the washcoat, thus it is only treated as a surface where the reactions take place. The kinetic expressions are based on findings in literature [3]. The kinetic parameters were calibrated using isothermal steady state data produced with small-scale monolith supplied with simulated exhaust gases. The objective function for the calibration results for the NH<sub>3</sub> can be seen in Fig. 2, with the model fit represented as crosses and the data as circles. The residuals are small, and the fit was considered satisfactory.

$$\frac{\partial c_{b,i}}{\partial t} = -u \frac{\partial c_{b,i}}{\partial z} - \frac{4k_g}{b} (c_{b,i} - c_{wc,i}) \quad (1)$$

$$\frac{\partial c_{wc,i}}{\partial t} = \frac{4k_g}{b} (c_{b,i} - c_{wc,i}) + \sum_i r_i \quad (2)$$

$$\frac{\partial T_b}{\partial t} = -u \frac{\partial T_b}{\partial z} - \frac{4h_{heat}}{b\rho_b c_{p,b}} (T_b - T_{wc}) \quad (3)$$

$$\frac{\partial T_{wc}}{\partial t} = \frac{4h_{heat}}{b\rho_b c_{p,b}} (T_b - T_{wc}) + \sum_i \Delta H_{r,i} r_i \quad (4)$$

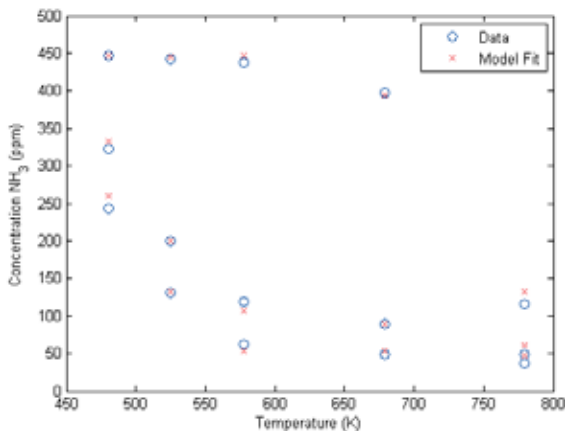


**Figure 2:** Calibration results for NH<sub>3</sub>. The circles represent the data and the crosses the model fit.

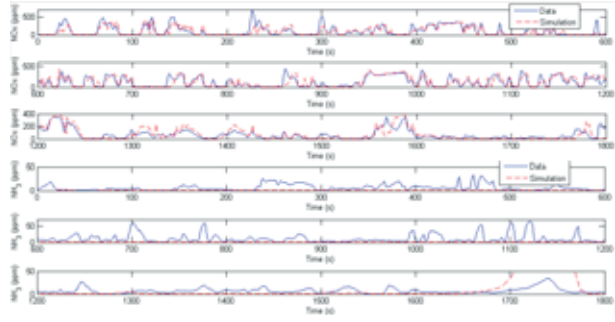


**Figure 3:** Validation results for the full-scale data. Three top figures are NO<sub>x</sub> results and three bottom pictures are NH<sub>3</sub> results. The dotted line is the model prediction and the full line is the data.

Figure 3 shows a simulation of a full-scale monolith with real truck engine exhaust gases as input to the catalyst. The full line shows the output measurement taken after the gases have passed through the catalyst, and the dotted line shows the model prediction. The NO<sub>x</sub> prediction is in good agreement with the data, especially in time but also in absolute value. The NH<sub>3</sub> simulation does not agree with data. The model predicts no NH<sub>3</sub>-slip, except for a big peak at the end of the test. Using isothermal data has likely not contained enough information to calibrate the kinetic reactions properly.

## Conclusions and Future Work

The developed first principles model was combined together with a kinetic model and calibrated with steady-state small-scale monolith data at isothermal conditions. The model was validated using full-scale monolith data with exhaust gases produced by a real diesel truck engine. The results showed that the model is capable of accurately predict the NO<sub>x</sub> output from the catalyst, but not the NH<sub>3</sub>-slip. Future work will include improving the models predictive capabilities regarding NH<sub>3</sub>. Possibly this will require using non-isothermal data. Control structures will be developed that will be used together with the model.

## Acknowledgement

This project is a collaboration between the CAPEC research center of DTU Chemical Engineering, Haldor Topsøe A/S and Innovation Fund Denmark.

## References

1. A. Fritz, V. Pitchon. The current state of research on automotive lean NO<sub>x</sub> catalysts, *Appl. Catal. B* 13 (1997).
2. W. A. Majewski, M. K. Khair, *Diesel Emissions and Their Control*, SAE International (2006)
3. L. Olsson, H. Sjövall, R. J. Blint, A kinetic model for ammonia selective catalytic reduction over Cu-ZSM-5. *Appl. Catal. B* 81 (2008)



Address:  
Department of Chemical and Biochemical Engineering  
Søltofts Plads, Building 229  
Technical University of Denmark  
DK-2800 Kgs. Lyngby  
Denmark

Telephone: +45 4525 2800  
Fax: +45 4588 2258  
E-mail: [kt@kt.dtu.dk](mailto:kt@kt.dtu.dk)  
Website: [www.kt.dtu.dk](http://www.kt.dtu.dk)

Print: GraphicCo.  
January 2016

Cover: Charlotte Brunholt

Cover photo: Christian Ove Carlsson

ISBN-13: 978-87-93054-79-0



